GEOLOGICAL SURVEY OF CANADA
COMMISSION GÉOLOGIQUE DU CANADA

PAPER / ÉTUDE
90-1C

CURRENT RESEARCH, PART C
CANADIAN SHIELD

RECHERCHES EN COURS, PARTIE C
BOUCLIER CANADIEN

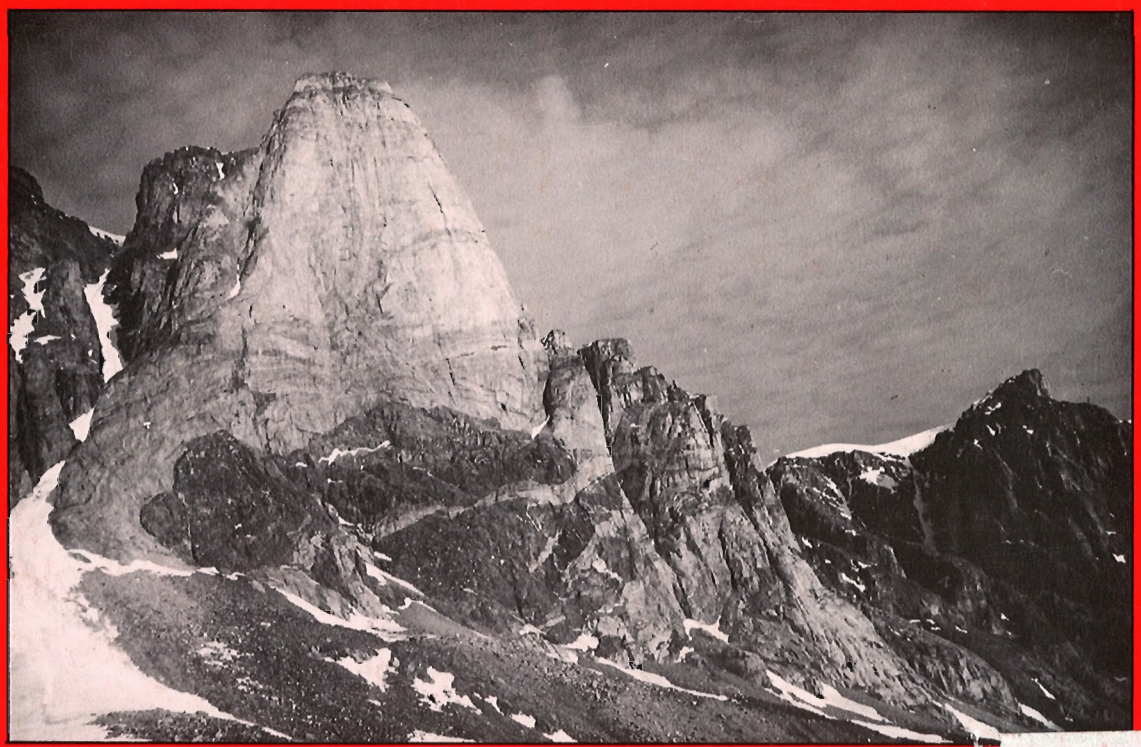

Energy, Mines and Resources Canada
Énergie, Mines et Ressources Canada

THE ENERGY OF OUR RESOURCES - THE POWER OF OUR IDEAS

L'ÉNERGIE DE NOS RESSOURCES - NOT

GEOLOGICAL SURVEY OF CANADA
COMMISSION GÉOLOGIQUE DU CANADA
PAPER/ÉTUDE 90-1C

CURRENT RESEARCH, PART C
CANADIAN SHIELD

RECHERCHES EN COURS, PARTIE C
BOUCLIER CANADIEN

1990

Available in Canada through

authorized bookstore agents and other bookstores

or by mail from

Canadian Government Publishing Centre
Supply and Services Canada
Ottawa, Canada K1A 0S9

and from

Geological Survey of Canada offices:

601 Booth Street
Ottawa, Canada K1A 0E8

3303-33rd Street N.W.
Calgary, Alberta T2L 2A7

100 West Pender Street
Vancouver, British Columbia V6B 1R8

A deposit copy of this publication is also available
for reference in public libraries across Canada

Cat. No. M44-90/1C
ISBN 0-660-55698-7

Cover description

A 1200 m peak on east side of Cambridge Fiord, Baffin Island showing large stacked mafic boudins near axis of recumbent fold dipping northeast.

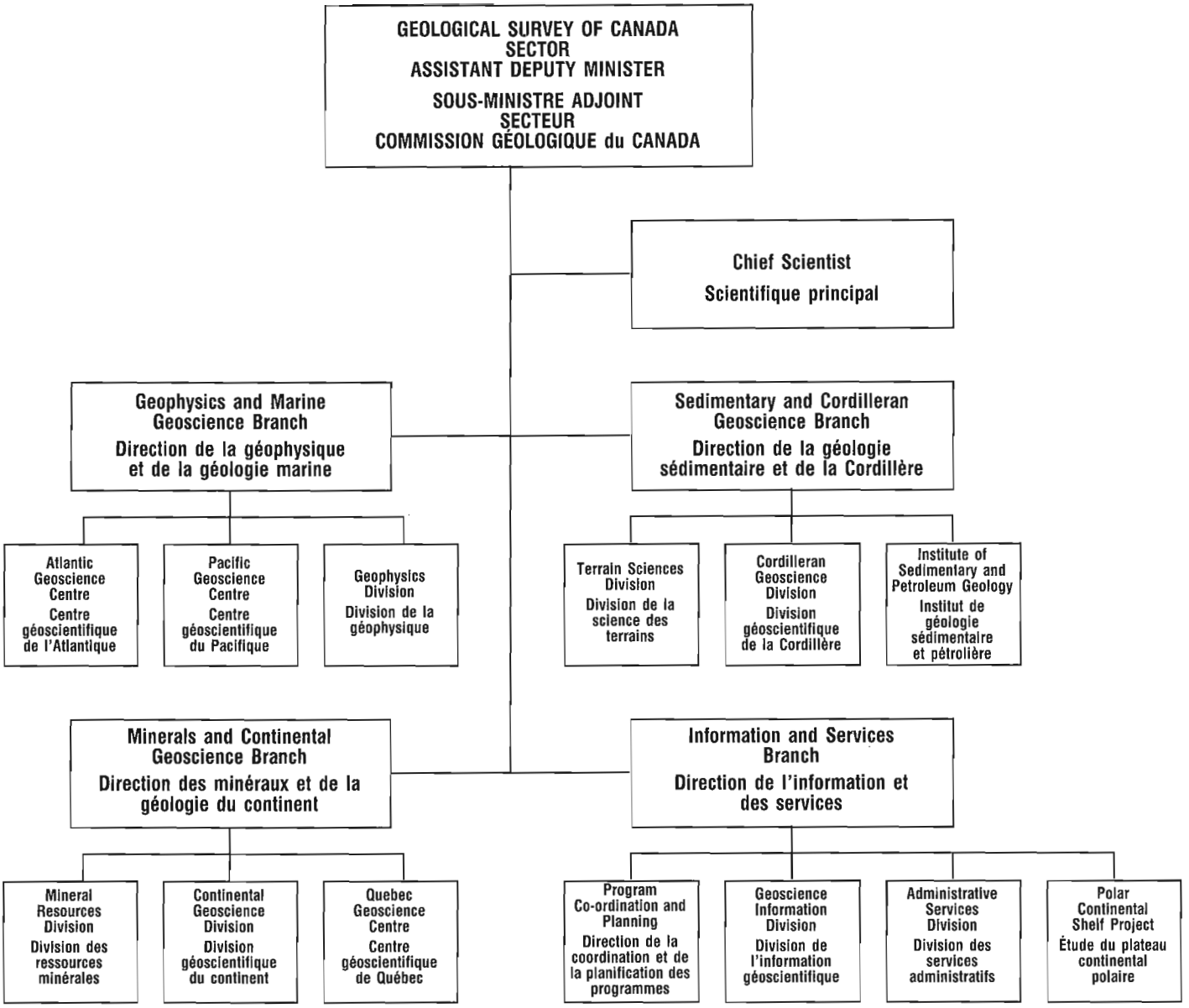
GEOLOGICAL SURVEY OF CANADA
SECTOR
ASSISTANT DEPUTY MINISTER
SOUS-MINISTRE ADJOINT
SECTEUR
COMMISSION GÉOLOGIQUE du CANADA
Chief Scientist
Scientifique principal
Geophysics and Marine Geoscience Branch
Direction de la géophysique et de la géologie marine
Sedimentary and Cordilleran Geoscience Branch
Direction de la géologie sédimentaire et de la Cordillère
Atlantic Geoscience Centre
Centre géoscientifique de l'Atlantique
Pacific Geoscience Centre
Centre géoscientifique du Pacifique
Geophysics Division
Division de la géophysique
Terrain Sciences Division
Division de la science des terrains
Cordilleran Geoscience Division
Division géoscientifique de la Cordillère
Institute of Sedimentary and Petroleum Geology
Institut de géologie sédimentaire et pétrolière
Minerals and Continental Geoscience Branch
Direction des minéraux et de la géologie du continent
Information and Services Branch
Direction de l'information et des services
Mineral Resources Division
Division des ressources minérales
Continental Geoscience Division
Division géoscientifique du continent
Quebec Geoscience Centre
Centre géoscientifique de Québec
Program Co-ordination and Planning
Direction de la coordination et de la planification des programmes
Geoscience Information Division
Division de l'information géoscientifique
Administrative Services Division
Division des services administratifs
Polar Continental Shelf Project
Étude du plateau continental polaire

Separates

A limited number of separates of the papers that appear in this volume are available by direct request to the individual authors. The addresses of the Geological Survey of Canada offices follow:

601 Booth Street,
OTTAWA, Ontario
K1A 0E8
(FAX: 613-996-9990)

Institute of Sedimentary and Petroleum Geology,
3303-33rd Street N.W.,
CALGARY, Alberta
T2L 2A7
(FAX: 403-292-5377)

Cordilleran and Pacific Geoscience Division,
100 West Pender Street,
VANCOUVER, B.C.
V6B 1R8
(FAX: 604-666-1124)

Pacific Geoscience Centre
P.O. Box 6000,
9860 Saanich Road
SIDNEY, B.C.
V8L 4B2
(FAX: 604-356-6565)

Atlantic Geoscience Centre
Bedford Institute of Oceanography,
P.O. Box 1006
DARTMOUTH, N.S.
B2Y 4A2
(FAX: 902-426-2256)

Quebec Geoscience Centre
2700, rue Einstein
C.P. 7500
Ste-Foy, Québec
G1V 4C7
(FAX: 418-654-2615)

When no location accompanies an author's name in the title of a paper, the Ottawa address should be used.

Tirés à part

On peut obtenir un nombre limité de « tirés à part » des articles qui paraissent dans cette publication en s'adressant directement à chaque auteur. Les adresses des différents bureaux de la Commission géologique du Canada sont les suivantes:

601, rue Booth
OTTAWA (Ontario)
K1A 0E8
(facimilé: 613-996-9990)

Institut de géologie sédimentaire et pétrolière
3303-33rd St. N.W.,
CALGARY, Alberta
T2L 2A7
(facimilé: 403-292-5377)

Division géoscientifique de la Cordillière et du Pacifique
100 West Pender Street,
VANCOUVER, Colombie-Britannique
V6B 1R8
(facimilé: 604-666-1124)

Centre géoscientifique du Pacifique
B.P. 6000,
9860 Saanich Road
SIDNEY, Colombie-Britannique
V8L 4B2
(facimilé: 604-356-6565)

Centre géoscientifique de l'Atlantique
Institut océanographique de Bedford
B.P. 1006
DARTMOUTH, Nouvelle-Écosse
B2Y 4A2
(facimilé: 902-426-2256)

Centre géoscientifique de Québec
2700, rue Einstein
C.P. 7500
Ste-Foy, Québec
G1V 4C7
(facimilé: 418-654-2615)

Lorsque l'adresse de l'auteur ne figure pas sous le titre d'un document, on doit alors utiliser l'adresse d'Ottawa.

CONTENTS

Structural observations in the Gilbert River belt, Grenville Province, southeastern Labrador

Simon Hanmer and David J. Scott[1].
Continental Geoscience Division

Hanmer, S. and Scott, D.J. Structural observations in the Gilbert River belt, Grenville Province, southeastern Labrador; in Current Research, Part C, Geological Survey of Canada, Paper 90-1C, 1-11, 1990.

Abstract

The Gilbert River belt is a bundle of elongate, syntectonically emplaced granitoids intruded into a corridor of upper amphibolite facies metasediments undergoing folding. Mylonites are volumetrically unimportant. Whereas the Gilbert River belt is not a crustal-scale shear zone, its southwestern margin is a 100 m wide zone of granoblastic mylonite which may represent the tectonic contact between the Mealy Mountains-Pinware terranes and the Lake Melville Terrane.

Résumé

La zone de Gilbert River est un faisceau de plutons granitiques allongés, mis en place pendant le plissement synmétamorphique (faciès des amphibolites) d'une ceinture de métasédiments. Les mylonites sont peu importantes. Bien que la zone de Gilbert River ne soit pas un cisaillement d'importance crustale, la lisière mylonitique qui forme sa bordure sud-ouest, large de 100 m, pourrait marquer le contact tectonique entre les terranes de Mealy Mountains et Pinware d'un côté et le terrane de Lake Melville de l'autre.

[1] Department of Geology, Queen's University, Kingston, Ontario K7L 3N6

INTRODUCTION

Recent regional mapping in the Port Hope Simpson — St. Lewis River area in the Grenville Province, southeastern Labrador has led to the identification of a 30 km wide, crustal-scale zone of intense deformation, the Gilbert River shear belt (Gower et al., 1987, 1988), referred to as the Gilbert River belt throughout this report. Compared with the areas on either side, the Gilbert River belt is a striking corridor of highly elongate map units (Gower, 1988a, b). According to Gower et al. (1988), the Gilbert River belt represents the southeastern extension of the Lake Melville Terrane and separates the Mealy Mountains and Pinware Terranes to the southwest from the Hawke River terrane to the northeast (Fig. 1). The potential tectonic significance of the belt is emphasized by the amplitude of the very pronounced discrete aeromagnetic low which underlies it (Gower et al., 1987). Furthermore, the northeastern margin of the Gilbert River belt coincides with the top of a very pronounced southwest facing slope in the regional gravity field, whose base coincides with a late fault developed within the Gilbert River belt, the Gilbert River fault (Gower et al., 1987). Gower and co-workers proposed that movement within the Gilbert River belt was predominantly dip-slip north of the Gilbert River fault and dextral strike-slip south of the fault. Our six weeks of fieldwork during the summer of 1989, undertaken at the invitation of C.F. Gower (Newfoundland Department of Mines), focussed on the structural aspects of the coastal exposure of the Gilbert River belt in the Alexis Bay — St. Lewis area. Principal field observations are:

(1) The WNW-ESE trending structural grain of the Gilbert River belt is marked by the elongate geometry of lenses of variably foliated granitoid and predominantly pelitic paragneiss. In the granitoids this grain is also marked by a single, sometimes composite, foliation. In the paragneisses the regional trend is generally marked by F2 fold axial planes. The regional extension lineation (Fig. 2a) in the granitoids is parallel to that in the paragneisses which is

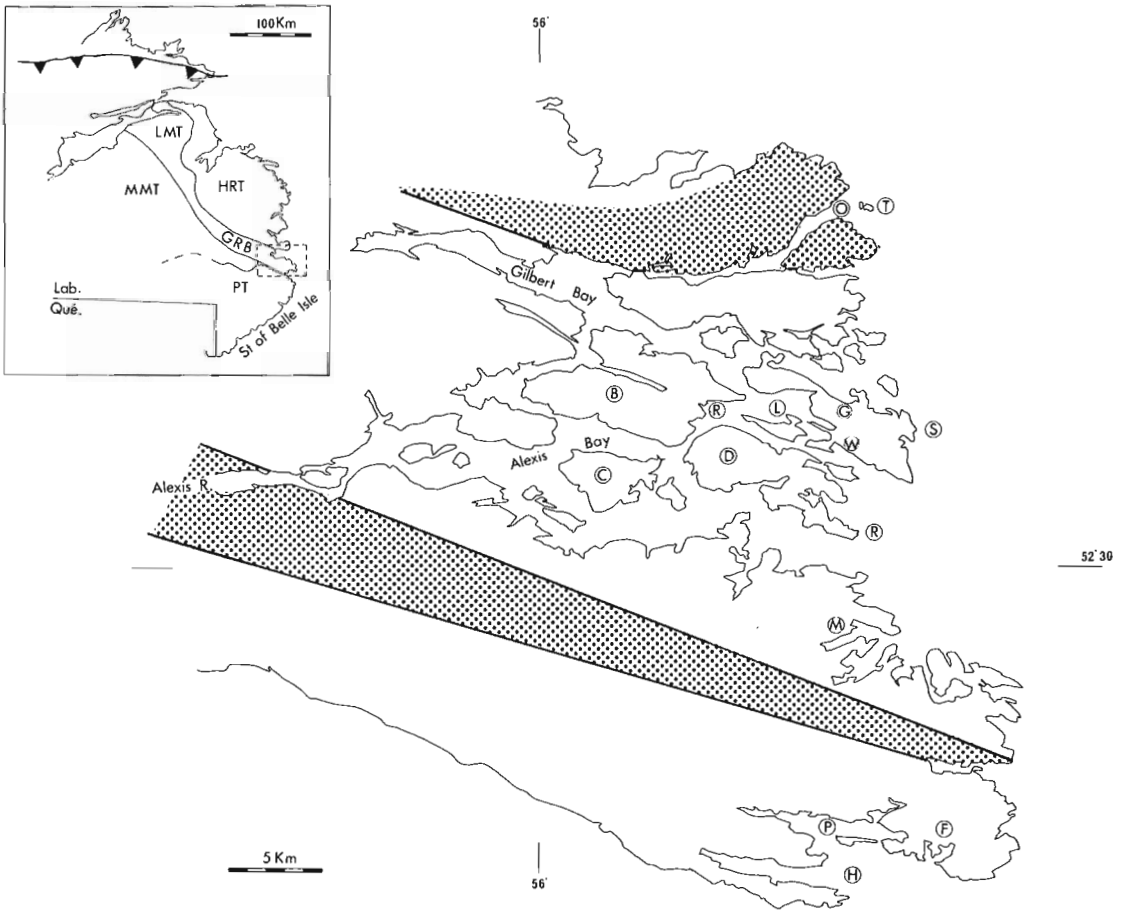

Figure 1. Location (inset) and geological summary of the study area (boxed) in the Grenville Province, southeastern Labrador. The toothed line is the Grenville Front. Abbreviations in the inset map are Mealy Mountains Terrane (MMT), Lake Melville Terrane (LMT), Gilbert River Belt (GRB), Hawke River Terrane (HRT), Pinware Terrane (PT). Shaded map units are the White Bear Arm mafic complex (north) and the Alexis River anorthosite and associated mafic rocks (south). Non-shaded areas are underlain by granitoids and semi-pelitic metasediments. Letter codes are Big Island (B), Cartwright Island (C), Denbigh Island (D), Cape St. Francis (S), Georges Cove (G), Leg Island (L), Long Harbour (H), Mecklenberg Harbour (M), Occasional Harbour (O), Port Marnham (P), Rexon's Cove (R, west), Red Point (R, east), St. Lewis (F), Twin Islands (T), Williams Harbour (W). Adapted from Gower et al., 1987, 1988.

coaxial with the F2 fold axes. In contrast to the consistently shallow WNW plunges reported from the inland continuation of the Gilbert River belt (Gower, 1988a), plunges in the coastal section are both steep and highly variable.

(2) Complex boudinage and 'lobe-and-cusp' folding of mafic dykes emplaced into granite host rocks in various states of deformation, indicate that both the granite host and the dykes were emplaced within a short time interval during the subsolidus cooling of the granites and are syntectonic with respect to at least part of the regional deformation at high metamorphic grade.

(3) Strain regime is variable and was strongly influenced by the material properties of the deforming rock. In layered paragneisses, small-scale shear-sense criteria are best observed on YZ surfaces perpendicular to the F2 fold axes and on XZ surfaces in the homogeneous granitoids. In the former case the shearing is a consequence of local layer-parallel slip during the folding process, whereas the latter case reflects a component of regionally imposed shear.

(4) Mylonites and strongly sheared rocks related to the regionally imposed shear component of the deformation are volumetrically unimportant. They occur in six ill-defined narrow corridors within which, with few exceptions, discrete mylonite zones are in the order of 10 m wide by up to several kilometres long. The mylonite zones occur either *en-echelon* or *en-relais*, rather than side-by-side. Mylonites were formed at upper amphibolite to greenschist facies.

(5) The most significant high grade mylonite zone forms the north shore of Long Harbour and comprises up to circa 100 m (width) of rectiplanar granoblastic straight gneiss. It constitutes the tectonic contact between the Gilbert River belt to the northeast and the Pinware Terrane to the southwest.

(6) The displacement pattern within the mylonites is variable and comprises components of dextral transcurrent and north-side-up slip.

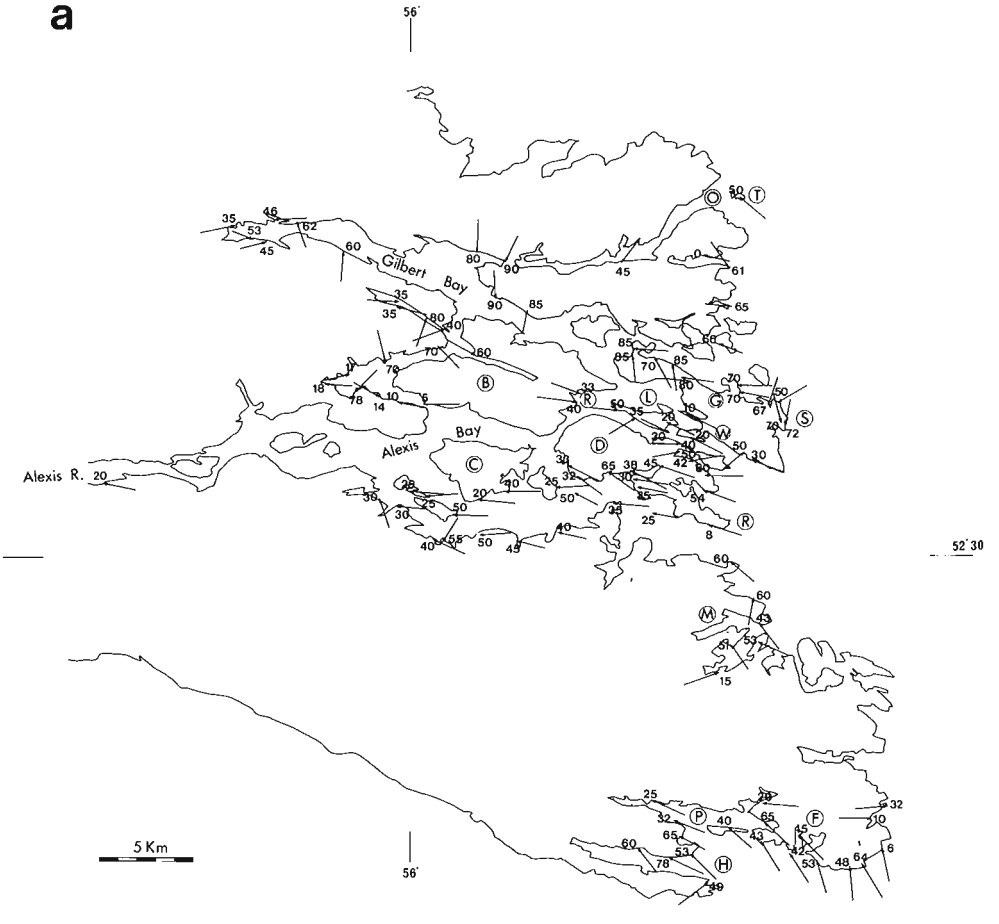

Figure 2. Structural data. (a) Extension lineations. (b) Locations of outcrops within zones (circa 10 m wide) of mylonitic rocks. Circles, squares and diamonds are protomylonite, mylonite, ultramylonite respectively. Solid symbols are greenschist facies, open symbols are high grade mylonitic rocks. (c) Distribution of observations of shear-sense criteria. Location abbreviations as in Fig. 1.

LITHOLOGICAL AND GEOMETRICAL SETTING

The southeastern end of the exposed Gilbert River belt is essentially composed of granitoids, semi-pelitic to pelitic metasediments and an association of meta-anorthosite and amphibolite (Fig. 1). The granitoids in particular are cut by an array of mafic dykes, which also occur to a lesser extent within the metasediments (see Gower et al., 1987, 1988 for detailed lithological descriptions and Gower, 1988a, b, for geological maps).

The metasediments range from homogeneous metapelites to rhythmically layered metapelite to siliceous semi-pelite and rare quartzite. The sillimanite — garnet — biotite — K feldspar mineral assemblages of much of the metasediment and the development of large and small-scale migmatitic structure are indicative of upper amphibolite facies metamorphism. However, metapelitic lithologies north of the Rexon's Cove mylonites (Fig. 2b; see below) and south of St Lewis are muscovite ± sillimanite bearing and represent middle amphibolite facies. An S1 foliation is developed parallel to the relict primary layering and the migmatitic banding in the metasediments. A coarse 'knotty' texture of K-feldspar and quartz — sillimanite ± magnetite aggregates is associated with S1. S1 is folded about upright F2 folds of variable plunge and scale, whose wavelength ranges from centimetres to hundreds of metres. The F2 fold style is scale-independent and comprises simple long limbs alternating with short limbs decorated with minor folds whose enveloping surface makes an high angle with the long limbs. F2 fold vergence is generally towards the north in the Alexis Bay area, but towards the south in the St Lewis area. An S2 axial plane foliation is variably developed in association with the F2 folds. Although commonly absent from the F2 hinge zones and short limbs, S2 is strongly expressed in the long F2 limbs. It develops either by the small-scale folding and complete transposition of the S1 'knotty' foliation into a new rectiplanar foliation or by the co-planar reworking of the S1 foliation as the F2 long limbs develop (Fig. 3a,b). In either case the development of S2 imparts a marked slabby appearance to the rock. The S2 fabric is not associated with retrogression of the S1 mineral assemblage.

A well developed extension lineation, commonly marked by aligned sillimanite, is present on both S1 and S2 surfaces (Fig. 2a and 3c). It is everywhere parallel to F2 fold axes (Fig. 3d), irrespective of fold tightness, indicating that the folds initiated coaxial with the lineation. Shear-sense indicators such as rotated winged feldspar porphyroclasts and sets of asymmetrical extensional shears are best observed on F2 long limbs in sections perpendicular to the extension lineation (YZ). In three dimensions it can be verified that the intersection of the extensional shears with the S1 and/or S2 foliation is parallel to the extension lineation. The shear-sense observed is systematically antithetic to the sense of rotation undergone by the fold limb during the progressive tightening of the fold. From this we conclude that the shearing observed in the metasediments is essentially a reflection of a local component of layer-parallel shear related to the folding process.

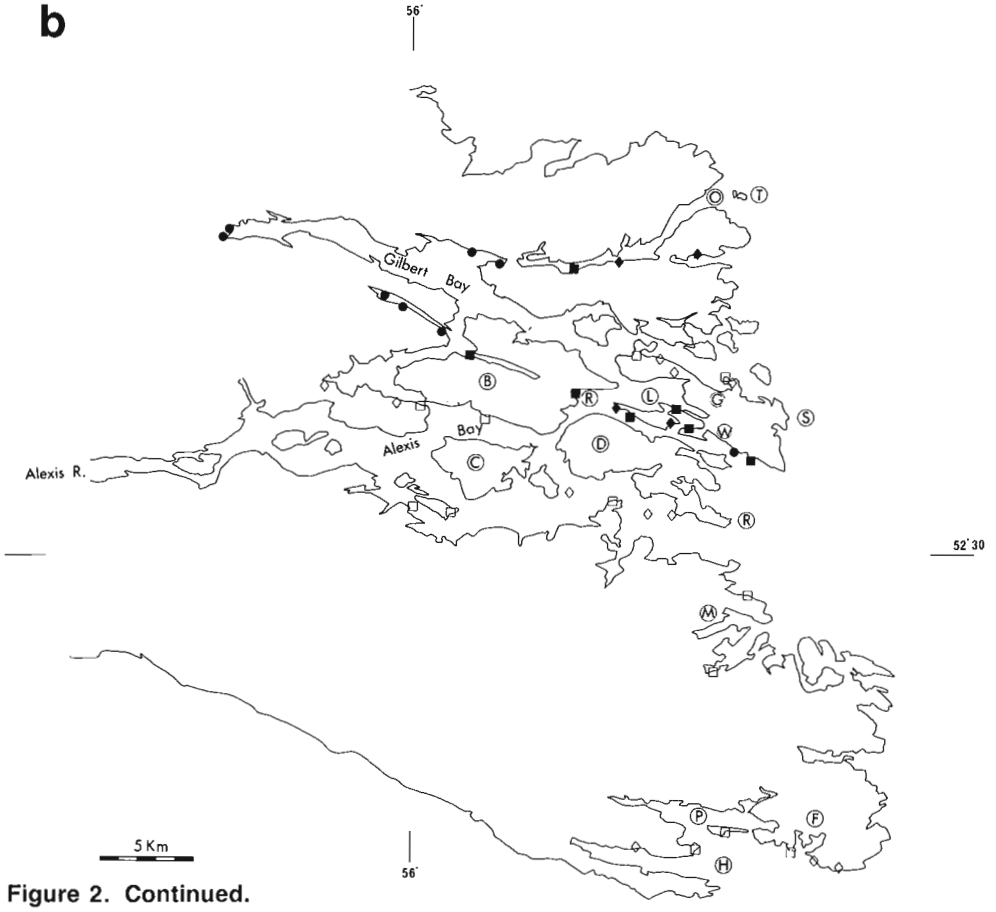

Figure 2. Continued.

The granitoids range from coarsely megacrystic through coarse to finer equigranular textures. The coarser granitoids are fairly rich in biotite. The distinction between megacrystic and coarse granitic texture with scattered large feldspars is not always clear cut. Much of the granitoid is moderately to well foliated, although large exposures on and southwest of Cartwright Island and on Denbigh Island show only mild foliation development. The salient point here is that the overall intensity of foliation development does not reflect an intense penetrative finite strain. For the most part the WNW trending foliation is simple and upright. It carries a variably WNW plunging extension lineation (Fig. 2a). Locally, sets of dextral asymmetrical extensional shears are developed which are best observed in sections parallel to the extension lineation (XZ plane of the finite strain ellipsoid), irrespective of its plunge.

Fine to medium grained equigranular leucogranite occurs in three distinct associations. The first is the late tectonic 1176 Ma (U/Pb on zircon; Gower, 1988a) Gilbert Bay pluton which straddles Gilbert Bay in the vicinity of the northeast corner of Denbigh Island (Gower et al., 1987). The second is as sub-concordant sheets, up to several tens of metres thick, intruded into the low grade Rexon's Cove and Occasional Harbour mylonites (Fig. 2b; see below). A composite C/S fabric is commonly developed within these leucogranite sheets. The dihedral angle between the C and the S planes is usually observed in planes parallel to the extension lineation (XZ). The third association comprises discrete, clearly intrusive sheets of white leucogranite, ± small pinhead garnets, which are spatially associated with the aluminous metasediments. The spatial relationship, the aspect of the granite and the high metamorphic grade are typical of migmatite terranes and suggest a local origin for the leucogranites. Such leucogranites were emplaced subparallel to S1 in the metasediments. Among them are those which carry an internal foliation parallel to S1; others do not. Both sets are folded by F2 and those sheets without an internal S1 develop a good S2 foliation. Excellent examples of both sets of leucogranite sheets are present in the metasediments at George's Cove and Cape St. Francis. Precise isotopic dating of the leucogranites would closely bracket both S1 and S2 in the paragneiss.

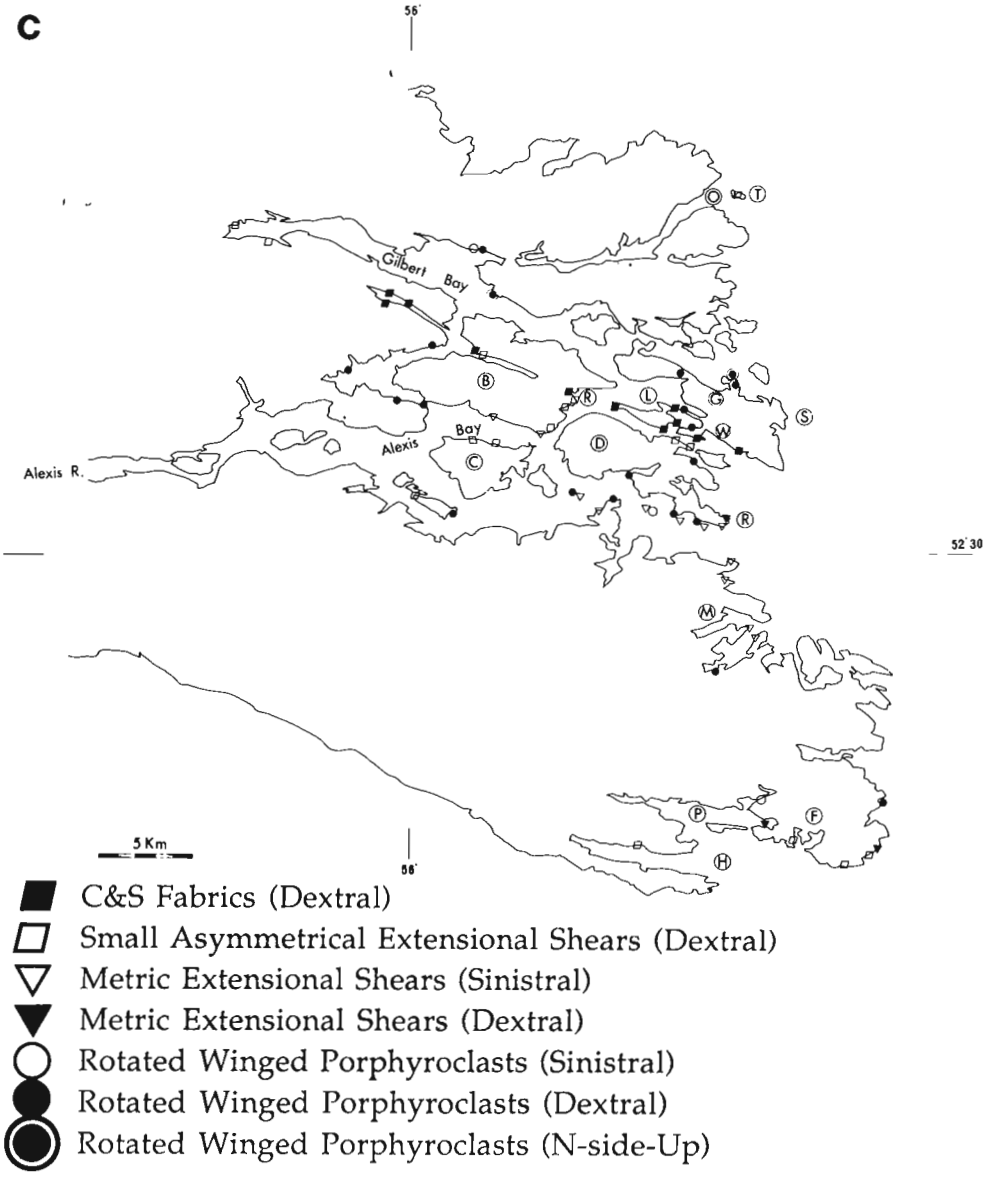

Figure 2. Continued.

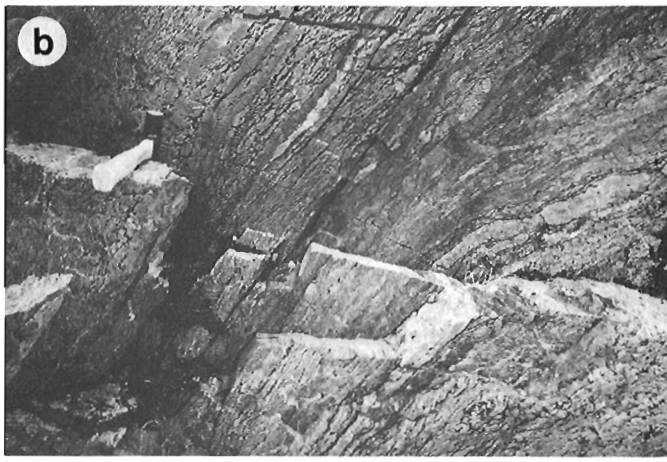

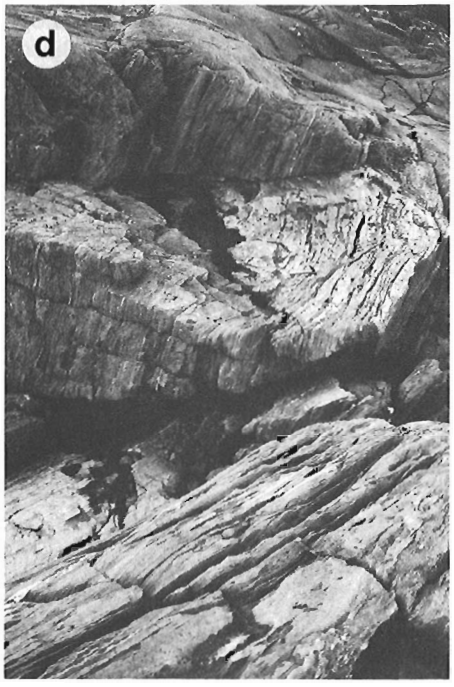

Figure 3. Deformation structures in metasediments. (a) Upright horizontal F2 fold of S1 foliation, hammer parallel to fold axis and to extension lineation; Red Point. (GSC 205022-W) (b) Detail of A to show strong reworking and grain size-reduction of S1 in developing F2 fold limb. Clearly the sense of shear is perpendicular to the extension lineation (hammer). (GSC-205022-V). (c) Dip-parallel extension lineation; south of Cape St. Francis. (GSC-205022-I). (d) F2 fold axis parallel to steeply plunging extension lineation. Shear direction on long limb is clearly perpendicular to the lineation; Cape St Francis. (GSC-205022-C).

A distinctive garnet ± sillimanite diatexite associated with sheets of white garnet leucogranite occupies much of the mouth of the Alexis River in the southwest corner of Alexis Bay. The north shore and islands within the river channel are underlain by a granitoid matrix charged with irregular, misoriented 10 cm to 5 m diameter inclusions of amphibolite and layered paragneiss, much of which is recognizable metatexite with compositionally controlled leucosome development. Although the inclusions are internally deformed, the diatexite is remarkable for its jumbled, poorly layered appearance. The south shore, west and south of Lazyman Island (southwest of Cartwright Island), is similar, but with much smaller amphibolitic inclusions. The principal difference with the north shore is the presence of 1-10 m thick concordantly foliated leucogranite sheets dipping systematically at 20 degrees to the southwest. This shallow-dipping layering is cut by a three-dimensional array of extensional shears, each up to a metre or so in width, which accommodate a steeply plunging principal direction of shortening. We cannot propose a well constrained explanation for this structure; we simply note the spatial coincidence of a poorly deformed diatexite structure with the only extensive flat-lying planar geometry in the study area. Such a configuration calls to mind the experimental rising dome models of Dixon (1975).

Anorthositic rocks form a strip in the southern part of the study area (Fig. 1). Essentially gabbroic anorthosite to leucogabbro for the most part, they present textures ranging from coarsely ophitic and manifestly igneous to strongly foliated and deformation induced. The vertical WNW trending foliation is a simple planar fabric, generally marked by deformed polycrystalline aggregates of amphibole ± garnet, set in a granoblastic isotropic plagioclase matrix. No lineation is preserved. However, the deformation foliations within the anorthositic rocks are themselves cut at high

angles by 25-50 cm wide veins of anorthosite (south shore, Alexis River). For this reason we consider much of the deformational structure of the anorthositic rocks to be of primary origin, related to emplacement of the igneous rock.

MYLONITES

Gower et al. (1987, 1988) have described the Gilbert River belt as a 30 km wide zone of intense right-lateral, strike-slip deformation. We examined and assessed all of the previously identified occurrences of mylonite (Fig. 4a) in the coastal section and sought to find others. The resulting map pattern (Fig. 2b) comprises six ill-defined, narrow corridors within which discrete narrow, mylonite zones are in the order of 10 metres wide by up to several kilometres long. Within the corridors the mylonite zones are arranged either *en-echelon* or *en-relais*, rather than side-by-side; it cannot be determined if they are arranged in an anastomosing or a segmented pattern. Because of the stepped arrangement of the mylonite zones, the corridors within which they occur are much wider (100-1000m) than the individual mylonite zones themselves. The proportion of intensely strained rocks within the coastal section of the Gilbert River belt is very small.

Metamorphically the mylonites fall into two groups (Fig. 2b). The high grade mylonites formed at amphibolite facies. The metamorphic correspondence between mineral assemblages within and outside of the mylonite zones, coupled with the development of progressive strain gradients at their margins, suggests that the mylonites are contemporaneous with the development of the foliation and folding in the intervening granitoids and metasediments. Consequently, the parallelism of mildly developed and mylonitic foliation planes suggests that the high grade mylonites formed under a bulk non-ideal shear regime (combined pure and simple shear). At Port Marnham the pelitic component of the mylonites contains a middle amphibolite facies sillimanite-muscovite assemblage. Pelitic components of the other high grade mylonites contain an upper amphibolite facies sillimanite — K feldspar bearing assemblage. The most important development of high grade mylonite occurs as a zone of now granoblastic, granitic and amphibolitic banded straight gneiss (Fig. 4b; see definition in Hanmer, 1988a), about 100 m thick. It lies directly along strike from the proposed boundary between the Pinware Terrane and the Gilbert River belt, a tectonic boundary which truncates the contact between the Mealy Mountains and Pinware Terranes (Gower et al., 1988).

The low grade mylonites formed at greenschist facies in two zones; the Rexon's Cove (Big Island — Rexon's Cove — Leg Island — Williams Harbour) and Occasional Harbour (Gilbert Bay — Occasional Harbour) mylonites (Fig. 2b). However, the abundant development of coarse white mica aligned in the extension lineation and S2 foliation in sillimanite paragneiss immediately adjacent to the Rexon's Cove mylonites suggests that the greenschist facies mylonite zones may have initiated at higher metamorphic grade and narrowed with cooling (e.g. Hanmer, 1988b). They are typically green in colour. Where the mylonitic rocks are coarse enough, as in the case of protomylonites, white mica is seen to accompany the chlorite. The green mylonites contain numerous bands of pink mylonite derived from syntectonically emplaced pink leucogranite (see below). The green and pink ultramylonites are locally cut by well developed pseudotachylite and disrupted by penetratively developed fracturing and minor cataclasis, especially in the Gilbert Bay — Occasional Harbour corridor.

Mylonite zones arranged in a segmented or anastomosing geometry are limited in the amount of displacement they can accommodate before a master slip surface (or zone) emerges. The only mylonite zones of demonstrably significant continuous strike length are the Rexon's Cove and Occasional Harbour greenschist facies mylonites (Fig. 2b). Higher grade mylonites at Long Harbour are probably part of a belt extending along the length of the southwest side of the Gilbert River belt (see Gower et al., 1988). However the mylonites identified in the Mecklenberg Harbour area have not been identified along strike. Mylonites identified south of Denbigh and east of Cartwright Islands do not continue into Cartwright Island. It is possible that they swing southwestward to link with the mylonites of Lazyman Island, southwest of Cartwright Island, but this remains unconstrained. In any event, the Lazyman Island mylonites do not continue into the adjacent mainland towards which they strike. Similarly, the mylonite corridor located between Cartwright and Big Islands does not continue onto the mainland to the west, nor into Denbigh Island to the east. Whereas it could pass between Cartwright and Denbigh Islands to link with the mylonites south of Denbigh Island, such a fortuitous deflection is purely speculative. High grade mylonites west of Georges Cove strike into Gilbert Bay. Whereas they could project along the 20 km length of Gilbert Bay, there is no evidence for this at the western end of the bay. Finally, the mylonites in the St. Lewis area do not continue onto the mainland west of Port Marnham.

From the foregoing, we conclude that, with the possible exception of the Long Harbour, Rexon's Cove and Occasional Harbour zones, the mylonites of the Gilbert River belt have not accommodated regionally significant displacements. However, given their generally narrow widths, this does not preclude them representing intense local strains.

Whatever the magnitude of offsets accommodated by the mylonite zones, there is a certain consistency to the complex displacement pattern (Fig. 2c). The low grade Rexon's Cove mylonites are dextral transcurrent and characterized by shallow to moderate ESE plunging extension lineations and transport directions. The resultant dip-slip component is north-side-down. The high grade mylonites to the north of the Rexon's Cove mylonites show a north-side-up dip-slip movement along a steeply westerly plunging to dip-parallel extension lineation (Fig. 4c). Those in the Long Harbour — St. Lewis area show a similar north-side-up motion along a moderately to steeply WNW plunging extension lineation. Those in Alexis Bay, south of the Rexon's Cove mylonites show a dextral transcurrent movement along a shallow to moderate WNW plunging extension lineation. The resultant dip-slip component is north-side-up.

The following observations suggest that the dextral transcurrent components of the high and low grade mylonites

are separated in time by an high grade pure shear event. The highly anisotropic high grade mylonites are commonly cut by asymmetrical extensional shears ranging in size from centimetres to metres long and millimetres to decimetres wide. Most of these shears make a clockwise angle of about 25 degrees with the mylonite foliation and have a dextral shear-sense. Thus, irrespective of their size, the asymmetrical extensional shears are kinematically compatible with the dextral shear-sense of the mylonites as deduced, for example, from rotated winged porphyroclasts. However, demonstrably dextral transcurrent mylonites in the southern part of Alexis Bay (Mecklenberg Harbour — Red Point — south Big Island) are cut by sinistral asymmetrical extensional shears which lie anticlockwise to the mylonite foliation (Fig. 2c and 4d). Such shears coexist with dextral rotated winged porphyroclasts enclosed in the mylonite foliation in the same outcrops. Clearly a set of sinistral shears has been imposed on the dextral mylonites. Since the metamorphic mineral assemblage within the later extensional shears is not retrograde, we conclude that the sinistral shearing occurred under similar conditions to the upper amphibolite facies mylonitization.

We propose the following scenario to account for the foregoing observations. It is well known that bulk pure shear may be accommodated by slip on conjugate shear planes. Furthermore, such shears may develop in a domainal pattern where contemporaneous dextral and sinistral shears are spatially mutually exclusive (e.g. Hanmer, 1979; Hoffman et al., 1984). We have identified a domain of sinistral asymmetrical extensional shears. A domain of their conjugates would not be readily identifiable in the northern part of Alexis Bay since such structures would be difficult to distinguish from similar structures generated during dextral shear. We therefore suggest that the Alexis Bay area was subjected to an episode of high temperature pure shear which postdated the formation of the high grade mylonites, accommodated by localized strain distributed in domains of

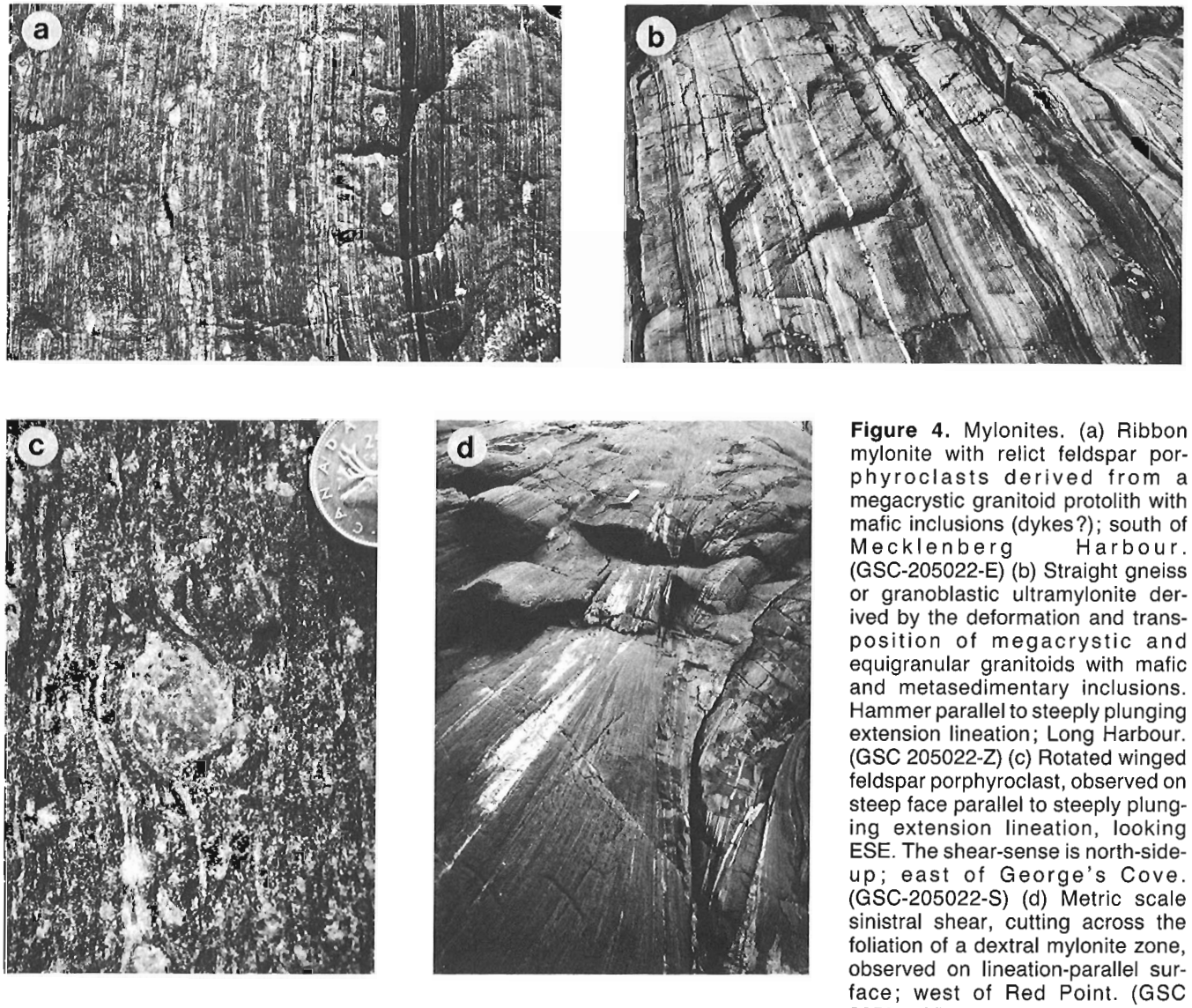

Figure 4. Mylonites. (a) Ribbon mylonite with relict feldspar porphyroclasts derived from a megacrystic granitoid protolith with mafic inclusions (dykes?); south of Mecklenberg Harbour. (GSC-205022-E) (b) Straight gneiss or granoblastic ultramylonite derived by the deformation and transposition of megacrystic and equigranular granitoids with mafic and metasedimentary inclusions. Hammer parallel to steeply plunging extension lineation; Long Harbour. (GSC 205022-Z) (c) Rotated winged feldspar porphyroclast, observed on steep face parallel to steeply plunging extension lineation, looking ESE. The shear-sense is north-side-up; east of George's Cove. (GSC-205022-S) (d) Metric scale sinistral shear, cutting across the foliation of a dextral mylonite zone, observed on lineation-parallel surface; west of Red Point. (GSC 205022-Y)

exclusive slip-sense. The metamorphic grade of the asymmetrical shears indicates that they formed prior to the low grade mylonites. This hypothesis is testable since excellent examples of intrusive sheets of fine to medium grained, equigranular, white garnet leucogranite are both emplaced into and deformed by the sinistral shears at Red Point. Precise isotopic dating of these sheets will yield the age of the pure shear event.

RELATIVE CHRONOLOGY

The Gilbert Bay pluton is everywhere isotropic to very poorly foliated and postdates the deformation in its immediate envelope. Accordingly, at least the high grade deformation in the Gilbert River belt is pre-1176 Ma. With very few exceptions, contacts between the other granitoids and the metasediments are concordant. One of the few exceptions is a 1 m wide subconcordant vein of very poorly foliated megacrystic granite which cuts across the S2 foliation of the metasediments at a low angle in George's Cove. In most cases, however, the simple foliation of the granitoid is parallel to the co-planar elements of the wall-rocks and inclusions (S1, F2 axial planes, S2, F2 long limbs). The question then arises as to whether the coarser granitoids are (i) pre-D1 and have acted as compositionally homogeneous bodies which did not register folding, or (ii) have only witnessed the D2 deformation. This question will be best addressed by precise isotopic dating of the leucogranite sheets emplaced between late D1 and pre-D2 in the paragneiss and comparing the results with similar study of the coarse granitoids themselves. The equigranular leucogranite sheets, spatially associated with the low grade Rexon's Cove and Occasional Harbour mylonites are demonstrably contemporaneous with the greenschist facies mylonitization. On the west side of Big Island, long, continuous, thin (10-25 cm) sheets of leucogranite lie concordant to the mylonite foliation, spaced at 10-25 cm intervals. Their internal structure ranges from isotropic granite to ribbon ultramylonite, the two extreme cases commonly occurring side by side. We conclude that the granite sheets were emplaced during the low grade mylonitization. Veins of medium grained equigranular leucogranite commonly cross-cut the foliation in the megacrystic granites. This, combined with the retrograde nature of the low grade mylonites (see below), indicates that the leucogranite sheets are younger than the coarser granitoids. For the moment we entertain the possibility that the leucogranite sheets could be contemporaneous with the superficially similar Gilbert Bay pluton.

Granitoids and mafic dykes

The coarse granitoids are intruded by a set of 25-200 cm wide mafic dykes (Fig. 5). These dykes are boudined and folded. However, the relationships between intrusion, subsolidus cooling and deformation warrant close examination, since they allow us to constrain the relative timing of part of the high grade deformation in the Gilbert River belt.

Vertical to upright fine grained, internally homogeneous mafic dykes, now metamorphosed to garnet amphibolite, intrude and cross-cut isotropic granitoids, foliated granitoids, F2 folded metasediments and syn to post-D2 mylonites. In the foliated granitoids, many outcrops contain an earlier sub-set of thin, drawn out, boudined dykes with ragged boundaries. These are cross-cut by a later sub-set of thicker, parallel-sided mafic dykes with discrete, planar boundaries. The thicker, discrete dykes are described in some detail below.

Heterogeneously extended mafic dykes occur as trains of blocky or barrel-shaped boudins in both isotropic and foliated megacrystic granite in Alexis Bay (Fig. 5a-c). Excellent examples are seen on islands southwest of Cartwright Island. Judging by the boudin gaps, extensions in excess of 50 % are not uncommon and local extensions greater than 100 % occur. The interboudin gaps are sometimes filled by a granitic material other than the host granite (Fig. 5a). However, we are particularly impressed by those cases where, in isotropic host granitoid, the interboudin gaps are occupied by apparently unmodified isotropic host (Fig. 5b,c). The absence of foliations related to flow of the host granitoid into the interboudin gaps suggests that the granitoid was stiff enough to fail by fracture, soft enough to flow as a continuous medium and hot enough to efface all trace of flowage by (re)crystallisation (Fig. 5a). In other examples straight, continuous dykes are strongly extended symmetrically along a NNE-SSW direction, whereas the granitoid carries a vertical tectonic foliation oriented ESE-WNW. Clearly the boudinage was not caused by the imposition of the tectonic foliation. Abstracting the foliation returns us to a case identical to that just described for an isotropic host granitoid.

Segments of mafic dyke, including parts of already boudined dykes, oriented at an high angle to the tectonic foliation in foliated coarse granitoid host rock, are usually folded. 'Lobe-and-cusp' folds of 5-50 cm wavelength systematically deform the dyke/granitoid contacts: without exception, the cusps are filled by the mafic material whereas the lobes are occupied by the granitoid (Fig. 5d-f). The tectonic foliation of the host granitoid is always axial planar to the fold (Fig. 5f), demonstrating their deformational, rather than primary, origin. Moreover, primary pillowed contacts between coeval mafic and felsic magmas would show the mafic material filling the lobes (e.g. Blake, 1981; Lindberg and Eklund, 1988; Wiebe, 1988). It has long been known that, in such a fold geometry, the material filling the lobes is more competent than that occupying the cusps (Ramsay, 1967, p. 383). We therefore are confronted with a paradoxical situation whereby some mafic dykes in the Gilbert River belt show evidence of initially competent, followed by later incompetent, behaviour compared with the granitoid host rocks. From personal experience in granulite facies terranes (Hanmer, 1984), mafic rocks, which are more competent than quartzo-feldspathic materials at lower metamorphic grades, may show incompetent behaviour at the highest temperatures of crustal metamorphism. However, metamorphic grade in the Gilbert River belt does not exceed upper amphibolite facies. Therefore, if the incompetent behaviour of the mafic rocks is thermally controlled, we must infer a source of heat other than regional metamorphism.

We propose the following scenario to account for the foregoing observations. After, or during the later stages of, emplacement, coarse granitoids at or close to their solidus were able to flow and even fracture at suitably rapid strain rates. Fractures were then occupied by narrow sheets of mafic magma. Because of the difference in solidus temperatures of the granitoid and mafic materials, the solid mafic material will be hotter than its granitoid host, even if only for a very short time interval. If a hot mafic dyke were extended at a sufficiently high strain rate, its rheology would

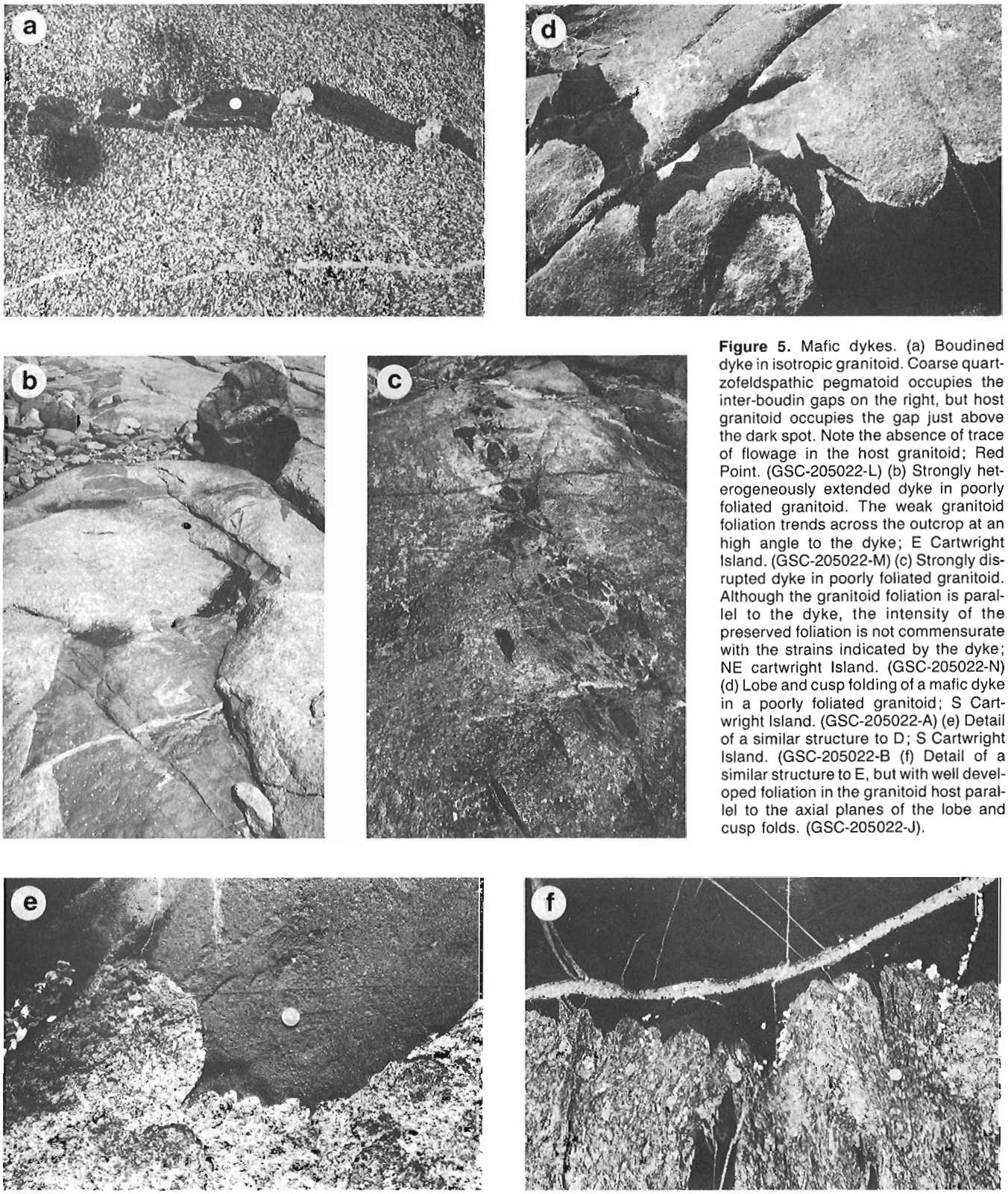

Figure 5. Mafic dykes. (a) Boudined dyke in isotropic granitoid. Coarse quartzofeldspathic pegmatoid occupies the inter-boudin gaps on the right, but host granitoid occupies the gap just above the dark spot. Note the absence of trace of flowage in the host granitoid; Red Point. (GSC-205022-L) (b) Strongly heterogeneously extended dyke in poorly foliated granitoid. The weak granitoid foliation trends across the outcrop at an high angle to the dyke; E Cartwright Island. (GSC-205022-M) (c) Strongly disrupted dyke in poorly foliated granitoid. Although the granitoid foliation is parallel to the dyke, the intensity of the preserved foliation is not commensurate with the strains indicated by the dyke; NE cartwright Island. (GSC-205022-N) (d) Lobe and cusp folding of a mafic dyke in a poorly foliated granitoid; S Cartwright Island. (GSC-205022-A) (e) Detail of a similar structure to D; S Cartwright Island. (GSC-205022-B (f) Detail of a similar structure to E, but with well developed foliation in the granitoid host parallel to the axial planes of the lobe and cusp folds. (GSC-205022-J).

reflect that strain rate and it would fracture and boudin i.e. it would show competent behaviour. If subsequently it were to deform at a slower strain rate without significant cooling, the combined effect of strain rate and high temperature could result in incompetent behaviour. This scenario requires that continued crystallization and recrystallization within the granitoid host is able to efface all trace of flowage of the granitoid into the interboudin gaps during initial extension of the dykes. As the granitoid host cools further, it is able to preserve a tectonically superimposed foliation. That this foliation is axial planar to the 'lobe-and-cusp' folds of the granitoid/mafic dyke interfaces indicates that some of the dykes were still undergoing subsolidus cooling at this tectonic stage. Therefore both the granitoid host rocks and the mafic dykes are syntectonic with respect to the imposed foliation. The regional significance of this deduction stems from the fact that the mafic dykes also cross-cut the foliation in the granitoids, the F2 folds in the metasediments and the high grade mylonites of the Gilbert River belt. Accurate isotopic dating of the granitoids and the mafic dykes will therefore allow us to closely gauge the rate of evolution of a deformation event — a rare opportunity in natural systems!

REGIONAL STRUCTURE

If, as we suggest here, the elongate nature of the map units within the Gilbert River belt is not a direct reflection of the degree of bulk strain, the question remains as to the regional significance of the belt. Moreover, difference in the lineation pattern within the coastal section of the Gilbert River belt compared with that of the more extensive inland portion, remains unexplained.

The first question can only be addressed after geochronological study of the igneous rocks both within and outside of the belt. If the former are younger than the latter then one might suggest that the belt was a preferred zone of shortening and syntectonic emplacement of granitoids whose primary shape was strongly influenced by the anisotropy of the already deformed wall-rock into which they were intruded, as well as by the kinematics of the deformation itself. Regarding the second question, we note that in the few outcrops where we could estimate the shape of the finite strain ellipsoid, e.g. in nests of sheath folds or deformed net-vein arrays, the total strain is markedly constrictional. Furthermore, such propitious outcrops all occurred within the zone of most steeply plunging lineations north of the Rexon's Cove mylonites. This observation leads us to suggest a causal relationship whereby a component of ESE-WNW shortening is linked to a steepening of the bulk finite extension direction. However, we cannot discriminate here between cause and effect.

Finally, we note that the structural signature of the northern part of the Gilbert River belt extends beyond the belt into the adjacent terrane to the north. For example, at Twin Islands, well within the White Bear Arm mafic complex (Gower et al., 1987), steeply NW plunging extension is associated with north-side-up oblique slip. From a structural standpoint, we do not feel that we have observed the northern limit of this structural signature. To the south, we suggest that the limit of the Gilbert River belt coincides with the Long Harbour granoblastic mylonites or straight gneisses which probably represent the terrane boundary between the Pinware Terrane and the Gilbert River belt, previously identified further north at St. Lewis (Gower et al., 1988).

ACKNOWLEDGMENTS

We would like to thank Charlie Gower, Newfoundland Dept of Mines, for inviting us to study the structural geology of a part of his regional mapping project area and for facilitating our orientation, arrival and accommodation ahead of the summer. We particularly thank the Russell family and other residents of Williams Harbour and Reg Russell of Port Hope Simpson, as well as Doreen Poole of Fox Harbour, for their warm hospitality. Ken O'Quinn and Wayne Tuttle, Goose Bay, maintained our contacts with the rest of the world. The manuscript was critically read and improved by Tony Davidson, Tony LeCheminant and Tony Peterson.

REFERENCES

Blake, D.H.
1981: Intrusive felsic-mafic net-veined complexes in north Queensland; Journal of Australian Geology and Geophysics, v. 6, p. 95-99.

Dixon, J.
1975: Finite strain and progressive deformation in models of diapiric structures; Tectonophysics, v. 28, p. 89-124.

Gower, C.F.
1988a: St. Lewis River; Newfoundland Department of Mines, Map 88-87, 1:100 000.

Gower, C.F.
1988b: Port Hope Simpson, Newfoundland Dept of Mines, Map 88-88, 1:100,000.

Gower, C.F., Neuland, S., Newman, M., and Smith, J.
1987: Geology of the Port Hope Simpson region, Grenville Province, Eastern Labrador; in Current Research, Newfoundland Dept of Mines, Report 87-1, p. 183-199.

Gower, C.F., Van Nostrand, T. and Smith, J.
1988: Geology of the St. Lewis River map area, Grenville Province, Eastern Labrador; in Current Research, Newfoundland Dept of Mines, Report 88-1, p. 59-73.

Hanmer, S.
1979: The role of discrete heterogeneities and linear fabrics in the formation of crenulations; Journal of Structural Geology, v. 1, p. 81-91.

Hanmer, S.
1984: Structure of the junction of three tectonic slices: Ontario Gneiss Segment, Grenville Province; in Current Research, Part B, Geological Survey of Canada, Paper, 84-1B, p. 109-120.

Hanmer, S.
1988a: Ductile thrusting at mid-crustal level, southwestern Grenville Province; Canadian Journal of Earth Science, v. 25, p. 1049-1059.

Hanmer, S.
1988b: Great Slave Lake Shear Zone, Canadian Shield: reconstructed vertical profile of a crustal-scale fault zone; Tectonophysics, v. 149, p. 245-264.

Hoffman, P.F., Tirrul, R., Grotzinger, J.P., Lucas, S.B. and Eriksson, K.A.
1984: The externides of Wopmay Orogen, Takijuq Lake and Kikerk Lake map areas, District of Mackenzie; in Current Research, Part A, Geological Survey of Canada Paper p. 84-1A, p. 383-395.

Lindberg, B. and Eklund, O.
1988: Interactions between basaltic and granitic magmas in a Svecofennian postorogenic granitoid intrusion, Aland, southwest; Lithos, v. 22, p. 13-23

Ramsay, J.G.
1967: Folding and Fracturing of Rocks; McGraw Hill, New York, 568 p.

Wiebe, R.A.
1988: Structural and magmatic evolution of a magma chamber: the Newark Island layered intrusion, Nain, Labrador; Journal of Petrology, v. 29, p. 383-411.

Review of the Federal — Provincial Mineral Development Agreement (1984-1989) aeromagnetic total field, vertical gradient, and electromagnetic surveys in Manitoba and Saskatchewan[1]

F.G. Kiss
Geophysics Division

Kiss, F.G., Review of the Federal-Provincial Mineral Development Agreement (1984-1989) aeromagnetic total field, vertical gradient, and electromagnetic surveys in Manitoba and Saskatchewan; in Current Research, Part C, Geological Survey of Canada, Paper 90-1C, p. 13-23, 1990.

Abstract

Combined aeromagnetic total field, vertical gradient and electromagnetic surveys were flown by contractors on behalf of the Geological Survey of Canada in Manitoba and Saskatchewan under the Federal-Provincial Mineral Development Agreement of 1984-89. The overall objective of these surveys was to provide detailed magnetic and electromagnetic coverage of areas having economic potential for gold and base metal exploration. Areas flown in Manitoba focused on the Archean volcanics and metasediments of the Lynn Lake, Leaf Rapids, Rice Lake and Flin Flon -Snow Lake greenstone belts. In Saskatchewan, the aeromagnetic survey of the Flin Flon and Kisseynew domains was extended west from the Manitoba-Saskatchewan provincial boundary to the Hanson Lake Block. Flying was also completed in the Waddy Lake area in the Central Metavolcanic Belt of the La Ronge Domain. Application of the results from these survey systems to mapping of bedrock geology is demonstrated by examples in selected survey areas.

Résumé

Des levés combinés du champ aéromagnétique total, du gradient vertical et de l'électromagnétisme ont été effectués au Manitoba et en Saskatchewan pour le compte de la Commission géologique du Canada dans le cadre de l'Entente fédérale-provinciale sur la mise en valeur des minéraux (1984-1989). Ces levés avaient pour objectif global de recueillir des données magnétiques et électromagnétiques détaillées de zones présentant des possibilités économiques pour l'exploration de l'or et des métaux pauvres. Les zones survolées au Manitoba ont été les roches volcaniques et les sédiments métamorphisés archéens des zones de roches vertes de Lynn Lake, Leaf Rapids, Rice Lake et Flin Flon-Snow Lake. En Saskatchewan, le levé aéromagnétique des domaines de Flin Flon et de Kisseynew a été prolongé vers l'ouest, au-delà de la frontière Manitoba-Saskatchewan jusqu'au bloc du lac Hanson. La zone du lac Waddy dans la zone volcanique métamorphisée centrale du domaine de La Ronge a également été survolée. L'application des données recueillies à la cartographie du socle est démontrée par des exemples de zones choisies.

[1] Contribution to the Canada-Manitoba and Canada-Saskatchewan Mineral Development Agreements 1984-1989. Project carried by the Geological Survey of Canada.

INTRODUCTION

At the conclusion of the Geoscience programs undertaken under the Federal-Provincial Mineral Development Subsidiary Agreement (MDA) of 1984-1989, a subagreement of the Economic Regional Development Agreement (ERDA), twelve aeromagnetic total field, vertical gradient and VLF-EM or time domain electromagnetic surveys were completed by contractors on behalf of the Geological Survey of Canada in Manitoba and Saskatchewan (Fig. 1).

A total of 78 109 km were flown by Kenting Earth Sciences Limited and Geoterrex Limited of Ottawa in ten survey areas in Manitoba and two in Saskatchewan (Table 1).

The overall objective of these airborne geophysical surveys was to provide accurate, high quality and the most detailed systematic magnetic coverage possible in areas deemed to have economic potential for gold and base metal exploration. The geophysical data compiled from these surveys should serve as an important mapping tool to be used in conjunction with parallel conventional detailed geological and geochemical mapping programs.

The surveys selected by the Manitoba Department of Energy and Mines in consultation with the exploration and mining industry and the Geological Survey of Canada focused on the Archean volcanics and metasediments of the Lynn Lake, Leaf Rapids, Rice Lake and Flin Flon-Snow Lake greenstone belts partly extending north over the Kisseynew Gneiss Complex and on the sub-Phanerozoic intrusives east and west of the Cormorant Lake area (Fig. 1).

In Saskatchewan, the aeromagnetic survey of the Flin Flon and Kisseynew domains was extended west from the Manitoba-Saskatchewan provincial boundary to the Hanson Lake Block. This survey included coverage of the Paleozoic carbonate sediments and underlying Precambrian basement rocks as far south as 56° N latitude. A smaller survey was also flown in the Waddy Lake area in the Central Metavolcanic Belt of the La Ronge Domain.

SURVEY SPECIFICATIONS

Most survey areas were flown at 300 m traverse line spacing with a distance of 10 km between control lines. The Lynn Lake northwest survey area was flown at a tighter traverse line spacing of 200 m to insure adequate ground coverage by the electromagnetic system. The survey height was maintained at 150 m above ground in all vertical gradient surveys and at 120 m for the Lynn Lake northwest aeromagnetic - electromagnetic survey.

PRODUCTS

The aeromagnetic total field, gradiometer, VLF-EM and time domain electromagnetic data were processed and archived as line data and gridded data sets and stored on a series of magnetic tapes in ASCII format.

The total field, gradiometer and conductivity data were compiled and printed in the form of contoured products at a scale of 1:20 000 on an NTS map sheet base. In addition, with the exception of the Lynn Lake northwest area, total field and gradient gridded data were each printed at a scale of 1:50 000 as multicoloured composite maps with VLF-EM profile data on the reverse side of each map.

These printed products are available through the Geological Survey of Canada, Publication Sales Offices in Ottawa

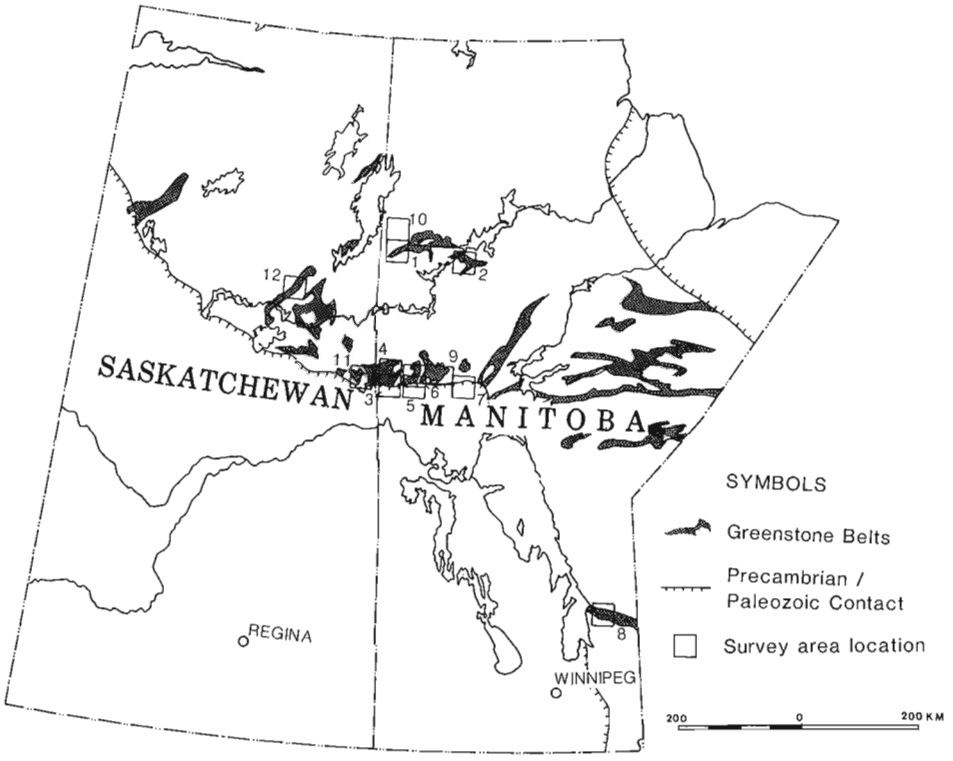

Figure 1. Distribution of greenstone belts in Manitoba and Saskatchewan. Numbered location of survey areas: 1. Lynn Lake southwest, 2. Rusty Lake, 3. Flin Flon-Root Lake, 4. Nokomis-Sherridon-Elbow Lake, 5. Moose Lake North, 6. Moose Lake South, 7. Hargrave River, 8. Rice Lake, 9. Snow Lake, 10. Lynn Lake northwest, 11. Amisk Lake, 12. Waddy Lake.

and Calgary. Digital archive magnetic tapes for these areas may also be purchased from the Geophysical Data Centre of the Geological Survey of Canada, Ottawa.

RESULTS

Since their development in the mid-seventies, aeromagnetic vertical gradient surveys have been used in mapping geological structure and lithology. The usefulness of this method lies in the ability to differentiate rock types by discriminating between differing magnetic properties of the rocks and using these characteristics to extend conventionally mapped geology into areas which may either be covered by overburden, under lakes or even below layers of non-magnetic sedimentary rocks.

Table 1. Aeromagnetic Surveys under Canada-Manitoba MDA Program (1984-1989).

Survey	Type	km	Line Spacing	Altitude	NTS Area Coverage
Lynn Lake SW (Dunphy Lake) (1984-85)	Aeromagnetic Total Field Gradiometer VLF	5,267	300 m	150 Radar	64C/11,12,14
Rusty Lake (Leaf Rapids) (1984-85)	Aeromagnetic Total Field Gradiometer VLF	5,239	300 m	150 Radar	64B/5,6,11,12
Flin Flon-Root Lake (Namew) (1985-86)	Aeromagnetic Total Field Gradiometer VLF	7,884	300 m	150 Radar	63K/3,4,5,6,12,13
Nokomis-Sherridon and Elbow Lake (1985-86)	Aeromagnetic Total Field Gradiometer VLF	6,887	300 m	150 Radar	63K/15,16 63N/1,2
Moose Lake North (1985-86)	Aeromagnetic Total Field Gradiometer VLF	2,289	300 m	150 Radar	63K/7,8
Moose Lake South (1986-87)	Aeromagnetic Total Field Gradiometer VLF	5,654	300 m	150 Radar	63K/1,2
Hargrave River (1986-87)	Aeromagnetic Total Field Gradiometer VLF	8,200	300 m	150 Radar	63J/6,7,10,11
Rice Lake (Bissett) (1986-87)	Aeromagnetic Total Field Gradiometer VLF	5,275	300 m	150 Radar	52L/13 62M/14
Snow Lake (1988-89)	Aeromagnetic Total Field Gradiometer VLF	8,180	300 m	150 Radar	63J/13 63K/15/16
Lynn Lake NW (McMillan Lake) (1988-89)	Aeromagnetic Total Field Electromagnetic	4,907	200 m	120 Radar	64C/13,14

Aeromagnetic Surveys under Canada-Saskatchewan MDA Program (1984-1989)

Survey	Type	km	Line Spacing	Altitude	NTS Area Coverage
Amisk Lake (Flin Flon) (1985-86)	Aeromagnetic Total Field Gradiometer VLF	18,787	300 m	150 Radar	63K/4,5,12,13 63L/1,8,9,10,16
Waddy Lake (1985-86)	Aeromagnetic Total Field Gradiometer VLF	4,779	300 m	150 Radar	64D/3,4,5,6 74A/1,8

TOTAL SURVEY LINE KILOMETRES: 78,109

Precision in the mapping of near surface features with the gradiometer system is an improvement in comparison to standard total field magnetic surveys. While closely spaced, vertically dipping geological units are better resolved, contacts between larger rock units can also be located with accuracy at the zero gradient contour level at higher magnetic latitudes (Hood and Teskey, 1989). The aeromagnetic gradiometer, therefore, was used as the primary survey system in this detailed airborne mapping program.

The use of Time Domain-EM in one area was a desirable option since the bedrock had been reported to be conductive (Hosain, 1981). Other auxiliary instrumentation such as the VLF-EM has been particularly useful in outlining faults and some lineations which exhibit long strike length and which are in many cases non-magnetic.

The following is a brief summary of some of the results obtained by the airborne survey systems in selected areas in Manitoba and Saskatchewan.

MANITOBA

Lynn Lake Greenstone Belt

The Lynn Lake Greenstone Belt recently mapped and described by Gilbert et al. (1980) is a domain of metavolcanic, metasedimentary and plutonic rocks of Aphebian age. Felsic plutons intrude and separate the greenstones into two separate northeasterly trending belts in the vicinity of Lynn Lake commonly referred to as the Northern and Southern belts.

Previous to the Canada-Manitoba Mineral Development Agreement (MDA) (1984-1989) program, detailed, high sensitivity aeromagnetic surveys in the area east of Lynn Lake had been initiated by the Geological Survey of Canada with the Queenair gradiometer system, and were completed successfully in 1984. The improved resolution offered by this system and the resulting airborne total field and vertical gradient maps produced from the data had proven to be an invaluable aid in detailed mapping of the area. As a result, surveying of the remaining western portion of the greenstone belt was resumed at the earliest phase of this MDA program.

Lynn Lake southwest area

The survey of this area of the greenstones from Lynn Lake to Zed Lake covering the Northern Belt and the length of the Southern Belt to the Manitoba-Saskatchewan border was commenced in 1985. Total field and vertical gradient magnetic maps with VLF-EM were released in 1986. Evaluation of the magnetic data clearly demonstrated the usefulness of the vertical gradient map as an aid to mapping stratigraphic units. Iron-rich horizons within the metaconglomerate formation which lies on the north flank of the Northern Belt near Motriuk Lake (A in Fig. 2, 3), are abundant throughout particular units across a thick stratigraphic sequence. These concentrations of iron within the units produce anomalous magnetic highs which are emphasized on the magnetic vertical gradient maps as narrow, linear bands.

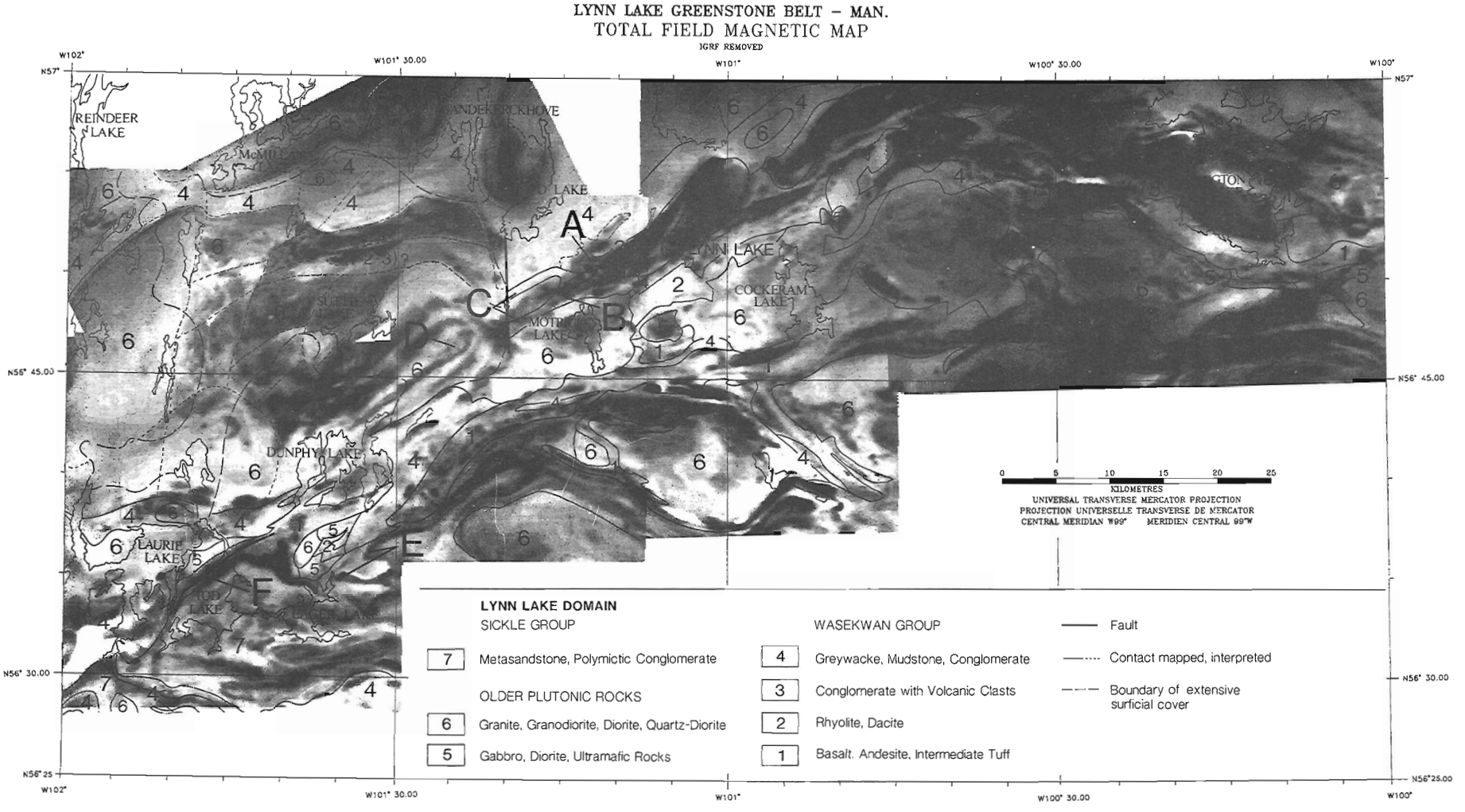

Figure 2. Lynn Lake, Manitoba - simplified regional geology superimposed on grey scale plot of composite total field aeromagnetic map. Mapped geology after Manitoba Energy and Mines (1986). Areas referenced in text are: (A) iron-rich horizons in metaconglomerate formation; (B and C)iron-rich horizons within volcaniclastic sediments; (D) banding of magnetic highs within gneiss; (E) distinct magnetic marker by member of Sickle Group conglomerate; (F) Tod Lake Fault.

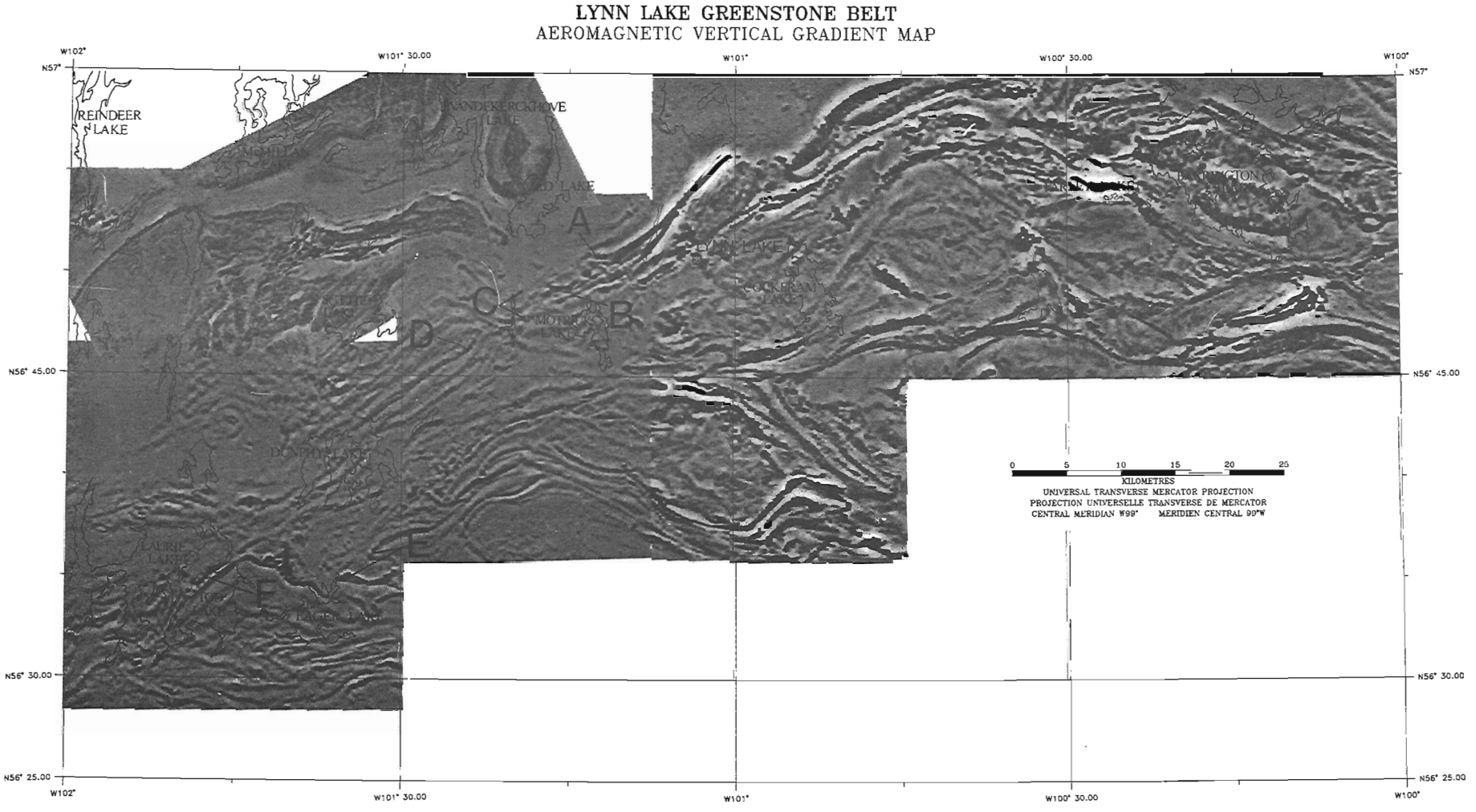

Figure 3. Lynn Lake, Manitoba - aeromagnetic vertical gradient composite map reproduced in grey tone. Areas of interest (A,B,C,D,E and F) described in text are referenced in Figure 2. Survey area east of 101 00'W was flown prior to this MDA program by the G.S.C. Queenair gradiometer system.

Farther south within the volcanics, accurate mapping of iron-formations within the Lynn Lake greenstone belt is significant factor in exploration for gold. In the Farley Lake area, gold occurs in replacement sulphide pockets in close association with iron-formations in a series of volcanic flows and volcaniclastic sediments. This mineralized region is generally referred to as the Agassiz Metallotect. Fedikow (1986) has observed the correlation of vertical gradiometer signatures to a number of these iron-formations within the metallotect. These formations have been extended westward (Ferreira, 1986) to Motriuk Lake (B in Fig. 2, 3). Although lack of outcrop farther west is a problem, there is some evidence of iron-rich horizons within the volcanogenic sedimentary sequence on the vertical gradient map (C in Fig.2, 3).

Farther to the southwest (D in Fig.2, 3), a broad terrain of metagreywackes, granodiorite and intruded gneissoid magnetite tonalite recently mapped by Cameron (1980), Gilbert et al, (1980) and McRitchie (1976) as part of the Kisseynew Complex exhibits lengthy, broad, ellipsoidal bands of magnetic highs lying along a northeasterly axis. The banding which reflects compositional variation and magnetite enrichment within the gneissic rocks is emphasized on the vertical gradient map. This feature is comparable to the banded appearance of the gneissic granodiorite intrusives mapped north of Mari Lake, Saskatchewan and also in the Kisseynew Complex, northwest of Flin Flon (Fig.5, 6).

In the area between the northeastern arm of Eager Lake and Tod Lake, a conglomerate member of the Sickle Group is found to be a distinct magnetic marker on earlier total field magnetic maps, and thus useful in mapping subsurface sedimentary units (Hall et al., 1981). The mapped results of the vertical gradient system have since been able to improve the definition of the same magnetic conglomerate member, showing its folded structure (E in Fig.2, 3) in clearer detail than was possible in earlier regional airborne geophysical surveys.

The VLF-EM instrumentation carried onboard the aircraft has been successful in delineating the Sickle Group conglomerate described above as well as other structural features in some areas. The Tod Lake fault (Gilbert et al., 1980) striking northeast from Tod Lake to Dunphy Lake (F in Fig.2, 3) is detected by all channels of the VLF-EM system.

Lynn Lake northweast area

The area from Zed Lake to the Manitoba-Saskatchewan border between 56°45′N and 57°N latitude has remained largely unmapped in detail to date, because more than 600 km^2 of the surface is blanketed by glacial drift.

For this detailed survey area, a combined total field magnetic and time domain electromagnetic system was used. Total field magnetic and conductivity contour maps at 1:20 000 scale were produced from the data, and released in 1989.

A gridded conductivity map produced from the electromagnetic data (Fig.4) shows that the metagreywackes of Whitesand Bay and Zed Lake are highly conductive and tentatively interpreted to be connected along a broad arc approaching the south shore of McMillan Lake and the southern tip of Vandekerckhove Lake. Approaching Zed Lake, the conductive zone is bifurcated suggesting that the metagreywackes are deflected primarily to the northeast and also to the southeast by a large intrusive body. The southeast arm appears to be segmented and much less conductive. The Zed Lake intrusive, possibly a dioritic mass, is strongly magnetic in contrast to the surrounding weakly magnetic metagreywackes. These metagreywackes are flanked to the south by non-conductive but highly magnetic rocks, possibly the magnetite granite and tonalite described by Cameron (1980).

A localized, anomalous conductivity high was produced over a long, narrow, northeasterly-striking magnetic high in the Reindeer Lake area, four kilometres south east of the southern tip of Whitesand Bay (A in Fig.4). This conductivity high is also coincident with weakly anomalous geochemical Cu, Zn, Fe lake sediment values recorded by regional geochemical surveys of the Geological Survey of Canada (GSC-Open File 999, 1983) in the area.

Flin Flon-Snow Lake greenstone belt and surrounds

A number of aeromagnetic gradiometer surveys, which have been contracted by the Geological Survey of Canada in the Flin Flon area, centred primarily on the highly prosperous base metal producing areas of the Precambrian greenstone belt and extending north into the Kisseynew Gneiss Complex and south to include the Paleozoic carbonate sediments and underlying Precambrian basement rocks.

The initial phase of airborne geophysical mapping of the greenstone belt was carried out with funds provided by the Federal-Provincial Interim Mineral Agreement of 1982-83. As an integral part of Project Cormorant, the airborne mapping program was not only intended to assist in the detailed mapping of the greenstone belt but more significantly, to delineate the extent and the constituents of the Precambrian rocks underlying the Paleozoic sediments and possibly outline new areas which may have potential for base metal deposits. The layout of this series of surveys consisted of a 20 km wide area on either side of a baseline corresponding generally with the Paleozoic-Precambrian contact extending from Flin Flon in the west to Hargrave Lake in the east.

Under the new Federal-Provincial Mineral Development Agreement of 1984-1989, the airborne program was expanded to include total field magnetic, gradiometer and VLF-EM mapping in six additional areas, totalling 39 094 line kilometres of survey flying.

The Flin Flon-Root Lake, Moose Lake north, Moose Lake south and Hargrave River surveys covered areas farther south and east over the Palaeozoic and underlying Precambrian basement rocks not flown in the first phase of the project.

Data from these aeromagnetic surveys were assembled and cross referenced with earlier total field and gradiometer

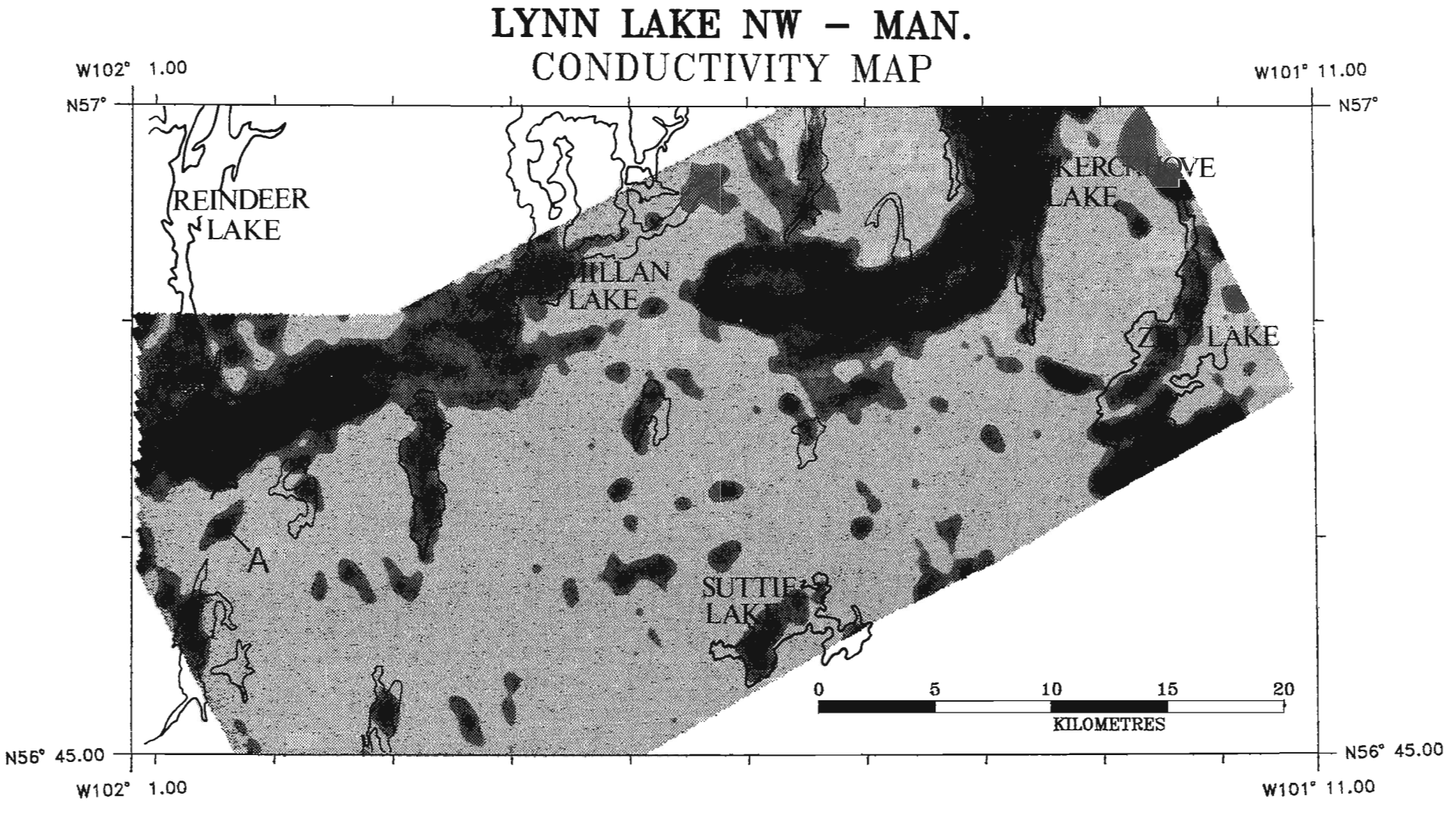

Figure 4. Lynn Lake northwest area, Manitoba - Conductivity map in grey tone. Dark areas are indicative of high conductivity. Isolated conductivity high (A) is coincident with a narrow magnetic high striking northeast. Extensive areas of high conductivity are predominantly related to metagreywackes and conglomerates of the Wasekwan Group.

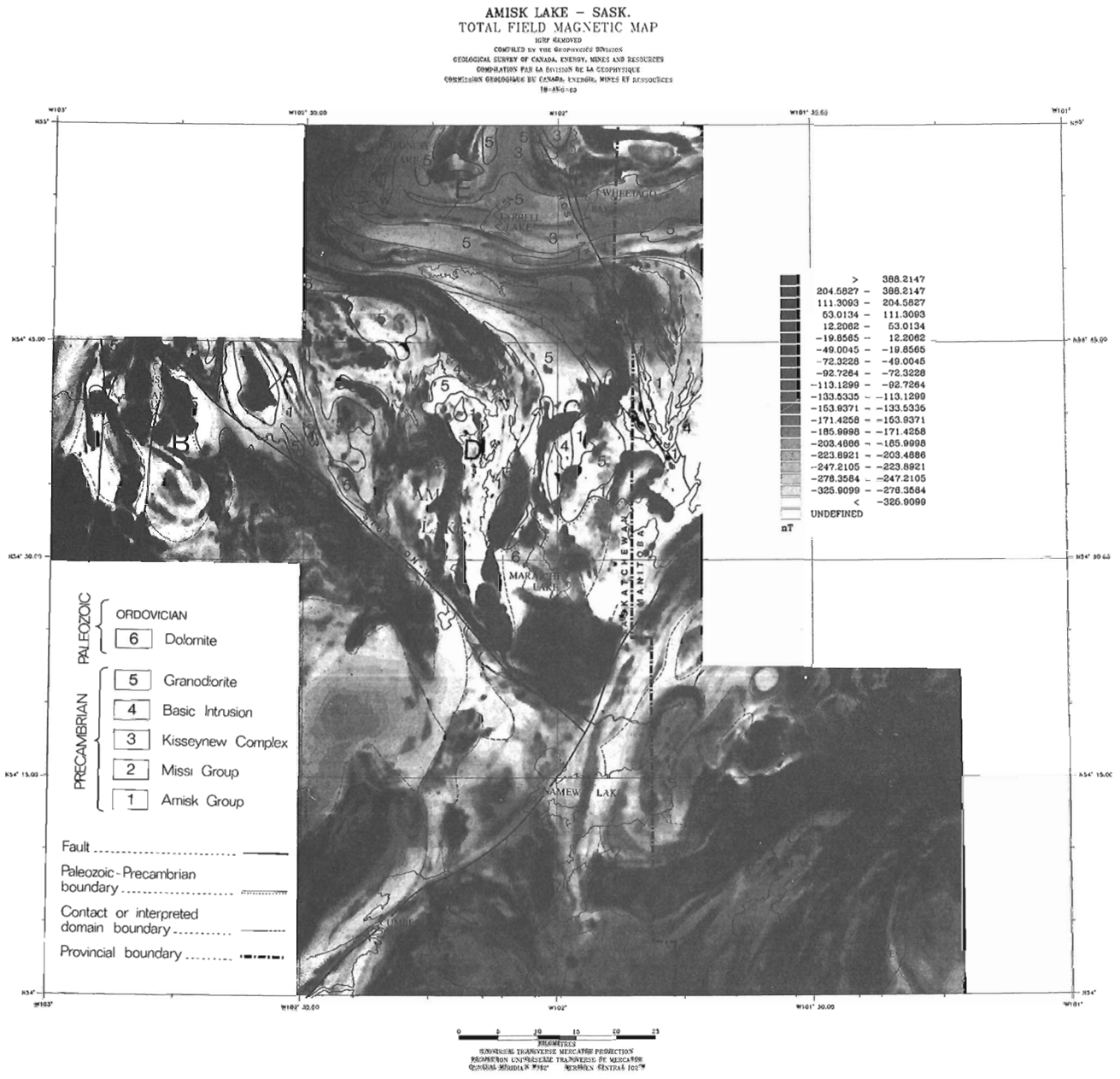

Figure 5. Amisk Lake, Saskatchewan - Simplified regional geology map of Precambrian in part after Froese, 1969 and Macdonald, 1981 superimposed on the composite grey tone aeromagnetic total field magnetic map. Sub-Paleozoic domain interpretation after Blair et al., 1988. Areas referenced in text: Snake River and Hanson Lake plutons (A) and (B) with high magnetic core; (C) Birch Lake - Table Lake gabbro; (D) Crater Island granodiorite; (E) interlayered gneisses at Tyrrell Lake.

data flown over exposed Precambrian geology, with airborne electromagnetic time domain data, drill core data and earlier geophysical interpretation (Hosain, 1984). Preliminary results were presented by Blair et al. (1988) outlining magnetic domains which when referenced to drill core data, provide a pseudo-geological map of the rocks below the Palaeozoic carbonate sediments. The southward continuation of the metavolcanic rocks below the carbonates, magnetite-poor granitic plutons, gabbroic bodies with layering or zoning and truncations of lineaments indicating faulting are cited in the structural and lithological interpretation.

This survey program was also extended northward to include two additional survey areas to cover the bulk of the metavolcanic rocks in the Kisseynew Gneiss Belt in the Elbow-Nokomis-Snow Lake triangle. These studies provided additional data to the detailed mapping and metallogenic studies within the Kisseynew belt which were being carried out concurrently under the MDA (1984-89) program.

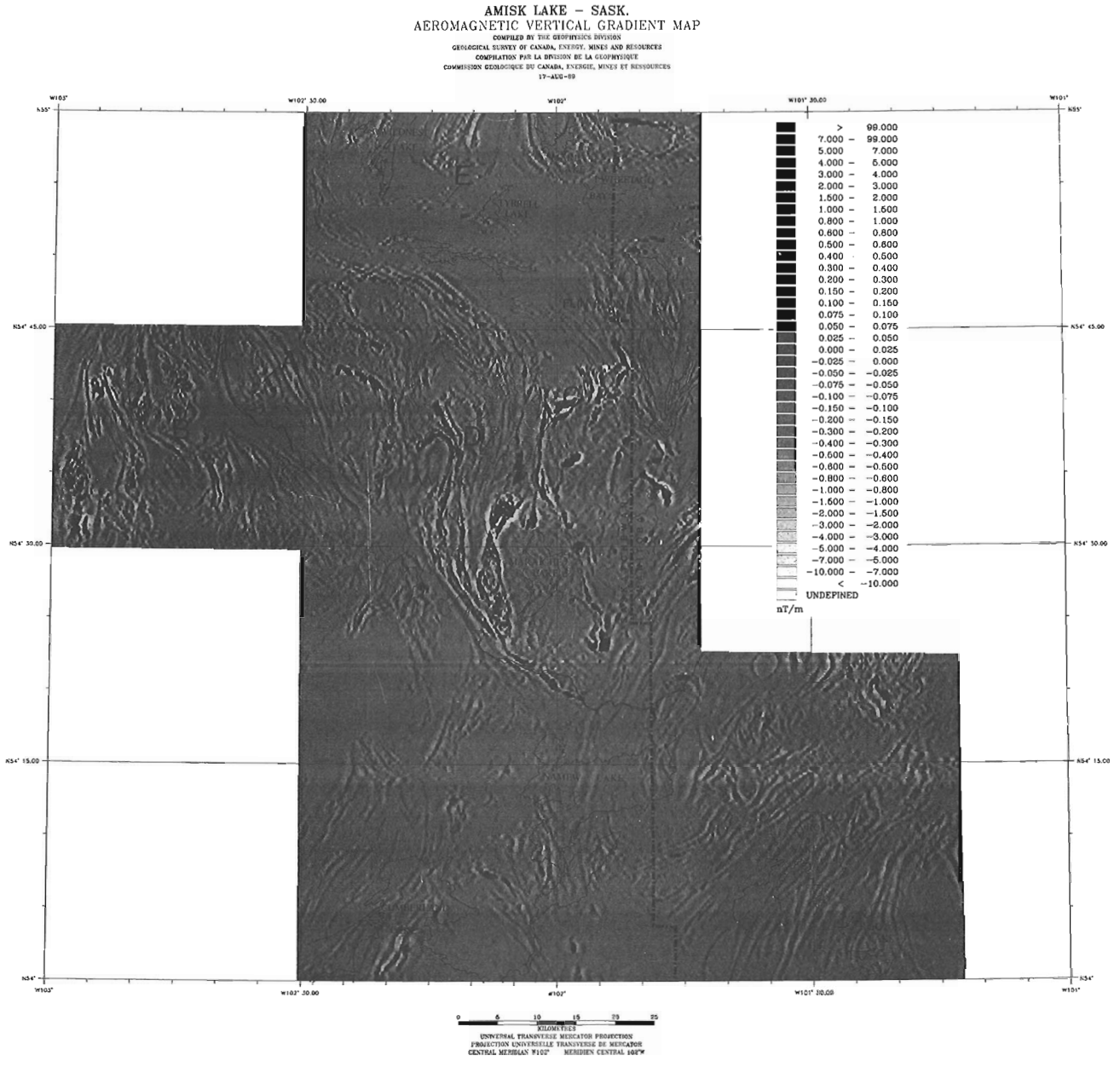

Figure 6. Amisk Lake, Saskatchewan - aeromagnetic vertical gradient composite grey tone map. Areas of interest (A,B,C,D, and E) described in text are referenced in Figure 5.

SASKATCHEWAN

Funding provided for the airborne geophysical phase of the Canada -Saskatchewan Mineral Development Agreement 1984-1989 program was directed towards the surveying of two main greenstone belts in east-central Saskatchewan. One selection covered all of the Flin Flon Domain and the Hanson Block which have had a long history of gold and base metal exploration and producing mines. Waddy Lake in the La Ronge Domain was chosen as the second area to be surveyed. This region has recently reached new heights in exploration activity after several significant new occurrences of gold were discovered in the Star Lake-Waddy Lake area in the early eighties.

Amisk Lake Area

The Amisk Lake survey was flown concurrently with the Flin Flon - Root Lake survey in Manitoba. Thus by 1986, the entire length of the Flin Flon greenstone belt from Wekusko Lake, Manitoba to Hanson Lake, Saskatchewan was detailed by aeromagnetic gradiometer/VLF coverage.

Figure 5 shows the general geology of the area superimposed on the total field aeromagnetic map resulting from the survey. In the west, the survey covers the Precambrian Hanson Lake Block consisting of metavolcanic, meta-arkose and granitoid rocks. The Sturgeon-Weir Thrust Fault separates this block from the greenstone belt consisting of

metavolcano-sedimentary and plutonic rocks of the Flin Flon Domain and the northern region of metamorphic rocks of the Kisseynew Complex. The rocks in the southern half of the survey area consist of a thin cover of Paleozoic dolomitic sediments which unconformably overly the Precambrian rocks. This boundary marks the edge of the Precambrian Canadian Shield.

On the total field magnetic map, a wide range of magnetic relief is evident. The most significant magnetic highs of several thousand nanoteslas are generally attributed to intrusive rocks of basic to ultrabasic composition, though some notable exceptions exist where granitic intrusives such as the Snake River (A in Fig.5) and Hanson Lake (B in Fig.5) plutons are highly magnetic in the central core of the plutons. The Birch - Table Lake gabbro (C in Fig.5) and the Crater Island granodiorites (D in Fig.5) are delineated as long, narrow, linear magnetic highs and enhanced on the aeromagnetic vertical gradient map (Fig.6).

While lower magnetic relief in the range of 300nT to 500nT is associated with the Missi Group sedimentary sequence, the Amisk Group volcanic flows and volcaniclastic rocks are well bellow this range. This magnetic distinction between the two groups in the greenstone belt can be applied to map higher grade metamorphic equivalents to the north in the Kisseynew Gneiss Complex (Pearson, 1972). Byers et al. (1965), Pearson (1972) and others have proposed that hornblende gneisses west of Weetago Bay represent metamorphosed volcanic rocks of the Amisk Group, and the interlayered biotite gneisses are equivalent to the Missi sedimentary strata. This interlayered association is demonstrated in the area of Tyrrell Lake (E in Fig.5, 6) by alternate bands of magnetic highs and lows corresponding respectively to the hornblende and biotite gneisses mapped in the region.

Examples of faulting can be seen in the Kisseynew Complex in the total field and gradiometer maps. A distinct northwesterly lineation extending from Flin Flon is traced by a magnetic low which traces the position of the Ross Lake Fault. In the south central part of the survey area, the Sturgeon-Weir Fault is similarly defined as a magnetic low and can be traced under the Paleozoic sedimentary cover.

Further detailed interpretive work by geologists and geophysicists at the Geological Survey of Canada and the Geological Survey of Saskatchewan is in progress in the southern half of the survey area to define domains within the Precambrian basement under the Paleozoic cover rocks. An outline of the preliminary domain divisions is presented in Figure 6 south of the Paleozoic - Precambrian demarcation line.

Waddy Lake Area

The area is about 40 km southwest of Southend, located at the southern extremity of Reindeer Lake. This survey focused on the northern part of the greenstones which are part of the Central Metavolcanic Belt of the La Ronge Domain. Recent interest in detailed geological mapping has developed and metallogenic studies by universities and federal and provincial agencies have accelerated as a result of new gold finds by the exploration industry in the metavolcanic and intrusive rocks in proximity to Byers Fault. This aeromagnetic geophysical survey provides additional data to assist in the detailed mapping of the geology by delineating faults and lithological boundaries based on their magnetic signatures.

A number of gold occurrences in the survey area are spatially related to the Byers Fault (Coombe et al., 1986), which is a major structural break striking predominantly east-west. This fault is visible on both the aeromagnetic and vertical gradient maps. The fault trace is most clearly defined on the vertical gradient map where it shows up as a strong high-low magnetic signature. The Oven Lake-Corner Lake fault subsets (Harper,1984) paralleling the Byers Fault are equally well defined on the aeromagnetic maps and supported by VLF-EM responses along strike (Fig.7). There are other examples of magnetic and VLF signatures throughout the metavolcanic sequence where east-west faulting is nearly parallel to the strike of the rocks, which are not easily recognized by conventional geological mapping. Numerous northeast striking fault sets in the Weedy Lake area and elsewhere throughout the survey area are also visible on the vertical gradient maps. Their fault trace is indicated by displacements or abrupt termination of the axes of east-west striking magnetic rocks.

CONCLUSION

The primary objectives of these airborne geophysical surveys have been achieved. The results improve the accuracy of geological maps by complementing other geoscience mapping projects and assist in outlining new areas of potential for mineral exploration.

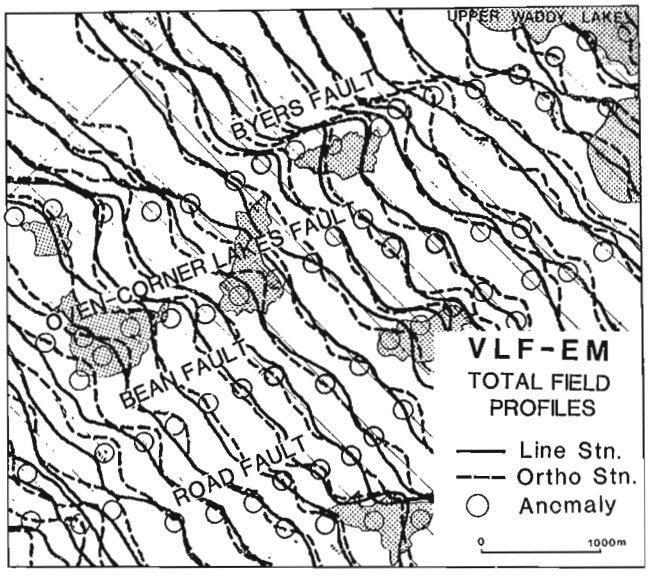

Figure 7. Waddy Lake, Saskatchewan - Total Field VLF-EM profile responses over Byers Fault and parallel subset faults reproduced from the reverse side of the aeromagnetic vertical gradient 1:50 000 scale maps.

These aeromagnetic maps have served as an effective and efficient tool in resolving structural and lithological features in great detail and have demonstrated their usefulness in defining lithology under surficial drift or deep below the cover of sedimentary rock. These products should also be a significant aid in base metal and gold exploration programs in the Precambrian Canadian Shield of Manitoba and Saskatchewan.

REFERENCES

Blair, B.B., Webster, W., Kornik, L.J. and Gordon, T.M.
1988: Project Cormorant: Interpretation of Sub-Paleozoic geology of the Cormorant Lake map area from geophysical and drill core data; Geoscience Canada, v.15, p. 98-100.

Byers, A.R., Kirkland, S.J.T. and Pearson, W.J.
1965: Geology and mineral deposits of the Flin Flon area, Saskatchewan; Saskatchewan Department of Mineral Resources Report 62, 95p.

Cameron, H.D.M.
1980: Geology of the McMillan Lake Area; *in* Manitoba Mineral Resources Division, Report of Field Activities, Report GS-1, p. 5-7.

Coombe, W., Lewry, J.F. and Macdonald, R.
1986: Regional geological setting of gold in the La Ronge Domain, Saskatchewan; *in* Gold in the Western Shield, ed. L.A. Clark, Canadian Institute of Mining and Metallurgy, Special Volume 38, p. 26-56.

Fedikow, M.A.F.
1986: Geology of the Agassiz stratabound Au-Ag deposit, Lynn Lake, Manitoba; Manitoba Mineral Resources Division, Open File Report OF85-5, 93p.

Ferreira, K.
1986: Geological investigations in the Sheila Lake-Margaret Lake area; *in* Manitoba Energy and Mines, Minerals Division, Report of Field Activities 1986, Report GS-2, p. 13-17.

Froese, E.
1969: General geology of the Coronation Mine area; *in* Symposium on the Geology of the Coronation Mine, Saskatchewan, Geological Survey of Canada, Paper 68-5, p. 7-36.

Geological Survey of Canada
1983: Regional lake sediment and water geochemical reconnaissance data, Manitoba NTS 64C; Geological Survey of Canada, Open File 999, NGR 64-1983, 133p., maps at 1:250 000 scale.

Gilbert, H.P., Syme, E.C. and Zwanzig, H.V.
1980: Geology of the metavolcanic and volcaniclastic metasedimentary rocks in the Lynn Lake area; Manitoba Mineral Resources Division, Geological Paper GP80-1, 118p.

Hall, D.H., Millar, T. and Mok, K.H.
1981: Interpretation of an aeromagnetic survey in the Lynn Lake area, Manitoba; Manitoba Mineral Resources Division, Open File Report OF81-1, 115p.

Harper, C.T.
1984: Geological mapping, Waddy Lake area (part of NTS 64D-4 and -5); *in* Summary of Investigations 1984, Saskatchewan Geological Survey, Miscellaneous Report 84-4, p.6-20, maps at 1:20 000 scale.

Hood, P.J. and Teskey, D.J.
1989: Aeromagnetic gradiometer program of the Geological Survey of Canada; Geophysics, v. 54, no. 8 (August), p. 1012-1022.

Hosain, I.T.
1981: Summary and evaluation of the geophysical data from the open assessment files of the Lynn Lake Greenstone Belt; Manitoba Department of Energy and Mines, Mineral Resources Division, Open File Report OF81-5, 40p., maps at 1:50 000 scale.
1984: Interpretation of airborne magnetic gradiometer surveys of the area south of the Flin Flon-Snow Lake belt (Parts of NTS 63K and 63J); Manitoba Department of Energy and Mines, Mineral Resources Division, Open File Report OF84-2, 26p.

Macdonald, R.
1981: Compilation bedrock geology: Pelican Narrows and Amisk Lake areas (NTS 63M, 63L, part of 63n and 63K); *in* J.E. Christopher and R. Macdonald, eds., Summary of investigations, Saskatchewan Geological Survey: Saskatchewan Energy and Mines Miscellaneous Report 81-4, maps at 1:250 000.

Manitoba Energy and Mines
1986: Bedrock Geology Compilation Map Series, Granville Lake, NTS 64C, 1:250 000.

McRitchie, W.D.
1976: Paskwaiowaka Regional Compilation; *in* Manitoba Mineral Resources Division, Report of Field Activities, p. 13-23.

Pearson, D.E.
1972: The location and structure of the Precambrian Kisseynew Gneiss Domain of Northern Saskatchewan; Canadian Journal of Earth Sciences, v.9, no.10, p. 1235-1249.

Résultats préliminaires sur les directions d'écoulement glaciaire dans la région de Salluit et des lacs Nuvilik, Nouveau-Québec

R.-A. Daigneault
Centre géoscientifique de Québec

Daigneault, R.-A., Résultats préliminaires sur les directions d'écoulement glaciaire dans la région de Salluit et des lacs Nuvilik, Nouveau-Québec; dans Recherches en cours, Partie C, Commission géologique du Canada, Étude 90-1C, p. 25-29, 1990.

Résumé

L'analyse de l'orientation des stries, des cannelures et des formes profilées indique que l'écoulement glaciaire dominant s'est effectué vers le nord, vraisemblablement à partir du centre de dispersion glaciaire de Payne (segment de la ligne de partage glaciaire du Labrador ancestral). Localement, des écoulements glaciaires plus récents succèdent au mouvement principal: vers l'ouest ou le nord-ouest au sud des monts de Povungnituk et vers le nord-est au sud du détroit d'Hudson. La dispersion glaciaire des blocs de dolomie du groupe de Povungnituk est reliée à la phase d'écoulement vers le nord.

Abstract

Glacial striations and grooves along with streamlined landforms record a main phase of regional northward ice-flow which presumably issued from the Payne outflow centre (segment of the Ancestral Labrador Ice Divide). Local evidence of subsequent ice-flow phases is also recorded: westward or northwesward ice-flow in an area south of the Povungnituk hills, and northeastward ice flow in an area south of Hudson Strait. Glacial dispersal of dolostone boulders derived from rocks of the Povungnituk Group is associated with the northward ice-flow phase.

INTRODUCTION

Dans le cadre d'un projet de cartographie des formations en surface de la partie septentrionale du Nouveau-Québec depuis le 61° de latitude nord, une étude des directions d'écoulement glaciaire a été effectuée. On présente ici les résultats préliminaires obtenus au cours de l'été 1989 dans la région de Salluit (35 J) et des lacs Nuvilik (35 G), soit entre 61°00′ et 62°25′ de latitude nord et entre 74°00′ et 76°00′ de longitude ouest (fig. 1.0). La présente étude se limitera à traiter essentiellement des directions d'écoulement glaciaire déduites à partir des marques d'érosion et des formes d'accumulation glaciaire ainsi que de la dispersion des blocs erratiques, les résultats d'analyse en laboratoire n'étant pas présentement disponibles.

GÉOLOGIE DU SUBSTRATUM

La région étudiée couvre en partie deux provinces structurales du Bouclier canadien, soit celle de Churchill au nord et celle du Lac Supérieur au sud (Stockwell et coll., 1979). Les roches volcaniques et sédimentaires de la zone de plissements du cap Smith (fosse de l'Ungava), dans la province de Churchill, occupent la partie centrale de la zone d'étude et constituent une bande d'environ 70 km de largeur, d'orientation est-ouest, séparant deux secteurs où dominent les gneiss granitiques et les granodiorites (Taylor, 1982; Lamothe, 1987). Régionalement, les roches de la Fosse de l'Ungava constituent donc de précieux traceurs pour l'étude de la dispersion clastique glaciaire. Localement, à l'intérieur de la bande du cap Smith, les quartzites, les calcaires et les dolomies du groupe de Povungnituk ainsi que les roches des intrusions ultrabasiques sont de bons marqueurs.

Des calcaires et des dolomies siluriennes occupent en partie le graben du détroit d'Hudson (Sanford et coll., 1979; MacLean et coll., 1986).

MÉTHODOLOGIE

Les travaux de terrain ont été réalisés entre le 1er août et le 11 septembre 1989. L'accès à la zone étudiée a été assuré essentiellement par hélicoptère à partir d'un camp de base situé à 22 km au sud-sud-est de Salluit, le long de la rivière Foucault. Outre la vérification sur le terrain des différentes unités lithostratigraphiques déduites à partir de séances de photo-interprétation préliminaires, on a procédé à un échantillonnage systématique du till (1 échantillon par 200 km^2). Les échantillons proviennent d'ostioles et ont été prélevés à une profondeur moyenne de 35 cm. La pétrographie des granules (2 à 6 mm) sera ultérieurement déterminée afin de définir le patron de la dispersion des débris de roches de la fosse de l'Ungava sur l'ensemble du territoire. Seule la présence de blocs de dolomie du groupe de Povungnituk a été notée sur le terrain.

L'orientation des stries, des cannelures et des formes profilées a été mesurée en tenant compte d'une déclinaison magnétique moyenne de 33° vers l'ouest. Une direction est attribuée aux stries lorsqu'elles ont une orientation similaire à celle des reliefs en dos de baleine observés à proximité.

TRAVAUX ANTÉRIEURS

Sur la péninsule de l'Ungava, les écoulements glaciaires sont principalement associés à la présence de la ligne de partage glaciaire du Labrador ancestral (localement nommée Payne par Bouchard et Marcotte, 1986) au Wisconsinien supérieur (Dyke et Prest, 1987a, 1987b). Cette ligne de partage glaciaire est responsable des écoulements radiaux observés de part et d'autre d'un axe nord-sud situé au centre de la péninsule (Lauriol, 1982; Gray et Lauriol, 1985; Bouchard et Marcotte, 1986; Delisle et coll., 1986). Dans la partie nord de la zone étudiée, les écoulements glaciaires sont généralement vers le nord (Matthews, 1967; Gray et Lauriol, 1985; Bruneau et Gray, comm. pers.) alors que dans la partie sud, aucun relevé systématique des marques d'écoulement glaciaire n'a été effectué jusqu'à présent. Toutefois, un écoulement vers le sud est suggéré pour expliquer la présence sporadique de roches de la fosse de l'Ungava au sud de leur région source (Currie, 1965; Taylor, 1982). Pour justifier ce phénomène, Bouchard et Marcotte (1986) proposent l'existence d'un centre de dispersion glaciaire (Ungava) antérieur à celui de Payne et localisé approximativement sur les monts de Povungnituk (fig. 2.0).

Enfin, au nord, Dyke et Prest (1987a, 1987b) suggèrent l'existence d'un courant de glace dans le détroit d'Hudson durant la majeure partie du Wisconsinien supérieur.

RÉSULTATS ET DISCUSSION

Les marques d'écoulement glaciaire

Les mesures de l'orientation des stries observées à 63 endroits et de celle des formes profilées (traînées morainiques, drumlins, drumlinoïdes) déduites par photo-interprétation indiquent la prédominance d'un mouvement dirigé globalement vers le nord sur tout le territoire étudié (fig. 1.0). Cet écoulement est vraisemblablement associé au flot Payne proposé par Bouchard et Marcotte (1986). Dans la région de Salluit, on observe une certaine déflection vers le nord-est, tant dans l'orientation des formes profilées que dans celle des stries. Cependant, le mouvement n'a pas l'étendue de celui proposé par Dyke et Prest (1987b) à l'appui de l'hypothèse selon laquelle un courant glaciaire se serait manifesté dans le détroit d'Hudson durant la majeure partie du Wisconsinien supérieur. De plus, contrairement au modèle proposé par ces auteurs, le mouvement vers le nord-est est postérieur à celui vers le nord. Au sud de la rivière Déception, seules des stries indiquent un mouvement vers le nord-est et on peut souligner qu'elles sont associées à un changement local dans la direction du retrait glaciaire. Dans la région du lac Allemand, on observe des stries, des reliefs en dos de baleine et des drumlins associés à un mouvement vers l'ouest ou le nord-ouest ainsi que des indices d'un mouvement vers le nord (figs 1.0 et 3.0). L'écoulement vers l'ouest ou le nord-ouest est compatible avec ceux proposés par plusieurs auteurs pour le secteur situé à l'ouest de la ligne de partage glaciaire du Labrador ancestral (Hillaire-Marcel et coll., 1980; Shilts, 1980; Dyke et coll., 1982; Lauriol, 1982; Bouchard et Marcotte, 1986; Gray et Lauriol, 1985). Dans l'un des endroits où les deux mouvements

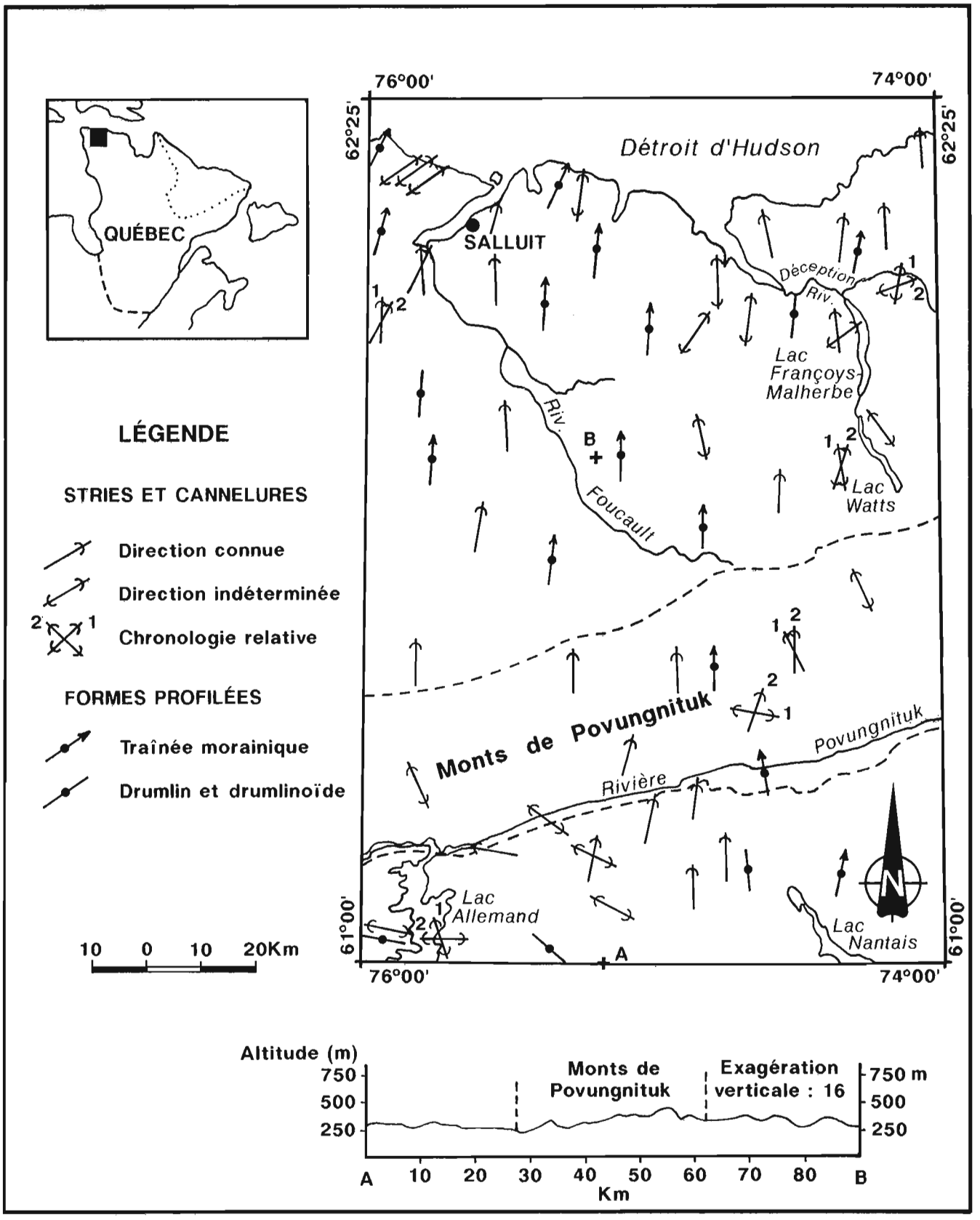

Figure 1. Région à l'étude: localisation, marques d'écoulement glaciaire et relief.

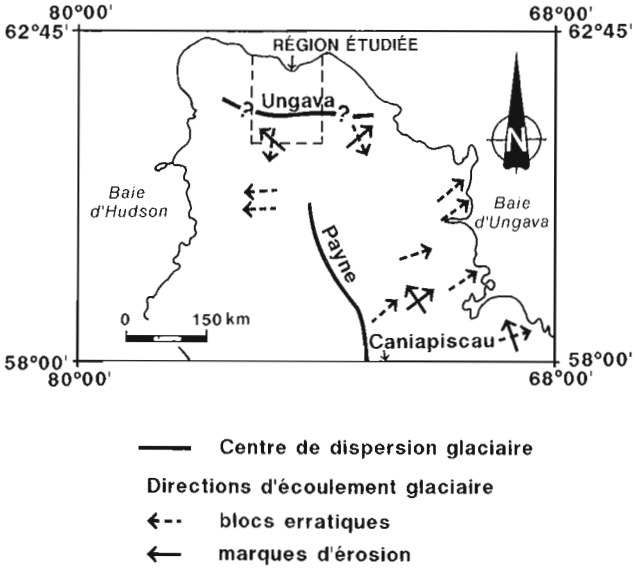

Figure 2. Les centres de dispersion glaciaires en Ungava d'après Bouchard et Marcotte (1986).

sont présents, des stries vers l'ouest recoupent de larges sillons vers le nord, phénomène qui semble indiquer que le mouvement vers l'ouest ou le nord-ouest succède à celui vers le nord. Présentement, on ne peut déterminer s'il s'agit d'un phénomène local lié à la déglaciation du secteur au sud des monts de Povungnituk ou d'un changement plus global dû à un déplacement de la ligne de partage glaciaire durant le Wisconsinien supérieur.

À l'intérieur des monts de Povungnituk, un site de stries laisse présumer un écoulement est-sud-est/ouest-nord-ouest antérieur à celui vers le nord. L'état actuel des recherches ne permet pas de préciser s'il s'agit d'un mouvement local ou s'il est associé avec le flot Ungava suggéré par Bouchard et Marcotte (1986; fig. 2.0). En effet, à 50 km au sud-sud-est de l'endroit mentionné, en périphérie du cratère du Nouveau-Québec, la direction de ce flot est de 110° (Bouchard et coll., 1989).

Transport des blocs erratiques

L'analyse qualitative (présence/absence) des blocs de dolomie du groupe de Povungnituk sur l'ensemble du territoire étudié révèle que le transport des blocs s'est effectué essentiellement vers le nord. Ainsi, alors que l'on dénombre plusieurs endroits caractérisés par la présence de ces dolomies au nord d'où elles affleurent, au sud aucune n'a été observée. La présence d'un de ces blocs à 8 km à l'ouest de la baie Déception semble indiquer une distance de transport vers le nord supérieure à 50 km.

L'analyse à la loupe binoculaire des granules des tills devrait permettre la vérification de l'hypothèse du transport glaciaire vers le sud proposée par Currie (1965) et Taylor (1982). Toutefois, il est intéressant de noter que Bouchard et Marcotte (1986) n'ont découvert aucun débris de roches de la Fosse de l'Ungava dans les granules des tills échantillonnés entre 58° et 61° de latitude nord, sur la péninsule

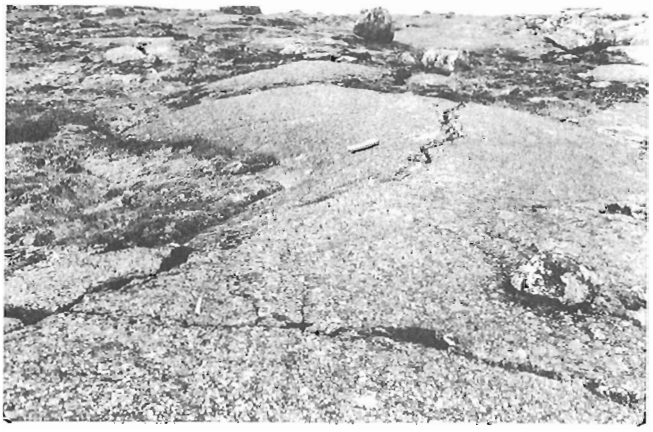

Figure 3. Vue vers l'ouest d'une surface rocheuse striée sur laquelle on observe deux orientations d'écoulement glaciaire: au centre un large sillon sud-nord et en bas des stries est-ouest. Le carnet au centre de la photo mesure 20 cm.

de l'Ungava. Bien qu'ils attribuent en partie leurs résultats à la faible densité de l'échantillonnage dans le secteur nord de leur zone d'étude, ces données contrastent avec les 4 % de fragments volcaniques et sédimentaires observés par Bouchard et coll. (1989) dans les environs du cratère du Nouveau-Québec (61°18′ de latitude nord et 73°40′ de longitude ouest). Pour l'instant, l'étendue de la zone touchée par le flot Ungava demeure largement indéterminée.

CONCLUSION

À la lueur des résultats préliminaires obtenus, il semble que l'écoulement glaciaire dominant provient du centre de dispersion glaciaire de Payne situé au sud de la région. Ce mouvement vers le nord est responsable de l'orientation de la plupart des stries, des cannelures et des formes profilées ainsi que de l'essentiel du transport.

Au sud des monts de Povungnituk et au sud du détroit d'Hudson, on observe des écoulements glaciaires plus récents, soit respectivement vers l'ouest ou le nord-ouest et vers le nord-est. Dans ce dernier cas, l'écoulement est relié à la déglaciation.

Aucun indice clair d'un mouvement le long du détroit d'Hudson n'a été observé par l'analyse des formes d'érosion et d'accumulation glaciaire. L'hypothèse d'une oblitération complète de cet ancien mouvement par celui vers le nord est possible bien qu'improbable. La poursuite des travaux de terrain de part et d'autre du secteur étudié devrait permettre la vérification de l'existence d'un courant glaciaire dans le détroit d'Hudson.

REMERCIEMENTS

L'auteur tient à remercier plusieurs personnes de la Commission géologique du Canada qui ont participé de près ou de loin à la réalisation de ces travaux: MM. Steve B. Lucas et Marc R. St-Onge pour leur soutien logistique et leur coopération enthousiaste sur le terrain; le groupe de l'Étude du

plateau continental polaire pour le soutien technique, ainsi que plusieurs chercheurs de la Division de la science des terrains pour leurs conseils scientifiques et techniques. Il adresse également sa reconnaissance au personnel de soutien du Centre géoscientifique de Québec.

BIBLIOGRAPHIE

Bouchard, M.A., and Marcotte, C.
1986: Regional glacial dispersal patterns in Ungava, Nouveau-Québec; *in* Current Research, Part B, Geological Survey of Canada, Paper 86-1B, pp. 295-304.

Bouchard, M.A., et collaborateurs
1989: Géologie glaciaire du cratère du Nouveau-Québec; *dans* L'histoire naturelle du cratère du Nouveau-Québec, M.A. Bouchard, éd., Collection Environnement et Géologie, Université de Montréal, V. 7, pp. 101-136.

Currie, K.L.
1965: The geologie of the New Quebec crater; Canadian Journal of Earth Sciences, v. 2, pp. 141-160.

Delisle, C.E., Bouchard, M.A., et André, P.
1986: Les précipitations acides et leurs effets potentiels au nord du 55° parallèle du Québec; Collection Environnement et Géologie, Université de Montréal, v. 2, 280 p.

Dyke, A.S., Dredge, L.A., and Vincent, J.S.
1982: Configuration and dynamics of the Laurentide ice sheet during the late Wisconsin maximum; Géographie physique et Quaternaire, v. 36, pp. 5-14.

Dyke, A.S., and Prest, V.K.
1987a: Late Wisconsinan and Holocene history of Laurentide ice sheet; Géographie physique et Quaternaire, v. 41, no. 2, pp. 237-263.
1987b: Paleogeography of northern North America, 18000-5000 years ago; Geological Survey of Canada, Map 1703 A, scale 1:12 500 000.

Gray, J.T., and Lauriol, B.
1985: Dynamics of the late Wisconsin ice sheet in the Unagava Peninsula interpreted from geomorphological evidence; Artic and Alpine Research, v. 17, no. 3, pp. 289-310.

Hillaire-Marcel, C., Grant, D.R., and Vincent, J.S.
1980: Comment and Reply on "Keewatin Ice Sheet-Reevaluation of the traditional concept of the Laurentide Ice Sheet" and "Glacial erosion and ice sheet divides, northeastern Laurentide Ice Sheet, on the basis of the distribution of limestone erratics"; Geology, v. 8, pp. 466-468.

Lamothe, D.
1987: Géologie et minéralisations de la Fosse de l'Ungava; Ministère de l'Énergie et des Ressources, Québec, document promotionnel 87-03, carte à 1/1 500 000.

Lauriol, B.
1982: Géomorphologie quaternaire du sud de l'Ungava; Collection Paléo-Québec, n° 15, 174 p.

MacLean, B., Williams, G.L., Sanford, B.V., Klassen, R.A., Blakeney, C., and Jennings, A.
1986: A reconnaissance study of the bedrock and surficial geology of Hudson Strait, N.W.T.; *in* Current Research, Part B, Geological Survey of Canada, Paper 86-1B, pp. 617-635.

Mathews, B.
1967: Late Quaternary events in northern Ungava; unpublished Ph. D. thesis, McGill University, Montréal, 283 p.

Sanford, B.V., Grant, A.C., Wade, J.A., and Barn, M.S.
1979: Geology of eastern Canada and adjacent areas; Geological Survey of Canada, Map 1401 A, scale 1:2 000 000.

Shilts, W.W.
1980: Flow patterns in the central North American ice sheet; Nature, v. 286, pp. 213-218.

Stockwell, C.H., McGlynn, J.C., Emslie, R.F., Sanford, B.V., Norris, A.W., Donaldson, J.A., Fahrig, W.F., et Currie, K.L.
1979: Géologie du Bouclier canadien; *dans* R.J.W. Douglas, éd., Géologie et ressources minérales du Canada, Commission géologique du Canada, Série de la géologie économique n° 1, pp. 50-165.

Taylor, F.C.
1982: Reconnaissance geology of a part of the Canadian Shield, northern Quebec and Northwest Territories; Geological Survey of Canada, Memoir 399, 32 p.

A preliminary report on the distribution of tourmaline in the northern Taltson Magmatic Zone, Northwest Territories, and its implication for base metal and tungsten prospecting

Hewitt H. Bostock
Continental Geoscience Division

Bostock, H. H. A preliminary report on the distribution of tourmaline in the northern Taltson Magmatic Zone, Northwest Territories, and its implication for base metal and tungsten prospecting; in Current Research, Part C, Geological Survey of Canada, Paper 90-1C, p. 31-41, 1990.

Abstract

The Taltson Magmatic Zone is an early Proterozoic, predominantly plutonic belt at the west edge of the exposed southwestern Churchill Province. Granitic batholiths contain widespread remnants of a supracrustal gneiss assemblage composed mostly of high grade pelitic to semipelitic gneisses. Tourmaline is absent in most of these rocks but is concentrated in five distinct areas. In one, all of the major lead-zinc showings are associated with amphibolites and haloed by tourmaline-bearing paragneiss. In one, most of the scheelite occurrences and minor amphibolite have associated tourmaline in paragneiss and minor veins at a lower level of concentration; but one occurrence of tourmalinite has been found. In one, tourmaline occurs in a local suite of small muscovite-bearing granite-pegmatite bodies. In the two remaining, association between ore metal occurrence and tourmaline in paragneiss is not clear. The compositions of these tourmalines closely reflect the compositions of the rocks within which they occur.

Résumé

La zone magnétique de Taltson en grande partie plutonique du Protérozoïque inférieur, située à l'extrémité ouest de l'affleurement sud-ouest de la province de Churchill. Les batholithes granitiques contiennent des restes répandus d'un assemblage de gneiss surpracrustal composé principalement de gneiss pélitique à semipélitique à haut degré de métamorphisme. La plupart de ces roches ne contiennent pas de tourmaline mais on en trouve dans des concentrations dans cinq zones différentes. Dans l'une, tous les indices importants de plomb-zinc sont associés à la présence d'amphibolites et sont auréolés de paragneiss à tourmaline. Dans une autre zone, la plupart des venues de scheelite et les faibles quantités d'amphibolites ont une faible teneur en tourmaline dans un paragneiss et des filons secondaires; une venue de tourmalinite a toutefois été découverte. Dans une autre zone, on trouve de la tourmalite dans une suite locale de petits massifs de granite-pegmatite à muscovite. Dans les deux dernières zones, l'association entre la venue de minerai métalique et la tourmaline dans le paragneiss n'est pas nette. Les compositions de ces tourmalines reflètent assez fidèlement les compositions des roches dans lesquelles elle se trouvent.

INTRODUCTION

Tourmaline is an accessory mineral in some granites and in some metasedimentary rocks. In sediments it can form through authigenesis, or it can be mechanically concentrated as a resistant heavy mineral. Borates, deposited in some evaporites, may be a source of boron for later tourmaline deposition. Tourmaline may be concentrated in greater proportions in pegmatites, in alteration zones, and in and around hydrothermal vents of various types. In this latter environment it is locally found in rock-forming proportions as tourmalinite. The tendency of boron to concentrate in some hydrothermal fluids, its scarcity in the earth's crust, and its entry into only one readily recognized, common mineral, tourmaline, makes tourmaline a pattern-forming mineral of special interest in regional petrography.

Recent investigations have concentrated on one aspect of tourmaline distribution patterns, that of tourmaline in the submarine volcano-hydrothermal exhalative environment, and its potential for use as a target mineral in exploration for certain types of base metal and tungsten-bearing ore deposits (Slack, 1984; Appel and Garde, 1987; Plimer 1988). This work implies that for some volcanic exhalites, ore minerals are precipitated locally whereas boron evolved from the same source may be somewhat less subject to immediate deposition, and can be dispersed to form a halo in the surrounding sediments. On the other hand because boron from normal sea water is known to be absorbed by clay minerals there is a problem that ore haloes of low boron content might be masked by normal boron deposition in argillaceous sediments. This problem is to some extent addressed if argillaceous tourmaline-bearing metasediments are surrounded in adjacent areas by similar metasediments which contain no tourmaline. It can then be argued that normal deposition, at least insofar as the particular area is concerned, did not concentrate enough boron in the argillaceous fraction to produce tourmaline. This is not to say however, that other peculiar situations, such as ones with indirect access to boron from evaporites or to terrestrial volcanism, may not result in local appearance of tourmaline in metasediments of marine origin that has no close relationship to ore deposition.

The purpose of this paper is to examine the overall tourmaline distribution in northern Taltson Magmatic Zone (TMZ), an Aphebian plutonic belt which follows the exposed western margin of the Canadian Shield from northern Alberta north to the Great Slave Lake Shear Zone. It indicates that there are distinct restricted areas within Taltson Magmatic Zone where tourmaline is present, and others displaying similar lithologies where it is not. Spatial association between tourmaline deposition and lead-zinc mineralization is clear in Thubun Lakes area (Fig. 1). A possible similar relationship with tungsten deposition as scheelite is suggested in the Rutledge River area. Data from these areas support the exhalative concept proposed by earlier workers. In one area, tourmaline occurs only in small muscovite granite bodies and does not appear to be related to volcanic exhalation. Similar small pretectonic granite bodies may have been the source of tourmaline in some gneiss that has undergone severe brittle-ductile shear. In some other areas of Taltson Magmatic Zone the exhalative model may apply but the picture is as yet unclear. Although the percentage of tourmaline in the metasediments is lower than that found in some other regions where an association between volcanism and lead-zinc or tungsten deposition has been indicated; nevertheless these areas appear to provide some of the best targets known in Taltson Magmatic Zone for further prospecting if these and related ore elements are sought.

Data for this paper are derived from 1:250 000 scale mapping between Alberta border (60 degrees North Latitude) and Great Slave Lake Shear Zone, and from the Paleozoic overlap east approximately to the 110th meridian. The area includes the Fort Smith sheet (75D), most of the Taltson Lake sheet (75E) and parts of the Little Buffalo River sheet (85A), Fort Resolution sheet (85H) and Hill Island Lake sheet (75C) are involved. The data largely comprise thin section petrography and field observations relating to tourmaline and its association with base metals and scheelite in Taltson Magmatic Zone north of the sixtieth parallel. In addition to work by the author it includes field observations and samples collected by the many students who have participated in reconnaissance mapping of the Precambrian rocks in this area. The report is preliminary because, although petrography of the Fort Smith quadrangle (NTS 75D) is essentially completed, that of much of Taltson Magmatic Zone farther north is yet to be done and very little detailed petrography has been undertaken in the Hill Island Lake area to the east.

GENERAL GEOLOGY

The region covered in this report can be divided into two principal geological terranes that are for the most part separated by a major fault zone (Fig. 1). These comprise a terrane of older crustal gneiss wedges on the east and a terrain occupied by the batholiths of Taltson Magmatic Zone on the west. The terrane of gneiss wedges may be further divided into two subzones: 1) a southwestern gneiss wedge along and within which minor plutons of Taltson age are present, and where remnants of an extensive paragneiss sequence are locally preserved; and 2) a north to eastern zone (here called the eastern wedges) which so far as is known, contains few or no remnants of pelitic paragneiss. The batholiths of Taltson Magmatic Zone, which occupy the western principal geological terrane, comprise the Deskenatlata Granodiorite (1986 Ma, U-Pb zircon), the Slave Monzogranite (1955 Ma, UPb monazite) and the Konth Syenogranite (1935 Ma, U-Pb monazite) together with remnants of a paragneiss sequence of similar lithology to that found within the southwestern gneiss wedge (Bostock et al., 1987).

The regional paragneiss is found as remnants within all of the batholiths of Taltson Magmatic Zone except Gagnon monzogranite. Paragneiss remnants within the southwestern gneiss wedge are thought to represent outliers of the same unit. The regional paragneiss consists primarily of quartzitic to pelitic biotite gneiss with some calc-silicate gneiss, quartzite, and amphibolite. Local graded beds are the only sedimentary structures recognized in these rocks. Bands of marble occur about Thubun Lakes and are present to a much more limited extent in the gneisses along strike to the south. The paragneiss has widely undergone a lower granulite to

upper amphibolite facies metamorphic maximum. In the southwestern wedge it has been variably retrograded to greenschist facies so that cordierite is completely altered but remnants of sillimanite and garnet persist. Hypersthene has been found in some bands in the paragneiss within the Konth and Slave batholiths. At Thubun Lakes (Fig. 2) the paragneiss has been intensely sheared under greenschist facies conditions along the axis of the southern lake and the high grade mineralogy, which preceded shearing, has been completely destroyed along this axis. Amphibolite of probable basic volcanic origin with minor meta-ultramafic rocks is most extensively exposed in the Thubun Lakes area (Fig. 2). Up to about 200 m of amphibolite occurs locally along the paragneiss remnant at and to the north of Fork Lake (Fig. 3). Scattered smaller remnants of amphibolite occur within the paragneiss north of Bedareh Lake (Fig. 5, but not independently shown). The Hill Island Lake paragneiss assemblage (Fig. 5) consists of the same pelitic sedimentary facies (turbidites) that is abundantly present in the regional paragneiss. Although it differs from the regional paragneiss in that metamorphism is prograde and reaches amphibolite facies only adjacent to the intrusive Natael muscovite monzogranite (1935 Ma, U-Pb monazite, Bostock et al., 1987) this does not preclude correlation suggested by similar lithology. As these two paragneiss units have not been observed in unfaulted contact their temporal sequence is unknown. Therefore, because it appears that the Hill Island Lake assemblage occurs only at the eastern margin of Taltson plutonism, and may have escaped the effects of high grade metamorphism for this reason, it is perhaps possible that these rocks form a particularly low grade outlier of the regional paragneiss assemblage.

Remnants of highly sheared, metamorphosed gabbro, anorthosite and ultramafic rocks have been found locally along the western edge of the eastern gneiss wedges. This contact therefore may represent a rifted plate margin which existed before shearing (Bostock, 1989). Whether deposition of the greywacke-mudstones, which now make up the major part of the regional paragneiss, can be related to the evolution of this margin, is unknown.

The eastern gneiss wedges are locally unconformably overlain by Nonacho Group (Aspler, 1985). The group is largely composed of fine to coarse, unmetamorphosed (except along some faults), terrestrial clastics. These rocks are deformed by sinistral shear thought to have occurred between 1935 and 1908 Ma (Bostock et al., 1988).

TOURMALINE AND ASSOCIATED ORE MINERAL OCCURRENCES

Introduction

Lead-zinc and scheelite occurrences, and even those of tourmaline, are not common in Taltson Magmatic Zone; nevertheless in two areas (Thubun Lakes, Fig 2; and Rutledge River, Fig. 3) ore mineral and tourmaline appear associated together. Several other areas contain tourmaline concentrations with only minor evidence of the presence of ore minerals discovered so far. It is germane therefore to consider such areas on the basis that ore minerals there may have been missed due to insufficient searching. The following section will describe first the two areas where both tourmaline and metals are concentrated, and will continue with descriptions of areas where only concentrations of tourmaline, without clearly related ore minerals, are presently evident.

Extensive thin section petrography of rocks in the Fort Smith quadrangle of Taltson Magmatic Zone (75D; south of 61° N, Fig. 1) has established that tourmaline over this large area is a rare accessory mineral. Less than one percent of those thin sections examined, contain it. However, those few that do are concentrated in two specific parts of the quadrangle (Fig. 1). Farther north in Fort Resolution (85H) and Taltson Lake (75E; both north of 61° N) petrography has suggested that, although tourmaline is a more common accessory, it is again concentrated in specific areas and is absent elsewhere. The tourmaline in all areas so far examined occurs predominantly within pelitic and semipelitic gneisses of the regional paragneiss and in associated conformable granitic to pegmatitic lenses. One layer of tourmalinite has been identified (about 60 % tourmaline). It also occurs within cross cutting granite veins, and within some small independent granitic bodies. Some has been found in Konth megacrystic syenogranite closely associated with paragneiss remnants, but it does not occur independently of the paragneiss in any of the batholithic granites so far examined.

The association of tourmaline with lead-zinc veins is suggested in the field through the appearance of medium-grained tourmaline in some of the local granitic sweats and dykes within paragneiss surrounding veins. The relationship however, is only substantiated when the distribution of accessory tourmaline evident in thin sections of rocks from the surrounding area is plotted with the veins.

Scheelite occurrences have been recognized using an ultraviolet lamp to examine all hand specimens returned to field camp. Observations positive for scheelite obtained by this method have all been checked by X-ray powder pattern identification. Because none of these occurrences was recognized at the time of collection of the specimens, little is known of the local extent or other mesoscopic characteristics of the mineralization.

Thubun Lakes (Fig. 2)

Tourmaline in the Thubun Lakes area occurs widely, mostly in paragneiss, but also in minor pegmatites and some quartz lenses. In paragneiss from two to ten sub-millimetre sized, rounded, olive-brown grains per thin section are typical in one third of the specimens examined, but in one specimen a 2mm lamella contains several percent tourmaline. Locally, diffuse bluish patches are present and in one sample these form diffuse cores. Within the zone of sinistral shear along south Thubun Lakes two or three angular fragments of tourmaline may be seen locally to lie along the same foliation plane suggesting that shearing has been responsible for disruption of a single larger crystal.

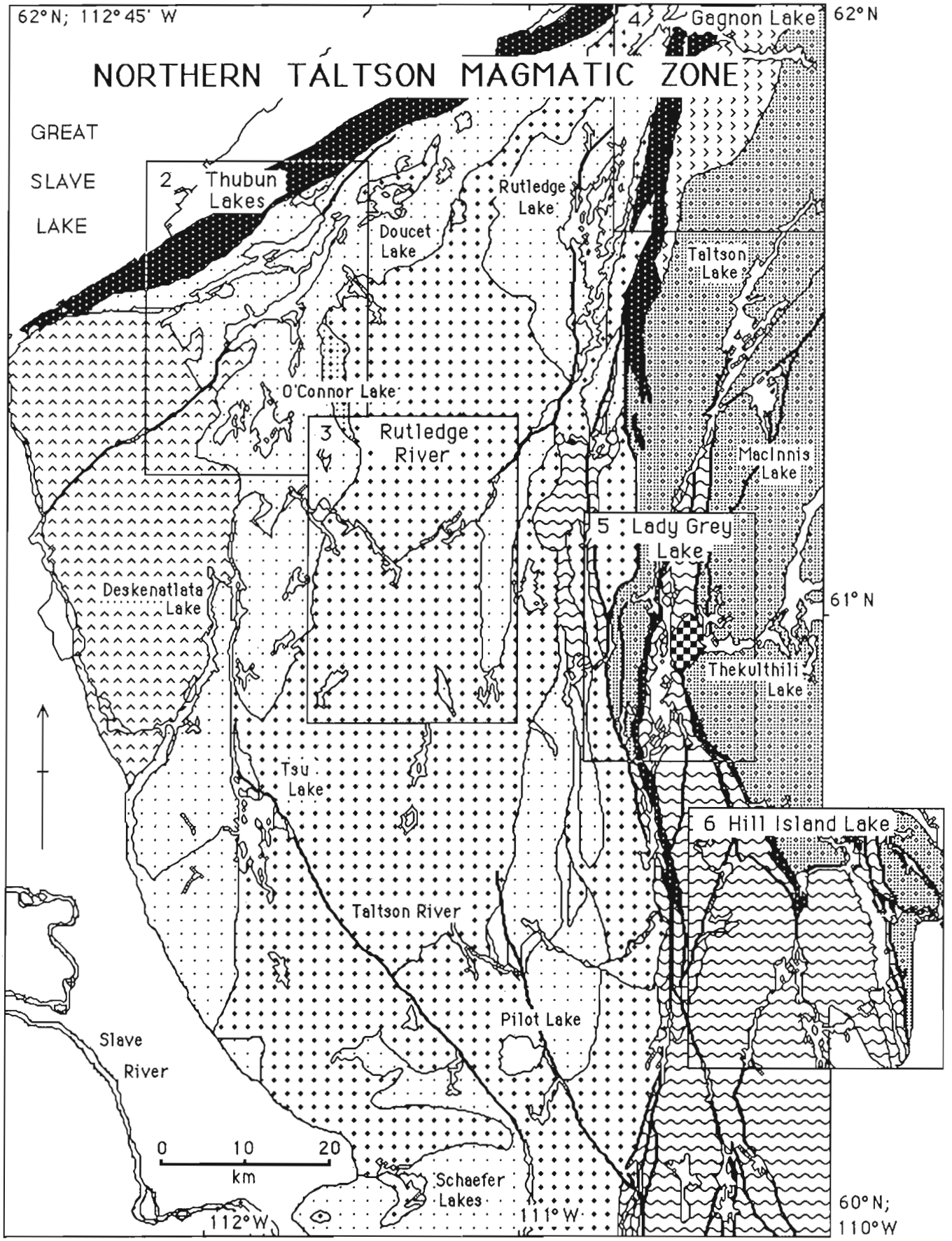
62°N; 112°45' W
NORTHERN TALTSON MAGMATIC ZONE
GREAT
SLAVE
LAKE
2 Thubun Lakes
4 Gagnon Lake
62°N
Rutledge Lake
Doucet Lake
Taltson Lake
O'Connor Lake
3 Rutledge River
MacInnis Lake
5 Lady Grey Lake
Deskenatlata Lake
61°N
Thekulthili Lake
Tsu Lake
6 Hill Island Lake
Taltson River
Pilot Lake
Slave River
0 10 20
km
Schaefer Lakes
112°W
111°W
60°N;
110°W

Quartz-galena commonly with sphalerite, some carbonate and locally with minor chalcopyrite occur near O'Connor Lake and along the shores of Thubun Lakes. Most of the showings are in quartz breccia veins with cocks comb texture common. The largest are near the southeast shore of O'Connor Lake where a vein mostly about 0.6m wide has been exposed for 75m and test pitted for a further 75m. The veins mostly clearly cross cut the regional trends, but one occurrence on the waterway between north and south Thubun Lakes is not clearly vein related. There, lenses of conformable pegmatite have intruded sulphide-bearing calcareous gneiss but are perpendicular to quartz gash. These pegmatites locally have rinds of green microcline that is fluorescent white under ultraviolet light suggesting a high lead content. It seems likely therefore that this lead mineralization predated emplacement of the pegmatites and likely predated the last metamorphism as well.

There is a strong spatial relation between the distribution of lead-zinc dominated occurrences and tourmaline in the Thubun Lakes area as shown in Figure 2. Both mineral groups occur along a belt stretching from O'Connor Lake northward into south Thubun Lakes and thence northeastward into north Thubun Lakes valley. This disposition appears to relate the arrangement of both mineral groups to the amphibolite belts of presumed volcanic derivation and their associated paragneiss. Given the complexity of intersecting structural trends in this area, the most likely explanation for the persistence of these congruent patterns would seem to be that of syndeposition of amphibolite, paragneiss, tourmaline and ore minerals. This however conflicts with the late cross cutting age of the galena-sphalerite veins. The possibility should therefore be considered that the Pb-Zn veins contain metals that have been remobilized from metasedimentary source beds that have not yet been recognized. Two further factors support this view: 1) At least one of the lead-zinc occurrences appears to have been through a period of high grade metamorphism and pegmatite intrusion, and 2) most of the tourmaline is very finely and sparsely dispersed through the paragneiss, whereas the lead-zinc is concentrated in the crosscutting veins. If boron were introduced at the time of lead-zinc veining and had access to the paragneiss only by similar cross-cutting fractures, it is difficult to see how it would attain a halo which is at the same time widely dispersed but sparsely disseminated.

Scheelite is present as 1 mm flecks irregularly but sparsely distributed through a coarsely recrystallized diopsidic zone in paragneiss at one locality in Thubun Lakes area about 2 km northeast of the northeast end of south Thubun Lake.

Lithological factors favouring volcanogenic ore deposition appear to be at a maximum for northern Taltson Magmatic Zone in the Thubun Lakes area. A substantial basic volcanic belt with possible acid volcanics masked by mylonitization occurs within a deformed carbonate-greywacke metasedimentary succession. A well developed, though volumetrically small, tourmaline halo surrounds a concentration of known lead-zinc occurrences. Minor scheelite has been found in the paragneiss near the northeast end of this tourmaline-defined halo which, by analogy with areas such as that described by Appel et al. (1987) in the Malene Gneisses of West Greenland, may also be exhalative in origin. Closer examination of this area for additional lead-zinc and tungsten mineralization may prove rewarding.

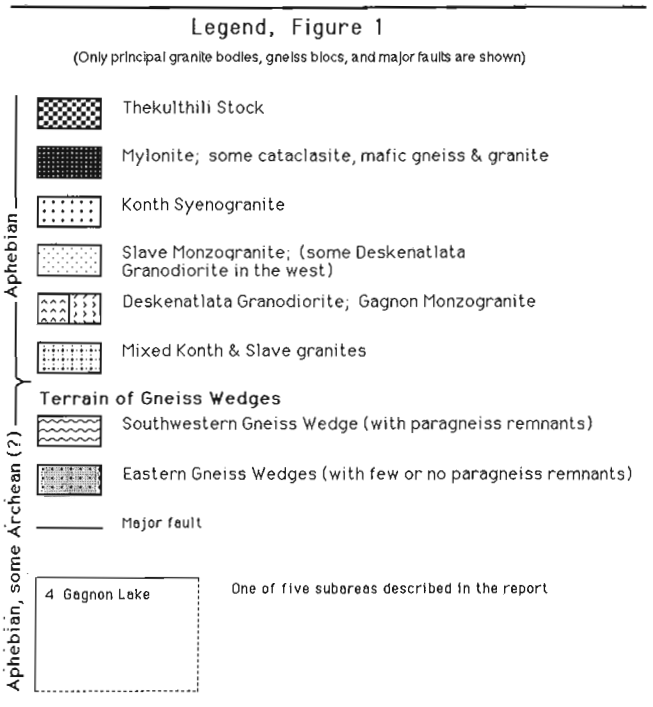

Figure 1. Regional Geological Map showing the main gneiss and plutonic rock units of northern Taltson Magmatic Zone.

Rutledge River (Fig. 3)

In the Rutledge River area tourmaline is for the most part a rare accessory mineral associated with paragneiss and with a group of minor cross cutting granite veins. One occurrence, which is so far unique within northern Taltson Magmatic Zone, fits the definition of tourmalinite.

Tourmaline as an accessory mineral associated with paragneiss occurs in two samples examined, one near the southeast end of a major lake on Rutledge River, and one with the narrower paragneiss screen farther north. In the southern occurrence a 1 cm thick band of fine grained biotite gneiss also contains minute disseminated grains of scheelite and accessory apatite is unusually abundant. The northern occurrence consists of accessory grains of tourmaline in megacrystic syenogranite immediately adjacent to paragneiss remnants. Tourmaline-bearing granite veins up to 15 cm wide are clustered in and between the northern paragneiss remnant and a dioritic body to the east. A minor granite vein with a few crystals of black tourmaline was observed in an isolated outcrop of gneiss within the paragneiss remnant along the east margin of the Rutledge River area.

The tourmalinite occurs on the west shore near the south end of a moderate sized lake (UTM coordinates, E492780;

N6765760 of Zone 12). There, quartz-rich paragneiss in 3 cm layers has local interbanded, slightly rusty, sillimanite-garnet-bearing pelitic gneiss up to 60 cm thick. This assemblage is intermittently exposed for about 50 m westward from the lake to the syenogranite contact. Near shore a fine grained, dark greenish, conformable layer up to about 30 cm thick has scattered small gossan patches distributed locally along it. The band mesoscopically resembles some minor amphibolites seen elsewhere in the Fort Smith area and was interpreted as such in the field. Thin section study shows it to consist of roughly 60 per cent fine grained, blue to yellow-brown tourmaline in radiating crystals, 20 per cent corundum, and 20 per cent biotite.

Four scheelite-bearing specimens were collected in this area, two on either side of Rutledge River where scheelite occurs both as minute veins and as very fine disseminations along a single lamella in paragneiss. The third specimen is from an amphibolite band about 3 m thick within paragneiss northwest of Nelson Lake. Scheelite forms as local, finely crystalline fracture coatings in the amphibolite. The fourth specimen is from a band of amphibolite about 20 m thick occurring within quartz-rich paragneiss (UTM coordinates E492200 N6768330 of zone 12) about 3 km north of the tourmalinite bed. The central 15 m of the amphibolite is broken into lenticular fragments, possibly derived from pillows, surrounded by thin seams of white granite. The outer 3 m on each side are of gneissic amphibolite possibly derived from tephra. Scheelite occurs as scattered patches up to 3 mm across in a sample from the central part of the amphibolite. Strong cream coloured fluorescence suggests that it is molybdenum-rich in comparison to other scheelites reported here.

The Rutledge River area includes the most numerous and most promising minor scheelite occurrences so far discovered in Taltson Magmatic Zone. No Pb-Zn mineralization has been found. Tourmaline appears to be associated with scheelite in the western paragneiss of the area, but the amount of tourmaline appears to be much less than at Thubun Lakes. The finely disseminated banded character of the scheelite at one locality is consistent with a stratabound origin and the close association with paragneiss suggests that the tiny vein occurrences represent remobilization of tungsten within or near the original paragneiss host. That these likely stratabound scheelite occurrences trend northward toward a concentration of tourmaline in paragneiss and granite veins suggests a tourmaline-rich target area that may warrant further prospecting for scheelite and related minerals. The occurrence of tourmalinite with its high content of boron may indicate proximity to an exhalative source. This and the absence of evidence of previous prospecting along the Fork Lake volcanic belt make this part of the Rutledge River area perhaps the best prospecting target yet found in this study.

Gangon Lake (Fig. 4)

In the Gagnon Lake area (Fig. 4) tourmaline was found in muscovite-tourmaline granitic dykes and apophyses in four places: one, on the west shore of Gagnon Lake, and the others farther south within an eastern gneiss wedge near the east contact of the Gagnon monzogranite pluton. With the exception of granite pegmatite associated with the Hill Island Lake assemblage (Fig. 6) no other bodies of this type have been found in northern Taltson Magmatic Zone. Because of the distinctive colour and form of typical tourmaline in a granitic matrix it is unlikely that many of these bodies would be missed in field work. Thus, unlike the other tourmaline occurrences, few more of them are likely to be discovered by thin section petrography. It can already be said therefore, that the concentration of these granite bodies of the Gagnon Lake area constitutes a distinctive pattern. No related ore mineral deposition is evident.

The Gagnon Lake occurrence consists of several dyke-like bodies of foliated lineated muscovite granite. The largest of these is about 12 m thick and strikes east-west with steep dip, cutting across the trend of the paragneiss. Tourmaline occurs in pencil-like quartz-tourmaline segregations that parallel the lineation and form about 10 per cent of the rock.

The northern occurrence along the Gagnon pluton contact comprises a small tourmaline-muscovite-albite quartz granite body of unknown size. Brown tourmaline discoloured bluish along fractures and locally at rims, forms about 1 per cent of the rock. Accessory purple fluorite is common.

The central locality along the Gagnon pluton contact comprises a group of narrow (0.6 m) fine grained muscovite granite dykes with local potash feldspar megacrysts along their margins. The dykes intrude a mixed granite-amphibolite gneiss and trend southeasterly with near vertical dips. Accessory tourmaline has irregular blue cores with pale brown to dark grey rims.

The southern locality comprises several muscovite granite-pegmatite bodies intrusive into biotite-quartz-feldspar gneiss with diffuse hornblende-bearing bands and scattered, lensoid, more mafic inclusions. The largest of these, about 11 m across, consists of rude layers of medium grained muscovite-tourmaline-rich granite and muscovite-poor, tourmaline-free pegmatite. In thin section the tourmaline is blue-grey with local blue cores.

A galena-bearing cocks comb quartz vein up to 6 cm wide is intermittently present along a breccia-fracture zone up to 15 cm wide and 50 m long cutting foliation in Slave monzogranite on the west shore of a deep bay south from Gagnon Lake. Galena and pink carbonate occur only locally in pockets along the vein. Trace galena was also observed within pyrite in a minor quartz vein within basal Nonacho conglomerate west of Taltson Lake.

Tourmaline in the Gagnon Lake area occurs only in small muscovite bearing granitic to pegmatitic intrusive bodies distinctly larger than the veins of the Rutledge River area. The three southern bodies are clustered along the east margin of Gagnon monzogranite pluton. They may represent late fluids related to emplacement of this pluton, but the presence of a similar granite body intruded within the regional paragneiss close to the Konth syenogranite along the west shore of Gagnon Lake may indicate that all are younger, and perhaps related to Konth Granite. The pattern

which these bodies display probably has something to say about late conditions of plutonism in northern Taltson Magmatic Zone that will become evident when the bodies themselves and the regional structural environment of their emplacement are better known. These small granitic bodies are significant here however, because, in addition to the evidence of boron mineralization which they provide, they represent concentrations of tourmaline large enough that they might be preserved locally through deformation of the type evident in the Lady Grey Lake area (Fig. 5).

Lady Grey Lake (Fig. 5)

In the Lady Grey Lake area tourmaline is present locally in the paragneiss and schlieren gneisses within, and along the fault bounded margins of, the southwestern gneiss wedge. Two accessory tourmaline occurrences are associated with linear bodies of granite-pebble-bearing biotite and muscovite-biotite schists along major faults. It is not clear whether these tourmalines are derived from Nonacho Group, from the regional paragneiss, or from combinations of these two; or whether the necessary boron might not have been introduced during early movements along the faults which these schists represent. Two specimens with accessory tourmaline are from biotite, schlieren-bearing gneiss possibly derived from intershearing of paragneiss with granite gneiss; and two are from garnet $\pm$ sillimanite paragneiss. One specimen is from an isolated exposure of muscovite granite gneiss with anastamosing zones of muscovite-biotite foliation. Common inclusions of grey quartz-tourmaline-rich rock up to 3 cm diameter are locally folded within the gneiss. Tourmaline forms up to about 20 per cent of these inclusions. Tourmaline concentrations of this size might originate in tourmalinite beds like that of Rutledge River area (Fig. 2), or perhaps in segregations of the type seen in the northwestern tourmaline-bearing granite locality at Gagnon Lake (Fig. 4). In thin section the matrix about quartz-tourmaline inclusions consists of albite phenoclasts and muscovite flakes in a quartz-feldspar mortar with scattered equant fragments of apatite to 1 mm in diameter. Tourmaline in all thin sections is olive brown with local bluish cores or irregular patches.

Scheelite occurs in one locality as tiny grey-white veins (2mm) with local purple fluorite in granite of a small apophyse near the east contact of the Thekulthili syenogranite stock. The apophyse intrudes a fringe of low grade laminated calcareous siltstone possibly correlative with the Hill Island Lake assemblage. Galena occurs in lenses with associated quartz in the eastern gneiss wedge (non paragneiss-bearing gneisses) about 4 km east of the exit of Thekulthili River from Thekulthili Lake. Three trenches occur over a strike length of about 20 m. The best showing exposes a galena lens up to 25 cm wide and about 1.5 m long in slightly feldspar-megacrystic biotite-chlorite gneiss.

In the Lady Grey Lake area (Fig. 5) neither lead-zinc nor tungsten mineralization appears to be closely related to tourmaline occurrence and the tourmaline is dispersed. Gneiss and granites of the southwestern gneiss wedge about Lady Grey Lake, with the exception of Thekulthili stock, have undergone exceptionally severe ductile deformation. The dispersed distribution of tourmaline in these rocks is consistent with its derivation from remnants of the regional paragneiss which have been infolded and dismembered within an older gneiss unit, and intruded by syntectonic granites. Combined dilution and remobilization implied by the complex geological paragenesis of these gneisses may also account for the absence of minor ore mineral occurrences in them. Those ore mineral occurrences which do occur are in special locations; one (scheelite) is related to the contact between Thekulthili granite stock and low grade metasediments that may be correlative to the Hill Island Lake assemblage (Fig. 6) The other (galena) is within the eastern gneiss wedges where no paragneiss has been recognized, and the derivation of the lead is unknown.

Hill Island Lake (Fig. 6)

In the Hill Island Lake area tourmaline has been found in the prograde metasediments of the Hill Island Lake assemblage west of Natael Bay, and in the Natael monzogranite pegmatite farther east, but no thin sections of metasediments east of the 110th meridian have been examined so far. The host rocks vary from chlorite zone siltstone and greywacke through cordierite zone to quartz-plagioclase biotite bands in migmatite and pegmatite. Tourmaline in these gneisses is commonly olive to yellow brown with diffuse bluish cores, but locally reddish brown cores are present. One specimen (sample 775, Table 1) was taken from a large, subangular, apatite-bearing pegmatite erratic probably not far from its place of origin.

The widespread occurrence of tourmaline at least in the northern exposures of these rocks, suggests boron concentration in this lithological unit, and by inference the possibility that local volcanogenic exhalative deposition of lead-zinc or tungsten may have been associated with it. On the other hand no volcanic rocks have been recognized in the Hill Island Lake assemblage. The presence of one scheelite occurrence in a calcareous bed, perhaps supported by the scheelite associated with similar rocks about Thekulthili stock in Lady Grey Lake area (Fig. 5), may be suggestive. The reconnaissance nature of the present study suggests further examination of this area.

TOURMALINE CHEMISTRY

Twelve hand specimens were selected from various parts of the Taltson Magmatic Zone where tourmaline was sufficiently abundant to suggest that an additional polished section would contain tourmaline. Analyses were obtained using a CAMECA CAMEBAX electron microprobe equipped with four wavelength dispersive spectrometers and automated to produce multielement analyses and data reduction using the CAMECA software ONPAQT on a PDP11/23 PLUS computer. The ONPAQT software uses the "PAP" matrix correction model developed by J.L. Pouchou and F. Pichoir (1984). The standards used were natural and/or synthetic minerals or metals. Accelerating voltage was 15 kV with a beam current of 30 nA. Electron microanalysis was done by M. Bonardi of the Mineral Resources Division, Geological Survey of Canada.

COMPOSITE INSET-MAP LEGEND

(Not all units appear on any one inset-map)

APHEBIAN

- Thekulthili syenogranite stock
- Mylonite
- Recrystallized mylonite, sheared granite and gneiss, some cataclasite
- Nonacho Group fine to coarse grained clastic sediments.
- Natael Muscovite Monzogranite (1935 Ma); mixed with Hill Island Lake assemblage (dashed-cross pattern)
- Konth Syenogranite (1935 Ma)
- Mixed Konth and Slave Granites
- Mixed Deskenatlata and Slave Granites with variable proportions of supracrustal inclusions
- Slave Monzogranite (1955 Ma)
- Deskenatlata Granodiorite (1986 Ma) & Gagnon Monzogranite
- Hornblende gabbro, hornblende plagioclase gneiss,
- Megacrystic granite, augen gneiss

APHEBIAN & ARCHEAN (?)

- Foliated granodiorite, diorite
- Hill Island Lake Assemblage: prograde greywacke-mudstone (diagonal dash pattern); schist (squared pattern)
- Regional Paragneiss: mostly high grade metaturbidites (light stippled); with amphibolite (dark stippled)
- Southwestern Gneiss Wedge (with local paragneiss remnants)
- Eastern Gneiss Wedges (with few or no paragneiss remnants)

Symbols

- tourmaline occurrence
- Tourmalinite occurrence
- Pb-Zn occurrence
- Scheelite occurrence

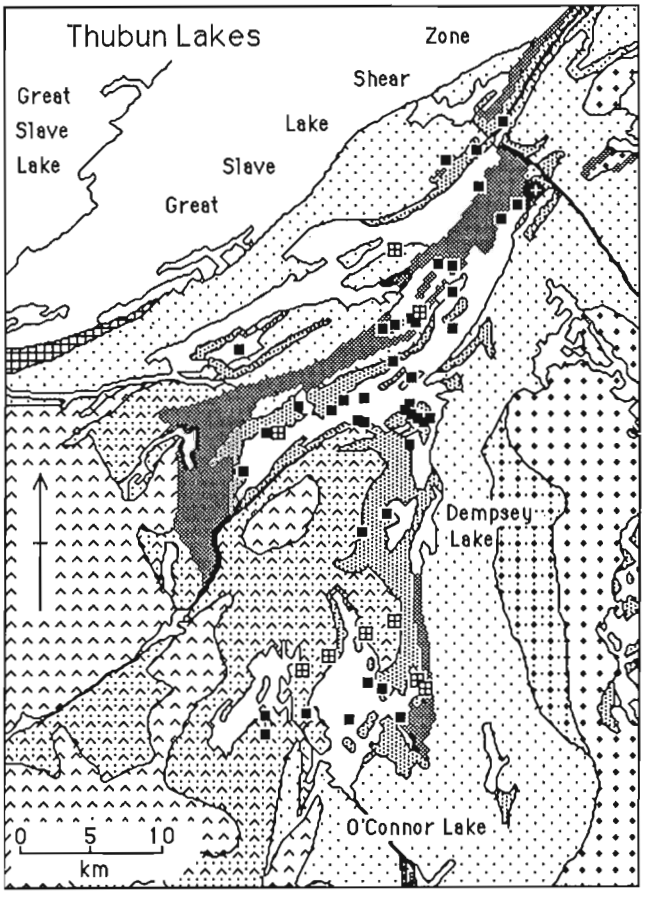

Figure 2. Geological map of the Thubun Lakes region showing the distribution of tourmaline, lead-zinc and scheelite occurences.

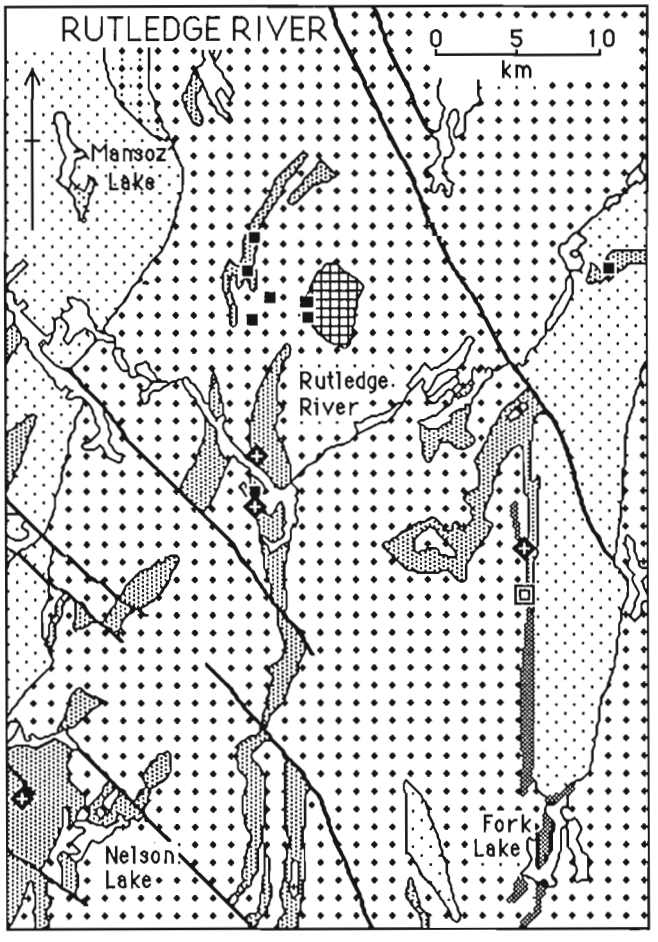

Figure 3. Geological map of the Rutledge River area showing the distribution of tourmaline, tourmalinite and scheelite occurrences.

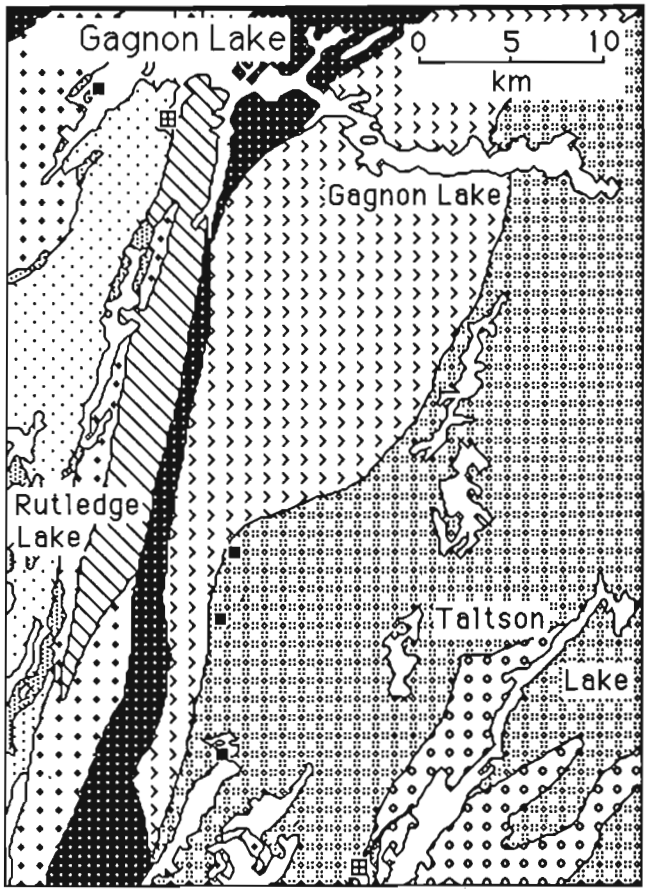

Figure 4. Geological map of the Gagnon Lake area showing the distribution of tourmaline and lead occurrences.

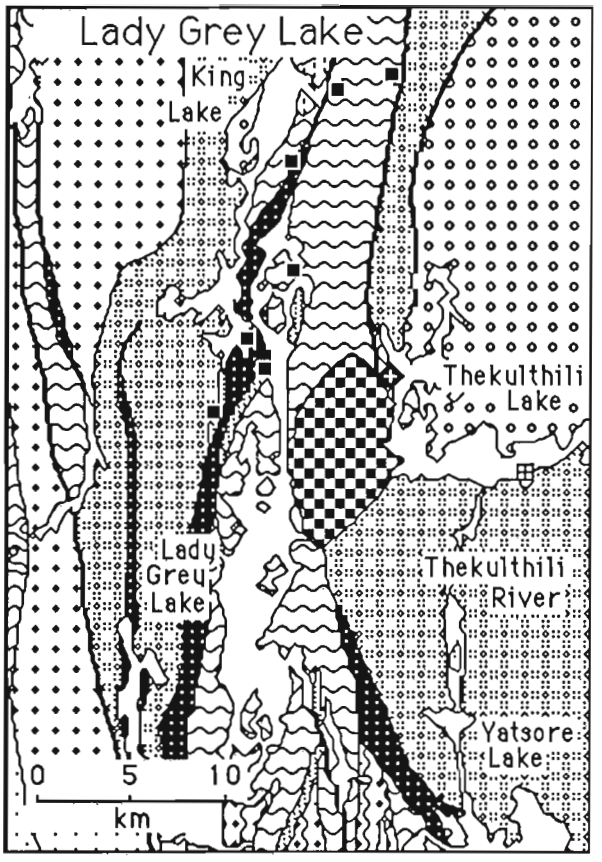

Figure 5. Geological map of the Lady Grey Lake area showing the distribution of tourmaline, lead and scheelite occurrences.

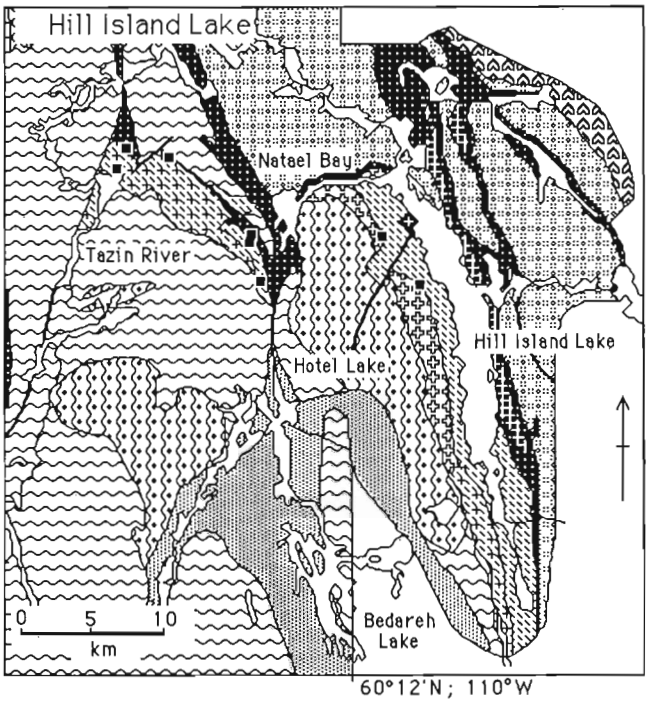

Figure 6. Geological map of the Hill Island Lake area showing the distribution of tourmaline and scheelite occurrences.

Table 1. Composition of Tourmaline from northern Taltson Magmatic Zone.

Sample	86BK-775b	85BK-569d	81BK-652a	85BK-81a	87BKO-430a	86BK-714a
Lithology	Apatite PEGM	Thubun PRGN	Natael GWKE	Thubun PRGN	Gagnon GRNT	Gagnon PEGM
Na2O	2.08	1.90	1.97	1.74	1.72	2.08
MgO	4.28	5.24	5.94	5.59	1.71	1.37
Al2O3	35.43	34.79	32.98	33.88	32.70	32.52
SiO2	36.14	36.12	36.92	35.95	35.27	34.67
k2O	0.04	0.05	0.04	0.06	0.05	0.05
CaO	0.44	0.72	0.52	1.23	0.19	0.16
TiO2	0.61	0.86	0.90	1.02	0.74	0.31
FeO	9.65	8.28	8.53	8.17	14.45	15.27
MnO	0.08	0.04	0.03	0.04	0.16	0.16
F	0.35	0.19	0.32	0.34	1.02	0.70
Cl	0.01	0.00	0.00	0.01	0.00	0.01
V2O5	0.01	0.07	0.04	0.07	0.01	0.01
Cr2O3	0.01	0.10	0.05	0.10	0.02	0.01
Total	89.12	88.36	88.23	88.20	88.05	87.30

Sample	81BK-650a	81BK-208a	87BKO-412d	87BK-606a	85BKJ-209a	86BK-370f
Lithology	Natael SLTN	Natael GWKE	Gagnon GRNT	Gagnon GRNT	GRNT vein	Tourmalinite
Na2O	1.97	2.01	2.12	1.96	2.42	1.73
MgO	4.67	6.02	2.04	2.09	3.09	5.75
Al2O3	33.25	33.84	33.61	31.98	33.09	36.22
SiO2	36.26	36.54	35.30	34.21	35.26	36.57
k2O	0.03	0.03	0.04	0.05	0.07	0.02
CaO	0.48	0.55	0.24	0.32	0.53	0.43
TiO2	0.73	0.75	0.70	0.49	0.76	0.17
FeO	9.75	7.66	13.57	14.03	13.65	6.58
MnO	0.04	0.03	0.16	0.13	0.03	0.01
F	0.30	0.23	0.82	0.48	0.77	0.23
Cl	0.00	0.00	0.01	0.01	0.01	0.01
V2O5	0.02	0.04	0.01	0.02	0.01	0.05
Cr2O3	0.03	0.03	0.01	0.01	0.01	0.02
Total	87.53	87.73	88.62	85.78	89.70	87.80

Abreviations: PEGM=pegmatite; PRGN= paragneiss; GWKE=greywacke; GRNT=granite; SLTN=siltstone

For this study 3 analyses were made across each of three tourmaline grains per specimen such that one core and two rim analyses were made on each grain. Comparisons suggest that there is a low level of significant zoning of Fe-Mg between cores and rims and some variation of alkalies between rims of crystals in the same specimen. These variations are sufficiently small that analyses for each sample have been averaged.

The data indicate that tourmalines from the metasediments have compositions that differ significantly from most of those from the granitic dykes and veins (Fig. 7, 8, 9). This supports the conclusion of Plimer (1988) that the tourmaline composition tends to reflect the bulk composition of the rock in which it occurs. In the case of the tourmalinite of which about 60 percent is tourmaline, the high alumina content reflects the presence of major corundum and the high magnesium content presumably the presence of high magnesium (?) biotite (see Fig. 7 and 8). Dispersion of the analyses for granitic tourmalines (Fig. 8) seems to suggest substitution of Al_2O_3 for SiO_2 whereas sympathetic variation is suggested for other tourmaline types. The two tourmaline paragneiss specimens from the Thubun Lakes area (specimens 81 and 569, Fig. 9) are significantly enriched in V_2O_5 and Cr_2O_3 with respect to all the others examined. This presumably results from increased concentrations of these elements in the environment at the time of deposition. It likely reflects the abundance of basic volcanic rocks (Fig. 2) but may also be related to syngenetic emplacement of minor ultramafics in the area, one of which has been reported within the amphibolites at O'Connor Lake (Bostock, 1987). Sample 775 is from an apatite-bearing pegmatite erratic near Natael Bay thought to represent pegmatite within the Hill Island Lake assemblage. The analysis of this tourmaline shows that it alone among the tourmalines from granitic rocks has some chemical characteristics of tourmaline from the paragneiss. Because all the other granitic tourmalines analyzed are from distinct crosscutting minor granitic intrusions further study will include comparison of tourmalines from conformable (synmetamorphic) granite veins with those from cross cutting bodies.

DISCUSSION

In the northern Taltson Magmatic Zone over large areas, the regional paragneiss appears to be devoid of tourmaline (the only common boron-bearing mineral). The boron contribution from normal marine sedimentation in such areas appears to have been too small to produce tourmaline in these gneisses. The tourmaline-bearing areas that exist must

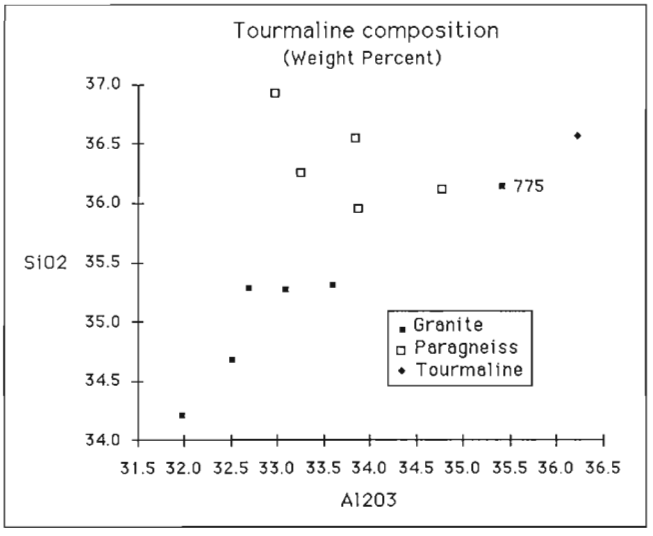

Figure 8. Scatter plot of SiO^2 vs. Al^2O^3 in tourmaline from northern Taltson Magmatic Zone.

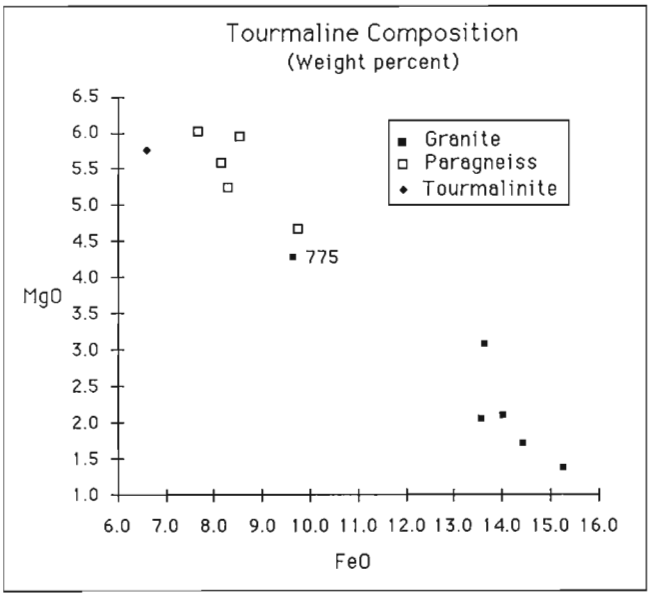

Figure 7. Scatter plot of MgO vs. FeO in tourmaline from northern Taltson Magmatic Zone.

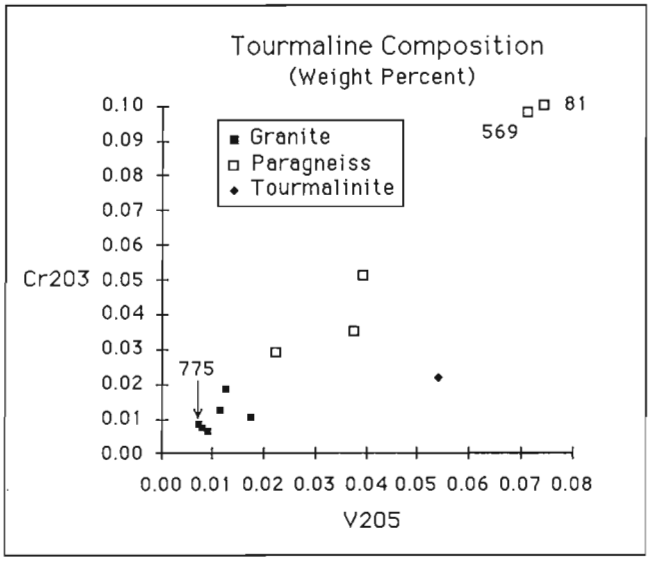

Figure 9. Scatter plot of Cr^2O^3 vs. V^2O^5 in tourmaline from northern Taltson Magmatic Zone.

therefore be unusual. Some, such as Thubun Lakes and eastern part of Rutledge River area are clearly prime candidates for tourmaline with a volcanic exhalative connection. In others, such as Hill Island Lake where tourmaline is a common accessory in the specimens so far examined, the situation is unclear. The absence of known lead-zinc and the single scheelite occurrence found in these rocks may reflect insufficient search. On the other hand other processes might account for tourmaline formation. It is possible that sedimentation in this part of the sedimentary basin may have had indirect access to boron from evaporites, perhaps through a particular local river delta; or such a river may have drained an area of terrestrial volcanism. No evidence for either of these alternatives has been found. Further investigation of Hill Island Lake area seems warranted before a submarine exhalative origin for boron concentration there can be rejected. Lady Grey Lake area seems less encouraging because of the absence of minor ore mineral occurrences in the regional paragneiss which contains the tourmaline, and because of the high degree of dismemberment to which the paragneiss has been subjected.

Other metallic mineral occurrences in Taltson Magmatic Zone do not appear to have associated tourmaline haloes. None has been found in the Rutledge Lake area where Cu-Ni occurrences are associated with minor ultramafic bodies mostly in paragneiss (Culshaw, 1984), and no tourmaline has been found in paragneiss in Tsu Lake area where molybdenite occurs in a breccia along the west contact of paragneiss with Slave Granite (Bostock,1980). None has been found in the area about minor loellingite-arsenopyrite concentrations in amphibolite bands west of Lady Grey Lake area (Bostock, 1982)

Concentration of small tourmaline-muscovite-bearing granitic bodies in the Gagnon Lake area and perhaps about Hill Island Lake is not evidently connected with ore mineral deposition. It represents concentration of "mineralizing fluids" not found in granitic bodies of similar size elsewhere in Taltson Magmatic Zone. In this respect the eastern margin of Taltson Magmatic Zone has also been found to be the locus of minor fluorite veins and accessory occurrences which however do not appear to be closely connected with the presence of tourmaline. This zone has therefore likely been one of mild concentration of a variety of such fluids.

REFERENCES

Appel, P.W.U. and Garde, A. A.
1987: Stratabound scheelite and stratiform tourmalinites in the Archaean Malene supracrustal rocks, southern West Greenland; Grnlands Geologiske undersgelse, Bulletin No. 156, p. 1-26.

Aspler, L. B.
1985: Geology of Nonacho Basin (Early Proterozoic) Northwest Territories; Ph.D. thesis, Carleton University, Ottawa, Ont., 385p.

Bostock, H.H.
1980: Reconnaissance Geology of the Fort Smith-Hill Island Lake Area, Northwest Territories; *in* Current Research, Part A, Geological Survey of Canada, Paper 80 1A, p. 153-155.

Bostock, H.H.
1982: Geology of the Fort Smith Map Area, District of Mackenzie, Northwest Territories (NTS 75D); Geological Survey of Canada, Open File 859, p 48.

Bostock, H.H.
1987: Geology of the south half of the Taltson Lake map area, District of Mackenzie; *in* Current Research, Part A, Geological Survey of Canada, Paper 87-1A, p. 443-450.

Bostock, H.H.
1989: The significance of ultramafic inclusions in gneisses along the eastern margin of the Taltson Magmatic Zone District of Mackenzie, N.W.T.; *in* Current Research, Part C, Geological Survey of Canada, Paper 89-1C, p. 49-56.

Bostock, H.H. and Loveridge, W.D.
1988: Geochronology of the Taltson Magmatic Zone and its eastern cratonic margin, District of Mackenzie; in Radiogenic Age and Isotopic Studies: Report 2, Geological Survey of Canada, Paper 88-2, p. 59-65.

Bostock, H.H., van Breemen, and Loveridge, W.D.
1987: Proterozoic geochronology in the Taltson Magmatic Zone, N.W.T.; *in* Radiogenic Age and Isotopic Studies: Report 1, Geological Survey of Canada, Paper 87-2, p. 73-80.

Culshaw, N.G.
1984: Rutledge Lake, Northwest Territories; A section across a shear belt within the Churchill Province; *in* Current Research, Part A, Geological Survey of Canada, Paper 84-1A, p. 331-338.

Plimer, I.R.
1988: Tourmalinites Associated with Australian Proterozoic Submarine Exhalative Ores; in Base Metal Sulfide Deposits, G.H. Friedrich, P.M. Herzig (Ed.), Springer-Verlag Berlin, p. 255-283.

Pouchou, J.L. et Pichoir, F.
1984: A new model for quantitative "X-ray microanalysis; Recherche Aerospecial, v. 84-3, p. 13-38.

Slack, J.F., Herriman, N., Barnes, R.G. and Plimer, I.R.
1984: Stratiform tourmalinites in metamorphic terranes and their geologic significance; Geology, v. 12, 713-716.

Further contributions to the stratigraphy and structure of the southwest part of the Tavani map area, District of Keewatin, N.W.T.[1]

Steven Ralser[2] and Adrian F. Park[2]

Ralser, S. and Park, A.F. Further contributions to the stratigraphy and structure of the southwest part of the Tavani map area, District of Keewatin, N.W.T.; in Current Research, Part C, Geological Survey of Canada, Paper 90-1C, p. 43-52, 1990.

Abstract

The basement, southwest of Rankin Inlet, is formed by the Archean Kaminak Group, a greenstone supracrustal sequence, overlain by the lower Proterozoic (?) Hurwitz Group. The Kaminak Group is divided into four volcanic and sedimentary formations (Atungag, Akliqnaktuk, Evitaruktuk, and Tagiulik). Mafic and felsic intrusions occur throughout the area. Two regional phases of Archean deformation are recognized. Localized, polyphase deformation occurs along a décollement zone at the base of the Tagiulik formation; this is progressive into D_1. D_1 is characterized by bedding-parallel high strain zones, a regionally pervasive S_1 foliation, and locally, F_1 folds. D_2 is characterized by open to tight folds and steeply dipping shear zones, both trending NE. These shear zones have a complex movement history. Granitoids were emplaced syn-D_1 and post-D_2. Metamorphic grade varies from sub-greenschist to upper amphibolite around granitoid complexes.

Résumé

Le socle du sud-ouest de l'inlet Rankin est constitué du groupe archéen de Kaminak, série supracrustale de roches vertes, recouvert du groupe de Hurwitz du Protérozoïque inférieur (?). Le groupe de Kaminak est réparti en quatre formations volcaniques et sédimentaires (Atungag, Aklignaktuk, Evitaruktuk et Tagiulik). On trouve dans toute la région des intrusions mafiques et felsiques. Deux phases régionales de déformation de l'Archéen sont identifiées. Une déformation polyphasique, d'expression locale, longe une zone de décollement à la base de la formation de Tagiulik; il s'agit d'une déformation progressive qui pénètre D_1 lequel se caractérise par la présence de zones de forte déformation parallèles à la stratification, une foliation S_1 régionalement pénétrative et, par endroits, des plis F_1. D_2 est caractérisé par des plis ouverts à fermés et des zones de cisaillement à fort pendange, tous les deux de direction NE. Ces zones de cisaillement partagent une histoire technique complexe. Les granitoïdes mis en place sont contemporains à D_1 et postérieurs à D_2. Les faciès métamorphiques varient du sous-faciès des schistes verts au sous-faciès supérieur des amphibolites autour des complexes granitoïdes.

[1] Contribution to Canada-Northwest Territories Mineral Development Agreement 1987-1991. Project carried by Geological Survey of Canada, Continental Geoscience Division.

[2] Geology Department, University of New Brunswick, Fredericton, N.B., E3B 5A3

INTRODUCTION

This report describes completion of the bedrock mapping undertaken in the southwest part of the 1: 250 000 Tavani map sheet (NTS 55K/3,4,5,6; Fig. 1; universal mercator grid is used to reference localities) and follows the work described by Park and Ralser (1989). In 1989 field work was concentrated in the south and west of the area.

STRATIGRAPHY

The Kaminak Group is divided (Fig. 2) into the Atungag formation, the Akliqnaktuk formation, the Evitaruktuk formation, and the Tagiulik formation (new names, the first three correspond to the Last Lake formation, and the last corresponds to the Mistake Bay formation of Park and Ralser, 1989). The Kaminak Group is overlain by the Hurwitz Group (Fig. 2), a lower Proterozoic quartz-rich sedimentary sequence described by Bell (1968) and Park & Ralser (1989). The distribution and relationships of the lithological units is shown in Figure 1.

Atungag formation

The Atungag formation consists of one lithofacies: massive mafic metavolcanic rocks, predominantly well-formed pillows and lava tubes, with minor interpillow material. Locally lavas are porphyritic. This formation is the equivalent of the Lower Volcanic unit of Miller (1989).

Akliqnaktuk formation

The Akliqnaktuk formation consists of ten distinct lithofacies (Fig. 3):

a) mafic pillowed flows with carbonate iron-formation
b) cherts and tuffs
c) mafic pillowed flows with breccia
d) granite conglomerate
e) carbonate exhalite
f) quartz arenites and quartz greywackes
g) variolitic mafic volcanic rocks
h) massive mafic volcanic flows with hyaloclastic breccias
i) black slate and green tuff
j) felsic volcanic and epiclastic rocks

The relationships of these lithofacies to each other is illustrated in the interactive stratigraphic column in Figure 3.

Evitaruktuk formation

The Evitaruktuk formation comprises cyclic units, of turbiditic origin, grading from coarse pebble conglomerate, through arenite to shales/slates. At "East lake" (GR815005) shales/slates dominate, with conglomerate present. West of Gill Lake (GR890240) only the arenite to shale portion of the cycle is preserved.

Tagiulik formation

The Tagiulik formation is described in detail in Park and Ralser (1989, p. 4), however it is more deformed and metamorphosed than previously thought (see below). A basal lithofacies is recognized, consisting of pelite-hosted carbonate- and sulphide-iron-formation, with chert, carbonate and breccia/conglomerate. This lithofacies is best developed around Mistake Bay (GR933954), but breccia/conglomerate is also seen at Gill Lake (GR948232). Where this lowermost succession is present, it lies above a major décollement, which obscures temporal relations with other formations. The entire Tagiulik formation is allochthonous.

INTRUSIVE ROCKS

Mafic Intrusive Rocks

Three suites of gabbros and related rocks are recognized; the Kiksautituk and Fat Lake suites are pretectonic and Archean in age. The third suite is (?) Early Proterozoic in age.

a) The Kiksautituk suite, consisting of dolerite and fine to coarse grained gabbros, locally porphyritic, and associated with diorites, tonalites, and trondhjemites. The gabbros are the most widespread of these lithologies; the whole suite is present at the northwestern end of Gill Lake (Kiksautituk). Primary layering is preserved locally (GR902877) in the gabbros.

b) The Fat Lake suite, consisting of porphyritic quartz gabbros and diorites. These are locally megacrystic, with both single and multiple crystal plagioclase megacrysts, up to 40cm in size. Concentrations of megacrysts define layers. The intrusions of the Fat Lake suite are not as widespread as those of the Kiksautituk suite, and are only found south of the Wilson River. At "Fat lake" (GR550875) the Fat Lake diorite contains gold-bearing quartz veins (Miller, 1989); quartz veins were not observed in any other intrusions of the suite.

c) Fine and even grained gabbros, with marginal diabase, occur near the contact of the Kinga and Tavani formations in the lower Proterozoic Hurwitz Group. Within the Tavani map area these are restricted to the Whiterock synform (e.g. GR620872).

Two suites of mafic dykes are recognized:

a) North-south trending diabase, locally porphyritic or plagioclase megacryst-bearing are correlated with the Kaminak swarm (Davidson, 1970).

b) Northwest-southeast trending diabase and gabbro dykes are correlated with the Mackenzie dyke swarm (Heywood, 1973).

Felsic Intrusive Rocks

Felsic intrusive rocks are of two types; granitoids and quartz feldspar porphyries. Major granitoid bodies occur around Gill Lake, Last Lake, and Tavani (Fig. 1); minor bodies occur at "East lake" and north of "Fat lake". They are subdivided, on the basis of their relationship to deformation, into syntectonic and post-tectonic groups (see below).

Quartz-feldspar and feldspar porphyries occur throughout the area, but predominantly in the mafic members of the Akliqnaktuk formation. In the Gill Lake area they occur as sheets two to three metres wide and tens of metres long. They contain large (up to 4 mm) euhedral plagioclase crystals, both euhedral and anhedral (rounded) quartz crystals (up to 5mm) and have a sheared quartz mica matrix. In larger bodies, such as that west of Last Lake (200 x 1500 m, GR525994) deformation is largely restricted to the margins.

Alkalic Intrusive Rocks

Biotite lamprophyre dykes (generally less than 1 m wide) occur throughout the area, trending northwest. Locally they contain abundant xenoliths of granitoid, gneiss, and quartzite. North of Last Lake (GR535992) a more substantial (50m x 10m)intrusive breccia has a complex matrix of micro-lamprophyre, biotite lamprophyre, fine and coarse grained syenite, and possible alkali pegmatite.

In two localities (GR518013 and GR 533011) east trending mafic dykes (up to 5m wide and 400m long) containing abundant xenoliths of anorthosite (up to 15cm across) occur within the Akliqnaktuk formation.

STRUCTURE

Three phases of regional deformation are recognized, in addition to an earlier, localized phase of intense deformation at the base of the Tagiulik formation. To better describe the Archean structures in the southern half of the mapped area, the area has been divided into four domains (Fig.4): Domain A - the central region, either side of the Ferguson River; Domain B - the area surrounding the Tavani Complex; Domain C - northwest of "Fat lake"; Domain D - the outcrop area of the Tagiulik formation. Structures to the north of the Wilson River are described in Park and Ralser (1989).

Domain A

D_1

D_1 structures in this domain are best displayed in the black slate/green tuff lithofacies of the Akliqnaktuk formation (GR650077). D_1 is represented by steeply plunging, stratabound sheath folds in crossbedded tuffs within black slates. Elsewhere in Domain A, D_1 is expressed as northeast trending shear zones, which show repeated movement throughout the Archean deformation history. Locally, in the Ferguson River area (GR735905) changes in facing direction in S_2 indicate the presence of F_1 fold hinges.

D_2

The dominant D_2 feature is a northeast trending synform in the "Fat lake" area (GR595963). This synform is open, upright to inclined (to the southeast) and shallowly plunging (both to NE and SW). In the eastern part of Domain A, D_2 is expressed by renewed movement on the northeast trending shear zones initiated during D_1.

Domain B

Domain B comprises the rocks surrounding the Tavani Complex. The structures in this domain are predominantly shear zones, of roughly similar orientation to the Tavani Complex boundary; i.e. northeast trending in the south, and east trending north of the complex. These shear zones show a long movement history, commencing in D_1 and continuing through D_2. This is indicated by the presence of both prograde and retrograde assemblages in different shear zones and their cross-cutting relationships. Although these shear zones show a steep mineral lineation, suggesting dip-slip movement, they also show features indicating strike-slip movement. The northernmost of these shear zones is the décollement at the base of the Tagiulik formation. All these shear zones appear to have complex movement histories involving reactivation.

Faulting between the décollement at the base of the Tagiulik formation and the Tavani Complex is responsible for the occurrence of a number of enclaves of the basal Akliqnaktuk formation within a section otherwise dominated by the Atungag formation. The same faulting is responsible for the repeated interleaving of tectonic units of greenschist and amphibolite facies assemblages. Some of this faulting is demonstrably extensional in both dip-slip and strike-slip modes.

Closer to the Tavani granite, in the margins of the Tavani Complex, mafic pillow lavas of the Atungag formation, gabbros and quartz-feldspar porphyry minor intrusions are deformed in a broad ductile shear zone. Along the margin of the Tavani granite offshoots of the main granite body and a suite of later mafic dykes occur in this shear zone, producing a mixed, locally stromatic, felsic to amphibolitic gneiss. This is the zone of migmatite identified by Heywood (1973), and although it is in part a deformed marginal agmatite to the Tavani granite, genuine metatexites do not occur. This zone is over a kilometre wide and can be traced for at least 100 km around the margin of the Tavani Complex, and to the south, around the eastern and southern margin of the Wallace River Complex (Eskimo Point Map Sheet, Davidson 1970). Kinematic indicators suggest a complex movement history, with both dip-slip and strike-slip components. A steep mineral lineation is pronounced and ubiquitous, however, other kinematic indicators imply major sinistral strike-slip movements across this zone.

Domain C

Domain C comprises the rocks surrounding the Last Lake Granitoid complex, and rocks to the west. Structurally, a similar situation occurs to that developed around the Tavani Complex (Domain B), although on a smaller scale.

D_1

D_1 is expressed as a strong foliation (S_1) on the exposed northern and southern contacts of the Last Lake complex. North of the contact S_1 is east-west, but swings into a north-south orientation in the west at Helika Lake (GR510145). On the southern margin S_1 is northwest trending away from the immediate contact zone. In the higher grade rocks adjacent to the granite contacts S_1 is defined by biotite and/or hornblende, while in the lower grade rocks it is defined by chlorite.

Pillows in the mafic volcanic rocks become progressively more strained towards the granite contact. This correlates with the increasing intensity of S_1.

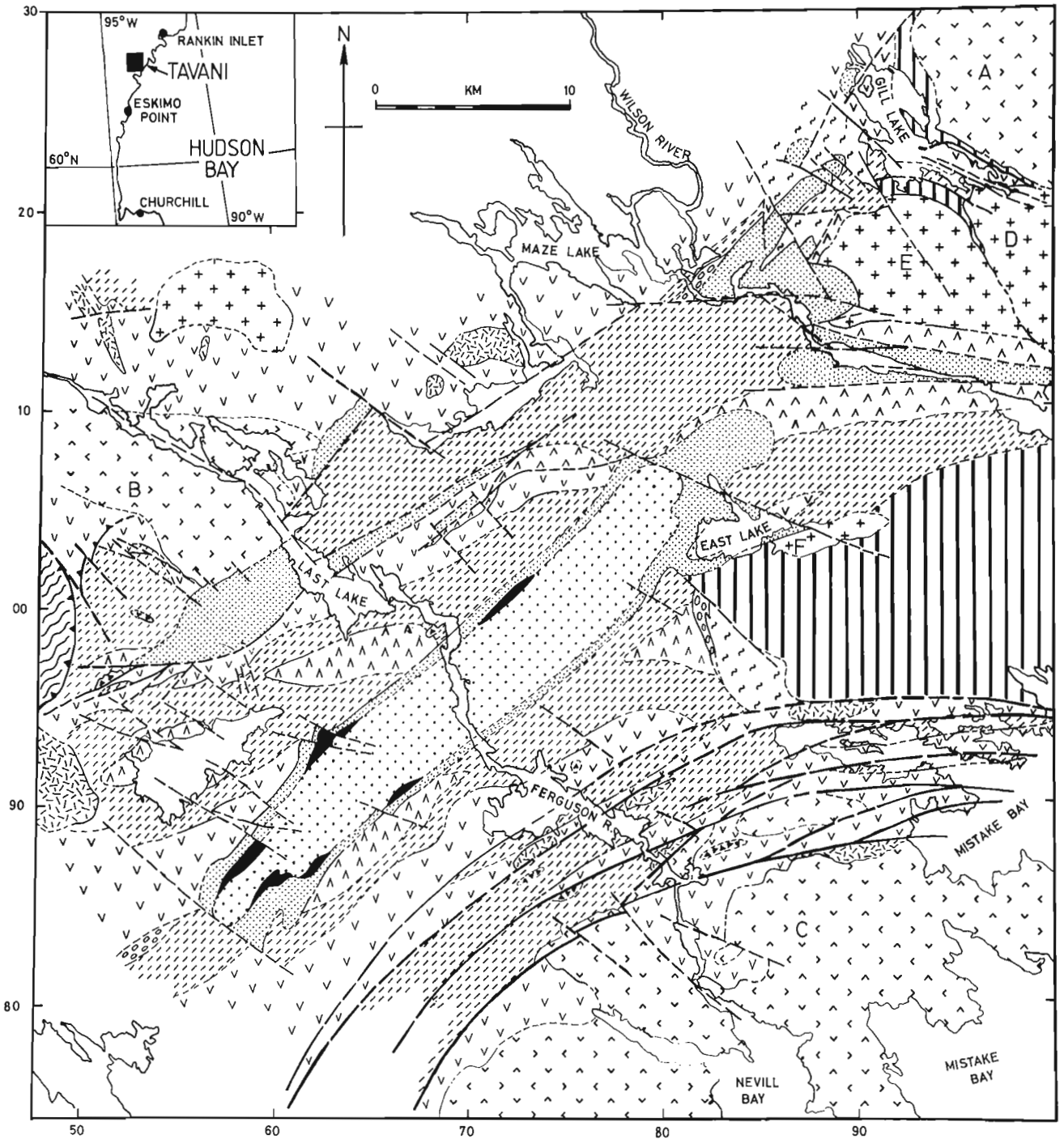

Figure 1. Simplified geology of the southwestern Tavani map area (55K3,4,5,6; modified from Heywood, 1973 and Park & Ralser, 1989).

Repetitions of the Atungag formation-Akliqnaktuk formation boundary (south of the Last Lake Granite complex), where S_0 and S_1 are parallel, suggest the presence of D_1 thrusts.

D_2

D_2 consists of northeast trending shear zones, generally dipping towards the northwest. A strong down-dip mineral lineation is associated with these shear zones.

A migmatite in the west of the area (GR490000) was thrust in from the west during D_2. In the mafic volcanic rocks immediately below the migmatite an L-tectonite, defined by hornblende growth, is developed. All the components of the migmatite were deformed during D_2 thrusting.

The folding of S_1 east of Helika Lake (GR510145) was a response to the D_2 deformation. At least one F_2 closure can be demonstrated.

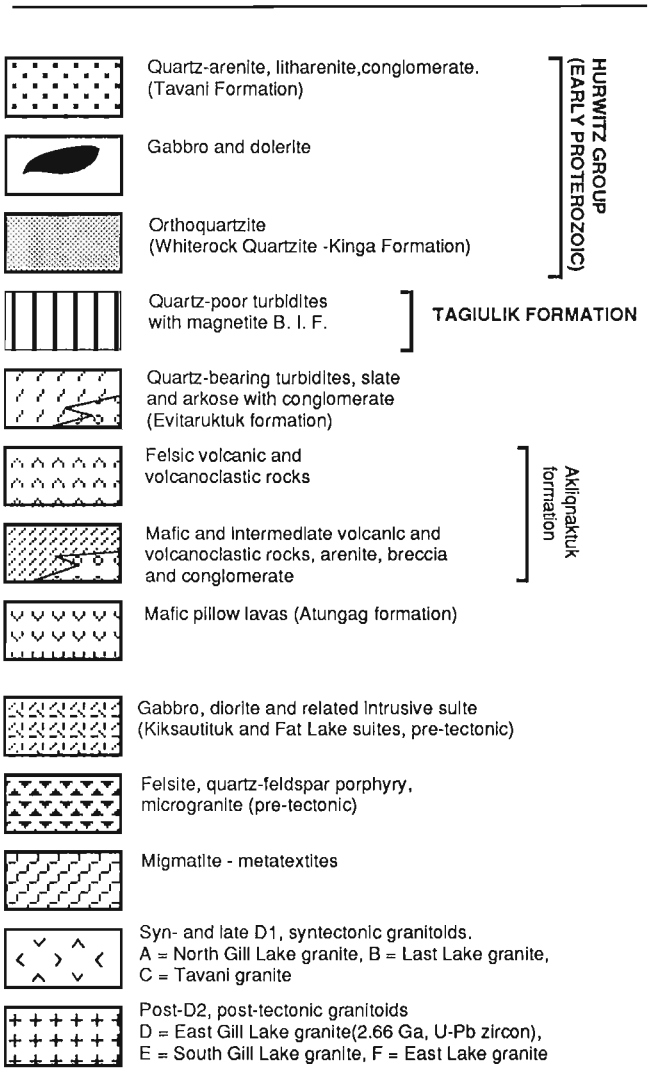

Domain D

Sediments of the Tagiulik formation show the most complex structures within the area (fig. 5).

Pre-D_1

Near the base of the Tagiulik Group (GR933954) small-scale (up to 20cm), steeply plunging, sheath folds are developed. Refolding relationships involving at least two generations of interfering sheath folds are apparent. These folds are all cut obliquely by the S_1 and S_2 cleavages. All the lithologies involved in this zone of progressive, intense deformation are basal Tagiulik formation sediments. The underlying rocks of the Akliqnaktuk and Atungag formations are not infolded, but are separated from the Tagiulik formation by a narrow, discrete shear zone. The interpretation offered here is that the sheath folds developed above and immediately adjacent to a décollement coincident with the stratigraphic base of the Tagiulik formation. This décollement is a very early feature (pre-F_1).

D_1

F_1 fold hinges are generally inferred from changes in facing direction in S_2. Near the base of the Tagiulik formation (GR933954) tight (wavelength of 40cm, amplitude of 10m) isoclinal F_1 folds are observed. The folds become more open and inclined farther from the base of the succession. F_1 fold hinges are also observed locally in some banded iron-formations (GR935983), and are tight or isoclinal. F_1 in this domain is generally east-west trending and shallowly plunging. S_1 cleavage is only observed locally in some fold

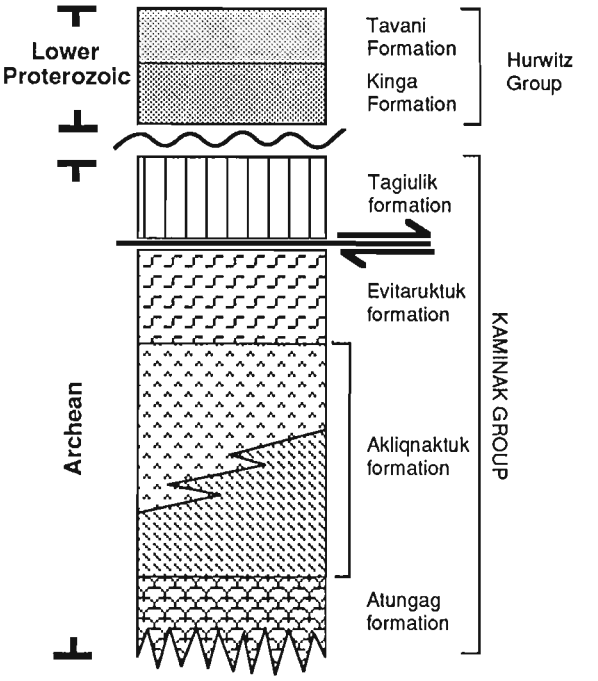

Figure 2. Stratigraphic column for Kaminak Group and Hurwitz Group.

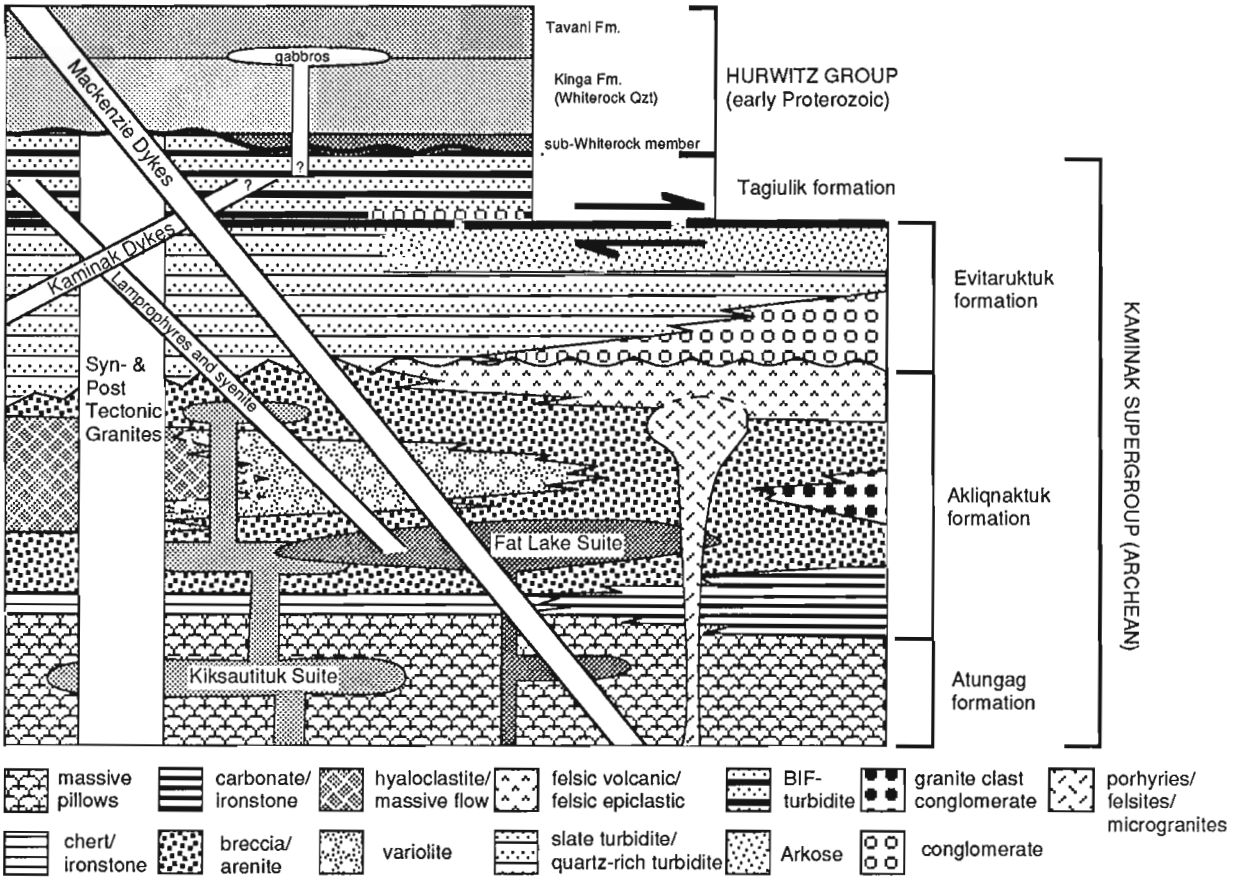

Figure 3. Interactive stratigraphic column for the southwestern Tavani map area.

hinges. D_1 deformation in the Tagiulik formation is similar to the D_1 deformation described in the Evitaruktuk formation west of Gill Lake (Park and Ralser, 1989).

The pre-D_1 and D_1 deformations are part of the same progressive deformational event related to the translation of the allochthon in which these metasediments are contained.

D_2

D_2, in the Tagiulik formation, is expressed as open to tight, generally northeast trending folds with an axial planar cleavage, S_2. The D_2 deformation becomes more intense towards the east (GR960001), with tighter F_2 folds and a more intense development of S_2. In the aureole of the East Lake Granite (GR815005), the S_2 cleavage is baked out of the rocks.

D_3

The final deformation phase, D_3, consists of the folds and fabrics found in the Hurwitz Group sediments, and related structures in the underlying Kaminak Group. These are described in Park and Ralser (1989).

METAMORPHISM

Regional Metamorphism

The regional metamorphism is best described in terms of the four structural domains.

Domain A

Sub-greenschist facies rocks occur in the northeastern part of Domain A (Fig.4, GR720090) with assemblages of vesuvianite-albite-stilpnomelane-zeolite. The remainder of this domain is metamorphosed under low to middle greenschist facies conditions, dominated by chlorite and/or epidote assemblages. On the Wilson River a quartz-talc-calcite-tremolite-magnesite assemblage, from which diopside is conspicuously absent, is present, indicating higher temperature greenschist facies conditions than are general in this domain.

Metamorphic grade increases to the north, south and west. In the Gill Lake area, to the north, metamorphism occurred under middle to upper greenschist facies conditions. Green amphibole (actinolitic) appears with chlorite in pillow lavas at the west end of this lake, and clinozoisite is a common component in the same assemblage elsewhere in this area. In pelitic and semipelitic rocks chlorite is accompanied by white mica (?muscovite) and epidote.

Relicts of higher grade assemblages are found in the shear zones around Gill Lake, usually in chlorite phyllonite derived from metagabbro or metadolerite. Such relicts (porphyroclasts) include ophitic-textured augite-plagioclase relicts, partly overgrown by hornblende-plagioclase, or by hornblende-zoisite assemblages. Actinolitic amphibole-clinozoisite-chlorite assemblages overgrow these amphibolite facies relicts, and are in turn replaced by chlorite or chlorite-epidote felts.

Domain B

Metamorphic grade increases towards the Tavani Complex, in Domain B. A rapid gradation is seen in mafic volcanic rocks, from epidote-chlorite assemblages, through actinolite and biotite, to hornblende-bearing amphibolites. Steps in this gradation coincide with tectonic breaks, and lower and higher grade enclaves survive within shear zones. At the highest grades close to the Tavani granite, migmatites are developed on a small scale, involving the development of leucogranite neosomes in amphibolite. From north to south across Mistake Bay (GR930920) the increase in grade from greenschist to hornblende-bearing amphibolite takes place in less than one kilometre. Lower grade enclaves are present in this section. This is accommodated, in part, by normal faults with a low angle to both bedding or layering, and, in part, the D_2 shear zones.

Domain C

In Domain C, to the west metamorphic grade increases through upper greenschist (chlorite-green amphibole) to a narrow zone (less than 100m) of upper amphibolite facies metamorphism (biotite-black amphibole). Structurally

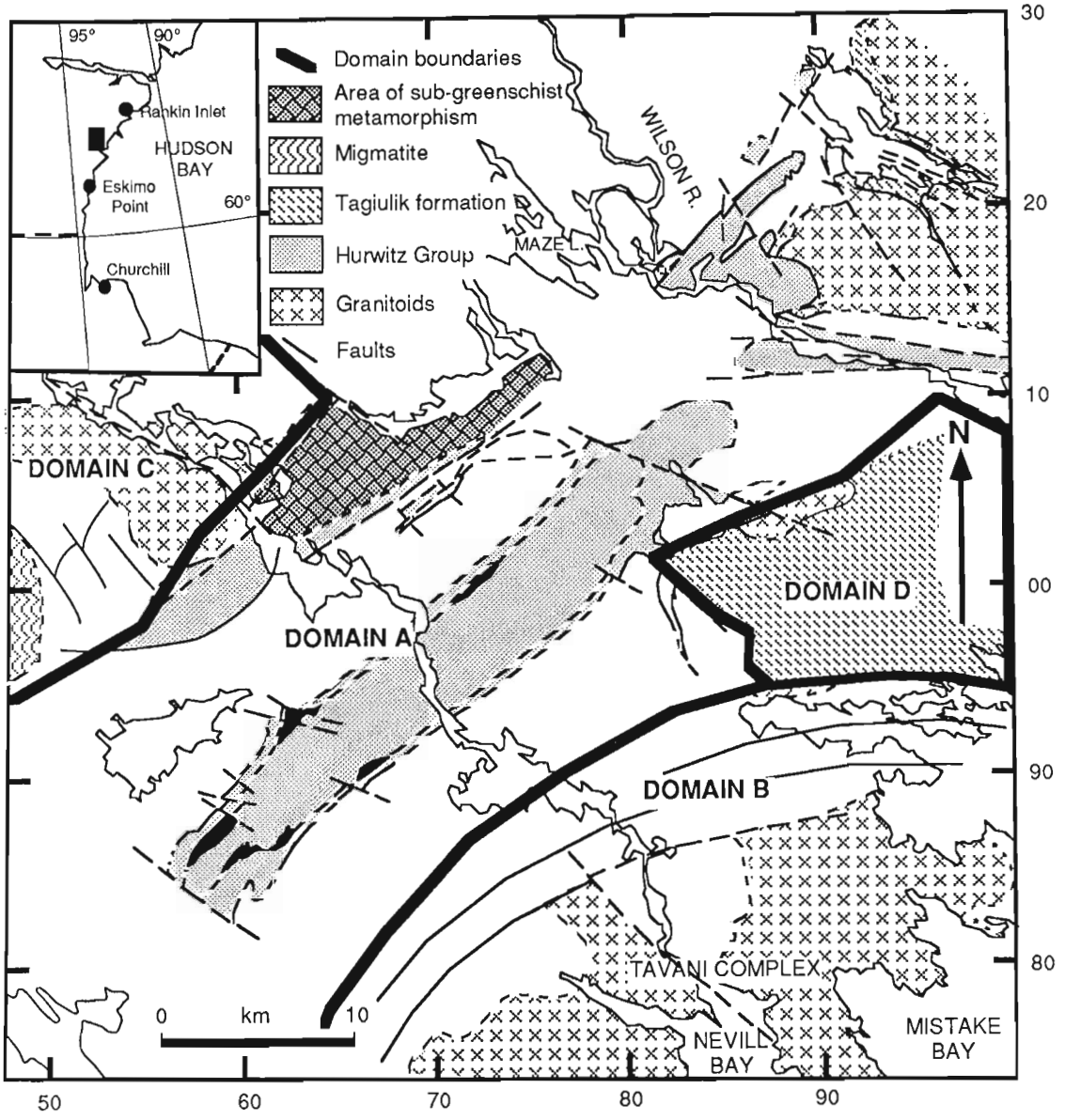

Figure 4. Simplified geological map of the southwestern part of the Tavani map area showing structural domains and areas of sub-greenschist metamorphism.

overlying the volcanic rocks is a migmatite. Metatexites, derived from *in situ* partial melting are well exposed in a number of localities (GR501005). Neosomes are composed of plagioclase-quartz-amphibole. Elsewhere in this body the lichen cover only permits recognition of granites or gabbros. This migmatite body was thrust in from the west, and is allochthonous on the underlying Atungag and Akliqnaktuk formations.

Domain D

The Tagiulik formation sediments, comprising Domain D, are metamorphosed in low to middle greenschist facies.

Contact metamorphism

Hornfels is developed in greywackes around most of the granite plutons in the area. In the turbidites of the Tagiulik formation, around the East Lake Granite, contact metamorphism has "baked out" all signs of earlier cleavage by the recrystallization of fine grained chlorite, leaving apparently pristine rocks. Scattered epidote clots are the only sign of metamorphism. This epidote growth becomes more prominent towards the granite. Approximately 500 m from the granite contact, diffuse, multigrain clots of epidote occur in a matrix that retains clastic textures. More coherent porphyroblasts occur nearer the contact, commonly taking the form of pure epidote pods (up to 2 cm diameter). Through the same zone carbonate-bearing magnetite-chert layers in the sequence are progressively replaced by epidote. In layers of particular composition replacement by epidote is total.

Turbidites of the Tagiulik formation around the south Gill Lake granite are more quartzo-feldspathic than those between "East lake" and Mistake Bay. The ironstone components show the same changes seen at "East lake", but the pelites and semipelites record the appearance of muscovite and epidote-actinolite some 200 m from the contact, clinozoisite and zoisite around 50 m, and microcline in the last 10 m of the contact zone. Epidote clots, like those at "East lake" are also present. Widths of mineral zones here are difficult to determine because the aureole is bounded, and modified, by later faults.

Sequential vein-fills are found both within the south Gill Lake granite and its envelope; earlier veins are deformed and cross-cut by later veins. The early fills include cummingtonite-tremolite-carbonate, followed by tremolite-zoisite and tremolite-clinozoisite. The latest vein-fills are epidote-chlorite-carbonate and epidote-chlorite-quartz. These veins are the products of hydrothermal activity during cooling of the south Gill Lake pluton.

Contact metamorphic effects are less obviously zoned around the other granitoids, but they include the development of biotite-sillimanite in the contact zone, and in xenoliths within, the north Gill Lake pluton.

Timing of Granite Emplacement During Deformation

The relationships to deformation of the Gill Lake granites and the East Lake granite are discussed in Park and Ralser (1989). Two groups of plutons are recognized. A syntectonic group, emplaced before D_2, includes the north Gill Lake, Tavani and Last Lake plutons. A post-tectonic group,

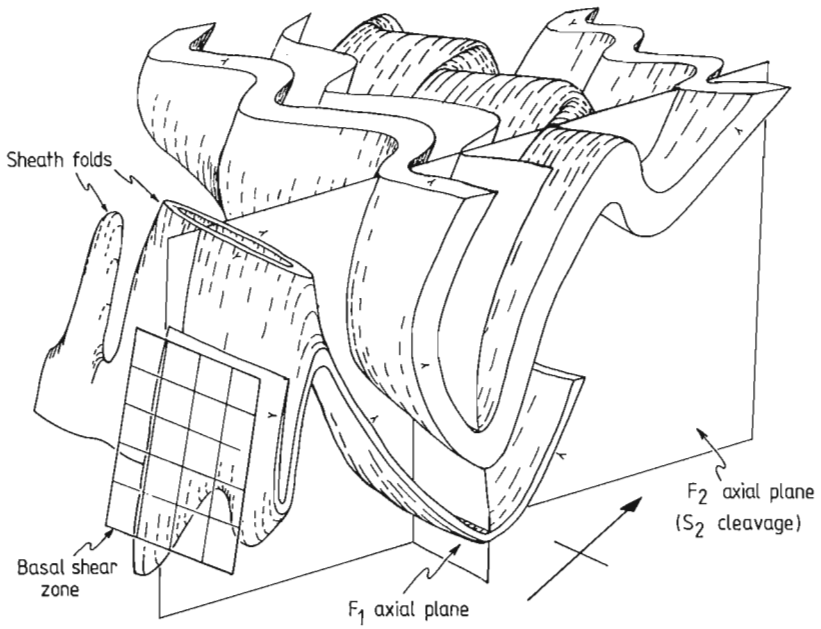

Figure 5. Schematic block diagram showing the structures developed near the base of the Tagiulik formation (Domain D).

emplaced late in, or after D_2 deformation, includes the east Gill Lake, south Gill Lake and East Lake plutons, and several other small stocks. A date of 2.66 Ga (U-Pb zircon; J.C. Roddick, pers. comm.) for the east Gill Lake granite constrains the minimum age for D_2.

In detail, the shape of the Tavani Complex is a D_2 structure. Apophyses of the granite are deformed in D_2 shear zones, but the relationship to D_1 is ambiguous. South of the Last Lake granite apophyses are discordant to the S_1 foliation. These apophyses are deformed in narrow shear zones parallel to S_1, which are subsequently cut by D_2 shear zones. North of the Last Lake granite, apophyses of granite are concordant with the strong S_1 foliation. These apophyses are only weakly foliated, whereas at the southern contact deformed granite may be mylonitic.

MINERALIZATION

Mineral deposits, and suitable hosts show both stratigraphic and tectonic controls. Chert-exhalite horizons are components of discrete lithofacies within the Evitaruktuk and Atungag formations, as are carbonate iron-formation and sulphidic pelites. Magnetite-chert and magnetite-pelite banded iron-formation are an important component of the Tagiulik formation. Carbonate and sulphide ironstones are restricted to the basal sequence of the Tagiulik formation. Quartz-carbonate veins, including sulphides (galena and several copper minerals), formed as a consequence of the hydrothermal cooling of post-D_2 granitoids. Elsewhere, quartz veining, including the gold-bearing veins at Fat lake, reflect competence contrasts between metagabbro bodies and their hosts during D_1 and D_2. A distinctive zone of diffuse to massive sulphide mineralization, hosted by amphibolite, is coincident with the major ductile shear zone forming the northern and western boundary to the Tavani Complex.

DISCUSSION AND CONCLUSIONS

1. The Kaminak Group is subdivided into four formations; a lowermost Atungag formation, dominated by pillow basalts; a middle Akliqnaktuk formation, dominated by volcanic rocks, epiclastic and pelagic sediments, with felsic volcanic rocks and epiclastites predominant at the top and mafic to intermediate material dominating the lower parts; and an uppermost Evitaruktuk formation, consisting largely of quartz-bearing turbidites with shaly and conglomeratic facies. The Tagiulik formation is allochthonous, lying above these three formations. The belt of mafic volcanic rocks between Last Lake and the Wilson River, formerly ascribed to the Happoytiyik Member (Hurwitz Group; Heywood, 1973), is now recognized as a distinctive lithofacies in the Akliqnaktuk formation.

2. The Tagiulik formation is completely allochthonous, contained within a nappe. Its depositional and chronological relationship to the other formations in the Kaminak Group is unknown.

3. Structure is dominated by open, upright F_2 folds and D_2 shear zones. D_1 features, including cleavage and minor fold developments, do not produce any major changes of younging or facing, indicating that the lack of large scale F_1 folds through most of the area is real, rather than being due to paucity of critical outcrop. Only in the relatively well-bedded Tagiulik and Evitaruktuk formations is a well-developed interference pattern between F_1 and F_2 folds apparent.

4. Metamorphism can be related to structure in that the various structural domains in the area coincide with metamorphic domains. Overall, greenschist facies or locally lower grade assemblages dominate; high grade rock, including amphibolites and migmatites, appears to the north, west and southeast. Shear zones contain both prograde and retrograde mineral assemblages. Metamorphic aureoles surround some of the late tectonic granitoids.

5. Structure, granite emplacement and metamorphism can be related closely in the Tavani Complex, a dome structure in which granite with marginal migmatite is mantled by amphibolite. The dome is circumscribed by high and low angle shear zones, across which there are rapid changes in metamorphic grade. Normal faults at low angle to the shear zones are widespread, producing many features consistent with its interpretation as a "metamorphic core complex" emplaced during D_2 deformation.

6. Three groups of syngenetic intrusions are recognized. The Kiksautituk suite of gabbro, diorite, granodiorite,tonalite and trondhjemite may be in part, co-genetic with the mafic volcanic rocks of the Atungag formation. The Fat Lake suite of porphyritic gabbro and diorite cross cuts the Kiksautituk suite; and a suite of felsites, quartz-feldspar porphyries and microgranites may be subvolcanic and related to the uppermost felsic component of the Akliqnaktuk formation.

7. Two phases of granitoid emplacement are recognised, syn-D_1 and post-D_2; both are Archean.

ACKNOWLEDGMENTS

We thank Subhas Tella of the Geological Survey of Canada and Paul Williams of the Department of Geology, University of New Brunswick for organizing the project and for their contribution to the mapping and interpretation through much useful discussion, and our field assistants Bob McNaughton, Rob Harriott and Jean-Luc Roy for their contributions. We also wish to thank the following: A. R. Miller, T. LeCheminant, and T. Frisch for much useful discussion; Sam Tatanuak for the expediting and radio schedules; our invaluable helicopter crew, Greg Bailey, Jim Prior, and Joe Nicholls; and Tongola Sandy, of Tungavik Federation of Nunavut for finding the Inuktitut place names. This study was carried out under contract no. 23233-9-0023/01-SZ.

REFERENCES

Bell, R.T.
1968: Preliminary notes on the Proterozoic Hurwitz Group, Tavani (55K) and Kaminak Lake (55L) areas, District of Keewatin; Geological Survey of Canada, Paper 68-36.

Davidson, A.
1970: Eskimo Point and Dawson Inlet map-areas (north halves) District of Keewatin 55E and 55F (north parts); Geological Survey of Canada, Paper 70-27.

Heywood, W.W.
1973: Geology of Tavani map-area, District of Keewatin; Geological Survey of Canada, Paper 72-47.

Miller, A.R.
1989: Highlights of gold studies in the Churchill Structural Province, Kaminak Greenstone Belt and Hurwitz Group, District of Keewatin, NWT; *in* Current Research, Part C, Geological Survey of Canada Paper 89-1C, p.127-134.

Park, A.F. and Ralser, S.
1989: Precambrian stratigraphy and structure of the southwest part of the Tavani map area, District of Keewatin, N.W.T.; *in* Current Research, Part C, Geological Survey of Canada Paper 89-1C, p.1-10.

Low- to medium-grade metamorphism of metabasites at Schist Lake, near Flin Flon, Manitoba

Scott Digel[1] and T.M. Gordon[1]

Digel, S. and Gordon, T.M. Low- to medium-grade metamorphism of metabasites at Schist Lake, near Flin Flon, Manitoba; in Current Research, Part C, Geological Survey of Canada, Paper 90-1C, p. 53-57, 1990.

Abstract

A prograde regional metamorphic sequence from prehnite-pumpellyite to lower amphibolite facies exists in basaltic metavolcanic rocks of the Early Proterozoic Amisk Group near Schist Lake. The lowest grade rocks are in the southeast part of the map area and contain prehnite and/or pumpellyite. To the northwest, prehnite and pumpellyite disappear, defining the boundary into the greenschist facies. In the northwest, mesoscopic actinolite and hornblende (?) appear at the expense of chlorite and epidote, suggesting the transition into the lower amphibolite facies. Preliminary kinematic studies of postmetamorphic block-bounding faults yield results consistent with the juxtaposition of differing metamorphic grade across some of the faults.

Résumé

Une séquence métarmorphique régionale prograde, du faciès à préhnite-pumpellyite au niveau inférieur du faciès des amphibolites, se trouve dans les roches volcaniques métamorphisées basaltiques du groupe d'Amisk du Protéozoïque inférieur près du lac Schist. Les roches à faible degré de métamorphisme se trouvent dans le sud-est de la zone illustrée par la carte et contiennent de la préhnite ou de la pumpellyite ou les deux. Vers le nord-ouest, la préhnite et la pumpellyite disparaissent, marquant la limite précédant le faciès des schistes verts. Dans le nord-ouest, l'actinolite et l'hornblende ? mésoscopiques prennent le pas sur la chlorite et l'épidote, indiquant la transition vers le niveau inférieur du faciès des amphibolites. Des études cinématiques préliminaires de failles post-métamorphiques en bordure de blocs ont donné des résultats compatibles avec la juxtaposition de différents degrés de métamorphisme à travers certaines failles.

[1] Department of Geology and Geophysics, University of Calgary, Calgary, Alberta, T2N 1N4.

INTRODUCTION

The Schist Lake area lies within the Flin Flon volcanic belt of the Churchill Province in northwestern Manitoba at approximately 54°45' N latitude and 101°45' W longitude. Prehnite and pumpellyite were first recognized in this area during 1:15 840 scale mapping by Bailes and Syme (1987) who mapped an isograd marking the disappearance of these two minerals in basaltic metavolcanics. The disappearance of both prehnite and pumpellyite and appearance of the assemblage actinolite-chlorite-epidote are considered to mark the boundary between the prehnite-pumpellyite and greenschist facies (Liou et al., 1985). The summer of 1989 was the first year of field work designed to investigate the nature of this isograd and to study the metavolcanics to the northwest, through increasing metamorphic grade, into the high grade Kisseynew Gneisses.

Preliminary investigations indicate that assemblages (see Table 1 for mineral abbreviations) diagnostic of three metamorphic facies (in metabasites) occur within the metamorphic sequence in the Schist Lake area. In order of increasing grade, the facies (and assemblages) are:

1) Prehnite-Pumpellyite (Prh-Pmp-Chl-Ep-Ab)
2) Greenschist (Act-Chl-Ep-Ab)
3) Greenschist-Amphibolite transition (Act-Hbl?-Pl)

These rocks provide a unique opportunity to study the metamorphism of basaltic rocks from low- to medium-metamorphic grade.

STRATIGRAPHY AND STRUCTURE

The oldest rocks in the area are volcanics of the 1886 Ma (Syme et al., 1987) Amisk Group which are unconformably overlain by sediments of the 1832 Ma (Gordon et al., in press) Missi Group. These rocks have in turn been intruded by plutons of varying ages. The timing of peak metamorphism has been estimated by Gordon et al. (in press) at approximately 1815 Ma.

Metavolcanics are restricted to the Amisk Group which outcrops extensively over the Schist Lake area. Minerals diagnostic of all three metamorphic zones are consistently best developed in rocks with abundant amygdules. The amygdaloidal units are pillowed flows (pillows) and mafic breccias composed of scoria and pillow fragments (scoria breccia). Diagnostic minerals are absent or rare in non-amygdaloidal tuffs, pillows, and synvolcanic dykes/sills.

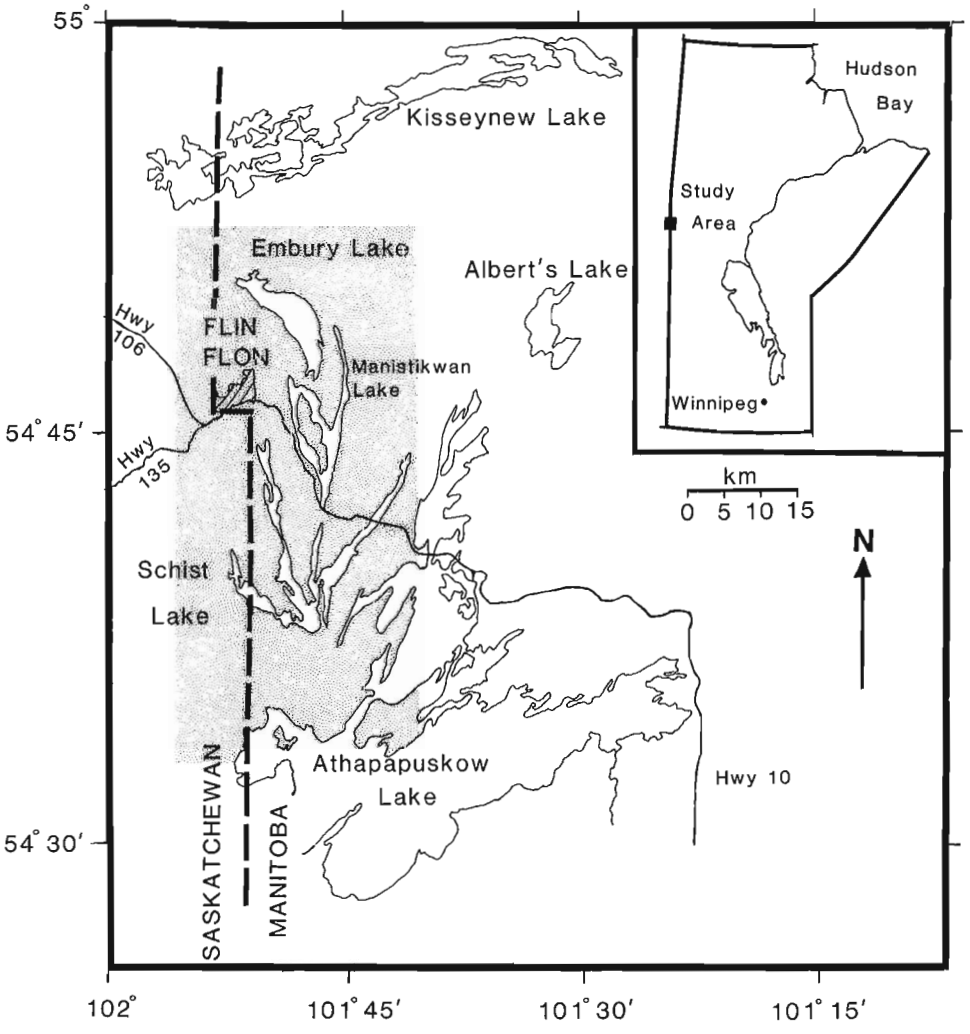

Figure 1. Location map of the Schist Lake area (stippled region).

Bailes and Syme (1987, 1989) and Syme (1986, 1987, 1988) described the local stratigraphy and structure in detail. They have subdivided the Flin Flon area into several blocks separated by block-bounding faults. Figure 2 has been modified from their work and shows the blocks pertinent to this study. Although the stratigraphy is consistent and well-defined within each block, specific stratigraphic units cannot be correlated across the block-bounding faults. The block-bounding faults juxtapose rocks of differing metamorphic grade (Fig. 2) and fault-related foliations overprint the metamorphic fabric, hence the faults must postdate the peak of metamorphism.

An effort is being made to determine the kinematics of the block-bounding faults in order to integrate the structural and metamorphic history. The Inlet Arm fault separates the subgreenschist Hook Lake and greenschist Bear Lake blocks (Fig. 2). Preliminary observations of kinematic indicators suggest that movement on the fault was oblique sinistral, consistent with the juxtaposition of low-grade on the west against higher-grade on the east. Further work on the other faults is planned for 1990.

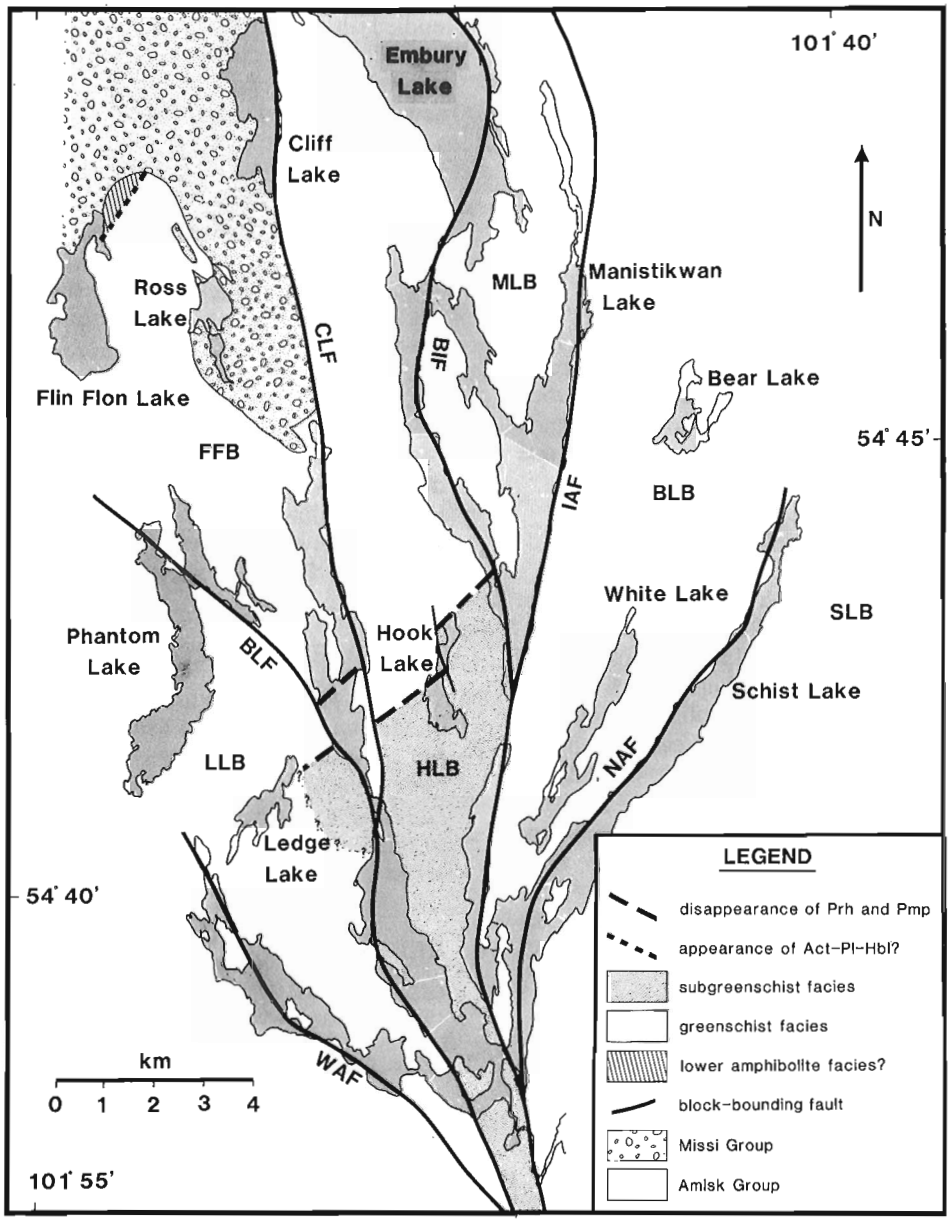

Figure 2. Simplified geological map of the Schist Lake area.
FFB- Flin Flon Block
LLB- Ledge Lake Block
HLBHook Lake Block
BLB- Bear Lake Block
SLB- Scotty Lake Block
MLB- Manistikwan Lake Block
IAF- Inlet Arm Fault
CLF- Cliff Lake Fault
BLF- Burley Lake Fault
WAF- West Arm Fault
NAF- Northeast Arm Fault
BIF- Big Island Fault

METAMORPHISM

The most complete metamorphic sequence is preserved in the Hook Lake (HL), Flin Flon (FF), and Ledge Lake (LL) blocks (Fig. 2). Subgreenschist minerals are found only within these three blocks, which are relatively free of large intrusions. The surrounding blocks are greenschist facies and show evidence of contact metamorphism produced by the intrusion of numerous plutons. Mineral assemblages and textures in pillow and scoria breccia units are compared from lowest to highest grade.

Prehnite-pumpellyite zone

Prehnite and pumpellyite are restricted to the southern portions of the Hook Lake, Flin Flon, and Ledge Lake blocks (Fig. 2) where they are most abundant in pillows and scoria breccia. Pillows typically have dark green pumpellyite-rich interiors with 2-15 mm quartz-prehnite amygdules and an outer 10-15 cm buff-brown margin with amygdules of prehnite, pumpellyite, quartz, and calcite. Two types of lapilli to block-size clasts are common in the scoria breccia unit. Type 1 clasts are buff-brown and contain 1-5 mm amygdules of pumpellyite, prehnite, and quartz. Type 2 clasts are similar to the pillows, interiors are dark green and pumpellyite-rich with prehnite amygdules, whereas 1-3 cm thick buff-brown outer rinds have pumpellyite amygdules. Both rock units are commonly cut by 5-50 cm wide, randomly oriented veins containing any or all of quartz, calcite, prehnite and epidote.

Greenschist Zone

Pillows and scoria breccia in the greenschist zone retain the mineralogical and colour zoning of their lower-grade counterparts although the minerals involved are diagnostic of the greenschist facies. Pillow interiors are up to 90 % epidote and are lighter green and harder than subgreenschist pillows. Amygdules contain quartz, epidote, calcite and rare actinolite. Pillow margins are composed of Ep-Chl-Ab-Qtz (Table 1) and have amygdules of these minerals. It is usually more difficult to distinguish Type 1 and 2 clasts in the scoria breccia at this grade. The fragments are usually buff-coloured with amygdules of quartz, epidote, chlorite, calcite, and occasional actinolite. Veins cutting these units contain any or all of epidote, quartz, and calcite (never prehnite or pumpellyite).

Table 1. List of mineral abbreviations (from Kretz, 1983).

Ab: Albite	Hbl: Hornblende
Act: Actinolite	Prh: Prehnite
Cal: Calcite	Pmp: Pumpellyite
Chl: Chlorite	Qtz: Quartz
Ep: Epidote/Zoisite	

Greenschist-Amphibolite Transition

A distinct change in the mineralogy and texture of pillows was mapped about 2 km northwest of Ross Lake (Fig. 2). Below the transition, the pillows contain abundant epidote and chlorite with mineralogical and colour zoning typical of greenschist facies pillows. Actinolite is difficult to see in hand specimen in these rocks. In the transition rocks (diagonally ruled zone on Figure 2), the amount of epidote and chlorite in the volcanics decreases drastically, accompanied by a corresponding increase in the amount and size of actinolite. The actinolite occurs as 1 to 4 mm needles and the rocks are much harder and darker in colour. Plagioclase is much more abundant in the transition rocks than the greenschist pillows. The change from greenschist to transition pillows is abrupt, occurring over less than 20 m. Definite amphibolite facies rocks were not identified in the area studied this summer. Amphibolite facies volcanics are located in the north and northwest parts of the study area (K. Ashton, pers. comm. 1989), 8 to 10 km south of Kisseynew Lake (Fig. 1) and will be examined in 1990.

CONCLUSIONS

Metavolcanics of the Early Proterozoic Amisk Group outcrop widely in the Schist Lake area. Mineral assemblages of metamorphic facies ranging from prehnite-pumpellyite in the southeast to lower amphibolite facies (Act-Hbl?-Pl) in the northwest are present in these rocks, providing a unique opportunity to study low- to medium-grade regional metamorphism of basaltic rocks.

Postmetamorphic faults juxtapose terranes (blocks) of different metamorphic grade. Kinematic studies of the block-bounding faults will be integrated with metamorphic studies in an effort to better understand the evolution of this part of the Flin Flon volcanic belt.

ACKNOWLEDGMENTS

The authors would like to thank E.C. Syme and A.H. Bailes of Manitoba Energy and Mines and E. Froese of the GSC for some useful discussions and for taking time out from their own summers to lead field trips in the area. Brad Cole and Lisa Kotowski provided good assistance and company in the field. E. Froese read an earlier draft of the manuscript.

REFERENCES

Bailes, A.H. and Syme, E.C.
1987: Geology of the Flin Flon-White Lake area; Manitoba Energy and Mines, Map GR87-1-1
1989: Geology of the Flin Flon-White Lake area; Manitoba Energy and Mines, Geological report, GR87-1.

Gordon, T.M., Hunt, P.A., Loveridge, W.D., Bailes, A.H., and Syme, E.C.
— U-Pb zircon ages from the Flin Flon and Kisseynew Belts, Manitoba: Chronology of crust formation at an Early Proterozoic accretionary margin; *in* The Early Proterozoic Trans-Hudson Orogen: Lithotectonic correlations and evolution; Geological Association of Canada, Special Paper, (*in press*)

Kretz, R.
1983: Symbols for rock-froming minerals; American Mineralogist, v. 68 , p 277-279

Liou, J.G., Maruyama, S., and Cho, M.
1985: Phase equilibria and mineral parageneses of metabasites in low-grade metamorphism; Mineralogical Magazine, v. 49, p. 321-333

Syme, E.C.
1986: Schist Lake area (Athapapaskow Lake Project); *in* Manitoba Energy and Mines, Report of Field Activities 1986, p. 30-39.
1987: Athapapaskow Lake Project; *in* Manitoba Energy and Mines, Report of Field Activities 1987, p. 30-39.
1988: Athapapaskow Lake Project; *in* Manitoba Energy and Mines, Report of Field Activities 1987, p. 20-34.

Syme, E.C., Bailes, A.H., Gordon, T.M., and Hunt, P.H.
1987: U-Pb zircon geochronology in the Flin Flon belt: Age of Amisk volcanism; *in* Manitoba Energy and Mines, Report of Field Activities 1987, p. 105-107

Archean granulites in the Lac à l'Eau Claire area, north Bienville Subprovince, Superior Province, Quebec

A. Ciesielski and L. Plante[1]
Continental Geoscience Division

Ciesielski, A. and Plante, L.; Archean granulites in the Lac à l'Eau Claire area, north Bienville Subprovince, Superior Province, Quebec; in Current Research, Part C, Geological Survey of Canada, Paper 90-1C, p. 59-67, 1990.

Abstract

The Lac à l'Eau Claire area, New Quebec, is dominated by the Bienville orthogneiss of granodioritic and granitic composition in which granulites, metabasic and metasedimentary rocks are minor phases. The granulite inclusions contain two pyroxenes, biotite-quartz symplectite, oligoclase, K-feldspar, magnetite and amphibole. The granulites were analyzed and compared to the Bienville orthogneiss. They are low in silica and potassium and high in iron and calcium and are considered to be restites or an intermediate product of the differentiation that gave rise to the Bienville orthogneiss.

Résumé

La région du lac à l'Eau Claire au Nouveau-Québec, est dominée par les orthogneiss de la sous-province de Bienville de composition granodioritique et granitique dans lesquels on retrouve des granulites, des métabasites et des roches métasédimentaires. Les granulites se composent de deux pyroxènes, de symplectites à biotite et quartz, d'oligoclase, de feldspath potassique, de magnétite et d'amphiboles. Les granulites ont été analysées et comparées avec les orthogneiss de Bienville. Elles sont pauvres en silice et en potassium et riche en fer et en calcium; on les considèrent comme des restites ou des produits de différenciation donnant naissance aux orthogneiss de Bienville.

[1] Geola Ltée, Val d'Or, Québec J9P 4P4

INTRODUCTION

Lac à l'Eau Claire, formerly Clearwater Lake, is located 1100 km north of Quebec City and is accessible from Kuujjuarapik (formerly Poste-de-la-Baleine and Great Whale) 220 km to the southwest, on the Nastapoka Arc of Hudson Bay (Fig. 1). The Lac à l'Eau Claire area (LEC) is dominated by the Bienville orthogneiss which contains large inclusions of granulite. A description of the different units in the LEC area is presented here along with chemical analyses (major, trace and rare earth elements) of the granulites which are compared with the Bienville orthogneiss. Preliminary examination indicates a chemical contrast between rock units.

Previous geological work in the area focussed on the meteoritic origin of the lake; it included drilling in the double crater of LEC by Earth Physics Branch (Dence, 1964, 1981), followed by geological studies of the west crater by Bostock (1969) and detailed study of the impact breccias and petrographic studies of the impactites (Phinney et al., 1978, Simonds et al., 1978). Regional and detailed geological studies were performed by Eade (1966), Stevenson (1968), Ciesielski (1983, 1984) and metamorphic and regional synthesis by Herd (1978) and Card and Ciesielski (1986).

Although previously included in the Minto Subprovince of the Superior Province (Ciesielski, 1983; Card and Ciesielski, 1986), characterized by large areas of opx-bearing rocks, LEC area is currently assigned to the northern part of the Bienville Subprovince given (1) the dominance of Bienville orthogneisses at amphibolite grade, (2) the relatively small proportion of granulite inclusions found in the LEC area (Fig. 2); small granulite grade meta-igneous inclusions are scattered elsewhere in the Bienville subprovince orthogneiss (Eade, 1966)), and (3) new geological mapping (by A.C. and L.P.). The boundary between Minto and Bienville subprovinces has been moved north of the LEC area, following a set of west-trending magnetic contrasts and an anomaly caused by a thin and elongated iron-formation northwest of LEC as outlined in Plante (1986) and Ciesielski (1989a) (Fig. 1).

The Bienville orthogneiss yields Archean ages; rocks from the southwest Bienville subprovince gives an imprecise discordia U-Pb (zircon) age of 2797 to 2819 Ma (Mortensen and Ciesielski, 1987) and orthogneiss around LEC yields a Rb-Sr age of 2562 +/-121 Ma. A Pennsylvanian age for the crater formation is indicated by an age of 287 +/-26 Ma of the impactites (Reimold et al., 1981). A paleontological study of the limestones and dolomites found as fragments in the impactites of the LEC west crater places them in the Middle or Upper Ordovician (Kranck and Sinclair, 1963).

This paper reports on mapping of LEC area carried out from 1980 to 1984 from two base camps of the Geological Survey of Canada and from the camp of Centre d'Etudes Nordiques de l'Université Laval (Quebec City).

GEOLOGICAL SETTING

Bienville orthogneiss

The Bienville orthogneiss is the main constituent of the western part of the Bienville subprovince (Ciesielski, 1984, 1989a). In the LEC area the orthogneiss constitutes the framework in which large porphyritic granodioritic phases and widespread inclusions of: (1) mesocratic granulite grade rocks, (2) basic and ultrabasic inclusions, (3) iron-formations and metasediments are found.

The gneisses are pink-grey and medium to coarse grained. The foliation is irregularly developed; the rock may be highly strained locally but is massive or weakly foliated elsewhere. There is variation in the amount of mafic minerals, textures and structures (breccias, schlieren, layering, homogeneous phase) and degree of granitic remobilization, partly related to fractures. The mineralogy is rather constant showing quartz, oligoclase, microcline (or perthite), hornblende, biotite with accessory sphene, apatite, allanite and zircon and scarce clinopyroxene. Biotite is in part altered to chlorite and locally forms symplectite with quartz. The rocks lie on a calc-alkaline trend with an increasing K_2O/CaO ratio toward the north of the Bienville subprovince (Ciesielski, 1984, 1989a).

Porphyritic granodioritic phase

This mappable unit shows gradational contact with the Bienville orthogneiss and is considered to be a cogenetic phase. The rock is mainly leucocratic and medium to coarse grained; it contains quartz, plagioclase, hornblende, traces of retrograded pyroxene and up to 45 % of K-feldspar (up to 5 cm long). Presence of large amounts of K-feldspar-rich phase in the Bienville orthogneiss in the northern part of the subprovince (LEC region, Fig. 1) is in agreement with the northward increase of K_2O/CaO ratios (Ciesielski, 1989a). This unit also contains metabasic inclusions and is interlayered with granulitic gneiss.

Granulite inclusions

This unit forms centimetric to mappable kilometric inclusions in the Bienville orthogneisses. It is composed of mesocratic to melanocratic greenish granoblastic rocks of medium to coarse grain; it shows plagioclase, biotite, ortho- and clinopyroxene, biotite-quartz symplectite associated in places with orthopyroxene, hornblende and K-feldspar, with accessory magnetite, sphene, apatite, and rare allanite. Plagioclase (An_{35}) is the main mineral; clinopyroxene may be altered to chlorite and some ortho- and clinopyroxene shows retrogression to hornblende. When present, the quartz appears as medium size lobate crystals, as aggregates or in biotite-quartz symplectite. Apatite and magnetite (<5 %) are ubiquitous and appear as small and medium size crystals associated with pyroxene and biotite; sphene and epidote are rare and associated with biotite and hornblende.

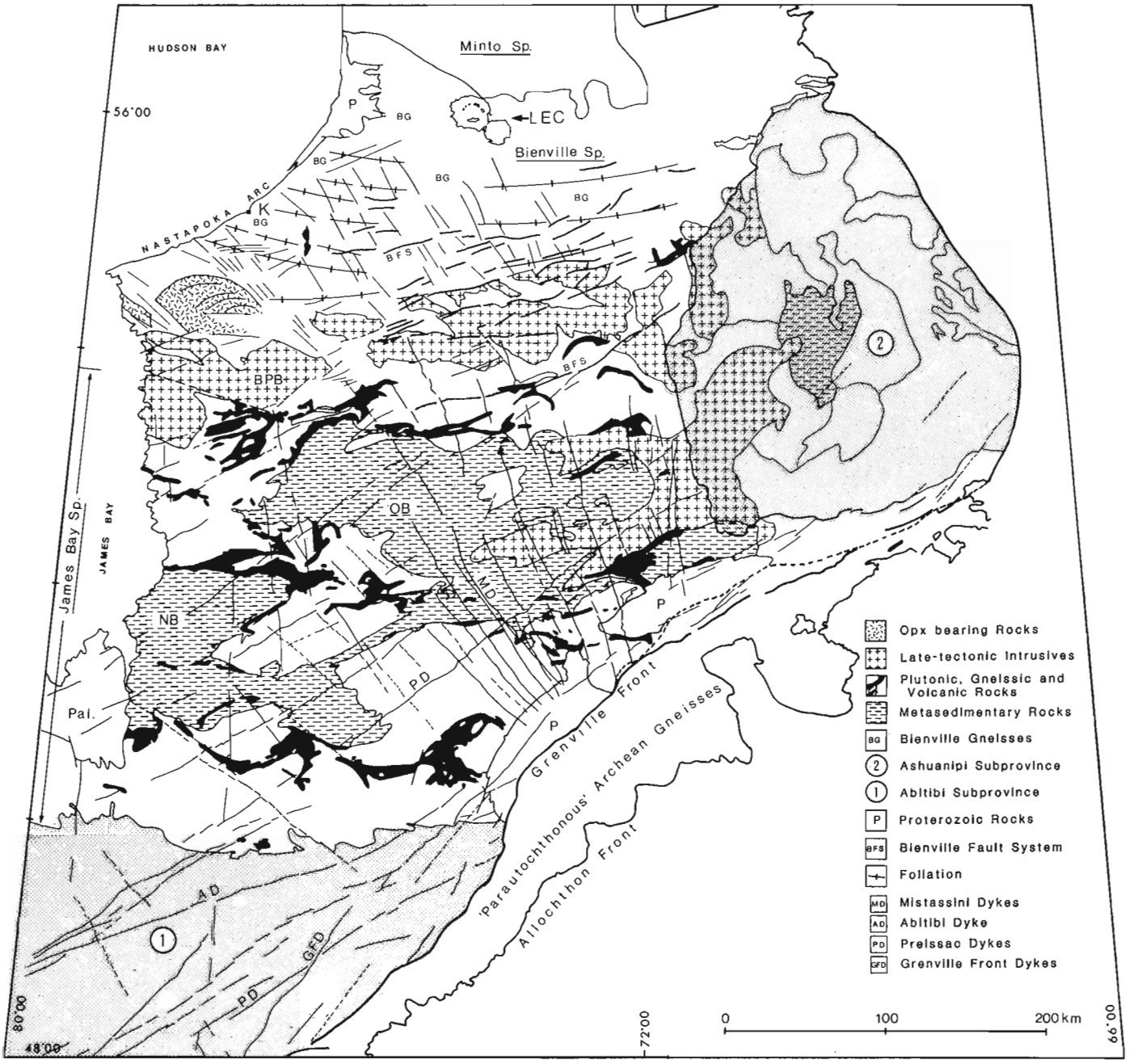

Figure 1. Geological map of the eastern Superior Province showing subprovinces defined either by lithologies or metamorphic grade (modified after Card and Ciesielski, 1986). The map show the Bienville Plutonic Belt (BPB) located at the southern limit of the Bienville subprovince along with the Bienville Fault System (BFS). The Ashuanipi subprovince is defined by the appearence of orthopyroxene in metasediments, diatexites, or late-plutonic intrusive rocks. The northern part of the Bienville subprovince lacks geological information; its limit is defined by magnetic contrasts due to iron formation in the northwestern part of LEC. The map also shows the distribution of four diabase dyke swarms of Early and Late Proterozoic age. The presence of Archean tonalitic gneisses south of the Grenville Front give the minimum southeast extent of the Superior Province prior to the Grenvillian Orogeny (Ciesielski, 1989b, Ciesielski and Madore, 1989). LEC: Lac-à-L'eau-Claire, K: Kujjuarrapik, OB: Opinaca "Basin", NB: Némiscau "Basin"

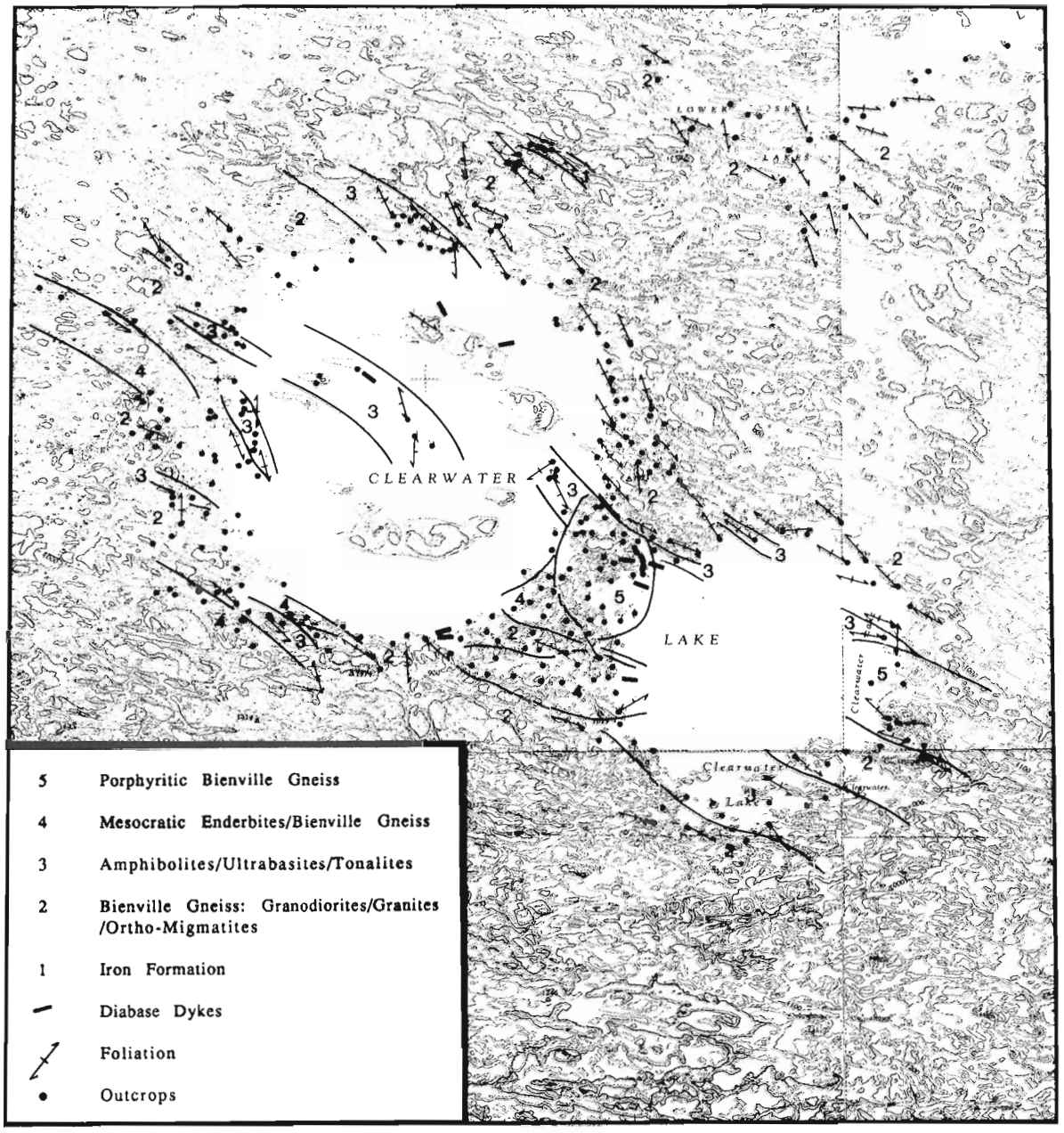

Figure 2. Geological map of the LEC area showing the distribution of granulites, Bienville orthogneiss, amphibolite and iron formation; note the constant northwest structural trends. Map after J. Rondot (unpublished data).

The granulites contain a K-feldspar porphyritic phase (reaching in places 40% of the rock), clinopyroxene-bearing "leuco-amphibolite" likely of metasedimentary origin, amphibolite and ultrabasite; they are cut by late pegmatite and pink granite. Rocks are massive or weakly foliated with foliation concordant with the host rock. The granulites are interlayered with porphyritic or biotite-rich Bienville granitic orthogneiss and show sharp or diffuse contacts parallel to the foliation. A number of compositional intermediates exist between the granulites and the host rocks, as many granulitic inclusions show gradational contacts and pass from green to pink without visible structural break (Plante, 1986).

Basic and ultrabasic rocks

These rocks may form mappable units in the granulites or the Bienville orthogneiss and comprise peridotite, metagabbro, and amphibolite associated with a tonalitic phase of partial melting origin. They form centimetric to decametric inclusions and have rounded, angular or stretched shape parallel to the foliation. In a drillhole located on the west basin of LEC, basic inclusions are numerous in a 250 m intersection and are cut by granite and pegmatite. An outcrop of websterite located on the Foreur Island (west basin of LEC) is composed of hypersthene, biotite, amphibole,

olivine, diopside, plagioclase and magnetite. A small inclusion of peridotite was found in the iron-formation northwest of LEC. Basic layers in the granulites and in the Bienville orthogneisses varying from 10 to 50 cm in width are folded, boudined and locally differentiated. Ciesielski (1983) described similar differentiated metabasites along the Nastapoka Arc (Fig. 1), interpreted as pre-Kenoran dykes.

Iron-formation

An iron-formation included in the Bienville orthogneiss was mapped 24 km north of the west basin of LEC (Fig. 2). Pyrite and magnetite facies are present (Gross, 1966) interlayered with quartzo-feldspathic and orthopyroxene-bearing metasediments and containing inclusions of serpentinized peridotite and chloritized amphibolite likely of volcanic origin. The iron-formation has a general northwest trend with 70° NE dip. The oxide facies is composed of quartz and magnetite layers, iron spinel (ceylonite; Plante, 1986), amphibole, pyroxene, feldspar, biotite and traces of pyrite and chalcopyrite. Quartzofeldspathic and biotite-rich bands (< 20 cm) are intercalated with the iron-formation. The sulphide facies comprises layers (> 1m thick) of biotite, quartz, feldspar, pyroxene and pyrite lenses. Traces of amphibole, magnetite and chalcopyrite are also present. The aeromagnetic anomaly associated to the iron-formation reaches 1000 nT and extends from the LEC east basin to the southeast part of Minto Lake; the presence of another northwest-trending elongated magnetic high located 100 km northeast of LEC might be stratigraphically related.

Diabase dykes

Altered dyke sets trending north, northeast and northwest were described by Bostock (1969) in the island ring of the LEC west basin. Fresh diabase dykes trending west and northwest intrude gneiss in the LEC area. The dykes are fine grained and have small phenocrysts of plagioclase and pyroxene, nodules of plagioclase-augite-pyrite (1-2 mm diameter), and well developed chilled margins. Both altered and fresh dykes predate impact and may correlate with dykes mapped outside the island ring, namely the Mistassini (north and northwest trends) and Preissac (northeast trends) swarms (Fig. 1) of Early Proterozoic age.

PETROCHEMISTRY OF GRANULITE INCLUSIONS

Table 1 shows the chemical analyses of the granulitic rocks from the islands separating the west and east basin of LEC. Plots of the Bienville orthogneisses shown in the different diagrams for comparison come from analyses of samples taken south and east of Richmond Gulf (Fig. 1); analyses are available upon request.

Major elements

The granulite inclusions are characterized by a low silica and high iron content compared to the Bienville orthogneiss and average 57.2 wt. % (standard deviation, s.d. 7.0) and 8.06 wt % (s.d. 3.31). In the granulites, calcium is higher but the alkalies are only slighly lower than the Bienville orthogneiss due to relatively high sodium content (Table 1). In both the granulite inclusions and the Bienville gneiss, phosphorus (0.29 wt. %, s.d. 0.23) and calcium (5.88 wt. %, s.d. 2.32) show a negative correlation with silica.

An-Ab-Or

The granulite inclusions (open symbols in Fig. 3) of LEC are classified in the O'Connor (1965) An-Ab-Or diagram modified after Barker (1979) and compared to the north Bienville orthogneiss (crosses in Fig. 3). Most of the samples fall in the tonalite or granodiorite field with average An content of 35 %. Given the amount of pyroxene and biotite (up to 35 %), they are designated as mesocratic enderbites (Streickeisen, 1974). Plante (1986) used the term "hypersthene leucodiorite" for the low-K granulite and "jotunite" for the K-feldspar-rich phase. The variation of normative orthoclase in the enderbite is principally related to variation of modal biotite. In contrast, most of the Bienville orthogneiss falls in the monzogranite (adamellite of O'Connor, 1965) or true granite field and show a fair variation in the amount of modal orthoclase.

K_2O-Na_2O-CaO and A-F-M

The enderbitic inclusions differ from the host rock, as shown by the calk-alkaline and AFM ternary diagrams. The enderbites show a gabbro-trondhjemitic affinity as opposed to the north Bienville gneiss that follow the calk-alkaline trend of Barker and Arth (1976) (Fig. 4a). In the AFM diagram, the granulite inclusions have the low relative alkaline values with Fe(t)/(Fe(t) + MgO) averaging 0.67 similar to the Bienville gneiss at 0.65 (Fig. 4b).

R2-R1

The R2-R1 diagram discriminates "granitic" suites on the basis of relation between rock bulk compositions the cationic compositions of the minerals (de la Roche, 1980). Figure 5 shows the quartz-saturation line along which liquids evolve as a primary differentiation from a ultrabasic or basic source. Arrows indicate various secondary differentiation trends from different liquid compositions according to different tectonic contexts (Batchelor and Bowden, 1985). The enderbites are scattered on the plot but are discriminated from the Bienville gneiss that cluster near the end of the differentiation path (Fig. 4a); the enderbites rest partly on the quartz-saturation line and some analyses show secondary differentiation reflected by increasing quartz and K-feldspar in thin section.

Trace elements

In both rock-units, Rb and K, and Sr and Ca vary in proportion. In the granulites, Rb/Sr ratios average 0.12 whereas in the Bienville gneiss they reach 0.39; K/Rb ratios are much the same in both units with an average of 331 and 335. In the enderbites, cobalt and nickel vary in inverse proportion with silica and barium and potassium in proportion with silica. In the Bienville gneiss, zirconium decreases with increasing silica as a result of increases of zircon content

Table 1. Chemical analyses of 33 samples of enderbites from the centre of LEC with averages and standard deviation. Major elements are in weight % and trace and rare earth elements in ppm.

(Rock samples were analyzed at the Geological Survey of Canada analytical chemistry laboratories. Major elements, Ba, Rb, Sr and Zr were determined by XRF wavelength dispersive analysis on fused disks; FeO was analyzed by rapid wet chemical method. $Fe_2O_3 = Fe_2O_3$ (XRF) - 1.11134*FeO (volumetric). Other trace elements were analyzed by ICP-TR1; 1.0g of sample dissolved in 10 % HCl and diluted to 100ml. REE were analyzed by ICP-RE1 on trace solution after x10 pre concentration and separation of majors using exchange resin).

Id/El	RSMF5	RSMF1A	W7	U1	R4	X2	U3	T9	S3A	T6	T4	F2	T11	T10	R7	N21	T2C	U8
SiO2 w%	69.3	48.6	67	51.5	61.1	49.4	58.5	57.2	55	63.9	59.1	52.6	52.1	53.9	63.2	65	57.9	74.6
Al2O3	15.3	17.9	17.4	19	15.7	12.6	18.9	17.6	15.1	15.3	15.5	17.3	17.5	19.2	14.6	15.5	17.1	13.8
Fe3O4	1.5	5	1.2	4.6	2.8	2.2	2.5	3.9	3.3	2.5	2.5	4.5	4.5	3.8	2.4	1.4	2.8	0.5
Fe2O3	1.5	5.1	1.2	5.1	4.1	7	2.6	3.7	6	2.3	3.8	5.6	5.2	3.8	3.9	3.2	3.9	1
Fe3O4(t)	3.165	10.661	2.532	10.261	7.351	9.97	5.386	8.007	9.96	5.053	6.718	10.716	10.272	8.018	6.729	4.952	7.129	1.61
MnO	0.05	0.11	0.04	0.12	0.08	0.17	0.08	0.09	0.09	0.07	0.1	0.15	0.13	0.07	0.08	0.08	0.08	0.01
MgO	0.99	4.79	0.77	3.85	3.27	11.79	1.66	2.56	4.19	2.34	4.74	4.71	3.88	2.81	2.81	2.58	3.67	0.45
CaO	3.18	9.38	3.95	7.86	4.98	10.58	4.18	4.85	4.9	3.63	5.37	8.37	6.54	4.84	3.94	3.95	5.31	1.74
Na2O	3.9	3.7	4.9	4.3	4.4	1.7	5.2	4.3	3.8	3.5	3.8	3.6	4.4	4.3	3.4	4	4.4	3.2
K2O	2.98	1.01	2.53	1.24	1.98	0.52	4.11	3.3	2.78	3.86	1.77	0.72	2.79	4.65	3.64	2.86	2.08	4.29
TiO2	0.33	0.85	0.34	1.29	0.75	0.47	0.64	0.98	1.62	0.56	0.57	0.73	1.22	0.7	0.1	0.5	0.58	0.19
P2O5	0.07	0.28	0.09	0.35	0.11	0.06	0.17	0.31	0.72	0.1	0.13	0.23	0.57	0.38	0.1	0.07	0.15	0.03
MnO	0.05	0.11	0.04	0.12	0.08	0.17	0.08	0.09	0.09	0.07	0.1	0.15	0.13	0.07	0.08	0.08	0.08	0.01
Ba (ppm)	902	475	815	782	257	291	874	1153	750	1235	431	205	635	2602	1045	619	561	1083
Rb	39	55	66	25	85	0	63	93	104	107	55	0	124	120	88	99	61	113
Sr	507	755	618	1118	446	984	451	886	541	555	481	702	573	1353	506	450	529	414
Zr	109	104	107	132	137	42	283	308	308	174	169	57	200	114	163	134	125	124
Co	9	42	9	27	21	59	14	19	30	17	25	35	28	18	19	17	20	8
Ni	15	41	15	33	37	190	18	24	60	32	72	33	27	7	28	38	43	11
La (ppm)	32	33	40	47	35	13	71	76	86	43	47	58	110	46	42	39	48	31
Ce	50	72	65	100	71	30	150	160	180	88	97	120	260	100	91	73	94	49
Nd	22	41	27	58	38	35	80	89	96	49	55	60	140	50	45	37	44	17
Sm	1.9	6.2	2.6	8.4	5.9	2.6	11	12	14	5.9	6.3	8.7	22	7.3	6.9	5.2	5.3	0.8
Eu	1.1	1.6	1.3	2.7	0.9	1.1	1.8	2.5	2.7	1.2	1.3	1.3	2.6	3.1	1.4	1.1	1.5	0.5
Gd	1.7	4.9	1.9	6.4	4.6	4.4	7.8	9	9.8	4.9	5.5	6.1	15	5.6	5	4.3	3.9	0.7
Dy	0.8	3.5	0.9	3.7	3.1	2.2	4.4	5	5.9	3.1	3.4	4	9	3.2	3.5	3.2	2.4	0.4
Yb	0.3	1.5	0.3	1.3	1.2	0.9	1.4	1.7	2.2	1.3	1.5	1.7	3.2	1.2	1.5	1.4	1	0.2
Qz	26.52	0	19.25	0.05	12.21	0	1.42	5.77	5.59	17.63	11.3	4.37	0	0	15.78	17.45	6.99	34.56
An	15.43	29.24	18	28.88	17.23	25.21	16.08	18.96	15.92	14.62	20	28.92	19.74	19.33	13.81	15.88	20.76	8.79
Or	17.62	5.99	14.97	7.34	11.73	3.07	24.31	19.53	16.46	22.85	10.48	4.25	16.53	27.52	21.54	16.93	12.31	25.39
Ab	33	31.31	41.46	36.39	37.23	14.39	44	36.39	32.16	29.62	32.16	30.46	37.23	34.12	28.77	33.85	37.23	27.08

Id/El	V1	W1	W3	V8	V10	V5	lec111	lec39	lec2B4	lecTN2	lec62	lec89Z	lec109	lec403	lec344	average(33)	standev
SiO2 w%	49.6	59	52.1	61.1	55.3	50.9	53.3	67.2	51.8	69.8	45.8	54.1	55.5	50.7	51.4	57.20	6.97
Al2O3	16.7	17.3	16.8	17.3	17.4	17.8	18.7	15.1	17	14.7	12.3	19	17	13.2	16	16.41	1.81
Fe3O4	5.5	4.2	2.9	3.1	2.9	4.4	4.5	0.4	5.5	1.9	7.9	2.4	3.6	3.9	5.2	3.34	1.57
Fe2O3	6.5	2.9	5.6	3	4.3	6.7	3.7	3.1	5.5	1.6	9	3.9	4.1	5.9	5.5	4.25	1.78
Fe3O4(t)	12.715	7.419	9.116	6.43	7.673	11.837	8.607	3.841	11.605	3.676	17.89	6.729	8.151	10.449	11.305	8.06	3.31
MnO	0.14	0.05	0.15	0.07	0.12	0.15	0.14	0.05	0.19	0.03	0.2	0.12	0.11	0.19	0.11	0.10	0.05
MgO	4.99	2.74	6.4	3.01	4.52	5.46	3.3	1.91	3.61	0.81	8.11	4.42	3.05	8.57	4.19	3.85	2.31
CaO	8.63	4.31	8.7	3.52	5.86	8.33	6.58	3.35	6.22	2.59	7.12	8.44	5.11	11.21	6.43	5.88	2.32
Na2O	3.6	4 6	3.6	4.6	4.5	3.7	4.9	3.4	4.5	3.7	3.4	4.5	4.3	3.1	3.5	3.96	0.66
K2O	0.99	2.04	1.54	1.89	2.18	0.72	1.27	3.51	1.01	3.46	1.09	0.77	3.04	0.81	2.3	2.23	1.17
TiO2	1.83	1	0.83	0.59	0.83	0.82	1.29	0.4	1.68	0.44	1.01	0.44	1.08	0.8	1.58	0.82	0.43
P2O5	0.55	0.28	0.28	0.23	0.26	0.52	0.6	0.11	0.72	0.17	0.18	0.08	0.53	0.14	0.99	0.29	0.23
MnO	0.14	0.05	0.15	0.07	0.12	0.15	0.14	0.05	0.19	0.03	0.2	0.12	0.11	0.19	0.11	0.10	0.05
Ba (ppm)	662	530	1059	671	488	216	452	951	294	1406	222	196	790	200	718	714.24	466.81
Rb	16	62	47	49	75	40	40	91	49	56	46	35	116	30	97	69.23	30.25
Sr	990	449	920	675	633	779	852	442	779	554	218	572	717	458	650	653.24	231.82
Zr	278	316	201	210	263	112	200	159	201	304	73	71	417	79	313	181.42	91.50
Co	34	17	43	22	27	47	26	19	31	11	70	32	27	44	36	27.36	13.93
Ni	47	25	84	24	67	48	37	24	39	5	51	34	29	65	30	40.39	32.14
La (ppm)	58	140	31	47	63	40	54	29	75	77	24	32	80	32	87	53.52	26.29
Ce	130	280	66	88	130	85	110	54	160	140	58	70	160	90	190	110.94	56.68
Nd	76	120	44	38	61	42	57	25	84	57	38	42	76	62	93	57.52	27.38
Sm	11	14	8.2	5.2	9.1	6.5	8.3	3.1	12	6.4	7.2	8.1	11	13	14	8.18	4.28
Eu	2.9	1.5	2.5	1.1	1.4	1.3	2.4	0.9	1.9	1.5	1.5	1.2	2.3	1.9	2.4	1.71	0.66
Gd	8.4	8.9	6.9	3.7	7.1	5.1	6.5	2.7	10	4.1	6.5	6.8	7.7	11	11	6.30	2.97
Dy	5	4.4	4.3	2.3	4.7	3.1	3.4	1.5	5.6	1.8	4.3	5.4	4	8.7	6.6	3.84	1.92
Yb	1.8	1.5	1.7	1.2	2.3	1.4	1.3	0.8	2	0.5	1.8	2.4	1.2	3.6	2.6	1.51	0.74
Qz	1.02	11.63	0	14.6	1.55	0.31	2.71	22.06	4.2	28.21	0	0.93	4.18	0	4.27	8.32	9.46
An	26.48	19.8	25.12	16.31	20.83	29.83	25.27	15.56	23.2	12.2	15.07	29.36	18.09	19.71	21.14	20.14	5.40
Or	5.86	12.08	9.12	11.19	12.91	4.27	7.52	20.77	5.98	20.47	6.46	4.56	18	4.8	13.62	13.23	6.92
Ab	30.46	38.93	30.46	38.93	38.08	31.31	41.46	28.77	38.08	31.31	28.77	38.08	36.39	26.23	29.62	33.45	5.58

in ferromagnesian minerals. Such a correlation does not occur in the enderbites because quartz is present with ferromagnesian minerals in Opx-Qz-Bio or Qz-Bio symplectites.

Rare earth elements

In the enderbites, all the REE except La and Ce show positive correlation with phosphorus. It may result from concentration of heavy rare earths (HRE) in apatite although partition into sphene, allanite, and zircon will also occur. In the Bienville orthogneiss, a positive correlation of HRE exists with phosphorus and zirconium suggesting partition into zircon and apatite. Europium anomalies (Eu*) vary from 0.41 to 2.04 in the granulites with an average of 0.86; in the Bienville orthogneiss europium anomalies vary from 0.46 to 2.62 with an average of 1.12. The slopes of the REE patterns are illustrated by the ratio $(La/Yb)_n$ in Figure 6 after Jahn et al.(1981). The granulites concentrate in the low La portion of the diagram, a result of relatively flattened REE slopes due to light rare earth (LRE) elements fractionation; the Bienville gneiss spread within the field of Archean TTG tonalite-trondhjemite-granodiorite (TTG) suites and show a continuous variation of ratios.

DISCUSSION

The enderbites differ from the Bienville gneiss by aspect, colour and chemistry. The enderbites have chemical characteristics of low silica and high iron content. The chemical contrasts and the gradational contacts between the enderbites and the Bienville gneiss can be explained by two different mechanisms.

One hypothesis is that the enderbites could result by CO_2 fluids circulating in the Bienville gneiss. It is widely hypothesized that carbonaceous fluids play a role in the formation of granulites and result in ion mobility (Condie et al., 1986; Clemens and Vielzeuf, 1987). This option is not supported by the presence of sharp contacts coexisting with diffuse and gradational contacts between enderbite and the Bienville orthogneiss nor by the chemical contrast between the two rock units.

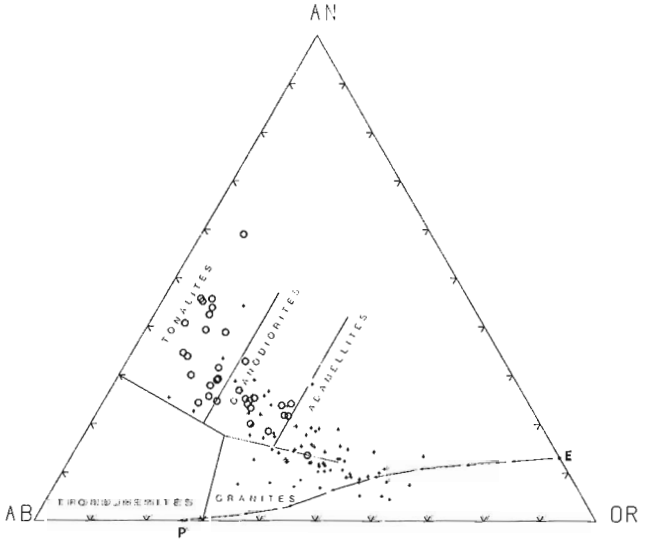

Figure 3. An-Ab-Or Granulite inclusions (open symbols) are classified and compared to the Bienville gneiss (crosses) in the normative feldspar ternary diagram of O'Connor (1965), modified by Barker (1979). EP represents the cotectic plane separating the K-feldspar from the plagioclase field. The granulite inclusions fall in the tonalite and granodiorite field and are designated by the term "mesocratic enderbites". They show an increase of normative Or due to variation of biotite and K-feldspar and a mean An content of 35.

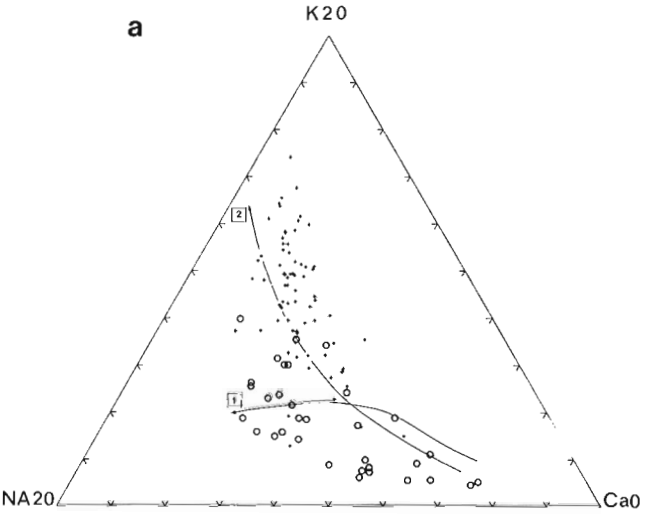

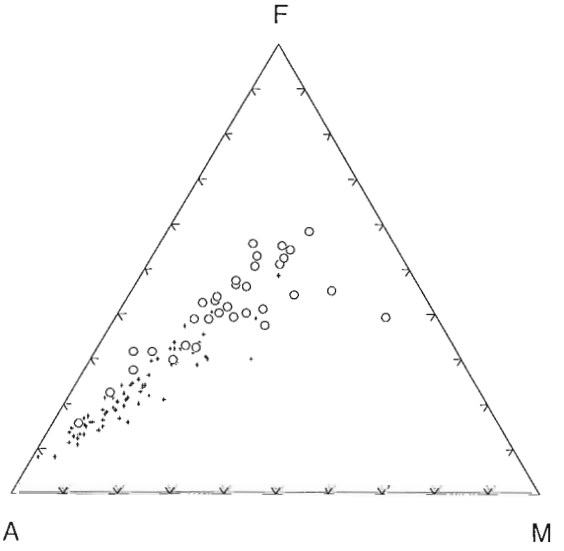

Figure 4a. In the calc-alkaline ternary diagram, the enderbites (open symbols) show trondhjemitic affinities (curve 1) as opposed to the Bienville gneiss (crosses) that show a strong K enrichment, the calc-alkaline trend (curve 2) of Barker and Arth (1976); the granitic part of the Bienville gneiss is considered as a final product of differentiation. The enderbite inclusions (open symbols) discriminate in the low alkalies portion of the AFM with a constant Fe/Mg ratio similar to the Bienville gneiss, (crosses).

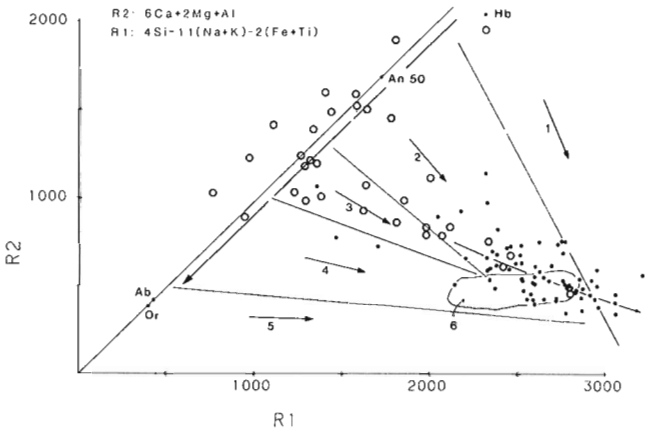

Figure 5. The R2-R1 plot discriminates different rock units on the base of the cationic composition of the rock-forming minerals (Batchelor and Bowden, 1985). The granulites (open symbols) evolve from a basic or ultrabasic source along the quartz-saturation line on which are located hornblende and plagioclase. 8 analyses show a secondary differentiation toward the quartz-enrichment field. The Bienville orthogneiss (dots) concentrates in the quartz-rich field and in part is considered as a final product of differentiation.

Trend 1: Mantle plagiogranites, 2: Pre-plate Collision Granitoids, 3: Caledonian Plutons (post-collision), 4: Sub-Alkaline Plutons, 5: Alkaline/Peralkaline Magmatism, 6: Partial Melt Granitoids.

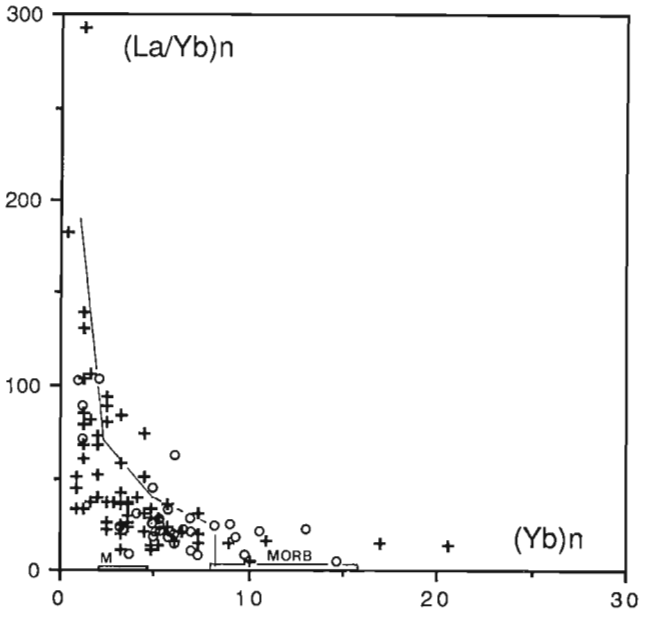

Figure 6. The slopes of REE are illustrated by the (La/Yb)n ratios (Jahn et al. 1981). The enderbites (open symbols) concentrate in the lower (La/Yb)n range due to LRE fractionation whereas the Bienville orthogneiss (crosses) shows a spread of the analyses in the field of Archean TTG granitoids of Martin (1986). M: mantle composition and MORB: oceanic basalt composition.

Another hypothesis states that the enderbites are restites or intermediate products of the differentiation giving rise to the Bienville orthogneiss, the source having been partly or totally melted at depth. This option agrees with the intermediate character of the enderbites as illustrated in Figures 3, 4b, 5 and 6. In Figure 4a, the enderbites show an apparent trondhjemitic affinity that is not confirmed by the Qz-Ab-Or diagram (not illustrated) in which tonalite-trondhjemite-granodiorite suites show decreasing potassium with increasing quartz (Barker, 1979). The enderbites could possibly be "in trend" with the Bienville gneiss in a calk-alkaline suite with a higher sodium content. Negative Europium anomalies (< 1.0) in the enderbites favour the restite scenario given presence of positive Eu anomalies and porphyritic K-feldspar phase in the Bienville gneiss.

The presence of orthopyroxene associated with the quartz-biotite symplectites reflects the relatively dry conditions in which mineral reactions took place in the enderbites. K-feldspar is not present in the symplectites but the presence of microcline in the mineral framework of some of the enderbites can be partly explained by K+ ion mobility during granulite grade metamorphism. Higher water activity in the Bienville orthogneiss is expressed by systematic presence of hornblendes and few clinopyroxenes which show hydrous alteration.

ACKNOWLEDGMENTS

Part of this paper comes from the MSc. thesis of the second author (L.P.). Thanks are due to J. Rondot who provided the geological map of LEC area. Support to L.P. from M.K. Seguin, and Centre d'Études Nordiques (Université Laval, Québec) is acknowledged. The manuscript was reviewed by M. Schau and A. Davidson of the Geological Survey of Canada.

REFERENCES

Barker, F., and Arth, J.G.
1976: Generation of tronhjemitic-tonalitic liquids and Archean bimodal trondhjemite-basalt suites; Geology, v. 4, p. 596-600.

Barker, F.
1979: Trondhjemites: definition, environment and hypotheses of origin; in Trondhjemites, Dacites and Related Rocks, F. Barker (ed.), Elsevier, Amsterdam, 1979, p. 1-12.

Batchelor, R.A., and Bowden, P.
1985: Petrogenetic interpretation of granitoid rock series using multicationic parameters; Chemical Geology, v. 48, p. 43-55.

Bostock, H.H.
1969: The Clearwater Complex, New Quebec; Geological Survey of Canada, Bulletin 178.

Card, K.D. and Ciesielski, A.
1986: Subdivisions of the Superior Province of the Canadian Shield; Geoscience Canada, v. 13, no. 1, p. 5-13.

Ciesielski, A.
1983: Cartographie d'une partie de la sous-province archéenne d'Ungava à la hauteur de Poste-de-la-Baleine, Québec; dans Recherche en Cours, partie B, Commission Géologique du Canada, Étude 83-1B, p. 109-119.
1984: Pétrologie des gneiss du domaine du lac Bienville, sous-province archéenne d'Ungava, Québec: Rapport d'étape; dans Recherche en Cours, partie B, Commission Géologique du Canada, Etude 84-1B, p. 1-10.
1989a: Orthogneiss and plutonic rocks of the Bienville and James Bay Subprovinces, Northeast Superior Province, Quebec; Geological Association of Canada, Program with Abstracts, p. A108, Montréal 1989.

1989b: Archean rocks of the Central Grenville Province, a reworked substrate of the Abitibi Belt, southeast of Chibougamau, Quebec; Geological Association of Canada, Program with Abstracts, p. A83, Montréal 1989.

Ciesielski, A. and Madore, C.
1989: Litho-tectonic map of the Grenville Front, the Archean Parautochthonous orthogneiss and Proterozoic dykes in the Central Grenville Province, southeast of Chibougamau, Quebec; Geological Survey of Canada, Open File 2059.

Clemens, J.D., and Vielzeuf, D.
1987: Constraints on melting and magma production in the crust; Earth and Planetary Science Letters, v. 86, p. 287-306.

Condie, K.C., Bowling, G.P., and Allen, P.
1986: Origin of granites in an Archean high-grade terranes, southern India; Contributions to Mineralogy and Petrology, v. 92, p. 93-103.

de la Roche, H., Leterrier, J., Grand Claude, P., and Marchal, M.
1980: A classification of volcanic and plutonic rocks using R2-R1 diagrams and element analyses - its relationships with current nomenclature; Chemical Geology, v. 29, p. 183-210.

Dence, M.R.
1964: A comparative structure and petrographic study of probable Canadian meteorite crater; Meteoritics, v. 2, p. 269-270.
1981: Meteorite Breakup; Nature, v. 289, p. 346-347.

Eade, K.E.
1966: Fort George and Kaniapiscau River (West-half) map-areas, New-Quebec; Geological Survey of Canada, Memoir 339.

Gross, G.A.
1966: Principal types of iron-formation and derived ores; Canadian Mining and Metallurgical Bulletin, v. 59, p. 150-153.

Herd, R.K.
1978: Notes on metamorphism in New-Quebec: in Metamorphism in The Canadian Shield; Fraser, J.A. and Heywood, W.W. (eds), Geological Survey of Canada, Paper 78-10, p. 74-83.

Jahn, Bor-ming, Glykson, A.Y., Peucat, J.J., and Hickman, A.H.
1981: REE geochemistry and isotopic data of Archean silicic volcanics and granitoids from the Pilbara Block, Western Australia: implications for the early crustal evolution; Geochimica et Cosmochimica Acta, v. 45, p. 1633-1652.

Krank, S.H. and Sinclair, G.W.
1963: Clearwater Lake, New-Quebec; Geological Survey of Canada, Bulletin 100.

Martin, H.
1986: Effect of steeper Archean geothermal gradiant on geochemistry of subduction-zone magmas; Geology, v. 14, p. 753-756.

Mortensen, J.K. and Ciesielski, A.
1987: U-Pb zircon and sphene geochronology of Archean plutonic and orthogneissic rocks of the James Bay region and Bienville Domain, Quebec; in Radiogenic Age and Isotopic Studies: Report I, Geological Survey of Canada, Paper 87-2, p. 129-134.

O'Connor, J.T.
1965: A classification for quartz-rich igneous rocks based on feldspar ratios; United States Geological Survey, Professional Paper 525-B, p. 79-84.

Phinney, W.C., Simonds, C.H., Cochran, A., and McGee, P.E.
1978: West Clearwater Quebec impact structure Part II: Petrology; in Proceedings of Lunar and Planetary Sciences 9th Conference, p. 2659-2693.

Plante, L.
1986: Modélisation géophysique des cratères météoritiques du lac-à-l'Eau-Claire, Nouveau-Québec; Mémoire de maîtrise inédit, Université Laval (Québec), 172 p.

Reimold, W.U., Grieve, R.A.F., and Palme, H.
1981: Rb-Sr dating of the impact melt from West Clearwater, Quebec; Contributions to Mineralogy and Petrology, v.76, p. 73-76.

Simonds, C.H., Phinney, W.C., McGee, P.E., and Cochran, A.
1978: West Clearwater Quebec impact structure, Part I: Field geology, structure and bulk chemistry; in Proceedings of the Lunar and Planetary Science 9th Conference, p. 2633-2658.

Stevenson, I.M.
1968: A geological reconnaissance of Leaf River map-area, New-Quebec and North-West Territories; Geological Survey of Canada, Memoir 356.

Streckeisen, A.
1974: How should charnockitic rocks be named; in Centenaire de la Société Géologique de Belgique, Géologie des Domaines Cristallins, Liège, 1974, p. 349-360.

Tectonic and petrological significance of regional lamproite-minette volcanism in the Thelon and Trans-Hudson hinterlands, Northwest Territories

T.D. Peterson and R.H. Rainbird[1]
Continental Geoscience Division

Peterson, T.D. and Rainbird, R.H. Tectonic and petrological significance of regional lamproite-minette volcanism in the Thelon and Trans-Hudson hinterlands, Northwest Territories; in Current Research, Part C, Geological Survey of Canada, Paper 90-1C, p. 69-79, 1990.

Abstract

Christopher Island Formation (lower Dubawnt Group) volcanic rocks at Dubawnt Lake, N.W.T., range from lamproitic lavas to mafic and felsic minettes. Syn- and post-depositional non-dilational, brittle normal faults are mostly parallel to the Bathurst (330) and McDonald (250) faults, which intersect in projection 150 km WNW of the study area. Later N- and NE-striking dilational faults, synvolcanic with middle Dubawnt Group Pitz Formation rhyolites, are interpreted as mostly west-side down normal faults. The style and composition of volcanism and sedimentation, together with the nature of deformation and the probable association with the Thelon and Trans-Hudson subduction-collisions, lead us to propose a tectonic model similar to models for the Tibetan and Colorado plateaus. Metasomatic enrichment of the sub-Churchill lithospheric mantle resulted from subduction at ca. 2.0-1.9 Ga, followed by thickening of the lithosphere during ca. 1.9-1.85 Ga continental collisions. Thermal relaxation in the enriched mantle, coinciding with the brittle Slave/Churchill indentation at ca. 1.84 Ga, produced ultrapotassic melts within phlogopite-enriched peridotite which reached the surface through brittle fractures.

Résumé

Les roches volcaniques de la formation de Christopher Island (base du groupe de Dubawnt), au lac Dubawnt (T.N.-O.), passent de laves lamproïtiques à des minettes mafiques et felsiques. Les failles normales cassantes sans dilatation, qu'elles soient syn-sédimentaires ou post-sédimentaires, sont pour la plupart parallèles aux failles de Bathurst (≈330°) et de McDonald (≈250°) qui recoupent en projection 150 km ouest-nord-ouest de la zone à l'étude. Des failles de dilatation à direction nord et nord-est synvolcaniques par rapport aux rhyolithes intermédiaires de la formation de Pitz du groupe de Dubawnt, sont interprétées comme des failles normales à compartiment ouest abaissé pour la plupart. Le style et la composition du volcanisme et de la sédimentation ainsi que la nature de la déformation et sa probable association avec les subductions-collisions théloniennes et trans-hudsoniennes, ont incité les auteurs à proposer un modèle tectonique semblable à ceux des plateaux du Tibet et du Colorado. L'enrichissement métasomatique du manteau lithosphérique sub-Churchill a été causé par une subduction vers 2, 0-1,9 Ga, suivie par un épaississement de la lithosphère pendant des collisions continentales vers 1, 9-1, 85 Ga. La relaxation thermique du manteau enrichi, coïncidant avec l'indentation cassante de Slave-Churchill vers 1,84 Ga, a produit des magmas ultra-potassiques au sein d'une péridodite enrichie de phlogopite qui ont atteint la surface par des fractures cassantes.

[1] *Department of Geology, University of Western Ontario, London, Ontario N6A 5B7*

INTRODUCTION

Minettes are potassic, calc-alkaline lamprophyres (phlogopite + clinopyroxene +/- sanidine) which often erupt on continental lithosphere which overlies an active subduction zone (Rock, 1987; Allan and Carmichael, 1984). Minettes also occur within some intracratonic uplifts, such as the Colorado Plateau (Roden et al., 1979). They are thought to originate within the metasomatized mantle which typically forms above subducting oceanic crust (e.g., Wallace, 1989). According to Bergman (1987), "Lamproites are, in general, the result of post-orogenic magmatic phenomena in regions that have experienced collisional orogenesis (with underlying fossil Benioff zones) several tens to many hundred million years prior to their eruption.". Lamproites are similar in several respects to minettes but are more primitive and often contain olivine phenocrysts. Bergman (1987) mentioned a possible genetic link between minettes and lamproites but noted that a direct field association had not been recorded. Lamproites can be diamondiferous.

Lower Dubawnt Group minettes erupted at ca. 1.85 Ga throughout a large part of the District of Keewatin (LeCheminant et al. 1987a). This event was exceptional for several reasons, including: (1) no concurrent basaltic or intermediate volcanism occurred in the area; (2) at least 2 km of flows and volcaniclastics accumulated in grabens presently exposed over an area of about 10 000 km^2, exceeding the total volume of minette flows elsewhere in the world by many times; and (3) stratigraphic successions from olivine minette (lamproite) through mafic, intermediate, and felsic minette are preserved. This paper presents a summary of the geology of the minettes at Dubawnt Lake, and a preliminary tectonic model for their origin.

In the Dubawnt Lake area gently to steeply dipping Proterozoic continental volcanic and sedimentary rocks (Dubawnt Group) unconformably overlie Archean, nondeformed to foliated mafic-to-granitic intrusions emplaced into an older mixed gneiss domain (Peterson et al., 1989). Mapping in 1988 and 1989 at 1:50 000 scale has established the local stratigraphy of the Dubawnt Group (summarized in Fig. 2) and the structural history of the grabens. A companion article on the physical volcanology and sedimentology of the lower Dubawnt Group (Rainbird and Peterson, 1990) follows this paper.

Exposures of the Dubawnt Group east and south of Dubawnt Lake have been studied by Blake (1980), LeCheminant et al. (1979, 1981), Tella and Eade (1980), and Tella et al. (1981). A petrological study of minette feeder dikes to the potassic volcanic rocks (Christopher Island Formation) was made by LeCheminant et al. (1987a). Previous geological studies of the northern Dubawnt Lake area (NTS 65N) were summarized by Peterson et al. (1989). A 1:250 000 geological map of the southern Dubawnt Lake area (NTS 65K) was published by Tella and Eade (1985), based on the mapping of Tella and Eade (1980) and Tella et al. (1981).

The Dubawnt Group (Donaldson, 1965) represents two continental volcanic-sedimentary cycles and a third sedimentary event. Minette flows, and pyroclastic and epiclastic rocks (Christopher Island Formation: CIF), locally with thin ($\leq$200 m) pre-volcanic conglomerate, are overlain by alluvial fan sedimentary rocks (Kunwak Formation: KF). These lower Dubawnt Group rocks are unconformably overlain by middle Dubawnt Group high-silica rhyolite (Pitz Formation) and associated sandstones. Regoliths are developed at the top of the Pitz Formation, beneath nearly flat-lying conglomerates and sandstones of the upper Dubawnt Group Thelon Formation. Minor basalts of uncertain stratigraphic position but closely associated with outcrops of Thelon Formation are assumed to be a minor aspect of Pitz volcanism, but may be extrusive equivalents of Mackenzie dykes, dated at 1.27 Ga (LeCheminant and Heaman, 1989).

A single U-Pb (zircon) age from a pyroxene syenite near Amer Lake, 350 km NE of Dubawnt Lake, of 1850 +30/-10 Ma (Tella et al. 1985) may date the Christopher Island Formation, which has syenitic equivalents. Fluorite-bearing rapakivi granite plutons, correlative with the extrusive Pitz Formation, have U-Pb ages ranging from 1.75 Ga (Loveridge et al., 1987) to 1.76 Ga (LeCheminant et al., 1987b). A U-Pb age from phosphatic cements in the Thelon Formation is 1720+/-6 Ma (Miller et al., 1989).

TECTONIC SETTING

Dubawnt Lake (Fig. 1), marks the western extremity of exposed lower Dubawnt Group basins. The Dubawnt Basin is defined here as the near-continuous exposure of Christopher Island Formation from northern Dubawnt Lake (NTS 65N) to Kamilukuak Lake (NTS 65K), and is 200 km long. Together with the 250 km long Baker Lake basin, the Dubawnt Lake basin and other erosional remnants define a 400x150 km NE trending belt of continental volcanic and sedimentary rocks.

Dubawnt Lake is equidistant (100 km) from the Chantrey and Tulemalu fault zones. The Chantrey Fault Zone separates the uplifted and granulitic Queen Maud Block (Hoffman, 1988) from the remainder of the Churchill Province. Field relations between lower Dubawnt Group basins and the Tulemalu Fault Zone (Tulemalu Fault Zone), a lineament separating the Rae and Hearne subprovinces of the Churchill Province and a possible suture zone (Snowbird suture: Hoffman, 1988) are unclear. The Tulemalu Fault Zone, which in the Tulemalu Lake area has an early ductile phase (Tella and Eade, 1986) truncates the Taltson Magmatic Zone and therefore is younger than 1.91 Ga, the youngest known intrusive in the Taltson Arc (Bostock and Loveridge, 1988). Ductile faulting is not known to affect the Christopher Island Formation, but it is affected by later brittle faulting along the Tulemalu Fault Zone (Tella and Eade, 1986).

The projected intersection of the brittle Bathurst and McDonald faults, 150 km WNW of Dubawnt Lake, is covered by the Thelon Basin. The McDonald fault postdates the Compton laccoliths, which intruded the Great Slave Supergroup at 1.86 Ga (Bowring et al., 1984). Both faults were formed by indentation of the Slave Province into the Churchill Province, in response to a continental collision on the western margin of the Slave Province (Johnny Hoe

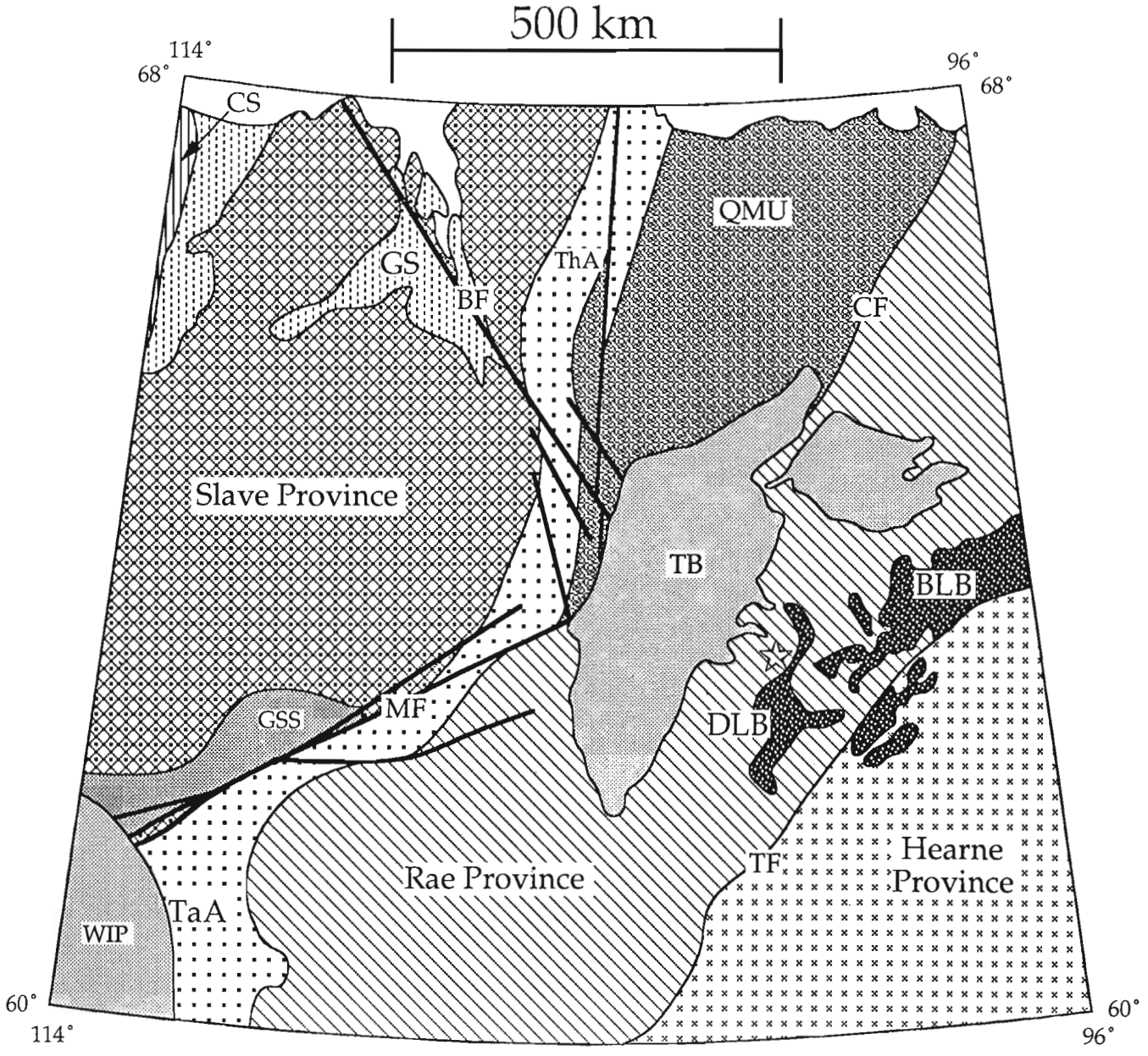

Figure 1. Tectonic elements in the region of the Slave and Churchill provinces. Dubawnt Lake is located by a star. BF = Bathurst Fault; CF = Chantrey Fault Zone; MF = McDonald Fault; TF = Tulemalu Fault Zone; CS = Coronation Supergroup; GS = Goulbourn Supergroup; GSS = Great Slave Supergroup; QMU = Quenn Maud Uplift; TaA = Taltson Arc; ThA = Thelon Arc; WIP = Western Interior Platform; BLB = Baker Lake Basin; DLB = Dubawnt Lake Basin; TB = Thelon Basin. Adapted from Hoffman (1988).

suture: Hoffman, 1988). Hoffman (1980) suggested that the feeder dykes to the Christopher Island Formation, which regionally average east-trending, were emplaced within crustal fractures related to this indentation. The Trans-Hudson orogen, at ca. 1.9-1.85 Ga, provided a NW dipping subduction zone along the southern margin of the Churchill Province which closely predates the Christopher Island Formation.

LOWER DUBAWNT GROUP AT DUBAWNT LAKE

Christopher Island Formation: geology and petrology

The terminology of the Christopher Island Formation lavas and dykes has varied from author to author. Blake (1980) compared the formation to potassic rocks in Papua, terming both shoshonites. Shoshonites, however, contain essential plagioclase feldspar (Nicholls and Carmichael, 1969) which is absent from any Christopher Island Formation rock.

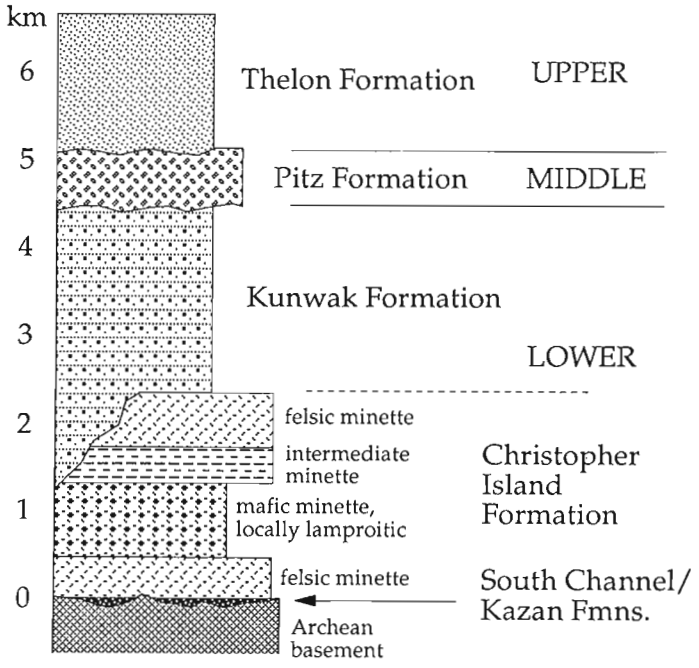

Figure 2. Summary stratigraphic section for the Dubawnt Group. Lower Dubawnt Group stratigraphy based on this study; middle and upper Dubawnt Group stratigraphy based on mapping throughout the District of Keewatin (see text for references). Thicknesses of units vary widely and are often uncertain due to fault repetitions; the total thickness of Christopher Island Formation indicated here is the minimum and is based on a nearly complete section at Lost Boat island (Peterson et al., 1989).

Wyman and Kerrick (1989) use the term "shoshonitic lamprophyre" (based on the classifications of Rock, 1984) for potassic Archean dyke rocks of the Superior Province similar to the Christopher Island Formation, but this term is self-contradictory, since lamprophyres by definition do not contain feldspar phenocrysts. LeCheminant et al. (1987a) fully discussed the mineralogy of the Christopher Island Formation dykes and recognized that they are minettes. Recent usage has extended the term minette, once reserved for dyke rocks, to include equivalent flows and pyroclastic rocks (e.g., Allan and Carmichael, 1984); 'lamproite' similarly refers to both intrusive and extrusive equivalents.

Most Christopher Island Formation flows and dykes are equivalent in all respects to well-characterized minettes, such as certain Quaternary eruptives in the Mexican Volcanic Belt (Allan and Carmichael, 1984). However, some Mg-rich flows and dykes (9-13 % MgO) are compositionally very similar to lamproites, although no Christopher Island Formation rocks have the very low Al_2O_3 contents typical of diamondiferous lamproites (Bergman, 1987). Many Christopher Island Formation rocks pass the major element screens of Foley et al. (1987) for their Group I ultrapotassic rocks (all lamproites), with the remainder generally classified as Group II (rift-related potassic rocks). The lamproitic Christopher Island Formation volcanic rocks differ from average lamproite (Bergman, 1987) in having slightly lower MgO and K/Al ratios; high K/Al ratios are considered particularly characteristic of lamproites. However, these quantities are positively correlated in the Christopher Island Formation rocks and the most mafic flows and dykes extend well into the lamproite field of Bergman (Fig. 3).

The Christopher Island Formation at Dubawnt Lake, generalizing from 5 measured sections, exhibits a felsic-mafic-felsic cycle. Flows at the basal unconformity are predominantly siliceous and poor in mafic minerals. Mafic minettes are rich in phlogopite ± clinopyroxene phenocrysts; olivine can only be identified in thin section and is with few exceptions altered to oxides plus carbonate, talc, or serpentine. Mafic minettes in some sections are overlain by aphanitic, grey-weathering lavas and very fine grained buff and grey or black-weathering tuffs. These eruptive rocks, with about 5% MgO, are intermediate between mafic and felsic minettes. In areas where intermediate minettes are absent, mafic minettes are sometimes separated from poorly exposed upper felsic minettes by lavas containing both clinopyroxene and sanidine phenocrysts, both of which appear resorbed. They are tentatively interpreted as mixed mafic/felsic magmas. The entire package is tentatively interpreted as a sequence of crustally contaminated magmas (felsic minette), followed by near-primary (lamproite and mafic minette) and fractionated (intermediate to felsic minette) magmas.

Some poorly exposed flows in the southern part of the map area contain 1 cm sanidine phenocrysts, and sparse biotite phenocrysts, in a siliceous matrix. These rocks appear transitional between Christopher Island Formation felsic minettes and Pitz Formation rhyolite porphyries, which may be as much as 90 Ma younger than the Christopher Island Formation. The field relations of the porphyries are not definitive, but petrological studies now in progress should resolve their nature.

Christopher Island and Kunwak Formations: structure

Exposures of Christopher Island and Kunwak formations in the Dubawnt Lake area, including major faults and generalized bedding data, are indicated in Figure 4. There are some differences in lithological interpretation between this map

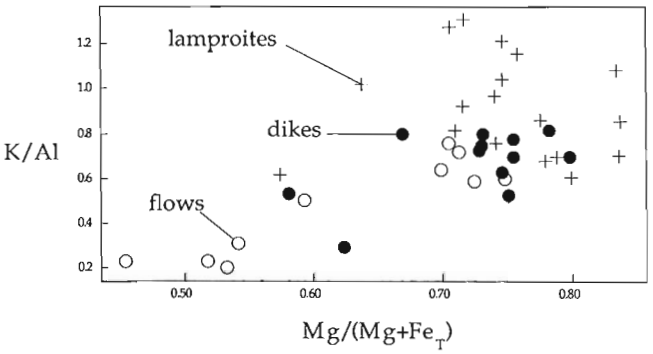

Figure 3. K/Al vs Mg (Mg + Fe +) for Christopher Island Formation flows from Dubawnt Lake (Peterson, unpub. data), Christopher Island Formation feeder dykes from across the District of Keewatin (LeCheminant, pers. comm.) and average lamproites from 19 worldwide occurrences (Bergman, 1987).

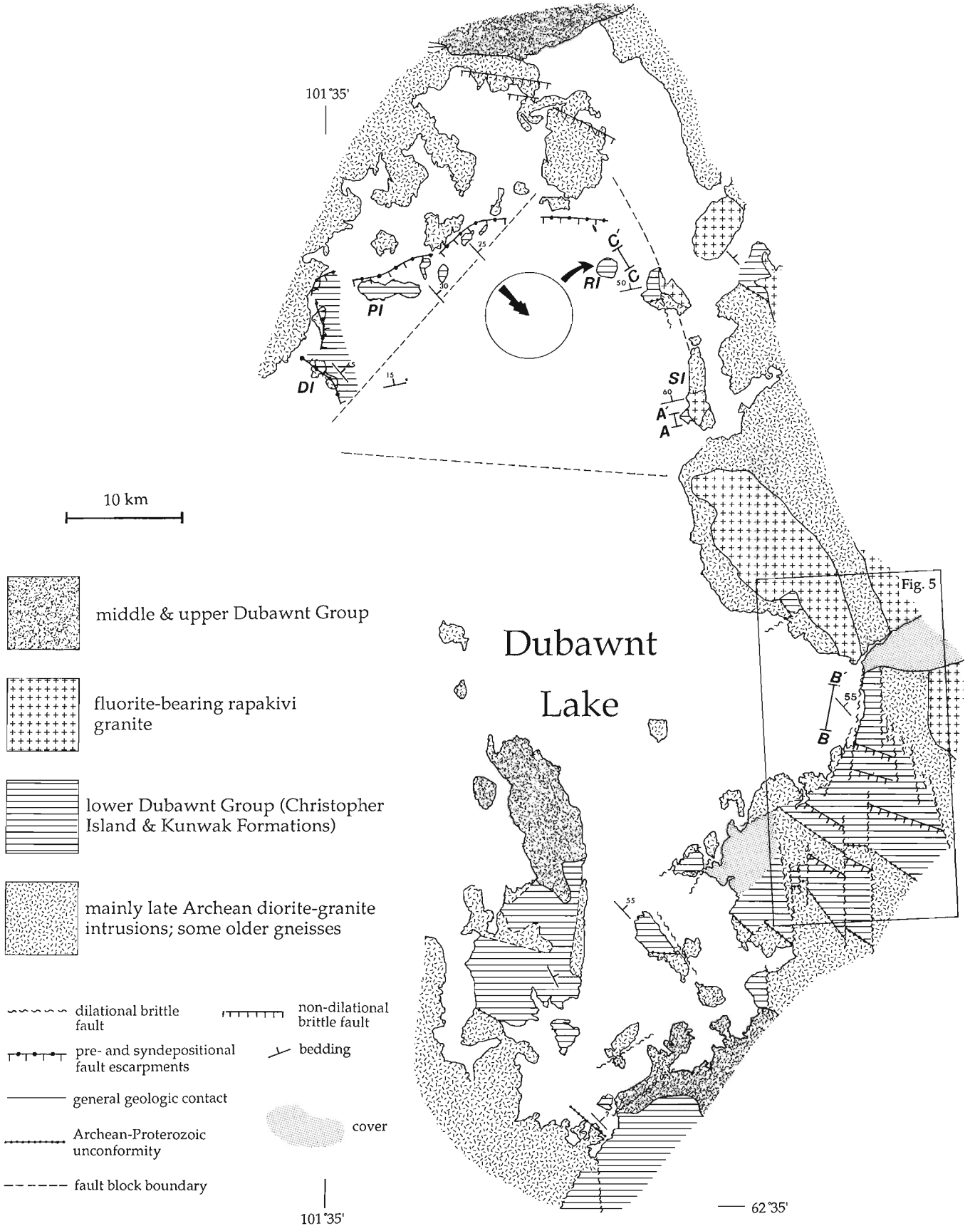

Figure 4. Bedrock geology of the Dubawnt Lake area. DI = Dumbell island; PI = Peanut island; RI = Round island; SI = South Long island. The paleocurrent rose diagram for Round island is based on 37 measurements of trough and planar crossbeds. Mapping by foot and boat traverses during 1988 and 1989, except for the southcentral portion which is partly based on mapping by Tella and Eade (1985). The area in figure 5 is indicated by the rectangle. Stratigraphic sections A-A', B-B', and C-C' are discussed by Rainbird and Peterson (1990).

and the map of Tella and Eade (1985). Some areas previously mapped as Christopher Island Formation have been reinterpreted as Pitz Formation and others as basalts of Pitz age or younger.

A detailed map covering the east-central shoreline is given as Figure 5; the major elements of the structure of lower Dubawnt Group rocks are present in this area. Limited outcrop renders linkages and offsets of some faults ambiguous, but two deformations are identified: (1) initial non-dilational brittle normal faulting, which rotated crustal blocks on presumed listric faults, and (2) later dilational brittle faulting of uncertain kinematics. Exposures of Christopher Island Formation on the east side of the lake are bounded by a system of these dilational faults which commonly were the site of later intrusions of rapakivi granite. To the northwest the Dubawnt Lake Basin is bounded by pre- or syndepositional fault escarpments, with both Christopher Island Formation and Kunwak Formation beds onlapping them at a high angle. To the south, the basal Dubawnt unconformity is repeated in a series of normal faults. Three structural domains, containing beds with contrasting strikes, have been identified but their contacts are below water. The interpreted contacts are indicated in Figure 4; they are presumed to correspond to normal faults.

The Kunwak Formation is restricted to the northwest sector of the lake. Paleocurrent measurements from cross-beds at Round island (Fig. 4) consistently indicate northwest transport. In contrast, paleocurrent measurements at Peanut island, where the basin margin is very close, are much more random. These data are consistent with the presence of a fault scarp to the NW, mapped in outcrop at Dumbell island, and tilting of crustal panels toward the escarpment during Kunwak time.

Non-dilational faults

The non-dilational faults are ubiquitously parallel in strike to bedding and, when stratigraphic relations are clear, are usually seen to place younger rocks south of older rocks. An exception is a fault which places intermediate minettes on the north side of mafic minettes at South Long island. These faults are interpreted as listric normal faults, usually southwest-dipping. In incompetent mafic minettes, the non-dilational faults typically consist of zones ≤ 50 m wide of hydrothermally altered rock containing anastamosing slip planes with no introduced material. In more competent intermediate and felsic minettes, discrete faults are observed (Fig. 6).

Northwest to westerly trending non-dilational faults have been mapped in the basement and in Christopher Island Formation. Beds of Christopher Island Formation are usually dipping at 40°-60°, rarely as steeply as 80, but Kunwak Formation alluvial fan conglomerates and sandstones have shallower dips of 25°-35°. This, and sedimentological evidence (Peterson et al. 1989; Rainbird and Peterson, 1990) indicate that deposition of the Kunwak Formation was largely in response to post-volcanic normal faulting and that Christopher Island Formation strata typically experienced more than one episode of normal faulting. Syndepositional faults are commonly observed in tuffs and epiclastic rocks within the Christopher Island Formation.

Rose diagrams of strikes of lower Dubawnt Group beds show a bimodal distribution, particularly for Kunwak Formation (Fig. 8D). The distribution peaks, at about 250° and 320°, can be identified in Christopher Island Formation strikes, but most of these form a larger peak at 290°. The poles to bedding for Christopher Island Formation strata are plotted in Figure 8A. The bedding attitudes can be interpreted as due to rotation of crustal blocks on listric faults commonly parallel in azimuth (but not dip) to the vertical Bathurst and McDonald faults, but occasionally of intermediate orientation; the greater scatter in Christopher Island Formation, as opposed to Kunwak Formation bedding, may reflect non-horizontal primary dips of tuffs and epiclastic rocks on volcanic edifices, or repeated faulting of the older Christopher Island Formation. Feeder dykes assumed to be initially vertical, now dipping south to west (Fig. 8C), indicate postvolcanic rotation of a sense consistent with the bedding data.

Dilational faults

The normal faults are cut at high angles by N to NE trending brittle faults. These are dilational faults with the introduced material being quartz or a quartz-chlorite mixture (Fig. 7). The observed apparent offsets in the basal unconformity and normal faults are sinistral (Fig. 5) but no data defining strike-slip motion is available. The offsets are consistent with vertical west-side-down motion on N-trending dilational faults (the west and central portions of Fig. 5), juxtaposing supracrustal rocks against the basement to the east, and SE-side-down motion on a system of dilational faults along the shoreline, placing basement rocks offshore. Both motions are consistent with the formation of pull-apart basins in a sinistral simple shear regime.

Some dilational faults were observed to cut Pitz Formation rhyolites, but rapakivi granites clearly intrude these faults at some locations (e.g., the north end of the map area of Fig. 5). They are therefore presumed to be synvolcanic with the Pitz Formation.

DISCUSSION: COMPRESSIONAL TECTONICS AND ORIGIN OF CHRISTOPHER ISLAND FORMATION

The lamproite-minette connection

The existence of the Christopher Island Formation minette suite, separate from any basaltic or intermediate volcanism, clearly shows that minette petrogenesis is decoupled from that of other magmas, and is not part of a basalt fractionation process or triggered by partial melting of metasomatized mantle by other primary magmas. *The involvement of large-scale mantle convection is contraindicated by the absence of basaltic rocks in the Christopher Island Formation.* This aspect of Dubawnt Group volcanism cannot be overemphasized, particularly in the context of its tectonic implications and the petrological implications of its most mafic products.

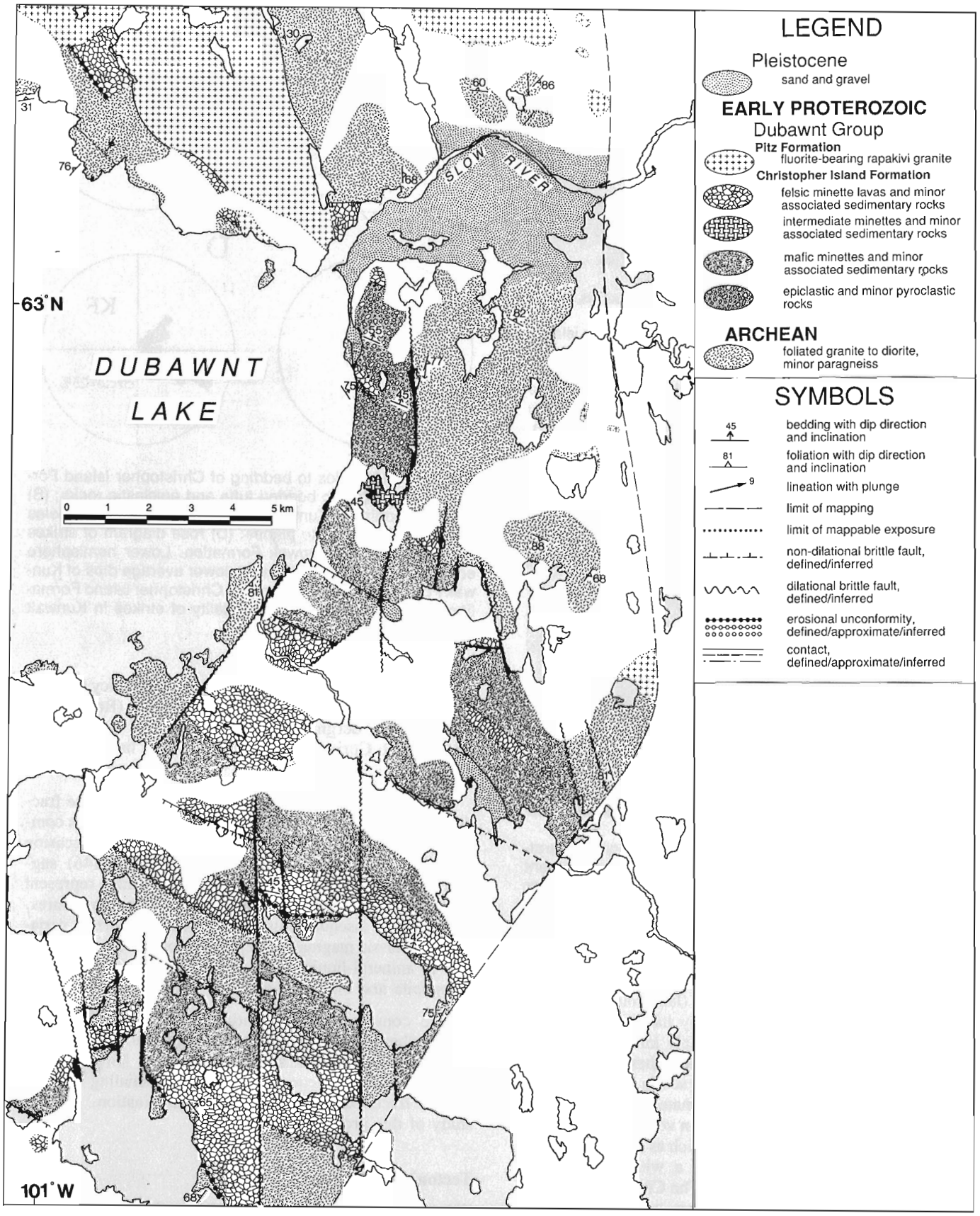

Figure 5. Geological map of the eastern shoreline of Dubawnt Lake south of Slow River. See Figure 4 for location. Exposures are of variable quality in the patterned areas and nonexistent in the blank ones.

Figure 6. Nondilational brittle fault, South Long island. Rapidograph pen on the fault trace for scale; 2/3 of the outcrop is under water. The fault, which is sensibly parallel to bedding, occurs in a homogeneous, aphanitic intermediate minette. The fault is one of 3 or 4 similar faults, over a space of 3 m, which place intermediate minette over flow breccia. Cleavage subparallel to the faults has been intersected at a shallow angle. GSC 205012-D.

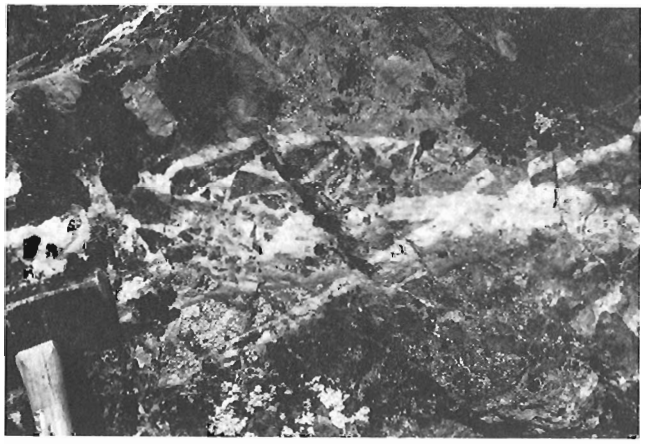

Figure 7. Dilational brittle fault from the fault zone separating Christopher Island Formation from Archean basement on the west side of the section marked B-B' (Fig. 4). Angular fragments of highly silicified minette are surrounded by milky quartz. GSC 205012-B.

For example, Foley et al. (1987, p. 96) have observed that, "The standard members of Group I (lamproites) occur in stable continental areas and normally have no associated non-ultrapotassic rocks, except possibly kimberlites in the case of Western Australia..." (our parentheses). Minettes, in contrast, typically occur as minor scoria cones and restricted flows in orogenic belts dominated by basaltic and intermediate volcanism (e.g., Mexican volcanic belt). Even intracontinental minette volcanism, such as on the Colorado Plateau, occurs in association with a wide spectrum of magma types (Roden et al., 1979). The Christopher Island Formation postdates the accretion of Laurentia, at 1950-1860 Ma (Hoffman, 1988) with the future minette-intruded lithosphere acting as hinterland to the Thelon and

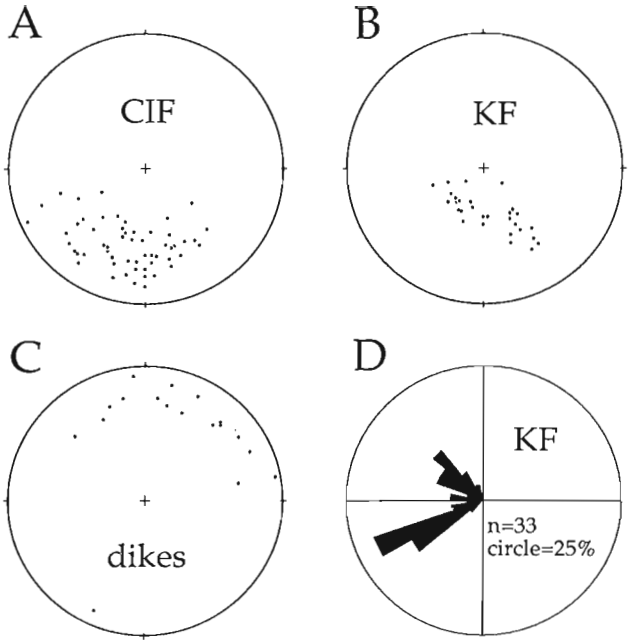

Figure 8. (A) Poles to bedding of Christopher Island Formation intravolcanic bedded tuffs and epiclastic rocks; (B) poles to bedding of Kunwak Formation sediments; (C) poles to minette feeder dyke planes; (D) rose diagram of strikes of bedding in the Kunwak Formation. Lower hemisphere equal area projections. Note the lower average dips of Kunwak Formation beds compared to Christopher Island Formation beds, and the strong bimodality of strikes in Kunwak Formation.

Trans-Hudson subduction-collisions. The tendency for lamproites to occur over fossil Benioff zones (Rowell and Edgar, 1983; Bergman, 1987) suggests that the potassic-ultrapotassic Christopher Island Formation has lamproitic affinities.

No study which we are aware of has identified the fractionation products of lamproites, although these rocks commonly occur as flows and should be associated on occasion with differentiated rocks. Bergman (1987, p. 146) suggested that lamproite and minette suites may represent broadly similar magmas crystallizing at different pressures. Pressure and disequilibrium reactions are important variables in potassic magmas, which are strongly heteromorphic due to mineral-liquid reactions involving (in this case) phlogopite and olivine (e.g., Yoder, 1986).

We consider that the intimate field association of Christopher Island Formation lamproites and minettes is evidence that magmas similar to average lamproite are related to *some* minettes, possibly differentiating by both crystal fractionation and crustal contamination. Further study of this problem is underway.

Tectonics and magma genesis

The nature of deformation of the lower Dubawnt Group is a constraint on the tectonic event which triggered production of potassic magmas. The strikes of Kunwak Formation

beds, and of the normal faults on which they rotated, are close to the orientations of the McDonald and Bathurst faults. The interpretation preferred here is that the non-dilational, pre- to postvolcanic brittle faulting at Dubawnt Lake reflects the propagation of extensions of these faults into the Dubawnt Lake area. Unfortunately, the age constraints on lower Dubawnt activity are poor. The error in the Amer syenite U-Pb age (1850+30/-10 Ma) is large, and it is not certain that this syenite is an intrusive equivalent of the Christopher Island Formation. Geochronological constraints on formation of the Christopher Island Formation are summarized in Figure 9.

Metasomatic enrichment of the mantle wedge overlying subducting oceanic lithosphere is probably responsible for considerable magma production in subduction zones (Tatsumi, 1989). Model Nd-Sm ages for the Christopher Island Formation, which are older than lithological ages, indicate an earlier episode of mantle enrichment (Esperanca and LeCheminant, 1986). The estimated time of enrichment, at ≈ 2.9 Ga, suggests that Thelon and Trans-Hudson subduction-collisions were not involved, but major-element modal metasomatism at ca. 2.0 Ga might be masked by an earlier event of trace element enrichment. Sr model ages for the Christopher Island Formation are 2.1 Ga. Poor correlation between the Sr and Nd isotopic systems is a common feature of potassic rocks (e.g., Bergman, 1987).

Extensively metasomatized mantle is more subject to partial melting than non-enriched mantle since phlogopite, amphibole, and carbonates melt completely near the solidus (Olafsson and Eggler, 1983). Wallace (in press) suggested that some minettes are derived from mantle so extensively metasomatized that olivine is completely replaced by phlogopite and clinopyroxene. This fact permits models which include either modest mantle uplift, or relatively inefficient heating of the lithospheric mantle, to produce potassic melts.

We propose the following model, elements of which have been suggested by A. LeCheminant, S. Tella, and P. Hoffman, which is consistent with known constraints summarized in Figure 9. (1) Subduction of oceanic crust beneath the Churchill Province (or beneath the Rae and Hearne provinces prior to their collision) occurred as a result of convergence of the Slave Province from the west (Thelon orogeny, ca. 2.0 Ga) and the Superior Province from the southeast (Trans-Hudson orogeny, ca. 1.9 Ga). Dehydration of the subducting lithosphere converted part of the overlying sublithospheric mantle to phlogopite peridotite by hydrous metasomatism. (2) Continental collision at ca. 1.9-1.85 Ga thickened lithosphere in the hinterland, forcing metasomatized mantle down into hotter asthenospheric mantle. (3) Brittle tectonics (McDonald and Bathurst faults, ca. 1.84 Ga) including possible gravitational collapse of the uplifted lithosphere on detachment faults, coincided with

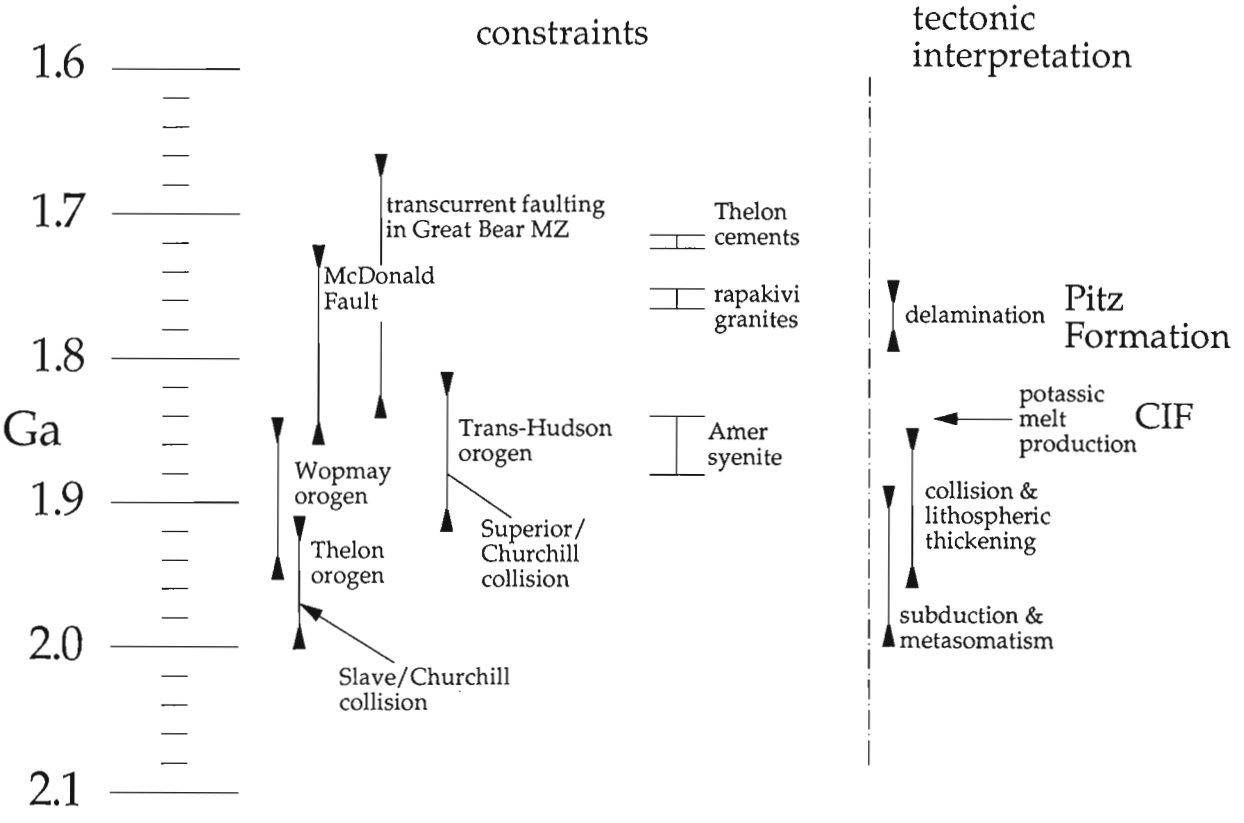

Figure 9. Tectonic constraints on Dubawnt Group volcanism and deformation, based on Hoffman (1988) and references therein. Bars for Thelon cements, rapakivi granites, and the Amer syenite represent U-Pb ages and errors. See text for discussion.

thermal relaxation in the metasomatized mantle and consequent production of ultrapotassic melts (CIF) which subsequently erupted through translithospheric fractures.

This model is similar to those proposed for the Gibraltar Arc (Platt and Visser,1989) and for the Tibetan Plateau (Molnar and Tapponnier, 1978; England andHouseman, 1988). Delamination and sinking of the dense lithospheric mantle root may follow formation of detachment faults. Such delamination would produce a thermal pulse in the suddenly thinned lithosphere, with the potential for melting of the lower crust. This could account for the anorogenic rapakivi granites and Pitz Formation rhyolites of the middle Dubawnt Group. An analytic model for delamination beneath the Colorado Plateau by Bird (1979) indicates that propagation of the delamination front over a distance of 400 km, the present length of combined lower Dubawnt Group basins, would take about 10 Ma and the resulting thermal anomaly would persist for about 50 Ma. The total is similar to the time gap between the Christopher Island Formation (assumed here to be 1.84 Ga) and Pitz Formation (ca. 1.76 Ga).

Pre-Christopher Island Formation sediments are thin to nonexistent in the Dubawnt Lake area, but reach thicknesses of about 2 km at the east end of the province, at Baker Lake (Blake, 1980).The sediments consist of basal conglomerate (South Channel, Angikuni Formations) and arkose (Kazan Formation). Paleocurrent data for the Kazan Formation near Baker Lake (Donaldson, 1965) and for the Kunwak Formation at Dubawnt Lake (this study) indicate northwesterly transport, suggesting downdropping of the west end of the lithosphere overlain by Christopher Island Formation rocks relative to its east end. If this is true, then volcanism must have begun earlier in the west, since prevolcanic sediments are thinnest there. This could be tested by precise dating across the volcanic province.

SUMMARY

The Christopher Island Formation (lower Dubawnt Group), a regionally developed suite of ultrapotassic and potassic lavas and volcaniclastic rocks, is dominantly of minette composition but has mafic members which are lamproitic. The absence of cogenetic basalts and of a nearby active subduction zone, but with evidence for earlier subduction, are hallmarks of lamproite volcanism and are characteristics of the Christopher Island Formation. Known geochronological, structural, sedimentological, and petrological constraints lead us to suggest the following scenario for Dubawnt time activity:

(1) Subduction of oceanic lithosphere at ca. 2.0 Ga (Thelon Arc) and at ca. 1.9 Ga (Trans-Hudson orogeny) resulted in metasomatic enrichment of the lithospheric mantle below the present Churchill Province.

(2) Lithospheric shortening and thickening in response to continental collisions at 1.9-1.85 Ga forced metasomatized lithospheric mantle down into hotter asthenospheric mantle.

(3) Thermal relaxation, and formation of primary ultrapotassic magmas (Christopher Island Formation), coincided with brittle tectonics and gravitational collapse of thickened lithosphere at ca. 1.84 Ga.

(4) Delamination of the lithospheric root indirectly produced anorogenic rhyolite volcanism at ca. 1.76 Ga (Pitz Formation), and renewed uplift and faulting.

Further structural and petrological studies, and above all geochronological data, are required to resolve the unique problems of the Dubawnt Group.

ACKNOWLEDGMENTS

We would like to thank Natalie Morisset, Bob Spark, and Bruce Kjarsgaard for their enthusiastic and capable assistance in the field. Paul Wallace, of the University of California, offered many useful observations in the field and counterpoint for discussions. T. Peterson gratefully acknowledges a field excursion led by Ian Carmichael to see minettes of the Mexican Volcanic Belt. The numerous contributions and invaluable assistance of A. LeCheminant (CGD) are gratefully acknowledged. The manuscript was critically reviewed by Paul Hoffman, with comments by J. Bédard (CGD).

REFERENCES

Allan, J.F., and Carmichael, I.S.E.
1984: Lamprophyric lavas in the Colima graben, SW Mexico; Contributions to Mineralogy and Petrology v. 88, p. 203-216

Bergman, S.C.
1987: Lamproites and other potassium-rich igneous rocks: a review of their occurrence, mineralogy and geochemistry; in J.G. Fitton, and B.G.J. Upton, (ed.) Alkaline Igneous Rocks, Geological Society Special Publication 30, p. 103-190

Bird, P.
1979: Continental delamination and the Colorado Plateau; Journal of Geophysical Research, v. 84, p. 7561-7571

Blake, D.H.
1980: Volcanic rocks of the Paleohelikian Dubawnt Group in the Baker Lake-Angikuni Lake area, District of Keewatin, N.W.T.; Geological Survey of Canada, Bulletin 309, 39 p.

Bostock, H.H., and Loveridge, W.D.
1988: Geochronology of the Taltson Magmatic Zone and its eastern cratonic margin, District of Mackenzie; in Radiogenic Age and Isotopic Studies: Report 2, Geological Survey of Canada, Paper 88-2, p. 59-65.

Bowring, S.A., Van Schmus, W.R., and Hoffman, P.F.
1984: U-Pb zircon ages from Athapuscow aulacogen, East Arm of Great Slave Lake, N.W.T., Canada; Canadian Journal of Earth Sciences v. 21, p. 1315-1324

Donaldson, J.A.
1965: The Dubawnt Group, Districts of Keewatin and Mackenzie; Geological Survey of Canada, Paper 64-20, 11 p.

England,P.C., and Houseman, G.A.
1988: The mechanics of the Tibetan plateau; Royal Society of London Philosophical Transactions, v. A326, p. 301-320

Esperanca, S. and LeCheminant, A.N.
1986: Isotopic evidence for multiple enrichment events from micalamprophyres in the District of Keewain, Canada; Geological Society of America, Program with Abstracts, v. 18, p. 595.

Foley, S.F., Venturelli, G., Green, D.H., and Toscani, L.
1987: The ultrapotassic rocks: characteristics, classification, and constraints for petrogenetic models; Earth Science Reviews, v. 24, p. 81-134.

Hoffman, P.F.
1980: Wopmay orogen: a Wilson cycle of early Proterozoic age in the northwest of the Canadian Shield; in: The Continental Crust and its Mineral Deposits, D.W. Strangway, ed. Geological Association of Canada, Special Paper 20, p. 523-549
1988: United Plates of America, the birth of a craton: early Proterozoic assembly and growth of Laurentia; Annual Reviews Earth and Planetary Science Letters, p. 543-603

LeCheminant, A.N., Leatherbarrow, R.W., and Miller, A.R.
1979: Thirty Mile Lake map area, District of Keewatin; in Current Research, Part B, Geological Survey of Canada, Paper 79-1B, p. 319-327

LeCheminant, A.N., Ianelli, T.R., Zaitlin, B., and Miller, A.R.
1981: Geology of Tebesjuak Lake map area, District of Keewatin: A progress report; in Current Research, Part B, Geological Survey of Canada, Paper 81-1B, p. 113-128.

LeCheminant, A.N., Miller, A.R., and LeCheminant, G.M.
1987a: Early Proterozoic alkaline igneous rocks, District of Keewatin, Canada: petrogenesis and mineralization; in T.C. Pharaoh, R.D. Beckinsale, and D. Rickard (ed), Geochemistry and Mineralization of Proterozoic Volcanic Suites, Geological Society of London Special Publication 33, p. 219-240.

LeCheminant, A.N., Roddick, J.C., and Henderson, J.R.
1987b: Geochronology of Archean and Early Proterozoic magmatism in the Baker Lake-Wager Bay region, N.W.T.; in Geological Association of Canada/Mineralogical Association of Canada, Program with Abstracts, v. 12, p. 66.

LeCheminant, A.N., and Heaman, L.
1989: Mackenzie igneous events, Canada: middle Proterozoic hotspot magmatism associated with ocean opening; Earth and Planetary Science Letters (in press).

Loveridge, W.D., Eade, K.E., and Roddick, J.C.
1987: A U-Pb age on zircon from a granite pluton, Kamilikuak Lake area, District of Keewatin, establishes a lower limit for the age of the Christopher Island formation, Dubawnt Group; in Radiogenic Age and Isotope Studies: Report 1, Geological Surevy of Canada, Paper 87-2, p. 67-71

Miller, A.R., Cumming, G.L, and Krstic, D.
1989: U-Pb, Pb-Pb, and K-Ar isotopic study and petrography of uraniferous phosphate-bearing rocks in the Thelon Formation, Dubawnt Group, Northwest Territories, Canada; Canadian Journal of Earth sciences v. 26, p. 867-880

Molnar, P. and Tapponnier, P.
1978: Active tectonics of Tibet; Journal of Geophysical research, v. 83, p. 5361-5375

Nicholls, J. and Carmichael, I.S.E.
1969: A commentary on the absarokite-shoshonite-banakite series of Wyoming, U.S.A; Schweizerische Mineralogische und Petrographische Mitteilungen 49, p. 47-64.

Olafsson, M. and Eggler, D.H.
1983: Phase relations of amphibole, amphibole-carbonate, and phlogopite-carbonate peridotite: petrologic constraints on the asthenosphere; Earth and Planetary Science Letters v. 64, P. 305-315

Peterson, T.D., LeCheminant, A.N., and Rainbird, R.H.
1989: Preliminary report on the geology of northwestern Dubawnt Lake area, District of Keewatin, N.W.T.; in Current Research, Part C, Geological Surevy of Canada, Paper 89-1C, p. 173-183

Platt, J.P., and Visser, R.L.M.
1989: Extensional collapse of thickened continental lithosphere: a working hypothesis for the Alboran sea and Gibraltar arc; Geology, v. 17, p. 540-543

Rainbird, R.H., and Peterson, T.D.
1990: Physical volcanology and sedimentology of lower Dubawnt Group strata, Dubawnt Lake, District of Keewatin, N.W.T.; in Current Research, Part C, Geological Survey of Canada, Paper 90-1C, p. xxx-xxx

Rock, N.M.S.
1984: The nature and origin of calc-alkaline lamprophyres: minettes, vogesites, kersantites and spessartites; Transactions of the Royal Society Edinborough, v. 74, p. 193-227
1987: The nature and origin of lamprophyres: an overview, in Alkaline Igneous Rocks, Fitton, J.G., and Upton, B.G.J., eds., Blackwell Scientific Publications, p. 191-226.

Roden, M.F., Smith, D., and McDowell, F.W.
1979: Age and extent of potassic volcanism on the Colorado Plateau; Earth and Planetary Science Letters v. 43, p. 279-284.

Rowell, W.F. and Edgar, A.D.
1983: Cenozoic potassium-rich mafic volcanism in the western USA: its relationship to deep subduction; Journal of Geology, v. 91, p. 338-341

Rowley, P.D., Anderson, J.J., Williams, P.L., and Fleck, R.J.
1978: Age of structural differentiation between the Colorado Plateau and Basin and Range provinces in southwestern Utah; Geology, v. 6, p. 51-55

Tatsumi, Y.
1989: Migration of fluid phases and genesis of basalt magmas in subduction zones; Journal of Geophysical Research, v. B94, p. 4697-4707

Tella, S., and Eade, K.E.
1980: Geology of the Kamilukuak Lake map area, District of Keewatin, a part of the Churchill Structural Province; in Current Research, Part B, Geological Survey of Canada, Paper 80-1B, p. 39-45
1985: Geology, Kamilukuak Lake, District of Keewatin, Northwest Territories; Geological Survey of Canada, Map 1629A, scale 1:250 000
1986: Occurence and possible tectonic significance of high-pressure granulite fragments in the Tulemalu fault zone, District of Keewatin, N.W.T., Canada, Canadian Journal of Earth Sciences, v. 23, p. 1950-1962.

Tella, S., Eade, K.E., Miller, A.R., and Lamontagne, C.G.
1981: Geology of the west half of the Kamilukuak Lake map area, District of Keewatin; a part of the Churchill structural province; in Current Research, Part A, Geological Survey of Canada, Paper 81-1A, p. 231-240.

Tella, S., Heywood, W.W., and Loveridge, W.D.
1985: A U-Pb age on zircon from a quartz syenite intrusion, Amer Lake, District of Keewatin, NWT; in Current Research, Part B, Geological Survey of Canada, Paper 85-1B, p. 367-370

Wallace, P.
— Minette lavas and associated leucitites from the western Front of the Mexican Volcanic Belt: petrology, chemistry, and origin; Contributions to Mineralogy and Petrology, in press.

Wyman, D.A. and Kerrick, R.
1989: Archean lamprophyre dikes of the Superior Province, Canada: distribution, petrology, and geochemical characteristics; Journal of Geophysical Research, v. 94, p. 4667-4696

Yoder, H.S.
1986: Potassium-rich rocks: phase analysis and heteromorphic relations; Journal of Petrology, v. 27, p. 1215-1228

Structural history and geotectonic evolution of the eastern Torngat Orogen in the North River map area, Labrador

Martin J. Van Kranendonk[1]
Continental Geoscience Division

Van Kranendonk, M.J., Structural history and geotectonic evolution of the eastern Torngat Orogen in the North River map area, Labrador; in Current Research, Part C, Geological Survey of Canada, Paper 90-1C, p. 81-96, 1990.

Abstract

The Early Proterozoic Torngat Orogen affects the western Nain and southeastern Rae provinces of the Laurentian Shield, and in the map area can be divided from east to west across strike into: 1) the foreland zone, 2) the Abloviak shear zone, and 3) the internides. The eastern orogen evolved in three stages. The effects of an early fold/thrust belt are preserved in the Aphebian Ramah Group. This was followed by the main stage of deformation at granulite- to amphibolite-grade, which involved sinistral simple shear and probable coeval E-W shortening in a transpressive collisional tectonic regime. The Ramah Group was affected by this deformation. E-W shortening across wide zones of steeply-lineated glassy ultramylonite outlived transcurrent shearing during uplift and cooling of the orogen. This sequence of deformation events is compared to that developed by previous workers farther north, and used to propose a geotectonic model for the evolution of the Torngat Orogen.

Résumé

L'orogène de Torngat du Protérozoïque précoce a des effets sur la partie ouest de la province de Nain et le sud-ouest de la province de Rae du Bouclier laurentidien, et, dans la zone illustrée sur la carte, il peut être divisé de l'est vers l'ouest, transversalement à la direction, en trois zones: 1) la zone d'avant-pays, 2) la zone de cisaillement d'Abloviak, et 3) les internides. L'orogène oriental s'est formé en trois étapes. Les effets dus à la formation précoce d'une zone de plissements-chevauchements ont laissé leurs traces dans le groupe de Ramah de l'Aphébien. Il s'ensuivit l'étape principale d'une déformation au degré de métamorphisme des granulites aux amphibolites qui a comporté un cisaillement simple senestre et un racourcissement est-ouest contemporain probable lors d'une phase tectonique de collision de transpression. Le groupe de Ramah a été affecté par cette déformation. Le raccourcissement est-ouest à travers de vastes zones d'ultramylonite vitreuse à linéation très inclinée a survécu à un cisaillement de coulissage durant le soulèvement et le refroidissement de l'orogène. Cette séquence de déformation est comparée à celle élaborée dans le passé par des chercheurs dans une zone plus septentrionale et elle est utilisée pour composer un modèle géotectonique de l'évolution de l'orogène de Torngat.

[1] Department of Geological Sciences, Queen's University, Kingston, Ontario, K7L 3N6.

INTRODUCTION

The Early Proterozoic Torngat Orogen (Mengel, 1988: Fig. 1) is well exposed between latitudes 57°30'N and 58°N inthe North River map area of Labrador (Fig. 2). It separates high-grade Archean gneisses of the Nain Province from Archean and Early Proterozoic gneisses of the southeastern Rae Province in the Laurentian Shield (Hoffman, 1988; Wardle et al., in press), and has been defined as a zone of granulite- to amphibolite-grade, sinistral shear deformation of Early Proterozoic age (Mengel, 1988). The northern part of the orogen was described by Taylor (1979), Morgan (1975), Ryan et al. (1983, 1984), Wardle (1983, 1984), Mengel (1984, 1985, 1988), and Korstgård et al. (1987). The southern extension, south of Hebron Fiord (Fig. 1), has been studied as part of a three year regional mapping project of the North River and Nutak map areas (NTS maps 14E and 14F) headed by I. F. Ermanovics of the Geological Survey of Canada (Ermanovics et al., 1988, 1989). The author's fieldwork during the project forms the basis for a PhD thesis at Queen's University. In this report, the geology of the eastern Torngat Orogen in the North River map area is described, and the structural history is compared to that established by previous workers farther north. Using these results, a geotectonic model for the evolution of the orogen is developed.

PRINCIPAL GEOLOGICAL ELEMENTS

Archean amphibolite- to granulite-grade gneisses of the Nain Province form the basement east of the orogen (*see* Ermanovics et al., 1988; Van Kranendonk et al., 1989), and have a geological history as old as 3.8 Ga (Schiøtte et al., 1989). Following Late Archean deformation at granulite- to amphibolite-grade, a swarm of Early Proterozoic diabase dykes (Napaktok dykes) intruded along NE-SW and NW-SE fractures at shallow crustal levels. This complex of gneisses and dykes is unconformably overlain by two Aphebian supracrustal successions; the Mugford Group in the east (Smyth, 1976), and the Ramah Group in the west (Morgan, 1975; Knight and Morgan, 1981) (*see* Fig. 1).

The Ramah Group in the map area is discontinuously preserved within a 75 km long by up to 2 km wide tectonic sliver that locally includes basement, and strikes parallel to the orogenic front at about 160° (Ermanovics et al., 1988, 1989; Van Kranendonk and Ermanovics, 1989: Fig. 2, 6, and 8). The Ramah Group is metamorphosed at upper amphibolite grade, and is predominantly composed of interbedded quartzite and pelite, diabase sills, and subordinate beds of quartz pebble conglomerate and calc-silicate. Bedding is commonly preserved, particularly in quartzite layers where crossbedding is locally evident. In the northern half of the map area (Fig. 6) the Ramah Group retains its unconformable relationship on pinkish-weathering, altered basement gneisses and dark green amphibolite Napaktok meta-dykes of the Nain Province (Ermanovics et al., 1988). At the unconformity, a distinctive zone up to 15 m thick is composed of $\leq$20% elliptical white clots (up to 2x5 cm) of quartz and sillimanite in a medium grained, pink, quartzofeldspathic matrix (Fig. 3a). This unit grades up through thinly interbedded quartz arenite and fine- to medium-grained, pink, meta-arkose (Fig. 3b), into orthoquartzites and conglomerate interbeds of the Ramah Group. This sequence locally contains up to 10% magnetite-bearing pegmatites, and may represent a metamorphosed regolith. In the southern map area, where the Ramah Group is more strongly deformed and more highly migmatized, contacts with the basement are tectonic.

Rocks of the Archean Nain Province and overlying Aphebian supracrustal sequences were deformed within the Early Proterozoic Torngat Orogen, which can been divided into three principal tectonic elements from east to west; 1) the foreland zone, 2) the Abloviak shear zone (ASZ), and 3) the "internides" (c.f. Korstgård et al., 1987: Fig. 1 and 2).

The foreland zone is a structurally complex region along the Nain-Churchill boundary as defined by Taylor (1971). It forms the focus of this report, and is described in the following section. Structures in the foreland zone grade westward into the ASZ, a granulite- to amphibolite-grade, subhorizontally lineated sinistral shear zone that extends northward for about 400 km from the map area to Abloviak Fiord in northeastern Quebec (Taylor, 1979; Korstgård et al., 1987: Fig. 1). In the map area, the ASZ is about 20 km wide and strikes about 160° (Fig. 2). It shows evidence of both sinistral simple shear and approximate E-W pure shear (i.e. L-S shear fabrics, extensional shear bands (Fig. 3c), and N-S trending buckle folds). Several lithological units are deformed within the ASZ. However, the bulk of this zone is underlain by a distinctive unit of quartz-feldspar-garnet-biotite-sillimanite-graphite paragneiss known as the Tasiuyak gneiss (Wardle, 1983). Up to 40 km wide in the map area, the Tasiuyak gneiss has been interpreted as a diatexite derived from aluminous metasedimentary protoliths (Ryan, 1983, 1984; Wardle, 1983, 1984) that are probably the southeasterly equivalents of the Aphebian Lake Harbour Formation (N. Goulet, pers. comm. 1989; Fig. 1).

The western margin of the ASZ is placed along a gradational boundary between straight, mylonitic gneisses of the shear zone proper, and the internides of the Torngat Orogen, in which large-scale, tight, upright folds of strongly deformed, though less highly strained, compositional layering can be recognized along a N-S trend (Fig. 3d). Folds of this style pass westward through the Tasiuyak gneiss into migmatitic orthogneiss and metasedimentary gneiss of the Lac Lomier complex.

Five lithological assemblages have been identified from east to west across the Torngat Orogen in the map area (Fig. 2).

1. Nain Province gneisses and Napaktok meta-dykes.
2. Ramah Group metasediments and metadiabase sills.
3. Tonalitic orthogneiss and migmatite, meta-anorthositic gneiss, and subordinate paragneiss of unknown age, but which are physically similar to Nain Province gneisses except that they lack Napaktok dykes.
4. Tasiuyak metasedimentary gneiss, and homogeneous, charnockitic gneiss.
5. Tonalitic orthogneiss and migmatite, mafic granulite, paragneiss, and homogeneous, charnockitic gneiss (identical to those of assemblage 4) of the Lac Lomier complex.

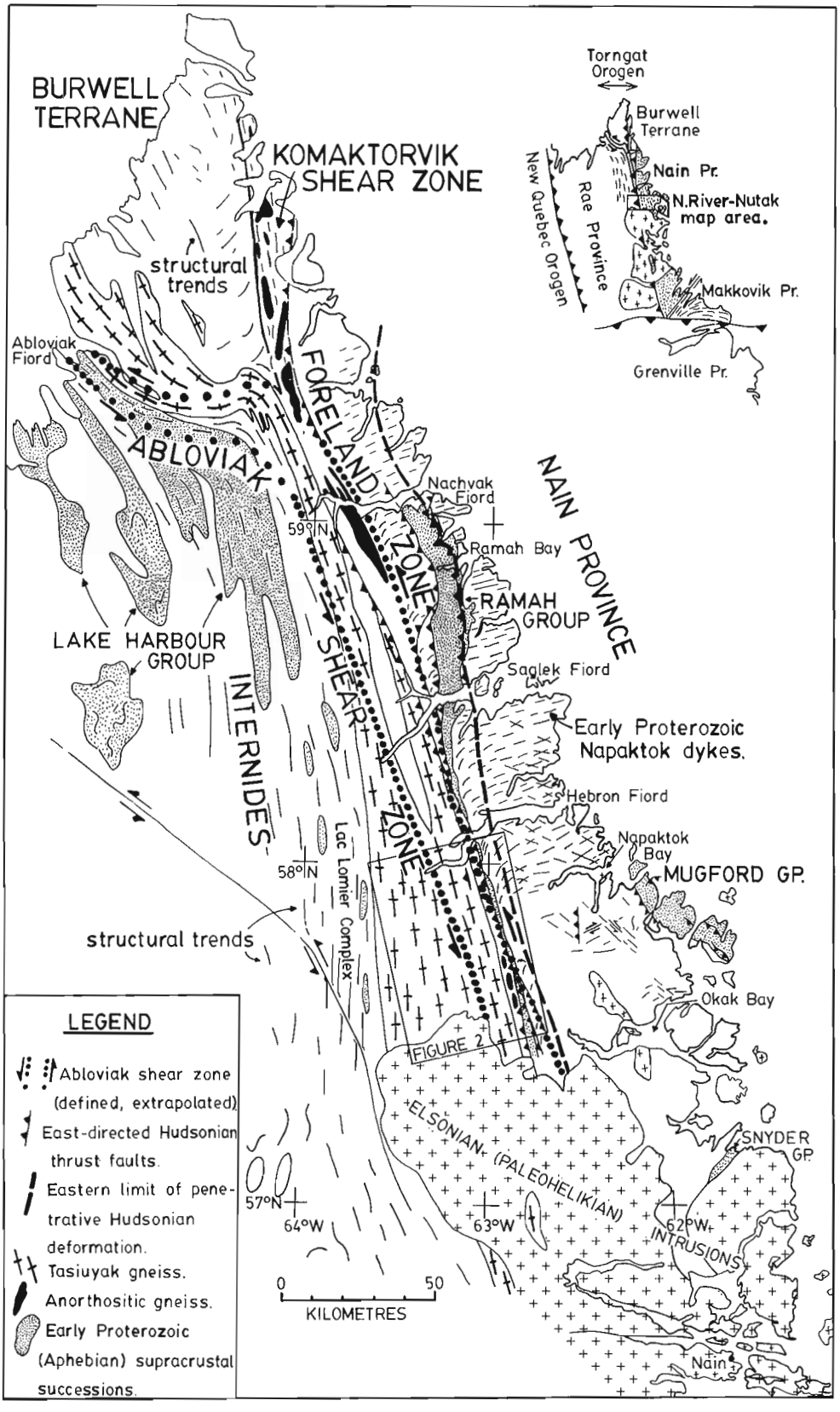

Figure 1. General geological map of northern Labrador, showing the principal geological and tectonic elements of the Torngat Orogen. Information compiled from Korstgard et al. (1987), Wardle et al. (in press), Taylor (1975), and N. Goulet and A. Ciesielski (pers. comm., 1989).

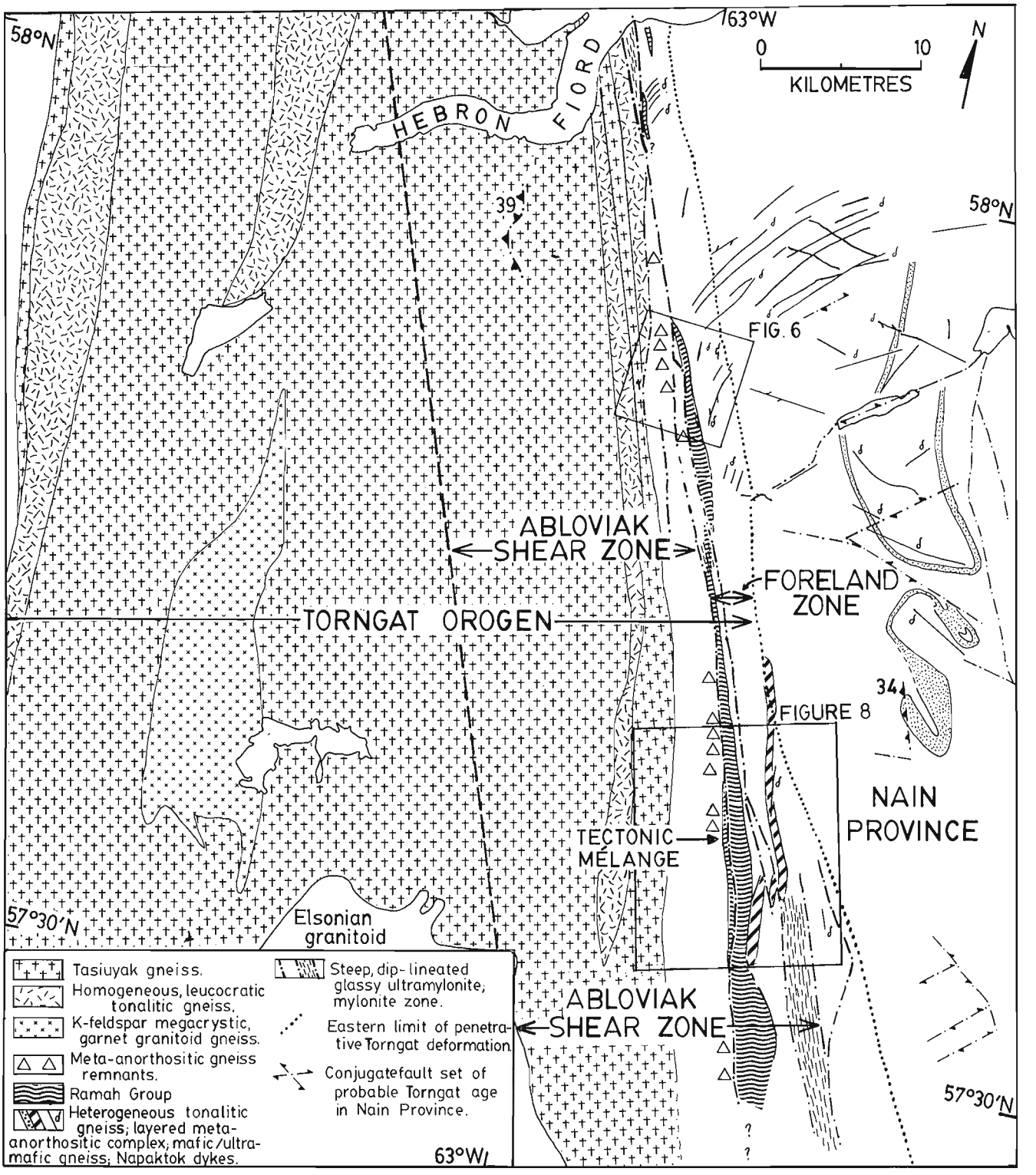

Figure 2. General geological map of the eastern Torngat Orogen in the North River map area. Notice that the Ramah Group is transgressed by the Abloviak shear zone in the southern map area.

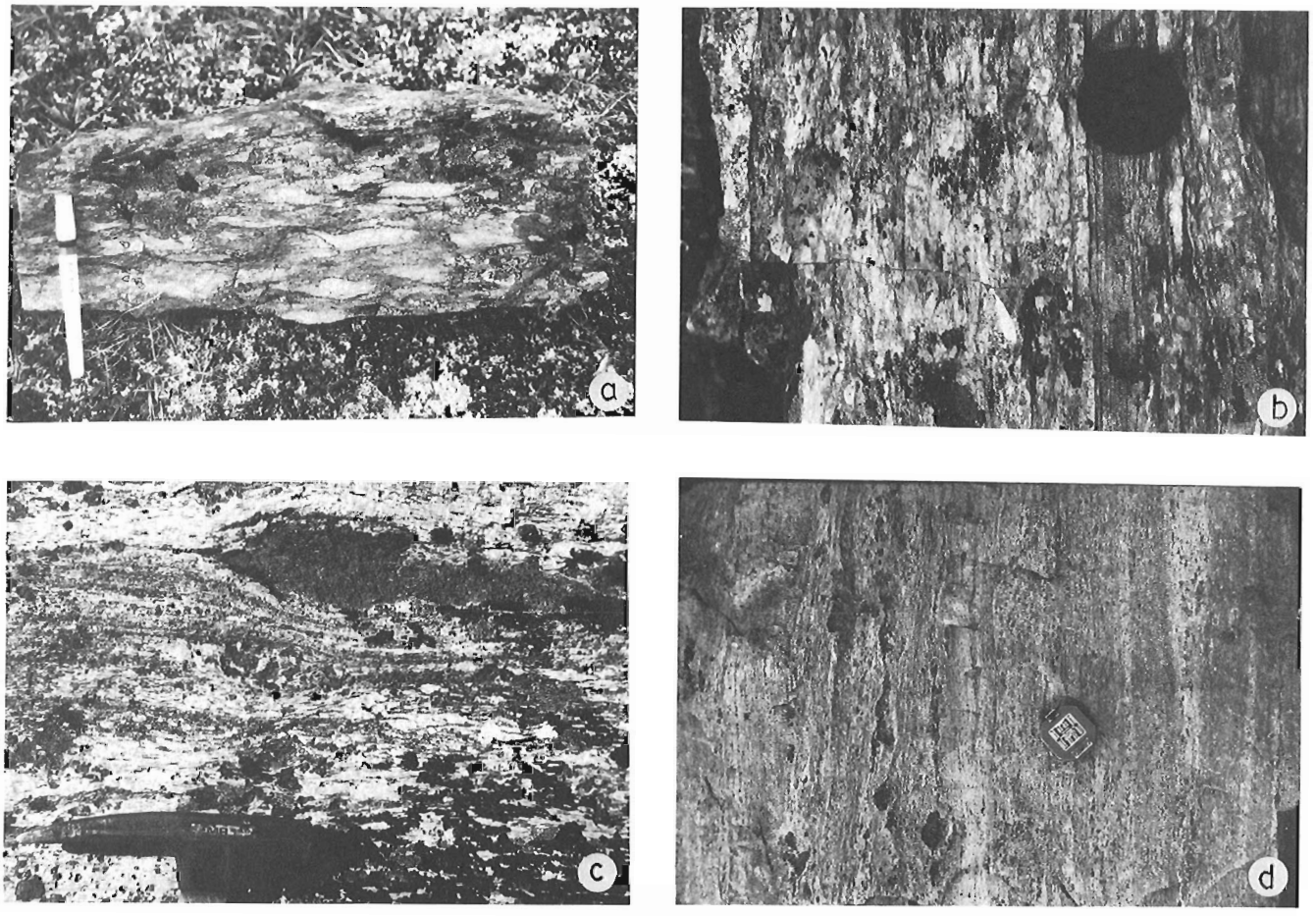

Figure 3. a) Clotty-textured unit of probable metamorphosed regolith near the unconformity between the Ramah Group and basement gneisses (x pattern in Fig. 6). Pen is 13.5 cm long. b) Transition between clotty-textured gneiss (left) and overlying, finely interbedded quartzite and arkose of the Ramah Group. Lens cap is 64mm in diameter. c) Sinistral extensional shear band in mylonitic Tasiuyak gneiss of the Abloviak shear zone. d) Compositional layering in lower-strained Tasiuyak gneiss from the internides of the Torngat Orogen. Brunton compass is about 8 cm wide.

These assemblages are continuous along the Torngat Orogen. In particular, note the train of meta-anorthositic gneiss bodies in lithological assemblage 3 (Fig. 1). The lithological contact between the Nain and Rae provinces is interpreted to lie between assemblages 2 and 3 (*see* Discussion).

EARLY PROTEROZOIC DEFORMATION

Early Proterozoic deformation affected the Nain Province as far east as the Mugford Group, 60km east of the orogenic front (Fig. 1). Deformation features in the Mugford Group include folds and northeast-verging thrusts developed at greenschist grade (Smyth, 1976; Ermanovics et al., 1989). In the Nain Province, effects of Early Proterozoic deformation include sheared Napaktok dykes and NNW-striking, shallow west-dipping mylonite and pseudotachylyte breccia zones that show west-side-up displacement. The dykes are sheared parallel to their conjugate NW-SE and NE-SW emplacement pattern (Fig. 4), and may show 100s of metres displacement across their borders. These deformation features indicate approximate E-W shortening across the Nain Province during Early Proterozoic orogenesis.

Approaching the foreland zone, Napaktok dykes and Archean structures in the Nain Province become deflected counterclockwise to NNW strikes by sinistral simple shear (Mengel, 1985). NE- to E-striking dykes are passively deflected, whereas NW striking dykes are buckled and strongly deformed. The eastern margin of the foreland zone is placed along the eastern limit of penetrative Early Proterozoic foliation that cuts Archean gneissosity (Fig. 5a) and is parallel to the orogenic front (Fig. 6). This boundary coincides roughly with the appearance of garnet-bearing mineral assemblages in Napaktok dykes, and of a pervasive hornblende overprint of Archean mineral assemblages in Nain Province gneisses. The western limit of the foreland zone is placed along the eastern limit of strongly lineated mylonitic gneisses of the ASZ whose L-fabric plunges shallowly to the north on subvertical schistosity planes.

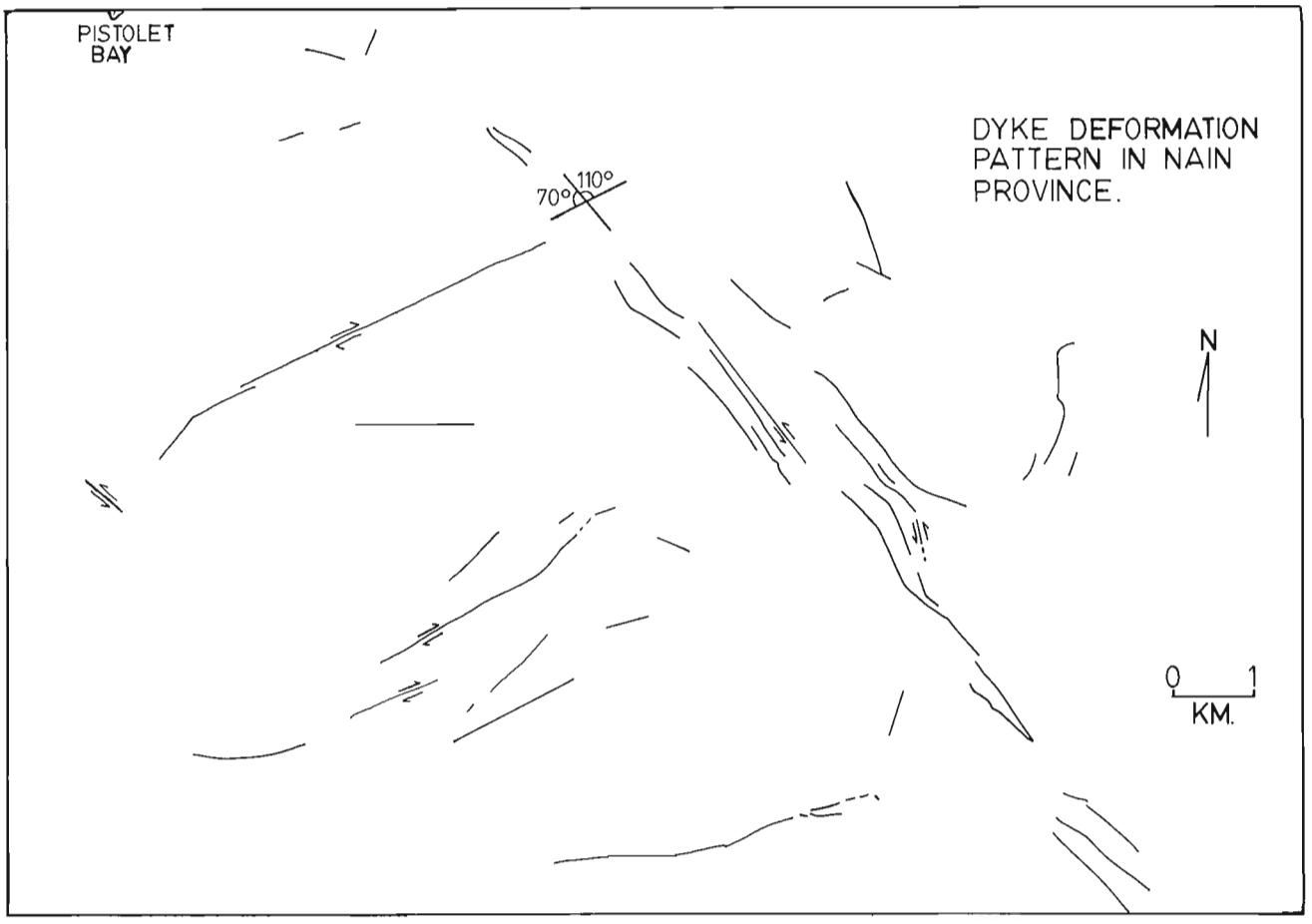

Figure 4. Map pattern of sheared Napaktok meta-dykes in the Pistolet Bay area of the Nain Province.

Three sets of Early Proterozoic structures are present in the foreland zone (Fig. 6). These include: 1) a set of early structures which are preserved only in the least deformed Ramah Group; 2) structures related to Abloviak sinistral shearing; and 3) subvertical zones of dip-lineated, porphyroclastic to glassy ultramylonite and pseudotachylyte breccia that strike parallel to the orogenic front across the ASZ/foreland zone transition.

Structures that were formed prior to Abloviak shearing are preserved in the least deformed Ramah Group, located in the foreland zone in the northern map area (Fig. 6). These structures include rootless isoclinal folds of bedding, and curviplanar dislocation surfaces which truncate bedding within the Ramah Group and juxtapose the Ramah Group against Archean basement gneisses (*see* Fig. 4a-c in Ermanovics et al., 1989). These dislocation surfaces are interpreted as early thrust faults which developed in a thickening fold and thrust belt. Notice the mini-duplex structure of early thrusts in the largest sliver of the Ramah Group illustrated in Figure 6, where three early thrust faults repeat the unconformity between the lowest structural occurrence of this distinctive zone and the roof thrust. A northeasterly component of tectonic transport during thrusting is indicated by the geometry of this duplex structure and by the asymmetry of a local set of thrust-related folds.

The second set of Early Proterozoic structures are related to Abloviak shearing, and overprint structures associated with the early fold/thrust belt in the Ramah Group. The intensity of the Early Proterozoic foliation increases westward within the foreland zone. In the northern map area (Fig. 6), this is accompanied by S-asymmetric folding of transposed Archean gneissosity in rocks derived from the Nain Province (Fig. 5b), of buckled Napaktok dykes (Fig. 5c), and of a metamorphic schistosity that is generally subparallel to bedding in the Ramah Group (Fig. 5d). In the easternmost foreland zone, these folds have steep to moderate south-plunging axes (Fig. 6). Westward within the foreland zone, fold axes become shallower and are subparallel to an increasingly more intense stretching lineation. Within the ASZ and the internides of the Torngat Orogen, folds and mineral stretching lineations plunge shallowly to the north (Fig. 7). Abundant indicators of sinistral displacement (i.e. the asymmetry of the folds where steeply-plunging, extensional shear bands, and rotated metamorphic porphyroblasts) show that these structures were formed during Abloviak shearing. The gradual east to west transition in the orientation and intensity of Abloviak-related structures is continuous into the Ramah Group (e.g. Fig. 6). The continuity of Abloviak-related structures between the Ramah Group and and adjacent reworked basement gneisses

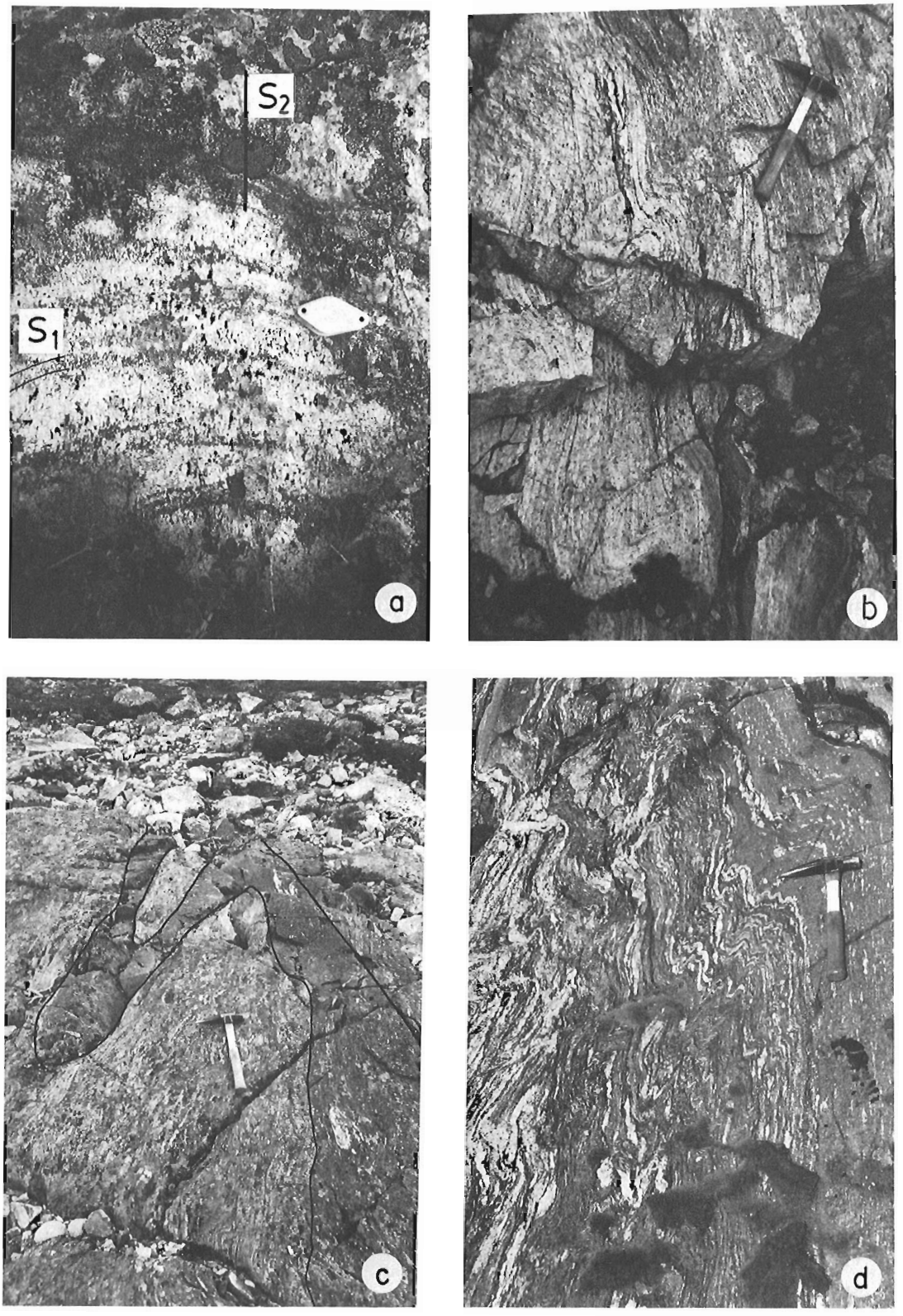

Figure 5. a) Early Proterozoic foliation (S .sub 2) cutting Archean gneissosity (S .sub 1) in the foreland zone of the Torngat Orogen. View to the SSE. Lens is 3cm long. b) S-folded gneissosity in Nain Province gneisses reworked by Early Proterozoic deformation within the foreland zone of the Torngat Orogen. c) S-folded apophysis of a Napaktok dyke (area inside ink lines), deformed and metamorphosed within the foreland zone of the Torngat Orogen. View is to the northwest. d) S-folded schistosity in metapelites from the eastern Ramah Group where it is deformed within the Abloviak shear zone in the southern map area. View to the NNW.

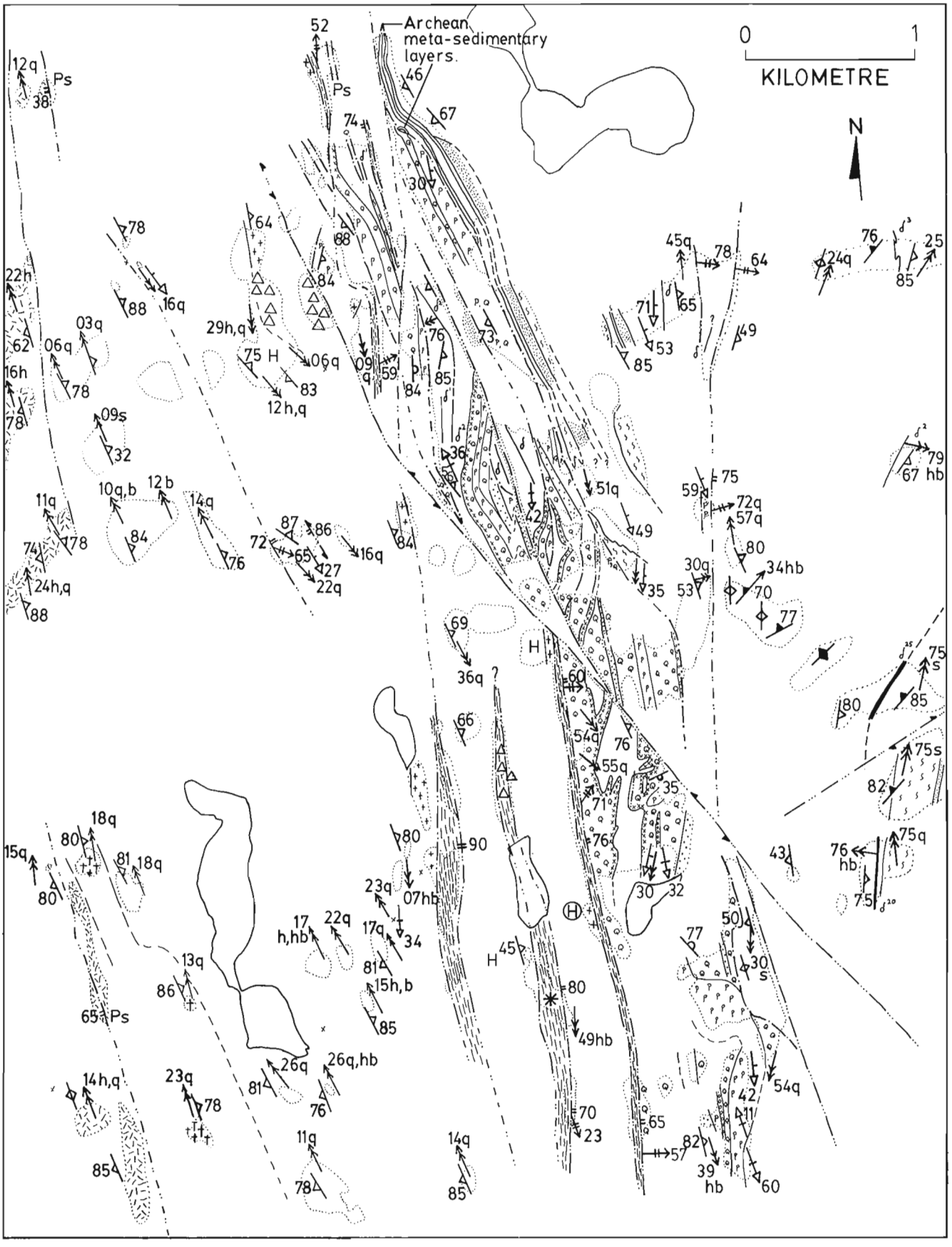
Archean meta-sedimentary layers.
0
1
KILOMETRE
N

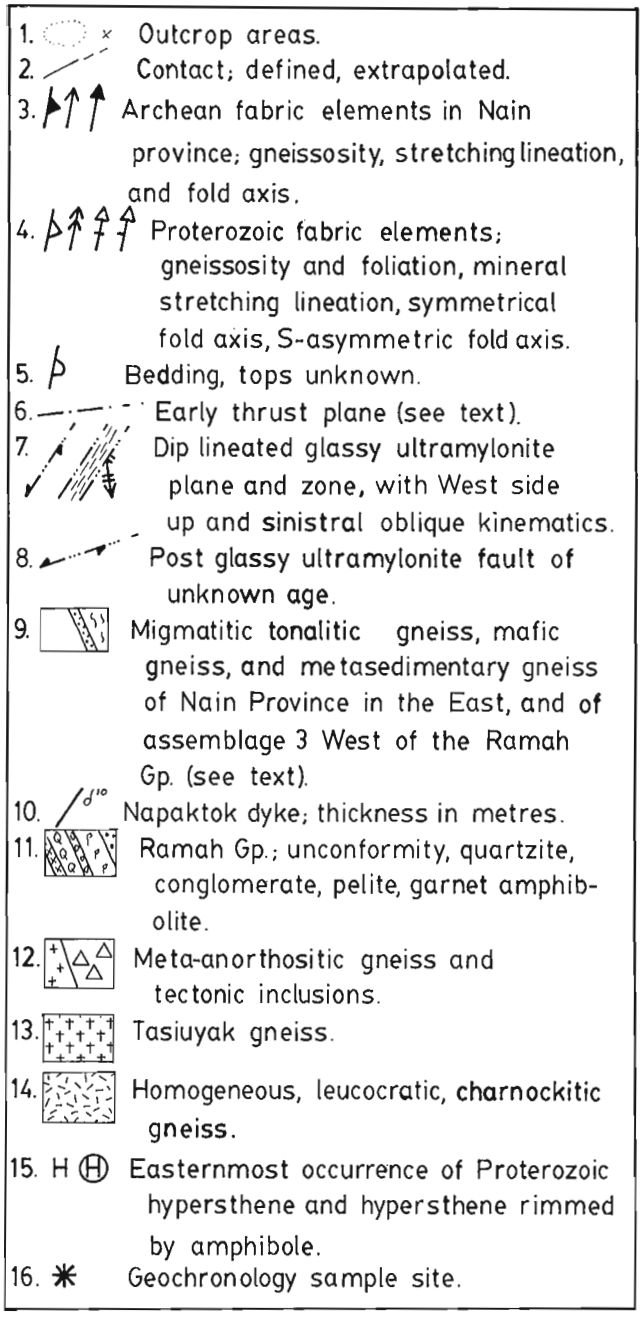

Figure 6. Detailed geological map of the Ramah Group in the northern part of the North River map area. In this region, the Ramah Group is deformed in the foreland zone of the Torngat Orogen and is in contact with gneissic Archean basement and Napaktok dykes across three types of curviplanar surfaces: i) unconformity (x — pattern), ii) early thrust faults (dash-dot lines), and iii) late, glassy ultramylonites with down-dip stretching lineations (dash-dot-dot lines). Note the duplex structure of early thrusts in the southern part of the largest sliver of Ramah Group, and the gradual east to west transition of Early Proterozoic fabric element orientations across the map area. Stereonet plots of these fabric elements are presented in Figure 7.

proves that the Ramah Group was deformed by Abloviak shearing in the Torngat Orogen (Van Kranendonk and Ermanovics, 1989).

The third set of Early Proterozoic structures consists of several steep zones of porphyroclastic to glassy ultramylonite and pseudotachylyte breccia (Fig. 9a) that cut all previous structures and telescope the metamorphic gradient associated with the main stage of Abloviak deformation (c.f. Mengel, 1988). These remarkable zones are up to 400m wide and strike parallel to the orogenic front (Fig. 2). They contain dip-parallel stretching lineations and kinematic indicators of west-side-up displacement, regardless of the dip of these zones, which changes across strike from shallow west-dipping in the ASZ, to steeply west-dipping, subvertical, and steeply east-dipping across the foreland zone (Fig. 6). These zones of glassy ultramylonite are analogous to the zones of west-side-up mylonite and pseudotachylyte breccia found across the Nain Province, and may be coeval with thrusting in the Mugford Group. U-Pb ages on two fractions of igneous zircon separated from a medium grained, pink granite sheet that was deformed only by the dip-slip movement within a glassy ultramylonite zone located just west of the Ramah Group (Fig. 6), gives a maximum age of this deformation at 1808 and 1805 ±5 Ma (C. Roddick, pers. comm., 1989).

A more complex set of structures occurs across the eastern Torngat Orogen in the southern map area, where mapping was conducted this summer by S. Hanmer (GSC) and D.J. Scott (Queen's University) (Fig. 8). In this region, the foreland zone is 1-2km wide, and the ASZ transgresses the Ramah Group at amphibolite grade for up to 4 km into rocks derived from the Nain Province. The western margin of the Ramah Group is bounded by a 200 m wide, steeply dipping zone of black, dip-lineated, porphyroclastic to glassy ultramylonite that grades westward into a 200 m wide tectonic mélange (Fig. 8). This unique zone strikes parallel to the orogenic front and gives way in the west to granulite grade, subhorizontally lineated mylonitic gneisses derived from lithological assemblages 3 and 4.

Pre-Abloviak structures are not preserved in the Ramah Group in the southern map area because of the very high strain that accompanied Abloviak shearing. The Ramah Group is preserved within a 2km wavelength, north-plunging, upright antiform, as seen from the symmetrical distribution of small-scale asymmetric folds across its strike length (Fig. 8). Interbedded quartzites and metapelites show alternating dip-parallel and subhorizontal stretching lineations respectively, on all scales down to several millimetre thick interbeds (Fig. 9b). Quartzite beds with dip-parallel lineations grade into the glassy ultramylonite zone in the west and show west-side-up kinematics, whereas metapelitic layers are tightly folded about subhorizontal axes whose plunge varies along the length of the orogen in the map area (*see* Fig. 3 in Ermanovics et al., 1989), and are strongly deformed by sinistral simple shear along the eastern limb of the fold where fabrics are parallel to those in adjacent mylonitic gneisses derived from the Nain Prov-

ince. Locally, non-coaxial folds formed in metapelitic layers through the interaction of these two structures, which appear to have developed at identical metamorphic conditions.

East of the Ramah Group, mylonitized Nain Province gneisses deformed within the ASZ under amphibolite grade conditions contain subhorizontal stretching lineations and fold axes for up to 4km east of the Ramah Group until they abut a ≤200 m wide unit of mafic and ultramafic rocks (Fig. 2 and 8). Immediately adjacent to the mafic rocks, orthogneiss contains Early Proterozoic dip-parallel stretching lineations and indicators of both west-side-up and sinistral movement (S. Hanmer, pers. comm., 1989). A similar situation was observed by the author in the foreland zone of the northern map area, where subhorizontally lineated orthogneiss is in many places juxtaposed against Napaktok metadykes which contain a steeply dipping stretching lineation of recrystallized plagioclase and hornblende aggregates (Fig. 6). In these areas, neither overprinting relationships of the two structures, nor difference in metamorphic grade of the two structures were observed.

On the western margin of the Ramah Group, the unit of tectonic mélange is composed of a garnetiferous and sillimanite-bearing quartzofeldspathic matrix derived from semipelitic compositions of the Ramah Group that contains about 25 % of tectonic inclusions of metasediment (quartzite, metapelite, calc-silicate, and locally marble) and garnet amphibolite that are also derived from the Ramah Group (Fig. 9c). Two slices of tonalitic orthogneiss are deformed within this zone, the eastern of which contains intensely folded and boudined, but nevertheless recognizable, Napaktok dykes, indicating derivation from Nain Province protoliths (I. Ermanovics, pers. comm., 1989). The eastern slice contains no dykes and is therefore grouped within lithological assemblage 3 (Fig. 8b).

Stretching lineations within the tectonic mélange zone vary from subhorizontal to subvertical in layers with no apparent rheological differences. Kinematic indicators in these layers (i.e. rotated inclusions and porphyroclasts, foliation "fish") show sinistral and west-side-up displacement respectively. In the adjacent porphyroclastic to glassy ultramylonite zone, stretching lineations are subvertical. However, kinematic indicators of both west-side-up and sinistral transcurrent displacement are abundant. Significantly, the structures in both the tectonic mélange and glassy ultramylonite zones formed under identical metamorphic conditions, with dip-slip zones containing stable amphibolite facies mineral assemblages identical to those preserved in adjacent regions deformed by transcurrent shearing. Locally, greenschist grade assemblages and pseudotachylyte in the dip-slip zones demonstrate that they acted as loci for continued deformation as the orogen was exhumed to shallow crustal levels.

These relationships in the southern map area can be explained by two models which, at this stage of the investigation, are equally tenable. The alternating structures in the Ramah Group could have resulted from either: 1) overprinting between early transcurrent shearing, whose fabrics are preserved in the east, and subsequent E-directed thrusting, whose fabrics are concentrated within quartzite beds and intensified from east to west across the Ramah Group toward the zone of glassy ultramylonite and tectonic mélange; or 2) coeval E-W shortening and sinistral simple shearing during oblique transpression in the main stage of Torngat orogenesis. In this model, relatively competent quartzite layers accommodated the bulk of the shortening strain by predominantly dip-parallel slip that was accompanied by only relatively minor buckling, whereas the less competent metapelitic layers absorbed the transcurrent component of the deformation and were strongly folded by the

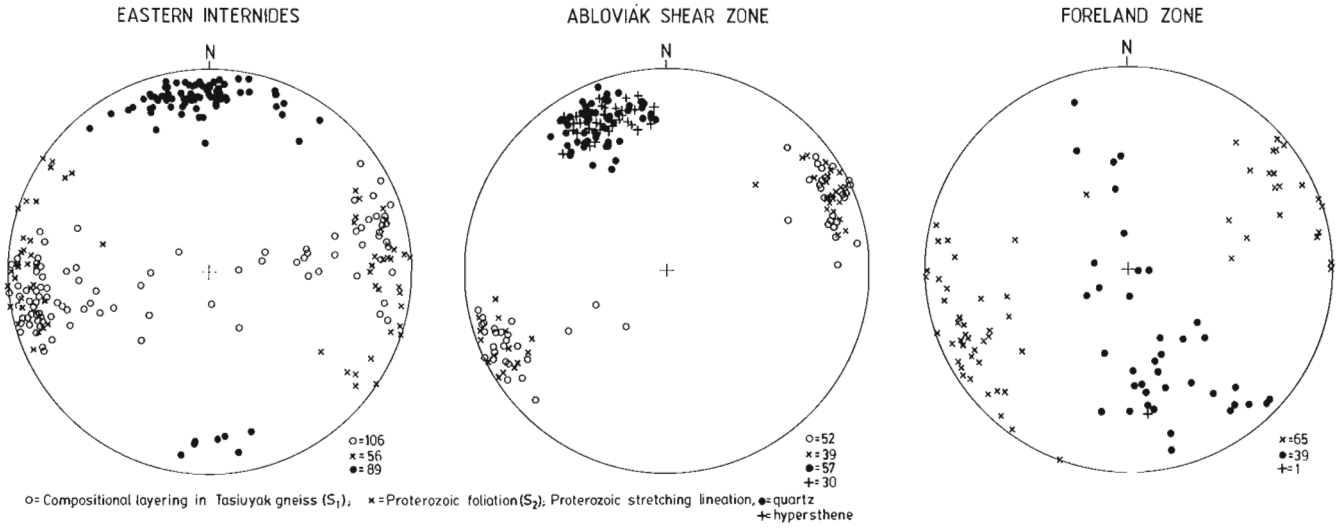

Figure 7. Lower hemisphere equal-area stereonet plots of Early Proterozoic fabric elements across the eastern Torngat Orogen in the northern map area, illustrated in Figure 6.

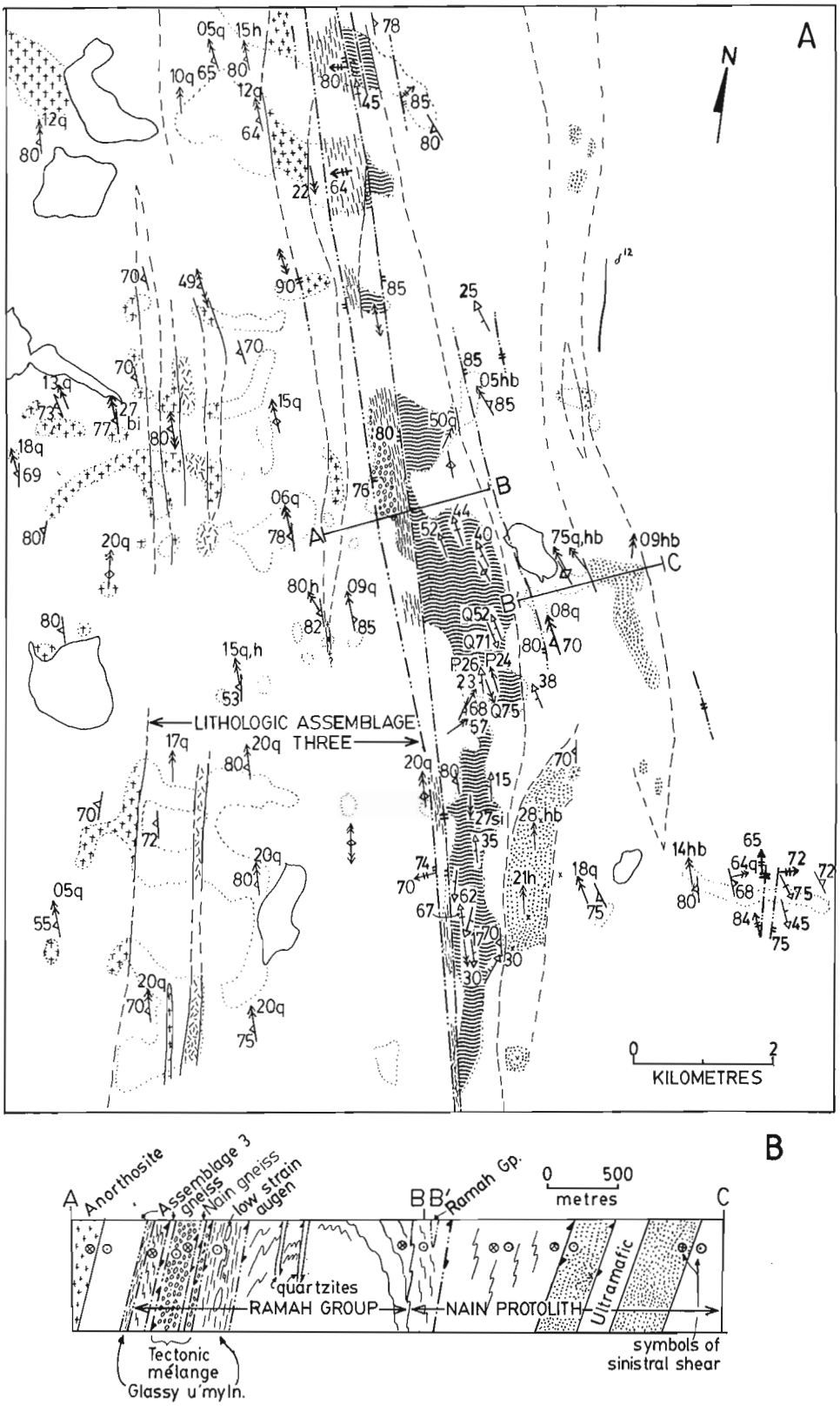

Figure 8. a) Geological map of the eastern Torngat Orogen in the southern map area. Notice the fold geometry of the Ramah Group, the location of the tectonic mélange zone, and the position of the cross-section profile A-B-C. Same legend as for Figure 6. b) Schematic cross-section of the eastern Torngat Orogen in the southern map area, showing the geometry of the folded Ramah Group and the principal elements of the tectonic mélange in profile.

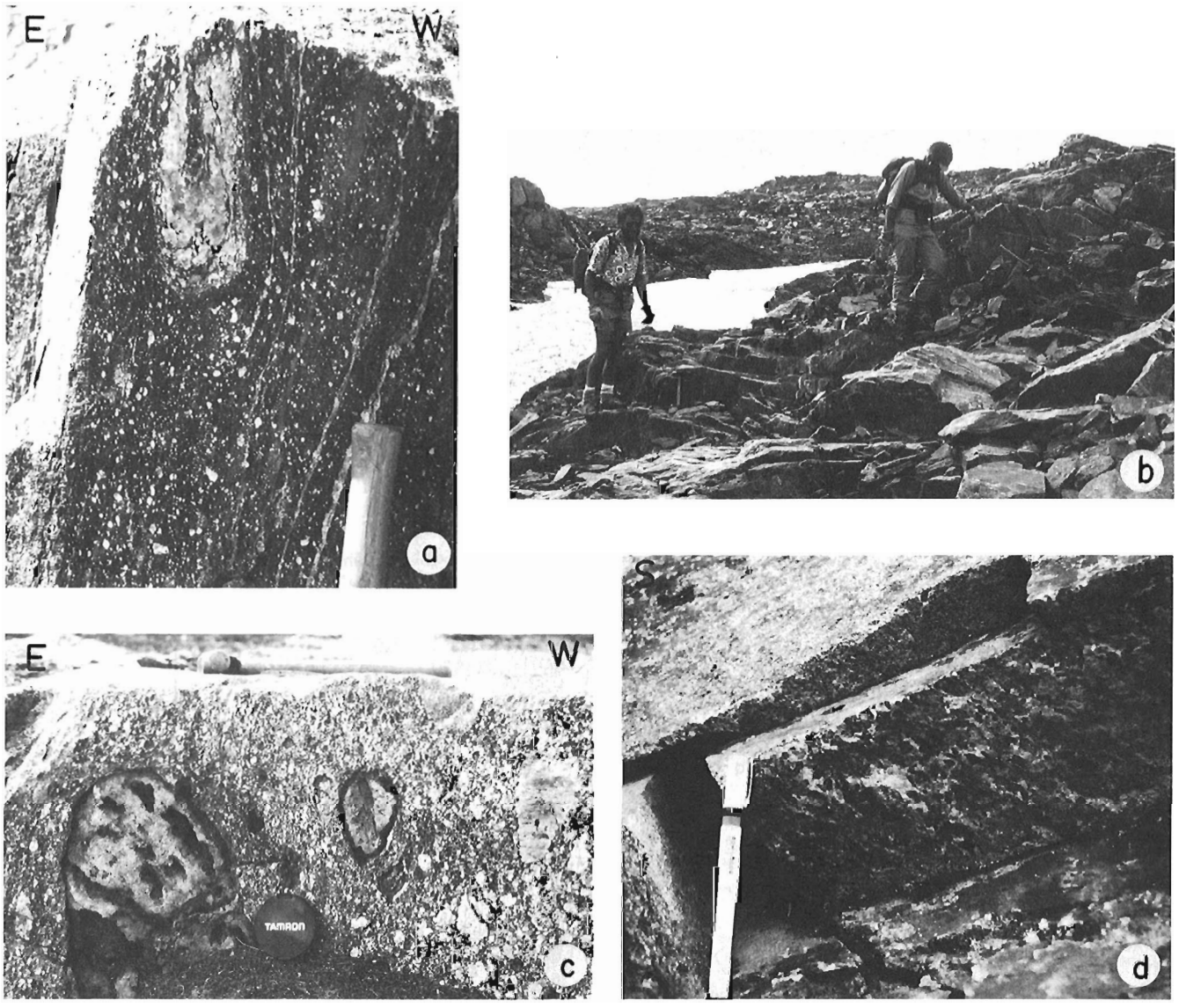

Figure 9. a) View to the south of a vertical plane through NNW-striking, dip-lineated porphyroclastic ultramylonite derived from coarse granitic material. From just east of the tectonic mélange zone in the southern map area. b) Alternating vertically and horizontally lineated quartzite and metapelitic layers of the Ramah Group deformed within the Abloviak shear zone in the southern map area. c) View to the south of a vertical plane through an outcrop of tectonic mélange. Blocks of calc-silicate are composed of actinolite rimmed by hornblende, and sit in a coarse grained quartzofeldspathic matrix containing garnet and sillimanite, all of which are derived from the Ramah Group. d) Moderately N-plunging lineated hypersthene in homogeneous charnockite of lithological assemblage 4 from the eastern Abloviak shear zone. Pen is 13.5 cm long.

shortening component of the deformation on subhorizontal axes whose plunge varied along strike (Fig. 10). The observed change in plunge of Early Proterozoic stretching lineations adjacent to mafic layers in reworked Nain gneisses can also be explained by the transpression model, which for this reason, is preferred at this time. The mafic layers are interpreted as having formed rigid butresses in relatively incompetent orthogneiss, thereby concentrating the E-W shortening component of the deformation. The zones of intense dip-slip shearing may have nucleated during transpression, and outlived the transcurrent component of the deformation as the orogen was exhumed.

METAMORPHISM

The metamorphism accompanying Early Proterozoic deformation caused a gradual transition from a greenschist grade overprint of Archean high grade mineral assemblages east of the foreland zone to a regional granulite grade metamorphism of all rock types west of the glassy ultramylonites. The grade of metamorphism in the Ramah Group is consistent with this transition, regardless of its position within the foreland zone or the ASZ. The Napaktok dykes also record this steady westward increase in metamorphic grade. Therefore, no field evidence was found in the map area to support

the hypothesis of two metamorphic events along the Nain-Churchill boundary zone (c.f. Mengel, 1988; Wardle et al., in press).

Metamorphism was coeval with deformation. This is supported by deformed, thermal peak minerals such as helicitic (snowball) garnet porphyroblasts in Ramah Group metapelites and amphibolites in the foreland zone, and aligned orthopyroxene in charnockitic rocks of the ASZ and core zone (Fig. 9d). In the foreland zone, thermal peak metamorphic fabrics are folded, indicating that transcurrent movement outlasted the peak of metamorphism. West of the foreland zone, however, recrystallization outlasted deformation, as shown by annealed polygonal textures in quartz and feldspar, and by growth of postkinematic garnet.

Some effects of retrograde metamorphism do occur in the map area, such as decompression rims on granulite grade assemblages (c.f. Mengel, 1988), and low grade features (greenschist facies mineral assemblages and pseudotachylyte) in long-lived zones of dip-slip movement. Although geochronological information and P-T determinations are required as proof, these retrograde features are interpreted as having formed during uplift of the orogen, and a second metamorphic event is not considered neccessary to explain their presence in the Torngat orogen.

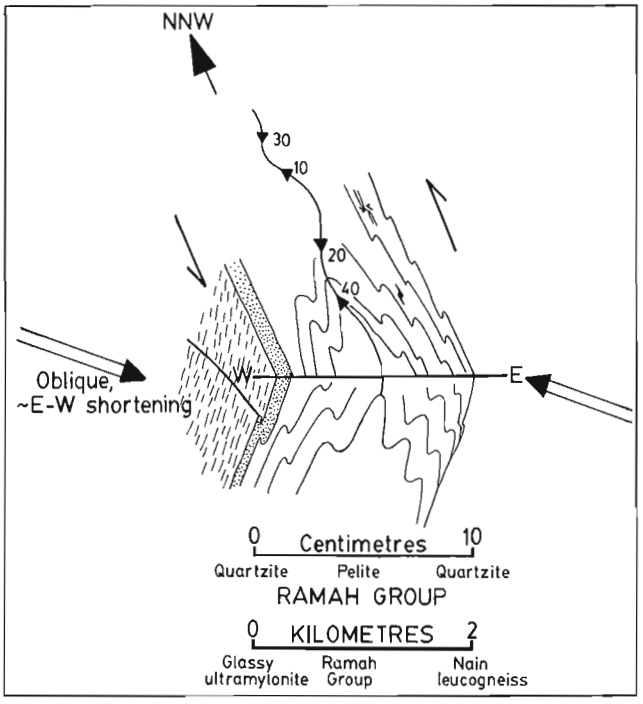

Figure 10. Schematic diagram of the transpressive deformational model to explain the features of the Ramah Group in the southern map area. In this model, E-W shortening was accommodated by buckle folding of less competent metapelitic layers on subhorizontal axes developed at the scale of individual beds (millimetre- to metre-scale) to the whole Ramah Group (2km wavelength fold), and by W-side-up reverse slip on more competent quartzite layers (small scale) to glassy ultramylonite zones (small to large scale). Sinistral simple shear was accommodated by slip within metapelites. Large scale non-coaxial folding reflects subvertical overall extension.

DISCUSSION

Three principal observations have been made regarding the geotectonic evolution of the Torngat Orogen: 1) the Aphebian Ramah Group was affected by early thrusting, by the high grade deformation associated with Abloviak shearing, and by late, E-directed thrusting; 2) Abloviak deformation probably involved coeval approximate E-W shortening and sinistral simple shearing in a transpressive collisional regime; and 3) metamorphic features in the Torngat Orogen are compatible with a single thermotectonic event. These observations are interpreted as showing that the geotectonic evolution of the Nain-Churchill boundary zone resulted from a single, protracted collisional event.

This interpretation can be applied north of the map area in the Hebron-Saglek region, where a similar sequence of deformation events has been observed in highly strained Ramah Group (B. Ryan, pers. comm., 1988). Farther north, in the Saglek-Nachvak region, the Ramah Group is preserved in a 20 km wide fold/thrust belt whose open, N-S trending folds of bedding and moderately W-dipping, E-verging thrusts indicate deformation by approximate E-W shortening (c.f. Morgan, 1975; Wardle, 1983; Mengel, 1984, 1988). Early Proterozoic granulite-grade gneisses deformed by sinistral simple shear in the foreland zone of the Torngat Orogen are thrust over amphibolite- to greenschist-grade Ramah Group across the Nachvak thrust (Morgan, 1975; Wardle, 1983; Mengel, 1988). These features led Mengel (1985, 1988) and Wardle et al. (in press) to propose that the Ramah Group had not undergone the high-grade sinistral transcurrent shear event, but was deposited afterwards. These authors ascribed all the deformation and metamorphism in the Ramah Group to a separate tectonic event, in which late, E-directed thrusting that possibly originated from the Hudsonian New Quebec Orogen, redeformed the Torngat Orogen. However, the findings in the North River map area are not consistent with the implications of this interpretation, and hence disprove it (Table 1).

The transpressive model developed for the map area can account for the features of the orogen in the Nachvak-Saglek region. There, the sinistral simple shear component of the Abloviak deformation did not affect the Ramah Group because the preserved portion of it lay beyond the eastern limit of transcurrent deformation, and only the E-W shortening component of the deformation was recorded. Farther north, the two components of the deformation are dramatically resolved into spatially separate zones that splay around the Burwell terrane (Fig. 1). Sinistral transcurrent movement occurred in the Abloviak shear zone, which wraps around the southern and western margins of the Burwell terrane, and dip-slip movement was localized on subvertical glassy ultramylonites along the Komaktorvik zone (as seen this summer with R. Wardle of the Newfoundland Department of Mines).

TABLE 1. Comparative sequence of events in the eastern Torngat Orogen as proposed for the Nachvak-Saglek region (Mengel, 1988), and the North River map area.

COMPARISON OF INTERPRETED EVENTS IN THE NAIN-CHURCHILL BOUNDARY ZONE

NORTH RIVER MAP AREA

CRATONIZATION AND DYKE EMPLACEMENT

UPLIFT AND EROSION

DEPOSITION OF RAMAH GROUP (RG)

-In foredeep environment during initial stages of foreland deformation?

DEFORMATION

1) EARLY THRUSTING AND ISOCLINAL FOLDING OF RG

2) SINISTRAL TRANSCURRENT SHEARING

-rotation of Archean structures and L. Proterozoic dykes into N-S trend

-S-folding of basement + RG; development of L-fabric

- granulite(W) - greenschist(E) metamorphism

3) DUCTILE THROUGH BRITTLE THRUSTING

-tectonic juxtaposition of lithologies and metamorphic facies

- glassy ultramylonites to brittle pseudotachylyte zones

-minor folding adjacent to thrusts

CAUSE OF DEFORMATION: OBLIQUE COLLISION OF NAIN-RAE PROVINCES

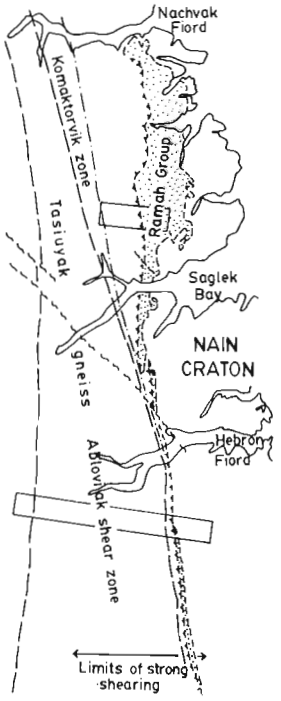

SAGLEK BAY AREA

CRATONIZATION AND DYKE EMPLACEMENT

TORNGAT OROGENY (ca. 1910 Ma)

SINISTRAL TRANSCURRENT SHEARING (L. Proterozoic)

-rotation of Archean structures and L. Proterozoic dykes into N-S trend

-granulite and amphibolite facies metamorphism: recrystallization of dykes

CAUSE OF TORNGAT DEFORMATION: NAIN-RAE OBLIQUE COLLISION, OR INTRA-NORTH ATLANTIC CRATON SHEARING. (Wardle et al., in prep.)

EROSION AND UPLIFT

DEPOSITION OF RAMAH GROUP

HUDSONIAN OROGENY (ca. 1800 Ma)

EASTWARD THRUSTING

-tectonic juxtaposition of lithologies and inversion of earlier (Torngat) metamorphic sequence

-crustal thickening; tectonic burial, deformation and metamorphism of RG

CAUSE OF HUDSONIAN DEFORMATION: SUPERIOR-RAE COLLISION (Wardle et al., in prep.)

From the conclusions reached in the North River map area and the observations on the deformation style in the Torngat Orogen along strike to the north, a geotectonic model is proposed. The Torngat Orogen is believed to have resulted from oblique collision between Rae and Nain provinces (c.f. Taylor, 1979; Korstgård et al., 1987). This probably included a component of underthrusting of the Nain Province, as suggested by the east-directed thrusting component of the deformation. The homogeneous charnockites found throughout the ASZ and Lac Lomier complex may be the exhumed magmatic products of this subduction. Aphebian supracrustal successions deposited on opposite flanks of these colliding blocks were deformed by Torngat orogenesis. On the western Rae block, the Tasiuyak gneiss is interpreted as being derived from the easternmost, deep-water facies of the Lake Harbour Formation, deposited in a passive marginal basin. The lower Ramah Group forms the eastern antithesis to the Tasiuyak gneiss, deposited as a shallow siliciclastic shelf sequence in a west-facing basin on the margin of the Nain craton (Knight and Morgan, 1981). The upper Ramah Group (Nullataktok to Cameron Brook formations) (ibid.) consists of euxinic, deepwater sediments that Hoffman (1987) interpreted as having been deposited in an eastward-prograding foredeep in front of a migrating fold/thrust belt. It is proposed that the suture zone between the colliding blocks is cryptic, and represented by the wide zones of very highly-strained glassy ultramylonite that are developed along the eastern margin of the ASZ in the southern Torngat Orogen, and in the Komaktorvik shear zone in the north. The Burwell terrane may represent a small crustal block of pre-Hudsonian age that became trapped between colliding Nain and Rae provinces (c.f. Hoffman, 1988). Deformation in the Komaktorvik and Abloviak shear zones in the northern Torngat Orogen was probably contemporaneous.

Of unknown origin in this model is the protolith of gneisses in lithological assemblage 3, located between the Ramah Group and the Tasiuyak gneiss. These gneisses are identical to Nain Province rocks, except that they lack Napaktok dykes. The gneisses could, therefore, have originated from the Nain Province in which dykes either were not emplaced, or passed through to higher levels. Alternatively, gneisses from lithological assemblage 3 could also have been derived from the Lac Lomier complex of the Rae Province, to which they also bear a striking resemblance. Another unsolved question concerns the origin and distribution of the train of meta-anorthositic gneiss bodies that occupy the same structural position in lithological assemblage 3 from Cape Burwell to the southern map area. This strip of rocks remain one of the most enigmatic features of the Torngat Orogen.

Numerous tests of the proposed geotectonic model can readily be made. Material has been collected from within the map area that will allow the absolute ages of the proposed sequence of deformational events to be constrained. Effort should also be made to determine the ages of Aphebian supracrustal successions in Labrador; particularly the Ramah Group, Lake Harbour Formation and the Tasiuyak gneiss. In order to determine the possibility of a cryptic suture, Sm-Nd model ages of the strip of gneisses located immediately west of the Ramah Group in the map area (lithological assemblage 3) should be compared to the Sm-Nd model ages for gneisses from the Nain Province and Lac Lomier complex. To test for subduction during the deformation, the chemistry of the homogeneous charnockites should be analyzed to determine if they reflect an arc/subduction component of magmatism. Finally, mapping of the Burwell terrane must be a priority if the geotectonic evolution of the Torngat Orogen is ever to be fully understood. At present, all hypotheses remain speculative until more is known about the geology of this key element in the tectonic puzzle of Labrador.

ACKNOWLEDGMENTS

This summary contains the ideas and suggestions of many visitors and co-workers in the North River map area over the past three years, including Simon Hanmer of the Geological Survey of Canada, Bruce Ryan and Dick Wardle of the Newfoundland Department of Mines, Flemming Mengel, and Herb Helmstaedt, Dugald Carmichael, and Dave Scott, all of Queen's University. Their input is gratefully acknowledged. I would particularly like to thank Dick for the excursion to Abloviak Fiord this summer, and Normand Goulet and André. Ciesielski for showing us some fantastic geology there. Their ideas are also included in this report. The mental stimulation and friendship of Flemming, Bruce, Simon, and Ingo Ermanovics made this project all that I could have wished for. Finally, thanks to Ingo for logistical, and continuing moral support over the years. This research is supported by a fellowship from Queen's University and by the GSC for summer mapping.

REFERENCES

Ermanovics, I.F., Van Kranendonk, M., Corriveau, L., Bridgwater, D., Mengel, F., and Schiøtte, L.
1988: Geology of the North River-Nutak map areas, Nain-Churchill provinces, Labrador; in Current Research, Part C, Geological Survey of Canada, Paper 88-1C, p. 19-26.

Ermanovics, I.F., Van Kranendonk, M., Corriveau, L., Mengel, F., Bridgwater, D., and Sherlock, R.
1989: The Boundary Zone of the Nain-Churchill provinces in the North River-Nutak map areas, Labrador; in Current Research, Part C, Geological Survey of Canada, Paper 89-1C, p. 385-394.

Hoffman, P.F.
1987: Early Proterozoic foredeeps, foredeep magmatism, and Supriortype iron-formations of the Canadian Shield; in Proterozoic Lithospheric Evolution, Ed. A. Kröner; American Geophysical Union, Geodynamic Series 17, p. 85-98.
1988: United Plates of America, the Birth of a Craton: Early Proterozoic Assembly and Growth of Laurentia; Annual Review of Earth and Planetary Science, 16, p. 543-603.

Knight, I. and Morgan, W.C.
1981: The Aphebian Ramah Group, northern Labrador; in Proterozoic Basins of Canada, ed. F.H.A. Campbell; Geological Survey of Canada, Paper 81-10, p. 313-330.

Korstgard, J., Ryan, B., and Wardle, R.
1987: The boundary between Proterozoic and Archean crustal blocks in West Greenland and northern Labrador; in Evolution of the Lewisian and Comparable Precambrian High Grade Terrains, ed. R.G. Park and J. Tarney; Geological Society of London, Special Publication No. 27, p. 247-259.

Mengel, F.C.
1984: Preliminary results of mapping in the Ramah Group and adjacent gneisses south of Saglek Fiord, northern Labrador; in Current Research, Newfoundland Department of Mines and Energy, Mineral Development Division, Report 84-1, p. 21-29.
1985: Nain-Churchill province boundary: a preliminary report on a cross-section through the Hudsonian Front in the Saglek Fiord area, northern Labrador; in Current Research, Newfoundland Department of Mines and Energy, Mineral Development Division, Report 85-1, p. 33-42.
1988: Thermotectonic evolution of the Proterozoic-Archean boundary in the Saglek area, northern Labrador; unpublished PhD thesis, Memorial University of Newfoundland, St. John's, Newfoundland.

Morgan, W.C.
1975: Geology of the Precambrian Ramah Group and basement rocks in the Nachvak Fiord-Saglek Fiord area, northern Labrador;Geological Survey of Canada, Paper 74-54, 42p.

Ryan, A.B., Martineau, Y., Bridgwater, D., Schiøtte, L., and Lewry, J.
1983: The Archean-Proterozoic boundary in the Saglek Fiord area, Labrador, report 1; in Current Research, Part A, Geological Survey of Canada, Paper 83-1A, p. 297-304.

Ryan, A.B., Martineau, Y., Korstgard, J., and Lee, D.
1984: The Archean-Proterozoic boundary in northern Labrador: report 2; in Current Research, Part A, Geological Survey of Canada, Paper 84-1A, p. 545-551.

Schiøtte, L., Compston, W., and Bridgwater, D.
1989: Ion probe U-Th-Pb zircon dating of polymetamorphic orthogneisses from northern Labrador, Canada; Canadian Journal of Earth Sciences, v. 26, no. 8, p.1533-1556.

Smyth, W.R.
1976: Geology of the Mugford Group, northern Labrador; in Report of Activities, Newfoundland Department of Mines and Energy, Report 76-1, p. 72-79.

Taylor, F.C.
1971: A revision of the Precambrian structural provinces in northeastern Quebec and northern Labrador; Canadian Journal of Earth Sciences, v.8, no. 5, p. 579-584.
1975: Geology, Pointe le Droite, Newfoundland-Quebec; Geological Survey of Canada, Map 1429A.
1979: Reconnaissance geology of a part of the Precambrian Shield, northeastern Quebec, northern Labrador, and Northwest Territories; Geological Survey of Canada, Memoir 393.

Wardle, R.J.
1983: Nain-Churchill Province cross-section, Nachvak Fiord, northern Labrador; in Current Research, Newfoundland Department of Mines and Energy, Report 83-1, p. 68-90.
1984: Nain-Churchill Province cross-section; Riviere Baudancourt-Nachvak Lake; in Current Research, Newfoundland Department of Mines and Energy, Report 84-1, p. 1-11.

Wardle, R.J., Ryan, B., Nunn, G.A.G., and Mengel, F.C.
in press: Labrador Segment of the Trans-Hudson Orogen: crustal development through oblique convergence and collision; in The Trans-Hudson Orogen of North America: Lithotectonic Correlations and Evolution, ed. by J.F. Lewry and M.R. Stauffer; Geological Association of Canada, Special Paper.

Van Kranendonk, M.J. and Ermanovics, I.
1989: Deformation of the Lower Proterozoic Ramah Group and implications for Nain-Churchill boundary zone evolution, northern Labrador, Canada; Geological Association of Canada-Mineralogical Association of Canada Annual Meeting, Program with Abstracts v.14, p. A39.

Van Kranendonk, M.J., Helmstaedt, H., and Ermanovics, I.
1989: Archean structural history of the Nain Province, northern Labrador, Canada: Evidence of Early Archean crustal imbrication; Geological Association of Canada-Mineralogical Association of Canada Annual Meeting, Program with Abstracts v.14, p. A123.

Archean deformation and metamorphism of metasedimentary rocks in the Contwoyto-Nose Lakes area, central Slave Province, N.W.T.[1]

C. Relf[2]
Continental Geoscience Division

Relf, C., Archean deformation and metamorphism of metasedimentary rocks in the Contwoyto-Nose Lakes area, central Slave Province, N.W.T.; in Current Research, Part C, Geological Survey of Canada, Paper 90-1C, p. 97-106, 1990.

Abstract

Archean metasedimentary rocks in the Contwoyto-Nose Lakes area of the Slave Structural Province have undergone regional high T/low P metamorphism. Two shallowly-dipping, gently undulating isograds separate the biotite, cordierite and sillimanite mineral zones. An isograd corresponding to the muscovite breakdown reaction has been obscured by the injection of abundant, externally-derived granitic veins, which impart a migmatitic texture to the rocks. Locally, fragmented beds of iron-formation can be traced through the migmatites. Fours sets of Archean structures have been recognized. D1 and D2 produced tight to isoclinal folds and associated cleavages. Two sets of late NE-and NW-striking cross folds are characterized by domains of open to tight mesoscopic folds and crenulations. The superposition of all four fold sets has resulted in complex but resolvable fold geometries. Regionally, the late cross folds have produced a dome and basin interference pattern of the syn-thermal peak cleavage (S2) and the isograd surfaces.

Résumé

Les roches sédimentaires archéenne dans la zone des lacs Contwoyto-Nose de la province structurale des Esclaves ont subi un métamorphisme régional à température élevée et à basse pression. Deux isogrades à faible ondulation et à pendage peu profond séparent les zones minérales de biotite, cordiérite et sillimanite. Un isograde carrespondant à leur réaction de fracturation de la muscovite a été masqué par l'injection de filons granitiques externes abondants qui donne une texture migmatitique aux roches. Localement, des couches fragmentées de formation ferrifère peuvent être retracées par le biais des migmatites. Quatre séries de structures archéennes ont été relevées. D1 et D2 ont produit des plis de serrés à isoclinaux et des clivages associés. Deux séries de plis transversaux récents à direction nord-est et nord-ouest sont caractérisés par des domaines de plis et de crénulations mésoscopiques d'ouverts à serrés. La superposition de ces quatre séries de plis produit des géométries de plis complexes mais néanmoins explicables. À l'échelles régionale, les plis transversaux les plus récents ont produit une configuration d'interférence en dôme et bassin du clivage sommital syn-thermal (S2) et des surfaces isogrades.

[1] Contribution to Canada-Northwest Territories Mineral Development Agreement 1987-1991. Project carried by the Geological Survey of Canada.

[2] Department of Geological Sciences, Queen's University, Kingston, Ontario, K7L 3N6

INTRODUCTION

The purpose of this study is to examine the structural and metamorphic evolution of the metasedimentary rocks in the Contwoyto-Nose Lakes area (Fig. 1) that host gold-bearing iron-formations. Results following the third summer of mapping (1989) in the study area are given here. The project is partially funded by a Canada — N.W.T. Mineral Development Agreement contract (Project C1.1.1), which is being carried out in conjunction with regional (1:000 000) geological mapping of the Contwoyto Lake 1:250 000 map sheet (NTS 76E) and the west half of the Nose Lake sheet (76F) (*see* King et al., 1988, 1989, 1990; Relf, 1989).

Previous geological mapping in the area has been discussed by King et al. (1988, 1989) and Relf (1989). For a more thorough discussion of results of the first two years' mapping, refer to King et al., 1988, 1989, and Relf, 1989.

Metasedimentary rocks (which include pelites, semipelites, psammites, volcaniclastic sediments and iron-formation) preserve four sets of Archean structures. Pre- and syn-thermal peak shortening, characterized by isoclinal folds and faults, were followed by post thermal peak regional compression, which produced two sets of (coeval?) upright cross folds. The timing of metamorphism with respect to deformation has been established from porphyroblast-fabric relationships (Relf and King, 1989). High T/low P regional metamorphism accompanied the second deformation, which was contemporaneous with extensive magmatism in the area (King et al., 1989). The morphology, timing and regional significance of the late cross folds are discussed in this paper, as well as the geometry of the resultant fold interference patterns. The map pattern defined by the metamorphic isograds, and textural changes which accompany mineralogical changes between different mineral zones are also described.

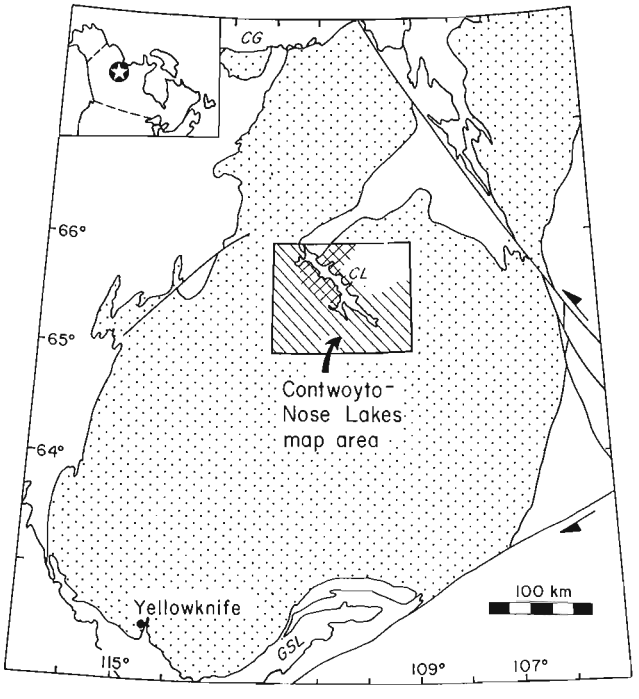

Figure 1. Location of Contwoyto-Nose Lakes area. Stippled area is the Slave Structural Province. Inset shows position of Slave Province in Canada. Diagonal lines show area covered to date by regional mapping (King *et al.*, 1990). Cross hatching shows area of detailed structural and metamorphic analysis. Abbreviations: C G = Coronation Gulf, C L = Contwoyto Lake, G S L = Great Slave Lake.

METAMORPHISM

Three distinct mineral zones — biotite, cordierite, and sillimanite (Relf, 1989; King et al., 1989) have been extended following 1989 mapping (Fig. 2). The highest grade rocks in the area contain assemblages which are above the muscovite breakdown reaction curve. However, the isograd corresponding to this reaction has been obscured by the injection of abundant granitic veins, which impart a migmatitic texture to the rocks. The transition from sillimanite-grade schists to migmatitic metasediments does not correspond to the muscovite breakdown isograd.

Near the isograds that separate mineral zones, distinct textural changes accompany or precede the first appearance of the characteristic mineral. For example, biotite-grade metapelites are slates, but coarsen to phyllites about 20 to 50 m below the cordierite isograd. Metapelites containing the first occurence of cordierite are texturally transitional between phyllites and schists.

Textural changes are also useful in mapping the sillimanite isograd in the field. Sillimanite first appears as very fine-grained needles of fibrolite which are very difficult to recognize in hand sample. The first sillimanite porphyroblasts visible in outcrop occur at least 50 m "upgrade" from the first appearance of fibrolite in thin section. However, the transition from cordierite to sillimanite zones is accompanied by a textural change which is easy to recognize. At or very near the first appearance of fibrolite, the metapelites contain small (1-2 mm) white "knots" which weather prominently on the outcrop surface. In thin section, these knots have been found to consist of quarzt + muscovite +/− fine-grained sillimanite. Although sillimanite may not be present in the white knots, fibrolite is almost always associated with biotite in the matrix of the rocks which contain the white knots.

The transition from sillimanite schists to migmatites is characterized by the presence of greater than 20% granitic veins which intrude along and across the foliation (King et al., 1990). This transition does not coincide with a metamorphic isograd, as the veins generally do not appear to have been generated in situ. Locally, small isolated pods and veinlets of granitic material may represent a minor component of partial melt derived from the metasediments. Mineral assemblages preserved in the melanocratic phase of the migmatites include biotite + muscovite +/− cordierite +/− garnet +/− sillimanite + quartz + plagioclase; or biotite + K- feldspar +/− sillimanite +/− cordierite +/− melt + quartz + plagioclase. The isograd corresponding to the breakdown of muscovite is therefore preserved within the migmatites, but could not be mapped due to the variable extent to which the country rock has been assimilated by the granitic portion.

As no muscovite-breakdown isograd could be distinguished, the mappable mineral zones are confined to the north-central part of the Contwoyto Lake map sheet (Fig. 2). Here, the isograds outline a thermal low which extends to the edge of the map sheet NE of Contwoyto Lake. In the vicinity of Lupin Mine (Fig. 2), the cordierite isograd is known from underground exposures to dip about 30° towards the south (Ralph Bullis, pers. comm., 1988). On the east side of Contwoyto Lake almost due east of the mine, the sillimanite isograd dips less than 10° west, based on its exposure at the surface and in drill core. Elsewhere the dips of the isograds are not known, but are thought to be shallow. For example, the map trace of the sillimanite isograd in the Butterfly Lake area trends southwards from Butterfly Lake with the "hot" side to the east (Fig. 2). In the rocks above the isograd, metapelites with the assemblage biotite, andalusite, muscovite +/− cordierite +/− garnet, and incipient fibrolite are found locally. Texturally these rocks resemble the white knot-bearing schists which characterize the cordierite/sillimanite zone transition. These rocks are not just restricted to a few tens of metres around the sillimanite isograd, but they are found in areas several kilometres to the east. The widespread occurrence of this assemblage and texture suggests that the sillimanite isograd has a very shallow dip in the area. These contraints on the dips of the isograds suggest that the termal low has a basin-like shape in the third dimension. The significance of this in terms of the regional structures is discussed below.

Mineral assemblages in metapelites and semipelites can be used to bracket the peak metamorphic conditions experienced by the rocks. Assemblages in the cordierite zone equilibrated in bathozone 1 or 2 of Carmichael (1978), which corresponds to pressures of about 1.0 to 3.6 kbar. Andaulsite in this zone is commonly observed replacing staurolite by one of the following reactions (Fig. 3):

1) staurolite + muscovite + quartz =
garnet + aluminosilicate + biotite + vapour,
or
2) staurolite + quartz =
garnet + aluminosilicate + vapour.

The upper P and T conditions for these reactions are about 3.6 kbar and 560 °C, based on the Holdaway (1971) triple point for aluminosilicates and a P-T grid for ideal pelites (Carmichael et al., 1987) (Fig. 3). Locally staurolite is preserved in the sillimanite zone, where it is replaced by sillimanite via reactions 1 or 2 above (Fig. 3). These reactions occur in bathozones 3 or 4 of Carmichael (1978), between about 3.6 and 5.6 kbar, and at approximately 560 to 600 °C (Fig. 3).

Mineral assemblages characteristic of particular metamorphic bathozones (Carmichael, 1978) have not been observed in the migmatites. However, as kyanite has not been recognized in the migmatites, the pressure cannot have exceeded approximately 7 kbar (ibid.). In fact, the maximum P was probably considerably lower than this. Preliminary geobarometry using the program "GEO-CALC" of Berman et al. (1987) has yielded a pressure estimate of 3.5 +/− 1 kbar for one sample of a migmatized metapelite (Relf and King, 1989). The sample was taken approximately 20 km northeast of Yamba Lake, and contains the assemblage biotite, muscovite, sillimanite, staurolite, garnet, quartz and plagioclase. The presence locally of mineral assemblages from above the muscovite breakdown reaction implies maximum T in the range of about 650 to 700 °C (Carmicheal, 1978; Winkler, 1979).

The regional thermal peak may have been followed by local contact metamorphism around late plutons. For example, north of Butterfly Lake, the trace of the sillimanite isograd follows the contact of a small tonalite pluton which crosscuts the syn-thermal peak schistosity, and therefore was emplaced following the regional thermal peak. Adjacent to the pluton, randomly-oriented sillimanite which transects the syn-thermal peak fabric was found in thin section. This sillimanite is thought to be related to contact metamorphism caused by heat introduced by the late pluton.

Effects of retrograde metamorphism recognized in the area include the alteration of poikiloblastic cordierite to muscovite, biotite, and quartz, and chloritization of biotite and garnet. Locally, large (up to 15 cm) retrograde andalusite crystals grow across the main syn-thermal peak schistosity within the sillimanite zone.

The protolith to the melanosome in the migmatites can be distinguished locally. A number of outcrop-sized areas have escaped extensive migmatization and preserve coherent metasedimentary rocks. Here, primary sedimentary structures such as concretions and graded bedding may be preserved. Iron-formation, distinguished by the assemblage hornblende + garnet +/− grunerite +/− sulphide minerals, has also been recognized within these areas (Fig. 2). Even where they have been migmatized, layers of iron-formation can be identified by their mineral assemblage, although they are extensively fragmented by intrusion and deformation, and commonly cannot be traced more than a few tens of metres.

DEFORMATION

Four sets of Archean structures have been identified in the map area (Relf, 1989; King et al., 1989). They are described below:

D1 — Pre-thermal peak isoclinal folding, faulting and cleavage development

Structures that predate the peak of metamorphism are characterized by tight to isoclinal folds of bedding. These folds have dominant wavelengths on the order of 100 m, and variable plunges due to subsequent deformations. A biotite +/− muscovite cleavage (S1) is preserved locally in microlithons between the S2 surfaces and as aligned mica inclusions within porphyroblasts. F1 and S1 have been described in more detail by King et al. (1988, 1989) and Relf (1989).

The S1 fabric is interpreted to be related to F1 folds, because in the rare localities where S1 is preserved in the hinge of an F1 fold, it appears to be axial planar. It is possible that F1 and S1 structures are not consanguineous but that they formed during two distinct deformational events, or

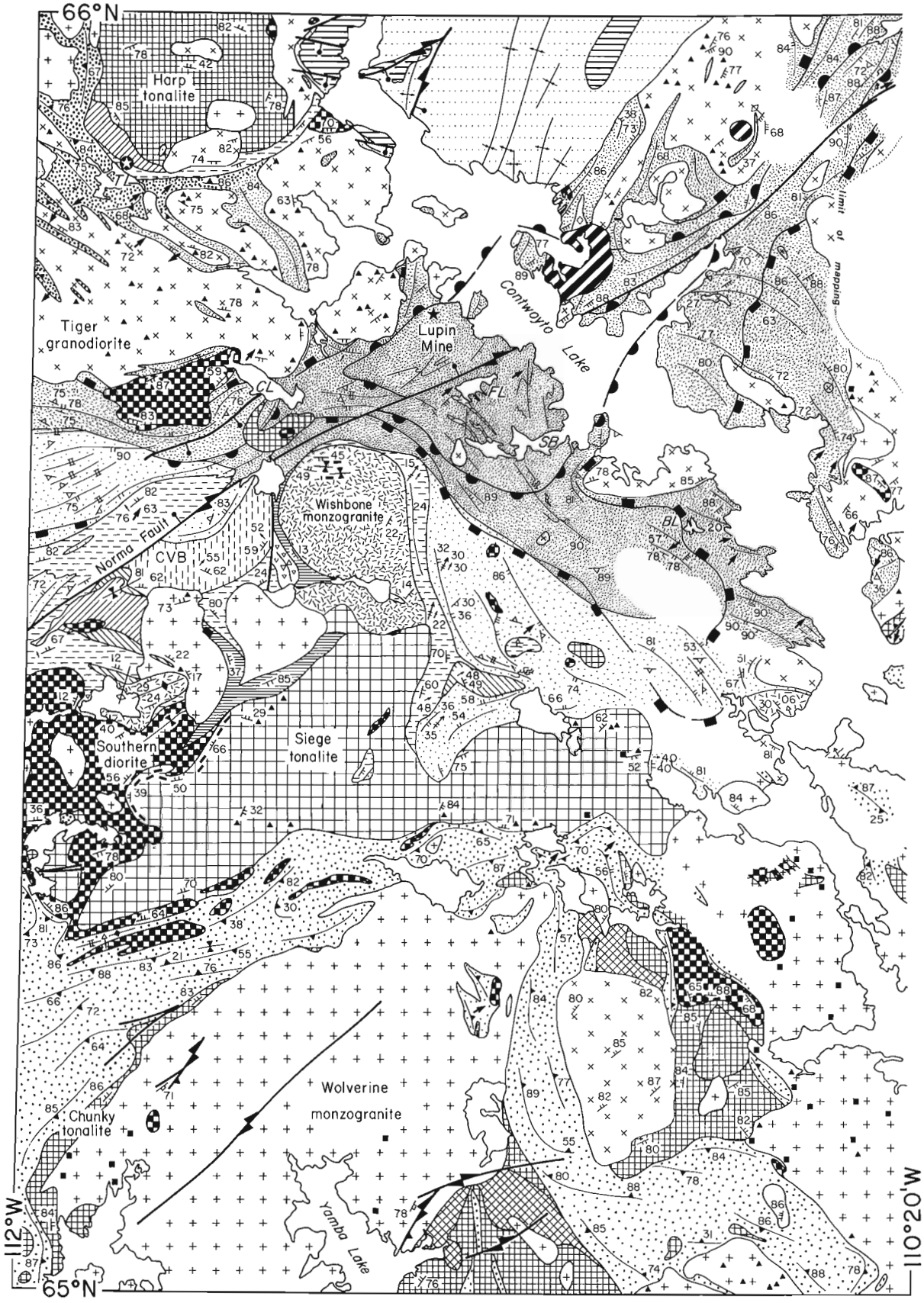

Figure 2. Simplified geological map of the Contwoyto-Nose Lakes area. Unpatterned areas are drift-covered ground through which geological contacts could not extrapolated. Location of iron-formation within the migmatites east of Contwoyto Lake marked with a circled cross. Abbreviation: C V B = Central Volcanic Belt: Bodies of water: C L = Contwoyto Lake, F L = Fingers Lake, S B = Shallow Bay, T L = Tuk Lake, B L = Butterfly Lake.

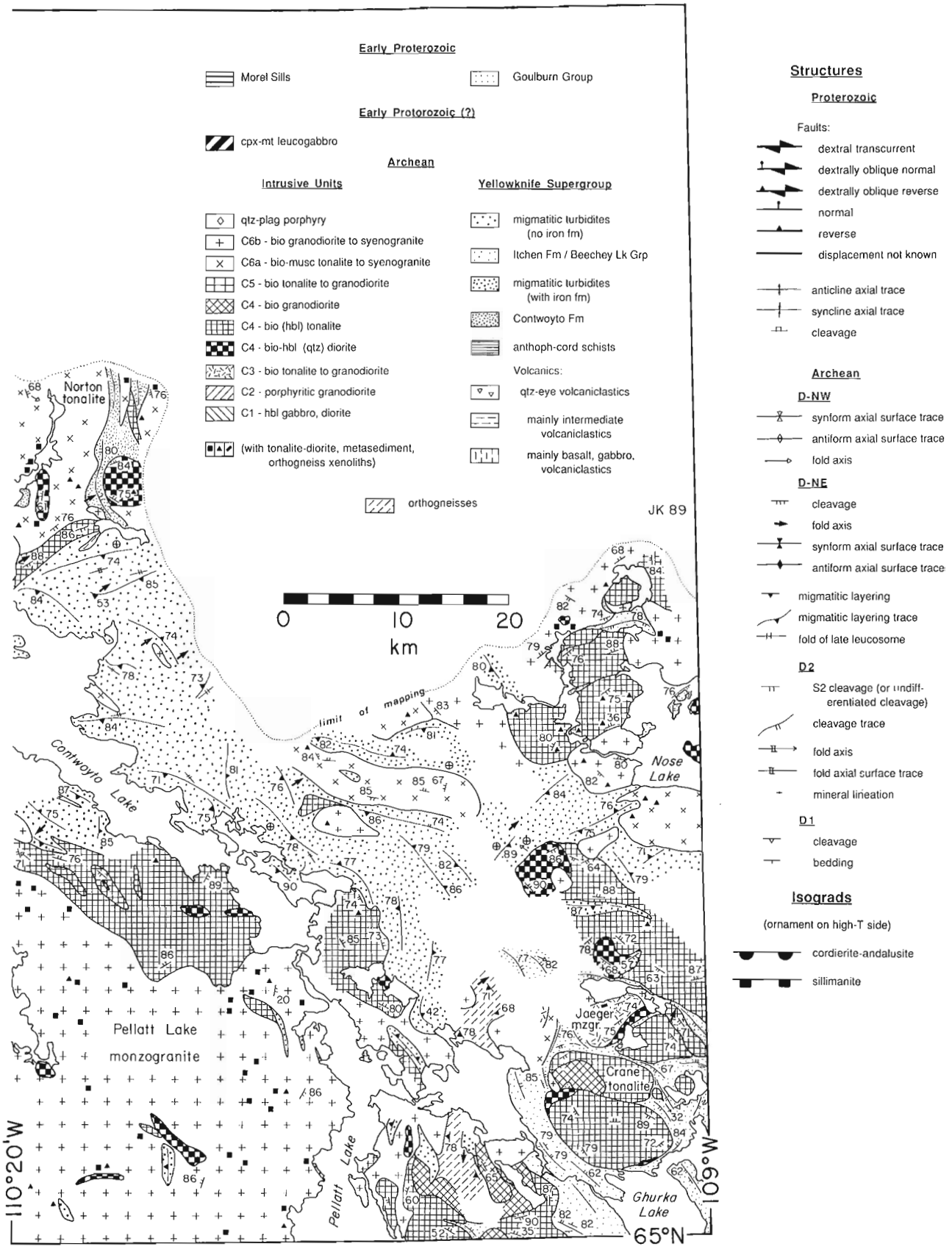

Structures

Proterozoic

Faults:
- dextral transcurrent
- dextrally oblique normal
- dextrally oblique reverse
- normal
- reverse
- displacement not known

- anticline axial trace
- syncline axial trace
- cleavage

Archean

D-NW
- synform axial surface trace
- antiform axial surface trace
- fold axis

D-NE
- cleavage
- fold axis
- synform axial surface trace
- antiform axial surface trace

- migmatitic layering
- migmatitic layering trace
- fold of late leucosome

D2
- S2 cleavage (or undifferentiated cleavage)
- cleavage trace
- fold axis
- fold axial surface trace
- mineral lineation

D1
- cleavage
- bedding

Isograds

(ornament on high-T side)
- cordierite-andalusite
- sillimanite

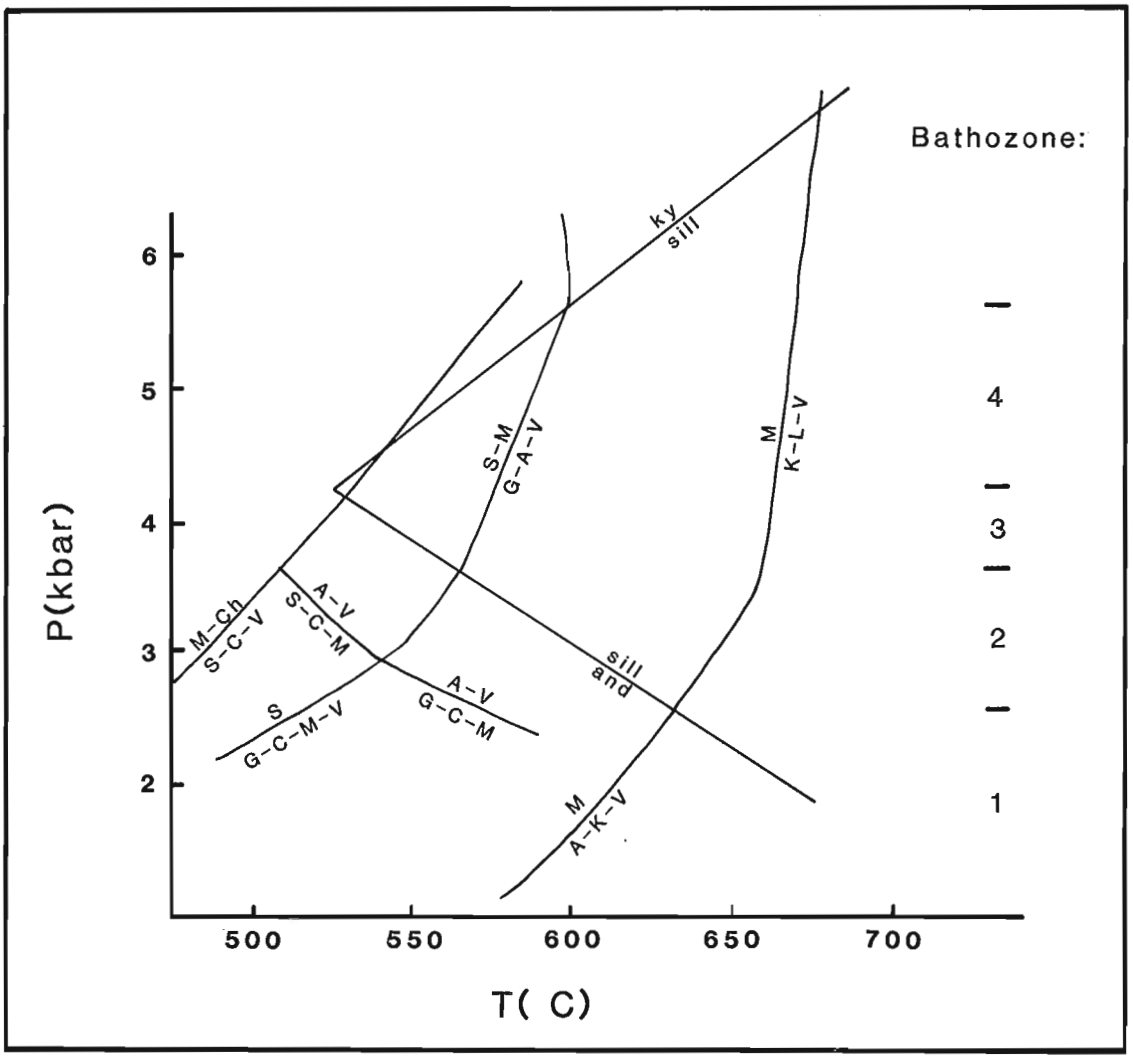

Figure 3. P-T grid for ideal pelite system, showing stability fields of aluminosilicate minerals, staurolite breakdown and muscovite breakdown reactions, as well as bathzones of Carmichael (1978). From Carmichael et al., 1987. Abbreviations: A = aluminosilicate, C = cordierite, Ch = chlorite, G = garnet, K = K-feldspar, L = liquid, M = muscovite, S = staurolite, V = vapour, and = andalusite, sill = sillimanite, ky = kyanite. All assemblages include quartz and plagioclase.

that some F1 folds are syn-sedimentary. As no evidence has been found so far to suggest that F1 and S1 are unrelated structures, they are currently assumed to be related.

Faults overprinted by the S2 cleavage occur locally in the map area. One such fault (Fig. 4) is folded about, and therefore predates, S2. It is not known whether these faults accompanied F1 folding. However, none have been observed to be folded by F1, nor have F1 folds been observed to be transected by pre-S2 faulting.

D2 — Syn-thermal peak isoclinal folding, faulting and cleavage development

Variably plunging, tight to isoclinal, F2 folds of bedding are the most dominant mesoscopic folds in the area. They range from a few millimetres to hundreds of metres in wavelength. They have an associated cleavage (S2) which is clearly axial planar and defines the main planar fabric in the metasediments through most of the map area. S2 formed during the regional thermal peak, and is a penetrative cleavage defined by biotite +/− muscovite at all metamorphic grades. Porphyroblasts of cordierite, andalusite and sillimanite lie in the S2 plane, and commonly define a mineral lineation parallel to the F2 fold axis, indicating that metamorphic mineral growth accompanied D2. S1 is transposed into S2 in many areas, making the two cleavages indistinguishable. More detailed descriptions of S2 and F2 have been presented by King et al. (1988, 1989) and Relf (1989).

Refraction of S2 across beds of differing mechanical properties (e.g. metapelites and metapsammites) is common, and can be extreme. At one locality, S2 is refracted by 75° through curved bedding in an F1 hinge zone. As the cleavage is refracted through a previously curved surface, S2 itself also appears to be folded. Care must be taken therefore in distinguishing between refracted and folded cleavages.

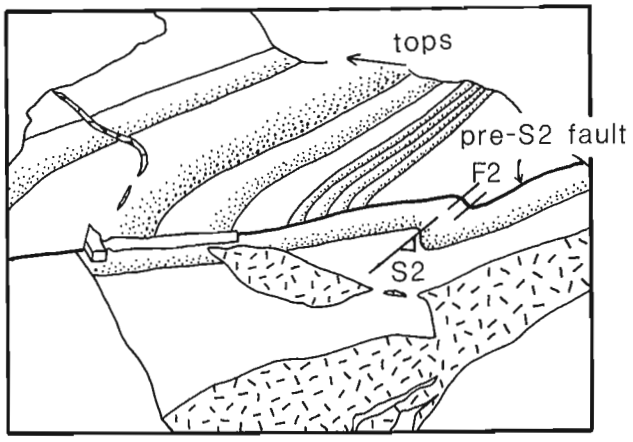

Figure 4. Pre-S2 faulted bedding, with thermal peak schistosity (S2) growing across it. Fault is folded about S2, and may have accompanied F1 folding. Sketch traced from photograph of outcrop. Hammer handle is 35 cm long.

The S2 surface varies in orientation from vertical to subhorizontal. Shallow dips of S2 are observed more commonly in the highest grade rocks (migmatites), although they are also found at lower grades. The original orientation of S2 is not known, but locally where upright NE- and NW-striking crossfolds have shallow to subhorizontal plunges, S2 is suspected to have been shallow.

D_{NE} and D_{NW} — Post-thermal peak NE- and NW-striking upright cross folding and crenulation cleavage development.

Two sets of upright NE- and NW-striking cross folds, previously referred to as D3 and D4, have been recognized (King et al., 1988, 1989; Relf, 1989). However, the domains of the two structure sets appear to be almost mutually exclusive, and thus their relative timing is ambiguous. The nomenclature D_{NE} and D_{NW} is therefore used here. "NE" and "NW" indicate the strike of the cleavage and the axial planes to folds, not the orientation of the stress fields which produced these structures.

King et al. (1988, 1989) and Relf (1989) described D_{NE} structures as open, upright cross folds and local crenulations. Following mapping in 1989, it was found that F_{NE} folds are tight in places, and locally have a well-developed crenulation cleavage defined by biotite. This cleavage ranges in strike from about 020 to 080°, and dips between 70° NW and 70° SE, with a near-vertical mean. Where S2 has been folded about S_{NE}, it may be transposed into S_{NE} along the limb of the fold, in which case the latter is the predominant planar fabric in the outcrop (Fig. 5).

F_{NE} folds deform bedding, S2 and locally crenulate syn-S2 porphyroblasts. These folds have subvertical axial surfaces which strike between about 020 and 080°. F_{NE} folds plunge down the limbs of D2 folds, and therefore have steep plunges where S2 is steep, and shallow plunges where S2 is shallow.

F_{NW} folds were described as open, upright, kilometre-scale NW-striking cross folds by King et al. (1989). Further

Figure 5. S2 transposed into S_{NE} along limb of F_{NE} fold (of S2), where angle between S2 and S_{NE} is small (bottom part of photograph). S2 is preserved in F_{NE} hinge zone in top half of photograph where it is nearly perpendicular to S_{NE}.

mapping revealed that these folds also occur on the centimetre to metre-scale. They are open to (rarely) tight folds and crenulations of S2 and porphyroblasts, with a local cleavage defined by biotite. The axial surfaces of F_{NW} folds are subvertical and vary in strike from about 280 to 340°.

At three localities (marked "A" on Fig. 2), upright NW folds are superposed on a spaced, NE-striking, post-thermal peak cleavage (Fig. 6). At a fourth locality (marked "B" on Fig. 2), NW-crenulations are deformed by NE-crenulations. These observations suggest that the two structure sets overlapped in time and therefore may be approximately contemporaneous.

Fold Interference

Complex interference patterns resulting from four superposed Archean fold sets are observed in the study area. Interference patterns resulting from F1 and F2 folding have been documented by Relf (1989). They correspond to Types 2 (mushroom-shaped) and 3 (coaxial) of Ramsay (1967). Where late mesoscopic NE or NW folds overprint steeply plunging F2 folds, Type 3 interference patterns of bedding are produced (Fig. 7). In places where the S2 surface is shallowly dipping, it defines a Type 1 (dome and basin) pattern as a result of NE and NW cross folding (Fig. 8).

Although poor exposure and multiple fold interference locally cause the map pattern to be seemingly unresolvable, the geometry of the fold pattern is at least locally predictable. Structures of different generations can be recognized by their relationship to thermal peak minerals. Post-thermal peak structures have systematic NE and NW orientations, which makes them easy to distinguish.

The regional structural grain, which is defined by S2 and isoclinally folded (F2) bedding, is deformed by a series of kilometre scale open folds with NE- and NW-striking axial surfaces. Structural domes of the S2 surface (e.g. the Olga dome; King et al., 1988) are preserved, and have been interpreted to result from superposed late upright cross folding.

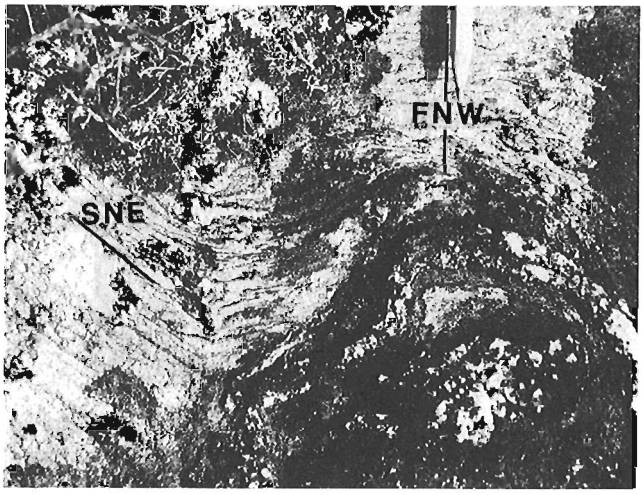

Figure 6. Spaced S_{NE} cleavage and S2-parallel quartz vein (slightly oblique) refolded about an upright NW fold. Pencil points towards NW.

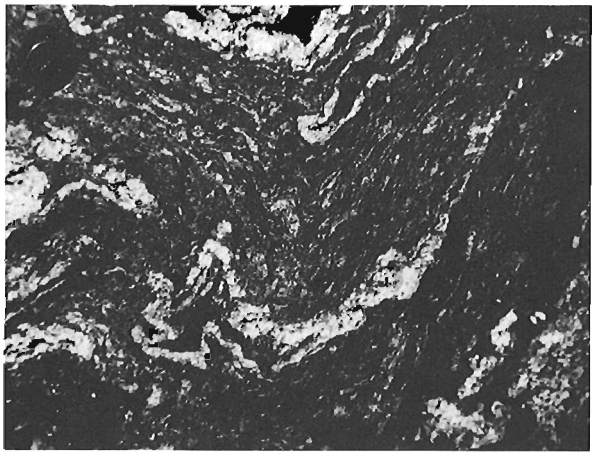

Figure 7. Type 3 interference of NE cross fold superposed on isoclinal F2 folds of migmatitic layering. Lens cap is 5.1 cm in diameter.

The role of the plutons in controlling the orientations of S2 is not certain. The intrusion of some of the late plutons may have reoriented S2 locally (cf. King and Helmstaedt, 1989). If this is the case, then the present map pattern is not entirely a product of late folding, but is due to a combination of late plutonism and regional cross folding.

As the thermal peak of metamorphism and D2 were coeval, the isograd surfaces must also have been affected by D_{NE} and D_{NW}. In their present orientation, the isograds define a large, shallowly dipping basin that undulates locally. High-angle upright cross folds could only produce such a geometry if the original isograd surface was near horizontal. The NE-trending thermal low on the north side of Contwoyto Lake is interpreted to represent the hinge zone of an F_{NE} synform. It narrows and widens along its length as a result of NW cross folding. An F_{NW} synform intersects it at the SW end, resulting in the basin-like topology of the isograds.

As a partial consequence of folding the isograds, the cross folds have caused metamorphic assemblages from different structural levels to be exposed at the present erosional surface. Other factors which may have controlled the erosional surface include differential regional uplift and isostatic recovery following glaciation. In total, as much as 10-12 km (corresponding to roughly 3 kbar) of structural relief may be observed in the area.

Timing of Deformation

All four structure sets described in the preceding section are interpreted to be Archean, based on relationships with plutons of known Archean age. King et al. (1988) recognized six distinct Archean plutonic episodes, informally named C1 to C6 in order of interpreted chronology of emplacement.

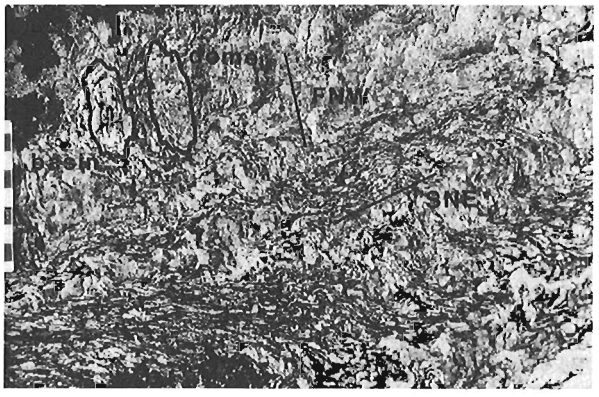

Figure 8. Dome and basin fold interference pattern defined by S2 due to superposition of F_{NE} and F_{NW}. Trace of F_{NE} hinge zone runs diagonally through the top part of photograph, from centre left to top right. S2 is subhorizontal in the hinge zone, and steep on the fold limb in bottom part of photograph. Open F_{NW} folds warp S2 into domes and basins in the area of the F_{NE} hinge zone. Top of photo is north.

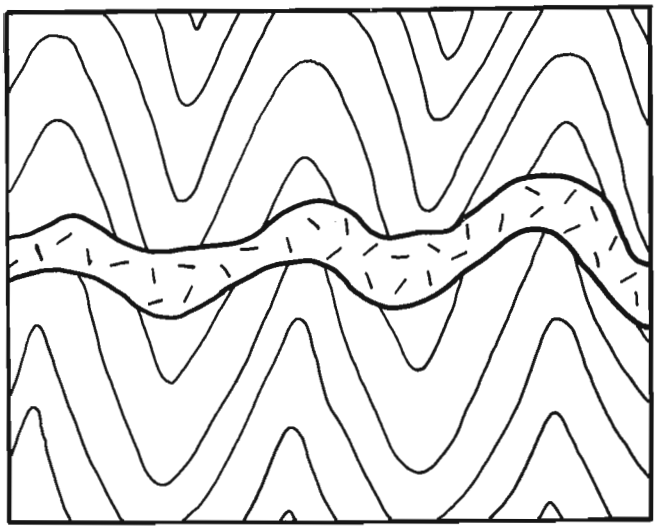

Figure 9. Idealized F_{NW} chevron folds of bedding, cross-cut by vein of pegmatitic syenogranite (C6). Vein is buckled about NW-striking axial plane, but cuts across hinge zones of folds of bedding, indicating emplacement during D_{NW}. Axial trace of folds trend approximately 330°. Vein width is 6 cm.

The timing of D2 with repect to plutonism has been discussed by King et al. (1988, 1989); and Relf and King (1989). D2 structures were interpreted to be contemporaneous with a pluton suite dated at about 2608 Ma, (van Breemen et al., 1989). The youngest (C6) plutons, with a mean age of about 2583 Ma, (van Breemen et al., 1989), are thought to be coeval with D_{NE} and D_{NW}. They have intruded both parallel to and across the S2 fabric, and therefore postdate S2. Locally C6 plutons contain a weak to moderate NE-striking foliation, and veins related to the plutons are folded about F_{NE} folds. D_{NE} is therefore interpreted to have overlapped in time with C6 plutonism. Elsewhere, veins related to C6 bodies were observed cutting across the hinge zones of F_{NW} folds. The veins have also been weakly buckled about a NW-trending axial trace (Fig. 9). Folding related to D_{NW} therefore appears to have accompanied the intrusion of C6 plutons.

SUMMARY

Mapping isograds can be facilitated by documenting textural changes which accompany the mineralogical changes. Slaty metapelites coarsen to schists at the cordierite isograd, and small white knots consisting of quartz + muscovite ± sillimanite appear in the schists at or near the sillimanite isograd. The transition from schists to injection migmatites occurs below the muscovite breakdown reaction, which cannot be mapped as an isograd due to the extent to which the metasediments have been assimilated by the migmatite leucosome.

Post-thermal peak F_{NE} and F_{NW} cross folding has complicated the interference patterns produced by pre- and syn-thermal peak F1 and F2 folding. However, the structures are still resolvable, and therefore geometries can be predicted. On a regional scale, the two sets of cross folds have played a significant role in producing the kilometre-scale structural domes defined by S2, and basins defined by the metamorphic isograds.

Implications for gold exploration

Despite extensive injection of granitic material, remnants of iron-formation can still be recognized in the migmatitic rocks. Such areas should therefore not be ignored as exploration targets for iron-formation-hosted gold mineralization.

Structures of different generations can be distinguished by carefully documenting their orientations, relative timing and relationships to thermal peak assemblages. Detailed structural mapping is important to determine the plunges of folds, and therefore the subsurface geometries of folded surfaces.

ACKNOWLEDGMENTS

Competent and enthusiastic field assistance was provided by Debbie MacPhedran. Janet King is thanked for numerous stimulating discussions in and out of the field. The manuscript benefitted from reviews by D. Carmichael, H. Helmstaedt, J. King. S. Lucas and M. van Kranendonk.

REFERENCES

Berman, R.G., Brown, T.H., and Perkins, E.H.
1987: GEO-CALC: Software for calculation and display of pressure-temperature-composition phase diagrams; University of British Columbia, 27 p.

Bostock, H.H.
1980: Geology of the Itchen Lake area, District of Mackenzie; Geological Survey of Canada, Memoir 391, 101 p.

Carmichael, D.M.
1978: Metamorphic bathozones and bathograds: a measure of the depth of post-metamorphic uplift and erosion on the regional scale; American Journal of Science, v. 278, p. 769-797.

Carmichael, D.M., Helmstaedt, H., and Thomas, N.
1987: A field trip in the Frontenac Arch with emphasis on stratigraphy, structure and metamorphism; Field Trip Guide, Meeting of the Friends of the Grenville.

Holdaway M.J.
1971: Stability of andalusite and the aluminosilicate phase diagram; American Journal of Science, v. 271, p. 82-85.

King, J.E. Davis, W.J., Relf, C., and Avery, R.W.
1988: Deformation and plutonism in the western Contwoyto Lake area, central Slave Province, District of Mackenzie, N.W.T.; *in* Current Research, Part C, Geological Survey of Canada, Paper 88-1C, p. 161-176.

King, J.E., Davis, W.J., Van Nostrand, T., and Relf, C.
1989: Archean to Proterozoic deformation and plutonism of the western Contwoyto Lake map area, central Slave Province, District of Mack-enzie, N.W.T.; *in* Current Research, Part C, Geological Survey of Canada, Paper 89-1C, p. 81-94.

King, J.E., Davis, W.J. Relf, C., and Van Nostrand, T.
1990: Geology of the Contwoyto-Nose Lakes map area, central Slave Province, District of Mackenzie, N.W.T.; *in* Current Research, Part C, Geological Survey of Canada, Paper 90-1C.

King, J.E. and Helmstaedt, H.
1989: Deformational history of an Archean fold belt, eastern Point Lake area, Slave Structural Province, N.W.T.; Canadian Journal of Earth Sciences, v. 26, p. 106-118.

Ramsay, J.G.
1967: Folding and Fracturing of Rocks; McGraw-Hill Inc., New York, 568 p.

Relf, C.
1989: Archean deformation of the Contwoyto Formation metasediments, western Contwoyto Lake area, Northwest Territories; *in* Current Research, Part C, Geological Survey of Canada, Paper 89-1C, p. 95-105.

Relf C. and King, J.E.
1989: Distribution of high T/low P metamorphic mineral zones in the central Archean Slave Province: Thermal and tectonic controls; *in* Geological Association of Canada Annual Meeting, Program with Abstracts, p. A24.

van Breemen, O., King, J.E., and Davis, W.J.
1989: U-Pb zircon and monazite ages from plutonic rocks in the Contwoyto-Nose Lakes map area, central Slave Province, District of Mackenzie; *in* Radiagenic Age and Isotope Studies, Report 3, Geological Survey of Canada, Paper 89-2.

Winkler, H.G.F.
1979: Petrogenesis of Metamorphic Rocks Springer-Verlag, New York, 348 p.

Georgian Bay geological synthesis: Twelve Mile Bay to Port Severn, Grenville Province of Ontario[1]

Nicholas Culshaw[2], David Corrigan[2], John Ketchum[2], and Peter Wallace[2]
Continental Geoscience Division

Culshaw, N., Corrigan, D., Ketchum, J., and Wallace, P., Georgian Bay geological synthesis: Twelve Mile Bay to Port Severn, Grenville Province of Ontario; in Current Research, Part C, Geological Survey of Canada, Paper 90-1C, p. 107-112, 1990

Abstract

Relationships within and between lithostructural domains in the southeast part of Georgian Bay are described. Go Home domain is composed of highly deformed granitoid gneiss with thin but persistent marble and graphite paragneiss units, all being intruded by younger orthogneiss. These rocks are structurally overlain by leucosome-rich migmatitic gneiss whose lower boundary is decorated with pods and layers of anorthositic gneiss and metabasite, near which lie larger masses of coronitic metagabbro and garnet-pyroxene granulite. NNW-trending, subhorizontal folds in this domain are deformed by WNW-trending structures associated with the basal detachment of the Moon River synform, within which gneisses have a simple, layered quasi-stratigraphy. Moon River gneiss overlies an attenuated tail of Parry Sound domain rocks at an anorthosite-quartzite marker unit. Parry Sound lithologies in turn overlie the Blackstone assemblage of northern Moon River subdomain.

Résumé

Les liens qui existent entre les domaines lithostructuraux du sud-est de la baie Georgienne et au sein de chacun d'eux sont décrits. Le domaine de Go Home est composé de gneiss granitoïde très déformé et de minces mais persistentes unités de marbre et de paragneiss à graphite, tous recoupés d'orthogneiss plus récent. Ces roches sont structuralement sous-jacentes à un gneiss migmatitique à haute teneur en leucosome dont la limite inférieure est orné de masses allongées et de couches de gneiss anorthositique et de basite métamorphisée, près desquelles reposent de grands massifs de gabbro coronitique métamorphisé et des granulites à grenat-pyroxène. Les plis subhorizontaux à direction nord-nord-ouest dans ce domaine sont déformés par des structures à direction ouest-nord-ouest associées au détachement basal de la structure synforme de Moon River dans laquelle les gneiss présentent une quasi-stratigraphie simple stratifiée. Le gneiss de Moon River repose sur une extrémité atténuée de roches du domaine de Parry Sound, là où se trouve une unité repère d'anorthosite-quartzite. Les roches de Parry Sound reposent à leur tour sur l'assemblage de Blackstone dans le sous-domaine septentrional de Moon River.

[1] Contribution to the Canada-Ontario Mineral Development Agreement 1985-1990. Project carried by the Geological Survey of Canada.

[2] Department of Geology, Dalhousie University, Halifax, Nova Scotia, B3H 3J5.

INTRODUCTION

This report outlines the preliminary results of the third of three seasons' mapping of a corridor across tectonic strike in the Central Gneiss Belt of the Grenville Province, Ontario. This work was funded by the Canada-Ontario Mineral Development Agreement 1984-1989 under Project C.2.3., "Georgian Bay Geological Synthesis". The corridor extends from Key Harbour, situated close to the Grenville Front Tectonic Zone, southeast to the neighbourhood of Port Severn, beyond which Paleozoic sedimentary rocks cover the Shield. An important aim of the traverse is to explore further the tectonic history of this part of the Grenville Province, building on the reconnaissance mapping of Davidson et al. (1982). Following work to the northwest in 1987 and 1988 (Culshaw et al., 1988, 1989), mapping was undertaken in 1989 in the southern part of the corridor, an area 35 km long and tapering in width southward from 25 km to 3 km. The northern part of the area is within parts of the Parry Sound domain and the Moon River subdomain (Davidson et al., 1982; Culshaw et al., 1983). The area has already received some attention from authors mainly interested in structural aspects (Waddington, 1973; Schwerdtner and Mawer, 1982; van Berkel and Schwerdtner, 1986); less attention has been paid to lithology (eg. Davidson et al., 1982), and many aspects of the geology remained poorly known.

SUMMARY OF FINDINGS

The following are the highlights of the mapping: (1) The relationship between the Moon River and Blackstone Lake gneiss associations, and the Parry Sound domain has been clarified (Fig. 1). This was necessary since last year's work (Fig. 2, Culshaw et al., 1989) left some uncertainty over the relationship between these units on the west side of the Moon River structure north and northeast of Twelve Mile Bay.

(2) Mapping of that part of the Moon River subdomain that lies within the study area has been completed. This shows that the synform is formed in a relatively simple succession of layered gneisses.

(3) The major effort was directed at mapping the segment of the Go Home subdomain that lies within the area. This is part of the lowest "deck" of the Central Gneiss Belt (Culshaw et al., 1983), possibly part of the parautochthon as defined by Rivers et al. (1989). It is divisible into three units, based on characteristic associations of gneissic rocks: a) the Honey Harbour gneiss, a predominantly quartzofeldspathic gneiss of which much probably had a plutonic parent; a metasedimentary component includes extensive but thin, folded sheets of marble and associated paragneiss. b) the Go Home granitoids which intrude the Honey Harbour gneiss; these granitoids are gneissic megacrystic granites, granodiorites, monzonites and associated mafic rocks, forming a large complex which dominates much of the east side of the mapped area. c) the Pine Island migmatites that form a structurally higher unit. This migmatite sheet is separated from the underlying Go Home granitoids and Honey Harbour gneiss by a tectonic contact decorated with small fragments and discontinuous layers of foliated anorthosite and small bodies of metabasite, including "pseudo-eclogite" (Culshaw et al., 1983).

Boundaries between the two lower units are at least in part tectonic. The results of the mapping support the concept that Go Home subdomain has structural and lithological similarities with Rosseau subdomain which lies northeast of Moon River subdomain and therefore that these two subdomains may be physically continuous beneath the Moon River synform (Culshaw et al., 1983; Davidson, 1984).

GO HOME SUBDOMAIN

Honey Harbour gneiss (gHH)

The main mass of the Honey Harbour gneiss occupies the south part of Go Home subdomain; to the northwest it forms a thin belt between the Go Home granitoids and the Pine Island migmatites (Fig. 1). It is composed mainly of fine grained, migmatitic, pink granitic or grey granodioritic gneiss, generally biotite-bearing but poor in hornblende. Although usually uniform in outcrop and lacking both well developed layering and the streaky shape fabric characteristic of a plutonic parentage, in several places the gneiss has preserved textures indicative of plutonic origin. Mafic gabbroic or dioritic gneiss interlayered with monzonite occur in the east, well exposed along Highway 69 (d, Fig. 1). Within the area southeast of Honey Harbour the gneiss includes several strips of strongly foliated monzonitic and granitic orthogneiss (m, Fig. 1). The age relationship of these, and other bodies too small to show in Figure 1, to the rest of the Honey Harbour gneiss is not known. In contrast, close to the margin of the Go Home granitoid complex the Honey Harbour gneiss is cut by small dykes of megacrystic granite related to that complex. To the east, in outcrops along Highway 69, the colour of fresh and weathered surfaces suggest that, although no orthopyroxene was observed in the field, the gneiss locally attained granulite facies.

Within the southern exposure of the Honey Harbour gneiss there are several extensive layers of marble associated with calc-silicate gneiss and rusty graphitic paragneiss (see Grant, 1985). Although very thin, these units are remarkably persistent and form excellent markers which trace out the major folds (Fig. 1). The marbles have a tectonoclastic fabric and adjacent quartzofeldspathic gneisses are commonly flaggy. The occurrence of these tectonic fabrics and the fact that two of the units of marble lie along the contact of the Honey Harbour gneiss with orthogneiss suggest that they may mark zones of displacement. The marble contains wollastonite, diopside and locally forsterite. The surrounding quartzofeldspathic gneisses usually contain only biotite and hornblende, but may be retrograded from granulite facies. The rusty paragneiss is commonly graphitic and in places it has been prospected by small-scale trenching. It is probable that sulphide- and graphite-rich zones are more common and extensive than previously known and may merit further prospecting.

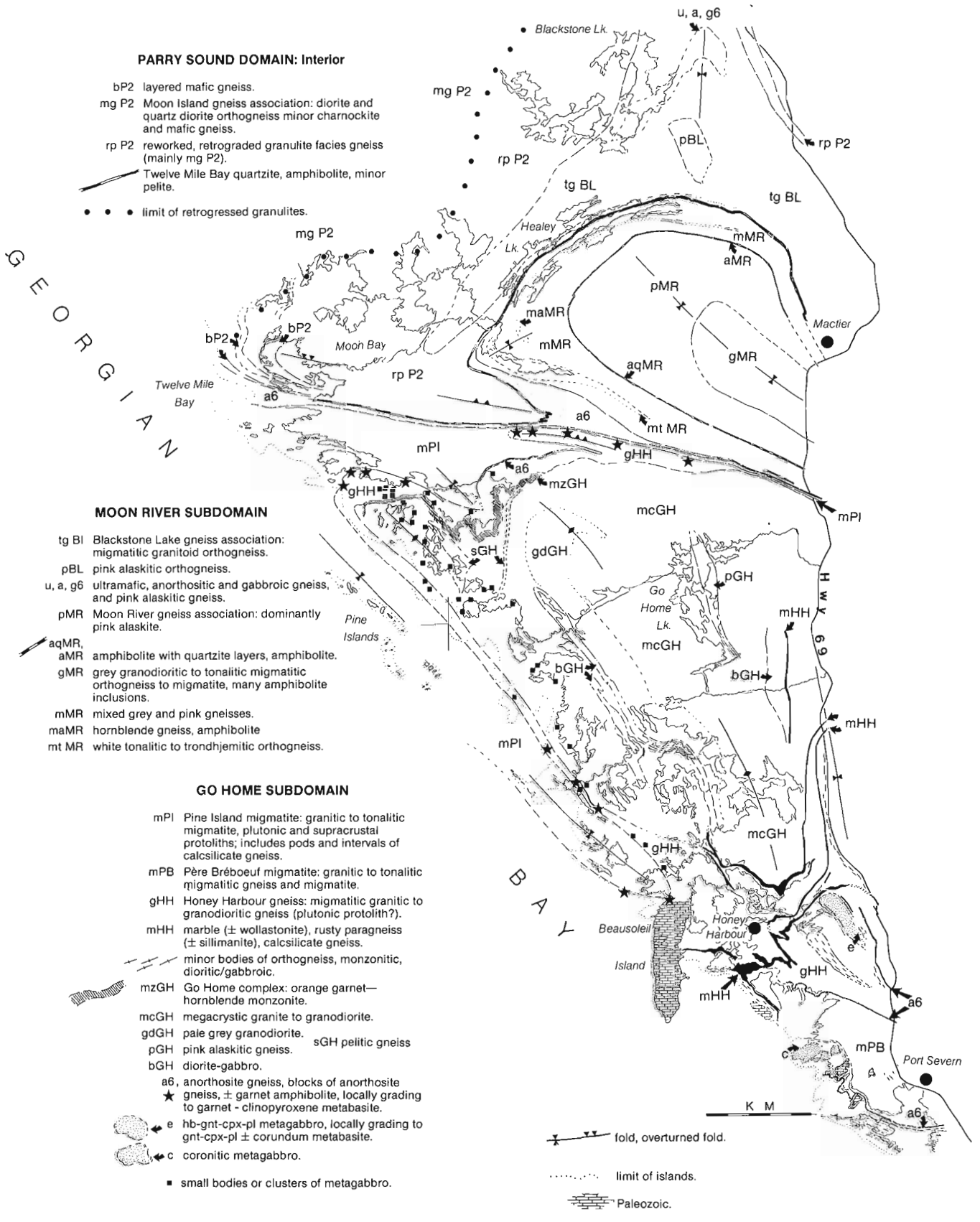

Figure 1. Geological map of the area west of Highway 69 from Moon Bay-Healey Lake-Mactier area to Port Severn.

Go Home complex

The most extensive unit in the map area is composed of strongly foliated granitoids of the Go Home complex (units mcGH, gdGH, pGH and bGH, Fig. 1). The predominant rock types are preliminarily identified as megacrystic monzogranite and granodiorite, containing biotite, hornblende and subordinate, sporadically developed garnet (unit mcGH). The northwestern boundary of the complex is marked by a thin folded sheet of orange garnet-hornblende monzonite (unit mzGH) and the centre is dominated by an elongate body of pale grey granodiorite to tonalite (unit gdGH). Elongate bodies of dioritic to gabbroic metaplutonic gneiss lie within the complex (unit bGH). The complex is deformed, being affected both by regional scale folds and pervasive outcrop scale deformation producing, for example, belts of flaggy and/or augen gneiss, zones of chaotic folding and shearing, or total destruction of orthogneiss fabric by mylonitization. These granitoids do not physically resemble the mid-Proterozoic plutons exposed within the Britt domain in the northern part of the transect (Davidson et al., 1982; "single-cycle orthogneisses" of Culshaw et al., 1988 and 1989). They differ in composition, texture and compositional range, resembling more closely some of the granitoid rocks of the Brandy Lake complex, which is situated within the Rosseau subdomain of the "lower deck". However, the age of the Brandy Lake complex (Muskoka granite) has been determined at 1414 Ma (U-Pb zircon; Krogh and Davis, 1969; recalculated in Easton, 1986), in the same age range as the single-cycle orthogneiss bodies in Britt domain (van Breemen et al., 1986).

Pelitic gneiss containing sillimanite (unit sGH) occurs in the northwest part of the Go Home complex. These are relatively poor in garnet and mica despite their aluminous nature; they have a distinctive quartzofeldspathic aspect, resembling certain metasedimentary rocks of the Key Harbour gneiss association (Culshaw et al., 1988).

Pine Island migmatite and related rocks (units mPI, mPB)

In the following descriptions, the term "migmatite" is used to distinguish rocks that are not only "mixed rocks" in the classical sense of the term but also which have a field-character determined by the presence of abundant leucosome (in field jargon, they are extremely "juicy"). Thus many quartzofeldspathic rocks in the study area are "migmatitic", having a minor amount of leucosome, whereas those referred to as "migmatite" may contain leucosome and host rock in equal proportions.

There are two distinct bodies of migmatite, as defined above, of which the Pine Island migmatite (unit mPI) is the largest. These bodies have a special structural relationship with their neighbouring rocks, described further below. The Pine Island migmatite is the structurally highest unit in the Go Home subdomain, forming a sheet folded along the outer coast into a large, northwest-trending synform. It overlies the Honey Harbour gneiss and the Go Home complex and dips northward beneath the thin anorthosite and enveloping gneisses along Twelve Mile Bay at the base of the Moon River structure (Fig. 1). It consists of a basal tonalitic migmatite overlain by simple biotite-bearing migmatite of granitic and granodioritic composition and sheets of pink alaskitic gneiss. There are also pods and thin intervals of calc-silicate gneiss and rare leucocratic granitic migmatite containing local occurrences of muscovite and sillimanite. For these a supracrustal origin is most likely.

The Pine Island migmatite is not cut by either the Go Home complex granitoids or plutonic members of the Honey Harbour gneiss. The boundary with the underlying Honey Harbour gneiss is generally the site of highly strained rock and is marked by a line of small anorthosite, garnet amphibolite and "pseudo-eclogite" bodies. The anorthosite bodies are mostly metre-scale rounded blocks of strongly foliated and totally recrystallized white anorthosite gneiss. These occur in trains set in a granitic or pegmatitic matrix; foliation within individual blocks is commonly disposed at a high angle to that in the country rock. Elongate, concordant lenses of anorthosite gneiss are also present, for example along the northern contact (Fig. 1). The blocks may therefore have originated by pull-apart and rotation of already ductilely deformed and strain-hardened rock. The presence of these blocks, the strongly developed fabric and the lithological break noted above is compatible with interpretation of the boundary of the Pine Island migmatite as a detachment, as has been suggested for comparable boundaries (Davidson, 1984).

A second body of migmatite is situated in the south where it is infolded with the Honey Harbour gneiss (unit mPB, Fig. 1). The boundaries of this body are also associated with both continuous elongate bodies of anorthosite gneiss and trains of fragments of anorthosite gneiss identical to those at the base of the Pine Island migmatite (cf. Grant, 1985, for previously recognized anorthosite). These migmatites contain tonalitic migmatite similar in part to the Pine Island migmatite but different in its content of migmatite derived from granitoid.

Mafic igneous rocks

The anorthosite bodies which lie along gneiss-migmatite boundaries are generally accompanied by small masses of garnet amphibolite. Some of these are demonstrably derived from garnet-clinopyroxene metabasite ("pseudo-eclogite") preserved in the cores of the masses. This association seems to be characteristic of tectonic boundaries within this part of the Central Gneiss Belt, the rock assemblage being present along the base of the Moon River structure along Twelve Mile Bay, in the southwest of Britt domain near Bateau Island (Culshaw et al., 1989, Fig. 1), and within Rosseau subdomain (see Davidson, 1990).

In contrast to the small metabasites associated with anorthosite, the South Bay metagabbro is relatively large (Fig. 1). It is mainly composed of fine grained plagioclase-hornblende-garnet-clinopyroxene but generally lacks preserved igneous texture. Assemblages dominated by clinopyroxene-garnet have been observed at one locality where they are accompanied by several metre-wide corundum-bearing zones. These features suggest the metagabbro has a "pseudo-eclogitic" affinity, compatible with its spatial association with the elongate anorthosite

gneiss which lies to the east of the body along the boundary between Honey Harbour gneiss and migmatite (Fig. 1).

To the northwest there are many small gabbroic bodies immediately below the anorthosite-decorated boundary of the Pine Island migmatites (Fig. 1). Most of these are thoroughly metamorphosed and texturally altered. The end product is a metabasite with a discontinuous, plagioclase-rich leucosome. Some of the larger bodies have metamorphic windows in which an earlier coronitic texture is evident. Since they are concentrated close to an important tectonic boundary they may be comparable with the metabasites concentrated along the tectonic boundary of the Nadeau Island gneiss association in the southern part of the Britt domain (Needham, 1987; Culshaw et al., 1989).

Equant bodies of coronitic olivine metagabbro near Port Severn, in contrast, are for the most part composed of texturally very well preserved rock containing primary igneous minerals with relatively narrow reaction rims (Grant, 1985). Parts of the contacts of these bodies show an intrusive relationship with the enclosing migmatitic gneiss, with fine grained gabbro cutting across earlier layering and leucosome. Other parts of the contacts, however, show involvement of the gabbro in high-grade ductile deformation, whereby elongate blocks and slivers of flattened, formerly coarse grained metagabbro are oriented within the foliation of well layered gneissic tectonites. U-Pb baddeleyite and metamorphic zircon ages of ca. 1170 Ma and 1050 Ma, respectively, obtained from this gabbro (Davidson and van Breemen, 1988) give a younger age limit for early leucosome formation and a possible age for the later deformation.

MOON RIVER SUBDOMAIN

Moon River gneiss association

The Moon River gneiss association ("assemblage" in Fig. 2, Culshaw et al., 1989) has a simple, layered quasi-stratigraphy above the thin anorthosite/quartzite/amphibolite marker which lies along the base of the structure (Fig. 1). Mixed pink and grey plutonic and supracrustal migmatitic gneisses (unit mMr) lie above the marker, and include units that are not continuous around the structure. For example, a white tonalitic or trondhjemitic orthogneiss (unit mtMR) which contains its own suite of mafic dykes forms an elongate lens along the western edge of the association, near the thickest part of the anorthosite (Fig. 1). This gives way along strike to the southeast to grey migmatitic biotite/hornblende/garnet gneiss (included in unit mMR). This combined unit is overlain by a thin but very persistent amphibolite which is associated for much of its length with three quartzite horizons (unit aqMR/aMR). Together these form a second marker which traces out the synform. For much of its length the amphibolite lies at the lower boundary of a large unit of pink leucocratic gneiss (unit pMR). This includes both layered and uniform, bright pink, equigranular to weakly streaky, biotite-magnetite granite gneiss. This type of rock is common elsewhere in the Georgian Bay transect where it has been referred to as "alaskite". For example, it occurs as layers within the Pine Island migmatite, in the southern Sand Bay gneiss association (unit pS?, Culshaw et al., 1989, Fig. 1), and in the Bayfield gneiss association (unit pB, Culshaw et al., 1988, Fig. 1). This unit also includes minor granodioritic gneiss and contains small pods of garnet amphibolite which are probably metagabbro. The core of the synform within the map area is formed of grey migmatitic gneiss (gMR), which has a tonalitic to granodioritic composition with minor variants (plagioclase-hornblende-biotite ± epidote ± K-feldspar). A characteristic feature is the abundance of blocky amphibolite boudins which form ca. 20-30 % of any outcrop. The rock has a uniform granoblastic texture lacking the streaky texture commonly associated with deformed plutonic rocks; however, its generally uniform composition suggests a plutonic precursor.

Blackstone Lake gneiss association

Granodioritic and granitic migmatites of the Blackstone Lake association (unit tgBL; see also Culshaw et al., 1989, Fig. 2) lie beneath the basal anorthosite/quartzite marker on the east side of the Moon River structure. These rocks are continuous with those along strike to the north and continue beyond the map area to the southeast. On the west side of the Moon River structure, north of Twelve Mile Bay, gneisses of Parry Sound domain can be traced continuously from within the area of retrograde granulites, eastward along the contact with the anorthosite-quartzite marker unit along Twelve Mile Bay, around the overturned antiform at Moon Bay, and eastward around the synform between overlying anorthosite-quartzite and underlying Blackstone Lake gneiss (Fig. 1). East of Healey Lake they have not been recognized and presumably pinch out along strike.

STRUCTURE

The oldest recognized structures within Go Home domain are the high strain fabrics represented by the folded tectonoclastic marbles and the basal fabric of the Pine Island migmatite (Fig. 1). These are folded by northwest-trending regional folds (F_2), an example being the synform in the Pine Island migmatite, a subhorizontal structure over 20 km along its axial trace (Fig. 1). Variability of plunge results in the cellular structure present in the south part of Go Home subdomain. Folds associated with the straight zone which extends east-southeastward from Twelve Mile Bay are younger (F_3), as is shown by the refolding of small- and large-scale F_2 folds. The latter are overturned with north-northeast-dipping axial surfaces in the vicinity of Twelve Mile Bay (Fig. 1). Smaller asymmetric folds of probably similar age occur on the east side of the synform in the region of Mactier (Fig. 1).

SUMMARY

Go Home subdomain within the transect has a three-fold lithological division: migmatite, megacrystic granitoids and older mixed gneisses. These rocks are part of the "lower deck" of the Central Gneiss Belt which itself contains anorthosite-decorated tectonic boundaries. As in Britt domain, there are subhorizontal structures tens of kilometres long. The intersection of two anorthosite-

decorated tectonic boundaries at the base of the Moon River structure and the Pine Island migmatites respectively suggests repetition of similar major structures. This geometry is repeated in Rosseau subdomain (Davidson et al., 1982, Davidson, 1990); such a scenario may imply the presence of a hidden floor thrust below the Go Home and Rosseau subdomains. The presence of rocks of the Parry Sound domain within what has previously been defined on lithological and structural grounds as the Moon River subdomain (Davidson et al., 1982) suggests that a distinction should be made between the Moon River structure (geometrical) and the Moon River subdomain (lithological).

REFERENCES

Culshaw, N.G., Check, G., Corrigan, D., Drage, J., Gower, R., Haggart, M.J., Wallace, P., and Wodicka, N.
1989: Georgian Bay geological synthesis: Dillon to Twelve Mile Bay, Grenville Province of Ontario; in Current Research, Part C, Geological Survey of Canada, Paper 89-1C, p. 157-163.

Culshaw, N.G., Corrigan, D., Drage, J., and Wallace, P.
1988: Georgian Bay geological synthesis: Key Harbour to Dillon, Grenville Province of Ontario; in Current Research, Part C, Geological Survey of Canada, Paper 88-1C, p. 129-133.

Culshaw, N.G., Davidson, A., and Nadeau. L
1983: Structural subdivisions of the Grenville Province in the Parry Sound - Algonquin region, Ontario; in Current Research, Part B, Geological Survey of Canada, Paper 83-1B, p. 243-252.

Davidson, A.
1984: Identification of ductile shear zones in the southwestern Grenville Province of the Canadian Shield; in Precambrian Tectonics Illustrated, edited by A. Kröner and R. Greiling, Schweizerbart'sche Verlagsbuchhandlung, Stuttgart, p. 263-279.

Davidson, A.
1990: Evidence for eclogite metamorphism in the southwest Grenville Province, Ontario; in Current Research, Part C, Geological Survey of Canada, Paper 90-1C.

Davidson, A. and van Breemen, O.
1988: Baddeleyite-zircon relationships in coronitic metagabbro, Grenville Province, Ontario: implications for geochronology; Contributions to Mineralogy and Petrology, v. 100, p. 291-299.

Davidson, A., Culshaw, N.G., and Nadeau, L.
1982: A tectono-metamorphic framework for part of the Grenville Province, Ontario; in Current Research, Part A, Geological Survey of Canada, Paper 82-1A, p. 175-190.

Easton, R.M.
1986: Geochronology of the Grenville Province; in J.M. Moore, A. Davidson, and A.J. Baer, ed., The Grenville Province; Geological Association of Canada, Special Paper 31, p. 127-173.

Grant, S.M.
1985: Coronitic gabbro and meta-anorthosite in the Central Gneiss Belt, Grenville Province of Ontario; in A. Davidson et al., Studies in the Grenville Province of Ontario; in Current Research, Part A, Geological Survey of Canada, Paper 85-1A, p. 474-478.

Krogh, T.E. and Davis, G.L.
1969: Old isotopic ages in the northwestern Grenville Province; in H.R. Wynne-Edwards, ed., Age Relationships in High-grade Terranes; Geological Association of Canada, Special Paper 5, p. 189-192.

Needham, T.W.
1987: Geological setting of two metagabbroic bodies, central Britt domain, southwestern Grenville Province; in Current Research, Part A, Geological Survey of Canada, Paper 87-1A, p. 507-603.

Rivers, T., Martignole, J., Gower, C.F., and Davidson, A.
1989: New tectonic divisions of the Grenville Province, southeast Canadian Shield; Tectonics, v. 8, p. 63-84.

Schwerdtner, W.M. and Mawer, C.K.
1982: Geology of the Gravenhurst Region, Grenville Structural Province, Ontario; in Current Research, Part B, Geological Survey of Canada, Paper 82-1B, p. 195-207.

van Berkel, J.T. and Schwerdtner, W.M.
1986: Precambrian geology of the Moon River area, Muskoka and Parry Sound Districts; Ontario Geological Survey, Geological Series Map P2954.

van Breemen, O., Davidson, A., Loveridge, W.D., and Sullivan, R.W.
1986: U-Pb zircon geochronology of Grenville tectonites, granulites and igneous precursors, Parry Sound, Ontario; in J.M. Moore, A. Davidson, and A.J. Baer, ed., The Grenville Province; Geological Association of Canada, Special Paper 31, p. 191-207.

Waddington, D.H.
1973: Foliation and Mineral Lineation in the Moon River Synform, Grenville Structural Province, Ontario; M.Sc. thesis, University of Toronto, Toronto, Canada.

Evidence for eclogite metamorphism in the southwest Grenville Province, Ontario

A. Davidson
Continental Geoscience Division

Davidson, A., Evidence for eclogite metamorphism in the southwest Grenville Province, Ontario; in Current Research, Part C, Geological Survey of Canada, Paper 90-1C, p. 113-118, 1990.

Abstract

Among several occurrences of garnet-studded mafic rock within the Central Gneiss Belt, Grenville Province, a few contain evidence for former eclogite assemblages. An example from a tectonically attenuated, metamorphosed basic igneous complex at Lake Rosseau, Ontario, is used to document this finding. Eclogite metamorphism is deduced to have taken place in situ, *implying that both the meta-igneous complex and its quartzofeldspathic country rocks have experienced higher pressure ($\geq \sim 1.3$ GPa) than is normally recorded in this region. Evidence for the high-pressure stage of the rocks' P-T-time path is preserved only in mafic rocks of appropriate bulk composition, and to date has been found only within the tectonically lowest structural domains.*

Résumé

Des nombreuses venues de roche mafique parsemée de grenat relevées dans la zone de gneiss centrale de la province de Grenville, quelques-unes seulement contiennent des indices d'anciens assemblages d'éclogite. Un exemple à partir d'un complexe igné basique, métamorphisé et tectoniquement atténué, au lac Rosseau (Ontario), est utilisé pour réaliser cette conclusion. Il est établi par déduction que le métamorphisme des éclogites aurait eu lieu in situ, *indiquant que le complexe igné métamorphisé et ses roches encaissantes quartzofeldspathiques ont été soumis à une pression plus élevée ($> \approx 1{,}3$ GPa) qu'habituellement enregistrée dans cette région. Des traces de pression élevée du parcours P-T-temps des roches n'ont été conservées que dans les roches mafiques de composition globale appropriée, et n'ont été relevées, à ce jour, que dans les domaines structuraux les plus tectoniquement inférieurs.*

INTRODUCTION

Tectonic lenses of mafic rock occur commonly within the Grenville gneiss terranes in Ontario, particularly in zones of high ductile strain. Among them are lenses and pods of mafic rock studded with garnet porphyroblasts, previously referred to as 'eclogite-like rock' (Davidson et al., 1982) or 'pseudo-eclogitic metagabbro' (Culshaw et al., 1983) because, despite its appearance, it contains plagioclase and augite, not omphacite. However, at an isolated occurrence near Arnstein (Davidson et al., 1982), garnet has a pyrope content as high as 55 mol per cent, kyanite forms embayed cores within corundum-spinel-sapphirine knots, and clinopyroxene with a maximum jadeite content of ~10 mol per cent is intimately intergrown with plagioclase. Grant (1987) obtained pressure and temperature estimates of ~1.5 ± 0.1 GPa and 825 ± 50°C for this rock, and did not hesititate to refer to it as meta-eclogite.

In some places, mafic rock composed of pyroxene, amphibole and plagioclase, studded with garnet porphyroblasts, is associated with anorthositic and related mafic gneiss in concordant layers or trains of lenses and pods that can be traced for several tens of kilometres within quartzofeldspathic gneiss (Fig. 1, inset). Detailed mapping of one of these units, located in Rosseau subdomain and previously reported to contain sapphirine-bearing gneiss of anorthositic affinity (Davidson et al., 1982), has revealed several pods and lenses of eclogite-like rocks distributed along a strike length exceeding 20 km (Fig. 1). This highly attenuated and metamorphosed basic igneous complex is rarely more than 200 m thick and contains rocks whose compositions range from pyroxenite to anorthosite. Primary igneous texture, usually distorted by flattening and only rarely nondeformed, is locally preserved in low-strain lenses within otherwise completely recrystallized and generally very fine grained, sugary textured, thinly layered gneiss composed predominantly of plagioclase and amphibole with or without garnet, pyroxene and biotite. The purpose of this paper is to present evidence that the eclogite-like rocks in these occurrences formerly contained the eclogitic assemblage omphacite-garnet-kyanite, now variably "retrograded" (the term "retrograded" is used here in the same sense as in most literature on altered eclogite (e.g. Dunn and Medaris, 1988), even though the secondary minerals may be "prograde" in terms of temperature (Griffin, 1987)).

ECLOGITIC ROCKS AT JUDDHAVEN

Among the least retrograded eclogitic rocks so far discovered are those occurring on the peninsula separating Lake Joseph and Lake Rosseau between Juddhaven and Minett (Fig. 1), where they form pods and layers associated with metapyroxenite, amphibole-plagioclase gneiss (metagabbro) and meta-anorthosite. The massive, dark green eclogitic rocks contain 10-50 per cent red garnet up to 15 mm in diameter in a medium to fine grained matrix composed principally of green clinopyroxene and dark green amphibole; plagioclase is rarely evident in hand specimen. In some rocks, large aggregates of pale amphibole and pyroxene with dark amphibole rims are pseudomorphous after some original mafic phase, possibly olivine, giving evidence for a formerly coarse grain size.

Thin sections show the following features: 1) Garnet porphyroblasts contain inclusions of kyanite, rutile, plagioclase, amphibole and rare quartz and clinopyroxene; they have embayed margins and are surrounded by radiating, relatively coarse amphibole-plagioclase symplectite that grades outward to amphibole with very little intergrown plagioclase (Fig. 2, A). 2) Clinopyroxene is intimately intergrown with plagioclase in the form of a fine, feathery symplectite (Fig. 2, B); small orthopyroxene grains are present in the outer margins of this symplectite, which is separated from garnet by amphibole-plagioclase symplectite. 3) Small knots of vermiform corundum, green spinel and pale blue sapphirine in a matrix of small, polygonal plagioclase grains are separated from garnet and clinopyroxene-plagioclase symplectite by amphibole-plagioclase symplectite; these knots are zoned, usually with corundum in the cores separated from outer sapphirine by a median zone of spinel, although some knots have spinel cores with sapphirine rims or are composed entirely of spinel. 4) All of the plagioclase is metamorphic in origin; there are no pseudomorphous forms suggesting former plagioclase laths. 5) Polygonal plagioclase grains in and around the aluminous mineral knots are reversely zoned and calcic, and in sharp contact with more sodic plagioclase associated with adjacent amphibole-plagioclase symplectite.

Electron microprobe analyses of the various mineral components are summarized below:

1) Garnet is weakly zoned, ranging from $Gr_{22}Al_{31}Py_{47}$ (core) to $Gr_{21}Al_{38}Py_{41}$ (rim) in one specimen, and $Gr_{21}Al_{41}Py_{37}$ (core) to $Gr_{22}Al_{34}Py_{44}$ (rim) in another.
2) Clinopyroxene in symplectite has a jadeite content ranging from 4.5 to 10.3 mol per cent and a comparable content of Tschermak's molecule. One analysis of a grain enclosed in garnet has a jadeite content of 13.4 mol per cent.
3) Amphibole is pargasite with Al = 1.75-1.9 T-site occupancy and X_{Mg} between 0.72 and 0.78.
4) Plagioclase intergrown with clinopyroxene has the range An_{34-40}. Plagioclase intergrown with pargasite ranges from An_{54} adjacent to garnet to An_{42} away from garnet. It has a similar composition between amphibole and aluminous mineral knots, adjacent to which it is reversely zoned with Ca-rich rims. Plagioclase within the aluminous mineral knots has the range An_{79-92}. One plagioclase inclusion in garnet analyzed as An_{29}.
5) Sapphirine is a highly aluminous variety, more so than the empirical 7:9:3 formula (Higgins et al., 1979); X_{Mg} is 0.85. Spinel, despite its dark green colour, has a relatively high Mg-spinel content ranging from 58 to 65 mol per cent.

The symplectitic intergrowths described above are interpreted as follows. *Clinopyroxene-plagioclase*: retrograde breakdown of former omphacitic clinopyroxene. Although omphacite *per se* has been found neither as preserved relicts within this symplectite nor as inclusions in garnet, this type of symplectite has long been recognized as the product of omphacite breakdown (e.g. Eskola, 1921; Alderman,

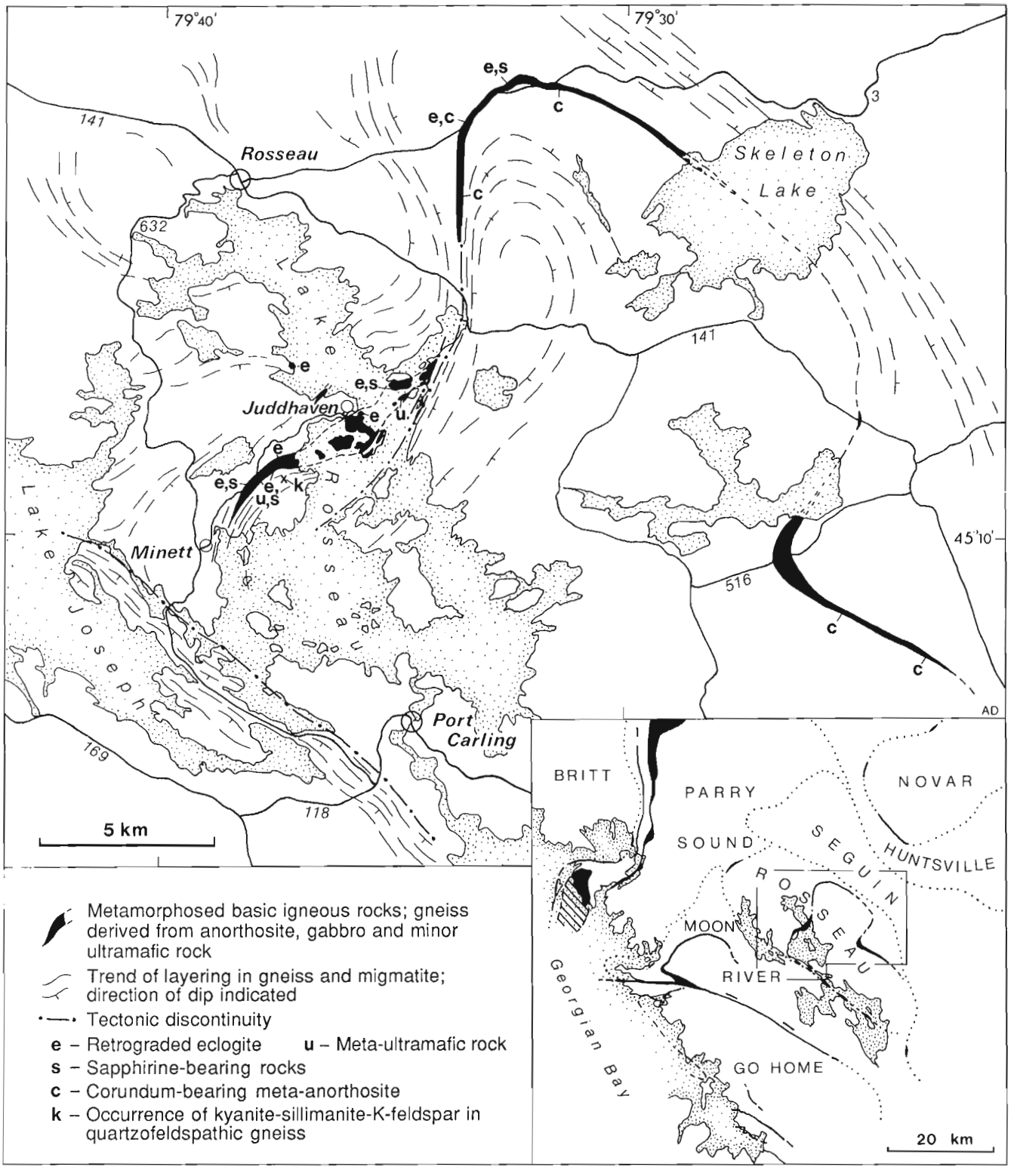

Figure 1. Distribution of anorthositic meta-igneous units in the Muskoka region, Ontario (inset), and details of the meta-eclogite-bearing unit in the Lake Rosseau area.

1936; Davidson, 1943; Boland and van Roermund, 1983). *Pargasite-plagioclase*: reaction between garnet and former omphacite; this type of symplectite is also commonly recorded in examples of partly retrograded eclogite (e.g. Dunn and Medaris, 1988). *Aluminous minerals-bytownite symplectite*: reaction involving kyanite or clinozoisite and garnet, perhaps omphacite. Although kyanite or clinozoisite relicts have not been observed in the cores of aluminous symplectite knots in the Juddhaven occurrence, kyanite forms large ragged cores in identical symplectites in retrograded eclogite near Arnstein (Fig. 2, C); similar replacements are known in retrograded eclogite occurrences elsewhere in the world (e.g. Bard et Caruba, 1982; Santallier, 1983). Grant (1987) observed clinozoisite in a similar relationship to corundum-spinel symplectite in meta-eclogite from near the west boundary of Algonquin Park. Moreover, where kyanite inclusions are exposed at embayed garnet rims, they are partly or wholly replaced by aluminous symplectite in examples from both Juddhaven and Arnstein (see Davidson et al., 1982, Plate 30.4, D).

Whole rock chemical analyses of Juddhaven retrograded eclogite (Table 1) indicate a precursor of slightly nepheline-normative olivine gabbro composition with about 60 mol per cent normative plagioclase ($\sim An_{70}$). Modal metamorphic plagioclase in these rocks is difficult to estimate on account of the extremely fine grain size of the clinopyroxene-plagioclase symplectite, but it does not exceed 25 per cent. Preliminary modelling using the above whole rock composition, thermodynamic data of Berman (1988) and the modelling program THERIAK (diCapitani and Brown, 1987) suggests that at 600°C the primary low-pressure assemblage olivine-plagioclase-diopside should be abruptly replaced by the eclogite assemblage garnet-omphacite-kyanite ± quartz at 1.28 GPa; the required pressure would be greater at higher temperature, similar to

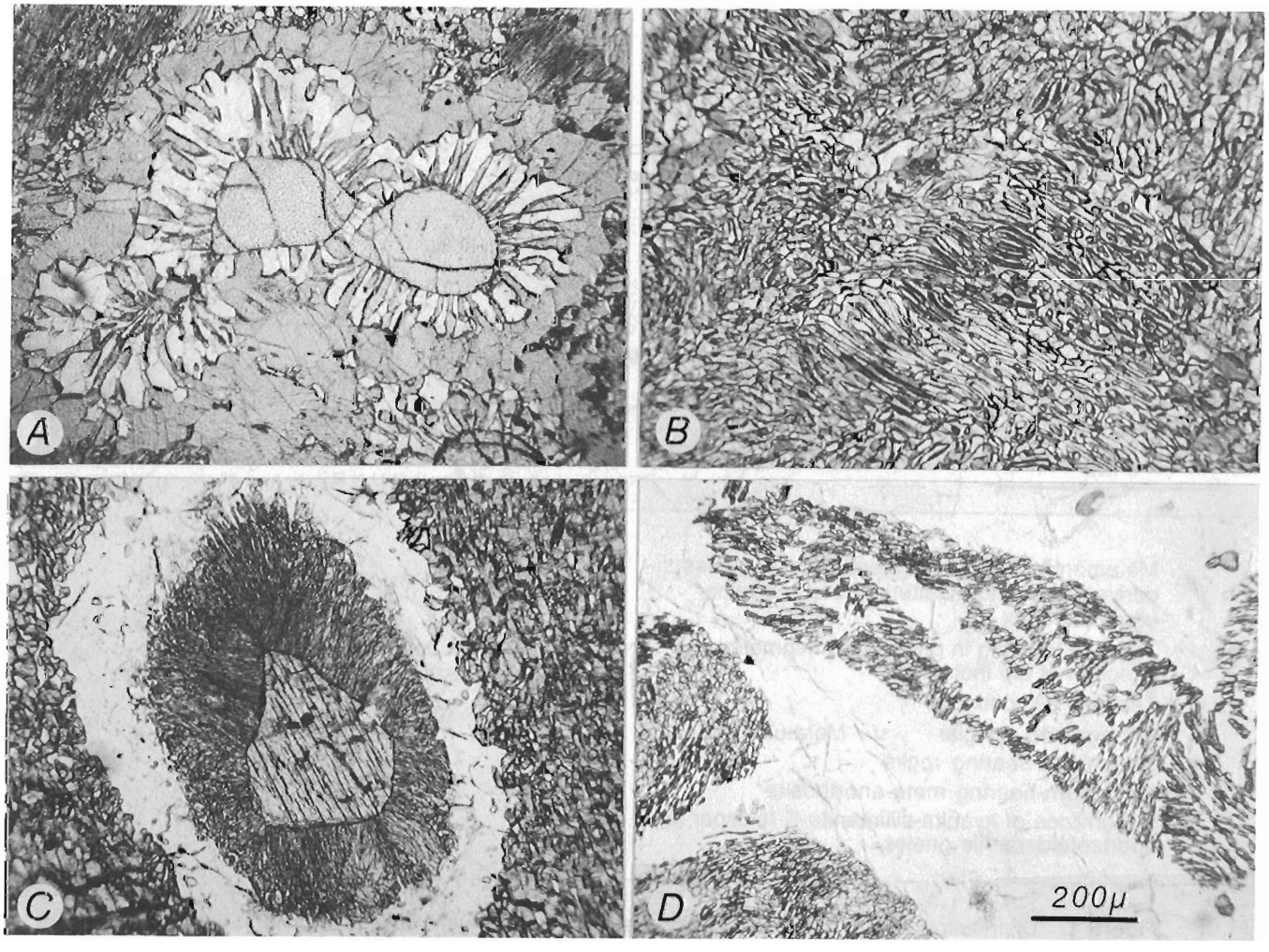

Figure 2. Photomicrographs of symplectitic intergrowths in meta-eclogite, plane light: **A.** garnet surrounded by plagioclase-pargasite symplectite with outer rim of pargasite against fine clinopyroxene-plagioclase symplectite. **B.** detail of clinopyroxene-plagioclase symplectite, interpreted to have formed from omphacitic clinopyroxene. **C.** corundum-spinel-sapphirine-plagioclase symplectite surrounding core of corroded kyanite. **D.** corundum knots in meta-anorthosite, pseudomorphous after an unknown former phase, possibly primary igneous Ca-plagioclase. All photomicrographs are at the same scale.

values obtained by Grant (1987). These estimates are higher than any paleopressures recorded in the country rock gneisses (0.8 - 1.1 GPa; Anovitz and Essene, in press).

INFERENCE OF ECLOGITE METAMORPHISM

The occurrence of retrograded eclogite associated with a highly attenuated but otherwise intact basic meta-igneous suite does not support the idea that the eclogite masses are tectonically emplaced fragments derived from deeper level, and out of metamorphic equilibrium with their enclosing rocks. Moreover, associated anorthositic and leucogabbroic rocks also contain evidence that they have undergone similar high pressure metamorphism. For example, some anorthositic layers are replete with vermiform corundum, spinel or sapphirine aggregates, commonly in the form of pseudomorphs after some unknown phase (kyanite, clinozoisite, Ca-plagioclase?) (Fig. 2, D); loosely knit aggregates of orthopyroxene, clinopyroxene and garnet, probably in replacement of primary olivine, have dispersed outer zones of sodium gedrite, an unusual mineral also reported from meta-eclogites in Norway (Smith, 1988). There is no evidence, however, that pressure was high enough for plagioclase to have become unstable on its own (i.e., anorthite → Tschermak's molecule + quartz; albite → jadeite + quartz). Nevertheless, plagioclase can be eliminated at lower pressure in rocks of suitable composition by reaction with mafic phases such as olivine; the balanced equation given as an example below has reactant albite, anorthite and olivine in essentially the same proportions as in the norm of the analysis given in Table 1:

13 plagioclase ($An_{69.2}$) + 7 olivine →
11 clinopyroxene ($Jd_{36.4}$) + 6 kyanite + 3 garnet ($Gr_{22.2}$)

Attenuated anorthositic gneiss units have been mapped in all domains of the Central Gneiss Belt in Ontario. Culshaw et al. (1983) suggested a stacking order for these domains, displaced northwestward on major ductile shear zones and implying a tectonic superposition. To date, units containing corundum-bearing anorthositic gneiss and associated retrograded eclogite have only been found in domains of the lowest structural deck (Britt, Go Home, Rosseau and parts of Algonquin domain).

Table 1. Whole rock analysis (weight per cent) and molecular norm of Juddhaven meta-eclogite

SiO_2	45.8	qz	0.0
TiO_2	0.35	or	2.8
Al_2O_3	19.3	ab	16.7
Cr_2O_3	0.05	an	40.8
Fe_2O_3	3.6	ne	1.7
FeO	5.6	cpx	12.0
MnO	0.16	opx	0.0
MgO	10.71	ol	21.7
CaO	11.48	mt	3.7
Na_2O	2.2	il	0.5
K_2O	0.49	ap	0.1
P_2O_5	0.04		
S	0.00		
CO_2	0.0	plagioclase	$An_{68.9}$
H_2O	0.9	mol. $Mg/Mg+Fe^T$	0.68
Total	100.68	normative C.I.	38.0

Secondary assemblages in the eclogitic and associated rocks (combinations of hypersthene, augite, garnet, pargasite, phlogopite, plagioclase, corundum, spinel, sapphirine and rutile) indicate adjustment to generally high-temperature conditions. If the earlier, relict eclogite metamorphism is not tectonically out-of-place, the surrounding quartzofeldspathic gneisses must also have been subjected to similar high-pressure conditions. That the country rocks record neither mineralogical nor textural evidence of such high-pressure metamorphism suggests that they have re-equilibrated at some later stage on their P-T-time paths, perhaps close to T_{max}. It is likely that re-equilibration was facilitated by continued recrystallization during the ductile flow recorded by the high-strain state preserved in most of the basic meta-igneous rocks and in the quartzofeldspathic gneisses that enclose them. The record of apparently *in situ* high-pressure metamorphism, preserved only in certain basic rocks, may therefore represent an earlier, higher pressure stage on the P-T-time path of all the rocks of the lower structural deck in this region of the Grenville Province. The timing of metamorphism is poorly constrained, however, and it is possible that the high-pressure metamorphism is not on a continuous P-T-time path with that which caused "retrogression" of the eclogitic assemblage.

REFERENCES

Alderman, A.R.
1936: Eclogites from the neighbourhood of Glenelg, Invernessshire; Geological Society of London, Quarterly Journal, v. 92, p. 488-530.

Anovitz, L.M. and Essene, E.J.
— Thermobarometry and pressure-temperature paths in the Grenville Province of Ontario; Journal of Petrology (in press).

Bard, J.-P. et Caruba, C.
1982: Texture et minéralogie d'une éclogite à disthène-sapphirine-hypersthène-quartz en inclusion dans les gneiss migmatiques des Cavalières, Massif de Sainte-Maxime (Maures orientales, France); Comptes Rendus des Séances de l'Académie des Sciences, v. 294, série II, p. 103-106.

Berman, R.G.
1988: Internally consistent data base for minerals in the system Na_2O-K_2O-CaO-MgO-FeO-Fe_2O_3-Al_2O_3-SiO_2-TiO_2-H_2O-CO_2; Journal of Petrology, v. 29, p. 445-522.

Boland, J.N. and van Roermund, H.L.M.
1983: Mechanisms of exsolution in omphacites from high temperature, type B eclogites; Physics and Chemistry of Minerals, v. 9, p. 30-37.

Culshaw, N.G., Davidson, A., and Nadeau, L.
1983: Structural subdivisions of the Grenville Province in the Parry Sound-Algonquin region, Ontario; in Current Research, Part B, Geological Survey of Canada, Paper 83-1B, p. 243-252.

Davidson, A., Culshaw, N.G., and Nadeau, L.
1982: A tectono-metamorphic framework for part of the Grenville Province, Parry Sound region, Ontario; in Current Research, Part A, Geological Survey of Canada, Paper 82-1A, p. 175-190.

Davidson, C.F.
1943: The Archaean rocks of the Rodil district, South Harris, Outer Hebrides; Royal Society of Edinburgh, Transactions, v. 61, p. 71-112.

diCapitani, C. and Brown, T.H.
1987: The computation of chemical equilibrium in complex systems using non-ideal solid solutions; Geochimica et Cosmochimica Acta, v. 51, p. 2639-2652.

Dunn, S.R. and Medaris, L.G., Jr.
1988: Retrograded eclogites in the Western Gneiss Region, Norway, and thermal evolution of a portion of the Scandinavian Caledonides; Lithos, v. 22, p. 229-245.

Eskola, P.
1921: On the eclogites of Norway; Videnskapsselskapets Skrifter. I. Matematisk-Naturvidenskabelig Klasse, no. 8, p. 1-118.

Grant, S.M.
1987: The petrology and structural relations of metagabbros from the western Grenville Province, Canada; Ph.D. thesis, University of Leicester, Leicester, U.K., 208 p.

Griffin, W.L.
1987: 'On the eclogites of Norway' - 65 years later; Mineralogical Magazine, v. 51, p. 333-343.

Higgins, J.B., Ribbe, P.H., and Herd, R.K.
1979: Sapphirine I. Crystal chemical contributions; Contributions to Mineralogy and Petrology, v. 68, p. 349-356.

Santallier, D.S.
1983: Les éclogites du Bas-Limousin, Massif Central français. Comportement des clinopyroxènes et des plagioclases antérieurement à l'amphibolitisation; Bulletin de Minéralogie, v. 106, p. 691-707.

Smith, D.C.
1988: A review of the peculiar mineralogy of the "Norwegian coesite-eclogite province", with crystal-chemical, petrological, geochemical and geodynamical notes and an extensive bibliography; in D.C. Smith, ed., Eclogites and Eclogite-facies Rocks; Developments in Petrology, v. 12, Elsevier, Amsterdam, 524 p.

Early Proterozoic collisional tectonics in the internal zone of the Ungava (Trans-Hudson) orogen, Lacs Nuvilik and Sugluk map areas, Québec

M.R. St-Onge and S.B. Lucas
Continental Geoscience Division

St-Onge, M.R. and Lucas, S.B. Early Proterozoic collisional tectonics on the internal zone of the Ungava (Trans-Hudson) orozen, Lacs Nuvilik and Sugluk map areas, Québec; in Current Research, Part C, Geological Survey of Canada, Paper 90-1C, p. 119-132, 1990.

Abstract

Mapping to the north of the Cape Smith Thrust Belt has shown that high grade plutonic-supracrustal terranes are accreted to the thrust belt along early Proterozoic thrust faults. The footwall to the belt is the Archean Superior Province basement, which is characterized by layered biotite and hornblende-biotite tonalites. The basal Cape Smith Belt thrust sheets are overrun by a large thrust package (Narsajuaq terrane) containing a suite of layered hornblende-biotite tonalites and diorites intruded by plutons of quartz diorite, tonalite and granite, and subsequently by peridotite sills. The granulite grade Sugluk terrane structurally overlies the Narsajuaq terrane, and is marked by tonalites and granites intruding highly deformed sequences of metasedimentary and metaplutonic (tonalite-diorite) rocks. The Narsajuaq and Sugluk terranes record complex deformation histories, with pre-accretion fabrics variably reworked during their emplacement in the thrust belt.

Résumé

La cartographie au nord de la zone de chevauchement du cap Smith a démontré que des terranes de roches plutoniques et supracrustales se sont ajoutés par accrétion à la zone le long de chevauchements datant du Protérozoïque inférieur. Le compartiment inférieur de la zone de chevauchement est le socle archéen de la province du lac Supérieur. Ce socle comprend des tonalites litées à biotite et à hornblende et biotite. Les nappes inférieures de la zone du cap Smith sont recoupées par un chevauchement important (le terrane Narsajuaq) qui comprend une séquence litée de tonalites à hornblende et biotite et des diorites pénétrées par des plutons de diorite quartzique, tonalite et granite et, plus tard par des filons-couches de péridotite. Le terrane Sugluk à faciès des granulites repose sur le terrane Narsajuaq et comprend des tonalites et granites mises en place dans une séquence métasédimentaire et métaplutonique déformée. Les terranes Narsajuaq et Sugluk font état des phases de déformation complexe qui ont touchées la région, et au cours desquelles des textures associées à une période antérieure à l'accrétion ont été reprises et modifiées au cours de l'évènement d'accrétion.

INTRODUCTION

A multidisciplinary geoscientific study of the northern Ungava Peninsula, Québec, was initiated in 1989 with 1:50 000-scale mapping north of the Cape Smith Belt (Fig. 1). The project has several objectives: (1) regional, 1:50 000 scale geological coverage of the project area, complementing the maps of the Cape Smith Belt published by the Geological Survey of Canada (GSC) (St-Onge and Lucas, 1990) and the Ministère de l'Énergie et des Ressources du Québec (Barrette, 1989, and references therein); (2) regional-scale assessment of economic mineralization; and (3) understanding the tectonic history of the map area through topical studies on its geochronology (R. Parrish, GSC; J. Dunphy, Université de Montréal), isotope geochemistry of plutonic units (J. Dunphy and J. Ludden, Université de Montréal), structural history (S. Lucas, GSC), metamorphic evolution (M. St-Onge, GSC), Quaternary geology (R. Daigneault, GSC), and geophysics (Mike Thomas, GSC). This report summarizes the tectonostratigraphy, structure, metamorphism and economic geology of the 1989 map area (see Fig. 1).

The northern Ungava Peninsula contains four principal tectonic elements (Fig. 1): (1) Superior Province basement, (2) Cape Smith Belt, (3) Narsajuaq terrane (new name), and (4) Sugluk terrane (Hoffman, 1985). Together these constitute the footwall, thrust belt and accreted terranes (fault bound, lithologically and metamorphically distinct tectonostratigraphic assemblages) of an ancient mountain belt, the Ungava segment (or northern Quebec segment of Hoffman, 1989) of the Trans-Hudson orogen. Here for conciseness we will use the term Ungava orogen. Mapping in 1989 focussed on the internal zone of the orogen (Fig. 1) where significant structural relief (> 10 km) exposes a deep crustal cross section. With the information provided by the cross section, we have been able to establish a framework for future geological, geophysical and geochronological studies.

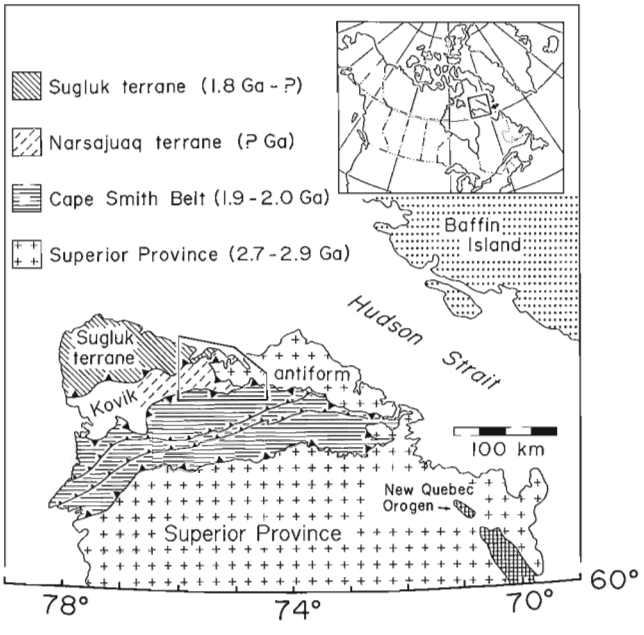

Figure 1. Map illustrating the location of the 1989 field area (outlined with box) and the tectonic elements in the Ungava orogen. Ages are from Parrish (1989).

TECTONOSTRATIGRAPHIC ASSEMBLAGES AND LATE INTRUSIVE SUITES

Five principal tectonostratigraphic assemblages have been documented in the map area (Fig. 2): parautochthonous Superior Province basement, the Spartan Group, the Watts Group, the Narsajuaq terrane and the Sugluk terrane. All units within these assemblages are deformed and metamorphosed, and so modifiers describing their deformation state (e.g., gneiss) or metamorphic character (e.g., meta-) are dropped for simplicity. The structural and metamorphic characteristics of these assemblages are discussed in subsequent sections.

Parautochthonous Superior Province basement

Superior Province gneisses forming the footwall basement to the Cape Smith Belt have been mapped unbroken from the south margin of the belt into the Sugluk Inlet-Deception Bay map area (Fig. 1; St-Onge et al., 1988). The Superior Province gneisses in the map area are termed parautochthonous because they developed a mylonitic foliation during displacement on the overlying basal décollement (Fig. 3), and were locally imbricated along late (out-of-sequence) thrust faults (Lucas, 1989; St-Onge and Lucas, in press). Both a basement slice and the footwall basement have been dated by the U-Pb method east of Deception Bay, yielding ages of 2780 Ma and 2882 Ma respectively (Parrish, 1989).

The principal rock type of the Superior Province basement is a medium grained, equigranular biotite or hornblende-biotite tonalite with a well developed gneissic foliation (Fig. 4). The hornblende-biotite tonalites are generally interlayered with hornblende-biotite diorite. However, diorite comprises less than 10 % of the rocks in the parautochthonous basement. Another relatively minor constituent of the tonalites is mafic (amphibolite) enclaves. The mafic minerals in the tonalites, coupled with the presence or absence of diorite layers or mafic enclaves has allowed the parautochthonous basement to be subdivided into three principal map units (Fig. 2): (1) dominantly biotite tonalite; (2) dominantly hornblende-biotite tonalite with local diorite interlayers; and (3) hornblende-biotite tonalite with mafic enclaves.

A well developed gneissosity in the Superior Province basement is largely due to the abundant presence of monzogranite veins and sheets (Fig. 4). Several generations of monzogranitic veins occur within some tonalite outcrops, with grain size ranging from fine to medium and texture from equigranular to K-feldspar megacrystic. Tabular bodies, up to 25 m thick, of K-feldspar megacrystic granodiorite to monzogranite also intrude the tonalite sequence (lac Arial vicinity, Fig. 2). The veins are typically deformed, and are generally sub-parallel to the tonalite foliation.

The tonalite with mafic enclaves unit (Fig. 2) is unique in the parautochthonous basement for the abundance of enclaves and also for the presence of kilometre-scale gabbro bodies. The enclaves are primarily composed of hornblende, biotite and plagioclase, with less common metamorphic garnet and clinopyroxene. The mafic enclaves in the tonalites may in part represent boudined dykes or sills.

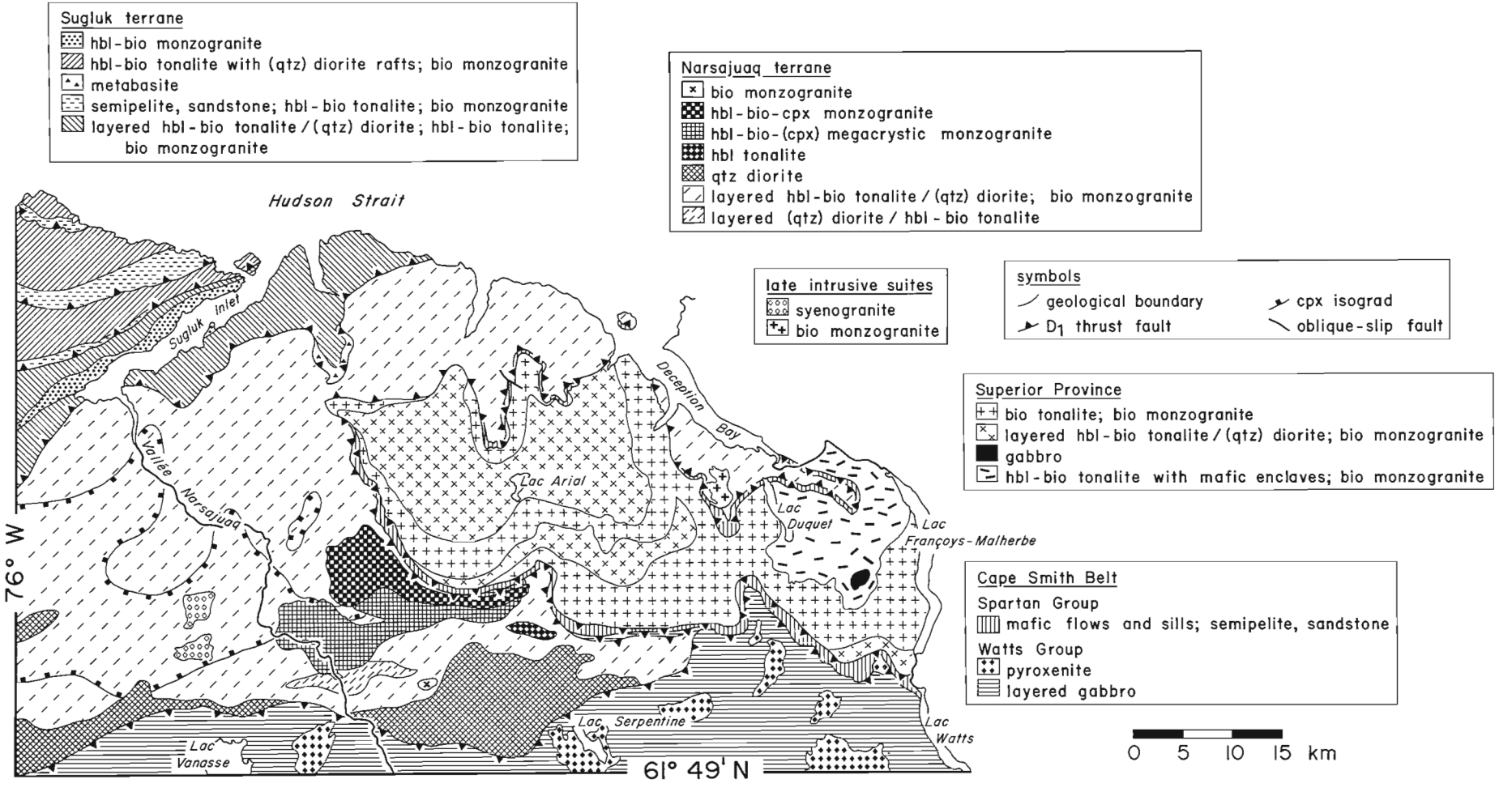

Figure 2. Geological compilation map for the Sugluk Inlet-Deception Bay area.

Several large (kilometre-scale) and intact, foliated gabbro sills occur west of lac Françoys-Malherbe. They are characterized by hornblende-plagioclase assemblages and are cut by relatively rare, deformed monzogranite veins.

Spartan Group

The Spartan Group generally represents the structurally lowest units of the Cape Smith Belt in the map area (Fig. 2, 3). The group is characterized by two principal units: a lower sequence of sedimentary rocks, overlain by a sheet of mafic rocks (flows and sills) (Fig. 5). The contact between these two units is unequivocally a fault because a slice of Superior Province basement is found juxtaposed between them to the west of lac Duquet (west edge of Fig. 5). The Spartan Group sedimentary rocks record a mixed siliciclastic and volcaniclastic provenance, and are interlayered with mafic flows and/or thin sills. Layers (transposed bedding) of arkosic sandstone, carbonate-cemented sandstone, semipelite, pelite and marble are intermixed with mafic schists of varying grain size and siliciclastic component. The base of the lower sedimentary thrust sheet is characterized by white arkosic sandstone beds which can be traced for tens of kilometres along strike (i.e., from south of lac Duquet to northeast of lac Arial, Fig. 2). Both the lower sedimentary and upper mafic thrust sheets are intruded by peridotite sills which range in strike length from several metres to several tens of metres. These deformed and metamorphosed sills are absent in the parautochthonous basement.

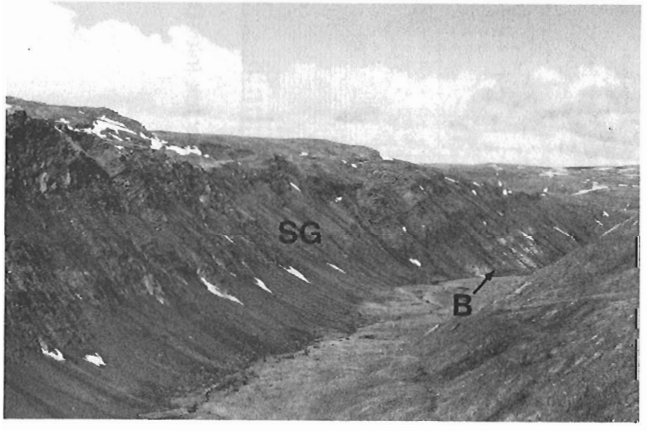

Figure 3. Basement-cover contact south of lac Duquet, looking north. Thrust sheets of Spartan Group (SG) structurally overlie the the parautochthonous Superior Province basement (B). The valley is 300 m deep. (GSC 205013-D)

Figure 4. Tonalite (dark bands) with monzogranite veins (light bands) from the Superior Province basement. Pen for scale is 15 cm long. (GSC 205013-A)

Watts Group

The Watts Group is represented in the map area by thrust sheets of layered mafic plutonic rocks, forming part of the mafic cumulate sequence of the Purtuniq ophiolite (St-Onge et al., 1988). As in the lac Watts — rivière Déception area to the east, the mafic cumulates are characterized by centimetre- to metre-scale layering of lithologies ranging from anorthosite to gabbro to pyroxenite. The layered mafic rocks are cut by intrusive bodies of pyroxenite and layered ultramafic cumulates in the structurally highest (most southerly) Cape Smith Belt thrust sheet (Fig. 2).

Narsajuaq terrane

The newly recognized Narsajuaq terrane consists of variably-deformed plutonic rocks of as yet unknown age and tectonic significance. The terrane is characterized by an older layered unit of tonalite and diorite which was intruded by sheet-like bodies of quartz diorite, tonalite and granite prior to pervasive, syn-deformation injection of monzogranite veins. The intrusive sequence for the apparently calc-alkaline plutonic units indicates a temporal calcic (e.g., quartz diorite and tonalite) to more potassic (e.g., granite) magmatic evolution.

Tonalite-diorite unit

Tonalites form the principal portion of the older layered unit in the Narsajuaq terrane, and are generally hornblende- and biotite-bearing (±clinopyroxene). Diorite represents less than 20% of this unit, but is inhomogeneously distributed. Many of the diorites may be quartz diorites, although thin section study is required to confirm this. Layered tonalite-diorite with subequal proportions of each lithology is found primarily in the vallée Narsajuaq area; a map-scale diorite-tonalite package is outlined approximately 35 km south of Sugluk Inlet (Fig. 2). In this area, tonalite and diorite form centimetre- to metre-scale layers that exhibit both sharp contacts (Fig. 6) and gradational contacts reflecting a continuous increase or decrease in the proportion of mafic minerals. These relationships suggest that the layered unit (Fig. 7) may have been built up by multiple intrusions of tonalite and diorite sheets. Field observations indicate that the most common intrusive relation is tonalite intruding diorite, establishing the possibility that some of the laterally less continuous diorite layers may be xenoliths in larger tonalite bodies.

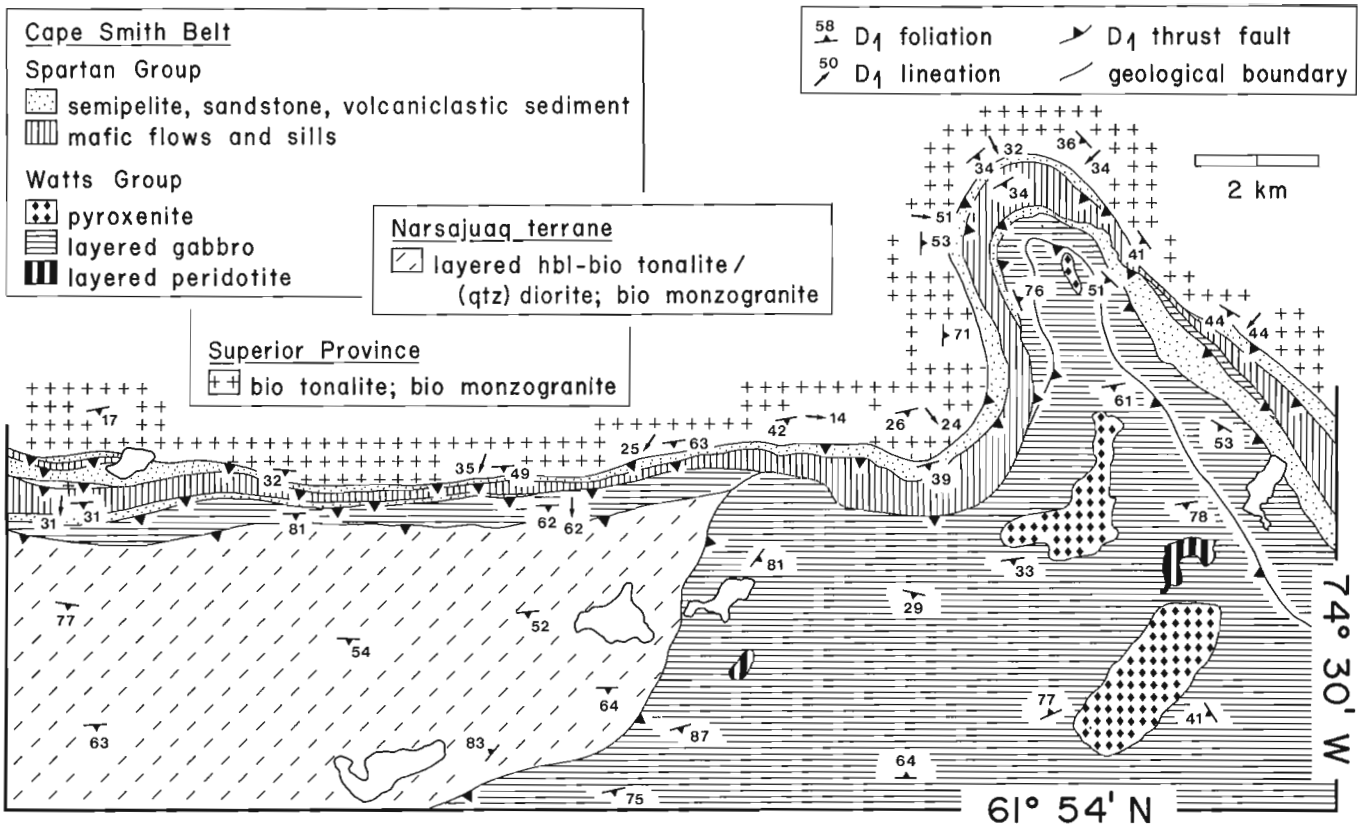

Figure 5. Detailed map of the north margin of the Cape Smith Belt in the area southwest of lac Duquet. The map illustrates the relationships between the Superior Province basement, the Cape Smith Belt and the Narsajuaq terrane.

Figure 6. Layered tonalite-diorite unit from the Narsajuaq terrane. Pen for scale is 15 cm long. (GSC 205013-V)

Tonalite and quartz diorite intrusions

Map-scale bodies of tonalite and quartz diorite which are clearly intrusive into the layered tonalite-diorite unit have been delineated in the Narsajuaq terrane. These units are marked by their lithological homogeneity, which contrasts with the finely-layered nature of the tonalite-diorite unit. Quartz diorite forms an extensive sheet-like body adjacent to the northern margin of the Cape Smith Belt in the lac Vanasse-lac Serpentine area (Fig. 2). The quartz diorite is medium to coarse grained and equigranular. The small tonalite body to the north of lac Serpentine also has a sheet-like geometry broadly concordant with the layering in the tonalite-diorite unit, and has hornblende as its only mafic phase. Veins of a similar tonalitic unit can be seen cutting the quartz diorite body, suggesting that emplacement of the tonalite may have followed quartz diorite intrusion. Both the quartz diorite and tonalite bodies are cut by veins of monzogranite (now deformed), thus constraining the minimum age for their emplacement.

Monzogranite plutons

Two prominent granite plutons occur east of vallée Narsajuaq and approximately 30 km south of Sugluk Inlet (Fig. 2). The plutons display sharp intrusive contacts against the layered tonalite-diorite unit. Cross-cutting relationships allow the relative ages of the plutons to be determined: the younger, more northerly "HBC" granite cuts the older "Two Rivers" granite at their eastern terminus. The "Two Rivers" monzogranite is a medium grained, K-feldspar megacrystic body containing up to three mafic phases: biotite-hornblende±clinopyroxene. The pluton is compositionally zoned to the extent that it has a more calcic rim of megacrystic tonalite to granodiorite. Finally, the "Two Rivers" monzogranite has a weak magnetic signature on the aeromagnetic map (Geological Survey of Canada, 1983).

The "HBC" pluton, in contrast, is a medium grained, equigranular monzogranite with ubiquitous hornblende, biotite and clinopyroxene. The clinopyroxene in the plutons may be of igneous origin, but records a retrograde metamorphic overprint in hornblende rims. The "HBC" monzogranite has a strong positive anomaly on the aeromagnetic map (Geological Survey of Canada, 1983). The overall geometry of the plutons is interpreted as sheet-like, with the map-view shape (Fig. 2) attributed to the effect of the two post-thrusting folding events.

Monzogranite veins and sheets

Most units in the Narsajuaq terrane are cut by veins and sheets of biotite monzogranite and granodiorite (Fig. 7). The only units that do not contain the pervasive veins are the two granite plutons discussed above. This suggests that the granite plutons may either be related to the regional granite veining event, or post-date it. The granitic to granodioritic veins and sheets range in thickness from several millimetres to over 10 m. The lateral extent of any one intrusive unit increases with its thickness, but can be up to several hundred metres. Several sets of granitic veins can be distinguished compositionally and texturally although they all appear to display similar timing relationships. The veins are all deformed and generally lie sub-parallel to the foliation in the host rock. A map-scale body of medium grained, equigranular biotite monzogranite was mapped to the northwest of lac Serpentine, and, given the similarity to veins in the surounding host rock, it appears to be a large sheet of the same late granitic suite.

Late ultramafic intrusions

The youngest intrusive unit in the Narsajuaq terrane predating the early Proterozoic deformation is peridotite sills. The ultramafic bodies range in size (strike length) from several metres to several tens of metres. The ultramafic sills occur in the layered tonalite-diorite unit and the younger diorite body, but are absent from the tonalite and granite intrusions.

Figure 7. Layered tonalite-diorite unit from the Narsajuaq terrane. Gneissic layering is defined by tonalite, diorite and monzogranite (vein) bands. Hammer for scale is 45 cm long. (GSC 205013-T)

The complete absence of ultramafic intrusions from the parautochthonous basement and the Sugluk terrane is notable. Although the absolute age of the ultramafic intrusions is not known, they postdate the monzogranite veins but predate cross-cutting syenogranite (pegmatite) dykes.

Sugluk terrane

Sugluk terrane represents a heterogeneous assemblage of sedimentary, volcanic (?) and plutonic rocks that have been engulfed by bodies of tonalite and granite during granulite grade, transcurrent bulk shear deformation. Subsequent thrusting and folding has produced a monoclinal stack of thrust imbricates which contain a number of distinct tectonostratigraphic units.

Tonalite-diorite unit

Well layered tonalite and diorite appears to form the oldest plutonic unit in the Sugluk terrane. The unit is best exposed in the southernmost imbricate of the terrane (Fig. 2), and comprises centimetre- to tens of metre-scale layers of tonalite and diorite (Fig. 8) with variable grain size and mineralogy. In general, the metamorphic mineralogy in Sugluk terrane is a function of the degree of hydration and retrogression from the once-pervasive granulite grade assemblages. As a result, mineral assemblages in the tonalite-diorite unit vary from biotite only (e.g., in tonalite) or hornblende-biotite (e.g., in diorite) to orthopyroxene-clinopyroxene-garnet-hornblende-biotite (e.g., in both tonalite and diorite). Tonalitic layers are generally medium grained and equigranular. Diorites, in contrast, range in texture from medium to coarse grained and in composition from leucocratic (quartz diorite) to more mafic diorite. The tonalite-diorite unit contains abundant layer-parallel (i.e., lit-par-lit) veins or sheets of apparently younger tonalite and monzogranite.

Sedimentary rocks

Three thrust imbricates of granulite grade sedimentary rocks occur in the Sugluk terrane. The lower contact of each

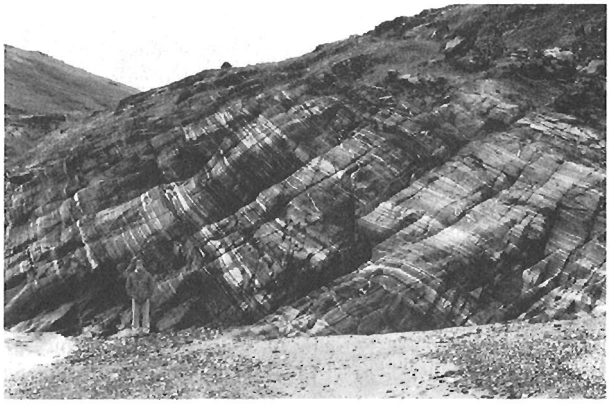

Figure 8. Layered tonalite-diorite unit of the Sugluk terrane. Person for scale is 2 m tall. (GSC 205013-R)

imbricate is interpreted as a thrust fault emplacing the sediment package on a tonalite body free of sedimentary rock inclusions. The upper contact of the sediment package is intrusive, defined as the last occurrence of significant sediment within the engulfing tonalite bodies. Sporadic centimetre- to metre-scale sedimentary xenoliths occur in the tonalite bodies, in addition to more common tonalite and diorite inclusions. Granite to granodiorite veins and sheets are commonly associated with the sedimentary rocks, suggesting that at least some of the granites may be locally derived by partial melting.

A heterogeneous assortment of highly deformed, siliciclastic and carbonate rocks occur in the sedimentary map unit of the Sugluk terrane. As previously described by Taylor (1982) and Doig (1987), sandstones (Fig. 9), semipelites, pelites, ironstones, marbles and calc-silicate rocks occur in intervals that are hundreds of metres thick. Semipelite represents the most abundant sedimentary rock, while rusty weathering pelite is relatively rare. Relatively homogeneous sandstone is interlayered with semipelite, pelite and mafic bands (Fig. 9). Marble and calc-silicate layers are less common but can form metre-scale intervals within the siliciclastic sequences. The supracrustal package also contains layers of garnet-clinopyroxene$\pm$orthopyroxene metabasite, which may represent either mafic flows, sills or volcaniclastic sediment. U-Pb geochronology of the sediments (Parrish, 1989) indicates that: (1) a garnet-biotite semipelite has zircon cores recording ages of >2230 Ma overgrown by metamorphic rims at 1825-1829 Ma; while (2) a sandstone has a population of young detrital igneous grains (1830-1863 Ma) and a population of older detrital grains (>2525 Ma with Proterozoic metamorphic overgrowths).

Tonalite and granite intrusions

Large bodies of hornblende-biotite-orthopyroxene tonalite and smaller bodies of granite dominate the Sugluk terrane (Fig. 2). These highly-deformed intrusive complexes form east-west striking, tabular bodies which are concordant with the layering in the sedimentary and layered tonalite-diorite units. The tonalites are generally medium grained, equigranular and have a leucocratic, tan (granulite) or grey-white (retrograded granulite) weathering appearance. Granites account for about 10 % of the younger intrusive units, and are emplaced in the sedimentary and the layered tonalite-diorite units. The larger granite bodies (e.g., Sugluk Inlet body, Fig. 2) commonly have a K-feldspar megacrystic monzogranite core and margins of megacrystic tonalite to granodiorite. The deformed tonalite and granite intrusions are characterized by abundant, centimetre- to tens of metre-scale xenoliths and rafts of sedimentary rocks and tonalite-diorite (Fig. 10). Orthopyroxenite and mafic inclusions also occur throughout the tonalite intrusions (Fig. 11), although their origin is enigmatic. The orthopyroxenite blocks, as shown in Figure 11, may represent boudins from a mafic dyke which intruded the tonalite during syn-metamorphic deformation. U-Pb studies (Parrish, 1989) have shown that one of the tonalites has both igneous and metamorphic zircons of 1830 Ma age. A granite body yields an igneous age of 1835 Ma and has metamorphic zircons ranging in age from 1825-1830 Ma (Parrish, 1989).

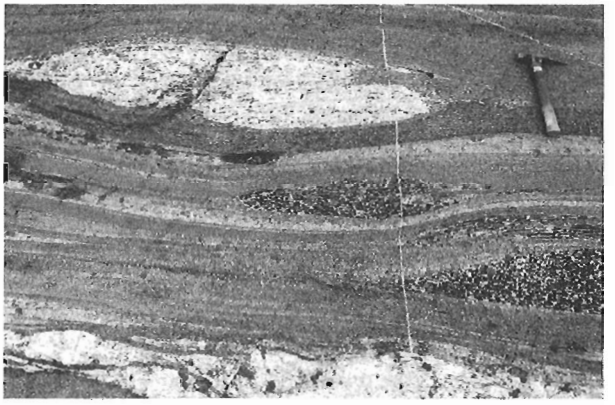

Figure 10. Tonalite and diorite inclusions in a large syn-tectonic tonalite of the Sugluk terrane. Hammer for scale is 34 cm long. (GSC 205013-P)

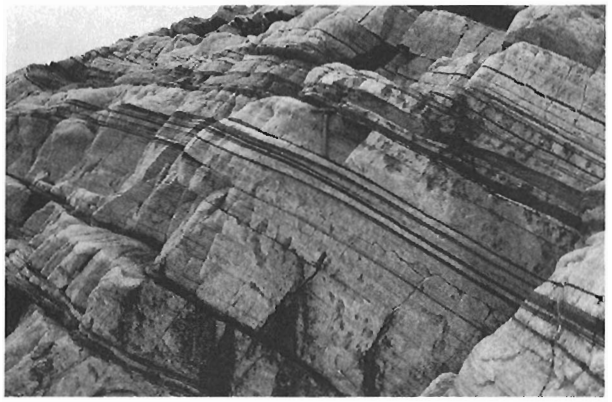

Figure 9. Thick sandstone section with thin mafic bands from the Sugluk terrane. Hammer for scale is 34 cm long. (GSC 205013-B)

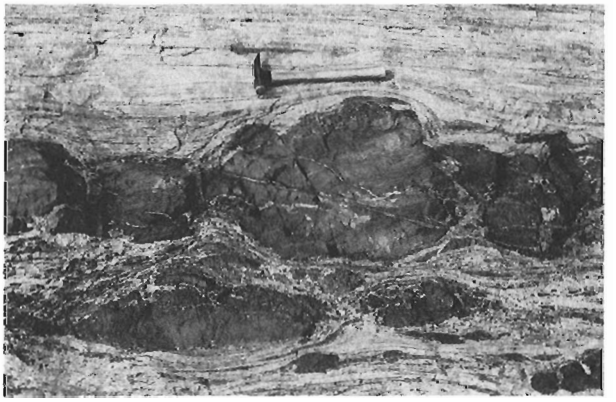

Figure 11. Orthopyroxenite boudins in a Sugluk terrane syn-tectonic tonalite. Hammer for scale is 34 cm long. (GSC 205013-J)

Late intrusions: tonalites and clinopyroxenites

Relatively small (tens of metres thick) tonalite and clinopyroxenite bodies appear to have intruded during the waning stages of the granulite grade deformation. Both types of intrusions include misoriented blocks of foliated country rocks (Fig. 12) but contain a relatively low-strain, syn-metamorphic foliation. The young hornblende-biotite-orthopyroxene±clinopyroxene tonalites occur in small pockets throughout the older tonalite and layered tonalite-diorite units of Sugluk terrane, suggesting that they may represent late phases of the older tonalite intrusions. The clinopyroxenites represent an ultramafic magma which incorporated, and to a large degree digested, blocks of tonalite or layered tonalite-diorite host rock. Spectacular hornblende reaction rims surround the inclusions, and mark the zone of hybridization of the clinopyroxenite-inclusion system.

Lac Duquet monzogranite pluton

An undeformed monzogranite pluton west of lac Duquet (Fig. 2) stitches the parautochthonous basement, the Spartan Group thrust slice and the Narsajuaq terrane rocks. The medium grained, equigranular biotite monzogranite pluton was emplaced principally within the layered tonalite-diorite unit of the Narsajuaq terrane, adjacent to the early Proterozoic thrust slice (Fig. 2). Apophyses and veins of the granite cut the thrust fault, the Spartan Group mafic rocks, and the footwall parautochthonous basement. The lac Duquet monzogranite pluton may be related (on the basis of its post-thrusting age) to the suite of tonalites to granites which intrude the internal Cape Smith Belt allochthons and have been dated at ca. 1840-1876 Ma (Parrish, 1989).

Syenogranite dykes and sills

A suite of syenogranite dykes (Fig. 13) and sills cut all tectonic elements in the map area (Fig. 1), but are concentrated in the Sugluk and Narsajuaq terranes. These bodies typically have a pegmatitic texture, marked by K-feldspar crystals up to 20 cm in length, and have biotite±muscovite±garnet± magnetite as accessory phases. Both the dykes and the sills are undeformed and cross-cut all structures defined in the map area. As a group, the pegmatitic dykes define a conjugate set with steeply-dipping, northeast- and northwest-trending orientations. Dykes also occur in steeply-dipping, east-west orientations, presumably representing the extensional fracture attitude for the conjugate set. The syenogranite sills locally form mappable bodies, which are shown in Figure 2. A syenogranite cutting Sugluk terrane tonalite gneisses has been dated at 1758 Ma (Parrish, 1989). Emplacement of the dykes into the Sugluk granulites results in a retrogression to amphibolite grade assemblages in centimetre- to metre-scale borders (Fig. 13).

STRUCTURAL HISTORY

A complex, multiple-event deformation history characterizes the tectonic elements of the Ungava orogen. Detailed structural and metamorphic studies in the Cape Smith Belt identified three principal deformation events which affected the early Proterozoic rocks of the belt (St-Onge et al., 1988; Lucas, 1989). These events are: D_1: development of a south-verging thrust belt during northward underthrusting of the Superior Province basement and its north-facing continental margin; D_2: folding of the thrust belt and its footwall (Superior Province) basement along east-west axes; and D_3: cross-folding of the thrust belt and footwall basement to produce a dome-and-basin fold interference pattern with significant structural relief on the flanks of the D_3 folds (up to 30 km in total). Structures related to each of these events have been recognized in the Narsajuaq and Sugluk terranes, interpreted to have been accreted to the thrust belt during D_1. In addition, fieldwork this summer has identified at least one older deformation event in each of the terranes and in the Superior Province basement.

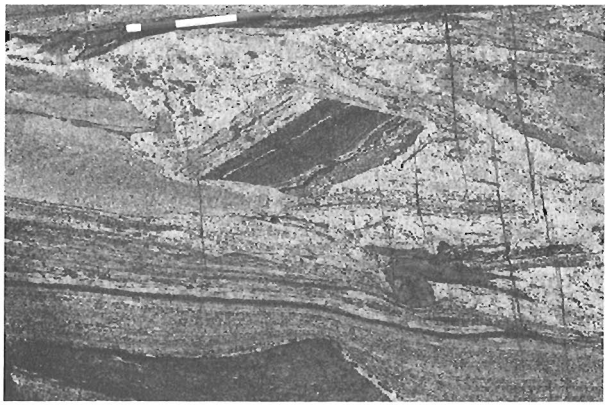

Figure 12. Late, syn-metamorphic tonalite in the Sugluk terrane containing misoriented xenoliths of deformed tonalite and diorite. Hammer for scale is 34 cm long. (GSC 205013-X)

Figure 13. Late syenogranite dyke cutting a Sugluk terrane tonalite. The light and dark amphibolite grade zones adjacent to the dyke contrast with the grey granulite grade tonalite to the left. Hammer for scale is 34 cm long. (GSC 205013-M)

Pre-D_1 deformation

All units within the parautochthonous Superior Province basement are characterized by a well developed gneissic foliation. The foliation within individual tonalite, diorite or monzogranite layers is generally defined by an alignment of biotite and/or hornblende, and, less commonly, by a shape fabric of deformed quartz and plagioclase. The overall gneissosity is produced by the interlayering of tonalite±diorite with monzogranite veins (e.g., Fig. 4). The gneissosity appears to have developed at amphibolite grade conditions, given the hornblende-biotite assemblage in deformed tonalite and diorite layers and in foliated amphibolite enclaves. The relative age of the gneissosity is clearly constrained to predate D_1 because the syn-D_1 reworking involves hydration of the gneisses and the development of retrograde metamorphic assemblages in the D_1 foliation (Lucas, 1989). Thus the outcrop-scale, amphibolite grade gneissosity represents a pre-D_1 fabric (even though it may have been reoriented to a D_1 attitude).

The layered tonalite-diorite unit of the Narsajuaq terrane displays a prominent gneissic foliation similar to that of the parautochthonous Superior Province basement (Fig. 7). It is defined by alternating bands of tonalite, diorite and/or monzogranite. In individual bands as well as in more lithologically homogeneous map units (e.g., granites), the foliation is delineated by aligned hornblende, biotite (Fig. 6), and where present, clinopyroxene grains and deformed quartz, plagioclase and K-feldspar grains or aggregates. These observations suggest that the foliation, and thus the larger-scale gneissosity, developed during syn-metamorphic (amphibolite grade) deformation. A pre-D_1 age for the gneissosity and the associated stretching lineation (generally defined by quartz-feldspar rodding) is suggested by two observations: (1) the gneissosity becomes reworked adjacent to the early Proterozoic thrust faults; and (2) the stretching lineations define a population significantly different from those measured in Cape Smith Belt rocks. The principal modifications to the Narsajuaq terrane gneissosity adjacent to the thrusts are that it becomes "flaggy" (i.e., more intense), angular discordances are "straightened", and that it can become reoriented into parallelism with the D_1 foliation in Cape Smith Belt rocks. The pre-D_1 stretching lineations trend basically east-west and plunge moderately (Fig. 14a), in contrast to the generally transverse, southwest or northwest trending D_1 lineations found in Cape Smith Belt rocks or Sugluk and Narsajuaq terrane rocks adjacent to D_1 thrust faults (Figs. 14b, c, d). The kinematics of the pre-D_1 deformation in the Narsajuaq terrane could not be unequivocally determined in the field, and require thin section study.

The Sugluk terrane records intense, pre-D_1, syn-granulite grade deformation which is broadly coeval with emplacement of the large tonalite bodies (Parrish, 1989). The principal planar fabric observed throughout the Sugluk terrane is a gneissic foliation defined by parallel lithological layers and intrusive units. Within individual lithologies, the syn-metamorphic nature of the foliation is evident from the alignment of orthopyroxene, clinopryroxene, hornblende and/or biotite crystals. Overprinting relationships allow the pre-D_1 stretching lineation to be distinguished from the D_1 lineation (Figs. 14d, e; 15). The pre-D_1 lineation, locally defined by aligned orthopyroxene crystals, is a subhorizontal, east-west trending structure (Fig. 14e). D_1 deformed zones are often associated with retrogression of the granulite grade gneisses, although this effect becomes less important in more internal (northern) thrust sheets. Within several hundred metres of the thrust faults, the effects of either or both the pre-D_1 and D_1 deformations (including lineations) may be present, as illustrated by the chocolate tablet boudinage in Figure 15. The maximum extension direction associated with the boudined mafic layers in the sandstone (Fig. 15) corresponds to the subhorizontal stretching direction. Pre-D_1 rotation of boudins (Fig. 16) is interpreted to result from slip along extensional shears at boudin ends in a sense that is synthetic to the dextral bulk shear flow in the sandstone (e.g., Hanmer, 1986). The dextral sense for pre-D_1 subhorizontal bulk shear flow is further indicated by the asymmetry of rotated, winged feldspars and folded monzogranite veins.

D_1 crustal thickening and bulk shear deformation

The D_1 crustal thickening event, responsible for the development of the Cape Smith Thrust Belt, generated the terrane-bounding, regional-scale faults mapped in the Sugluk Inlet-Deception Bay area (Fig. 2). Syn- to post-thermal peak reimbrication of the Cape Smith Belt allochthons and penetrative bulk shear of the internal zone units were concurrent with accretion of the tectonostratigraphic terranes. These faults are similar to those described as out-of-sequence structures in the Cape Smith Belt to the east (St-Onge et al., 1988; Lucas, 1989). The top-to-the-south thrust sense of displacement on the internal zone faults was established through analysis of D_1 stretching lineations and kinematic indicators such as C/S fabrics and rotated inclusions (Hanmer, 1986). D_1 stretching lineations generally trend northwest or southwest (recording the effects of D_2 and D_3 deformation; Fig. 14b,c,d) and are transverse. The thrust faults bounding the Spartan Group slice, and thus separating the Narsajuaq terrane from the parautochthonous basement (Fig. 2), are syn-metamorphic. In contrast, the Watts Group/Narsajuaq terrane fault to the west of lac Serpentine and the fault emplacing the Sugluk terrane on the Narsajuaq terrane (Fig. 2) are post-thermal peak structures. The thrust faults within Sugluk terrane are defined by tectonostratigraphic repetitions, and are assumed to be post-thermal peak in age because they are associated with the steep (overprinting) stretching lineations (Figs. 14d, 15) which also characterize the post-thermal peak, terrane-bounding fault.

Penetrative bulk shear deformation during D_1 affected rocks of the Cape Smith Belt, the Superior Province basement and the two terranes. Syn- and post-thermal peak mylonitic foliations occur in the Spartan and Watts Group units. In the Superior Province basement, reorientation of the gneissic foliation into parallelism with Cape Smith Belt foliations was accompanied by the development of a D_1 stretching lineation (Fig. 14f). In the Narsajuaq terrane, significant strain gradients, indicating intense D_1 deformation, are restricted to areas adjacent to thrusts. Throughout most of the Narsajuaq and Sugluk terranes, reorientation of

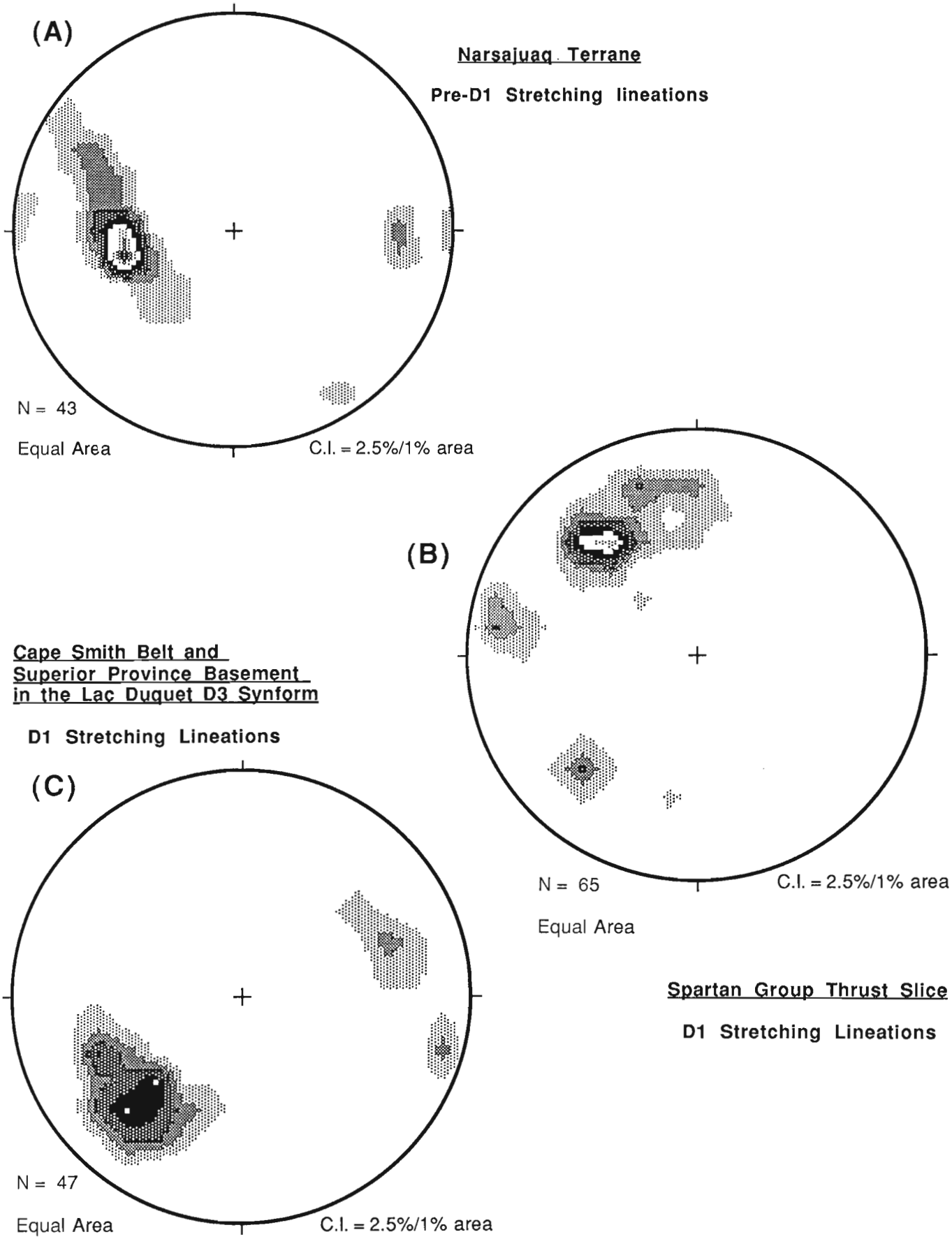

Figure 14. Equal area, contoured stereonet plots of stretching lineations.

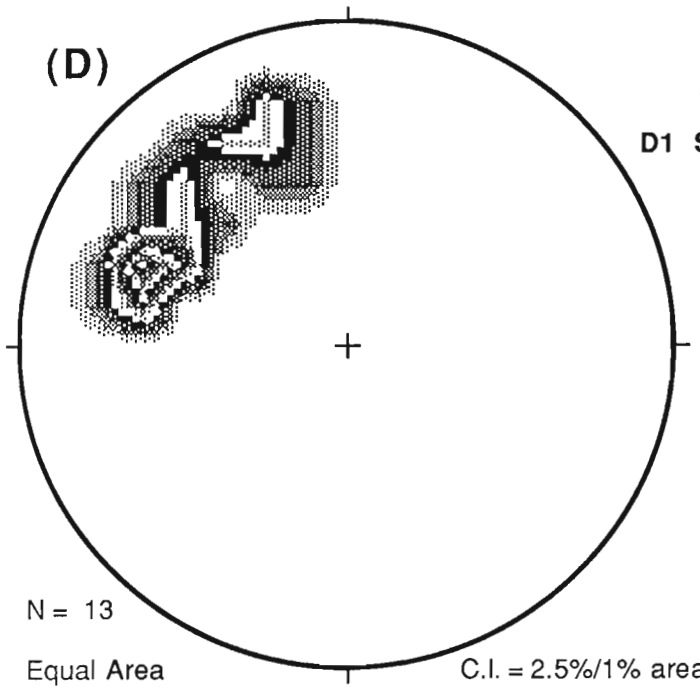

Sugluk Terrane

D1 Stretching Lineations

N = 13

Equal Area

C.I. = 2.5%/1% area

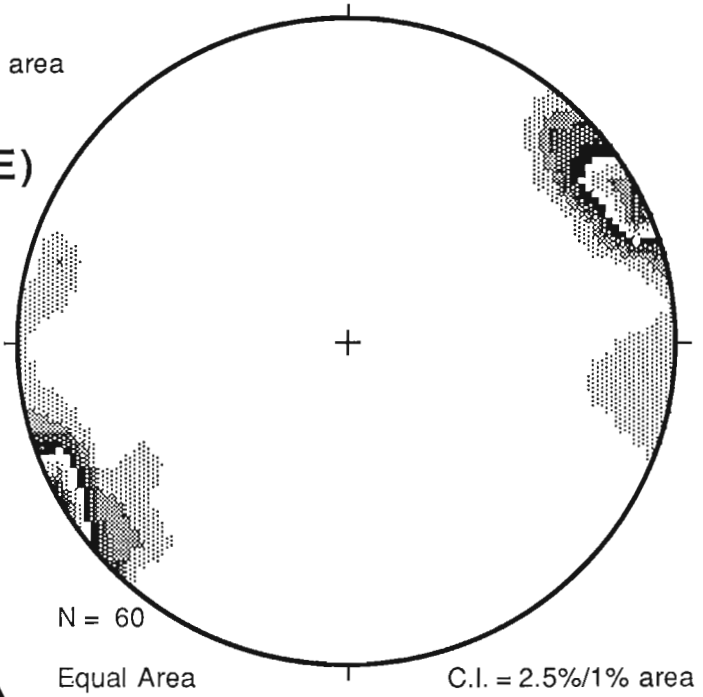

N = 60

Equal Area

C.I. = 2.5%/1% area

Parautochthonous Superior Province Basement

D1 Stretching Lineations

Sugluk Terrane

Pre-D1 Stretching Lineations

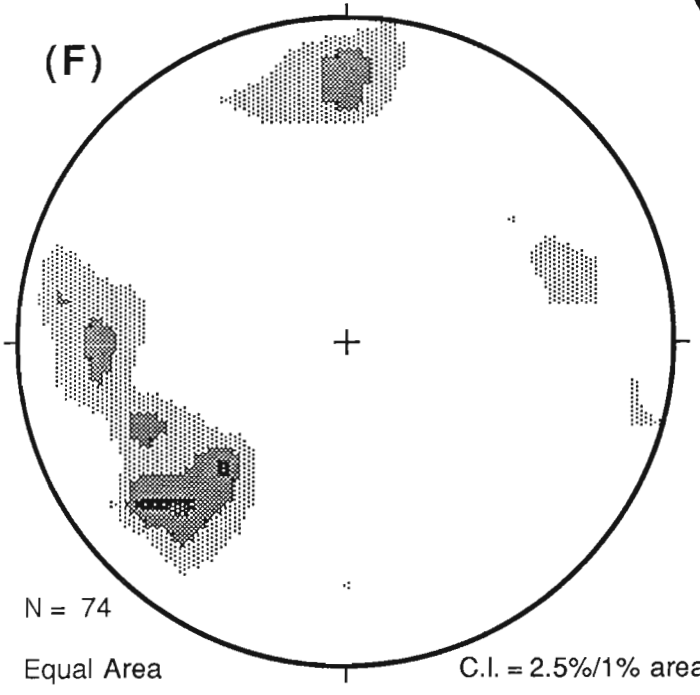

N = 74

Equal Area

C.I. = 2.5%/1% area

fabric elements such as stretching lineations is minor (Fig. 14a, e), suggesting that penetrative D1 deformation is not as pervasive as in the Superior Province basement.

D_2 and D_3 crustal-scale folding events

All tectonic elements of the map area were deformed during the D_2 and D_3 events. The east-west trending (D_2), median Kovik antiform (Hoffman, 1985) is a regional-scale structure apparently extending from Hudson Strait to Hudson Bay (Fig. 1). The Spartan Group thrust slice closes to the west across the west-plunging crest of the antiform (Fig. 2). The southern limb of Kovik antiform changes along strike from a relatively simple south-dipping homocline in the lac Duquet-lac Françoys Malherbe area (Fig. 2) to a sharply overturned panel extending west from the lac Serpentine area. Similar map-scale overturned structures are observed to the east along the northern margin of the Cape Smith Belt (see Lucas, 1989; St-Onge and Lucas, in press). The D_2 structures are deformed by D_3 folds to form a map-scale dome-and-basin interference pattern. This pattern is readily seen in the map trace of the thrust faults separating the Narsajuaq terrane from the parautochthonous basement (Fig. 2). The dispersive effect of D_2 and D_3 deformation on the orientations of D_1 (and pre-D_1) fabric elements can be observed in the stereonet plots of stretching lineations (Fig. 14).

Figure 15. Chocolate tablet boudinage in a Sugluk terrane sandstone. The two extension directions correspond to the two stretching lineation orientations illustrated in Figure 14d and e. Pen for scale is 15 cm long. (GSC 205013-W)

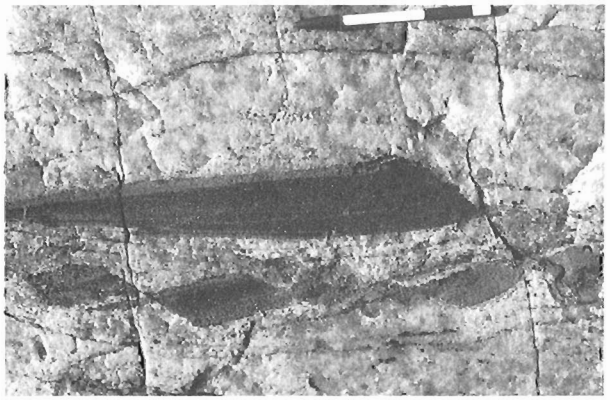

Figure 16. Back-rotated mafic boudins indicating dextral bulk shear flow in the Sugluk terrane sandstone outcrop illustrated in Figure 15. North is to the top the photograph and the stretching lineation is oriented east-west. See text for discussion. Pen for scale is 15 cm long. (GSC 205013-S)

METAMORPHIC HISTORY

Exposure of Spartan Group rocks across the crest of Kovik antiform (Fig. 2) has revealed a thermal peak metamorphic zonation within the mafic and sedimentary rocks. Along the north margin of the Cape Smith Belt (Fig. 2), mafic assemblages include hornblende-actinolite±garnet, while east of the present map area, St-Onge and Lucas (in press) have shown that Spartan Group pelites contain kyanite-muscovite-garnet-biotite assemblages (Fig. 17). Mafic rocks on the northern limb of the antiform contain

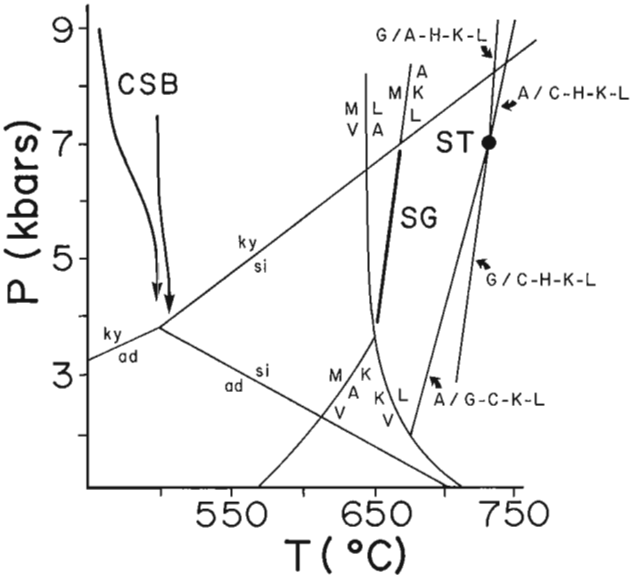

Figure 17. Metamorphic pressure (P)-temperature (T) grid illustrating the position of the following pelitic assemblages: (CSB) Spartan Group pelites from the north margin of the Cape Smith Belt to the east of lac Watts (Fig. 2) (see St-Onge and Lucas, in press b); (SG) Spartan Group pelites from the thrust slice exposed along Deception Bay (Fig. 2); (ST) Sugluk terrane pelites. Abbreviations refer to the following phases: A-aluminosilicate; ky-kyanite; si-sillimanite; ad-andalusite; G-garnet; C-Cordierite; H-hypersthene; K-K-feldspar; M-muscovite; L-melt; V-vapour phase.

hornblende-garnet/clinopyroxene assemblages while pelites locally contain univariant K-feldspar-sillimanite-melt ± muscovite assemblages (Fig. 17).

The Narsajuaq terrane is marked by a wide expanse of amphibolite grade hornblende-biotite assemblages in tonalites and diorites (Fig. 2). This metamorphic homogeneity is interrupted in several locations by both higher and lower grade assemblages. Greenschist grade actinolite-chlorite-biotite replace hornblende-biotite assemblages in the quartz diorite found adjacent to the post-thermal peak fault carrying Watts Group rocks in the lac Serpentine-lac Vanasse area (Fig. 2). Higher grade, hornblende-biotite-clinopyroxene (with hornblende rims) rocks are found regionally in the area surrounding the vallée Narsajuaq south of Sugluk Inlet (Fig. 2).

The Sugluk terrane granulite grade event is coeval with intense bulk shear deformation and intrusion of large tonalite and granite bodies (see also Parrish, 1989). Thermal peak assemblages in the syn-tectonic tonalites are generally hornblende-biotite-orthopyroxene, with clinopyroxene and garnet appearing in zones rich in layered tonalite-diorite xenoliths. A variety of mineral assemblages are present in the sedimentary rocks of the terrane. Pelites generally contain sillimanite-K-feldspar-garnet-biotite-melt, with local sillimanite-hypersthene-cordierite-K-feldspar-garnet-biotite-melt assemblages (Fig. 17). Calc-silicate rocks contain diopside-garnet-phlogopite-calcite-spinel assemblages, while sandstones are garnet, orthopyroxene and/or clinopyroxene-bearing. Retrograde metamorphism in Sugluk terrane appears to be related to two tectonic/magmatic events. The first is interpreted to result from emplacement of the Sugluk terrane on the Narsajuaq terrane at post-thermal peak (upper amphibolite grade) conditions. The second event is related to the intrusion of the syenogranite dykes. Amphibolite grade, hornblende-biotite ± clinopyroxene ± garnet assemblages characterize the relatively narrow (centimetre- to metre-scale) retrograde borders adjacent to the dykes (Fig. 13).

ECONOMIC GEOLOGY

The results of fieldwork during 1989 have important implications for mineral exploration in northern Québec. First, ultramafic bodies occur throughout the Narsajuaq terrane, and could be related to the mafic-ultramafic magmatic event which gave rise to the lac Cross, Katinik and Raglan (Donaldson) orebodies in the Cape Smith Belt (see Giovenazzo et al., 1989). Second, detailed mapping of the Narsajuaq terrane-Cape Smith Belt contact in the lac Serpentine-lac Vanasse area has moved the contact southward from previous compilations (e.g., Taylor, 1982) and has reduced the interpreted size of layered ultramafic rocks of the Watts Group (Purtuniq ophiolite). Finally, rare copper mineralization (chalcopyrite-malachite) is associated with the late syenogranite dykes. The mineralization is restricted to several metre-scale occurrences which are too small to be shown on the compilation map.

DISCUSSION

Evidence to date suggests that the internal zone of the Ungava (Trans-Hudson) orogen in northern Québec is characterized by two distinct tectonostratigraphic terranes thrust onto the allochthons of the Cape Smith Belt. While the Superior Province basement and Narsajuaq terrane appear to have similar layered tonalite-diorite sequences, the distinct character of the Narsajuaq terrane is indicated by the presence of the younger quartz diorite, tonalite, granite and peridotite intrusions. Relations between the terranes, the Cape Smith Belt rocks, and the parautochthonous Superior Province basement should be clarified with further mapping and isotopic studies. The newly recognized Narsajuaq terrane and the apparently young (ca. 1830 Ma) Sugluk terrane may hold the keys, along with the enigmatic Spartan Group volcano-sedimentary package, to understanding the regional tectonics of the early Proterozoic Ungava orogen and the tectonic setting for the 1998 Ma Purtuniq ophiolite (Parrish, 1989).

ACKNOWLEDGMENTS

Janet Dunphy (U. de Montréal) and Emmanuel Saydeh (U. d'Ottawa) are acknowledged for their careful mapping. Robin Roots is lauded for keeping us well fed and entertained. Jacques Dorion (pilot) and Al Singh (engineer) are thanked for the expert flying and trouble-free operation of the helicopter. The Polar Continental Shelf Project is thanked for providing half of the helicopter hours. Robert Daigneault (GSC) contributed significantly to camp life. Randy Parrish (GSC) and Dave Pattison (U. of Calgary) are gratefully acknowledged for contributing to the mapping program. Mark Okituk (Salluit Qarqalik Landholding Corporation) and Paul Papigatuk (Salluit Municipal Council) are thanked for their co-operation and generous hospitality. John Percival and Tony Davidson are acknowledged for a careful review of the manuscript.

REFERENCES

Barrette, P.D.
1989: Géologie de la région du lac Bolduc, Fosse de l'Ungava; Ministère de l'Énergie et des Ressources du Québec, carte préliminaire, DP 88-17.

Doig, R.
1987: Rb-Sr geochronology and metamorphic history of Proterozoic to early Archean rocks north of the Cape Smith Fold Belt, Quebec; Canadian Journal of Earth Sciences, v. 24, p. 813-825.

Geological Survey of Canada
1983: Magnetic anomaly, Rivière Kovic, Quebec and Northwest Territories; Geological Survey of Canada, Map NP 17-18-AM.

Giovenazzo, D., Picard, C., and Guha, J.
1989: Tectonic setting of Ni-Cu-PGE deposits in the central part of the Cape Smith Belt; Geoscience Canada, v. 16, p. 134-136.

Hanmer, S.
1986: Asymmetrical pull-aparts and foliation fish as kinematic indicators; Journal of Structural Geology, v. 8, p. 111-122.

Hoffman, P.F.
1985: Is the Cape Smith Belt (northern Quebec) a klippe?; Canadian Journal of Earth Sciences, v. 22, p. 1361-1369.

Hoffman, P.F.
1989: Precambrian geology and tectonic history of North America; in The Geology of North America-An Overview, A.W. Bally and A.R. Palmer (ed.); Geological Society of America, The Geology of North America, v. A, p. 447-512.

Lucas, S.B.
1989: Structural evolution of the Cape Smith Thrust Belt and the role of out-of-sequence faulting in the thickening of mountain belts; Tectonics, v. 8, p. 655-676.

Parrish, R.R.
1989: U-Pb geochronology of the Cape Smith Belt and Sugluk block, northern Quebec; Geoscience Canada, v. 16, p. 126-130.

St-Onge, M.R., and Lucas, S.B.
1990: Geology, eastern portion of the Cape Smith Thrust-Fold Belt, parts of the Wakeham Bay, Cratere du Nouveau-Québec and Nuvilik Lakes map areas, northern Québec; Geological Survey of Canada, Maps 1721A to 1735A.

St-Onge, M.R., and Lucas, S.B.
in press b: Evolution of the Cape Smith Belt: Early Proterozoic continental underthrusting, ophiolite obduction and thick-skinned folding; in The Early Proterozoic Trans-Hudson Orogen: Lithotectonic Correlations and Evolution, J.F. Lewry and M.R. Stauffer (ed.); Geological Association of Canada, Special Paper, in press.

St-Onge, M.R., Lucas, S.B., Scott, D.J., Bégin, N.J., Helmsteadt, H., and Carmichael, D.
1988: Thin-skinned imbrication and subsequent thick-skinned folding of rift-fill, transitional-crust and ophiolite suites in the 1.9 Ga Cape Smith Belt, northern Quebec; in Current Research, Part C, Geological Survey of Canada, Paper 88-1C, p. 1-18.

Taylor, F.C.
1982: Reconnaissance geology of a part of the Canadian Shield, northern Québec and Northwest Territories; Geological Survey of Canada, Memoir 399, 32 p.

A geological transect of northeastern Superior Province, Ungava Peninsula, Quebec: the Lake Minto area

J.A. Percival, K.D. Card, R.A. Stern and N.J. Bégin[1]
Continental Geoscience Division

Percival, J.A., Card, K.D., Stern, R.A., and Bégin, N.J. A geological transect of northeastern Superior Province, Ungava Peninsula, Quebec: the Lake Minto area; in Current Research, Part C, Geological Survey of Canada, Paper 90-1C, p. 133-141, 1990.

Abstract

The Minto subprovince, a poorly known part of the Superior Province characterized by northwesterly structural trends, was mapped in the Lac Minto- Leaf River area. Sparse metavolcanic and metasedimentary remnants were successively intruded by four plutonic suites: 1) deformed, metamorphosed, two-pyroxene-biotite diorite; 2) massive to weakly foliated hornblende ± two pyroxene granodiorite to diorite; 3) inclusion-rich, biotite ± orthopyroxene ± garnet diatexite; and 4) massive to foliated leucogranite. Some mineral potential exists in the small, widely distributed remnants of greenstone, iron-formation and pyroxenite lenses.

Résumé

La sous-province de Minto, partie peu connue de la province du lac Supérieur caractérisée par des directions structurales nord-ouest, a été cartographiée dans la région du lac Minto-rivière Leaf. Les restes volcaniques et sédimentaires métamorphisés éparses ont été successivement recoupés par quatre suites plutoniques: 1) une diorite à biotite (deux pyroxènes) métamorphisée et déformée; 2) une hornblende de massive à faiblement feuilletée ± granodiorite à diorite à deux pyroxènes; 3) une biotite ± orthopyroxène ± diatexite à grenat comportant de nombreuses inclusions, et 4) un leucogranite de massif à feuilleté. Les petits restes largement répartis de lentilles de roches vertes, de formation ferrifère et de pyroxénite pourraient contenir des minéraux exploitables.

[1] Department of Geological Sciences, Queen's University, Kingston, Ont. K7L 3N6

INTRODUCTION

This report describes the first results of a three year project aimed at assessing the mineral potential and geological evolution of a large, poorly known region of the northeastern Superior Province known as the Minto subprovince (Card and Ciesielski, 1986). The approach is to map a geological transect approximately 100 km in width, from Hudson Bay to Ungava Bay, at 1: 500 000 scale; the latitude of Lake Minto and Rivière aux Feuilles was chosen to take advantage of the access these waterways provide. During the 1989 field season, the western part of the region was examined.

Previous reconnaissance work (Stevenson, 1968) showed low mineral potential. However, changing exploration strategies, driven by discoveries of gold in iron-formations (e.g., Ashuanipi complex; Lapointe, 1986) and small greenstone belts (e.g., Big Bell, Australia; Phillips and De Nooy, 1988) in high-grade metamorphic terranes, require a re-assessment of the geology of the Minto subprovince to better define the potential of mineralized environments. Sulphide-rich samples taken from Stevenson's collection and from initial reconnaissance in 1988 returned gold assays of up to 35 ppb.

GENERAL GEOLOGY

The Minto subprovince, a 250 000 km^2 high-grade gneiss terrane, underlies most of the Ungava Peninsula (Fig. 1); its prominent NNW structural and aeromagnetic grain (Stevenson, 1968) distinguish it from the southern Superior Province, where dominantly easterly trends prevail (Card and Ciesielski, 1986). The subprovince consists mainly of felsic, orthopyroxene-bearing plutonic rocks and minor supracrustal remnants. To the south, the Bienville plutonic domain is distinguished on the basis of its easterly structural trends, paucity of supracrustal lithologies and lack of orthopyroxene. The Minto subprovince is flanked to the west, north and east by belts of early Proterozoic age.

LITHOLOGY

The region is underlain by igneous and metamorphic rocks that form several lithologically distinct, mappable units (Fig. 2). These are described below in approximate chronological order.

As: *Metasedimentary rocks* occur primarily as inclusions of variable size within intermediate and felsic intrusions. Greywacke compositions predominate and pelite, minor iron-formation, rare quartzite and calc-silicate gneiss are also present. Bedding is rarely preserved in greywacke-pelite sequences, which are generally migmatitic paragneisses containing assemblages of garnet - biotite - plagioclase - quartz ± sillimanite ± orthopyroxene ± cordierite ± pyrite, pyrrhotite. Garnet occurs as porphyroblasts up to 10 cm in diameter, commonly surrounded by haloes depleted in mafic constituents. Granitic leucosome veins on the millimetre-centimetre scale constitute 10-50 % of the metasedimentary rock and larger pods of garnet-bearing leucogranite are also common. Paragneiss grades to inhomogeneous diatexite (Brown, 1973; see below) with increasing volume of leucosome.

Two types of iron-rich rocks are commonly associated with the paragneiss: 1) banded (millimetre scale), quartz - magnetite iron-formation (Fig. 3) with coarse, recrystallized magnetite; and 2) rusty zones of siliceous, sulphide - garnet - orthopyroxene rocks forming concordant lenses in paragneiss. Five iron-rich samples from Stevenson's collection contain 3-6 ppb gold.

Rare calc-silicate gneiss occurs in association with metavolcanic rocks and as isolated inclusions in plutonic rocks. These thinly-layered, greenish-white rocks contain assemblages of carbonate - clinopyroxene ± garnet (andradite?).

Av: Rare mafic units occur as kilometre-scale inclusions in granitoid rocks, mainly in the western part of the area. The largest body, about 1 by 3 km, in the central Lake Minto area, consists of heterogeneous, gneissic orthopyroxene - clinopyroxene - hornblende and garnet - clinopyroxene - hornblende mafic rocks, containing pods of hornblende - pyroxene ultramafic rocks and interlayered with units of thinly-layered, fine grained rocks of felsic composition. Zircons with an igneous appearance from a felsic unit yield a preliminary U-Pb age of 2695 ± 5 Ma (J.K. Mortensen, pers. comm., 1989). Sulphide-rich zones, abundant at lithological contacts, contain gold contents in the 5 - 35 ppb

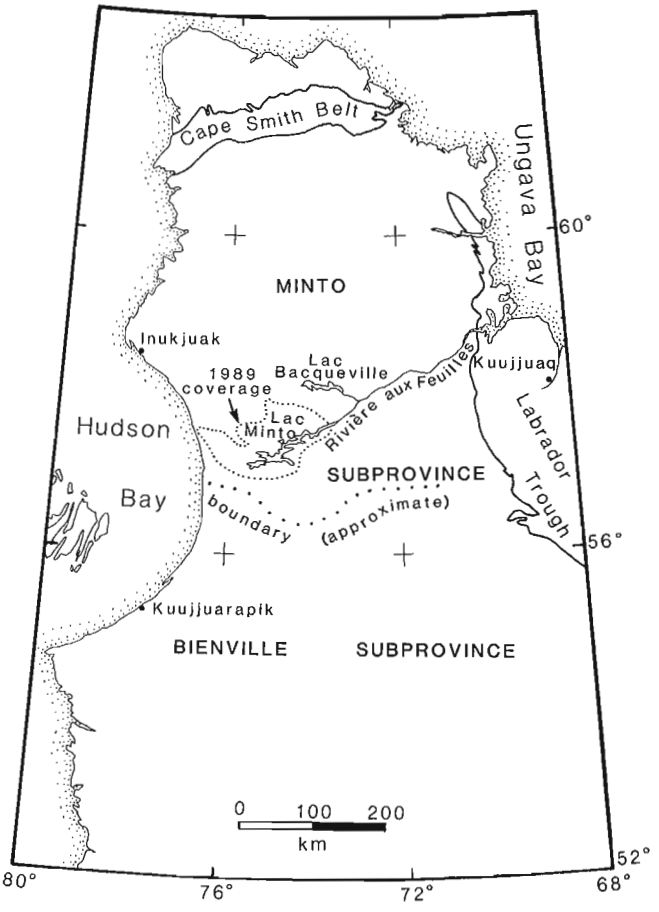

Figure 1. Location map showing major geological features of the Ungava Peninsula and the position of the Lake Minto-Rivière aux Feuilles transect.

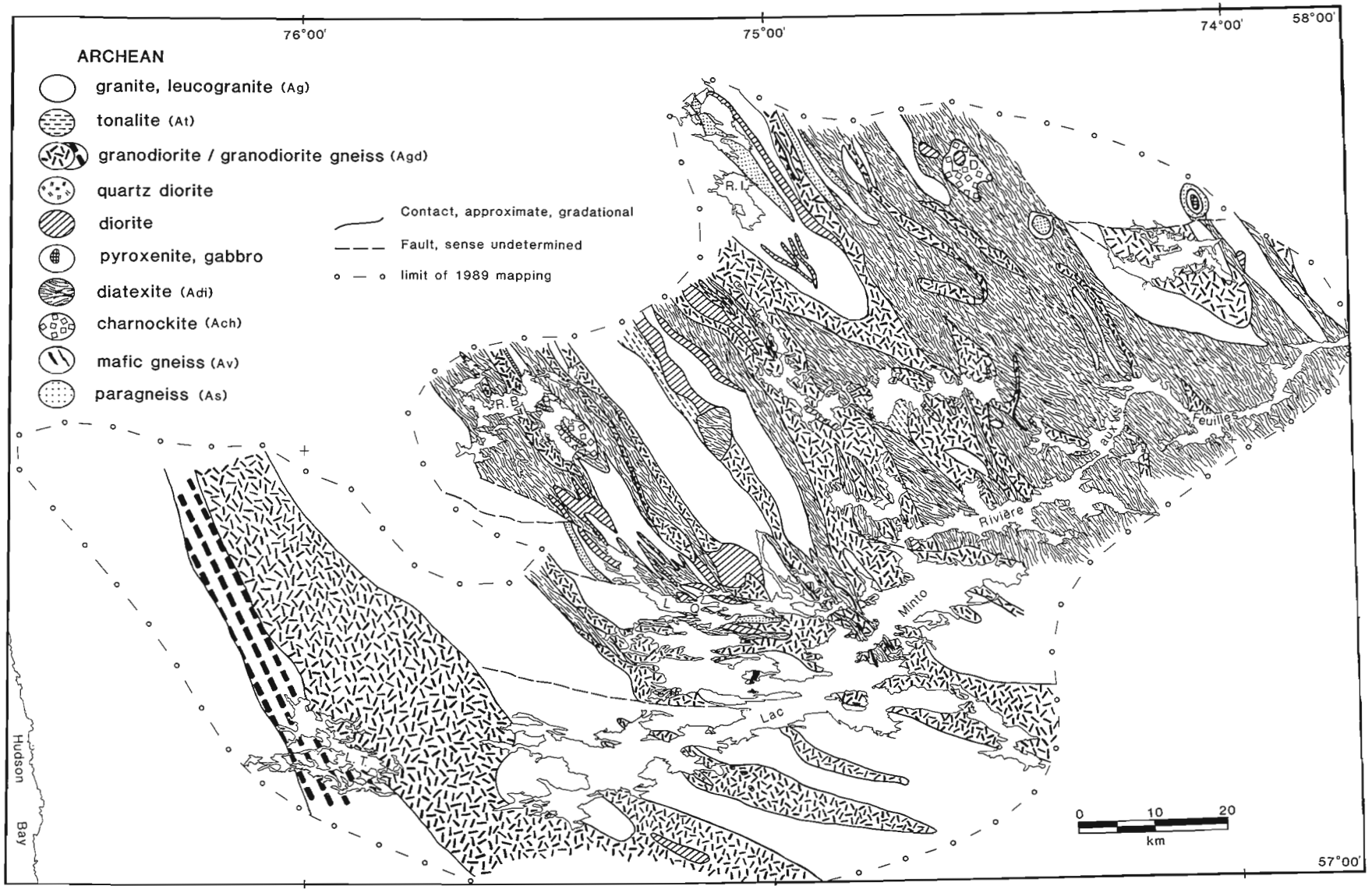

Figure 2. Sketch map of the geology of the Lake Minto area. Field observations were recorded on air photographs, plotted at 1:50 000 and compiled at 1:250,000. L.D.. Lake Descarreaux; L.Q.: Lake Qullinaaraaluk; L.T.: Lake Tikkerutuk; R.B.: Boniface River; R.I.: Inuksuak River.

range, based on five grab samples. Minor units of garnet-biotite paragneiss and calc-silicate gneiss occur at the margins of the volcanic unit.

Mafic units at several localities have possible volcanic origin. Associations of mafic rocks and iron-formation suggest a supracrustal origin. Fine grained mafic units with plagioclase megacrysts (Fig. 4), associated with paragneiss east of Lake Qullinaaraaluk, are possible flows or subvolcanic sills (cf. Phinney et al., 1988). Rare irregular clinopyroxene-rich patches and stringers in mafic rocks could represent pillow selvages. Small xenoliths of fine- to medium-grained, foliated to gneissic mafic rock occur in plutonic bodies throughout the area and may represent fragments of a greenstone association. Although primary structures were not observed, the association of fine grained mafic and felsic rocks with paragneiss, calc-silicate rocks and iron-formation provides circumstantial evidence for a supracrustal, possibly volcanic origin.

Ad: A suite of homogeneous plutonic rocks, generally of *dioritic* composition, but ranging to tonalite, gabbro and associated with some pyroxenite, occurs both as inclusions in younger plutons and as kilometre-scale bodies. In the larger bodies, primary igneous textures and mineralogy are preserved, whereas smaller inclusions generally have gneissic and migmatitic structure. Well-preserved units in the Lake Bacqueville area (Fig. 1) consist mainly of diorite with some tonalite, gabbro and minor pyroxenite, with characteristic texture formed by oikocrystic ortho- and clinopyroxene. At outcrop scale, the appearance varies from preserved medium-grained oikocrystic to fine- to medium-grained gneissic structures with coarse ortho-and clinopyroxene in migmatitic leucosome. Diorite grades with increasing mafic mineral content to biotite-bearing gabbro and locally to pyroxenite. Sulphide-rich zones occur locally at decimetre-scale within the more mafic members of the suite.

Large (kilometre-scale) pyroxenite inclusions, associated with gabbro and diorite, occur sparsely within granite and granodiorite throughout the area. They commonly contain a foliation or migmatitic layering discordant to the host intrusion. Pyroxenites are characteristically invaded by granite along joint networks, giving the rock an agmatitic appearance (Fig. 5). Enclaves of pyroxenite breccia locally, as at Lake Tikkerutuk, have a pyroxenitic matrix.

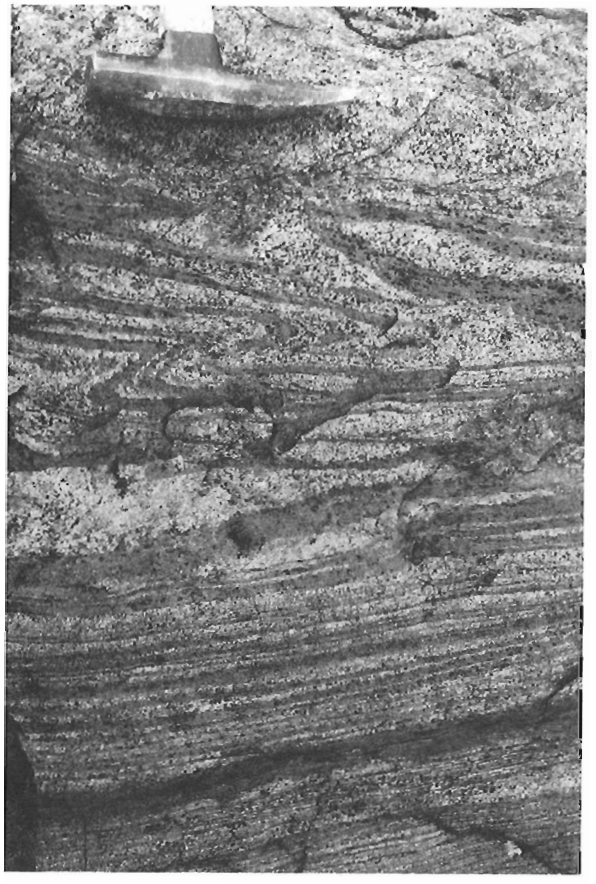

Figure 3. Thinly-laminated quartz-magnetite iron-formation showing typical contorted structure; photo from a 2 m^2 inclusion in diatexite. Hammer head is 17 cm long. (GSC 205004)

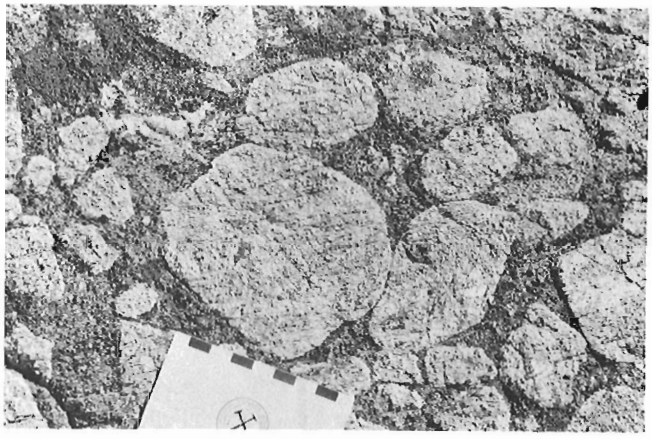

Figure 4. Plagioclase megacrysts in a fine grained mafic unit, possibly a volcanic flow or sill, interlayered with paragneiss. Scale in centimetres. (GSC 205004-E)

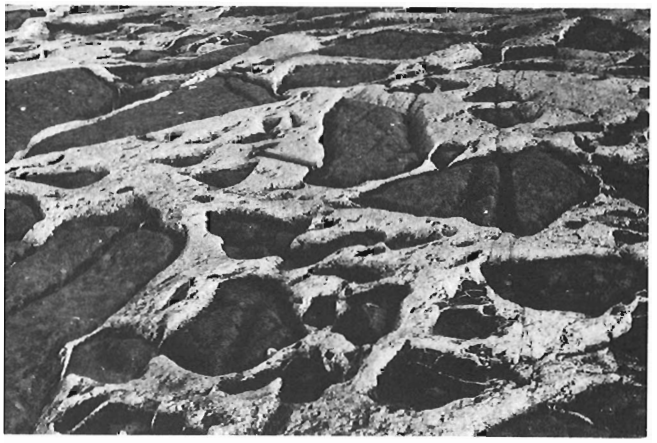

Figure 5. Pyroxenite xenoliths in granite, developing agmatitic structure. More common is granite with sparse pyroxenite xenoliths; granite-veined pyroxenite occurs locally. Hammer handle is 30 cm long. (GSC 205004-C)

Am: A suite of texturally and structurally distinct *mafic* rocks occurs as inclusions in diatexite, granodiorite and granite. The bodies have a geometry suggestive of dykes, but commonly occur as trains of blocky fragments (Fig. 6), readily distinguished from adjacent gneissic inclusions by their massive, homogeneous textures and common reaction rims against the host intrusion. Generally gabbroic to dioritic, the bodies are fine to coarse grained and locally plagioclase porphyritic. Local cross-cutting relationships between fine and coarse types is evidence for multiple intrusion. The overall character of these bodies suggests injection of mafic dykes into still molten or plastic felsic magmas, giving rise to the dyke-like inclusion trains.

Agd: A suite of hornblende-bearing rock types, mainly *granodiorite*, but including quartz diorite, diorite, gabbro and pyroxenite, forms a distinct mappable unit. These homogeneous, equigranular, medium- to coarse-grained rocks are generally massive to weakly foliated (Fig. 7); granodiorite is variably gneissic in some bodies. The mafic mineral assemblage includes hornblende and biotite, with variable amounts of orthopyroxene and clinopyroxene; olivine occurs in some ultramafic compositions. Mineral proportions vary within individual bodies; hornblende and biotite commonly increase at the expense of ortho-and clinopyroxene toward foliated margins. Hornblende occurs both as rims on pyroxene and as a matrix mineral. Sulphide-rich zones are common in the more mafic members. The mineral assemblages and massive, coarse textures suggest an igneous origin for the suite.

Gradational relationships among the various rock types were observed at several localities. For example, near Lake Qullinaaraaluk, diorite grades with increasing mafic mineral content to gabbro and with increasing quartz and feldspar content to monzodiorite, leucodiorite and granodiorite. Granodiorite, regionally the most extensive unit of the suite, commonly contains diorite and gabbro inclusions, along with rare paragneiss and foliated to gneissic diorite to quartz diorite. The hornblende-bearing rocks are cut by and enclosed within younger granite and granodiorite. The relationship between units of this suite and granodiorite of the diatexite suite (see below) is enigmatic. Neither includes xenoliths of the other, but the two are locally closely associated or interlayered on a scale of 5-50 m, where they have similar grain size and texture. The two suites may thus be contemporaneous.

Hornblende-bearing diorites are readily distinguished from older, two-pyroxene - biotite diorites by their coarse grain size, general lack of tectonic fabric and presence of abundant hornblende.

At: Small bodies of *tonalite* constitute a minor lithological component. They are medium grained, homogeneous, generally foliated rocks with assemblages of biotite-quartz-plagioclase ± hornblende ± orthopyroxene.

Adi: *Diatexite* (Brown, 1973) underlies large parts of the western Lake Minto and Rivière aux Feuilles areas. The name is used to describe a lithologically heterogeneous unit (Fig. 8) consisting of three main components: 1) 50-95 % medium- to coarse-grained, homogeneous, massive granodiorite to granite, with assemblages of biotite-quartz-plagioclase-K-feldspar ± orthopyroxene ± garnet ± cordierite;

Figure 6. Dyke-like trains of mafic fragments in inhomogeneous diatexite. Note the homogeneous and discordant nature of the mafic bodies in contrast to the gneissic character of enclaves in diatexite. Width of centre of photograph is 2 m. (GSC 205004-A)

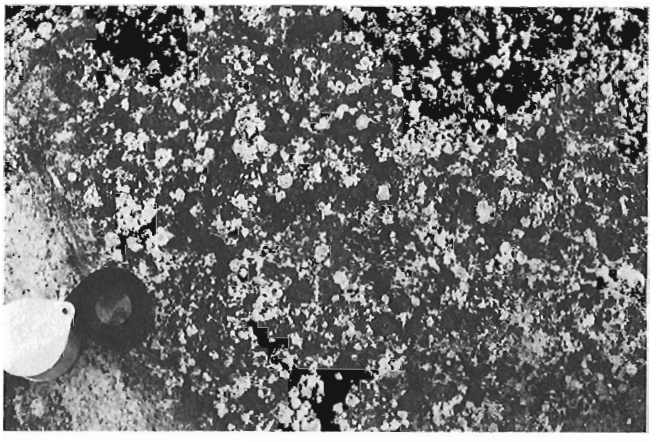

Figure 7. Massive, coarse grained, hornblende-clinopyroxene-orthopyroxene quartz diorite, typical of textures in the hornblende-bearing plutonic suite. Hand lens is 2.5 cm in diameter. (GSC 205004-D)

2) inclusions (5-50 %) of paragneiss,iron formation, diorite, mafic gneiss, dyke remnants and rare tonalitic gneiss; and 3) concordant sheets of white or pink biotite ± garnet ± orthopyroxene leucogranite. Intercalation of these components in different proportions at centimetre-kilometre scales gives the rock a gneissic character at hand specimen, outcrop or map scale. The granodiorite "matrix" phase itself is commonly heterogeneous, with coarse grained leucocratic granite segregations containing centimetre-sized orthopyroxene. Diatexite forms mappable units of 'homogeneous' (>75 % granodiorite) and 'inhomogeneous' (<75 % granodiorite) varieties although these are not distinguishable at the scale of Figure 2.

Mineral assemblages in the granodiorite component of the diatexite vary with inclusion type: garnet- and rare cordierite-bearing granodiorites, which form discrete units at 0.5-5 km scale, are generally associated with garnet-bearing paragneiss enclaves; orthopyroxene - biotite varieties commonly have orthopyroxene - clinopyroxene - biotite diorite inclusions. In some areas inhomogeneous diatexite is gradational to migmatitic paragneiss and has a migmatitic appearance. Hornblende occurs rarely as rims on orthopyroxene.

The diatexite suite constitutes migmatitic rocks containing >50 % neosome (e.g., Brown, 1973). Homogeneous varieties may represent melt fractions of greater than 75 %.

Ach: Rocks termed *charnockite* are coarse grained, brown, homogeneous, massive to foliated granite to granodiorite. They contain biotite (5-10 %), orthopyroxene (5-15 %), rare hornblende, and common aligned K-feldspar megacrysts up to 2 cm in size. Mafic and dioritic inclusions make up less than 1 % of most outcrops. Orthopyroxene and biotite locally occur in discrete, irregular domains on a 5-10 cm scale. Local alteration has converted charnockite to pink biotite granite with some preserved orthopyroxene cores. The coarse grain size and lack of tectonic fabric suggests an igneous origin for the orthopyroxene, rather than metamorphic recrystallization of a coarse grained igneous rock.

Figure 8. Inhomogeneous diatexite, containing ~ 25% inclusions of paragneiss. Leucogranitic pegmatites are a common component of diatexite. Hammer handle is 30 cm long. (GSC 205004-B)

Aggn: Foliated to *gneissic granodiorite to granite* generally occurs in diffuse contact zones between granodiorite and granite. Layers and schlieren of darker, biotite-rich granodiorite to diorite occur within lighter, leucocratic granite resulting in a gneissosity at the hand specimen to outcrop scale. Mafic minerals include biotite and magnetite, with smaller amounts of hornblende, clinopyroxene and rare orthopyroxene. The gneisses are cut by and included within massive biotite granite (Ag).

Ag: *Granite* weathers pink or pink-white and forms bodies ranging from centimetre-sized dykes to batholiths exposed in rugged, well-jointed outcrops with glacially polished surfaces. Granite varies texturally from massive and homogeneous, with medium, coarse or pegmatitic grain size, to foliated or gneissic, containing wispy, biotite-rich septa. Mafic minerals are typically biotite ± magnetite (2-20 %) with minor hornblende, clinopyroxene, orthopyroxene or garnet. Alteration to assemblages of epidote, hematite and chlorite is common, particularly in late shear zones. Inclusions of all the previously-described units were observed in granite; together with its generally massive nature this implies emplacement late in the tectonomagmatic history of the area.

Granite that forms part of the diatexite unit locally shows complex intermingling with granodiorite. Irregular and gradational contacts suggest contemporaneous magmas, either from distinct sources, or through late magmatic segregation.

Proterozoic Dykes: At least three sets of mafic dykes occur in the region. An earlier set of clinopyroxene - plagioclase diabase trends NNW (330°) and is cut by olivine diabase striking WNW (285°). WNW dykes lacking olivine are also present; their age with respect to the other dyke sets is unknown.

STRUCTURE

At the outcrop scale most rock types carry the characteristic regional NNW structural trend, defined by a mineral foliation, gneissic layering, migmatitic veins or inclusion alignment (D_2). Rare examples of structures predating the dominant set include discordant gneissic layering in inclusions and locally preserved, kilometre-scale oval structures (D_1; see below).

The regional NNW (D_2) trend, well illustrated on aeromagnetic maps (e.g., G.S.C., 1988), is made up of alternating lithological units on a 0.1-20 km scale. Contacts between and within the concordant bodies include both sharp and gradational igneous contacts as well as diffuse, *lit-par-lit* migmatitic injection zones.

From cross-cutting and inclusion-host relationships, a relative lithostructural chronology has been established (Table 1). The oldest preserved structures include rare sedimentary bedding in paragneiss and iron-formation (As), as well as lithological contacts between metavolcanic (Av) units. Early intrusions into the supracrustal sequence are the two-pyroxene-biotite Ad suite, including diorite and rare tonalite, gabbro and pyroxenite. Although the diorites occur mainly as strongly foliated to migmatitic inclusions in younger intrusions, larger oval bodies are preserved in places.

At Lake Bacqueville (Fig. 1; outside the zone of continuous regional coverage of Fig. 2, two topographically-defined oval structures, about 5 km in size, are made up mainly of migmatitic diorite; one contains a core of paragneiss. An early (D_1) migmatitic layering dips steeply inward, defining conical structures, and is variably folded and transposed into NNW (D_2) orientations. Diatexite, which surrounds one oval and forms concordant intrusive sheets within the sequence, has only the NNW fabric. Other topographic oval structures are also conical in the third dimension but are lithologically distinct. The Lac Descarreaux structure (Fig. 2) has a core of gabbro and diorite, a rim of paragneiss and is engulfed by charnockite. A 3 km oval west of Lake Depocas consists of a pyroxenite core and paragneiss rim, and is surrounded by granite. Both examples may represent D_1 structures.

The younger plutonic rocks may be syntectonic with respect to the major NNW fabric-forming event (D_2). Rocks of the hornblende granodiorite (Agd) and diatexite (Adi) suites generally contain gneissic inclusions and are themselves massive to foliated and rarely gneissic. Granite (Ag) is generally massive to weakly foliated except where involved in narrow, late, high-strain zones. Gneissic granite that occurs locally in massive granite may represent an earlier generation of granite. A prominent swing in the orientation of units and structures, from NNW to EW, most obvious in the Lake Qullinaaraaluk area, defines a sinistral shear, possibly of D_2 age.

High-strain zones (D_3), generally formed in granite, are steep and strike WNW to NW. They occur mainly as zones up to 1 km thick of platy foliation defined by ribbon quartz and granular feldspar and are associated with brittle offsets. Lineations and kinematic indicators are rare but generally suggest strike-slip displacement. The Lake Qullinaaraaluk swing is accompanied by a high-strain zone of D_3 style.

Late brittle faults (D_4?) are marked by narrow topographic depressions trending NNW, NW and E-W. Rocks within and adjacent to these zones have cataclastic textures with platy quartz and feldspar augen. Alteration to hematite, chlorite and epidote is accompanied rarely by the formation of quartz vein systems and pseudotachylite seams. Such rocks commonly have significantly lower magnetic susceptibility than their unaltered counterparts, suggesting magnetite destruction during alteration.

IGNEOUS AND METAMORPHIC PETROLOGY

Stevenson (1968) noted the widespread presence of orthopyroxene in the Minto subprovince. Based on re-examination of assemblages and textures in rocks from Stevenson's collection, Herd (1978) concluded that the terrane underwent metamorphism to granulite facies, followed by variable retrogression to amphibolite and greenschist facies. The distribution of orthopyroxene in the Lake Minto area is portrayed in Figure 9, based on the 1989 field observations. Orthopyroxene occurs mainly in plutonic rocks with igneous textures; only a small proportion of the terrane is made up of rocks containing metamorphic orthopyroxene. Thus the distribution of orthopyroxene in Figure 9 indicates granulite facies in metamorphic rocks and low water fugacity during crystallization of the igneous rocks. The orthopyroxene zone is bounded by biotite granite and hornblende-biotite granodiorite to the south and west.

Paragneiss (As) is generally migmatitic and contains assemblages, developed both in paleosome and neosome, of:

i) biotite - plagioclase - quartz
ii) garnet - biotite - plagioclase - quartz
iii) garnet - cordierite - biotite - plagioclase - quartz
iv) garnet - sillimanite - biotite - plagioclase - quartz
v) garnet - orthopyroxene - biotite - plagioclase - quartz
vi) garnet - cordierite - sillimanite - biotite - plagioclase - K-feldspar - quartz

One occurrence of sapphirine in biotite schist was noted. Assemblage v) indicates metamorphism to granulite facies and the other assemblages are permissive of this grade. Common garnet-cordierite assemblages indicate pressures below 700 MPa (7 kb) (Holdaway and Lee, 1977). Geothermobarometric work is underway to assess possible variations in exposure level within the terrane.

Metavolcanic rocks are homogeneous to migmatitic. Mafic units consist of the following assemblages:

vii) orthopyroxene - clinopyroxene - hornblende - plagioclase
viii) garnet - clinopyroxene - hornblende - plagioclase

Units of two-pyroxene - biotite diorite have similar assemblages in paleosome and neosome. Although oikocrystic pyroxene in the paleosome may be an inherited igneous feature, coarse pyroxenes in neosome indicate metamorphism to granulite facies.

The widespread occurrence of orthopyroxene in the igneous rocks suggests hot, dry magmatic conditions.

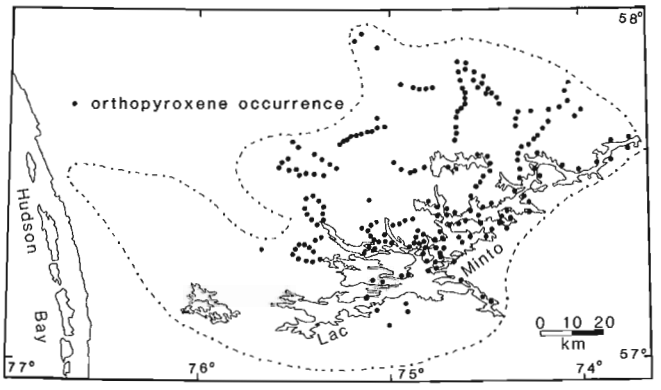

Figure 9. Distribution of orthopyroxene in the Lake Minto region. The occurrences reflect partly the extent of coverage and partly a change from dominantly hornblende- and biotite-bearing assemblages in the south and west, to orthopyroxene-bearing rocks in the north and east. The presence of orthopyroxene is lithologically controlled to some extent.

Although such conditions are considered normal for dioritic and gabbroic compositions, the occurrence of orthopyroxene in granodiorite and granite also indicates high liquidus temperatures. Coarse granitic segregations in granodiorite, presumably a late-crystallizing fraction in a cool, fluid-rich environment, contain fresh orthopyroxene, indicating relatively anhydrous conditions. Recently, Peterson and Newton (1989) showed experimentally that significant quantities of CO_2 are soluble in granitic melts. Such liquids would have reduced water activity through their crystallization history and could remain in equilibrium with orthopyroxene. Tests for this possibility will include calculation of water activity from equilibria involving biotite and a search for grain-boundary graphite films which may precipitate from CO_2-rich fluids during cooling (Frost et al., 1989).

RELATIVE CHRONOLOGY

Based on cross-cutting relationships and relative ages of plutonic and structural events, the oldest units recognized are paragneiss and metavolcanic rocks, inferred to be supracrustal (Table 1). The oldest intrusions belong to the diorite-tonalite-gabbro suite, generally foliated to gneissic and locally observed to have cut paragneiss. A D_1 deformation and probable metamorphism produced gneissic and migmatitic structures in these older units, before intrusion of the hornblende-bearing plutonic suite. The hornblende-bearing suite may have been approximately coeval with production and intrusion of the diatexite suite; both are massive to weakly foliated and neither contains inclusions of the other. Evidence of coeval mafic magmatism comes from the mafic dyke-like inclusions in granodiorite and diatexite. Intrusion of large volumes of generally massive granite closed the Archean magmatic history.

The dominant NNW structural grain is made up of NNW-oriented masssive and foliated plutonic units as well as late brittle faults. Based on their internal and external geometry, intrusion of the hornblende granodiorite and diatexite suites may have occurred broadly synchronously with a D_2 deformation event. Brittle-ductile shear zones that involve otherwise massive granite are assigned to a D_3 event, whereas brittle faults probably relate to a D_4 event. Three sets of Proterozoic dykes cut all of the foregoing rock units and structural elements.

MAGNETIC CHARACTER

The magnetic anomaly map (G.S.C., 1988) is characterized by short-wavelength (10-20 km), NNW-oriented, parallel high and low anomalies, truncated by broad lows oriented NW and E-W. Larger-scale (100-200 km) domains with distinct intensity and relief have northerly orientations.

A portable magnetic susceptibility meter was used on the outcrop to determine values for the various map units (Table 2). In general, diorites are the most magnetic, followed by granodiorites and diatexites. Granites are intermediate whereas paragneiss has very low susceptibility. In general there is a good correlation, at local scales, between the distribution of units and magnetic anomalies.

Table 1: Relative chronology of lithological units and structural elements in the Lake Minto area.

Unit	Lithology		
Pd3	NNW Cpx-Plg dykes		
Pd2	NNW Ol-Cpx-Plg dykes		
Pd1	NW Cpx-Plg dykes		
	D_4 faults		
	D_3 ductile shear zones		
Ag	Granite		
Am	Dyke fragments	}	
Adi	Diatexite	}	D_2 deformation
Agd	Hornblende granodiorite	}	
	D_1 deformation		
Ad	Pyroxene-biotite diorite		
As, Av	Sedimentary, volcanic rocks		

Table 2: Average magnetic susceptibility (SI units) of major rock types.

Rock type		n	avg
As	(excluding BIF)	17	198
Ad	diorite	13	4998
	tonalite	8	2775
Agd	granodiorite	10	2840
	diorite	16	3612
	gabbro	8	1147
	pyroxenite	2	3250
	granite	4	1230
Adi	Opx-Bt Dtx	18	2382
	Gt Dtx	20	1063
Ach	charnockite	14	2057
Ag	granite	75	2109
	granodiorite	22	1680

MINERAL POTENTIAL

Several geological environments in the Lake Minto area are potentially interesting for mineral exploration. Pyroxenite, although generally in small, discontinuous bodies, contains numerous sulphide-rich zones that are currently being assessed for PGE potential. Gold potential may exist in iron-formations and sulphide-rich zones in paragneiss, based on showings in similar environments in the Ashuanipi complex in the Schefferville area to the south (Lapointe, 1986; Thomas and Butler, 1987; Percival, 1987). Grab samples from sulphide showings in metavolcanic rocks at Lac Minto returned Au assays in the 5-35 ppb range. The large iron-formations noted by Stevenson (1968) may have better exploration potential than the small, discontinuous bodies encountered in the present survey.

REGIONAL CONSIDERATIONS

The northerly magnetic and structural trends of Minto subprovince contrast with large-scale easterly structures in the

southern Superior Province. Based on interpretation of magnetic patterns at the Minto-Bienville boundary, Card and Ciesielski (1986) speculated that the Minto subprovince could be an older block onto which the 3.0 - 2.7 Ga belts of the southern Superior Province had been accreted. However, the limited geochronology does not support this hypothesis: metavolcanic rocks from Lake Minto are ~ 2.7 Ga (J.K. Mortensen, pers. comm., 1989) and a granodiorite from Rivière aux Feuilles is 2.72 Ga (Machado et al., 1989). It is more likely that the Minto subprovince represents a relatively late addition to the Superior Province.

Structural trends in the high-grade Ashuanipi complex to the south are dominantly WNW, projecting toward the Minto subprovince, but separated from it by the Bienville domain. There are several lithological and structural similarities between parts of the Ashuanipi (Percival and Girard, 1988; Percival, 1989) and Minto subprovinces: 1) dominantly metasedimentary supracrustal lithologies, cut by 2) early, pyroxene-oikocrystic biotite diorite-tonalite, locally preserved in oval, cone-shaped structures, subsequently intruded by 3) homogeneous and inhomogeneous diatexite, and by 4) late biotite granite. Based on the existing mapping, the proportion of late granite is higher in the Minto than in the Ashuanipi subprovince. However it appears that similar histories characterize the two terranes; geochronology is in progress to establish absolute ages as a basis for detailed comparison and possible correlation.

By lithological criteria, the Minto subprovince most closely resembles the plutonic terranes of the Superior Province, for example Berens River subprovince (e.g., Card and Ciesielski, 1986). However the widespread presence of primary orthopyroxene in plutonic rocks is a significant difference that requires explanation. Although it is possible that Minto subprovince represents a deeper and therefore hotter and drier crustal level than normally exposed in Superior Province, the presence of garnet-cordierite assemblages and preliminary unpublished geobarometry indicating 400-500 MPa (4-5 kb) metamorphic pressures permit only marginally deeper exposure levels. The magmatic orthopyroxene may relate to conditions of igneous generation or emplacement; work is underway to define these pressure, temperature and fluid activity parameters.

ACKNOWLEDGMENTS

Capable field assistance was provided by A. Therriault (University of Houston) and S. Castonguay (Université du Québec à Montréal). Logistic and air support were handled from Kuujjuarapik by the Centre d'Études nordiques and Air Saguenay. M.R. St-Onge and A. Davidson made helpful comments on the manuscript.

REFERENCES

Brown, M.
1973: The definition of metatexis, diatexis and migmatite; Proceedings of the Geological Association, v. 84, p. 371-382.

Card, K.D., and Ciesielski, A.
1986: Subdivisions of the Superior Province of the Canadian Shield; Geoscience Canada, v. 13, p. 5-13.

Frost, B.R., Fyfe, W.S., Tazaki, K., and Chan, T.
1989: Grain-boundary graphite in rocks and implications for high electrical conductivity in the lower crust; Nature, v. 340, p. 134-136.

Geological Survey of Canada
1988: Magnetic anomaly map, Lake Minto; Geological Survey of Canada, Map NO 18-M, scale: 1:1 000 000.

Herd, R.K.
1978: Notes on metamorphism in New Québec; Geological Survey of Canada, Paper 78-10, p. 79-83.

Holdaway M.J. and Lee, S.M.
1977: Fe-Mg cordierite stability in high-grade pelitic rocks based on experimental, theoretical and natural observations; Contributions to Mineralogy and Petrology, v. 63, p. 175-198.

Lapointe, B.
1986: Reconnaissance géologique de la région du lac Paillerаut- Territoire du Nouveau Québec; Ministère d'Énergie et des Ressources du Québec, MB85-73, 10 p.

Machado, N., Goulet, N., and Gariépy, C.
1989: U-Pb geochronology of reactivated Archean basement and of Hudsonian metamorphism in the northern Labrador Trough; Canadian Journal of Earth Sciences, v. 26, p. 1-15.

Percival, J.A.
1987: Geology of the Ashuanipi granulite complex in the Schefferville area, Quebec; in Current Research, Part A, Geological Survey of Canada, Paper 87-1A, p. 1-10.
1989: Geology of the Ashuanipi complex in the Schefferville area; Geological Survey of Canada, Open File 2050.

Percival, J.A., and Girard, R.
1988: Structural character and history of the Ashuanipi complex in the Schefferville area, Quebec-Labrador; in Current Research, Part C, Geological Survey of Canada, Paper 88-1C, p.51-60.

Peterson, J.W., and Newton, R.C.
1989: CO_2-enhanced melting of biotite-bearing rocks at deep-crustal pressure-temperature conditions; Nature, v. 340, p. 378-380.

Phillips, G.N., and De Nooy, D.
1988: High-grade metamorphic processes which influence Archaean gold deposits, with particular reference to Big Bell, Australia; Journal of Metamorphic Geology, v. 6, p. 95-114.

Phinney, W.C., Morrison, D.A., and Maczuga, D.E.
1988: Anorthosites and related megacrystic units in the evolution of Archean crust; Journal of Petrology, v. 29, p. 1283-1323.

Stevenson, I.M.
1968: A geological reconnaissance of Leaf River map-area, New Quebec and Northwest Territories; Geological Survey of Canada, Memoir 356, 112p.

Thomas, A., and Butler, J.
1987: Gold reconnaissance in the Archean Ashuanipi complex of western Labrador; in Current Research, Newfoundland Department of Mines and Energy, Report 87-1, p. 237-255.

Altered and mineralized rocks at Echo Bay, N.W.T., and their relationship to the Mystery Island intrusive suite[1]

Nancy C. Reardon[2]

Reardon, N.C., Altered and mineralized rocks at Echo Bay, N.W.T., and their relationship to the Mystery Island intrusive suite; in Current Research, Part C, Geological Survey of Canada, Paper 90-1C, p. 143-150, 1990.

Abstract

The intermediate plutons of the Mystery Island intrusive suite are associated with broad zones of altered rocks which contain albite, magnetite + apatite + actinolite and/or pyrite. Pitchblende, native Ag, Ni-Co arsenide veins, many of which have been mined, are spatially, but not temporally, associated with the plutons and their altered wallrocks. However, the chemical milieu provided by the altered rocks could have preferentially reacted with younger mineralizing fluids to localize some pitchblende, native Ag, Ni-Co arsenide deposits. Reconnaissance whole-rock oxygen isotope analyses rule out a meteoric geothermal system and high water/rock ratios, but are comparable to those from geothermal systems in which the fluids are evolved seawater or highly-evolved meteoric water.

Résumé

Les plutons intermédiaires de la suite intrusive de l'île Mystery sont associés à de vastes zones de roches altérées qui contiennent de l'albite, de la magnétite + apatite + actinolite et(ou) de la pyrite. Des filons de pechblende, d'argent natif, d'arséniure de Ni-Co dont plusieurs ont été exploités, sont spatialement mais non temporellement associés aux plutons et à leurs roches encaissantes altérées. Cependant, le milieu chimique lié à la présence de ces roches altérées pourrait avoir réagi de préférence avec des fluides de minéralisation plus récents et formé ainsi localement quelques gisements de pechblende, d'argent natif et d'arséniure de Ni-Co. Des analyses isotopiques de l'oxygène sur la roche entière excluent l'hypothèse d'un système géothermique météorique et des rapports eau-roche élevés pour se rapprocher plutôt de systèmes géothermiques dans lesquels les fluides sont formés d'eau de mer évoluée et d'eau météorique très évoluée.

[1] Contribution to Canada — Northwest Territories Mineral Development Agreement 1987-1991. Project carried by Geological Survey of Canada, Continental Geoscience Division

[2] Department of Geology, University of Ottawa, Ottawa, K1N 6N5

INTRODUCTION

Pitchblende, native Ag, Ni-Co arsenide veins in the western Great Bear magmatic zone have been mined intermittently since the 1930s. The veins are spatially, but not temporally, associated with intermediate plutons of the Mystery Island intrusive suite (Fig. 1) and their altered wallrocks, which are current exploration targets for silver and uranium. Large-scale alteration of the rocks and its effect on later mineralizing fluids is important in understanding the geological history of the mineralization. The present study attempts to establish the relationship of the plutons to their altered wallrocks, and to pitchblende, native Ag, Ni-Co arsenide mineralization in the Echo Bay area by examining field relations, mineralogy and stable isotopic compositions.

The results of seven weeks of field work during the summer of 1989 are summarized in this report. Petrographic data as well as reconnaissance whole-rock oxygen isotope data from the Contact Lake and Glacier Lake plutons and their altered host rocks are also presented. Emphasis is placed on: 1) altered rocks in the Port Radium area (Fig 2); and 2) quartz-carbonate ± sulphide veins in the Port Radium area.

PREVIOUS WORK

Although the mineralized veins in the Echo Bay and Conjuror Bay-Camsell River areas have been extensively studied (Kidd, 1932; Furnival, 1935; 1939; Campbell, 1955; Jory, 1964; Robinson, 1971; Thorpe, 1971; 1974; Badham et al., 1972; Mursky, 1973; Robinson and Ohmoto, 1973; Shegelski, 1973; Changkakoti et al., 1986), little work has been carried out on the plutons of the Mystery Island intrusive suite and their altered wallrocks. A study by Furnival (1939) of the geology in the Contact Lake area included modal analyses of the Contact Lake pluton. Cherer (1988) studied the petrology and geochemistry of the Contact Lake pluton and the southern portion of the Glacier Lake pluton. Hildebrand (1982, 1986) mapped altered rocks above and within the Rainy Lake and Balachey plutons (Fig. 1) and carried out detailed petrological and geochemical studies of the rocks. He recognized the alteration assemblages and divided the altered rocks into three zones: 1) albite; 2) magnetite-apatite-actinolite; and 3) pyrite. Pb-isotope (Jory, 1964; Thorpe, 1971) and oxygen, carbon and sulphur isotope studies (Robinson and Ohmoto, 1973) were carried out on the mineralized veins at Port Radium. However, no oxygen isotope data are available for the altered host rocks.

GEOLOGY

The Mystery Island intrusive suite (Hildebrand, 1981) consists of six semi-concordant, epizonal plutons of intermediate composition which crop out within two areas in the 1.87 Ga Great Bear magmatic zone separated by faults and younger granitoid plutons (Hoffman and McGlynn, 1977; Hildebrand et al., 1986). The plutons are sill-like in cross-section, up to 10 km long and 2 km thick, and intrude sedimentary and volcanic rocks of the LaBine Group (Hoffman, 1984). The plutons and their host rocks were folded at about 1.843 Ga (Bowring, 1984), exposing the plutons and their altered wallrocks in oblique cross-section. After 1.84 Ga, younger northeast-striking transcurrent faults cut the folded plutons and their host rocks (Hoffman, 1980; Hildebrand et al., 1986). The transcurrent faults are cut by Cleaver diabase (Hoffman, 1984; Hildebrand, 1982) which are unconformably overlain by the 1.663 Ga Hornby Bay Group (McGrath and Hildebrand, 1984; Bowring and Ross, 1985). Many of the transcurrent faults were reactivated during a period of normal faulting which occurred during the late stages of, or after, the deposition of the Hornby Bay Group (Hildebrand, 1988). Gabbro sills known as Western Channel diabase are the youngest rocks in the area (Hildebrand, 1982).

Altered rocks

All of the plutons of the Mystery Island intrusive suite have altered wallrocks. The altered rocks comprise zones up to 1 km in thickness which are divided into three zones in the field: 1) a zone of albitized rock present above, and locally below, the roofs of the plutons; 2) a magnetite-apatite-actinolite zone present at some distance above the plutons; and 3) an outer zone of pyrite (Hildebrand, 1986; Reardon, 1989). The zones are somewhat discontinuous laterally, and in some areas overlap substantially. Locally, the albite zone, and to a lesser extent, the magnetite-apatite-actinolite and pyrite zones, are superimposed on the plutons. The distribution of the zones in the Port Radium area is shown in Figure 2.

Albite zone

The albite zone is characterized by varying degrees of albitization; altered rocks vary in colour from reddish to pale pink. Extremely altered rocks, found in close proximity to the plutons, are white both on the fresh and weathered surfaces, with the only mafic constituent being small wisps of chlorite. Veins and pods of albite are present in highly altered areas. The recognition of albitized rocks in the field becomes increasingly difficult with increasing distance from the plutons, since other processes, such as hematization, and variation in lithology, affect the colour of the altered rocks. A second criterion used in the field for determining the degree of albitization of lava flows is the apparent corrosion of plagioclase phenocrysts.

Magnetite-apatite-actinolite zone and breccias

This zone is defined by the presence of at least two of the three minerals: magnetite, apatite and actinolite. Actinolitic amphibole, referred to here simply as actinolite, is the most abundant of the three and is widely distributed throughout the area both within the magnetite-apatite-actinolite zone, and as a singular alteration mineral. The most common assemblages of the minerals in this zone are: 1) actinolite + magnetite; 2) actinolite + apatite; and 3) magnetite + apatite + actinolite. The assemblage actinolite + pyrite ± quartz is present locally. The paragenetic sequence of these minerals is actinolite-magnetite or magnetite-actinolite, and

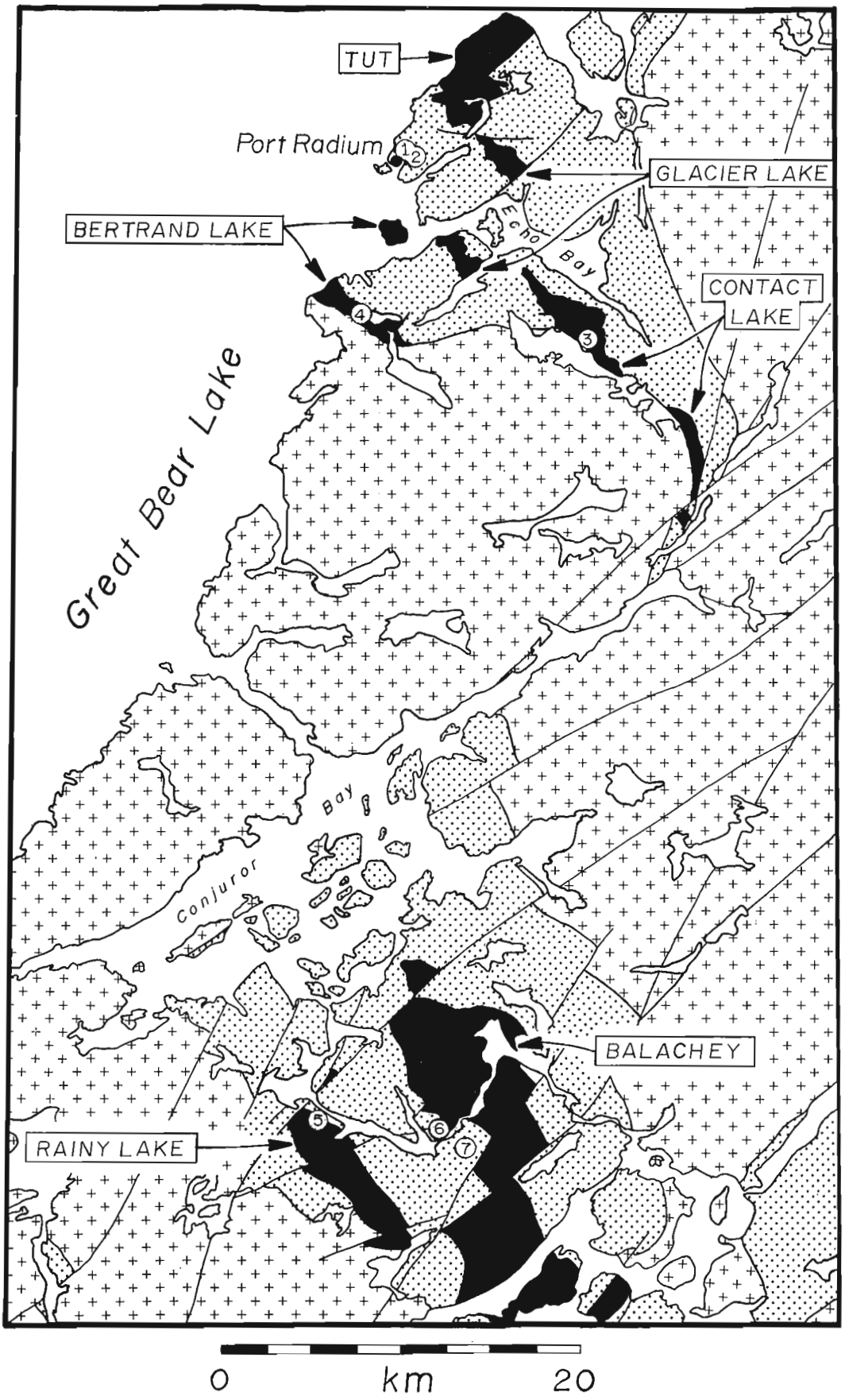

Figure 1. Location map of the Mystery Island intrusive suite modified after Hildebrand (1986) and Reardon (1989). U-Ag-Co-Ni arsenide deposits: 1 = Eldorado, 2 = Echo Bay, 3 = Contact Lake, 4 = Bonanza Group, 5 = Terra, 6 = Federated, 7 = Norex and Smallwood.

when all three minerals are present, magnetite-actinolite-apatite or actinolite-magnetite-apatite. Some magnetite-apatite-actinolite veins elsewhere in the Great Bear magmatic zone contain pitchblende and chalcopyrite (Gandhi, 1988; Gandhi and Bell, 1989).

Magnetite, apatite and actinolite occur as veins and pods or as disseminated crystals. The veins are not very continuous; are generally exposed along strike for less than 1 m; and are up to 1 m in width. The veins have various orientations, but generally strike E-W and N-S; follow fracture systems; and are steeply dipping. Pods are generally less than 1 cm, and locally up to several centimetres across. Disseminated crystals of magnetite, apatite and actinolite replace country rocks locally. An excellent example of this replacement is found above the Contact Lake pluton. There, strongly albitized rocks containing disseminated magnetite, apatite and actinolite are also cut by magnetite + apatite + actinolite veins.

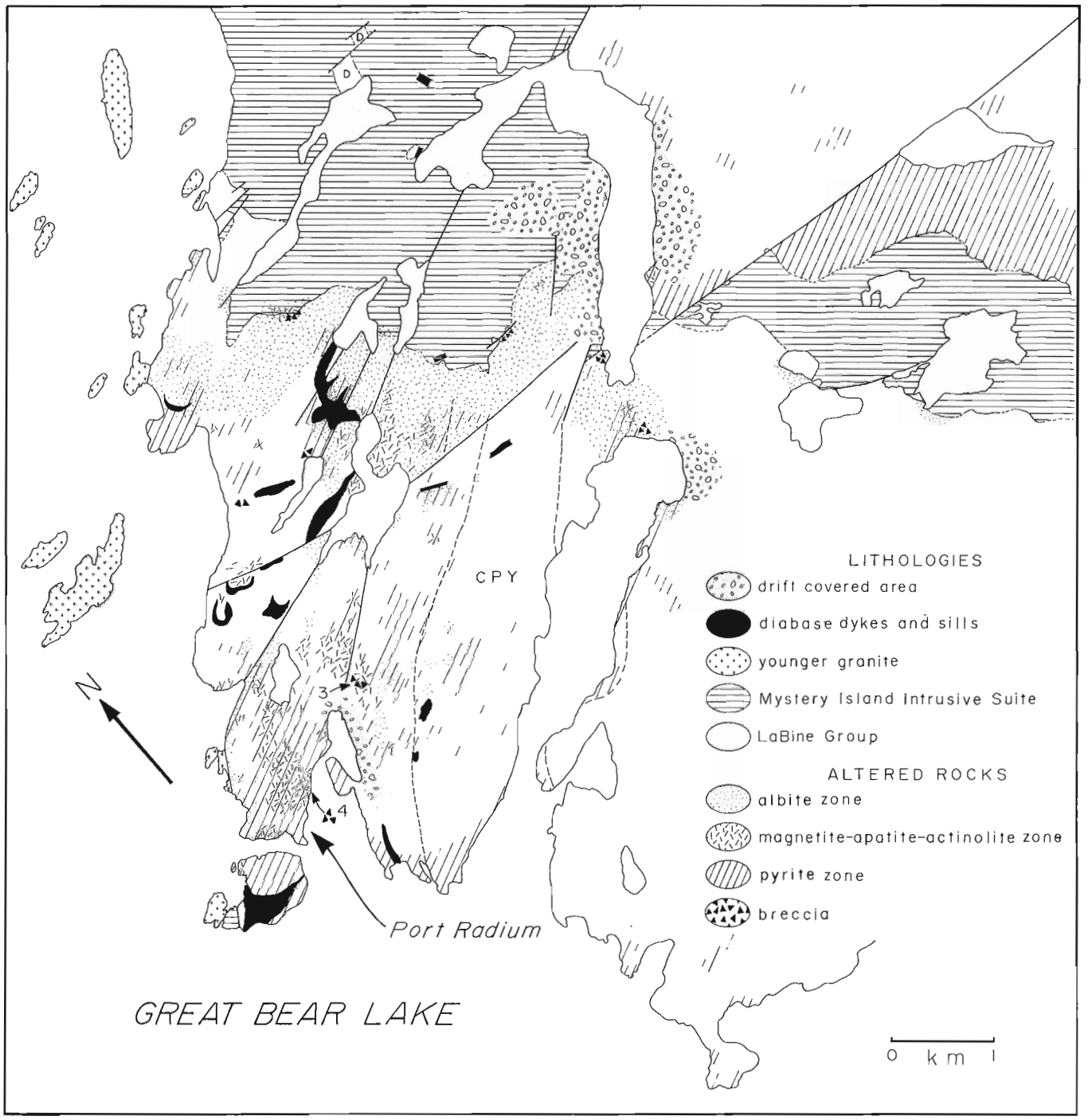

Figure 2. Geological sketch map of altered rocks in the Port Radium area, showing the distribution of the albite, magnetite-apatite-actinolite and pyrite zones. A chalcopyrite subzone is indicated by dashed lines. The breccias illustrated in Figures 3 and 4 are indicated by "3" and "4" respectively. D = diorite.

The mode of occurrence of magnetite, apatite and actinolite varies with original lithology. In andesites, these minerals are usually present in veins or pods, whereas in sedimentary rocks alteration minerals are disseminated throughout the rock, replacing individual beds. Some pervasively altered rocks are cut by veins and pods of magnetite-apatite-actinolite or magnetite-actinolite (Fig 3). Breccias which consist of pink, probably albitized, fragments in a matrix of finely disseminated actinolite and magnetite are common and are usually present near the plutonic contacts (Fig 2.). Magnetite-apatite-actinolite breccias (Fig. 4) comprise angular to rounded fragments of country rock to 1 m in diameter enclosed in a matrix of (in order of formation) medium- to coarse-grained magnetite ($\pm$ sulphides), actinolite, apatite, $\pm$ epidote and albite. The locations of the breccias are shown in Figure 2.

Robinson and Ohmoto (1973) suggested that actinolite-magnetite veins in the Port Radium area were related to the diabase dykes and sills in the area. This hypothesis is unlikely as the diabase sills are younger than the veins, and the diabase dykes are not large or widespread enough to have produced this alteration.

Pyrite zone

This zone is characterized by the presence of pyrite as disseminated crystals or centimetric pods which form visible gossan in the field. The zone is generally found at some distance above the roofs of the plutons, although one large gossan is present directly above the northern portion of the Glacier Lake pluton, and small amounts of gossan are present below some of the plutons. Locally, magnetite-apatite-actinolite veins and breccias contain pyrite. Within the pyrite zone, higher concentrations of pyrite are present in sedimentary rocks than in andesites. This could be due to differences in porosity, permeability and/or composition of the two lithologies. In the Echo Bay and Conjuror Bay-Camsell River areas, pitchblende, native Ag, Ni-Co arsenide veins are spatially associated with the pyrite zone (Hildebrand, 1986, 1988). Economic mineralization is not restricted to this zone, however, as demonstrated by the Contact Lake silver deposit (Fig. 1), which is hosted by the Contact Lake pluton.

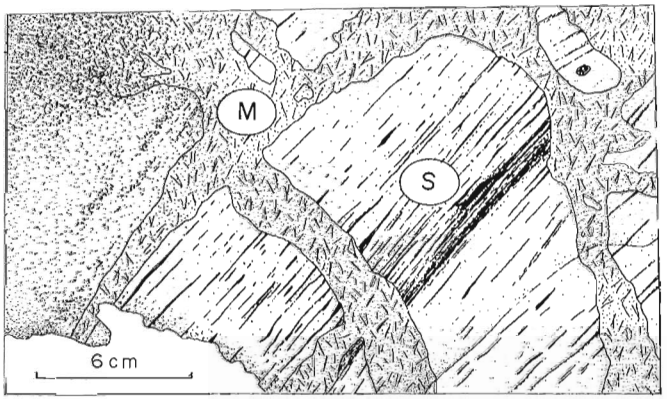

Figure 3. Sketch of sedimentary rocks replaced by disseminated actinolite and magnetite (S) in a matrix of magnetite and actinolite (M).

A zone of chalcopyrite was recognized east of Port Radium (Fig. 2). The zone is characterized by the presence of finely disseminated chalcopyrite within the groundmass and amygdules of andesitic lava flows. This could represent a subzone of the pyrite zone, and is apparently controlled by stratigraphy.

Altered rocks at Port Radium

Robinson and Ohmoto (1973) attributed alteration of rocks in the Port Radium area to contact metamorphism due to the intrusion of a younger granitic pluton immediately west of Port Radium. However, altered rocks at Port Radium are similar to those adjacent to the plutons of the Mystery Island intrusive suite in that they contain zoned alteration assemblages of albite, magnetite-apatite-actinolite and pyrite. Rocks along the shore of Great Bear Lake are strongly albitized, with albitization decreasing eastward. A magnetite-apatite-actinolite zone trending parallel to the lakeshore (approximately NNE) is present 500 m southeast of the shoreline. A zone of pyrite overlaps both the albite and magnetite-apatite-actinolite zones but is strongest 300 to 500 m from the shoreline (Fig. 2). This suggests the former presence of a pluton of the Mystery Island intrusive suite offshore (R.S Hildebrand, pers. comm., 1988). A small, fault-bounded remnant of a pluton compositionally and texturally similar to the plutons of the Mystery Island intrusive suite discovered during the 1989 field season on Cobalt Island, immediately southwest of Port Radium, supports this hypothesis.

OXYGEN ISOTOPE RECONNAISSANCE STUDIES

Sixty-six whole-rock oxygen isotope analyses were completed from samples collected within, below and above the Contact Lake pluton and the southern portion of the Glacier Lake pluton. Preliminary whole-rock results indicate that variation of $\delta^{18}O$ within the plutons and their altered zones is limited. $\delta^{18}O$ ranges from +6.3 to +10.3 for altered

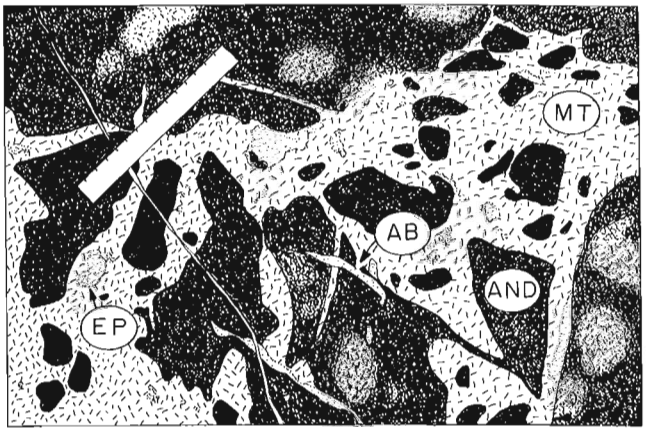

Figure 4. Sketch of brecciated andesite (AND) in a matrix of magnetite with lesser actinolite (MT) and epidote (EP). Discontinuous albite veins (AB) cut both the andesite and the matrix. A calcite veinlet cuts the andesite, matrix, and albite veins. Scale = 15 cm.

andesites, whereas plutons tend to have slightly higher $\delta^{18}O$ values, from +8.1 to +12.3. A histogram of the $\delta^{18}O$ values is presented as Figure 5. The data rule out a meteoric geothermal system with high water-rock ratios, since $\delta^{18}O$ values of rocks altered by meteoric geothermal waters are typically lower than those observed, and often record large geographic variations in $\delta^{18}O$. The $\delta^{18}O$ values are comparable to those from geothermal systems in which the fluids were evolved seawater or highly evolved meteoric water in a system which had low water/rock ratios. More detailed work is underway to attempt to define both regional and small-scale variations.

QUARTZ-CARBONATE ± SULPHIDE VEINS

Quartz-carbonate veins, many of which contain sulphides, are found throughout the study area. Some of the veins are mineralized and have been mined for uranium, silver, and copper. The following descriptions refer to veins mapped during the 1988 and 1989 field seasons and do not include veins which were mined.

Mineralogy and paragenesis

The principal minerals of the veins are quartz, calcite, siderite, chalcopyrite, hematite and pyrite. Minor amounts of nickel-cobalt arsenides are present locally. Most of the veins contain fragments of country rock which are strongly chloritized, or, less commonly, hematized. The veins are divided into several types according to their mineralogy: 1) quartz (± carbonate), 2) quartz + hematite (± carbonate) 3) quartz (± carbonate) + chalcopyrite (± pyrite). In all veins quartz grew first, followed by hematite or sulphides. Most of the veins contain carbonate, usually siderite, which is younger than quartz. Where carbonate and sulphide minerals are both present, the sulphides are found within the carbonate. Veins of calcite and siderite are common and some contain sulphides. Locally, veins of siderite transect quartz-siderite-sulphide veins.

Distribution and geometry

The veins are present throughout the study area, but are more abundant in the Port Radium area than elsewhere. They range from a few centimetres to greater than 1 m in width. Many of the veins are continuous for several metres, and up to 300 m, along strike. Most of the veins strike northeast and north, although a few strike northwest; the mineralized veins at Port Radium generally strike northeast. All of the veins in the area are steeply-dipping, typically greater than 65°. Campbell (1955) argued that many of the veins filled faults and tension fractures related to the NE-trending transcurrent faults. However, large transcurrent faults in the area, which strike approximately northeast, are not known to contain mineralized veins.

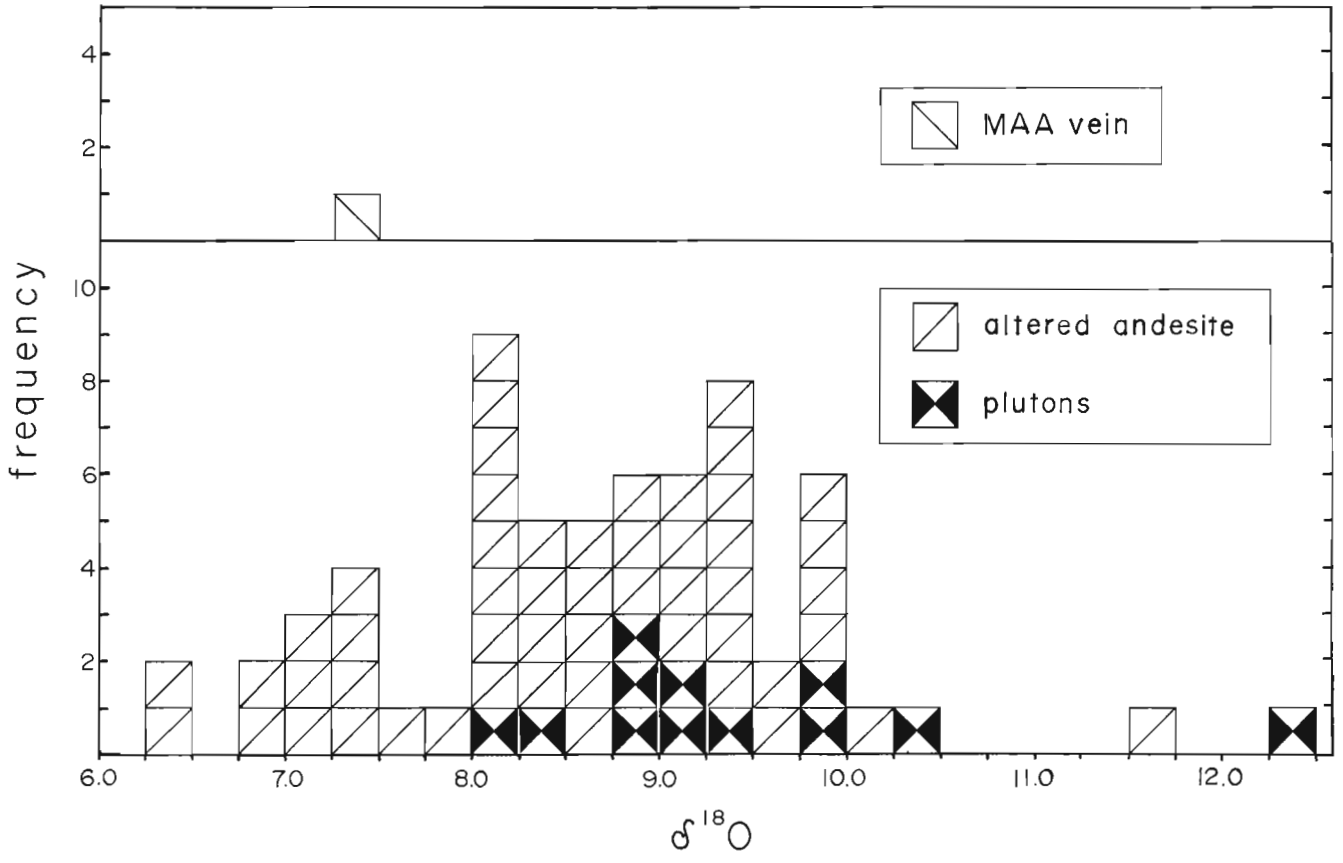

Figure 5. Histogram of $\delta^{18}O$ values for the Contact Lake pluton and the southern portion of the Glacier Lake pluton and their altered wallrocks.

Age relationships

Jory (1964) described a diabase dyke in the Eldorado mine (Fig. 1) at Port Radium which intersects and is diverted by quartz veins. The dyke is brecciated by later movement on the veins and healed by vein mineralization. Jory (1964) also reported that a diabase sill in the mine is not offset by quartz veins, but is affected by late mineralization. Robinson (1971) concluded that diabase dykes in the Eldorado mine are younger than the initial development of the vein structures but older than most of the vein minerals. Robinson (1971), in agreement with Jory, concluded that a diabase sill in the mine cut all but the latest stages of mineralization. Robinson and Ohmoto (1973) argued that diabase dykes and sills, actinolite-magnetite veins and pitchblende, native Ag, Ni-Co arsenide veins are closely related in time, and were formed at about 1450-1400 Ma based on: K-Ar ages of 1400 Ma for a diabase sill in the Port Radium area (Wanless et al., 1968), and 1420 Ma for actinolite-magnetite veins in the Echo Bay mine (Robinson and Morton, 1972); a U-Pb age of 1450 Ma on pitchblende from mineralized veins at Port Radium (Jory, 1964); and cross-cutting relationships, as described above. However, Thorpe (1971) reported a Pb-Pb age for galena in mineralized veins of 1625 Ma.

Since most mineralized veins strike northeast, it might seem reasonable to relate them to northeasterly-striking transcurrent faults. However, the largest transcurrent faults in the area are not known to be mineralized, although they contain quartz stockworks up to 30 m wide. Furthermore, as strike-slip faults only develop dilatant zones at bends, it is difficult to explain how mineralized veins, up to 1.5 km long and with features characteristic of extension, would be generated along such faults. Furnival (1939) recognized two periods of quartz deposition in northeast-striking fault zones: one that predated deposition of the Hornby Bay Group; and another which cuts the Hornby Bay Group. The cross-cutting relationships of the veins and diabase dykes and sills described by Jory (1964) and Robinson (1971) agree with two ages of veins within fault zones at Port Radium, the latter being mineralized. A number of workers have identified west-side-down normal faults along the western side of the Great Bear magmatic zone which placed rocks of the lower Hornby Bay Group against rocks of Wopmay orogen (Kerans et al., 1981; Hildebrand, 1982; Hoffman, 1984; McGrath and Hildebrand, 1984; Ross and Kerans, 1989). The presence of mineralization in northeasterly-striking fault zones can be explained by relating the timing of mineral deposition to west-side-down normal faulting, as proposed by Hildebrand (1988). The hydrothermal cells which were responsible for the mineralization may have been driven by 1663 ± 8 Ma (Bowring and Ross, 1985) magmatism of the lower Hornby Bay Group. U-Pb dates of carbonate cements and veins elsewhere in Wopmay orogen (Bowring et al., 1989) support this model in that their ages are about 1667 Ma, within analytical error of Hornby Bay magmatism.

ECONOMIC IMPLICATIONS

Shegelski and Scott (1975), Hoffman et al. (1976) and Hildebrand (1984) noted that all mines in the Echo Bay and Conjuror Bay-Camsell River areas occur either within the plutons of the Mystery Island intrusive suite or their altered wallrocks. Most pitchblende, native Ag, Ni-Co arsenide veins are spatially associated with the pyrite zone (Hildebrand, 1988), although economic mineralization is not restricted to these zones, as demonstrated by the Contact Lake mine (Fig. 1). The chemical environment created by the sulphides could have served to precipitate ore minerals from fluids passing through this zone. The association between mineralization and the presence of sulphides has also been observed in the Terra Mine (Fig. 1), where concentrations of ore minerals within silver-bearing veins are significantly greater where the veins intersect a large sulphide zone (S. Gandhi and S. Roscoe, pers. comm., 1989). This suggests that the pyrite zone associated with the Mystery Island intrusive suite is a good exploration target for economic concentrations of U and Ag.

ACKNOWLEDGMENTS

Field work was supported financially by the Geological Survey of Canada and a Canada-Northwest Territories Mineral Development Agreement. Costs for isotopic analyses were paid by an NSERC research grant to Bruce Taylor. I would like to thank Robert Hildebrand and Bruce Taylor for critically reviewing the manuscript. Thanks to CEGB for the use of their Cessna. Special thanks to my assistant, Stephane Lagace.

REFERENCES

Badham, J.P.N., Robinson, B.W., and Morton, R.D.
1972: The geology and genesis of the Great Bear Lake silver deposits; 24th International Geological Congress, Montreal 1972, Section 4, p. 541-548.

Bowring, S.A.
1984: U-Pb geochronology of early Proterozoic Wopmay orogen, N.W.T., Canada: an example of rapid crustal evolution; Ph.D. thesis, University of Kanasas, 148 p.

Bowring, S.A. and Ross, G.M.
1985: Geochronology of the Narakay Volcanic Complex: Implications for the age of the Coppermine Homocline and Mackenzie igneous events; Canadian Journal of Earth Sciences, v. 22, p. 774-780.

Bowring, S.A., Housh, T.B., Heatherington, A.L. and Grotzinger, J.P.
1989: U-Pb isotopic analysis of carbonate cements, early Proterozoic Rocknest Formation: evidence for differential element mobility during diagenesis; *in* Abstracts with programs, Geological Association of Canada-Mineralogical Association of Canada v. 14, p. A 78.

Campbell, D.D.
1955: Geology of the pitchblende deposits of Port Radium, Great Bear Lake, N.W.T.; Ph. D. thesis, California Institute of Technology, 323 p.

Changkakoti, A., Morton, R.D., Gray, J. and Yonge, C.J.
1986: Electron microprobe analyses of native silver and associated arsenides from the Great Bear Lake silver deposits, Northwest Territories, Canada; Canadian Journal of Earth Sciences, v. 23, p. 1470-1479.

Cherer, R.M.
1988: Petrology and geochemistry of three plutons of the Mystrey Island Intrusive Suite, District of Mackenzie, Northwest Territories; B.Sc. thesis, University of Toronto, Toronto.

Furnival, G.M.
1935: The large quartz veins of Great Bear Lake, Canada; Economic Geology, v. 30, p. 843-850.
1939: Geology of the area north of Contact Lake, N.W.T.; American Journal of Science, v. 237, p. 478-489.

Gandhi, S.S.
1988: Volcano-plutonic setting of U-Cu bearing magnetite veins of the FAB claims, southern Great Bear magmatic zone, Northwest Territories; *in* Current Research, Part C, Geological Survey of Canada, Paper 88-1C, p. 177-187.

Gandhi, S.S. and Bell, R.T.
1989: Magnetite deposits of the Great Bear magmatic zone, Canada; *in* abstracts with Programs, Geological Society of America, v. 21, no. 6, p. A33

Hildebrand, R.S.
1981: Early Proterozoic LaBine Group of Wopmay Orogen: Remnant of a volcanic arc developed during oblique convergence; *in* Proterozoic Basins of Canada, ed. F.H.A. Campbell; Geological Survey of Canada, Paper 81-10, p. 133-156.
1982: Geology, Echo Bay — MacAlpine Channel area, District of Mackenzie, Northwest Territories; Geological Survey of Canada, Map 1546A, scale 1:50 000.
1984: Geology of the Rainy Lake and White Eagle Falls map areas, District of Mackenzie: Early Proterozoic cauldrons, stratovolcanoes and subvolcanic plutons; Geological Survey of Canada, Paper 83-20, 42 p.
1986: Kiruna-type deposits:their relationship to intermediate subvolcanic plutons in the Great Bear magmatic zone, northwest Canada; Economic Geology, v. 81, p. 640-659.
1988: Ore deposits in the Great Bear magmatic zone, an early Proterozoic arc terrane in Wopmay orogen, northwestern Canadian Shield; International field conference on the tectonic setting of Proterozoic volcanism and associated ore deposits, Turku, Finland, abstract volume, August 1988, p. 12.

Hildebrand, R.S., Hoffman, P.F. and Bowring, S.A.
1986: Tectono-magmatic evolution of the 1.9-Ga Great Bear magmatic zone, Wopmay Orogen, northwestern Canada; Journal of Volcanology and Geothermal Research, v. 32, p. 99-118.

Hoffman, P.F.
1980: Conjugate transcurrent faults in north-central Wopmay Orogen (early Proterozoic) and their dip-slip reactivation during post-orogenic extension, Hepburn Lake map-area (86J), District of Mackenzie; *in* Current Research, Part A, Geological Survey of Canada, Paper 80-1A, p. 183-185.
1984: The Northern Internides of Wopmay Orogen; Geological Survey of Canada, Open File 832, scale 1:250 000

Hoffman, P.F. and McGlynn, J.C.
1977: Great Bear Batholith: volcano-plutonic depression; *in* Volcanic Regimes in Canada, ed. W.R.A. Baragar, L.C. Coleman and J.M. Hall; Geological Association of Canada, Special Paper 16, p. 170-192.

Hoffman, P.F., Bell, I.R. and Tirrul, R.
1976: Sloan River map-area (86K), Great Bear Lake, District of Mackenzie; *in* Report of Activities, Part A, Geological Survey of Canada, Paper 76-1A, p. 353-358.

Jory, L.T.
1964: Mineralogical and isotopic relations in the Port Radium pitchblende deposit, Great Bear Lake, Canada; Ph.D. thesis, California Institute of Technology, 275 p.

Kerans, C., Ross, G.M., Donaldson, J.A., and Geldsetzer, H.J.
1981: Tectonism and depositional history of the Helikian Hornby Bay and Dismal Lakes groups, District of Mackenzie; *in* Proterozoic Basins of Canada, ed. F.H.A. Campbell; Geological Survey of Canada, Paper 81-10, p. 157-182.

Kidd, D.F.
1932: A pitchblende-silver deposit, Great Bear Lake, Canada; Economic Geology, v. 27, p. 145-159.

McGrath, P.H. and Hildebrand, R.S.
1984: An estimate, based on magnetic interpretation, of the minimum thickness of the Hornby Bay Group, Leith Peninsula, District of Mackenzie; *in* Current Research, Part A, Geological Survey of Canada, Paper 84-1A, p. 223-228.

Mursky, G.
1973: Geology of the Port Radium map area, District of Mackenzie; Geological Survey of Canada, Memoir 374, 40p.

Reardon, N.C.
1989: The Mystery Island intrusive suite and associated alteration haloes, Great Bear Lake, District of Mackenzie, N.W.T.; *in* Current Research, Part C, Geological Survey of Canada, Paper 89-1C, p. 37-42.

Robinson, B.W.
1971: Studies on the Echo Bay silver deposit, N.W.T., Canada; Ph.D. thesis, University of Alberta.

Robinson, B.W. and Morton, R.D.
1972: The geology and geochronology of the Echo Bay area, N.W.T., Canada; Canadian Journal of Earth Sciences, v. 9, p. 158-171.

Robinson, B.W. and Ohmoto, H.
1973: Mineralogy, fluid inclusions, and stable isotopes of the Echo Bay U-Ni-Ag-Cu deposits, Northwest Territories, Canada; Economic Geology, v. 68, p. 635-656.

Ross, G.M. and Kerans, C.
1989: Geology, Hornby and Dismal Lakes groups, Coppermine Homocline, District of Mackenzie, Northwest Territories; Geological Survey of Canada, Map 1663 A, scale 1:250 000 (with descriptive notes).

Shegelski, R.J.
1973: Geology and mineralogy of the Terra silver mine, Camsell River, N.W.T.; M.Sc. thesis, University of Toronto, 169 p.

Shegelski, R.J. and Scott, S.D.
1975: Geology and mineralogy of the silver-uranium-arsenide veins of the Camsell River District, Great Bear Lake, N.W.T.; *in* Abstracts with programs, Geological Society on America, v. 7, no. 6, p. 857-858.

Thorpe, R.I.
1971: Lead isotopic evidence on age of mineralization, Great Bear Lake; Geological Survey of Canada, Paper 71-1, Part B, p. 72-75.
1974: Lead isotope evidence on the genesis of the silver-arsenide vein deposits of the Cobalt and Great Bear Lake areas, Canada; Economic Geology, v. 69. p. 777-791.

Wanless, R.K., Stevens, R.D., Lachance, G.R. and Edmonds, C.M.
1968: Age determinations and geologic studies. K-Ar isotopic ages, Report 8, Geological Survey of Canada, Paper 67-2, Part A.

Stratigraphy, facies and structure in volcanic and sedimentary rocks of the Archean Back River volcanic complex, N.W.T.[1]

M.B. Lambert, G. Burbidge[2], C.W. Jefferson[3], C. Beaumont-Smith[4], and R. Lustwerk[3]
Continental Geoscience Division

Lambert, M.B., Burbidge, G., Jefferson, C.W., Beaumont-Smith, C. and Lustwerk, R., Stratigraphy, facies and structure in volcanic and sedimentary rocks of the Archean Back River volcanic complex, N.W.T., in Current Research, Part C, Geological Survey of Canada, Paper 90-1C, p. 151-165, 1990.

Abstract

Volcanic and sedimentary facies bordering this Archean, calc-alkaline stratovolcano record transitions from subaerial lavas, domes and related clastic aprons and alluvial fans of the emergent edifice through shallow marine conglomerates, oolitic/stromatolitic carbonates, and a rhyolitic fan delta, to deeper water volcaniclastic turbidites and crystal tuffs. Amalgamated sandy turbidites occupy submarine fan channels directed radially away from the volcano.

Three iron-bearing sedimentary sequences punctuate volcanic and sedimentary stratigraphy: A — sulphidic calcite-cemented volcaniclastics, magnetitic chert and slate within the volcanics; B — cherty iron-formation, including oolitic/stromatolitic carbonate, magnetite-, sulphide- and siderite-chert, sulphidic volcaniclastics, graphitic slate, and stratabound auriferous quartz veins between the volcanic pile and overlying greywacke-turbidites; C — argillitic to cherty magnetite- and sulphide- iron-formation, graphitic slate near or laterally equivalent to volcaniclastics within the greywacke-turbidites.

The volcanic complex was a competent mass enclosed by less competent turbidites which record four deformational events.

Résumé

Les faciès volcaniques et sédimentaires bordant ce stratovolcan calco-alcalin d'âge archéen, révèlent les transitions qui ont eu lieu de laves et de dômes subaériens et de plaines d'épendage et de cônes alluviaux connexes de roches clastiques liés à l'édifice émergeant à travers des conglomérats, des roches carbonatées oolitiques et stromatolitiques et un cône de déjection rhyolitique de milieu marin peu profond, à des turbidites volcanoclastiques et des tufs cristallins de milieu marin plus profond. Des turbidites sableuses amalgamées occupent des chenaux de cônes sous-marins dirigés radialement vers l'extérieur du volcan.

[1] Contribution to Canada-Northwest Territories Mineral Development Agreement 1987-1991. Project carried by Geological Survey of Canada.
[2] Department of Geology, University of Ottawa, Ottawa, Ontario K1N 6N5
[3] Mineral Resources Division
[4] Department of Geology, University of New Brunswick, Fredericton, N.B. E3B 5A3

Trois séquences sédimentaires ferrifères distinguent la stratigraphie volcanique et sédimentaire: A — des roches volcanoclastiques à ciment de calcite sulfurées, du chert et de l'ardoise magnétiques au sein des roches volcaniques; B — une formation de fer cherteuse, comprenant des roches carbonatées oolitiques et stromatolitiques, des cherts à magnétite, sulfure et sidérite, des roches volcanoclastiques sulfurées, des ardoises graphitiques et des filons de quartz aurifère logés au sein d'une strate unique, entre l'amas volcanique et les turbidites à grauwacke sus-jacentes; C — une formation ferrifère à magnétite et sulfure dont la nature varie d'argilitique à cherteuse, une argile graphitique adjacente ou latéralement équivalente aux roches volcanoclastiques contenues dans les turbidites à grauwacke.

Le complexe volcanique était un massif compétent contenu dans des turbidites moins compétentes qui ont été le siège de quatre événements de déformation.

INTRODUCTION

Field work in the 1989 season focused on refining stratigraphy within major volcanic units, sedimentological studies in volcaniclastic rocks and in turbidites of the Beechy Lake Group of the Yellowknife Supergroup, extending mapping of iron-formations, structural studies in metasediments surrounding the volcanic complex, and geochronological sampling of all major volcanic units, mafic dykes and plutons.

Highlights of the work include discovery of five new Archean stromatolite localities, recognition of volcanic turbidites in the stratigraphy, documenting vertical and lateral facies changes of three iron-bearing sedimentary sequences, confirming a structural model for deformation of the volcanic edifice, and discovery of a minor archeological site.

STRATIGRAPHY

Several publications (Lambert, 1976, 1977,1982a, 1982b; Moore, 1977; Frith, 1987; Jefferson et al. 1989) present preliminary stratigraphy of the Back River volcanic complex and Figures 1 and 2 serve as a generalized guide in lieu of a formal revised stratigraphy (in preparation). Herein we present (1) new findings that will form the basis of subdividing and understanding previously undivided large volcanic and sedimentary units, and (2) detailed accounts of selected areas that illustrate how well facies relations, volcanic and sedimentary processes can be documented.

Unit 2 'Andesites'

The area (unit 2 ,Fig. 1), between the outer and inner ring features (defined by arcuate zones of felsic intrusions, domes, breccias and carbonate impregnation; Lambert 1978) containing massive to pillowed lavas, tuffs, various types of breccias (pyroclastic, epiclastic lava flow, and debris flow) and undifferentiated volaniclastic rocks was previously mapped as a single unit Lambert, 1982b) thought to be dominantly of andesitic composition. The unit contains an abundance of volcaniclastic rocks, some of which contain ubiquitous felsic (rhyolitic and dacitic) clasts that should be regarded as possible debrites and not bear the compositional term 'andesite'. Moreover, some of the lava flows are dacite. The deposits generally appear to be massive, large-volume units that were spread over broad areas (tens of kilometres present strike-length). Thin-bedded volaniclastic sequences commonly define boundaries between large, massive units.

Critical to understanding the volcanic stratigraphy is the realization that boundaries of these large units locally are marked by fluvial deposits (e.g. Boomerang Lake braidplain) that broad areas of debris flows can be subdivided by intervening pyroclastic flows and lavas, that lava field lies west of Gold Lake, and most of the massive units within the southern part of the complex are gently dipping.

'Boomerang Lake' braidplain

East of Thwelycho Lake (near 'Boomerang Lake', local name, locality 3, Fig. 1) flat-lying cross-bedded volcanic sandstones and conglomerates separate very thick, massive andesitic pyroclastic flows. Weathering of the carbonate-impregnated matrix has emphasized sedimentary textures and structures, revealing large (up to 4 m) planar-tabular crossbeds in poorly to moderately sorted coarse volcarenites (Fig. 3). Bimodal distributions of planar-tabular crossbed directions within the volcarenites suggest linguoid bars. Many of the (west-dipping) large planar-tabular crossbeds have east-verging ripples and crossbeds on their foresets indicating migration of small dune forms up the planar-tabular (bar) foresets in separated flow (Fig. 4). Other sedimentary features include large (up to 1 m) trough crossbeds with easterly plunges; a 1.8 m thick unit of intraclastic breccia (Fig. 5); and local scours and channels cut into an underlying massive, probably tuffaceous, andesitic unit. Detailed mapping of these exposures revealed a braided cluster of easterly-trending channels cut into thick andesite tuffs. Elongate erosional remnants of the underlying tuff are interpreted as bars separating epiclastic channels. The preferred interpretation for this deposit is a subaerial braidplain marking a short hiatus in ashflow volcanism on the southwest flank of the stratovolcano.

Lavas near Gold Lake

The eastern tip of a lava field, that undoubtedly extends to the west, has been partially mapped west of Gold Lake. This unit comprises a succession of subaerial lavas with flow boundaries defined by thick zones of flow breccia. Four flows have been defined: two plagioclase-phyric andesite flows are overlain by two dacite flows. Andesite flows are about 6 m thick and flow breccias make up about 1/4 to 1/2 the flow thickness. Dacite flows have much thicker flow breccias than the andesite flows.

Massive parts of flows form blocky to prismatic jointed cliffs whereas recessive weathering flow breccias form the tops of most slopes. This topographic expression combined with the gentle dips of the flows (20-30° E near Gold lake, approaching subhorizontal northwesterly toward the centre of the complex) causes an erroneous impression of an unusually large proportion of breccia in the area. Much of the gently sloping present topography, which gradually rises toward the centre of the complex, consists of dip slopes marking lava flow units. Although only a small part of the lava field was mapped in detail, we now realize that individual lava flow units can be mapped and lava flows make up a greater part of the stratigraphy than previously realized.

RHYOLITES OF THE INNER AND OUTER RING FEATURES

Intrusive and extrusive (dome/flow complexes) rhyolite/dacite units (unit 5, Fig . 1) mark local centres of volcanic effusion along inner and outer ring fracture zones (Lambert, 1977,1978). Some of these bodies in the southern part of the outer ring intrude and include slivers of the adjacent andesite. Similarity of lithology throughout both inner- and outer-ring felsic bodies generally makes subdivision impractical. Criteria for subdivision only apply locally within each body. No marker unit has been traced far enough to show that the various rhyolite bodies were ever part of a single unit.

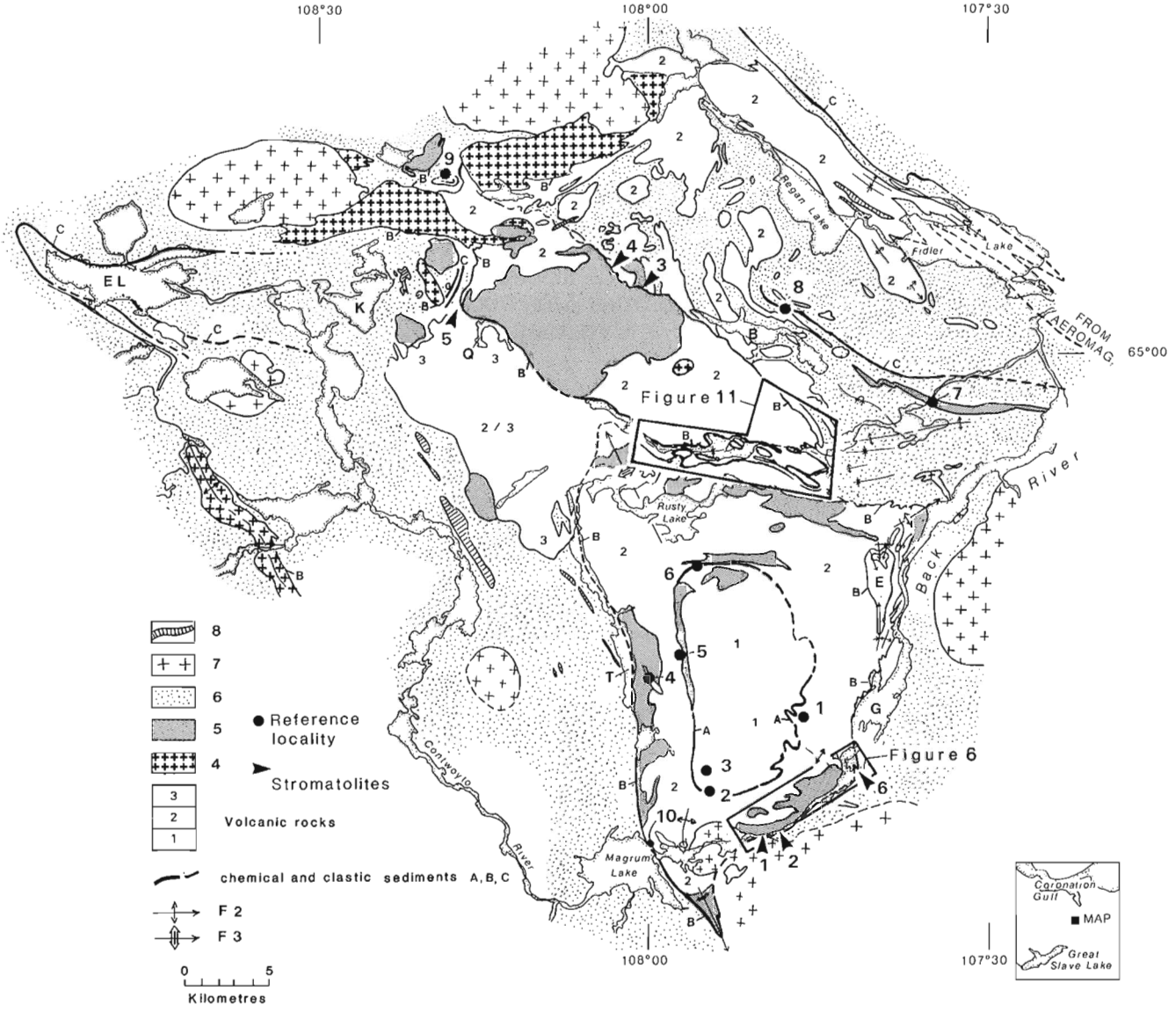

Figure 1. Simplified geology of the Back River volcanic belt. B — Boucher Lake, E — Eastring Lake syncline, EL — Esker Lake, G — Gold Lake, K — Keish Lake, Q — Quatermoon Lake, T — Thlewycho Lake. Location of iron-formation in the Esker Lake area is from unpublished data provided by Sirius Energy Corp. Ltd. and partners. 1-dacitic to andesitic tuffs and breccias; 2-volcaniclastic rocks, breccias, andesitic and dacitic lavas; 3-felsic breccias, volcarenites; 4-basalt; 5-rhyolite domes and flows, tuffs in turbidites of unit[6]; 6-turbidites, Beechy Lake Group; 7-plutonic suite; 8-mafic dykes and sills.

Outer-ring rhyolite at Thlewycho Lake

The 1.5 by 10 km rhyolite complex along the southeast side of Thlewycho Lake (locality 4) is divisible longitudinally into 2 parts by a basaltic unit in the southern part and bedded felsic tuffs, at about the same stratigraphic level, in the northern part. The dividing basaltic unit is a 100 m-thick westward dipping and facing sequence, mainly of coarsely amygdaloidal massive to pillowed flows and pillow breccias. They are underlain by a 10 m basal clastic sequence which includes very thick-bedded, massive, non-sorted basalt breccia, 2 thin interbeds of graded, ripple-marked basaltic wacke, and thin basal lenses of shale and quartz-rich fine sandstone. The bedded sequence, breccias and amygdules are all accentuated by abundant carbonate impregnation.

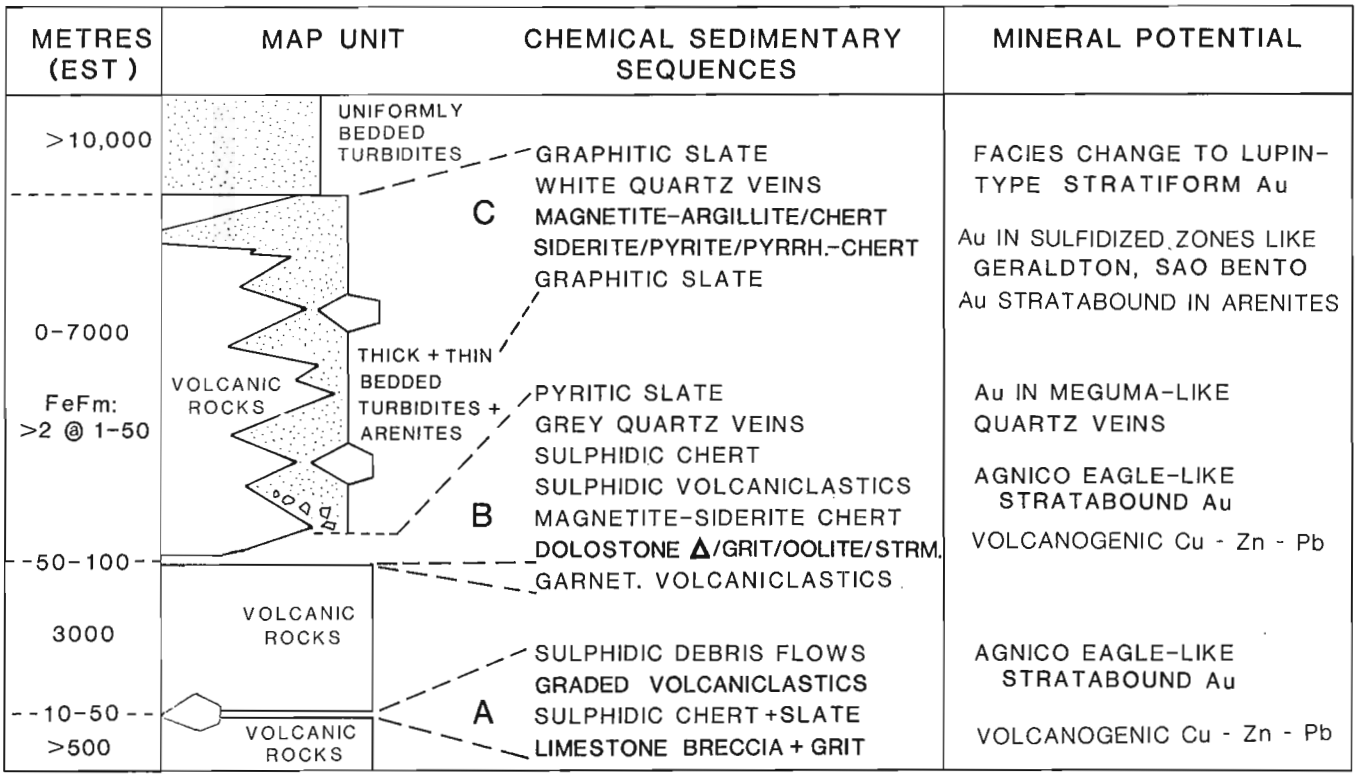

Figure 2. Generalized facies relationships in northeastern Slave Province (C.W.J.)

Figure 3. Large planar-tabular crossbeds in pebbly rhyolite volcarenite. Crossbeds are emphasized by selective carbonate replacement along tops of foresets. Distance across outcrop is about 15m. Locality 1. G.S.C 205025-I.

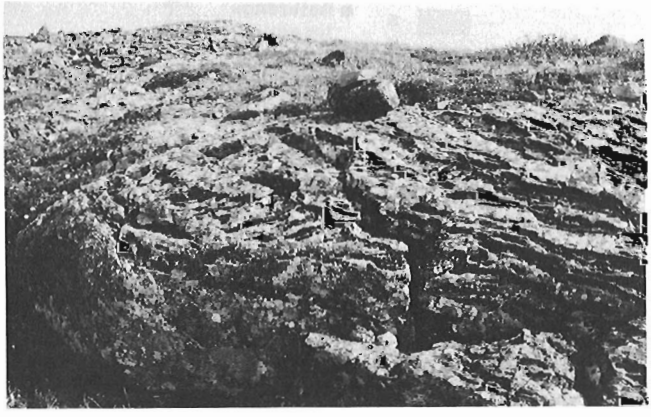

Figure 4. Small trough crossbed (arrow) migrating up planar-tabular crossbed foreset. Hammer is 35 cm long. GSC 205034-A.

The 72 m dividing tuffaceous section at the north end of the Thlewycho Lake rhyolite complex consists of parallel-bedded, finely laminated to medium-bedded white porcellanite (rhyolite), dark grey to green chloritized quartz phyric dacitic to ?andesitic tuff, heterolithic volcaniclastic rock (?lithic tuff or epiclastic rock), 1.5 m of thin-bedded couplets with porcellanite grading to shale and 3 m of black mudstone. The succession is interpreted as dominantly air-fall, fine rhyolitic ash.

These two successions represent a temporary cessation, between the main eruptions of the rhyolitic lava dome, during which a different magma source was tapped to erupt basalt lava into a shallow subaqueous environment in the south while frequent and probably minor explosions continued from a rhyolite centre to the north with the deposition of fine ash.

Rhyolites of the inner ring structure

A pause in the eruption of a rhyolite dome/flow of the inner ring (locality 5) fracture zone is recorded by a 50 m clastic section, from bottom to top as follows: 1) more than 13 m of massive, very poorly sorted, coarse rhyolite-block breccia and minor conglomerate, 2) 8 m of fine-laminated to thin-bedded trough-cross-bedded sand, and 3) 29 m of crudely thin- to thick-bedded rhyolite pebble to boulder conglomerate. The well-rounded clasts in the conglomerate and the sedimentary structures in sandy units are dramatically accentuated by selective carbonate replacement of the conglomerate matrix.

This section of crossbedded rhyolite sands and well rounded pebble/boulder conglomerate are interpreted as a paleo beach deposit marking the shoreline of an emergent portion of the dome.

Facies of the Gold Lake dome/flow complex

The Gold Lake felsic dome/flow complex (Fig. 6) is a large (1.5 km by 8 km) body comprising rhyolitic to dacitic domes, lavas and related clastic aprons that represent ring-fracture volcanism during one of the last stages of eruption along the southeast flanks of this volcano. This well exposed (80 % outcrop) southern part of the volcanic complex clearly records the diverse volcanic and sedimentary facies changes at a transition from subaerial to subaqueous environments.

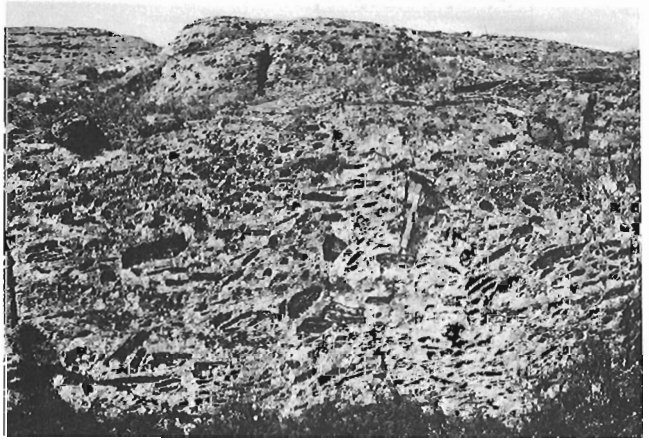

Figure 5. Intraclastic breccia unit 1.8 m thick containing clasts selectively replaced by carbonate (dark). Matrix is poorly sorted coarse volcarenite. GSC 205025-G.

Facies of the dome complex (Fig. 6b) from the massive interior through the marginal clastic aprons are 1) 'massive' rhyolite/ dacite (most of the body), 2) in situ breccia carapace, 3) aprons of coarse breccia and 4) carbonate-impregnated bedded, pebbly, poorly-sorted volcarenite with some primary carbonate percipitates indicated by local occurrence of ooliths and stromatolites.

This succession is overlain by bedded carbonate and iron-formation, of Sequence B, followed by turbidites of the Beechy Lake Group.

The western and southern parts of the complex overlies tuffs and breccias of unit 2(andesites).

The dome and its breccia aprons

'Massive' portions of the body comprise several lithological phases (aphanitic to porcellaneous rhyolite, abundantly quartz-feldspar phyric rhyolite, feldspar phyric grey dacite). These rocks are massive, flow-layered (rare), microcfactured felsites, with minor autoclastic breccia.

The term 'carapace breccia' is used to designate areas along margins and locally within the body where massive rhyolite grades from highly fractured felsite to 'in situ' breccia (tightly packed monolithologic angular to rounded blocks of rhyolite with intervening rhyolite breccia). These breccias are interpreted as flow breccia or carapace crumble breccia at the top and sides of domes.

Breccia aprons comprise dominantly monolithological rhyolite/ dacite derived from the dome complex and minor exotic fragments. Deposits are very poorly to moderately sorted with pervasive carbonate impregnation in the matrix.

Facies are different on the western (landward) sides of the complex than on the eastern (seaward) side (Fig. 6b). On the west sides of the dome the coarse breccias locally grade into scree breccia and carbonate occurs only as sporadic patches locally replacing matrix of some breccias — there is no wholesale carbonate impregnation of breccia. Some of these are flow breccias. Where flows thin out on hill tops above underlying tuffaceous and debris flow deposits, boundaries vary from sharp to gradational within 50 m. Along the eastern side of the dome, massive rhyolite or carapace breccia grade into a clastic apron generally comprising coarse rhyolite scree or landslide breccias, overlain by well bedded rhyolite sandstones, carbonates, and turbidites of the Beechy Lake Group. The breccia zones are intensely impregnated with carbonate, and locally contain bedded carbonate, the latter commonly oolitic and more rarely stomatolitic. Locally carbonate lies directly on massive rhyolite.

Near the north end of the complex, a 400 x 1500m, northwesterly elongate, breccia deposit (Unit 7, Fig. 6) overlies dacitic flows and flow breccias on its west side and

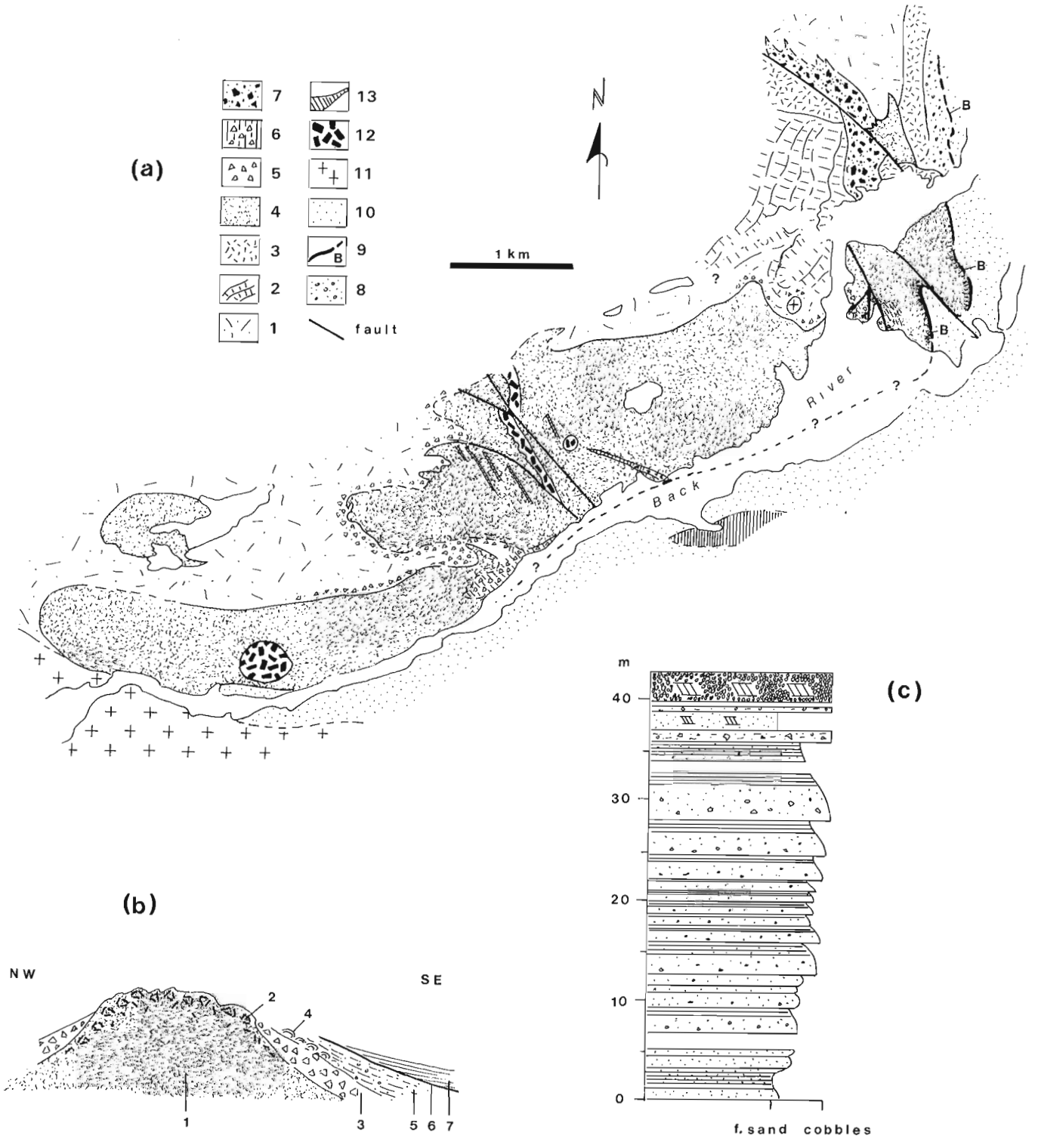

Figure 6. The Gold Lake dome/flow complex (a) Map — location shown in Figure 1, 1- volcaniclastic rocks and lavas, undifferentiated; 2 — andesite and dacite lavas; 3 — dacite; 4 — rhyolite/dacite dome; 5 — rhyolite breccia; 6 — carbonate impregnated felsic breccia; 7 — avalanche breccia; 8 — rhyolite pebble arenite to lutite; 9 — iron-formation of Sequence B; 10 — turbidites of the Beechy Lake Group; 11 — granodiorite; 12 — hornblendite; 13 — gabbro, diabase. (b) Generalized facies across the dome: 1 — massive rhyolite; 2 — crumble breccia; 3 — breccia apron; 4 — stromatolitic and oolitic carbonate; 5 — pebbly rhyolite volcarenite (fan delta); 6 — iron formation; 7 — turbidites of the Beechy Lake Group. (c) Stratigraphy of rhyolite fan delta — unit 5 of (b).

massive to brecciated rhyolite on its east side. This is a very thick massive unit comprising very poorly sorted, closely packed, intact angular to subrounded blocks up to 3 m across in a poorly sorted granule breccia matrix. Clasts have dominantly felsic (rhyolitic and dacitic) and minor mafic compositions. Lenses of volcarenite and rhyolite pebble and boulder conglomerate appear locally within the section.

Cliffs in a bay in Gold Lake, exposing a 30 m high section across the unit, show that the deposit occupies a steep sided valley between the lava succession to the west and the rhyolite to the east. The unit is interpreted as landslide or avalanche deposits, formed by partial collapse of parts of the dome complex. A thin rhyolite dyke, presumably related to the dome, cutting this deposit suggests that the breccia was deposited during development of the dome complex.

Volcaniclastic turbidites

A 40m section (Fig. 6c) of thin- to thick-bedded, graded, horizontally stratified, pebbly rhyolitic sandstone lies below the Yellowknife turbidites and above the bedded breccias and conglomerate along the west shore of the Back River above Gold Lake. The beds, which coarsen and thicken upward through the section, are interpreted as deposits from high-concentration turbidity flows (amalgamated a, a_2 a_3, b_2 turbidites of Cas, 1979). This section is overlain by moderately- to well-sorted crossbedded sandstone to rounded pebble and cobble conglomerate, with bimodal (north and west) paleocurrents suggesting current activity in a nearshore, shallow marine environment. Extensive carbonate replacement within the matrix of the conglomerates, and in-situ stromatolites in oolitic carbonates at the same stratigraphic level farther upriver support a shallow marine interpretation. The above facies probably represent a fan-delta, in which the stratified breccias and coarse grained turbidites comprise the subaerial and submarine components respectively.

Figure 7. Laterally linked domal stromatolites developed immediately above boulder breccia interpreted as a marginal marine fan-delta deposit. Pen is 14 cm long. Locality 2. GCS 205025.

CARBONATES

Carbonate occurs as replacement of primary features, notably in ring fracture zones (Lambert, 1978), in the matrix of breccias bordering domes, permeable parts of conglomerate, sandstone and tuffaceous sediment beds, fracture fillings, and remobilized carbonate in tectonic breccias. It is less common as primary chemical sediment in the form of interlayered carbonate in cherty iron formations and stratified carbonate locally containing ooliths and stromatolites.

Stromatolites of Sequence B were discovered in 5 separate localities (1 to 5 in Fig. 1, and may be present at locality 6.The co-ordinates are:

Locality	*Latitude*	*Longitude*
1	64°45′08″N	107°49′47″W
2	64°44′57″N	107°50′45″W
3	65°02′10″N	108°01′15″W
4	65°03′15″N	108°06′25″W
5	65°02′00″N	108°14′30″W
6	64°45′00″N	107°46′40″W

Localities 1 and 2 are exposed in steep sloping outcrops at the water's edge on the west side of the Back River. Stomatolites are laterally linked domes, 15-20 cm in diameter (Fig. 6) that occur in situ in oolitic carbonate lenses (or?beds), at least 40 cm thick, overlying carbonate impregnated breccia. At locality 1 the stomatolites have grown over irregular surfaces of blocks in carbonate impregnated breccia. Laterally-linked domes 10 cm in section at locality 3 (Fig. 8) are found in poorly exposed frost-heaved outcrop. Locality 4 exposes stratiform cryptalgalaminate (Fig. 9) that occur in beds at least 2 m thick that are exposed for at least 200 m along strike. Locality 5 contains laminated and bun-shapes (Fig. 10). All localities lie near the base of Sequence

Figure 8. Laterally linked domal stromatolites, Locality 3. GSC 205027-P.

B, the boundary between late stage (ca. 2692 Ma; van Breemen et al., 1987; Lambert and Henderson, 1980) rhyolite dome complexes and overlying turbiditic sedimentary rocks of the Beechy Lake Group. It is likely that several other localities along this horizon, where carbonate is laminated and oolitic (e.g. locality 6), also contain stromatolites.

These localities represent the second discovery of stromatolites of Archean age in the Slave Province (see Henderson, 1975).

IRON-BEARING SEDIMENTARY SEQUENCES

Jefferson et al.(1989) described three lithologically and stratigraphically distinct iron-rich chemical sedimentary sequences that punctuate sedimentary and volcanic strata in the eastern part of the Back River complex. Field work in the summer of 1989 confirmed the sequences throughout the complex and extended them to the west (Fig. 1).

We have documented lateral as well as vertical facies changes in each of the sequences. Walhter's Law is applied to the second sequence, in that the vertical sequence is also a lateral sequence. This application is limited to the maximum 100 m of iron-rich sedimentary rocks within the sequence, in that the underlying volcanic rocks are never seen to interdigitate with the iron-rich strata.

The three sequences,labelled A, B and C, (Fig. 1,2) record chemical sedimentary events at times of volcanic quiescence. The iron-rich strata constitute stratigraphic and structural markers which, combined with geophysical data, have proven indispensable for tracing complex fold geometries (e.g. Fig. 11).

A: Ferruginous sedimentary rocks within the volcanic pile

Sequence A refers to the thickest of several thin sedimentary units which mark temporary cessation of volcanism and partial reworking of volcanic protoliths. This outward dipping sequence has been traced around 4/5 of the inner ring structure with the poorly exposed northeast corner being the only exception. It is lithologically diverse, containing calcite-cemented volcanic breccia to gritty limestone, magnetitic chert, graded volcaniclastic rocks and slate, all of which are variably sulphidic and iron-rich.

Figure 9. Cryptalgalaminate, Locality 4. Pencil is 8mm thick. GSC 205025-B, 2052025-D (right photo).

Facies changes in this sequence are more dramatic than those of the other two sequences. The initial section described by Jefferson et al. (1989) at reference locality 1 contains no carbonate rock or slate. At locality 2, Sequence A includes the sulphidic chert, sulphidic breccia and graded sulphidic epiclastic rocks of the initial section, as well as a thick underlying zone of calcite impregnated breccia, conglomerate and grit.

The section of Sequence A, south of Rusty Lake (locality 6), closely resembles Sequence B. Here, carbonate-impregnated heterolithic, granule to pebble conglomerate overlies felsic volcanic rocks and is overlain in sequence by pyritic slate, chert-rich iron-formation (magnetite, carbonate and pyrite), and locally derived turbidites. The pyritic slate contains pyrite nodules like those in the slates of Sequence B at 'Pyrite Ball Bay'.

No significant gold occurrences are known from Sequence A, although it is extensively covered by mineral claims.

B. Ferruginous sedimentary rocks between the volcanic pile and overlying greywacke-turbidites

Sequence B separates continuous volcanic rocks from overlying turbidite-dominated strata. Lean cherty iron-formation (IF) characterizes Sequence B which, from bottom to top, includes: 1) locally oolitic or stromatolitic dolomite to siderite breccia and grit, 2) magnetite-, sulphide- and siderite-chert iron formation, 3) a middle semi-continuous clastic marker unit (greywacke, slate or sulphidic heterolithic breccia) 4) sulphide-chert iron-formation, and 5) carbonaceous slate which grades upward into turbidites. Previously described stratabound, grey, sulphidic quartz veins (Jefferson et al., 1989) are the most auriferous rocks in Sequence B.

Figure 10. Bun-shaped stromatolite, Locality 5. GSC 205027-L.

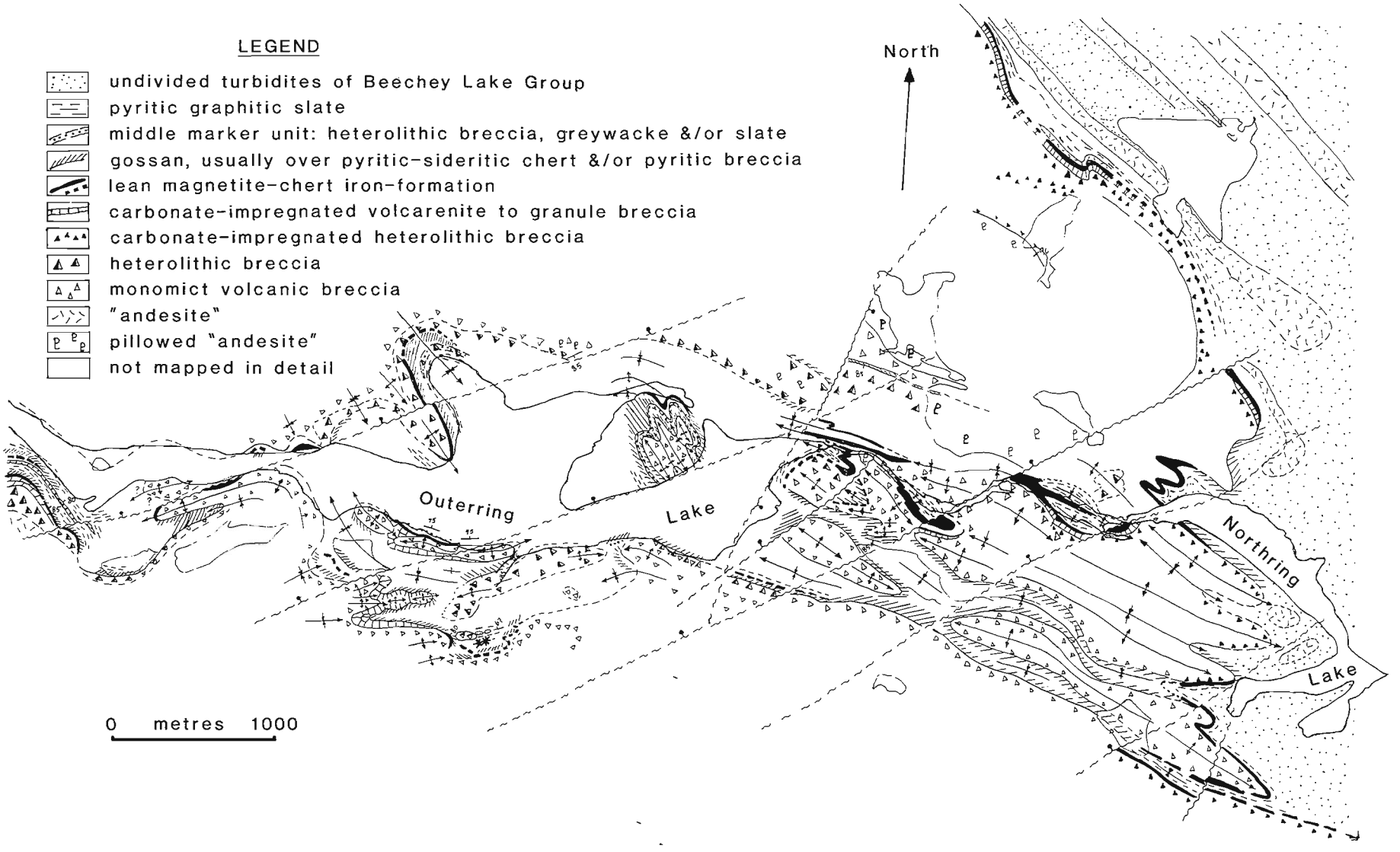

Figure 11. Sketch map of Sequence B facies changes and complex folds in the Outerring Lake area (location in Fig. 1).

Local changes in thickness and facies of carbonates iron-formations and the middle clastic marker suggest changes in both paleotopography and paleoenvironment. Figure 11 illustrates these lateral facies changes together with structural complexity in the Outerring Lake area.

C. Ferruginous sedimentary rocks within the greywacke-turbidites

Sequence C is hosted by turbidites mainly in northern parts of the area. In map pattern (defined largely by aeromagnetic and electromagnetic data, because of poor outcrop) it appears to be laterally adjacent to rhyolite units within the turbidites, particularly in the northwest, although it is not possible to trace units continuously from iron-formation into any particular volcanic unit. Iron-formation of this sequence occurs within 10 to 100 m (stratigraphic distance) of tuff or volcaniclastic sedimentary beds.

The appearance of the iron-formation varies markedly from place to place, as metamorphic grade in this northern part of the area ranges from lower greenschist facies in the east to upper amphibolite facies in the west (near Esker Lake).

Sequence C comprises 1) basal and capping graphitic slate, 2) extensive argillitic to cherty magnetite iron-formation (Fig. 12) with intense magnetic signature, 3) local sulphide — silicate iron-formation with subdued magnetic expression and moderate to weak conductivity, 4) chert nodules, and 5) cross-cutting, white quartz veins. Although quartz veins also occur in adjacent rocks, their association with sulphide, garnet, amphibole and chlorite alteration, and with gold and arsenic, is limited to the iron-formation strata.

Lateral facies changes in Sequence C take place over distances of kilometres. For example, Sirius Energy Corporation Ltd. and partners (information used with permission) have traced continuously (around a large syncline) an iron-formation that varies from magnetite-chert iron-formation within felsic tuff on the northern side of Esker Lake to silicate iron-formation (hornblende-garnet-pyrrhotite rock with no magnetite) that contains meta-chert nodules (Fig. 13) on the south side.

Gold in iron-formation has been sought in the Slave Province mainly in turbidite settings (Padgham, 1986). This study suggests that Sequence C is in the same facies association as the Lupin iron-formation (King et al., 1989) and that both lateral and vertical primary facies changes are present. Radiometric dating (in progress) may determine whether they are the same age.

YELLOWKNIFE SUPERGROUP TURBIDITES

Paleocurrent data

Sparse paleocurrent data from Beechy Lake Group turbidites immediately adjacent to the east, west and south sides of the Complex (Thwelycho, Jim Magrum, and Gold lakes, respectively) indicate paleoflow radially away from the complex with a significant component perpendicular to these directions along the margins of the complex. In Gold Lake the turbidites can be subdivided into six facies: 1. Thin-bedded, bottom- to mid-cutout "distal" turbidites; 2. Medium- to thick-bedded T_{ae} to (rarely) T_{abcde} turbidites; 3. Thickly bedded, amalgamated, crossbedded medium to coarse sandstone; 4. Thick to very thick mudshale and very thin to thick-bedded muddy turbidites; 5. Medium to very thick beds of brecciated (slumped) turbidites; 6. Tidally-reworked very thin sand/mud couplets. Paleocurrent data from flutes (Fig. 14), ripples, and crossbeds suggest that the thick and amalgamated turbidites were deposited within submarine fan channels, directed away from the complex, and that the thinner turbidites, mudshale, and muddy turbidites are overbank and levee deposits. The relative abundance of slump breccias may be attributed to 1. Failure of levee slopes; 2. steep slopes on juvenile volcaniclastic fans; 3. frequent seismic activity. The tidally-reworked (herringbone) facies, which occur just above the amalgamated coarse sands, may represent the activity of reversing tidal currents in a submarine canyon.

Figure 12. Banded iron-formation north of Boucher Lake, Locality 8, Figure 1. GSC 205027-O.

Figure 13. Chert nodules in garnet-hornblende iron-formation, cut by tensional quartz veins on south shore of Esker Lake. Knife is 8 cm long. GSC 205027-E.

Volcaniclastic deposits in turbidites

Dancing Goose volcanic turbidites

A 300 m-thick section through volcaniclastic turbidites is exposed at 'Dancing Goose Lake '(local name). The section (Fig. 15; locality 7, Fig 1) comprises ten thinning- and fining-upward cycles, from 5 to 32 m thick, averaging 19 m thick. The coarsest (basal) beds of the cycles vary from very coarse sand to small rhyolite pebble conglomerate. The beds in the lower 50-100 % of the cycles are amalgamated; mudshale clasts are present in the basal part of three of the cycles. The entire 10-cycle package is overlain and underlain by thin-bedded mud-rich turbidites to mudshale. Sole marks and ripples indicate northerly paleoflow. Such thinning- and fining-upward cycles in turbidites have been attributed to the repeated gradual abandonment of distributary channels in a mid-fan environment (Walker and Mutti, 1973; and Walker, 1970). This unit represents a rhyolitic epiclastic fan within the Beechy Lake turbidites derived from a felsic portion of the volcanic pile.

Ash in turbidites

Volcanic ash interbedded with the turbidites establishes a temporal link between volcanism and deposition of the Beechy Lake turbidites in this area.

Ash beds are common in the sediments in the northwest corner of the area. Northeast of Keish Lake (locality 9) three units of crystal rich tuff, interbedded with the turbidites, have crystal content similar to the nearby rhyolite/dacite dome. These volaniclastic deposits have ubiquitous flame structures at the bases suggesting that they may have been emplaced as subaqueous mass flow (possibly pyroclastic flows). The Beechy Lake turbidites in this area are mud-rich.

A very thick bed of massive, ungraded, moderately sorted crystal tuff occurs within thin- to medium-bedded Beechy Lake turbidites on an island in Gold Lake. The rock comprises 35 % euhedral, blocky feldspar crystals and crystal fragments and minor quartz crystals in a grey aphanitic matrix. Crystal content of this rock is similar to an abundantly porphyritic phase of the Gold Lake rhyolite/dacite dome 2 km to the west.

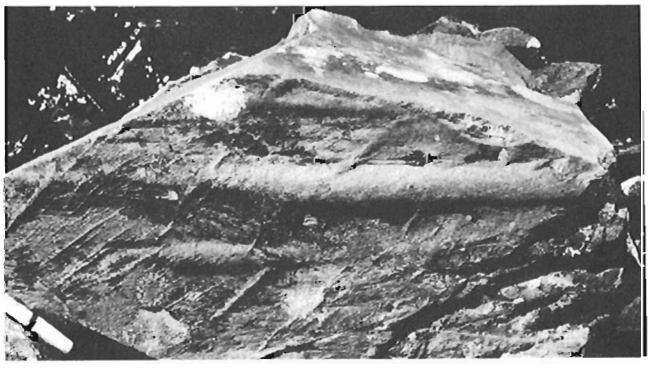

Figure 14. Spindle flutes on sole of a medium bedded turbidite. Gold Lake. Pen is 1 cm wide. GSC 205025-C.

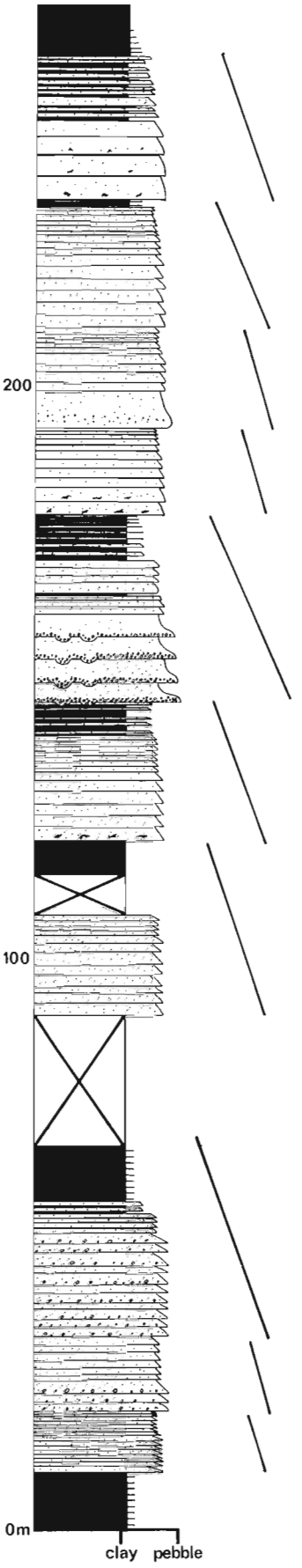

Figure 15. Stratigraphic section through rhyolite turbidites near 'Dancing Goose' Lake. Inclined lines to the right of figure indicate fining upward cycles.

DEFORMATION

Four generations of structures (three penetrative events followed by a fourth weakly developed local event), showing considerable overlap in style, deform sedimentary and volcanic rocks of the Back River area. Most structural analysis is from within the metaturbidite package and extrapolated into the volcanic complex.

The oldest structures (D_1) are tight to isoclinal folds (F_1) and associated slaty cleavage (S_1). Generally these folds are intrafolial but can occur at all scales. The Eastring Lake synform (E, Fig. 1) is an example of a kilometre scale F_1/F_2 interference structure. Doubly plunging intrafolial F_1 folds (Fig. 16) suggest that D1 is noncylindrical. Most commonly, F_1 folds are recognized by reversals in facing direction of metaturbidite sequences. S_1 slaty cleavage is

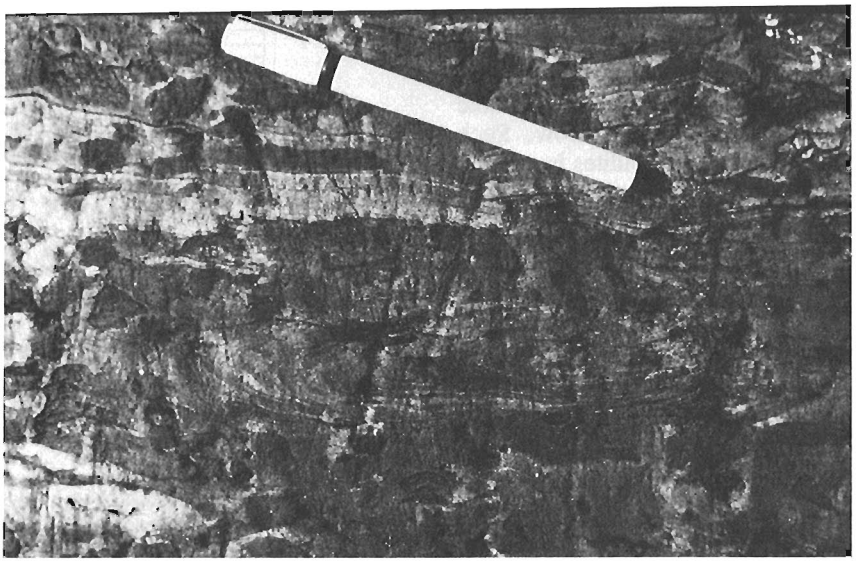

Figure 16. Intrafolial F_1 sheath fold in turbidites southeast of Jim Magrum Lake. S_2(not visible) parallels pen.

Figure 17. Tight F_2 fold refolded by F_3. Pen parallel S_3 (Gold Lake).

only developed locally and overlaps in style with S_2 cleavages.

Second generation of structures (D_2) are tight to isoclinal folds (Fig. 17) occurring at all scales. They plunge moderate to steeply, but adjacent to the east side of the volcanic complex, are highly asymmetrical and plunge steeply (varying through vertical) parallel to the boundary. This local noncylindrical behaviour is most easily explained by high strain along the volcanic-sedimentary contact.

Axial plane slaty cleavage (S2) is ubiquitous but may change morphology abruptly to a well developed crenulation cleavage, with a good crenulation lineation on S_0, in areas where S_1 is developed. The overlap in style between D_1 and D_2 folding and cleavage development makes identification of fold generations problematic especially within the volcanic complex where generally folds are rare and cleavage development is poor.

D_2 appears to be pre- to syn-peak metamorphic conditions. Metamorphic aureoles containing cordierite-biotite and cordierite-andalusite-staurolite-(biotite) surround granodiorite intrusions of the Regan Lake Intrusive Suite to the south of the volcanic complex. In these aureoles helicitic cordierite includes S_1/S_2 crenulation cleavages which subsequently have been rotated during D_3. This feature appears to be widespread in the central Slave (King et al., 1988, 1989; Relf. 1989).

S_2 is the regional cleavage (Jefferson et al., 1989). However, near the boundary of the volcanic complex, it parallels the contact between the volcanic rocks and the metaturbidites indicating that strain concentrated along this contact. This feature also explains the apparent noncylindrical nature of F_2 near the contact and suggests that the volcanic complex acted as a competent mass enclosed in a less competent turbiditic rocks. This competency contrast is also reflected in folding. Where the volcanics and turbidites are involved they form cuspate-lobate folds as demonstrated south of Gold Lake.

The youngest penetrative structures (D_3) are open (locally tight, Fig 18) folds and kinks (F3) and an associated crenulation cleavage. The S_3 cleavage varies from a fracture cleavage and weak intersection lineation in areas of poor fabric development to well developed differentiated crenulation cleavage and crenulation lineation in areas of abundant F_3 folding. Locally F_3 folding and cleavage completely transpose older structures. This feature combined with the fact that S_3 is generally present without folding creates a considerable style overlap with S_2. Fortunately, S_3 has a consistent west-northwest orientation in the western and southern areas of the complex and commonly transects F_2. The significance of this style overlap occurs in the volcanic complex where folding and multiple cleavages are rare. Unfortunately, it is tenuous to apply the notion of a regional cleavage in an area such as this where outcrop is discontinuous, usually intensely lichen covered and where the dominant rock type is massive and poorly foliated.

Near Gold Lake S_2 and S_3 commonly form a herring-bone cleavage interference pattern in well graded turbidites. Psammitic horizons preserve S_2 whereas pelitic horizons contain a well developed S_3 crenulation cleavage oriented at about 60° to S_2. In one outcrop herring-bone cleavage is folded by open kinks (F4) — the youngest structures in the Back River area (Fig. 19). These F_4 folds are poorly developed, lack penetrative cleavage and do not appear to represent a significant deformational event.

Macroscopic geometry of the southern portion of the volcanic complex can be explained by deformation of the margin of a major volcanic pile (primary dome) by D_2 and D_3. The northeastern, southeastern and southwestern 'corners of the complex are F_2 folds. In these areas F_2 minor folds verge toward the major hinges. The northwest corner (near Rusty Lake), however, may be a D_3 structure. F_2 folds in metasedimentary rocks west of Thleywcho Lake verge southwesterly. This is contrary to the vergence expected if the northwest corner was an F_2 structure. Hence this northwest corner is tentatively interpreted as a major F_3 fold.

Figure 18. Shallow plunging F3 folds south of Gold Lake.

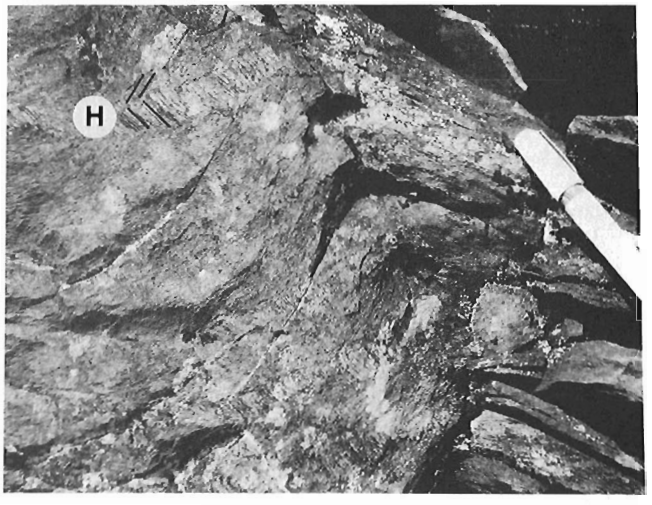

Figure 19. F4 fold east of Gold Lake. F_4 folds S_2/S_3 herringbone cleavage (H).

ARCHEOLOGICAL SITE — HEADWATERS OF THE BACK RIVER

An archeological site (locality 10) was found on a point providing a broad vista where Jim Magrum Lake drains into Back River. The find comprises lithic debitage, including flakes (up to 5 cm) of medium-grey to brownish-grey slate (mudshale), minor pale grey rhyolite, white vein quartz and cream chert having greasy lustre (a lithology not known locally), exposed on the surface of a frost boil (Fig. 20). This scenic location is on the east shore of Jim Magrum Lake (64°44'27''N, 108°00W), about 1 km northeast of the confluence of two major waterways: Contwoyto River and Back River.

INTERPRETIVE SUMMARY

Throughout the history of this volcano volcanism was punctuated by periods of erosion with deposition of fluvial fans, and deposition of three iron-rich chemical sedimentary units. The mineral potential of these units is summarized in Figure 2.

Diverse processes that occurred penecontemporaneously during the final stages of volcanism include quiet effusion of andesitic and dacitic lavas, emplacement of rhyolite/dacite dome complex (multistage processes) explosive eruption and deposition of tuffs, partial destruction of the domes by explosion, gravity collapse and erosion to produce broad, thick clastic aprons that spanned the emergent volcanic pile and adjacent seas. During quiescent periods chemical sediments formed near the shores of shallow marginal seas.

Tuffs and radiating submarine volcarenite (rhyolitic) fans interbedded with turbiditic sediments surrounding the complex link the volcanism with deposition of the Beechy Lake Group.

Figure 20. Lithic debitage on frost boil at archeological site, Jim Magrum Lake. GSC 205034.

Four folding events (D_2 to D_4 deform the complex. Second generation folds associated with pre- to syn- peak metamorphism dominate regional structure. The volcanic complex was a competent mass enclosed by less competent turbidites: strain concentrated along the contact. The macroscopic geometry of the southern portion of the complex is explained by deformation of the margin of the volcanic pile (a primary dome) by D_2 and D_3.

There is no evidence for a major structural break at the boundary between the volcanic pile and sedimentary rocks of the surrounding Beechy Lake Group.

ACKNOWLEDGMENTS

We thank Paul Williams and C.van Stall (G.S.C.) for guidance in unravelling structural problems, Brian Bluck for discussions and insight into stratigraphic interpretations and Frank Dudas for assistance in the field and Rod Stone for efficient expediting. Jim Mortensen helped in selecting and collecting samples for geochronology. Polar Continental Shelf Project provided 10 hours of helicopter time to CWJ. Friendly hospitality, logistic support and unpublished information were provided to CWJ by the Esker Lake Joint Venture (includes Sirius Energy Corporation Ltd., Argus Resources Ltd. and Equity Silver Mines Ltd.). Robert Baragar is thanked for critical reading of the manuscript.

REFERENCES

Cas, R.
1979: Mass-flow arenite from a Paleozoic interarc basin, New South Wales, Australia: Mode and environment of emplacement; Journal of Sedimentary Petrology, v. 49/1, p. 29-44.

Frith, R.A.
1987: Precambrian geology of the Hackett River area, District of Mackenzie, N.W.T.; Geological Survey of Canada, Memoir 417, 61 p.

Frith, R.A. and Percival, J.A.
1978: Stratigraphy of the Yellowknife Supergroup in the Mara-Back Rivers area, District of Mackenzie; *in* Current Research, Part C, Geological Survey of Canada, Paper 78-1C, p. 89-98.

Henderson, J.B.
1975: Archean stromatolites in the northern Slave Province, Northwest Territories, Canada; Canadian Journal of Earth Sciences, v. 12, p. 1619-1630.

Hill, J.D. and Frith, R.A.
1982: Petrology of the Regan Intrusive Suite, in the Nose Lake-Beechy Lake map-area, District of Mackenzie, N.W.T.; Geological Survey of Canada, Paper 82-8.

Jefferson, C.W., Beaumont-Smith, C.J. and Lustwerk, R.L.
1989: Stratigraphy and structural setting of iron-formations and gold in the Back River area, District of Mackenzie, N.W.T.; *in* Current Research, Part C, Geological Survey of Canada, Paper 89-1C, p. 293-304.

King, J.E., Davis, W.J., Relf, C. and Avery, R.W.
1988: Deformation and plutonism in the western Contwoyto Lake map area, central Slave Province, District of Mackenzie, N.W.T.; *in* Current Research, Part C, Geological Survey of Canada, Paper 88-1C, p. 161-176.

King, J.E., Davis, W.J., Van Nostrand, T. and Relf, C.
1989: Archean to Proterozoic deformation and plutonism of the western Contwoyto Lake map area, central Slave Province, District of Mackenzie, N.W.T.; *in* Current Research, Part C, Geological Survey of Canada, Paper 89-1C, p. 81-94.

Lambert, M.B.
1976: The Back River Volcanic Complex, District of Mackenzie; *in* Report of Activities, Part A, Geological Survey of Canada, Paper 76-1A, p. 363-367.
1977: The southwestern margin of the Back River Volcanic Complex; *in* Report of Activities, Part A, Geological Survey of Canada, Paper 77-1A, p. 153-158.
1978: The Back River Complex — a cauldron subsidence structure of Archean age; *in* Report of Activities, Part A, Geological Survey of Canada, Paper 78-1A, p. 153-158.
1982a: Felsic domes and flank deposits of the Back River volcanic complex, District of Mackenzie; *in* Current Research, Part A, Geological Survey of Canada, Paper 82-1A, p. 159-164.
1982b: The Back River Volcanic Complex, District of Mackenzie, N.W.T.; Geological Survey of Canada, Open File 848, 1:50 000 scale map.

Lambert, M.B. and Henderson, J.B.
1980: A uranium-lead age of zircons from volcanics and sediments of the Back River volcanic complex, eastern Slave Province, District of Mackenzie; *in* W.D. Loveridge, Rubidium-Strontium and Uranium-Lead Isotopic Age Studies, Report 3; *in* Current Research, Part C, Geological Survey of Canada, Paper 80-1C, p. 239-242.

Moore, D.W.
1977: Geology and geochemistry of a gold-bearing iron-formation and associated rocks, Back River, Northwest Territories; MSc. thesis, University of Toronto, 186 p.

Padgham, W.A.
1986: Turbidite-hosted gold-quartz veins in the Slave Structural Province, NWT; *in* Turbidite-hosted gold deposits, ed. J. Duncan Keepie, R.W. Boyle, and J.S. Haynes, Geological Association of Canada, Special paper 32, p. 119-134.

Relf, C.
1989: Archean deformation of the Contwoyto Formation metasediments, western Contwoyto Lake area, Northwest Territories; *in* Current Research, Part C, Geological Survey of Canada, Paper 89-1C, p. 95-105.

van Breemen, O., Henderson, J.B., Sullivan, R.W. and Thompson, P.H.
1987: U-Pb, zircon and monazite ages from the eastern Slave Province, Healey Lake area, N.W.T.; *in* Radiogenic Age and Isotopic Studies: Report 1, Geological Survey of Canada, Paper 87-2, p. 101-110.

Walker, R.G.
1970: Review of the geometry and facies organization of turbidites and turbidite-bearing basins; *in* J. Lajoie, (ed.) Flysch Sedimentology in North America; Geological Association of Canada, Special Paper 7, p. 219-251.

Walker, R.G. and Mutti, E.
1973: Turbidite facies and facies associations; in Turbidites and Deep-Water Sedimentation, ed. G.V. Middleton and A.H. Bouma; Society for Economic Paleontologists and Mineralogists, Short Course, Anaheim California, p. 119-158.

The medial zone of Wopmay orogen, District of Mackenzie

R.S. Hildebrand, S.A. Bowring[1], and T. Housh[1]
Continental Geoscience Division

Hildebrand, R.S., Bowring, S.A., and Housh, T., The medial zone of Wopmay orogen, District of Mackenzie; in Current Research, Part C, Geological Survey of Canada, Paper 90-1C, p. 167-176, 1990.

Abstract

The "Wopmay fault zone", which bisects Wopmay orogen, contains a spectrum of rock types, formed and deformed at different times, and juxtaposed along faults, intrusive contacts and unconformities; however, the structure is dominated by northerly-striking folds formed about 1.84 Ga. Therefore, we propose to rename the zone the medial zone of Wopmay orogen, No exposures of Slave craton are known west of the zone nor is it likely that Slave craton exists in the subsurface. A large klippe of Hottah terrane occurs east of the medial zone, where it occupies a substantial portion of the internal zone of Wopmay orogen. Major unresolved questions include the extent of Hottah terrane within the internal zone, the nature of the Hottah-Akaitcho contact, and the origin of cross-folding of the medial zone.

Résumé

La « zone de failles de Wopmay » qui découpe en deux parties égales l'orogène de Wopmay, contient divers types de roches, formées et déformées à différentes époques et juxtaposées le long de failles, de contacts intrusifs et de discordances; cependant, la structure est surtout caractérisée par des plis à direction nord datant de 1,84 Ga environ. Par conséquent, une redésignation de cette zone par zone médiane de l'orogène de Wopmay est proposée. Il n'existe aucun affleurement connu du craton des Esclaves à l'ouest de la zone, lequel ne serait pas non plus présent dans le sous-sol. Une grande klippe du terrane de Hottah se trouve à l'est de la zone médiane où elle occupe une partie importante de la zone interne de l'orogène de Wopmay. Parmi les principales questions non résolues, mentionnons l'étendue du terrane de Hottah au sein de la zone interne, la nature du contact Hottah-Akaitcho et l'origine du plissement transversal de la zone médiane.

[1] *Department of Earth and Planetary Sciences, Washington University, St. Louis. Mo. 63130, U.S.A.*

INTRODUCTION

During the summer of 1989 six weeks were spent in the field mapping rocks in the Calder River (86F) map area. The map area includes: (1) Archean gneisses and granitoid rocks of the Slave province; (2) rocks of Hottah terrane, interpreted as an exotic terrane that collided with the western margin of the Slave craton during the Calderian orogeny (Hildebrand et. al., 1983); (3) rocks of Akaitcho Group, interpreted as a rift succession deposited on the western margin of the Slave craton prior to the Calderian orogeny (Easton, 1980; Hoffman and Bowring, 1984); (4) plutons of the syn-collisional Hepburn batholith (Lalonde, 1986); and (5) rocks of the Great Bear batholith, a post-collisional magmatic arc (Hildebrand et. al., 1986). Previous investigations within the Calder River area are listed in Hildebrand et al. (1987). The major aims of the project are to unravel the geological evolution of the central Great Bear magmatic zone; the "Wopmay fault zone" and the western part of the internal zone of Wopmay orogen. The purpose of this report is to summarize some of the geological results of the summer's field work, with particular emphasis on the "Wopmay fault zone"; report preliminary geochronological results; and to explore some of their implications for Wopmay orogen.

WOPMAY FAULT ZONE

Background

The major linear that bisects Wopmay orogen, and separates the Great Bear magmatic zone from the internal zone, has long been considered to be a major fault termed the Wopmay River fault (Fraser et. al., 1972; Hoffman, 1973; McGlynn, 1975). Work done in the north during the 1970s led to the idea that the fault was a normal or oblique-slip fault active during Great Bear magmatism, but overstepped during later sedimentation (Hoffman et al., 1976; Hoffman and McGlynn, 1977). Easton (1981) coined the term Wopmay fault zone to refer to a zone of northerly-striking mylonites and faults of unknown age. He considered the westernmost fault of the zone as the boundary between the Great Bear and internal zones and coined the name, Grant subgroup, for a package of volcanic and sedimentary rocks of different metamorphic grades that occurs within the fault zone. St-Onge et al. (1982; 1983; 1984) also considered the internal zone-Great Bear boundary to be a fault and argued that the mylonitic rocks of the zone, and northwesterly-oriented folds in the Hepburn metamorphic-plutonic zone, were formed by dextral transpression during the Calderian orogeny. Subsequent normal faulting juxtaposed various blocks during uplift and erosion of the internal zone. Hoffman (1984b) argued that the Wopmay fault zone marked the western limit of non-stretched Archean crust and that as such it behaved as a buttress during subsequent orogenic events.

During the course of the present study Hildebrand and Bowring (1988) demonstrated that within the Calder River map area the boundary between the Great Bear and internal zone is an unconformity, similar to relations in the north (Hoffman and McGlynn, 1977). Locally, small displacement west-side-down normal faults appear to have been active during the early stages of Great Bear magmatism as evidenced by sedimentary facies and sequences within the Dumas Group (Hildebrand and Bowring, 1988). They also found that the northwesterly-striking folds within the Great Bear magmatic zone were progressively rotated into a northerly direction along the eastern margin of the zone. Furthermore, they argued that northwest-striking folds within the internal zone also rotated progressively into a northerly direction as one went westward and were generated by the same deformational episode as the Great Bear folds. This created a northerly-striking corridor dominated by tight, gently-plunging to horizontal, northerly-striking folds within a broad zone of northwesterly-oriented folds (see figures in Hildebrand and Bowring, 1988). The age of folding is about 1843 Ma as determined by U-Pb dating of zircons separated from folded volcanic rocks dated at 1844 $\pm$4 Ma and a granitic pluton, dated at 1843$\pm$5 Ma, which clearly postdates the folding (Bowring, 1984).

Redefinition and new name

Because there has been so much confusion within the literature as to what constitutes the Wopmay River fault or the "Wopmay fault zone", and because we now recognize that the zone is dominated by northerly-striking folds, not faults, it is proposed here to rename the corridor the *medial zone of Wopmay orogen*. The zone, which bisects the orogen, is located near the boundary between the Great Bear magmatic zone and the internal zone where northwesterly-striking folds of the internides and the Great Bear magmatic zone strike northerly. To the west, rocks of the medial zone are intruded by the youngest plutons of the Great Bear magmatic zone and to the east by plutons of the Bishop intrusive suite. In such areas the boundary of the medial zone is an intrusive contact and easily defined: elsewhere, it is gradational. Although the medial zone contains a wide spectrum of rock types, formed and deformed at different times and juxtaposed along faults, intrusive contacts and unconformities of different ages, when taken together they define a corridor of northerly-striking folds formed during a regional deformational episode that occurred about 1.843 Ga. Redefining the zone in this manner will allow future workers the freedom necessary to designate units, structures and events within the zone.

Geology and geochronology

Figure 1 is a mapped transect across the medial zone at the Wopmay River. It serves as an example of the geological map units of the medial zone and the complexity of their relations to one another. The units are described from east to west.

a.) The most easterly unit of the medial zone is a complex assemblage of orthogneisses, in part mylonitic (Fig. 2). Tonalitic, monzodioritic, and granitic layers dominate, although boudinaged mafic dykes and gneisses of possible volcanic parentage are common. The contact with rocks to the west is a fault that is concordant with fabric both above and below. Kinematic indicators suggest eastward top-over-bottom movement.

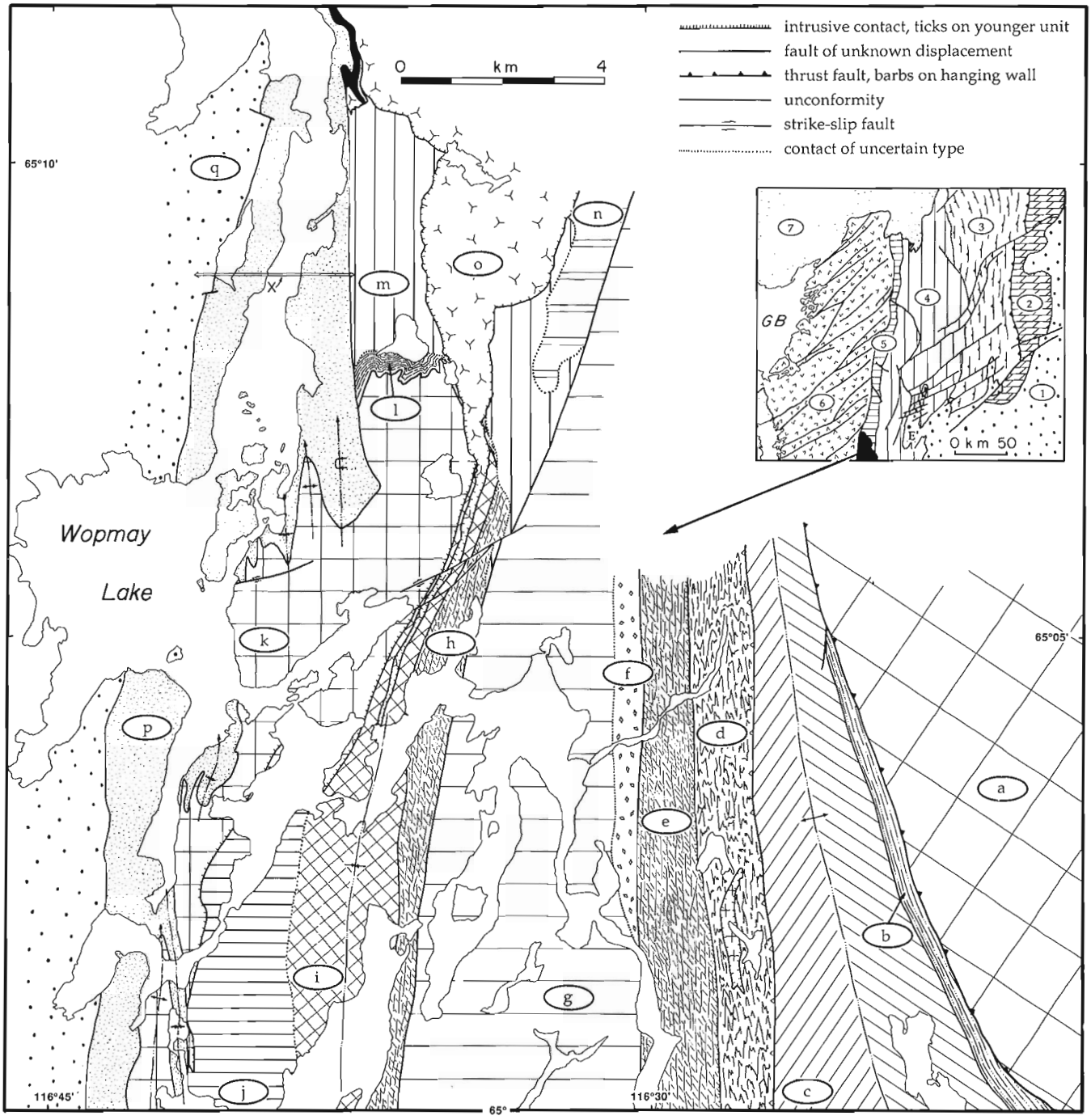

Figure 1. Geological sketch map showing distribution of lithological units within the medial zone at Wopmay Lake. Inset map shows location of main figure and major subdivisions of Wopmay orogen. 1 = Archean Slave craton; 2 = autochthonous strata of Wopmay orogen; 3 = Asiak thrust-fold belt (external zone); 4 = internal zone; 5 = medial zone; 6 = Great Bear magmatic zone; 7 = early Proterozoic and Paleozoic cover; E = Exmouth massif; GB = Great Bear Lake. a = Hottah orthogneiss; b = metasedimentary rocks; c = Archean mylonitic gneiss; d = migmatitic paragneiss; e = protomylonitic granite; f = muscovite-andalusite-garnet schist; g = low-grade sedimentary rocks, basalt and gabbro; h = protomylonitic granite; i = granitic and supracrustal gneisses; j = tonalitic and granitic gneiss; k = biotite granite, mylonite; l = siltstone, sandstone, carbonate; m = biotite-garnet-sillimanite gneiss; n = pillow basalt and gabbro; o = cpx-hornblende-biotite monzogranite; p = Dumas Group; q = foliated biotite granite; solid black areas = post-Dumas gabbro; X = line of section in Figure 12. The unconformity between rocks of the Dumas Group and unit o is exposed just east of the gabbro in the northern part of the figure.

A sample of unit a, an intimately-interlayered quartz monzodioritic and monzogranitic mylonitic gneiss (HWA-87Zr-21), was collected at 64° 59′ N, 116° 17′ W for U-Pb zircon geochronology. Preliminary results for four fractions are shown in Figure 3 and listed in Table 1. Two populations of zircon are present: light-brown, euhedral zircons and yellowish, subrounded zircons. Two fractions of light-brown euhedral zircons yield $^{207}Pb/^{206}Pb$ ages of 2.010 and 2.019 Ga and define a chord with an upper intercept of about 2.040 Ga. We interpret this as a preliminary estimate of the age of the quartz monzodioritic portion of the rock. Two fractions of subrounded yellow grains yield slightly younger $^{207}Pb/^{206}Pb$ ages of 1.991 and 1.995 Ga, which we infer were derived from the granitic material.

Based on these ages, gneisses of unit a are considered to be part of Hottah terrane, which has ages ranging from 1.914-2.278 Ga (Bowring, 1984). Based on the sense of movement and the fact that the Hottah rocks lie structurally above rocks of Slave craton, the fault is interpreted to be an eastward-vergent thrust fault. If correct, then rocks of unit a form a klippe in the internal zone. Reconnaissance done during the summer indicates that the western contact of the klippe may continue for over 100 km to the north. The eastern contact of the klippe remains unmapped and its relationship to rocks of the Akaitcho Group is unknown.

b.) Metasedimentary rocks dominate this unit, which sits unconformably upon unit c and is structurally overlain by unit a. The succession contains quartzites, garnet amphibolite and thinly-layered biotite-quartz-feldspar-garnet rocks. Rocks of this succession are folded about axial planes that dip easterly at 50°-70°, the same inclination as both the upper contact and the gneissic layering in the rocks of Hottah terrane. Additionally, the folds have an asymmetry compatible with an eastward vergence of the overlying thrust fault.

c.) This unit comprises annealed mylonitic gneisses derived mostly from plutonic rocks. The gneisses are lithologically heterogeneous at outcrop scale (Fig. 4) and comprise dominantly granitic, tonalitic, and amphibolitic layers. They are folded to form an anticline with steeply-dipping limbs (>50°) and a gentle northward plunge (0°-35°). To the southeast, the fold limbs shallow and the axial trace strikes northwest. Mineral lineations are gently-plunging and coaxial with the fold axis.

Figure 2. Typical mylonitic gneisses of unit a, which is interpreted on the basis of geochronology to be part of Hottah terrane. Note the disrupted granitic veins which yield a younger age than the surrounding quartz monzodioritic layers. GSC 205000-C.

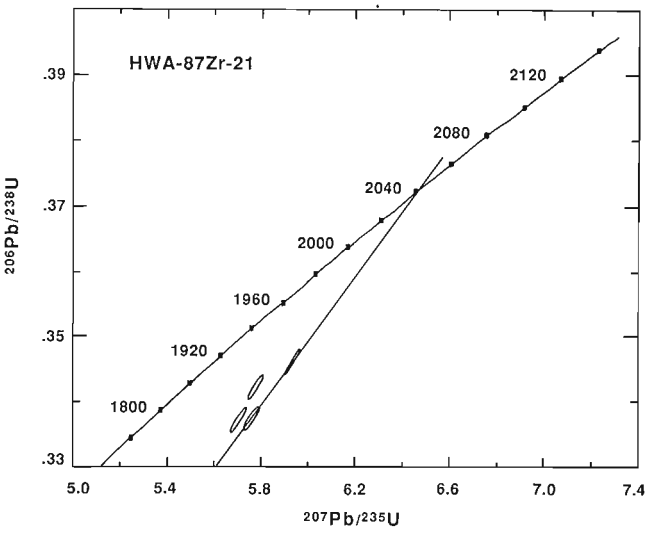

Figure 3. Concordia diagram showing U-Pb isotopic data for sample collected from unit a (HWA-87Zr-21).

Table 1. Isotopic data

Zircon fractions			Concentrations		Measured	Atomic ratios corrected for blank and common Pb				Age (Ga)
No.	*Properties*	*Weight (mg)*	*U (ppm.)*	*Pb (ppm.)*	$^{206}Pb/^{204}Pb$	$^{208}Pb/^{206}Pb$	$^{206}Pb/^{238}U$	$^{207}Pb/^{235}U$	$^{207}Pb/^{206}Pb$	$^{207}Pb/^{206}Pb$
					HWA-87Zr-21					
1	nm1	0.6905	701	258	5556	0.11502	0.34223	5.77548	0.12240	1.991
2	m2,eu,tan	0.2630	630	241	6141	0.14973	0.34621	5.93513	0.12433	2.019
3	m3,eu,tan	0.5045	566	210	4461	0.14168	0.33737	5.75521	0.12372	2.010
4	m4,yel,sbr	0.1867	724	260	11082	0.11171	0.33725	5.70342	0.12265	1.995
					HWA-89Zr-8					
5	nm2,B	0.8575	120	67	2067	0.09755	0.48730	13.5093	0.20106	2.834
6	nm2,eu	0.6661	242	132	3041	0.09205	0.48328	13.3213	0.19992	2.826
7	d-3	0.1260	253	138	15691	0.09454	0.48802	13.4892	0.20047	2.830
8	nm4	0.6434	146	77	1846	0.09028	0.46148	12.4908	0.19631	2.796

nm=nonmagnetic; m=magnetic; d=diamagnetic; number following refers to degrees of tilt on the Franz Isodynamic Separator; eu=euhedral; yel=yellow; sbr=subrounded

A sample of mylonitic syenogranite from unit c (HWA-89Zr-8) was collected at 64° 57′ N, 116° 18′ W for U-Pb zircon geochronology. Four fractions of light-brown euhedral zircons were analyzed and the results yield a discordant array (Fig. 5). $^{207}Pb/^{206}Pb$ ages of three fractions cluster together around 2.83 Ga and the other fraction has a $^{207}Pb/^{206}Pb$ age of about 2.8 Ga (Table 1). The upper intercept of a line regressed through the points is 2.925 ± 0.017 Ga.

d.) West of the Archean gneisses is a northerly-striking belt of recessively-weathering migmatitic paragneisses (Fig. 6) with a 70°-85° westward dipping fabric defined by cleavage and detached fold limbs. Their age is undetermined. They are intruded by variably-deformed, white-weathering, biotite granites, also of unknown age, that contain inclusions of granitic ultramylonite. The contact with the Archean gneisses is poorly-exposed but appears to be a concordant mylonite zone, 1-2 m thick. The granites, which are common within the paragneisses, are completely absent in rocks east of the contact. The occurrence of a mylonitic zone and the lack of the distinctive biotite granites in the Archean gneisses suggests that the contact is a fault.

Figure 4. Unit c showing heterogeneous character of the gneisses. Pen in top centre for scale. GSC 205000-A.

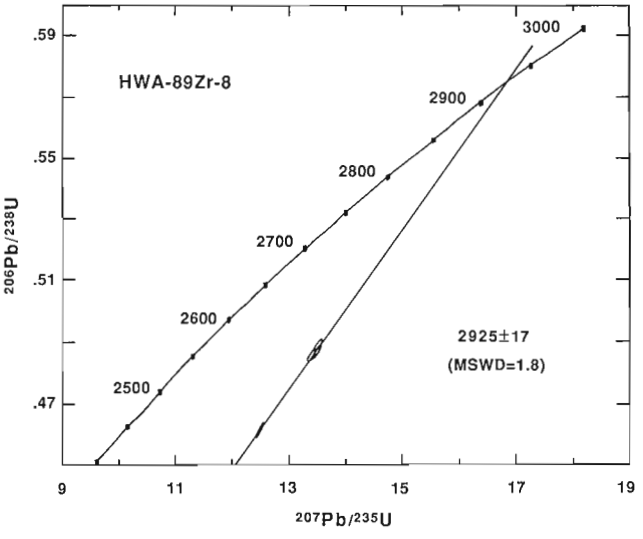

Figure 5. Concordia diagram showing U-Pb isotopic data for sample collected from unit c (HWA-89Zr-8).

e.) This unit is dominated by white-weathering, protomylonitic biotite granite (Fig. 7). Potassium feldspar phenocrysts range up to 10 cm across and sit in a medium- to coarse-grained groundmass of feldspars, quartz, and biotite. S-C fabrics are well-developed and there is typically a gently-plunging (0°-35°) mineral lineation. The granite contains enclaves, some to 8m, of sillimanite-garnet-biotite schist with local centimetre-thick layers of garnet. The porphyritic granite is intruded by variably-deformed medium-grained biotite granites similar to those intruding unit d paragneisses and, in many places, the contact between the granite of unit e and the paragneisses is obscured by the younger granites. Where the contact was observed the porphyritic granite contains abundant xenoliths of paragneiss.

f.) Juxtaposed against the porphyritic granite by a fault of unknown displacement is a westward-dipping belt of metapelites and psammites. Cleavage dips 75°-80° to the west; bedding typically dips 50°-60° to the west. Mineral lineations plunge less than 10° north or south. The age of the rocks is undetermined but they are part of a group of metasedimentary rocks, ranging continuously in metamorphic grade from muscovite-andalusite-garnet (Fig. 8) to above the production of granitic melts and muscovite breakdown, found within the medial zone for a strike length of

Figure 6. Typical appearance of sheared migmatitic paragneisses of unit d. Note the well-developed shear-bands in lower right. GSC 205000-J.

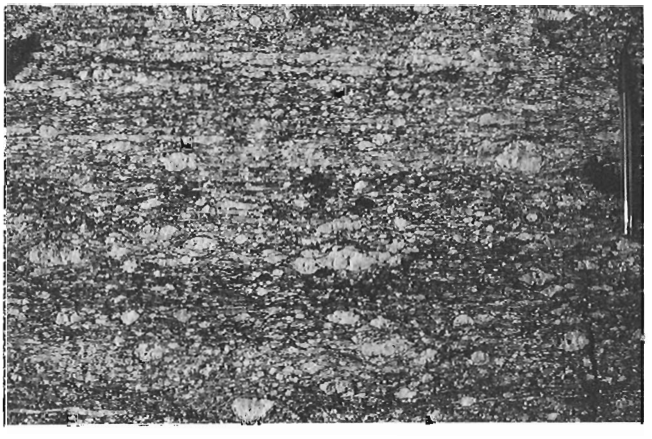

Figure 7. Protomylonitic granite characteristic of unit e. GSC 205000-V.

at least 100 km (Easton, 1981; St-Onge et. al., 1982; 1983; 1984). They are typically in contact with chlorite-grade sedimentary rocks, basalts and gabbros of unit g along a fault or unconformity. Easton (1981) included both the higher-grade rocks and the chlorite-grade rocks in the Grant subgroup. Here we prefer to avoid the term Grant subgroup because we are not certain that the low- and high-grade rocks are parts of the same stratigraphic package.

g.) West of unit f is a low-grade assemblage of rocks which Easton (1981) also included in the Grant sub-group. It is dominated by gabbroic sills that intrude a chlorite grade succession of quartz arenites, semipelites, dolomite-argillite rhythmites, cryptalgal dolomite, minor spherulitic rhyolite, and pillow basalts. The lowest part of the succession comprises siliciclastic sedimentary rocks, overlain by rhythmites (Fig. 9) and capped by cryptalgal dolomite. The upper part of the section is composed of pillow basalts but the contact between the basalts and sedimentary rocks was not observed due to the intrusion of numerous gabbroic sills. A rhyolite within the basalts yielded a U-Pb age of about 1.9 Ga (Bowring, 1984). The contact between units g and f was not exposed. The contact with units to the west was not observed by the authors but Easton (1981) found a 2-3 m-wide belt of ultramylonite.

Figure 8. Close-up of muscovite-garnet-andalusite schist (unit f) showing well-developed andalusite porphyroblasts. GSC 205000.

Figure 9. Carbonate-argillite rhythmites of unit g. Note the lack of penetrative fabric. Compare with Figure 11. GSC 205000-B.

h.) This unit is similar to unit e in that it is a white weathering, potassium feldspar porphyritic, biotite granite with a well developed s-c fabric and a sub-horizontal mineral lineation. It contains numerous enclaves of amphibolite and metasedimentary rocks, especially along its western margin where it intrudes a package of gneisses of supracrustal origin. Its age is undetermined but it appears to be basement to a low-grade sedimentary package discussed below (unit l).

i.) This unit is a heterogeneous assemblage of gneisses derived from sedimentary and volcanic protoliths. Common lithologies include quartzite, semipelite, garnet-plagioclase-biotite rocks considered to be meta-andesites, and a variety of siliceous lavas or hypabyssal porphyries. Granitoid intrusions cut the supracrustal rocks and, with a few exceptions, were deformed with them. The foliation defines a shallow northward-plunging synform with limbs that dip mostly between 60°-85°. Mineral lineations are also gently plunging. This unit, along with units h, j, and l, forms part of the basement upon which undated sedimentary rocks of unit l were deposited.

j.) Undated tonalitic and granitic gneiss containing boudinaged mafic dykes (Fig. 10) constitutes the bulk of this map unit. The unit has a well-developed gently-plunging mineral lineation and a steep, westward-dipping foliation. Its contact with unit i is possibly a fault. It is intruded on its western flank by granite of unit k.

k.) This map unit comprises variably-strained, pink weathering, biotite granite. It is mostly an l-s tectonite but in places there is no visible planar fabric, only a lineation. In some areas the rock is mylonitic. The granite is unconformably overlain by rocks of the Dumas Group and adjacent to the contact a well-developed weathered zone up to 10 m thick is developed. Numerous siliceous and intermediate composition porphyritic dykes, most varieties of which also cut the overlying Dumas Group, intrude the granite.

l.) This unit is a succession of low-grade sedimentary rocks, similar in lithology and metamorphic grade to unit g, that lies unconformably upon deformed granite of unit k but is itself unconformably overlain by rocks of the Dumas

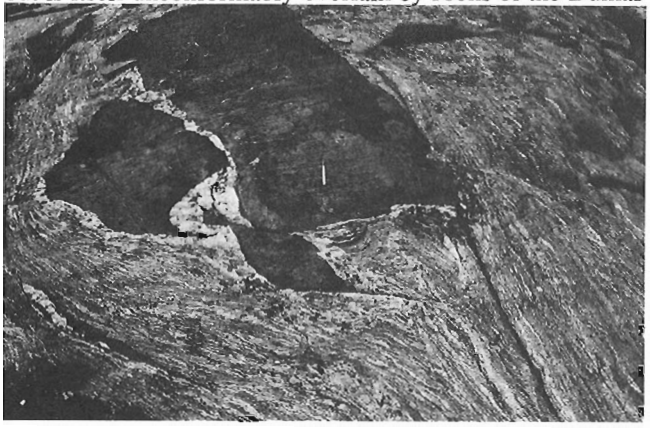

Figure 10. Typical appearance of unit j. Pen in lower part of large boundin for scale. GSC 205000-T.

Group (unit p). The lower 10-20 m are dominated by quartz arenite, arkose and siltstone, with minor intercalated beds of volcaniclastic sandstone. The siliciclastic sequence is overlain by several metres of finely-interbedded carbonate and argillite, which passes upward into 5-10 m of more massive, brown-weathering, cryptalgal dolomite. The section is structurally overlain by gneisses of unit m.

m.) This map unit comprises biotite-garnet-sillimanite gneisses of sedimentary origin. Layering is typically 1-3 cm thick and contorted (Fig. 11). Its contact with the low-grade sedimentary rocks of unit l occurs within a valley and is not exposed. However, it appears to structurally overlie that unit. The dramatic jump in metamorphic grade and the juxtaposition of high-over-low grade rocks suggests that the contact may be a thrust fault.

n.) This unit is mostly pillow basalt and gabbro metamorphosed under greenschist facies conditions except within a few metres of a large pluton (unit o) where it is metamorphosed to amphibolite. It is similar to the upper mafic part of unit g in that it comprises pillow basalts, gabbroic intrusions, and small amounts of rhyolite. Its relationship to the biotite-garnet-sillimanite gneisses (unit m) is unclear as the contact was not exposed. The top of the unit was not found.

o.) This unit, included as a member of the Bishop intrusive suite by Lalonde (1986), is a clinopyroxene-hornblende-biotite quartz monzonite-monzogranite pluton that intrudes units i, k, l, m, and n. Locally, there is a well-developed clinopyroxene-biotite-hornblende dioritic border phase. In general, the main body of rock is coarsely porphyritic with potassium feldspar phenocrysts to 4 cm. Biotite defines a foliation, especially adjacent to the intrusive contacts. The pluton is unconformably overlain by rocks of the Dumas Group (unit p) and is therefore older than 1:75 Ga.

p.) Rocks of this unit are part of the Dumas Group, which is the oldest group of rocks in the eastern Great Bear magmatic zone (Hildebrand et. al., 1986). In this area the group comprises laminated siltstone and sandstone, dolomite, siliceous ash-flow tuff, basaltic lavas, pebbly sandstone and conglomerate. U-Pb zircon geochronology indicates that an ash-flow tuff within the sequence was emplaced at 1.875 Ga (Hildebrand et. al., 1987). The supracrustal rocks are intruded by a variety of intermediate and siliceous porphyritic dykes. Rocks of the group unconformably overlie units j, k, l, m, n, o, and q. Similar rocks outcrop all along the eastern boundary of the Great Bear magmatic zone and, within most of the Calder River map area, occupy the core of an overturned syncline with an axis that plunges 0°-5° to either the north or south (Hildebrand and Bowring, 1988). At Wopmay Lake fold axes and mineral lineations plunge 35° to the north and deeper structural levels are seen. The plunge was utilized to construct the cross-section shown as Figure 12.

q.) This unit lies unconformably beneath the Dumas Group on the western side of an overturned syncline down the entire length of the Calder River map area (Hildebrand et. al., 1987; Hildebrand and Bowring, 1988). It comprises coarsely-porphyritic biotite granite dated at 1890±5 Ma (Hildebrand and Bowring, 1988). The rock is characterized by 2-6 cm potassium feldspar phenocrysts, anhedral quartz phenocrysts to 1 cm, and subhedral-euhedral plagioclase to 5 mm, in a matrix of quartz, feldspars, and biotite. Biotite defines a well-developed, steep (>75), westerly-dipping foliation, especially near the unconformity.

Figure 11. Typical contorted layering in biotite-garnet-sillimanite gneisses of unit m. Contrast the deformational style with Figure 9. GSC 205000-U.

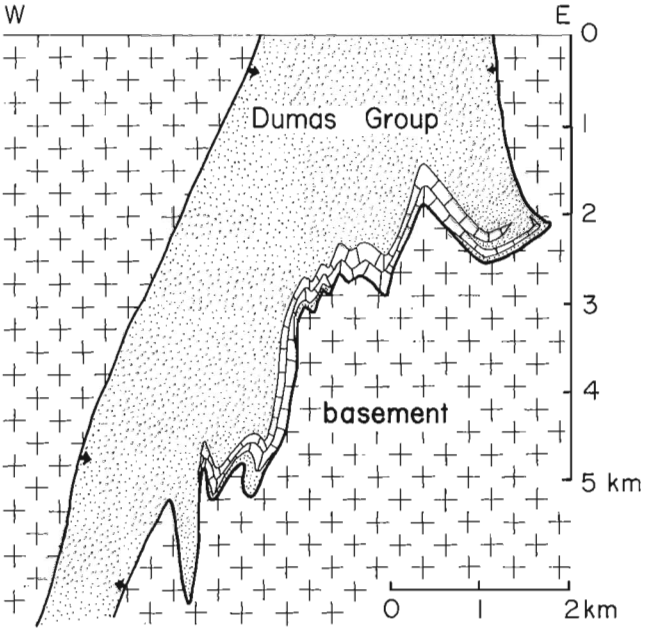

Figure 12. Down-plunge projection through the Dumas Group and its basement at Wopmay Lake showing style of folding. The overall structure is an overturned syncline with infolded rocks of the Dumas Group flanked by older rocks on both limbs. Basement on the west is unit q; on the east, units j, k, l, m, n, and o. Arrows indicate younging directions in Dumas Group. Note the overturned unconformities at the surface on both limbs of the syncline. Carbonate pattern = dolomite in lower Dumas Group. In places the dolomite sits directly on basement. The rheological difference between the basement and the carbonate could be responsible for the short wave length folds. Location is indicated in Figure 1.

CROSS FOLDING

For most of the length of the Calder River map area folds in the medial zone have horizontal, or very gently-plunging, axes. However, in the Wopmay Lake area most fold axes and mineral lineations plunge northward at about 35°. The northward plunge of linear elements in the area suggests that there is a deformational event which refolded the folds of the medial zone. As this region is directly west of a major westerly-striking cross-fold (Redrock culmination) that exposes Exmouth massif within the internal zone (Fig. 1 and see Hoffman et. al., 1988), it may be a continuation of that fold. However, Redrock culmination has been interpreted to be one of many east-northeast-trending folds (Tree River folds) that formed shortly after the Calderian orogeny but prior to magmatism of the Great Bear magmatic zone (St-Onge et. al., 1984; King, 1986; Hoffman et. al., 1988). The cross-folding that refolds rocks of the medial zone cannot predate rocks of the Great Bear magmatic zone as the folding involves those rocks. Conceivably, there were two distinct periods of cross-folding, but if the cross-folds in rocks of the medial zone were generated by the same event as that which generated Redrock culmination then there are two possibilities: (1) the Tree River folds postdate Great Bear magmatism; or (2) the Redrock culmination is not a Tree River fold. Additional work in the medial zone to the south should clarify this problem.

LINEATION WITHIN THE INTERNAL ZONE

The occurrence of the pervasive north-south oriented lineation that affects all rocks of the medial zone, including the Dumas Group, may have implications regarding interpretation of similar north-south mineral lineations of unknown origin within the western internal zone. Hoffman et al. (1988) suggested that the north-south oriented mineral lineations within the internal zone developed during the Calderian orogeny by strain partitioning. That is, the collision between Hottah terrane and Slave craton was oblique such that it had a strong strike-slip component (King, 1986). Whereas the kinematics of such a model are identical to those suggested by the event that generated the northwesterly and northerly-striking folds of the Great Bear magmatic zone, the medial zone, and the internal zone, it may be that some of the lineations within the internal zone were generated during the late folding event and not the Calderian orogeny. This is testable because lineations of Calderian age within the internides should be folded by the northwest-striking folds rather than coaxial with them.

DISCUSSION

Recent work by Bowring and Grotzinger (1989) and Bowring and Podosek (1989) suggests that in northern Wopmay orogen most of the Akaitcho Group is exotic with respect to Coronation margin and Slave craton. Additionally, they argued that magmas of the Akaitcho Group did not interact with Slave Craton but rather with Hottah terrane. The discovery last summer of a klippe of Hottah terrane within the internal zone, and the isotopic similarities of the Akaitcho Group to Hottah terrane, raise the question of whether or not rocks of the Akaitcho Group constitute a cover sequence on Hottah terrane. At present the eastward extent of the klippe and its contact with the Akaitcho Group remain unmapped so this question is not answerable; however, tectonic models proposed for Wopmay orogen hinge on its resolution.

SUMMARY OF THE MEDIAL ZONE

A summary of the major characteristics of the medial zone and their significance is listed below.

1. The fundamental structure of the medial zone is a group of shallowly-plunging, north-striking folds. Northwesterly-striking folds in both the Great Bear and internal zones tighten and trend progressively more northerly as the medial zone is approached until they strike northerly to define the zone (see Hildebrand and Bowring, 1988). Thus, the overall form of the fold system indicates that it formed as the result of dextral transpression. The age of folding is about 1.843 Ga as determined by U-Pb dates on zircons separated from granitic plutons and volcanic rocks in the Great Bear magmatic zone.

2. Most rocks within the medial zone, except for a few competent lithologies such as basalt and gabbro, have a well-developed mineral lineation that is coaxial with the folds. This suggests that the lineation formed contemporaneously with folding.

3. Numerous lithologies of various ages are exposed within the medial zone. They are separated by faults of unknown displacement, unconformities, thrust faults and contacts of unresolved type.

4. The contact between the Great Bear magmatic zone and the internides is nearly everywhere an unconformity, but minor west-side-down normal faults were active during sedimentation of the Dumas Group. Within the northern half of the orogen it is this unconformity, now rotated near vertical by folds of the medial zone, that forms the dominant photolinear, visible even from space (see McGlynn, 1981).

5. At first approximation the line forms a domain boundary between northeasterly-striking, right-lateral transcurrent faults to the west and northwesterly-striking, left-lateral faults to the east (Hoffman, 1984a; Hildebrand and Bowring, 1988). Within the medial zone many of the right-lateral faults of the Great Bear zone appear to turn northward until they parallel bedding and cleavage in sedimentary rocks of the Dumas Group where they disappear. Northwesterly-striking left-lateral faults of the internal zone transect the medial zone.

6. There are no known exposures of Archean rocks west of the medial zone. Neodymium and lead isotopic data from igneous rocks of the Great Bear zone indicate that the magmas did not interact with Archean crust (Bowring and Podosek, 1989; Housh et. al., 1989). Thus, even in the subsurface there may be no Archean crust west of the medial zone.

7. Rocks of Hottah terrane occur east of the medial zone where they form a klippe that forms part of a package of rocks thrust eastward over the Slave craton and its cover.

The klippe comprises a sizable portion of the internal zone, but the eastward extent of the klippe, and the nature of its contact with the Akaitcho Group, are unknown.

8. In the Wopmay Lake area north-striking folds of the medial zone are refolded by easterly-striking cross-folds. The relationship of the cross-folds to the Redrock culmination and the Tree River folds is unknown at present.

ACKNOWLEDGMENTS

We wish to thank our expeditor, Rod Stone, for his capable and efficient assistance and M. G. Hildebrand for cooking. Discussions with P.F. Hoffman were helpful. Raimo Lahtinen (Geological Survey of Finland), Magnus Ripa (Lund University), and Bruce Nocita (University of South Florida) shared our enthusiasm for the geology. J.E. King and A.N. LeCheminant critically read the manuscript.

REFERENCES

Bowring, S.A
1984: U-Pb zircon geochronology of early Proterozoic Wopmay orogen, N. W. T., Canada: An example of rapid crustal evolution; Ph.D. thesis, Lawrence, University of Kansas, 148 p.

Bowring, S.A. and Grotzinger, J.P.
1989: Implications of new U-Pb dating and physical stratigraphy for interbasinal correlations and the early Proterozoic evolution of the NW Canadian shield; *in* Geological Society of America, Abstracts with Programs, v. 21, p. A374.

Bowring, S.A. and Podosek, F.A.
1989: Nd isotopic evidence for 2.0-2.4 Ga crust in western North America; Earth and Planetary Science Letters, v. 94, p. 217-230.

Easton, R.M.
1980: Stratigraphy and geochemistry of the Akaitcho Group, Hepburn Lake map area, District of Mackenzie: An initial rift succession in Wopmay orogen (early Proterozoic); *in* Current Research, Part B, Geological Survey of Canada, Paper 80-1B, p. 47-57.
1981: Geology of Grant Lake and Four Corners map areas, Wopmay Orogen, District of Mackenzie; *in* Current Research, Part B, Geological Survey of Canada, Paper 81-1B, p. 83-94.

Fraser, J.A., Hoffman, P.F., Irvine, T.N., and Mursky, G.
1972: The Bear Province; *in* Variations in Tectonic Styles in Canada; R.A. Price and R.J.W. Douglas, ed., Geological Association of Canada, Special Paper 11, p. 454-503.

Hildebrand, R.S. and Bowring, S.A.
1988: Geology of parts of the Calder River map area, central Wopmay orogen, District of Mackenzie; *in* Current Research, Part A, Geological Survey of Canada, Paper 88-1C, p. 199-205.

Hildebrand, R.S., Hoffman, P.F. and Bowring, S.A.
1986: Tectono-magmatic evolution of the 1.9-Ga Great Bear magmatic zone, Wopmay orogen, northwestern Canada; Journal of Volcanology and Geothermal Research, v. 32, p. 99-118.

Hildebrand, R.S., Bowring, S.A., Steer, M.E., and Van Schmus, W.R.
1983: Geology and U-Pb geochronology of parts of the Leith Peninsula and Riviere Grandin map areas, District of Mackenzie: *in* Current Research, Part A, Geological Survey of Canada, Paper 83-1A, p. 329-342.

Hildebrand, R.S., Bowring, S.A., Andrew, K.P.E., Gibbins, S.F. and Squires, G.C.
1987: Geological investigations in Calder River map area, central Wopmay orogen, District of Mackenzie; *in* Current Research, Part A, Geological Survey of Canada, Paper 87-1A, p. 699-711.

Hoffman, P.F.
1973: Evolution of an early Proterozoic continental margin: The Coronation geosyncline and associated aulacogens of the northwestern Canadian Shield; Royal Society of London, Philosophical Transactions, v. 273, ser. A, p. 547-581.
1984a: The northern internides of Wopmay orogen; Geological Survey of Canada Map 1576A (with marginal notes).
1984b: Wopmay fault zone and its role in the evolution of Wopmay orogen; *in* Geological Association of Canada, Abstracts with Programs, v. 9, p. 74.

Hoffman, P.F. and Bowring,
1984: Short-lived 1.9 Ga continental margin and its destruction; Geology, v. 12, p. 68-72.

Hoffman, P.F., and McGlynn, J.C.
1977: Great Bear Batholith: a volcano-plutonic depression; *in* W.R.A. Baragar, L.C. Coleman and J.M. Hall, ed., Volcanic Regimes in Canada; Geological Association of Canada, Special Paper 16, p. 170-192.

Hoffman, P.F., Bell, I.R., and Tirrul, R.
1976: Sloan River map area (86K), Great Bear Lake, District of Mackenzie; *in* Report of Activities, Part A, Geological Survey of Canada, Paper 76-1A, p. 353-358.

Hoffman, P.F., Tirrul, R., King, J.E., St-Onge, M.R., and Lucas, S.B.
1988: Axial projections and modes of crustal thickening, eastern Wopmay orogen, northwest Canadian Shield; *in* S.P. Clark, ed., Processes in Continental Lithospheric Deformation; Geological Society of America, Special Paper 218, p. 1-29.

Housh,T., Bowring, S.A., and Villeneuve, M.
1989: Lead isotopic study of early Proterozoic Wopmay orogen, NW Canada: Role of continental crust in arc magmatism; Journal of Geology, v. 97, p. 735-747.

King, J.E.
1986: The metamorphic internal zone of Wopmay orogen (early Proterozoic), Canada: 30 km of structural relief in a composite section based on plunge projection; Tectonics, v. 5, p. 973-994.

Lalonde, A.E.
1986: The intrusive rocks of the Hepburn metamorphic-plutonic zone of the central Wopmay orogen, N.W.T.; Ph.D. thesis, McGill University, Montréal, Québec, 258p.

McGlynn, J.C.
1975: Geology of the Calder River map area (86F), District of Mackenzie; *in* Report of Activities, Part A, Geological Survey of Canada Paper 75-1A, p. 339-341.

McGlynn, J.C.
1981: Wopmay fault system; *in* Slaney, V.R., ed., Landsat images of Canada-a geological appraisal; Geological Survey of Canada, Paper 80-15, p. 44-45.

St-Onge, M.R., King, J.E., and Lalonde, A.E.
1982: Geology of the central Wopmay orogen (Early Proterozoic), Bear Province, District of Mackenzie: Redrock Lake and the eastern portion of the Calder River map areas; *in* Current Research, Part A, Geological Survey of Canada, Paper 82-1A, p. 99-108.

St-Onge, M.R., King, J.E., and Lalonde, A.E.
1984: Deformation and metamorphism of the Coronation Supergroup and its basement in the Hepburn metamorphic-plutonic zone of Wopmay orogen: Redrock Lake and the eastern portion of the Calder River map areas, District of Mackenzie; *in* Current Research, Part A, Geological Survey of Canada, Paper 84-1A, p. 171-180.

St-Onge, M.R., Lalonde, A.E., and King, J.E.
1983: Geology, Redrock Lake and eastern Calder River map areas, District of Mackenzie: The central Wopmay orogen (early Proterozoic), Bear Province, and the western Archean Slave Province; *in* Current Research, Part A, Geological Survey of Canada, Paper 83-1A, p. 147-152.

Stacey, J.S., and Kramers, J.D.
1975: Approximation of terrestrial lead isotope evolution by a two-stage model; Earth and Planetary Science Letters, v. 26, p. 207-221.

ANALYTICAL PROCEDURES

Zircons were separated using standard techniques, dissolved in Teflon micro-bombs spiked with a mixed ^{208}Pb-^{235}U tracer solution, and analyzed in single-collector mode using a VG-354 mass spectrometer. Radiogenic ^{206}Pb and ^{207}Pb were calculated by correcting measured ratios with measured blank Pb and the model Pb of Stacey and Kramers (1975) corresponding to the age of the zircons for the original non-radiogenic component. During the course of analyses blanks were < 10 pg ^{206}Pb and < 15 pg total U. Uncertainties on the $^{207}Pb/^{206}Pb$ and U-Pb determinations, estimated from the long-term reproducibility of standards and samples, are $\pm 0.1\,\%$ for $^{207}Pb/^{206}Pb$ and $^{208}Pb/^{206}Pb$ at the 2σ level and $\pm 0.4\,\%$ for $^{235}U/^{207}Pb$ and $^{206}Pb/^{238}U$.

Geology of the Contwoyto – Nose Lakes map area, central Slave Province, District of Mackenzie, N.W.T.

J.E. King, W.J. Davis[1], C. Relf[2], and T. Van Nostrand[3]
Continental Geoscience Division

King, J.E., Davis, W.J., Relf, C., and Van Nostrand, T., Geology of the Contwoyto – Nose Lakes map area, central Slave Province, District of Mackenzie, N.W.T.; in Current Research, Part C, Geological Survey of Canada, Paper 90-1C, p. 177-187, 1990.

Abstract

Metaturbidites of the Contwoyto and Itchen formations and those of the Beechey Lake Group appear to be coextensive although an extensive domain of injection migmatite obscures the relationship between them. Most of the leucosome in the migmatites was injected at the exposed structural level and the margins of the migmatized domains therefore do not coincide with a metamorphic isograd. Orthogneisses comprising hornblende-biotite-plagioclase units injected by tonalite are preserved within the migmatite domain. Two C3 (syn-volcanic) tonalite to monzogranite bodies were recognized, indicating that this phase of magmatism is more extensively preserved than previously thought. Numerous syn-D_2 hornblende-biotite gabbro to granodiorite and post-D2 muscovite-biotite tonalite to syenogranite bodies occur across the entire map area. Previously defined structural elements (D_1 to D_4) are also present across the area although D_3 and D_4 may have been contemporaneous and have been redesignated as D_{NE} and D_{NW}, respectively.

Résumé

Des turbidites métamorphisées des formations de Contwoyto et d'Itchen et celles du groupe de Beechey Lake semblent de même étendue bien qu'un vaste domaine de migmatite d'injection masque le lien qui existe entre elles. La grande partie du leucosome contenu dans les migmatites a été injecté au niveau structural exposé et dans les bordures des domaines migmatisés; il ne coïncide donc pas avec un isograde métamorphique. Des orthogneiss comprenant des unités de hornblende-biotite-plagioclase dans lesquelles s'introduisent de la tonalite ont été conservés dans le domaine migmatitique. Deux massifs de tonalite à monzogranite (syn-volcaniques) C3 ont été identifiés, indiquant que cette phase de magmatisme est spatialement mieux conservée que prévu. De nombreux massifs de gabbro à horblende-biotite à granodiorite, synchroniques à D2, et des massifs de tonalite à muscovite-biotite à syénogranite, postérieurs à D_2, traversent toute la zone illustrée sur la carte. Des éléments structuraux antérieurement définis (de D_1 à D_4) traversent également la zone; toutefois, D_3 et D_4 ont pu être contemporains et ont été redésignés D_{NE} et D_{NW}, respectivement.

[1] *Department of Earth Sciences, Memorial University of Newfoundland, St. John's, Newfoundland, A1B 3X5*
[2] *Department of Geological Sciences, Queen's University, Kingston, Ontario, K7L 3N6*
[3] *184 University Ave., St. John's, Newfoundland, A1B 1Z7*

INTRODUCTION

This report presents the results of the third field season of a four-year project in the central Slave Province during which the Contwoyto Lake (76E) and the west half of the Nose Lake (76F) map areas are being mapped at a scale of 1:100 000 (Figs. 1, 2). An associated project that involves detailed structural-metamorphic analysis of the medium-grade metasedimentary rocks is reported in Relf (1990).

The map area is underlain by metaturbidites and metavolcanics of the Yellowknife Supergroup (Henderson, 1970) that were intruded by at least six groups of plutons between about 2660 and 2580 Ma. The area was metamorphosed under high-temperature — low pressure conditions and has experienced four phases of Archean deformation. Previous work, general geology and previously mapped units in the area have been described by King et al. (1988, 1989). The geochronology has been summarized by Mortensen et al. (1988) and van Breemen et al. (1989). This report will focus on new results and new perspectives derived from work during 1989.

TURBIDITIC UNITS

Three metaturbiditic units, the Contwoyto and Itchen Formations (both part of the Cogead Group of Henderson, 1988) and the Beechey Lake Group have been defined in the central Slave Province but the relations between them are obscured by complex deformation, poor exposure, or migmatization. The Contwoyto Formation is "a unit consisting predominantly of the metamorphic equivalents of greywackes and mudstones of turbidite origin, but the definition includes the essential presence of scattered discontinuous bands and lenses of silicate, sulphide or oxide facies ... iron-formation" (Bostock, 1980, p. 21). The Itchen Formation is "the metamorphic equivalents of greywackes and mudstones ... which are similar to those of the Contwoyto Formation but lack the iron-formation lenses" (Bostock, 1980, p. 31-32). Bedding within the Itchen Formation was recognized to be generally thicker than in the Contwoyto Formation and to contain calcareous concretions (Bostock, 1980; King et al., 1988). The contact between the Contwoyto and Itchen formations is defined by the last occurrence of iron-formation. The Contwoyto and Itchen formations occur in the Point — Itchen — Contwoyto Lakes area. The Beechey Lake Group, which occurs in the Nose Lake — Back River area, has been defined as being "made up mostly of bedded greywackes ... and mudstones ... and their metamorphosed equivalents" with "minor rocks (<2 %) that include carbonaceous mudstone, banded silicate and oxide iron formation, chert and pyroclastic rocks" (Frith, 1987, p. 21). The Beechey Lake Group has not been subdivided and it is not obvious from the published descriptions whether mappable facies associations similar the Contwoyto and Itchen Formations can be identified in the Beechey Lake Group. That part of the Beechey Lake Group that occurs in the southeast corner of the Contwoyto-Nose Lakes map area (Ghurka Lake area, Fig. 2) was not observed to contain iron-formation and may therefore have been correlative with the Itchen Formation.

The Beechey Lake Group metaturbidites in the map area are separated from the Contwoyto and Itchen Formations by a zone of migmatization through which it is not possible to trace the contact between the two formations. Five locations of iron-formation were observed in the migmatites east of Contwoyto Lake (Fig. 2), suggesting that the rocks of the Contwoyto Formation continue through them. However, metaturbidites at Nose and Ghurka lakes (Fig. 2) are devoid of iron-formation and contain calcareous concretions. Fifteen kilometres east of Ghurka Lake, at Esker Lake, metaturbidites host gold-mineralized iron-formation (N.W.T. Chamber of Mines, 1988; Lambert et al., 1990). These relationships imply that either the Contwoyto and Itchen formations are complexly interfolded within the migmatite terrain or that the distinction between the two formations breaks down east of Contwoyto Lake.

MIGMATIZED TURBIDITES

Migmatized turbidites occur in a broad area that extends across the central part of the map area (Fig.2). They consist of varying percentages of biotite schist, derived from both metagreywacke and metamudstone, and granitoid leucosome (Fig.3). The latter is dominated by injected veins, although small, fine-grained irregular pods and veinlets that are intimately interspersed with metamorphic matrix

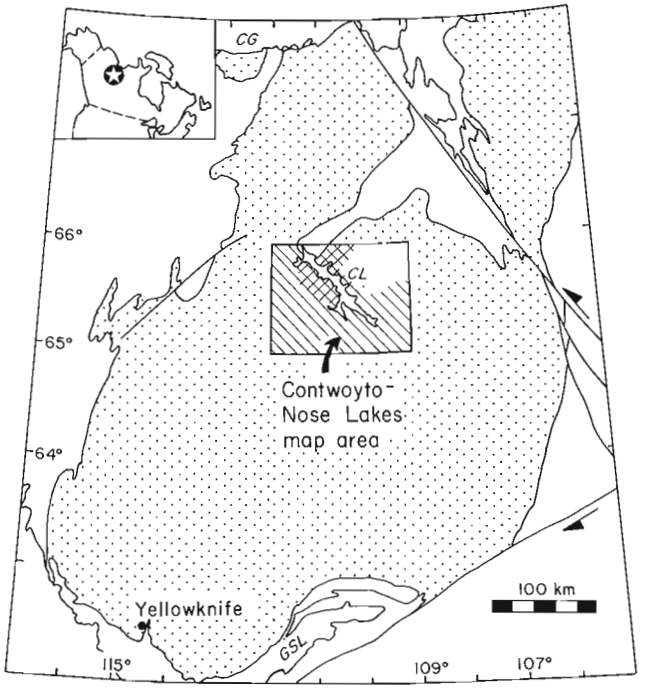

Figure 1. Location of the Contwoyto-Nose lakes project area. Stippled area is the Slave Structural Province. Inset shows the position of the Slave Province in Canada. Diagonal lines show the area covered to date; cross-hatch shows area of detailed structural-metamorphic analysis (Relf 1989, 1990). CG Coronation Gulf; CL — Contwoyto Lake; GSL — Great Slave Lake

minerals may represent *in situ* melt. There are two dominant types of injection leucosome (Fig. 3). The older of the two is typically a fine- to medium-grained, biotite tonalite to granodiorite that is equigranular to seriate in texture. In the western part of the map area, this leucosome was correlated with C4 tonalite intrusives on the basis of lithological similarity and spatial association (King et al., 1989). The younger leucosome is a biotite +/- muscovite leuco-granodiorite to leuco-monzogranite that characteristically contains grey K-feldspar and has associated pegmatites. It is the volumetrically dominant leucosome throughout most of the migmatitic terrane but has not been correlated with any of the C1-C6 groups of intrusions. Both types of leucosome occur as discrete centimetre- to metre-scale veins in veined migmatites or as pervasive leucosome in schlieric migmatite (cf. King et al., 1989). The later leucosome also occurs as small, schlieren-rich, irregularly-shaped bodies. Aluminous minerals such as cordierite, sillimanite and andalusite are present as xenocrysts or as apparently stable phases in both leucosomes (cf. King et al., 1989).

The distinction between units designated as metasedimentary formations (Contwoyto and Itchen Fms) and those as migmatites is based on the presence of sufficient leucosome to impart a migmatitic aspect to the rock (approximately 20-30 %). They are not fundamentally different rocks. The units are distinguished in Figure 2 in order to inform the reader of where to expect coherent, schistose turbidites rather than disrupted, migmatized turbidites. Because most of these veins are injected and not in situ melts, the distinction is not directly representative of a change in metamorphic grade.

ORTHOGNEISS

Orthogneisses, composed of interlayered hornblende + plagioclase +/-biotite units and biotite tonalite occur in five localities in the migmatitic paragneisses and as enclaves in the Wishbone and Jaeger plutons (Fig. 2, 3). Individual layers range in thickness from millimetres to metres, have sharp contacts and are continuous at the outcrop scale. The units are characterized by a medium grained, granoblastic texture and a weakly to moderately developed foliation defined by the planar alignment of ferromagnesian minerals or flattened feldspar and quartz. The layering could be a product of very discrete 'lit-par-lit' style of tonalite intrusion, but we consider this unlikely due to the narrow widths and continuity of some of the layers. This type of layering resembles deformation-enhanced layering. If this is so, structures related to the deformation, such as lineations and strong foliations, have been obliterated by recrystallization.

The plutons which contain the orthogneiss enclaves are interpreted to be part of the C3b group (see below) and so the orthogneisses must predate them. The tonalitic component of the orthogneiss enclaves is distinct from their hosts but are similar to phases of the C3a Olga tonalite (see below). This tentative correlation will be tested by U-Pb zircon dating. Where preserved outside of the C3 plutons, the orthogneisses are intruded by C6 units, but their contact relations with other units is not known. The hornblende-biotite-plagioclase component may be metamorphosed basalt/andesite or gabbro/diorite.

PLUTONIC UNITS

Plutonic units in the area have been classified by relative emplacement age into six groups referred to with the nomenclature C1, C2 ... C6 ('C' denotes geographic location near Contwoyto Lake) (King et al., 1988, 1989). Initial U-Pb dating substantiates the relative ages interpreted from field relations (Table 1). Nomenclature of the rock types follows Streckeisen (1976). Bodies mapped in 1989 include two that are interpreted to be part of the C3 group, the eastern extent of the C5 Siege tonalite, and numerous new C4 and C6 bodies.

C3 — Biotite tonalite to monzogranite

Plutons in the C3 group were previously subdivided into two types (C3a, C3b) (King et al., 1988). The first-recognized C3a body, the Olga tonalite, is a composite body comprising multiple sheets of biotite quartz diorite to tonalite. Individual sheets range in thickness from centimetres to tens of metres. The 'type' C3b body, the Wishbone tonalite, is medium to coarse-grained, quartz-rich and contains biotite as a ferromagnesian phase. It is also composite, but its component units are larger in size (greater than several metres) than in the C6a Olga tonalite. Emplacement predates the metamorphic thermal peak and C3 bodies are strongly recrystallized. The Olga tonalite has been dated at 2650 Ma (Table 1).

Biotite tonalite, very similar in composition and intrusive style to the C3a Olga tonalite occurs in the orthogneisses described above. In that unit, the tonalite commonly forms centimetre-scale veins interlayered with hornblende-biotite-plagioclase layers in the orthogneiss unit. Some parts of the orthogneiss package are composed of centimetre-scale, sheet-like bodies of tonalite with little or no metabasite component.

Two plutons, one on the west shore of Contwoyto Lake and the other between Ghurka and Nose Lakes (Fig. 2), are compositionally and texturally similar to the C3b Wishbone tonalite and therefore interpreted to be part of the C3b group of plutons. Their most distinctive features are extensive recrystallization and abundant, coarse quartz (Fig. 5). The bodies are equigranular , medium- to coarse-grained (2-8 mm) and contain irregular bodies and veins of pegmatite. Biotite comprises 2-10 % of the rock. A well-developed foliation is defined by the alignment of biotite and the shape of quartz and feldspar. Locally, quartz and feldspar shapes are linear.

C4 — Hornblende +/- biotite gabbro, diorite, quartz diorite, tonalite and granodiorite

The C4 group of intrusions includes hornblende +/biotite gabbro to granodiorite (with minor hornblendite and monzodiorite) that are characterized by poorly- to well-developed foliations. C4 bodies are typically sheet-like or oval in map view, with their long axes parallel to the structural grain of the host rocks. Two C4 plutons have yielded U-Pb zircon ages of 2608 Ma (Table 1). Interpretation of

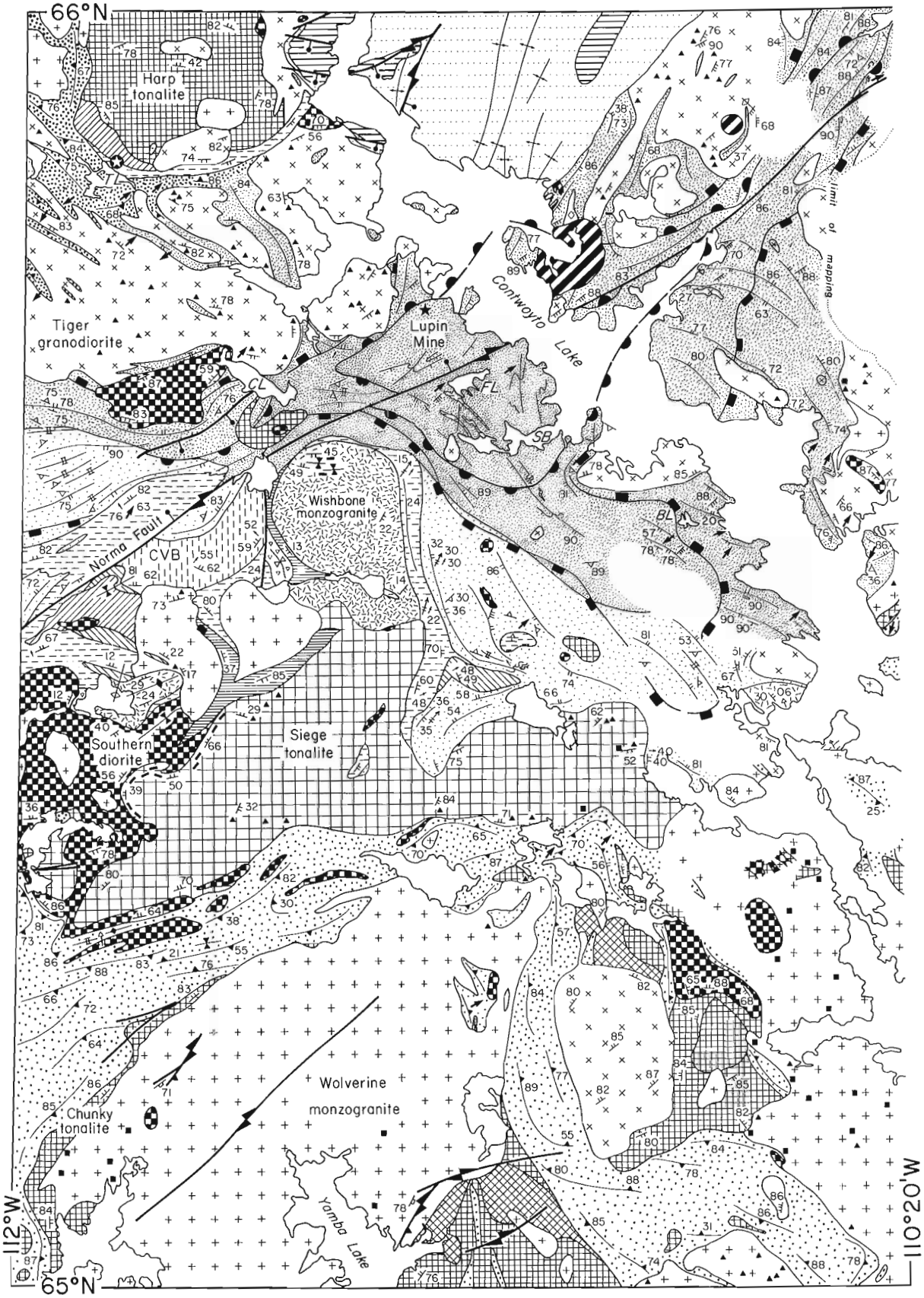
66°N
65°N
112°W
110°20'W
Harp tonalite
Tiger granodiorite
Lupin Mine
Contwoyto Lake
limit of mapping
Wishbone monzogranite
Norma Fault
CVB
CL
FL
SB
BL
Southern diorite
Siege tonalite
Wolverine monzogranite
Chunky tonalite
Yamba Lake

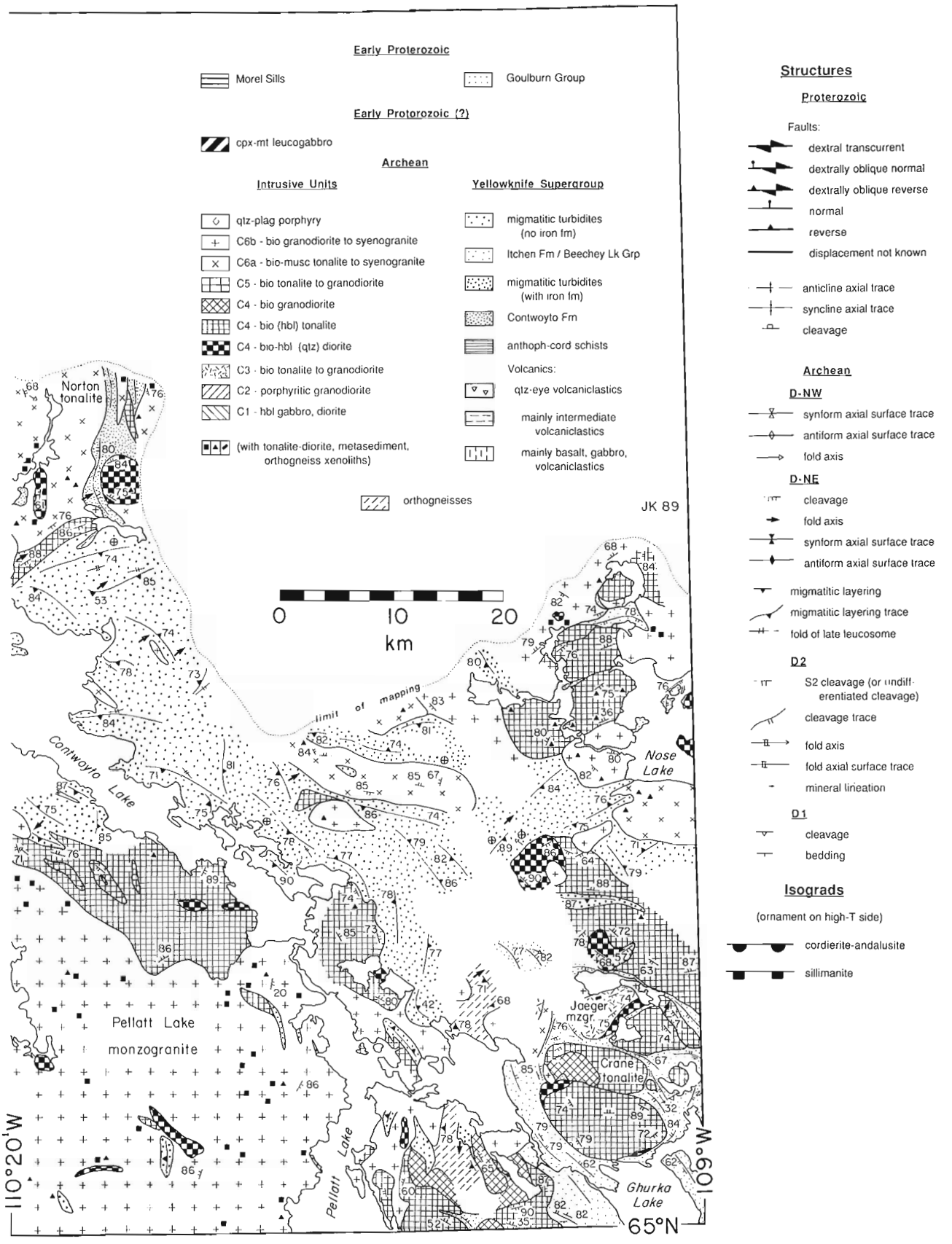

Figure 2. Simplified geological map of the Contwoyto — Nose lakes area. Unpatterned areas are drift-covered ground through which geology could not be extrapolated. Locations of iron formation within the migmatites east of Contwoyto Lake are marked with a circled cross.
Abbreviations: CVB — Central Volcanic belt; Bodies of water: CL Concession Lake; FL — Fingers Lake; SB — Shallow Bay; TL — Tuk lake.

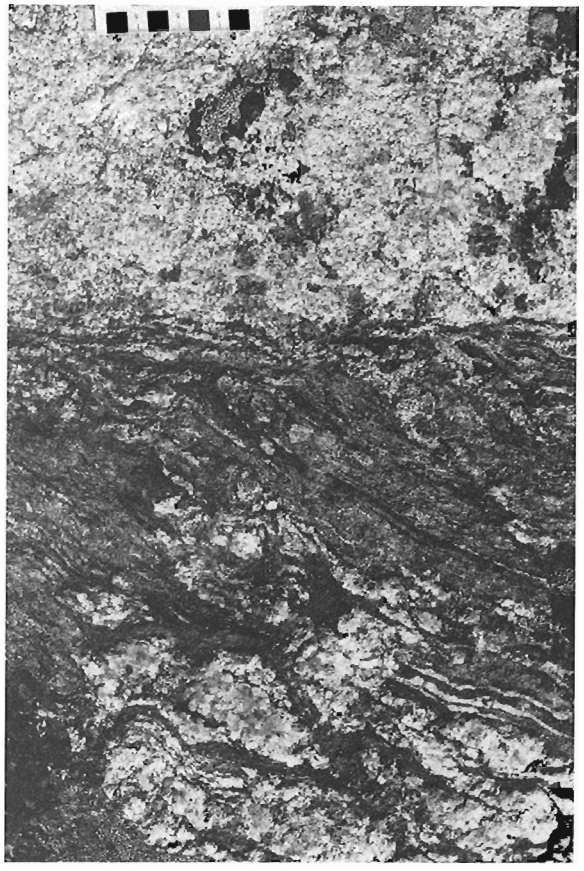

Figure 3. Migmatized metaturbidites intruded by fine-grained, thin veins of tonalite (C4?) and medium- to coarse-grained, thick veins of monzogranite leucosome. The monzogranite leucosome cuts the tonalite and is deformed about the (S_2?) foliation. Scale is in centimetres. (GSC 205003-I)

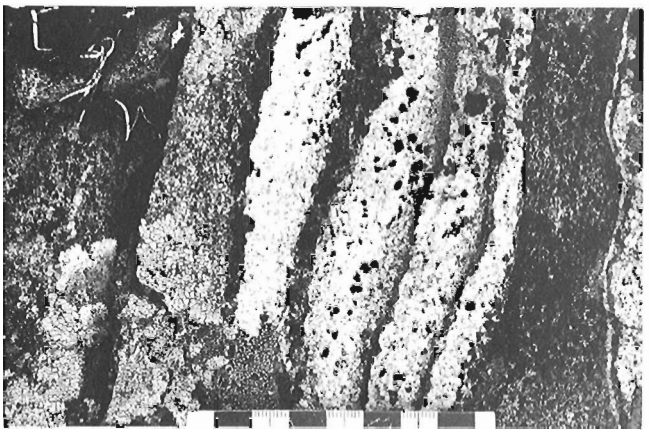

Figure 4. Orthogneiss composed of interlayered metabasite and tonalite. Scale is in centimetres. (GSC 205003-V)

Figure 5. Recrystallized and foliated monzogranite of the C3b Jaeger monzogranite. Scale is in centimetres. (GSC 205003-C)

preliminary geochemical data suggests that this group of rocks may have affinities to of modern continental margin-type magmatism (Davis, 1989).

The C4 plutons typically contain a very weakly to moderately developed foliation that is most commonly defined by the alignment of ferromagnesian minerals and more rarely by the shape of plagioclase and quartz. It is therefore best expressed in more mafic bodies. The foliation is continuous with, and is correlated with S_2 in the host rocks.

The lithologies, map pattern and strain state of the C4 group of plutons are very similar to that of the the dioritic to granodioritic intrusions included in the Regan Intrusive Suite described immediately east of the present map area (Hill and Frith, 1982; Frith, 1987; Frith and Fryer, 1985). Although these authors include some 'granite' bodies in the Regan Intrusive Suite no granites were recognized as part of the C4 group in the Contwoyto-Nose lakes map area.

Numerous plugs of hornblendite, hornblende gabbro and biotite-hornblende gabbro, only tens to hundreds of metres in size, are included in the C4 group because of their composition and relatively low strain state. These plugs intrude the metasedimentary rocks and are preserved as xenoliths within younger plutonic rocks.

The quartz diorite on the south shore of Nose Lake (Fig. 2) locally contains up to 75 % (by surface area) enclaves. The enclaves vary in composition from biotite-hornblende diorite to biotite-hornblende tonalite and have varied igneous textures (equigranular, seriate, porphyritic). The enclaves range in diameter from 1 cm to 2 m and are rounded to subangular. Where elongate they are mutually aligned. Both enclaves and host quartz diorite have only a very weak tectonic foliation although elongation may be up to 5:1 . The alignment of enclaves is therefore interpreted to be related to magmatic processes. 'Budding' of a contact was observed in one locality. The enclaves do not appear to be xenoliths from any exposed units. These observations are compatible with an interpretation of their origin through

magma mingling (Vernon, 1983). The variety of enclaves suggests that repeated or progressive magma mingling occurred. Microdioritic enclaves 1-30 cm in size are common in other C4 diorites and quartz diorites.

Where oval-shaped C4 plutons intrude sillimanite-muscovite schists near Ghurka Lake (Fig. 2), the S_2 foliation in the pluton and host rock is concordant except for triple points near either 'end'. No overprinting structures, besides those developed regionally, were recognized within these triple points. The lack of complete concordance and any overprinting structures illustrate that, in contrast to the interpretation of Hill and Frith, (1982), the orientation of the foliation is probably not related to stresses imposed soley by inflation of the C4 bodies but is more likely related to interference between regional and local strain fields (e.g. Ledru and Brun, 1977; Brun and Pons, 1981). At the east end of the C4 Crane tonalite (Fig. 2), a much smaller C4 tonalite has been emplaced within one of the triple points (Fig. 2, 6). In map view, this satellitic pluton has a tadpole shape with a 'tail' that narrows to a width of 1 metre and extends out of the triple point zone parallel to the regional orientation of S_2. This two dimensional form suggests that a tabular body (dyke) utilizing the S_2 foliation plane was able to inflate within the triple point adjacent to the Crane tonalite. This may be evidence that the triple point was a relatively low stress zone during C4 intrusion, thus consistent with the C4 intrusive event being synchronous with D_2.

C5 — Biotite tonalite to granodiorite

The Siege tonalite and one small satellitic body are the only known C5 bodies (Fig. 2). They are leucocratic, equigranular and fine- to medium-grained. Accessory apatite, magnetite and muscovite and biotite-rich enclaves and schlieren are common throughout (King et al., 1988, 1989). The two-dimensional form of the Siege tonalite is distinctly lobate (Fig. 2).

C6a — Muscovite — biotite tonalite to syenogranite

Plutons included within the C6a group are fine- to coarse-grained, muscovite-biotite tonalite to monzogranite with accessory apatite, tourmaline and garnet and abundant associated pegmatitic dykes and pods. One of the C6a plutons, near Lupin Mine, has been dated at about 2581 Ma (Table 1). C6a bodies are most abundant in the north part of the map area, where they form large composite bodies with numerous screens, xenoliths and schlieren of metasedimentary rocks. In the south they occur as isolated plutons, up to 10 km wide, that contain relatively few metasedimentary xenoliths (Fig.2).

S_3 foliations occur within C6a plutons and therefore the emplacement of the plutons is interpreted to have predated or was synchronous with D_3 (King et al., 1989). However, biotite in two plutons that are lithologically similar to the

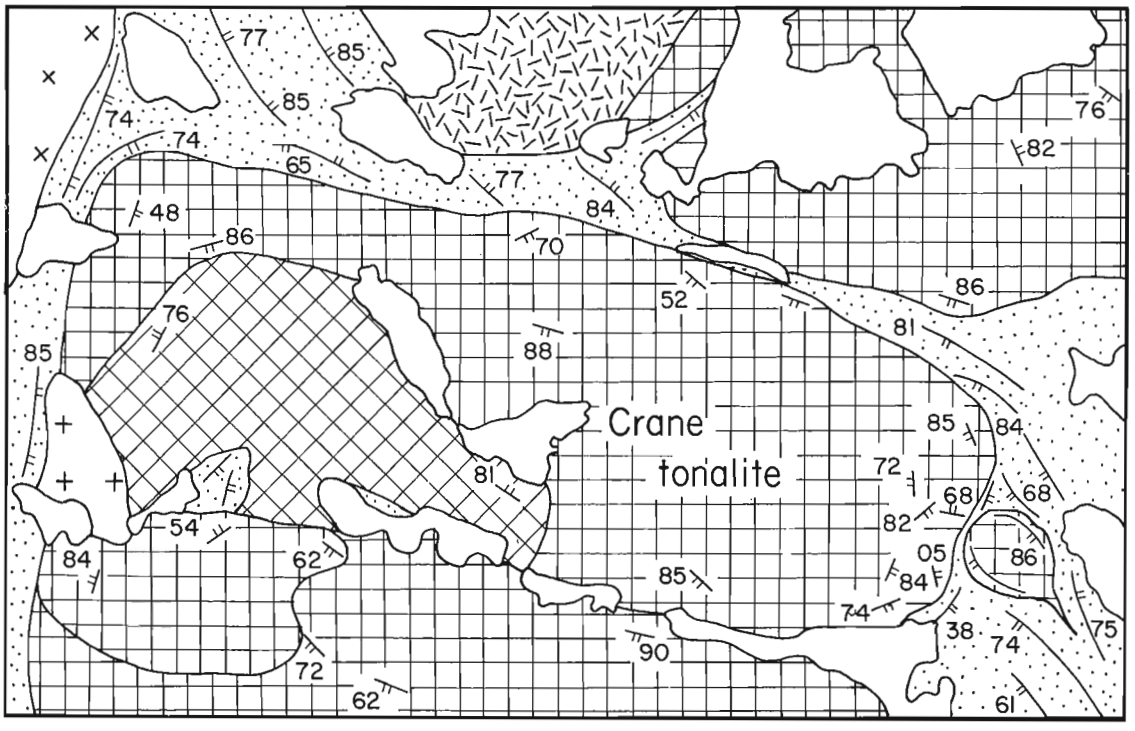

Figure 6. Detail of foliation trajectories around C4 Crane tonalite and satellite C4 pluton. Symbols same as Figure 2. The number of data points represent area of more detailed observations, not intensity of foliation development. Regional trend of S_2 through this area is NW-SE (Fig. 2).

C6a group, the Norton tonalite on the east shore of Contwoyto Lake and a pluton midway between Contwoyto and Nose lakes, contain biotite that is aligned parallel to S_2 in their host rocks (Fig. 2). Similarly, veins of a muscovite monzogranite (C6a?) are isoclinally folded about an axial plane that is parallel to the local S_2. These bodies may therefore have intruded during D_2. However, the foliations strike northwest and northeast and the fold axial plane strikes northeast. It is possible that the structures are the northeast-striking S_3 and F_3 and northwest-striking S_4 (see below).

C6b — Biotite monzogranite to syenogranite

C6b plutons are medium- to coarse-grained biotite granodiorite to syenogranite that are commonly K-feldspar porphyritic and have only minor associated pegmatitic veins and pods. In contrast to the C6a group, C6b plutons occur mainly as large sheet complexes in the south part of the map area (Fig. 2). Ages derived from three different C6b bodies range from 2585-2582 Ma (Table 1).

C6b plutons constitute the composite Pellatt Lake monzogranite (Fig.2). This body comprises an unknown number of units that range in composition from biotite tonalite to biotite syenogranite although its most common rock type is medium- to coarse-grained biotite monzogranite in which K-feldspar is commonly porphyritic. Parts of the body are characterized by a heterogeneous rock composed of a 'background' of equigranular, medium-grained biotite tonalite to granodiorite that contains veins, irregular patches, or randomly distributed pink K-feldspar crystals. Enclaves of foliated hornblende-biotite diorite, biotite tonalite and metasedimentary rocks, similar to the surrounding host rocks are present within the plutons. The enclaves range in size from metres to several kilometres and are either sharply bounded or partially assimilated.

C6b bodies are typically non-foliated although they are folded by F_3 and F_4. Locally they do contain foliations defined by the alignment of biotite and flattened quartz and feldspar (Fig. 7). These foliations may be S_3 and S_4 but their age cannot be unambiguously determined. In Figure 2 they are drawn as undifferentiated foliations. Discrete

Figure 7. Disharmonically folded veins of leucomonzogranite in migmatized turbidite. Pen is 13.5 cm. (GSC 205003-L)

Table 1. U-Pb ages from the Contwoyto-Nose Lakes area. The age of the intermediate tuff is from Mortensen et al. (1988) (all other ages are from van Breemen et al., 1989).

Unit	Age	Mineral
C6a monzogranite	2581 +9/-5 Ma	monazite
C6b Wolverine monzogranite	2582 +/-4 Ma	monazite
C6b pegmatitic syenogranite	2584 +/-4 Ma	monazite
C6b monzogranite	2585 +/-4 Ma	monazite
C4 Southern diorite	2608 +/-1 Ma	zircon
C4 Chunky tonalite	2608 +5/-3 Ma	zircon
C3a Olga tonalite - melanocratic phase	2649 +/-2 Ma	zircon
- leucocratic phase	2650 +/-5 Ma	zircon
C2 qtz-porphyritic granodiorite	2660.4 +0.9/-0.5 Ma	zircon
intermediate tuff, Central volcanic belt	2667.6 +3/-1.6 Ma	zircon

zones of moderately developed foliation, 1-2 m in width and striking northeast, occur within the Pellatt Lake monzogranite. The age of these is not known but the zonal character and orientation suggest that they may be shear zones, possibly related to a regionally developed set of Proterozoic faults (King et al., 1989). In both the Wolverine and Pellatt Lake monzogranites there are local zones of 'ghost foliation' in which a vague layering is defined by variations in composition and texture. There is a continuum between this vague layering and well-defined metasedimentary xenoliths. The 'ghost layering' is therefore interpreted to be represent digested inclusions.

MARA RIVER COMPLEX

The Mara River complex is an undivided unit adjacent to the east boundary of the present map area that comprises granitoid gneiss, migmatite, plutons of the Regan Intrusive Suite and granitoid rocks that may predate the Yellowknife Supergroup (Frith, 1987, p. 29). Where the complex extends into the Contwoyto-Nose lakes map area, it has been subdivided into migmatized turbidite, C4 diorite — tonalite and C6 tonalite monzogranite units (Fig. 2). C4- and C6-type bodies are not unique to the Mara River complex, but occur throughout the central Slave Province. The distinctive feature of the complex appears to be the migmatitic character of the host rocks. Because the component lithological units were distinguished, the term "Mara River Complex" is not used in the Contwoyto-Nose Lakes area.

STRUCTURE

Previous analysis (King et al., 1988, 1989; Relf, 1989) has shown the western part of the map area to be affected by four sets of Archean structures. The structures were designated as F_1-F_4 and S_1-S_4 and the inferred deformation events were designated D_1-D_4. The numbered nomenclature refers to the relative chronological sequence and does not necessarily imply that each deformation represents a discrete event. The structural sets included: D_1 — isoclinal folds, pre-thermal-peak (biotite-muscovite) cleavage and cleavage-parallel faults; D_2 — isoclinal folds, syn-thermal-peak cleavage, and cleavage-parallel faults; D_3 — open fold to tight folds and domainally-developed, post-thermal-peak crenulation cleavage that trend northeast; D_4 — open folds with local axial planar biotite cleavage that strike northwest. The same nomenclature is used here with the exception that D_3 and D_4 have been recognized to have varied relative time relations and are herein referred to as D_{NE} and D_{NW}. They are discussed further in this section.

The pre-thermal-peak S_1 is now recognized across the entire map area within porphyroblasts and in microlithons between S_2 cleavage surfaces. Pre-S_2 folds and faults were also observed in the newly mapped area. However, the relationship of these to S_1 could not be determined (see Relf, 1990).

S_2, interpreted to have formed coevally with the thermal peak (King et al., 1988), is the predominant cleavage across the map area. Its development is regionally consistent and is not spatially related to any single intrusion. S_2 is continuous with the layer-parallel biotite foliation in the migmatitic turbidites and the foliation in the migmatites is therefore interpreted to have formed during D_2.

Structures described previously (King et al., 1988, 1989; Relf, 1989) as post-thermal-peak D_3 and D_4 structures are also recognized across the map area but their relative chronology is now known to be variable. NE- and NW-trending post-thermal-peak structures, previously interpreted as D_3 and D_4 structures respectively, appear to be almost mutually exclusive in their distribution and information on overprinting relations is therefore sparse. At four localities where overprinting relations were exposed, three showed that the NW-trending folds postdated the NE-trending ones (Relf, 1990). The fourth showed the reverse. Because of these ambiguous relationships, Relf (1990) suggested that these sets of structures may have formed contemporaneously and therefore redesignated them as D_{NE} and D_{NW} (the 'NE' and 'NW' designation refers to the regional strike of the structures, not to the direction of the compressional stress).

The development of D_{NE} structures is strongly domainal. Open F_{NE} and weak crenulations are present throughout the map area, but there is a 'corridor' of intensely developed F_{NE} and S_{NE} that extends northeastward from Shallow Bay (Fig. 2). Within this 'corridor' there is a strongly developed S_{NE}, which locally transposes S_2 and becomes the dominant mesoscopic fabric (see Fig. 5 of Relf, 1990). The domainal nature of the D_{NE} structures may be a result of a heterogeneous regional stress field or of heterogeneous thermal softening during D_{NE}. No systematic asymmetry of the D_{NE} structures was recognized.

D_2, D_{NE} and D_{NW} structures are recognized in the migmatitic turbidites. The main foliation, defined by the alignment of biotite, is interpreted to be S_2. This main foliation is axial planar to folded biotite tonalite leucosome (C4) and these folds are therefore interpreted as F_2 (King et al., 1989). Post-thermal-peak NE- and NW-trending crenulations are interpreted as F_{NE} and F_{NW}.

The migmatized turbidites are also deformed by folds that are recognized only in the migmatized domain. The leuco-monzogranite leucosome transects S_2, and is folded by F_2 (Fig. 3). However it is also folded together with S_2 (Fig. 3). Fold styles range from harmonic chevrons or isoclines to extremely disharmonic and variably-oriented folds, the latter style occurring where there is a high percentage of leucosome (Fig. 7). The unpredictable fold style in leucosome-dominated migmatites reflects the response of melt-dominated materials to deformation (McLellan, 1984). Axial traces of harmonic folds are typically at 10°-40°, to the local trend of the predominant foliation (S_2). They are deformed by D_{NE} and D_{NW} structures. The folds formed after structures interpreted as S_2 and F_2 but before D_{NE} and D_{NW}. The fold style implies that the rocks were still hot during folding and the deformation therefore probably occurred closer in time to D_2 than to D_{NE} and D_{NW}.

METAMORPHISM

The biotite, cordierite and sillimanite mineral zones of King et al. (1988, 1989) and Relf (1989) were extended northeast of Contwoyto Lake following 1989 mapping (Fig. 2). The cordierite and sillimanite mineral zones narrow near the head of the northeast arm of Contwoyto Lake, then widen toward the northern map boundary, leaving a 5 km wide zone of biotite-grade slates and cordierite-grade schists (Fig. 2). Relf and King (1989) and Relf (1990) suggested that the present configuration of metamorphic zones is a function of both original thermal topology and post-metamorphic folding (D_{NE}, D_{NW}). The northeasterly oriented thermal 'synform' (Relf, 1990) is thought to have been formed at least in part by F_{NE} and its narrowing and widening by F_{NW} (King et al., 1989; Relf, 1990). Pressures and temperatures inferred from mineral assemblages remain within the 1.0-5.6 kb and 450°-640° C range previously established (Relf and King, 1989; Relf, 1990).

The trace of the sillimanite isograd, which regionally is not spatially related to any one pluton, is sharply deflected about a C6a pluton on the west shore of Contwoyto Lake (Fig. 2). Sillimanite adjacent to the pluton overgrows the S_2 foliation that everywhere else is syn-thermal-peak (Relf, 1990). This C6a pluton must therefore have been hot enough to impose a post-D_2, sillimanite-grade contact aureole on the host andalusite schists.

Metamorphic grade in the migmatized turbidites is difficult to determine because of the lack of diagnostic mineral assemblages. In the metaturbiditic melanosome both sillimanite K-feldspar — cordierite and sillimanite-muscovite assemblages were observed. The muscovite-breakdown isograd therefore occurs within the migmatized turbidites but it could not be mapped due to the variable extent to which the metaturbidites have been assimilated by the leucosome. Small, fine grained, irregular pods and veinlets of granitic composition that are intimately interspersed with the metamorphic mineral phases may represent in situ partial melt although it is difficult to unambiguously identify because of the pervasiveness of injected leucosome. The presence of cordierite in both the leucosome and the biotite schists suggests relatively high peak temperatures (Spear and Cheney, 1989).

SUMMARY

An extensive domain of migmatization masks the relationship between the Contwoyto and Itchen Formations and the Beechey Lake Group. Most leucosome was injected into its present site; in situ partial melt composes only a small percentage of observed leucosome. The margins of the migmatized domain therefore do not directly represent an increase in metamorphic grade. Mineral assemblages typical of high grades occur within the domain but high-grade isograds cannot be mapped. Orthogneiss composed of hornblende-biotite-plagioclase units injected by tonalite may represent basic to intermediate volcanic or intrusive rocks preserved in the migmatized domain.

Two newly mapped plutons are interpreted on the basis of field characteristics to be correlative with the ca. 2650 Ma C3 group of tonalite to monzogranite plutons. They must be radiometrically dated, but the correlation suggests that this phase of magmatism may more extensively preserved than previously thought. Plutons of the C4 group of biotite +/- hornblende gabbro to granodiorite plutons (ca. 2608 Ma) were emplaced during D_2 across the map area.

Pre-thermal-peak D_1 and syn-thermal-peak D_2 structures (cleavage, folds, faults) are preserved in the non-migmatized turbidites across the map area. Post-thermal-peak, NE- and NW-trending regional cross folding also affects all areas mapped to date. The late folds are domainal and almost mutually exclusive. They may have been broadly synchronous. Large volumes of ca. 2585-2580 Ma muscovite-biotite monzogranite were emplaced before and/or during the late cross folding. At least one of the late plutons carried sufficient heat to impose a sillimanite-grade contact aureole on its host rocks.

In summary, volcanic rocks, syn-volcanic intrusions and turbiditic metasedimentary rocks experienced a pre-thermal-peak compressional deformation at some time after 2650 Ma. They subsequently experienced further compression at around 2608 Ma contemporaneously with the emplacement of of biotite-hornblende gabbros to granodiorites (C4) and the thermal peak of a high — T / low — P metamorphism. Some muscovite-biotite tonalite plutons may also have been emplaced during this deformation. Large volumes of muscovite-biotite tonalite to syenogranite were emplaced at about 2585-2580 Ma before and/or during post-thermal-peak, possibly conjugate, regional cross folding.

ACKNOWLEDGMENTS

Mike Wingate and Debbie McPhedran were both superior assistants and contributed considerably to the mapping. Janien Schwarz continued to provide outstanding meals in often exceptional circumstances. We would like to thank our expeditor, Rod Stone, for his capable and efficient services. Discussions in the field with Jim Mortensen, Brian Bluck, Brian Fryer and Herb Helmstaedt were much appreciated. Critical reading by Robert Hildebrand improved the text.

REFERENCES

Bostock, H.H.
1980: Geology of the Itchen Lake area, District of Mackenzie; Geological Survey of Canada, Memoir 391, 101 p.

Brun, J.P. and Pons, J.
1981: Strain patterns of pluton emplacement in a crust undergoing non-coaxial deformation, Sierra Morena, Southern Spain; Journal of Structural Geology, v. 3, p. 219-229.

Davis, W.J.
1989: Geochemistry of ca. 2.6 Ga calc-alkaline plutonism in the central Slave Province; Geological Association of Canada, Mineralogical Association of Canada, Program with Abstracts, v. 14, p. A24.

Frith, R.A.
1987: Precambrian geology of the Hackett River area, District of Mackenzie, N.W.T.; Geological Survey of Canada, Memoir 417, 61 p.

Frith, R.A. and Fryer, B.J.
1985: Geochemistry and origin of the Regan Intrusive Suite and other granitoids in the northeastern Slave Province, northwest Canadian Shield; Canadian Journal of Earth Sciences, v. 22, p. 1048-1065.

Henderson, J.B.
1970: Stratigraphy of the Archean Yellowknife Supergroup, Yellowknife Bay — Prosperous Lake area, District of Mackenzie; Geological Survey of Canada, Paper 70-26, 12 p.
1988: Keskarrah Bay Area, District of Mackenzie, Northwest Territories; Geological Survey of Canada, Map 1679A, scale 1:50 000.

Hill, J.D. and Frith, R.A.
1982: Petrology of the Regan Intrusive Suite, in the Nose Lake — Beechey Lake map area, District of Mackenzie, N.W.T.; Geological Survey of Canada, Paper 82-8, 26 p.

King, J.E., Davis, W.J., Relf, C., and Avery, R.W.
1988: Deformation and plutonism in the western Contwoyto Lake map area, central Slave Province, District of Mackenzie, N.W.T.; *in* Current Research, Part C, Geological Survey of Canada, Paper 88-1C, p. 161-176.

King, J.E., Davis, W.J., Van Nostrand, R., and Relf, C.
1989: Archean to Proterozoic deformation and plutonism of the western Contwoyto Lake map area, central Slave Province, District of Mackenzie, N.W.T.; *in* Current Research, Part C, Geological Survey of Canada, Paper 89-1C, p. 81-94.

Lambert, M.B., Burbridge, G., Jefferson, C.W., Beaumont-Smith, C., and Lustwerk, R.
1990: Structure, stratigraphy and facies changes in volcanic and sedimentary rocks of the Back River Complex, N.W.T.; *in* Current Research, Part C, Geological Survey of Canada, Paper 90-1C.

Ledru, P. and Brun, J-P.
1977: Utilisation des fronts et des trajectoires de schistosit dans l'étude des relations entre tectonique et intrusion granitique: exemple du granite de Flamanville (Manche); Comptes Rendus de l'Académie des Sciences, v. 285, p. 1199-1202.

McLellan, E.
1984: Deformational behaviour of migmatites and problems of structural analysis in migmatite terrains; Geological Magazine, v. 121, p. 339-345.

Mortensen, J.K., Thorpe, R.I., Padgham, W.A., King, J.E., and Davis, W.J.
1988: U-Pb zircon ages for felsic volcanism in Slave Province, N.W.T.; *in* Radiogenic Age and Isotopic Studies: Report 2, Geological Survey of Canada, Paper 88-2, p. 85-95.

Northwest Territories Chamber of Mines
1988: Slave Province Gold; Northwest Territories Mining Industry News, v. 1, no. 2, p. 3.

Relf, C.
1989: Archean deformation of the Contwoyto Formation metasediments, western Contwoyto Lake area, Northwest Territories; *in* Current Research, Part C, Geological Survey of Canada, Paper 89-1C, p. 95-105.
1990: Archean deformation and metamorphism of metasedimentary rocks in the Contwoyto-Nose Lakes area, Central Slave Structural Province, N.W.T.; *in* Current Research, Part C, Geological Survey of Canada, Paper 90-1C.

Relf, C. and King, J.E.
1989: Distribution of high-T / low-P metamorphic mineral zones in the central Archean Slave Province: Thermal and tectonic controls; Geological Association of Canada, Mineralogical Association of Canada, Program with Abstracts, v. 14, p. 24.

Spear, F.S. and Cheney, J.T.
1989: A petrogenetic grid for pelitic schists in the system SiO_2 — Al_2O_3 — FeO — MgO — K_2O — H_2O; Contributions to Mineralogy and Petrology, v. 101, p. 149-164.

Streckeisen, A.
1976: To each plutonic rock its proper name; Earth Science Reviews, v. 12, p. 1-33.

van Breemen, O., King, J.E., and Davis, W.J.
1989: U-Pb zircon and monazite ages from plutonic rocks in the Contwoyto-Nose Lakes map area, central Slave Province, District of Mackenzie; *in* Radiogenic Age and Isotopic Studies: Report 3, Geological Survey of Canada, Paper 89-2, in press

Vernon, R.H.
1983: Restite, xenoliths and microgranitoid enclaves in granites; Journal and Proceedings, Royal Society of New South Wales, v. 116, p. 77-103.

Basement-cover relations between the Archean Sleepy Dragon Complex and the Yellowknife Supergroup in the Brown Lake area, Slave Province, Northwest Territories[1]

Donald T. James[2]

James, D.T. Basement-cover relations between the Archean Sleepy Dragon Complex and the Yellowknife Supergroup in the Brown Lake area, Slave Province, Northwest Territories; in Current Research, Part C, Geological Survey of Canada, Paper 90-1C, p. 189-195, 1990

Abstract

Archean rocks in the Brown Lake area may be subdivided into four lithological-structural domains consisting of gneisses and metaplutonic rocks of the Sleepy Dragon Complex, metavolcanic rocks of the Cameron River belt, metamorphosed greywacke-mudstone turbidites of the Burwash Formation, and unmetamorphosed porphyritic granite. The Burwash Formation domain also includes a thin belt of metavolcanic rocks west of Van Lake. The contact zone between the Sleepy Dragon Complex and the Cameron River metavolcanics is commonly deformed by moderately- to steeply-west-dipping high strain ductile structures that deform rocks in both domains. Kinematic indicators from the contact zone indicate both an east-vergent thrust displacementand a normal displacement. These conflicting indicators suggest that the zone may have an early thrust history related to early-syn and syn-metamorphic east-west shortening of the supracrustal rocks and a late-syn or post-metamorphic history of normal (west-side-down) displacement.

Résumé

Les roches archéennes de la région du lac Brown peuvent être divisées en quatre domaines lithostructuraux composés de gneiss et de roches plutoniques métamorphisées du complexe de Sleepy Dragon, de roches volcaniques métamorphisées de la zone de la rivière Cameron, de turbidites à grauwacke-mudstone métamorphisé de la formation de Burwash et de granite porphyritique non métamorphisé. Le domaine de la formation de Burwash comprend également une mince zone de roches volcaniques métamorphisées à l'ouest du lac Van. La zone de contact entre le complexe de Sleepy Dragon et les roches volcaniques métamorphisées de la rivière Cameron sont en général déformées par des structures ductiles de moyennement à très inclinées vers l'ouest qui affectent les roches de ces deux domaines. Les indicateurs cinématiques de la zone de contact indiquent un déplacement par chevauchement à vergence est et un déplacement normal. Ces indicateurs contradictoires laissent supposer que la zone a pu subir un chevauchement précoce lié à un raccourcissement est-ouest des roches supracrustales au début et au cours du métamorphisme et un déplacement normal (compartiment ouest abaissé) pendant la fin du métamorphisme ou après.

[1] Contribution to Canada — Northwest Territories Mineral Development Agreement 1987-1991. Project carried by the Geological Survey of Canada, Continental Geoscience Division.

[2] Shield Research Canada, 95 King Street East, Kingston, Ontario K7L 1Z2

INTRODUCTION

The objectives of this project are to map the part of the Archean, Cameron River metavolcanic belt between Fenton Lake and Brown Lake in the Slave Structural Province and to make a stratigraphic, structural and metamorphic analysis of the metavolcanic belt and adjacent metasedimentary, gneissic and granitoid terranes. The 1989 field season involved geological mapping at a scale of 1:50000 and was a continuation of a mapping project that was initiated in 1988 (see James, 1989). Mapping has resulted in a better understanding of the nature and significance of the contact zones between the major lithological — structural domains in this part of the Slave Province. This project represents a continuation of the 1:50 000-scale mapping of the Cameron River metavolcanic belt by Lambert (1988) south of 63° N.

The area mapped in 1989 is entirely within the Carp Lakes 1:250000 sheet (NTS 85 P) mapped by Moore et al. (1951). Mapping in 1989 occurred north of 63° 15′ N and includes parts of NTS map sheets 85 P/6 and P/7. The geology between 63° N and 63° 15′ N shown in Figure 1 is described by James (1989).

The geological map (Figure 1) shows that the area between Rick Lake and Brown Lake may be subdivided into four, Archean lithological — structural domains. The domains are composed of gneissic and metaplutonic rocks (units 1 and 2) that are presumed to be basement to the supracrustal rocks, metavolcanic rocks of the Cameron River metavolcanic belt (unit 3), metamorphosed greywacke — mudstone turbidites (unit 5), and unmetamorphosed porphyritic granite (unit 6). Each domain contains sets of structures that, with few exceptions, do not overprint structures in other domains. The contacts between the gneissic and metaplutonic domain and the Cameron River metavolcanic domain, and between the porphyritic granite domain and the Cameron River metavolcanic domain, are variably strained. This is in contrast to the nature of the same contacts that were mapped in 1988 in the Fenton Lake, Suse Lake and lake 355 (unofficial name) areas where a high strain zone is ubiquitous in the contact zone (James, 1989).

The area west of Van Lake may be similarly subdivided into lithological — structural domains consisting of unmetamorphosed granite, and a heterogeneous unit of interlayered metavolcanics and minor metasediments, and greywacke — mudstone metasediments. The granite domain in this area also contains occurrences of gneissic rocks that are identical in appearance to the gneissic rocks that occur at Brown Lake.

LITHOLOGY

Archean Pre-Yellowknife Supergroup Gneissic and Metaplutonic Rocks

Sleepy Dragon Complex

Gneissic and meta-plutonic rocks in the Brown Lake and Rick Lake areas are correlated on the basis of lithological similarity with the gneisses and metaplutonic rocks of the Sleepy Dragon Complex described by Henderson (1985). Rocks of the Sleepy Dragon Complex form part of a major block of gneisses, metaplutonic rocks and unmetamorphosed granitic plutons that extends for approximately 25 km east, 65 km south and 45 km to the north of Brown Lake. Henderson et al. (1987) reported U-Pb zircon ages of 2819 +40/-31 Ma for granitoid gneisses in the Sleepy Dragon Lake area, and 2663 +7/-5 Ma for the Turnback Rhyolite that occurs in Yellowknife Supergroup metavolcanics at the south end of the complex. These ages support the thesis that the gneisses and metaplutonic rocks of the Sleepy Dragon Complex are basement to the Yellowknife Supergroup. Geochronological studies necessary to confirm this relationship in the Fenton Lake and Brown Lake areas are in progress.

The gneisses of the Sleepy Dragon Complex (Fig. 1) are composed dominantly of tonalite gneiss and migmatitic tonalite (unit 1). Rocks contain biotite and hornblende and are intruded by at least two phases of metamorphosed and deformed tonalite veins. At Sherman lake (unofficial name), the gneissic unit also contains rare occurrences of strongly foliated, metamorphosed hornblende granite.

The gneissic unit also includes deformed and metamorphosed mafic dykes which increase in abundance towards the contact with the metavolcanic rocks. Adjacent to the metavolcanics, the gneisses also include deformed and metamorphosed ultramafic dykes. Neither the mafic nor the ultramafic dykes have been traced from the gneisses into the metavolcanic belt. Where strain along the contact between the Sleepy Dragon gneisses and the metavolcanics is high, the dykes are extensively boudinaged and folded producing a distinctive structural mélange of mylonitic gneiss and mafic and ultramafic dyke fragments.

The gneisses are intruded on all scales by unmetamorphosed granite and pegmatite. Pegmatite occurrences are very common along the contact between the gneisses and the metavolcanics.

The Sleepy Dragon Complex also contains a body of metamorphosed and variably foliated alkali feldspar porphyritic granite (unit 2, Fig. 1) that has been informally named the Suse Lake granite (James, 1989). The Suse Lake granite contains xenoliths of Sleepy Dragon gneiss demonstrating that the Suse Lake granite is younger than the gneisses. The absence of xenoliths of Yellowknife Supergroup rocks in the Suse Lake granite and the absence of intrusions of Suse Lake granite in Yellowknife Supergroup rocks, and the discordance between structures in the Suse Lake granite and the adjacent Yellowknife Supergroup metavolcanics suggests that the Suse Lake granite is older than the Yellowknife Supergroup.

Yellowknife Supergroup

Cameron River Metavolcanics

The metavolcanic rocks in the Yellowknife Supergroup (unit 3, Fig. 1) are part of the Cameron River metavolcanic belt that has been mapped from Brown Lake to Upper Ross Lake, 70 km to the south. Parts of the belt have been previously mapped by Henderson (1941b), Moore et al. (1951),

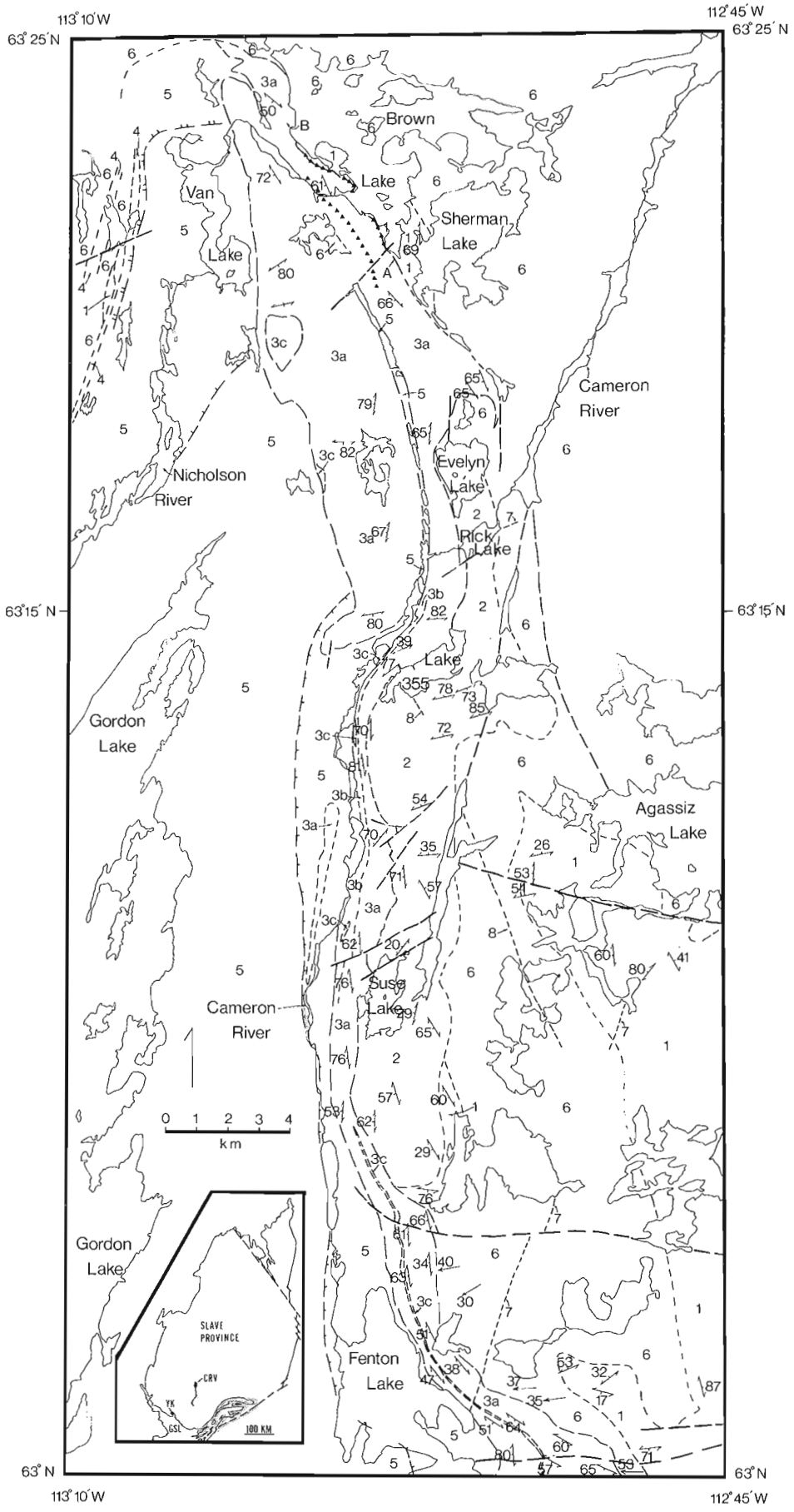

Legend

Lithological Units

Middle Proterozoic
- 8 Mackenzie diabase dykes

Early Proterozoic
- 7 diabase dykes

Archean
- 6 porphyritic granite

Yellowknife Supergroup
- 5 Burwash Formation
- 4 Nicholson River Metavolcanics
- 3 Cameron River Metavolcanics
  - 3a mafic metavolcanics
  - 3b mafic to intermediate metavolcanics
  - 3c meta-rhyolite triangular symbol represent iron formation

Sleepy Dragon Complex
- 2 Suse Lake granite
- 1 heterogeneous orthogneiss

geological contact (approximate, assumed)

foliation

mineral elongation lineation

fault trace

cordierite-in isograd

cordierite-out isograd (ornamentation on isograds is on the high-grade side)

Figure 1. General geology of the Cameron River Metavolcanic Belt between Fenton Lake and Brown Lake, Slave Province. Location map (inset) Yellowknife (YK) and Great Slave Lake (GSL).

Lambert (1974, 1977, 1982, 1988), Henderson (1985), Cullen (1988) and James (1989). Several kilometres northwest of Brown Lake the metavolcanic belt becomes dramatically thinner and appears to be eliminated by younger porphyritic granite. However, a prominent positive aeromagnetic anomaly that is continuous from the the Cameron River belt towards the northwest (Geological Survey of Canada aeromagnetic Map 2983 G) suggests that the metavolcanic belt may be continuous for at least another 10 km to the northwest.

In the Rick Lake, Evelyn Lake and Brown Lake areas the Cameron River metavolcanics occur in an approximately 700 m thick, west dipping, strongly flattened and folded succession. To the west, the metavolcanics are conformably overlain by greywacke — mudstone metasediments of the Burwash Formation. To the east, the metavolcanics are in tectonic contact with rocks of the Sleepy Dragon Complex. Dykes and small bodies of unmetamorphosed porphyritic granite (unit 6, Fig.1) within the Cameron River belt demonstrate that the granite is intrusive into the metavolcanic belt. In the Brown Lake area, the contact between the metavolcanic belt and the large granite body that occurs to the east is variably sheared.

The Cameron River metavolcanic belt is composed mainly of amphibolite-facies mafic amphibolites. The amphibolites occur as highly flattened and elongated pillowed and brecciated mafic volcanics, as fine grained, layered and non-layered, variably foliated amphibolites, and as medium-grained, massive to foliated hornblende — plagioclase rocks that are interpreted to be metagabbros. Metagabbro dykes/sills occur throughout the Cameron River belt; but they are most abundant as thin structurally continuous units near or at the base of the metavolcanic belt. Metagabbro makes up less than 10 % of the volcanic succession.

Locally, the metavolcanic belt contains distinctive, white and black-weathering mafic-to-andesitic pillow volcanics and pillow breccias where the pillows have relatively felsic margins and more mafic cores, and are surrounded by a mafic matrix. Locally the matrix is garnet-rich.

The Cameron River metavolcanic belt in the Brown Lake area also contains a minor amount of ultramafic metavolcanics. At location A on the map, the base of the Cameron River belt contains a 75 m thick zone of strongly deformed, green-, black- and dung-brown-weathering ultramafic rocks that have relict layering, and are intruded by massive, green-weathering ultramafic dykes. The ultramafic rocks are overlain by a 20 m thick meta-gabbro that is overlain by mafic pillow metavolcanics. This succession is continuous for less than 1 km, although smaller ultramafic occurrences are present along the same contact in the Brown Lake area.

Occurrences of felsic metavolcanics are not common in the area mapped in 1989 (Fig. 1). The most extensive occurrence of felsic rocks is 1 km southeast of Van Lake. In this area the metavolcanic belt contains an approximately elliptical, 2 km^2 rhyolite dome. Rocks are white-weathering, fine-grained and non-foliated. Locally, the unit contains thin (less than 1 m thick) shear zones. This rhyolite dome is shown in Moore's (1951) map as granite.

West of Evelyn Lake, along the contact between the Cameron River belt and the Burwash Formation, the Cameron River belt contains a thin body of rhyolite. These rocks have a relict porphyritic texture with blue quartz phenocrysts, or both quartz and feldspar phenocrysts.

In the Brown Lake area, the metavolcanic belt contains several occurrences of iron-formation (solid triangular symbol). The most extensive occurrence is along the contact between the Sleepy Dragon Complex and the Cameron River belt at Brown Lake. Banded chert-magnetite iron-formation is exposed along this contact somewhat discontinuously for 4 km. Locally, this iron-formation is 10 m thick. At several localities, the iron-formation is separated from the Sleepy Dragon gneisses by rocks that may be quartzitic metasediments. These potential metasediments require further study.

A zone of chert-magnetite iron-formation, garnet-amphibole rocks, metagreywacke, sulphide-rich zones and rare, felsic metavolcanics occurs within the metavolcanic belt approximately 400 m west of Brown Lake (Fig. 1).

Nicholson River metavolcanics

Interlayered amphibolites and metasedimentary rocks that occur west of Van Lake are herein informally named the Nicolson River metavolcanics (unit 4, Fig. 1). To the west, the Nicholson River metavolcanics have been intruded by granite and, locally, they are in tectonic contact with tonalite gneisses that are presumed to be relics of Sleepy Dragon Complex preserved along the Nicholson River metavolcanic — granite contact. The Nicholson River metavolcanics are conformably overlain by Burwash Formation metasediments.

The Nicholson River metavolcanics are composed mainly of well-layered amphibolites with alternating mafic and felsic layers. Locally, the well-layered amphibolites are interlayered with iron-formation and sulphide-stained zones. The unit also includes metagreywacke with minor, interlayered mafic amphibolites, and metagabbro. Primary volcanic structures were not recognized.

Structural repetition by folding of Burwash Formation metagreywacke and Nicholson River amphibolites cannot account for the distribution of rock types in the Nicholson River metavolcanic unit. Therefore, the intercalation of amphibolitic rocks and metagreywackes in interpreted as a primary compositional layering.

Burwash Formation

Metamorphosed greywacke and greywacke-mudstone turbidites that occupy the western part of the map area are correlated with the Burwash Formation as defined at Yellowknife by Henderson (1970) as they may be traced continuously to Yellowknife where the formation has been studied in detail by Henderson (1972, 1975). During the 1989 field season, mapping of the Burwash Formation was

concentrated mainly in the Van Lake area and along the contact between the metasediments and the Cameron River metavolcanics. The Burwash Formation south of 63° 15′ N has been previously mapped by Henderson (1941a).

The contact between the Cameron River metavolcanics and the Burwash Formation is poorly exposed, although the location of the contact is apparent on aerial photographs as it is marked by a distinct topographic break with the metavolcanics forming a steep scarp that rises above the metasediments. At all localities observed, the contact is sharp and marked by strongly foliated, commonly lineated, and steeply west-dipping metavolcanics that structurally underlie Burwash Formation metasediments. In contrast to some of the areas mapped in 1988, the Cameron River metavolcanics were not found to contain interlayered metasediments near the contact with the Burwash Formation. Burwash Formation metasediments adjacent to the contact with the metavolcanics are not appreciably different with respect to composition or structure from metasediments that are several kilometres away from the Cameron River belt.

The Burwash Formation consists mainly of metamorphosed, interbedded greywacke and mudstone that are characteristically of uniform thickness and are laterally continuous across the exposed area. Greywacke is the dominant lithology in most outcrops. Greywacke beds are light-grey- or tan-weathering and generally less than 2 m thick. Mudstone beds are black-weathering and commonly less than 0.2 m thick. Greywacke beds commonly show a colour, grain size and compositional variation from light-coloured and relatively quartzo-feldspathic bases to grey- or black-weathering, finer-grained, pelitic tops.

In the Van Lake area the Burwash Formation commonly contains undeformed and unmetamorphosed dykes of granite that may be several tens of metres wide, and dykes of pegmatite that are commonly tourmaline-bearing.

From the north end of Gordon Lake, metamorphic grade in the Burwash Formation increases to the north, towards the granite which surrounds the supracrustal rocks. Two mineral isograds marking the appearance and disappearance of cordierite were mapped. Above the cordierite-in isograd rocks contain cordierite with biotite and muscovite, and locally andalusite. Rarely the rocks contain garnet and biotite as the metamorphic assemblage. Above the cordierite-out isograd rocks locally contain sillimanite-quartz nodules and up to 20 % deformed granitic veins (in situ derivation?). The concentric zonation of isograds about the granite contact suggests that the metamorphism of the supracrustal rocks is related to the intrusion of the granite.

Post-Yellowknife Supergroup intrusive rocks

Porphyritic Granite

Rocks of the Yellowknife Supergroup and the Sleepy Dragon Complex are surrounded by unmetamorphosed and massive porphyritic granite (unit 6, Fig. 1). Contacts between rocks of the Sleepy Dragon Complex and the porphyritic granite units are gradational, marked by zones of a heterogeneous mixture of granite and gneiss that are locally greater than 1 km wide. Approximate contacts on the map are placed where the proportion of granite becomes greater than that of gneiss. In contrast, the contact between the Cameron River metavolcanics and the porphyritic granite is sharp. Commonly the contact is tectonic and is marked by a zone that is several hundred metres wide of varied but progressively stained granite where strain increases towards the contact. Locally, xenoliths of Cameron River metavolcanics occur in the granite within a few metres of the contact, unequivocally demonstrating the intrusive relationship. North and west of Van Lake the contacts between the Burwash Formation and Nicholson River metavolcanics, and the granite are somewhat gradational and are marked by an increasing abundance of granite and pegmatite in the supracrustal rocks towards the contact.

The granite is white- or pink-weathering and occurs as both an alkail feldspar porphyritic granite and as an equigranular granite. Contacts between the two textural variations are gradational and occur at all scales. This unit contains less than 10 % biotite and muscovite. Muscovite is not ubiquitous. This unit also contains a minor amount of pink or white, muscovite-pegmatite and dykes of fine grained, equigranular leucogranite. East of Brown Lake the granite commonly contains up to 10 %, fine- to coarse-grained garnet.

Diabase dykes

All of the lithological units are intruded by three sets of unmetamorphosed, massive, Proterozoic diabase dykes with strikes appromixately 020°, 085° and 340°. Ages of the 020° and 085° dykes are uncertain (Indin and Dogrib respectively?). The 340° striking dykes belong to the Mackenzie (1220 Ma) set (Fahrig and West, 1986).

STRUCTURAL GEOLOGY

In this section the geometric and kinematic aspects of the structural geology are described and a tentative deformation history is proposed.

Mapping has shown that the area can be subdivided into four lithological — structural domains that contain sets of structures of distinctly different styles and, in some cases, orientation. With a few exceptions, structures from different domains do not overlap in space and their relative timing therefore cannot be unequivocally demonstrated.

Geometric and kinematic description of structures

Sleepy Dragon Complex Domain

Gneisses within the Sleepy Dragon Complex record at least two phases of deformation. The youngnest and most prominent deformation is a high ductile strain that has produced a strong foliation and protomylonitic to ultramylonitic structures that have in most places obliterated older foliations and folds of the gneissosity.

The development of the high-ductile-strain-structures is of varied extent in the gneisses. Commonly, the most

highly-strained gneisses occur 300-400 m east of the contact between the gneisses and the Cameron River metavolcanics and are separated from the metavolcanics by a zone of significantly less-strained rocks. The contact between the gneisses and the metavolcanics is commonly marked by mylonitic rocks, however, locally the gneisses adjacent to the contact have not been significantly affected by the high strain. Mineral elongation lineations in highly strained Sleepy Dragon gneisses plunge moderately to sleepy from the west to the southwest. Kinematic indicators are uncommon or equivocal, although several occurrences of asymetric feldspar porphyroclasts, shear band structures and pull-apart structures in deformed pegmatites suggest a west-side-down (i.e. normal) sense of displacement.

The Suse Lake granite contains an older, north-northeast-striking foliation that becomes progressively overprinted towards the contact with the Cameron River metavolcanics by protomylonitic and mylonitic structures. The high-ductile-structures occur in a zone of varied width adjacent to the contact, up to several hundred metres wide, and include west- to southwest-trending mineral elongation lineations. Kinematic indicators are rare, but rocks at Rick Lake contain several occurrences of shear band structures that indicate a west-side-up (i.e. thrust) sense of displacement.

Cameron River metavolcanic domain

The Cameron River metavolcanics occur in a strongly flattened and folded succession. The geometry of the contact between the Burwash Formation and the Cameron River metavolcanics and minor structures within the metavolcanics indicate that the volcanics have been folded about approximately north-northwest-striking F_1 axial surfaces and approximately west-southwest-striking F_2 axial surfaces to produce the elongate dome-shaped map pattern of the Cameron River belt.

The main metamorphic foliation throughout the Cameron River belt is approximately parallel to the margins of the belt and is axial planar to minor, isoclinal F_1 folds of the compositional layering. The prominent lineation, defined by elongation of pillows and metamorphic minerals, is west- to southwest-trending and moderately to steeply plunging. Commonly the main foliation is overprinted by a west-southwest- to southwest-striking foliation that is presumed to be axial planar to F_2. Locally, the rocks are overprinted by a third, northwest-striking foliation.

Commonly, metavolcanics adjacent to the contact with the Sleepy Dragon Complex are highly-strained within several metres of the contact. At Brown Lake (e.g. location B in Fig. 1), however, there also occurs a high strain zone that follows a prominent topographic lineament that parallels the Cameron River metavolcanic - Sleepy Dragon Complex contact. Across this zone is a significant strain gradient marked by highly stained pillow volcanics. The asymmetry of gently-plunging folds in deformed granitic veins at location B suggest a thrust sense of displacement in this zone. The extent, significance and age of this zone is uncertain.

Burwash Formation

Only a brief examination of structures in the Burwash Formation in the Van Lake area was made in 1989. To the south of Van Lake, in the Gordon Lake area, structures in the Burwash Formation have been previously described by Henderson (1941a) and Fyson (1975). In the Van Lake area, the structure in Burwash Formation metasediments is dominated by generally north-trending, tight to isoclinal and closely spaced folds that are recognized by reversals in stratigraphic facing direction. Folds have vertical- to steeply-dipping axial surfaces and steeply-plunging fold axes. The main penetrative cleavage in mudstone in this area is approximately parallel to bedding and axial planar to the folds. Rarely, the rocks display cleavage-absent, isoclinal folds that demonstrate that the dominant, map-scale folds in the Burwash Formation are not the youngest structures.

Locally, the main penetrative cleavage in mudstone beds is overprinted by a northwest-striking cleavage and both of these cleavages are overprinted by a prominent south-southwest- to southwest-striking crenulation cleavage. The second and third cleavage appear to be restricted to rocks below the cordierite-out isograd.

Porphyritic granite domain

The porphyritic granite within the area mapped is either massive or strongly deformed. The strongly deformed rocks arer restricted to the area adjacent to the contact between the Cameron River metavolcanics and the granite. Occurrences of protomylonitic to mylonitic granite form a zone that is several metres to several hundred metres thick. The principal foliation in this zone parallels the contact with the metavolcanics and the rocks may contain steeply-oblique to down-dip mineral elongation lineations. Mesoscopic kinematic indicators were not recognized in the deformed granite.

Deformation history

Pre-mylonitic structures in the gneisses and metaplutonic rocks of the Sleepy Dragon Complex are truncated by the Cameron River belt suggesting that the pre-mylonitic structures of the Sleepy Dragon Complex are older than structures in the Yellowknife Supergroup supracrustal.

The general similarity in structural style and orientation, in the Cameron River metavolcanic belt and the Burwash Formation suggests that the development of the main map-scale folds in both belts is the same age. The approximate north-south-striking isoclinal folding and steep elongation of the rocks reflects a major east-west shortening of Yellowknife Supergroup supracrustal rocks that is early syn- to syn-metamorphic. Detailed difference between the styles and orientations of structures in the metavolcanic and metasedimentary belts can be attributed to the significant contrasts in lithology.

The conflicting senses of kinematic indicators from rocks in the highly-strained contact zone between the Cameron River metavolcanics and the Sleepy Dragon Complex suggests that the contact zone may have a long and complex

history. Part of the deformation in this zone may be synchronous with the main deformation of the supracrustal rocks. The youngest ductile strain is unequivocally post-porphyritic granite and thus postdates the main deformation in the supracrustal rocks. Kinematic indicators with a thrust sense from the Suse Lake granite at the contact at Rick Lake, and from Cameron River metavolcanics in a high strain zone that parallels the contact at Brown Lake, may indicate that the contact zone had an early history of east-vergent thrusting of the metavolcanic rocks over the Sleepy Dragon Complex. Thrusting may have beem synchronous with early syn- to syn-metamorphic east-west shortening and the main deformation of the supracrustal rocks. Kinematic indicators with a normal sense in Sleepy Dragon gneisses that occur several hundred metres from the contact at Brown LAke, and from the Suse Lake granite and porphyritic granite (James 1989) indicates that the contact zone had a late history of relatively low-grade west-side down (i.e. normal) displacement. Normal displacement was late-syn- or post-prophyritic granite and may be related to post-metamorphic extension that followed the major episode of east-west shortening in this part of the Slave Province.

Metamorphic, petrofabric and geochronological studies that are currently in progress will help to substantiate or modify this tentative deformation history.

ACKNOWLEDGMENTS

My sincere thanks to Anne G. Sherman for her excellent assistance in the field. Expediting was provided by Rod Stone with the assistance of the Geology Office, Indian and Northern Affairs Canada in Yellowknife. Cees Van Staal and Dan Roach made visits to the field area. Maurice Lambert and Peter H. Thompson are thanked for critical reviews of this report.

REFERENCES

Cullen, R.
1988: Geology and structure of the Cameron River belt, Fenton Lake area; parts of NTS 85 I/15, P/2; Geology Division, Indian and Northern Affairs Canada, Yellowknife, 2 maps with notes.

Fahrig, W.F. and West, T.D.
1986: Diabase dyke swarms of the Canadian Shield; Geological Survey of Canada, Map 1627A.

Fyson, W.K.
1975: Fabrics and deformation of Archean metasedimentary rocks, Ross Lake — Gordon Lake area, Slave Province, Northwest Territories; Canadian Journal of Earth Sciences, v. 12, p. 765-776.

Geological Survey of Canada
1963: Muir Lake, District of Mackenzie, Northwest Territories, sheet 85 P/6, aeromagnetic anomaly map 293 G, Geophysics Paper 2983.

Henderson, J.B.
1970: Stratigraphy of the Yellowknife. Yellowknife Bay-Prosperous Lake area, District of Mackenzie; Geological Survey of Canada, Paper 70-26, 12 p.
1972: Sedimentology of Archean turbidites at Yellowknife, Northwest Territories; Canadian Journal of Earth Sciences, v. 9, p. 882-902.
1975: Sedimentology of the Archean Yellowknife Supergroup at Yellowknife, District of Mackenzie, Geological Survey of Canada, Bulletin 246, 62 p.
1985: Geology of the Yellowknife-Hearne Lake area, District of Mackenzie: a segment across an Archean basin; Geological Survey of Canada, Memoir 414, 135 p.

Henderson, J.B., van Breemen, O., Loverridge, W.D.
1987: Some U-Pb zircon ages from Archean basement, supracrustal and intrusive rocks, Yellowknife — Hearne Lake area, District of Mackenzie, NWT; *in* Radiogenic Age and Isotopic Studies, Geological Survey of Canada, Paper 87-2, p. 111-121.

Henderson, J.F.
1941a: Gordon Lake, District of Mackenzie, Northwest Territories; Geological Survey of Canada, Map 644A.
1941b: Gordon Lake south, District of Mackenzie, Northwest Territories; Geological Survey of Canada, Map 645A.

James, D.T.
1989: Basement-cover relations between the Archean Yellowknife Supergroup and the Sleepy Dragon Complex north of Fenton Lake, District of Mackenzie, N.W.T., *in* Current research, Part C, Geological Survey of Canada, Paper 89-1C, p. 29-36.

Lambert, M.B.
1974: Archean volcanic studies in the Slave-Bear province; *in* Report of Activities, Part A, Geological Survey of Canada, Paper 74-1A, p. 177-179.
1977: Anatomy of a greenstone belt, Slave Province, Northwest Territories; *in* Volcanic Regimes in Canada, ed. W.R.A. Baragar, L.C. Coleman and J.M. Hall; Geological Association of Canada, Special Paper 16, p. 331-340.
1982: Synvolcanic intrusions in the Cameron River volcanic belt, District of Mackenzie; *in* Current Research, Part A, Geological Survey of Canada, Paper 82-1A, p. 165-167.
1988: The Cameron River and Beaulieu River volcanic belts, District of Mackenzie, Northwest Territories; Geological Survey of Canada, Bulletin 382, 145 p.

Moore, J.C.G. Miller, M.L., Barnes, F.Q.
1951: Carp Lakes, Northwest Territories; Geological Survey of Canada, Paper 51-8, map with descriptive notes.

Puskuta Lake shear zone and Archean crustal structure in the central Kapuskasing Uplift, northern Ontario[1]

Alain D. Leclair[2]
Continental Geoscience Division

Leclair, A.D., Puskuta Lake shear zone and Archean crustal structure in the central Kapuskasing Uplift, northern Ontario; in Current Research, Part C, Geological Survey of Canada, Paper 90-1C, p. 197-206, 1990.

Abstract

The late Archean Puskuta Lake shear zone is a steep, west- to northwest-trending, dextral transcurrent, brittle-ductile shear structure, at least 60 km long, bounding the Kabinakagami Lake metavolcanic belt of the Wawa Subprovince. Its nature and close spatial relation with multilayered metavolcanic lithologies make this deformation zone a structurally-favourable site for possible gold mineralization. Two main episodes of Archean intrusions preceded emplacement of Proterozoic dykes. Four generations of Archean structures are recognized. These dykes and structures are transected by an extensive system of Proterozoic brittle faults. The crustal structure of the central Kapuskasing uplift is represented by a set of exposed lithostructural levels corresponding to a vertical section of an Archean greenstone belt down to paleodepths of 30-35 km. The composite crustal column reconstructed from the Groundhog River, Val Rita and Chapleau blocks and Abitibi Belt depicts a gross lithological transition from the lower to upper crust.

Résumé

La zone de cisaillement du lac Puskuta de la fin de l'Archéen est une structure de cisaillement cassante, ductile et abrupte, à direction d'ouest à nord-ouest et à coulissage dextre, mesurant au moins 60 km de longueur, limitant la zone volcanique métamorphisée du lac Kabinakagami de la sous-province de Wawa. Sa nature et son lien spatial étroit avec des lithologies volcaniques métamorphisées à plusieurs couches rendent cette zone de déformation structuralement favorable à une minéralisation aurifère. Deux épisodes importants d'intrusions archéennes ont précédé la mise en place de dykes protérozoïques. Quatre générations de structures archéennes ont été déterminées. Ces dykes et structures sont recoupées par un vaste système de failles cassantes protérozoïques. La structure crustale du centre du soulèvement de Kapuskasing est représentée par une série de niveaux lithostructuraux affleurants, correspondant à une coupe verticale d'une zone de roches vertes archéennes atteignant des paléoprofondeurs de 30 à 35 km. La colonne crustale composite reconstruite à partir des blocs de la rivière Groundhog, de Val Rita et de Chapleau et du domaine d'Abitibi révèle une transition lithologique globale, de la croûte inférieure à la croûte supérieure.

[1] Contribution to Canada-Ontario Mineral Development Agreement 1987-1990. Project carried by Geological Survey of Canada
[2] 510-200 Lafontaine Ave., Vanier, Ontario K1L 8K8

INTRODUCTION

The premise that the Kapuskasing uplift of the central Superior Province reveals an oblique crustal cross section of an Archean greenstone belt down to paleodepths of about 30 km (Percival and Card, 1983, 1985) warrants further investigation and full documentation for economic and scientific reasons. This project, supported by the Canada-Ontario Mineral Development Agreement (Project C.7.3), is part of a multidisciplinary study of the uplift (see G. West, Kapuskasing Structural Zone Transect) staged mainly by university and government to improve our knowledge of three-dimensional aspects of the central Superior Province. The fault-bounded Groundhog River, Val Rita and northern Chapleau blocks of the central Kapuskasing uplift (Percival, 1985; Percival and McGrath, 1986) (Fig. 1) are each characterized by distinct lithology, internal structure, metamorphic conditions and geophysical signatures (Leclair and Nagerl, 1988; Leclair and Poirier, 1989), suggesting that each tectonic block corresponds to a specific lithostructural level of the Archean crust (Leclair, 1989). Regional mapping and complementary field-oriented research in the central Kapuskasing uplift, which represents the deep crustal root of adjacent mineral-rich areas of the Abitibi and Wawa belts, are necessary and important steps to fully understand deep geological processes that may have induced mineralization at higher crustal level and for future mineral exploration in the region.

Geological mapping of the 16 500 km² Kapuskasing area (Fig. 2; see Fig. 3 for legend) was concluded during the summer of 1989 with two months of field work mainly in the Wawa and Quetico belts. This report complements two earliers one by Leclair and Nagerl (1988) and Leclair and Poirier (1989) and is, in part, based on preliminary results of ongoing laboratory studies. It contains: a) a generalized geological map of the Kapuskasing area b) a description of the newly discovered Puskuta Lake shear zone and a brief discussion on its possible regional continuation and economic significance, c) the presentation of a chronological scheme for igneous and deformational events, and d) a composite crustal column for the central Kapuskasing uplift. Description of lithological units and structural elements are given in the previous reports.

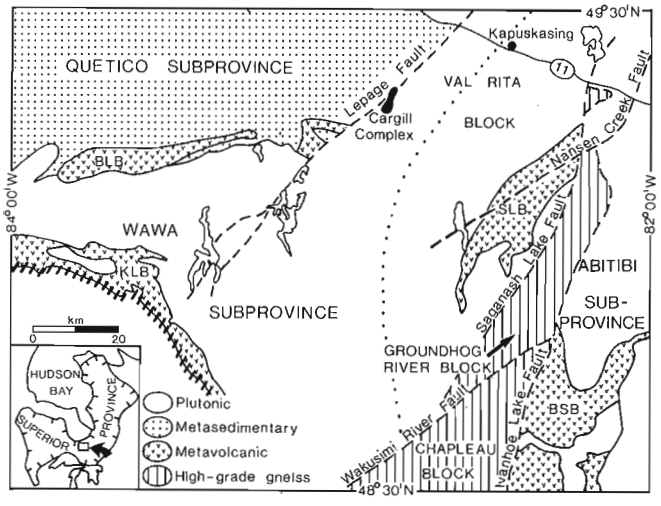

Figure 1. Location of major geological features in the Kapuskasing area showing subprovinces of the central Superior Province and regional structural elements of the Kapuskasing uplift (after Card and Ciesielski, 1986; Percival and McGrath, 1986). Inset shows the position of the Kapuskasing area in the Superior Province. Heavy diagonal lines show approximate extent of Puskuta Lake shear zone. Dotted line represents approximate axis of arcuate gravity and aeromagnetic anomalies of the Val Rita block. Metavolcanic belts are: BSB, Belford-Strachan belt; SLB, Saganash Lake belt; KLB, Kabinakagami Lake belt; BLB, Buchanan Lake belt.

PUSKUTA LAKE SHEAR ZONE

Systematic regional mapping in the southwestern part of the Kapuskasing area has outlined an arcuate, concave to the southwest, regional-scale deformation zone, Puskuta Lake shear zone, that bounds the Kabinakagami Lake metavolcanic belt on its south side (Fig. 1, 2). The shear zone was recognized by an abrupt northward transition from coarse crystalline rocks in the south to well-developed L-S tectonites. It extends for at least 60 km within the Wawa belt, from east of the Missinaibi River to the western limit of the study area, and perhaps beyond. The Puskuta Lake shear zone swings from a westerly orientation near the western edge of the map area into a northwesterly strike to the southeast, conformable with the general trend of the Kabinakagami Lake belt. It is approximately 1-2 km wide, but may exceed that where continuous compositional layering, with consistent attitude, in adjacent metavolcanic rocks is assumed to be the product of the nearby shearing process. Northeast-trending brittle faults which create subtle topographic effects transect the shear zone at several places.

North of the shear zone, the rhythmic succession of felsic, intermediate and mafic metavolcanic rocks of the Kabinakagami Lake belt coincides with a strong southeast-trending positive aeromagnetic anomaly (Geological Survey of Canada, 1984). These rocks, especially those in the southern part of the belt, are most commonly fine- to locally medium-grained with well-developed, strain-induced compositional layering. There is no direct field evidence that they had a volcanic precursor, because any primary features would have been obliterated by the intense deformation and amphibolite-facies metamorphism. However, they represent the along-strike easternmost extremity of the extensive Kabinakagami Lake metasedimentary-metavolcanic belt in the adjacent map-area to the west (cf. Thurston et al., 1977). Within the Puskuta Lake shear zone, rocks of this belt have been subjected to extreme deformation primarily in the ductile regime, followed by an episode of brittle faulting. A pluton of massive, biotite-bearing, K-feldspar megacrystic granite, with foliated margins, occurs within the widest part of the belt. The metavolcanic rocks are also intruded by foliated and gneissic hornblende-biotite tonalite plutons. To the north, the Kabinakagami Lake belt is intruded by a large batholith of dominantly massive, fine- to medium-grained, white, biotite leucogranodiorite and associated pegmatite, containing numerous xenoliths of psammitic metasedimentary rocks of uncertain provenance. The northern exposures

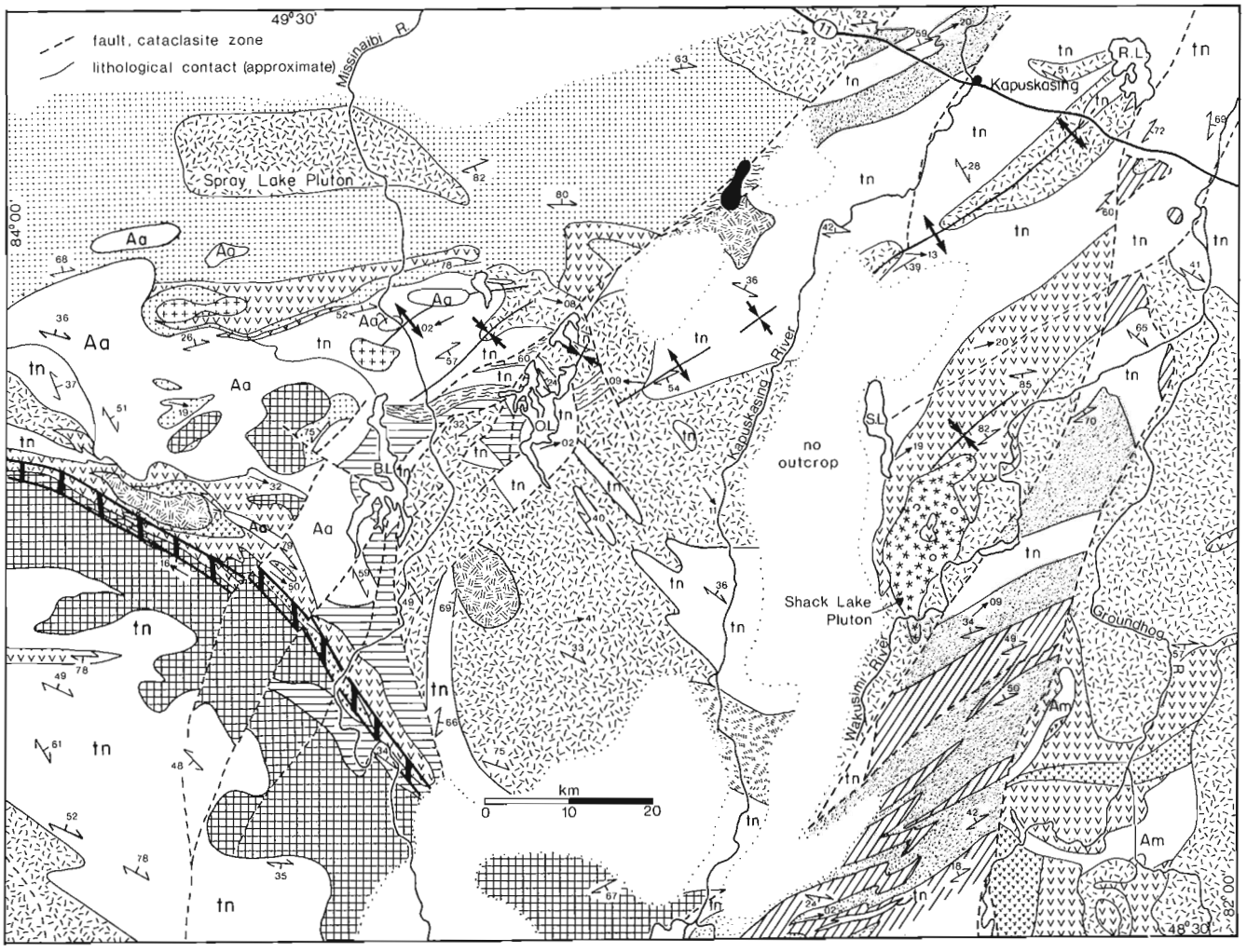

Figure 2. Generalized geological map of the Kapuskasing area, comprising the south half of Kapuskasing (NTS 42G) and the north half of Foleyet (NTS 42B) map areas. It includes areas originally mapped by McMurchy (1960), Bennett et al. (1967), Bennett (1969), Thurston et al. (1977). and Berger et al. (1986). R.L. - Remi Lake; S.L. - Saganash Lake: O.L. - Opasatika Lake; B.L. - Brunswick Lake. See figure 3 for legend.

LITHOLOGIC UNITS

Proterozoic

carbonatite complex

Archean or Proterozoic

syenite-monzonite-diorite

Archean

massive intrusive rocks

Aa — Bi leucogranodiorite, Bi±Mu±Ga pegmatite

Hn-Bi quartz monzonite, granodiorite, monzogranite

granite (locally megacrystic)

foliated to massive Bi-Ep±Mt granodiorite to tonalite

porphyritic Hn quartz diorite to diorite (~2691 Ma)

Am — diorite, gabbro, pyroxenite

foliated Bi-Hn mafic tonalite (homogeneous)

tn — Hn-Bi tonalite to granodiorite gneiss (xenolithic)

gneissic granite

psammitic metasediments

felsic metavolcanic rocks

mafic to intermediate metavolcanic rocks

migmatitic paragneiss

migmatitic mafic gneiss

STRUCTURES

fault, cataclasite zone

shear zone

F_3 synform axial trace

F_3 antiform axial trace

46 — F_2 fold axis lineation

46 — S_1 foliation, layering

Figure 3. Legend for geological map of Kapuskasing area shown in Figure 2. Preliminary U-Pb age determination is from Leclair and Sullivan (unpublished data).

of the batholith have an aluminous mineralogy, characteristic of S-type granitoids of the Quetico subprovince (Percival, 1988a). This could be used to imply that the Quetico-Wawa subprovince boundary is farther south than previously suggested by Berger (1985).

The Puskuta Lake shear zone grades to the south into medium- to coarse-grained, white to light pink, hornblende-biotite granodiorite to quartz monzonite with subordinate monzogranite. Away from the high-strain zone, these granitoid rocks are massive and homogeneous, to locally mildly foliated. They contain accessory epidote and sphene and less than 1 % mafic xenoliths composed of hornblende-plagioclase-quartz ± clinopyroxene. Some outcrops display a porphyritic texture with K-feldspar phenocrysts up to 1 cm long. Field relationships suggest that this unit is intrusive into biotite-epidote ± sphene ± magnetite tonalitic gneisses in the southwest corner of the map area. Along the southern flank of the shear zone, the granitoid has been transformed into a very distinctive L-S tectonite (Fig. 4), in sharp contrast with its originally undeformed, isotropic state.

The segment of the Puskuta Lake shear zone within the map area defines the contact between the felsic to mafic metavolcanic rocks of the Kabinakagami Lake belt and the pluton of granodiorite-quartz monzonite to the south. This highly sheared contact is interpreted to have been previously intrusive based on the occurrence of tectonically transposed, thin, leucocratic granitoid dykes in well-layered amphibolite and felsic rocks, and elongated lenses of layered amphibolite enclosed in sheared granitoid. Thus, the protomylonites and mylonites in the shear zone are demonstrably derived, in part, from a protolith of medium- to coarse-grained, isotropic, hornblende-biotite granodiorite and, in part, from the closely interlayered lithologies of the Kabinakagami Lake belt. The latter appears to constitute the predominant protolith, although tectonically degraded plutonic rocks are not everywhere distinguishable from the fine-grained metamorphic rocks. At some localities southeast of Puskuta Lake, grey to light grey, very fine-grained, laminated, flinty mylonites are possibly derived at the expense of felsic metavolcanic rocks. Thin seams of ultramylonite have also been observed in these rocks. Numerous, discrete, outcrop-scale, high-strain zones are recognized troughout the metavolcanic belt, and possibly represent splays of the main shear zone. The intense ductile deformation more or less coincident with the volcano-plutonic contact generated a roughly 2 km-wide corridor of mixed tectonites.

The tectonites within and adjacent to the shear zone have steeply north- to northeast-dipping foliation and subhorizontal stretching lineation. In the mylonitic metavolcanic rocks, the foliation is defined by millimetric to centimetric compositional layering (Fig. 5) and a mineral alignment of mainly hornblende. The granodiorite tectonite has a pervasive biotite foliation that dips systematically between 65 and 90 degrees toward the north and northeast. A stretching lineation, expressed as streaked-out and elliptical quartzofeldspathic aggregates, quartz aggregates and mineral alignment, is generally well developed in the mylonitic granodiorite but uncommon in the metavolcanic rocks. It undulates gently in the plane of the steep foliation, with a plunge that varies between 25 degrees and the horizontal in either direction. Dispersed K-feldspar porphyroclasts (less than 0.5 cm across) in the granodiorite tectonite are extremely sericitized but retain a subangular shape, whereas quartz occurs typically in the form of ribbons. The mylonitic fabric is broadly concordant with the regional fabric in the enclosing, less-deformed rocks, but is not necessarily contemporaneous.

The absolute age of the Puskuta Lake shear zone has not been determined. However, field relations provide some constraints on the relative age. All granitoid rocks and associated cross-cutting pegmatites have been affected by the deformation within the zone, with the exception of one set of late, undeformed pegmatite dykes that cut mylonites. Preliminary U-Pb age results on some massive and foliated

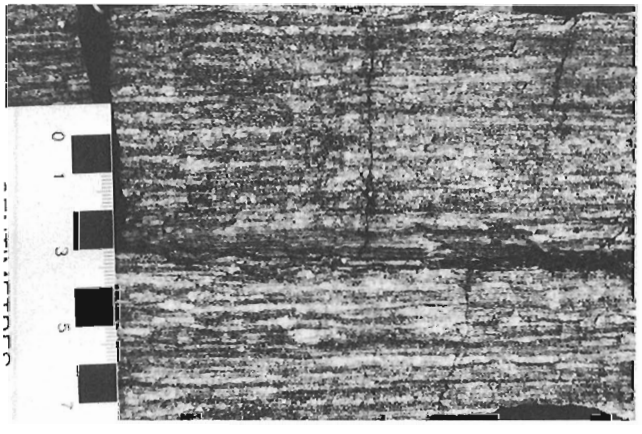

Figure 4. Well-developed L-S tectonite in the Puskuta Lake shear zone derived at the expense of hornblende-biotite granodiorite and showing ribbon quartz and a stretching lineation expressed by quartzofeldspathic aggregates. Scale is in centimetres. (GSC 205018-D).

Figure 5. Highly sheared, interlayered mafic to felsic metavolcanic rocks of the Kabinakagami Lake belt in the Puskuta Lake shear zone displaying well-developed, millimetric to centimetric, strain-induced compositional layering. (GSC 205018-B).

granitoid rocks in the Kapuskasing area indicate crystallization between 2686 Ma and 2700 Ma (Leclair and Sullivan, unpublished data), consistent with similar age for post-tectonic plutons in the Wawa gneiss terrane (Frarey and Krogh, 1986; Corfu and Muir, 1989). This is interpreted as representing an approximate upper age limit for the deformation zone. The lower age limit is provided by the north-northwest-trending mafic dykes of the Hearst swarm, which cut cleanly across the mylonitic fabric (Fig. 6). U-Pb systematics for zircons from a Hearst dyke in the southern Kapuskasing uplift yield a precise age of 2454 Ma (Heaman, 1988). Major displacement along the Puskuta Lake shear zone thus occurred in the late Archean (post-2686 Ma and pre-2454 Ma), similar in timing to several regional-scale deformation zones elsewhere in the central Superior Province (cf. Osmani et al., 1989). Work is underway to obtain a more accurate age, by dating euhedral sphene, believed to have crystallized during the high-temperature deformation.

The steep mylonitic foliation and complementary subhorizontal stretching and mineral lineations in the tectonites attest to dominantly transcurrent displacement along the Puskuta Lake shear zone. Kinematic indicators such as z-style asymmetric folds, rolled K-feldspar porphyroclasts and rare asymmetric pressure shadows demonstrate a dextral sense of shear. The broad clockwise deflection of the prominent southeast-trending magnetic signature produced by metavolcanic rocks of the Kabinakagami Lake belt also suggests a dextral shear sense. A planned follow-up study of oriented samples should corroborate field indications. The finite dextral displacement along the zone is unknown. However, the possibilities that the Puskuta Lake shear zone dissipates or is offset by faults before reaching the Kapuskasing zone should be considered, as no mylonite could be found along the southeastern projection of the deformation zone.

There is some evidence to suggest that comparable grades of metamorphism occur on both sides of the Puskuta Lake shear zone. Mafic xenoliths in granitoid rocks to the south consist of hornblende, plagioclase, quartz with or without clinopyroxene, diagnostic of amphibolite-facies metamorphism. North of the shear zone, mafic metavolcanic rocks are amphibolites, some containing garnet porphyroblasts. Also, pelitic schist containing the assemblage garnet-staurolite-biotite-muscovite-plagioclase-quartz occurs at one locality within the Kabinakagami Lake belt. Within the shear zone itself, tectonite with stable hornblende suggests that ductile deformation occurred at amphibolite facies conditions. Some mylonites contain secondary chlorite, indicative of waning temperature effects or later alteration.

DISCUSSION

Regional continuation of the Puskuta Lake shear zone

The westward continuation and linkage of the Puskuta Lake shear zone with previously mapped regional-scale deformation zones, with respect to geological setting and field relations, are discussed in this section. First, the Puskuta Lake shear zone occurs in the northern part on the Wawa belt and generally separates granitoid batholiths of this belt from a transitional zone of mixed supracrustal and intrusive rocks with both Wawa- and Quetico-belt affinities (Leclair and Poirier, 1989). At 49°N near the western edge of the map area, L-S tectonites within the shear zone display a well-developed mylonitic fabric that strikes west. Assuming that the zone remains generally parallel to the dominant structural grain, the Puskuta Lake shear zone projects toward Killala Lake shear zone which stretches along similar latitude in an east-west direction. The latter is a moderately north-dipping, dip-slip, ductile deformation zone which parallels the stratigraphy and broadly corresponds with the northern boundary of the Wawa belt (Williams, 1987, 1988). However, the Killala Lake shear zone predates the emplacement of granitoid batholiths, in apparent contradiction with the timing of the Puskuta Lake shear zone discussed above. On the other hand, motion along both shear zone appears to have occurred under prograde or high-grade conditions, coeval with amphibolite-facies metamorphism. As a result, a possible connection between the Puskuta Lake and Killala Lake shear zones is enigmatic. Nonetheless, the regional continuation of these deformation zones bears significantly upon their tectonic importance and should be considered in future models of large-scale belt accretion.

Economic significance

Shear zones are commonly mineralized, as indicated by the voluminous literature on the subject (e.g. Bursnall et al., 1989; references therein); and the Puskuta Lake shear zone may be no exception. In the Kapuskasing area, there is evidence for at least minor mineralization in the sheared metavolcanic rocks of the Kabinakagami Lake belt. At a few localities, rusty, sulphide-rich veins and pods, up to several metres long, occur in highly fractured, siliceous mylonitic rocks, possibly derived from a felsic volcanic protolith. These mineralized zones are commonly associated with segregations of quartz which also form a network of cross-cutting veins throughout the metavolcanic suite. All of these features appear to be related to a brittle deformational event

Figure 6. Mylonitic fabric developed in leucocratic granodiorite tectonite transected by an undeformed mafic dyke of the Hearst swarm, with white plagioclase phenocrysts. (GSC 205018-A).

that is relatively younger than ductile shearing. Several mineralized zones of the Kabinakagami Lake belt, with possible economically viable deposits, are under investigation by exploration firms.

In many regions of northern Ontario, gold mineralization is commonly associated with generally east-trending, major, transcurrent shear systems that tend to follow granite/volcanic contacts because of competency contrasts (e.g. Colvine et al., 1988; Osmani et al. 1989; references therein). The Puskuta Lake shear zone offers this sort of geological setting over a distance of several tens of kilometres. The mixed felsic to mafic metavolcanic rocks of the Kabinakagami Lake belt represent a potential source for gold and other precious metals and possess the contrasting rheological properties that encourage mineralization (cf. Kerrich, 1989a, b). The ductile and brittle nature of the Puskuta Lake shear zone and its close spatial relation with this multilayered volcanic sequence classify this deformation zone as a structurally favourable site and potentially important target for gold mineralization.

CHRONOLOGY

A tentative chronological scheme for igneous and deformational events in the Kapuskasing area based on field relations and age determinations is outlined below. It is subject to revision, pending additional geochronological results (Leclair and Sullivan, in preparation). The main regional-scale episodes of magmatism and deformation are included in this generalized scheme, with some local events.

Igneous events

Archean

1) tonalitic magmatism: emplacement of tonalite sheets and formation of a tonalitic to granitic leucosome phase defining the gneissic layering, coeval with regional metamorphism and deformation.
Late: cross-cutting hornblende-bearing tonalitic sweats in tonalite gneiss.
2) emplacement of a voluminous suite of massive to foliated, syn- to post-tectonic granitoid plutons and formation of pegmatites from about 2700 to 2686 Ma.
Late: intrusion of a least two sets of late-stage pegmatite dykes of mainly granitic composition.

Proterozoic

3) emplacement of north- to northwest-trending diabase dykes of Hearst/Matachewan swarm.
4) emplacement of northeast-trending quartz diabase dykes of Preissac swarm.
5) emplacement of northeast-trending diabase dykes of Kapuskasing swarm.
6) intrusion of the Cargill carbonatite complex and associated ultramafic to felsic dykes along the trace of the Lepage fault.

Deformational events

Archean

1) production of pervasive foliation and gneissic layering (S_1).
2) development of mesoscopic, tight to open folds (F_2) of the S_1 surface, with rare axial-surface fabrics.
3) development of megascopic, northeast-trending, tight to gentle, upright folds (F_3) without an associated planar fabric.
Late: rare extensional shears bounding less-deformed "lozenge" structures in tonalite gneisses, and possibly related to a conjugate set of roughly northwest-striking ductile shear bands.
4) transcurrent, ductile movement along the northwest- to west-striking, 2-km wide Puskuta Lake shear zone.

Proterozoic

5) regional brittle faulting possibly associated with displacement along major north- to northeast-trending faults.

ARCHEAN CRUSTAL STRUCTURE

The distinct lithological, structural, metamorphic and geophysical character of the fault-bounded Groundhog River, Val Rita and Chapleau blocks in the central Kapuskasing uplift (Leclair and Nagerl, 1988; Leclair and Poirier, 1989) is interpreted as a first approximation that each tectonic block corresponds to a specific lithostructural level of the crust (Leclair, 1989). In order to eliminate the geological and geophysical disparities that are due to inherent lateral variability of the rocks, lithostructural domains are defined primarily based on their calculated paleodepths from metamorphic geobarometry. These different lithostructural domains have been juxtaposed as a result of large movement on late faults, some of which have crustal dimensions. Major movement may have preceded emplacement of the arcuate Hearst/Matachewan dyke swarm at 2454 Ma (Percival et al., 1989), but an episode of regional brittle faulting must have occurred in the interval between the emplacement of the Kapuskasing dyke swarm and Cargill carbonatite complex, dated respectively at 2040 Ma (Hanes et al., 1986) and 1888 Ma (Heaman, pers. comm., 1988). Estimates of vertical displacement on major faults derived from paleopressure determinations (Fig. 7) using various mineralogical geobarometers range between about 5 and 15 km (Percival and McGrath, 1986; Leclair, unpublished data). Consequently, it is estimated that structural levels representing up to approximately 20 km of vertical section are exposed in the Kapuskasing area. A reconstruction permits conclusions on the gross Archean crustal structure of the region.

Lithostructural character

In general, there is a relationship between the lithology and metamorphic grade within the Kapuskasing area. The regional pattern can be read directly from the combined geological and metamorphic pressure maps (Fig. 2, 7).

Interlayered migmatitic mafic gneiss and paragneiss in the granulite facies (7-10 kbar) are restricted to the Groundhog River, northern Chapleau and northwestern Val Rita blocks. The Goundhog River block also includes upper amphibolite facies tonalite gneiss. The Val Rita block consists mainly of heterogeneous and xenolithic tonalite gneisses in the amphibolite facies (5-7 kbar) and a voluminous suite of foliated and massive granitoid plutons (4-5 kbar). Metavolcanic rocks, metamorphosed to greenschist and amphibolite facies (4-5 kbar), and associated massive intrusive rocks occur in the eastern Val Rita block, Wawa and Abitibi belts. Psammitic metasedimentary rocks of the Quetico belt have comparable metamorphic grades. The map pattern of these lithological metamorphic packages reflects a set of crustal megalayers (cf. Percival and Card, 1985; Percival, 1989b) presumed to have had a vertical arrangement prior to being transected and shifted by major faults. Large displacements on these structures resulted in the juxtaposition of different lithostructural domains of the lower, middle and upper crust (Leclair, 1989).

A map summarizing trends of the foliation across the map area (see Fig. 5 in Leclair and Nagerl, 1988) indicates a regional variation in structural style concomitant with changing lithologies and grades of metamorphism. For instance, granulite-facies gneisses of the Groundhog River and northern Chapleau blocks as well as those along the western edge the Val Rita block have consistent gentle to moderate northwest-dipping foliation. This abruptly changes to moderately-dipping and subhorizontal rolling geometries, with an overall chaotic orientation, in amphibolite-facies tonalite gneisses of the Val Rita block. A subvertical foliation is restricted to greenschist and amphibolite facies metasedimentary and metavolcanic belts in the area.

Vertical crustal reconstruction

The vertical reconstruction of the Archean crust in the central Kapuskasing uplift is based on interrelations displayed between paleopressure estimates, lithological, structural

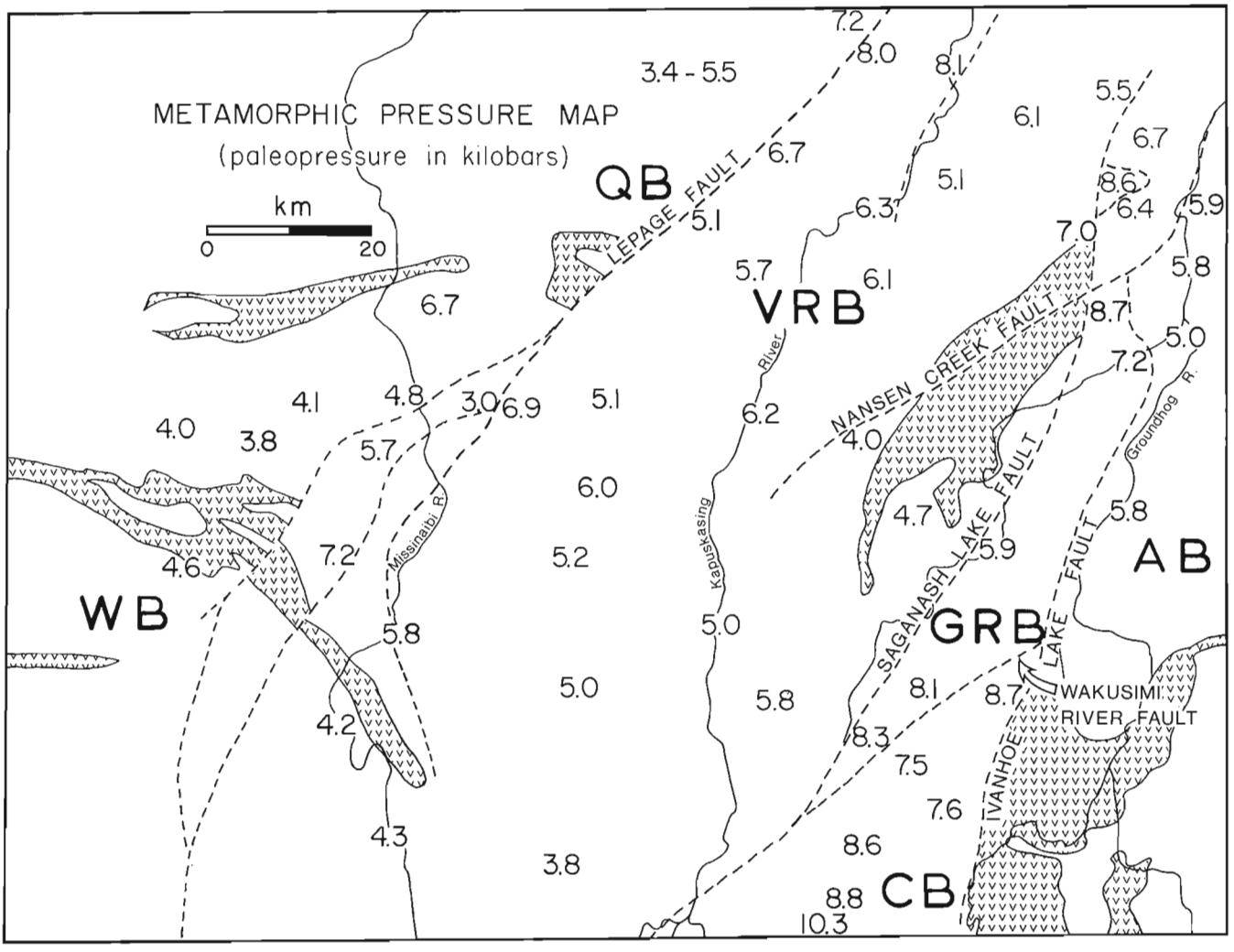

Figure 7. Simplified metamorphic pressure map showing preliminary results of paleopressure estimates, derived form various mineralogical geobarometers (Leclair, 1989; unpublished data), for the Groundhog River (GRB), Val Rita (VRB) and northern Chapleau (CB) blocks, and adjacent Quetico (QB), Wawa (WB) and Abitibi (AB) belts. Compare with Figures 1 and 2.

and geophysical data (Leclair, 1989; unpublished data). From this information, it is suggested that lithostructural domains realigned in their original configuration display a section of the crust from paleodepths of 10-15 km to those of 30-35 km. The diagrammatic crustal columns of the Groundhog River, Val Rita and northern Chapleau blocks and westernmost Abitibi belt, with their inferred tectonic relationships, are shown in Figure 8. Together, they depict a gross and continuous lithological transition toward successively higher structural levels from mafic gneiss, paragneiss, tonalite gneiss, foliated granitoid, to metavolcanic and associated massive intrusive rocks. The lithological package of dominantly granulite gneisses of the Chapleau block is interpreted as representing the deepest available window to the lower crust in the central Kapuskasing uplift. It displays some geological and geophysical characteristics distinct from those of the Groundhog River block (Leclair, 1988), implying juxtaposition of two originally separated rock assemblages, with the Chapleau block most likely derived from a slightly deeper level. The regional pattern in the paleopressure estimates across the normal-fault-bounded Val Rita block (Fig. 7; Leclair, unpublished data), which corroborates a paleodepth gradient predicted from gravity modelling (Percival and McGrath, 1986), translates into a complete lithological transition from the lower to upper crust. Greenstone-granite terranes of the Abitibi belt represent the highest crustal levels of the section. They probably correspond to a similar lithological 'package' that capped the granitoid rocks of the Val Rita block prior to regional uplift.

SUMMARY

The newly discovered, arcuate, brittle-ductile Puskuta Lake shear zone bounds the Kabinakagami Lake metavolcanic belt of the Wawa subprovince. Dextral transcurrent displacement of unknown magnitude along this steep shear structure has produced a roughly 2-km wide belt of mixed

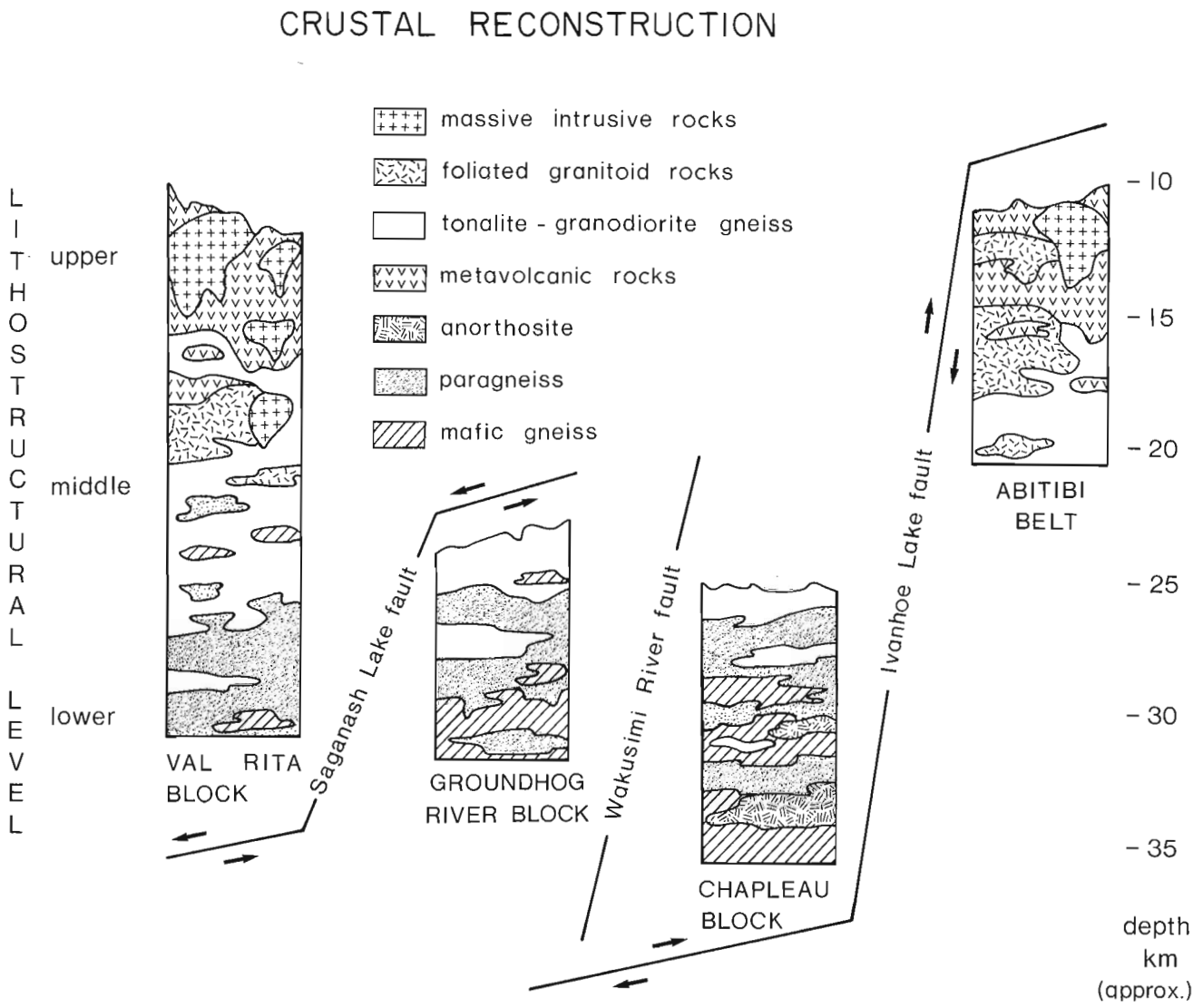

Figure 8. Diagrammatic vertical crustal reconstruction of the Archean crust revealed in the central Kapuskasing uplift, and inferred tectonic relationships between the Groundhog River, Val Rita and Chapleau blocks and westermost Abitibi belt.

L-S tectonites derived at the expense of hornblende-biotite granodiorite and mafic to felsic metavolcanic rocks. Puskuta Lake shear zone is part of an extensive network of regional-scale deformation zones that parallel subprovince boundaries in the Superior Province and are commonly mineralized.

In a generalized chronological scheme for igneous and deformational events, two main episodes of Archean magmatism and three set of Proterozoic diabase dykes, followed by emplacement of the alkalic/carbonatite Cargill complex, are recognized in the central Kapuskasing uplift. Three generations of Archean structures predate the emplacement of a voluminous suite of massive granitoid plutons. Transcurrent movement along the Puskuta Lake shear zone postdates the emplacement of these plutons. An extensive brittle fault system developed after emplacement of the Proterozoic dykes and before that of the Cargill complex.

The geological and geophysical disparities displayed within and among tectonic blocks of the central Kapuskasing uplift are interpreted to reflect different lithostructural levels of the crust, that were juxtaposed as result of about 5 to 15 km of vertical displacement along major northeast-trending faults. These lithostructural domains, defined primarily on the basis of their calculated paleopressures, represent approximately 20 km of vertical section exposed in the Kapuskasing area. The composite crustal column reconstructed from lithostructural domains in the Groundhog River, Val Rita and Chapleau blocks and Abitibi belt depicts the gross crustal structure of an Archean greenstone belt down to paleodepths of 30-35 km.

ACKNOWLEDGMENTS

John Everest (Carleton University) is thanked for able and enthusiastic field assistance. Field visits by and discussions with John Percival, John Bursnall, Gordon West, Cathy Shrady, John Hanes, Mike Perz and Cindy Harnett (Northern Times staff reporter) are greatly appreciated. Marc Lévesque (Lévesque Lumber Ltd.) is thanked for his information on the accessibility of some areas and his interest and help in our mapping program. Richard Lambert and Rainy Gruenewald (Ministry of Natural Resources) supplied up-to date air photos, without which mapping would have been impractical in a labyrinth of newly constructed logging roads. George Thériault (Air Ivanhoe Ltd.) and Ed. Coulombe (Hearst Air Service Ltd.) provided fixed-wing transportation to remote areas. Wayne Bolen (Huisson Aviation Ltd.) guaranteed skillful and safe helicopter landings. Brigitte Leclair helped with the drafting of figures. John Percival and Tony Davidson critically read the manuscript. Lithoprobe contribution no. 22.

REFERENCES

Bennett, G.
1969: Geology of the Belford-Strachan area, District of Cochrane; Ontario Department of Mines, Geological Report 78, 30 p.

Bennett, G., Brown, D.D., George, P.T., and Leahey, E.J.
1967: Operation Kapuskasing; Ontario Department of Mines, Miscellaneous Paper 10, 98 p.

Berger, B.R.
1985: Hearst-Kapuskasing area, District of Cochrane; Ontario Geological Survey, Miscellaneous Paper 126, p. 95-98.

Berger, B.R., MacMillan, D.W., and Roy, P.L.
1986: Precambrian geology of Rykert, Fergus and parts of Abbott and Opasatika Townships, Hearst-Kapuskasing area, Algoma and Cochrane Districts; Ontario Geological Survey, Preliminary Map p. 2962, scale 1:31,680.

Bursnall, J.T., Hodgson, C.J., Hubert, C., Kerrich, R.W., Marquis, P., Murphy, J.B. Osmani, I., Poulsen, H., Robert, F., Sanborn-Barrie, M., Stott, G., and Williams, H.R.
1989: Mineralization and Shear Zones; Geological Association of Canada, Short Course Notes, v. 6, 299 p.

Card, K.D., and Ciesielski, A.
1986: Subdivisions of the Superior Province of the Canadian Shield; Geoscience Canada, v. 13, p. 5-13.

Colvine, A.C., Fyon, J.A., Heather, K.B., Marmont, S., Smith, P.M., and Troop. D.G.
1988: Archean lode gold deposits in Ontario; Ontario Geological Survey, Miscellaneous Paper 139, 136 p.

Corfu, F., and Muir, T.L.
1989: The Hemlo-Heron Bay greenstone belt and Hemlo Au-Mo deposit, Superior Province, Ontario, Canada; Chemical Geology, v. 79, p. 183-223.

Frarey, M.J. and Krogh, T.E.
1986: U-Pb zircon ages of late internal plutons of the Abitibi and eastern Wawa subprovinces, Ontario and Quebec; *in* Current Research, Part A, Geological Survey of Canada, Paper 86-1A, p. 43-48.

Geological Survey of Canada
1984: Magnetic anomaly map. Timmins (NM-17); Map NM-17-M; scale 1:1 000 000.

Hanes, J.A., Archibald, D.A., and Lee, J.K.W.
1986: Reconnaissance $^{40}Ar/^{39}Ar$ geochronology of Kapuskasing, Matachewan, and Hearst dykes in the Kapuskasing structural zone and adjacent Abitibi and Wawa greenstone belts, Ontario; Geological Association of Canada, Program with Abstracts, v. 11, p. 77.

Heaman, L.M.
1988: A precise U-Pb zircon age for a Hearst dyke; Geological Association of Canada, Program with Abstracts, v. 13, p. A53.

Kerrich, R.
1989a: Geodynamic setting and hydraulic regimes: shear zone hosted mesothermal gold deposits: *in* Mineralization and Shear Zones, ed. J.T. Bursnall, Geological Association of Canada, Short Course Notes, v. 6, p. 89-128.
1989b: Geochemical evidence on the sources of fluids and solutes for shear zone hosted mesothermal Au deposits; *in* Mineralization and Shear Zones, ed. J.T. Bursnall, Geological Association of Canada, Short Course Notes, v. 6, p. 129-197.

Leclair, A.D.
1988: Geological and geophysical characteristics of the northern Kapuskasing uplift; *in* Scientific Drilling: The Lower Crust and Kapuskasing Structural Zone, ed. M.J. Drury, Canadian Continental Drilling Program Report 88-1, p. 16.
1989: The third dimension of the central Kapuskasing uplift interpreted from geological and geophysical data; Geological Association of Canada, Program with Abstracts, v. 14, p. A102.

Leclair, A.D., and Nagerl, P.
1988: Geology of the Chapleau, Groundhog River and Val Rita blocks, Kapuskasing area, Ontario; *in* Current Research, Part C, Geological Survey of Canada, Paper 88-1C, p. 83-91.

Leclair, A.D., and Poirier, G.G.
1989: The Kapuskasing uplift in the Kapuskasing area, Ontario; *in* Current Research, Part C, Geological Survey of Canada, Paper 89-1C, p. 225-234.

McMurchy, R.C.
1960: Geology of the Saganash-Wakusimi Lake area; Ontario Department of Mines, v. 69, Part 3, 19 p.

Osmani, I.A., Stott, G.M., Sanborn-Barrie, M., and Williams, H.R.
1989: Recognition of regional shear zones in south-central and northwestern Superior Province of Ontario and their economic significance; *in* Mineralization and Shear Zones, edited by J.T. Bursnall, Geological Association of Canada, Short Course Notes, v. 6, p. 199-218.

Percival, J.A.
1985: The Kapuskasing structure in the Kapuskasing-Fraserdale area, Ontario; *in* Current Research, Part A, Geological Survey of Canada, Paper 85-1A, p. 1-5.
1989a: A regional perspective of the Quetico metasedimentary belt, Superior Province, Canada; Canadian Journal of Earth Sciences, v. 26, p. 677-693.
1989b: The Kapuskasing uplift: A window on the deep crust of the Superior Province; Geological Association of Canada, Program with Abstracts, v. 14, p. A102.

Percival, J.A., and Card, K.D.
1983: Archean crust as revealed in the Kapuskasing uplift, Superior Province, Canada; Geology, v. 11, p. 323-326.
1985: Structure and evolution of Archean crust in central Superior Province, Canada; *in* Evolution of Archean Supracrustal Sequences, ed. L.D. Ayres et al., Geological Association of Canada, Special Paper 28, p. 179-192.

Percival, J.A., and McGrath, P.H.
1986: Deep crustal structure and tectonic history of the northern Kapuskasing uplift of Ontario: An integrated petrological-geophysical study; Tectonics, v. 5, p. 553-572.

Percival, J.A., Green, A.G., Milkereit, B., Cook, F.A., Geis, W., and West, G.F.
1989: Lithoprobe reflection profiles cross exposed deep crust: Kapuskasing uplift, Nature, v. 342, p. 416-420.

Thurston, P.C., Siragusa, G.M., and Sage, R.P.
1977: Geology of the Chapleau area, Districts of Algoma, Sudbury, and Cochrane; Ontario Division of Mines, Geoscience Report 157, 293 p.

Williams, H.R.
1987: Structural studies in the Beardmore-Geraldton belt and in the Quetico and Wawa subprovinces; *in* Summary of Field Work and Other Activities 1987, ed. R.B. Barlow et al., Ontario Geological Survey Miscellaneous Paper 137, p. 90-92.
1988: Geological studies in the Wawa, Quetico, and Wabigoon subprovinces, with emphasis on structure and tectonic development; *in* Summary of Field Work and Other Activities 1988, ed. R.B. Barlow et al., Ontario Geological Survey Miscellaneous Paper 141, p. 169-172.

Physical volcanology and sedimentology of lower Dubawnt Group strata, Dubawnt Lake, District of Keewatin, N.W.T.

R.H. Rainbird[1] and T.D. Peterson
Continental Geoscience Division

Rainbird, R.H. and Peterson, T.D., Physical volcanology and sedimentology of lower Dubawnt Group strata, Dubawnt Lake, District of Keewatin, N.W.T.; in Current Research, Part C, Geological Survey of Canada, Paper 90-1C, p. 207-217, 1990.

Abstract

The Christopher Island and Kunwak formations were deposited between about 1.9-1.8 Ga in a series of narrow east-northeast-trending fault-bounded basins exposed on the north and southeast margins of Dubawnt Lake. The Christopher Island Formation comprises a suite of potassic and ultrapotassic lavas and subordinate pyroclastic rocks possibly erupted from fissures developed along basin margin faults. Intercalated alluvial conglomerates and debris-flow breccias represent subaerial reworking of these deposits. A subsequent episode of uplift and faulting without associated volcanism controlled deposition of the overlying Kunwak Formation, a sequence of alluvial conglomerates and associated braidplain deposits. These rocks form exceptionally thick accumulations deposited perhaps by "conveyor belt" stacking adjacent to strike-slip (?) fault scarps from which they were derived.

Résumé

Les formations de Christopher Island et de Kunwak se sont déposées entre 1,9 et 1,8 Ga environ, dans une série d'étroits bassins limités par des failles à direction est-nord-est qui affleurent sur les bords nord et sud-est du lac Dubawnt. La formation de Christohper Island comprend une suite de laves potassiques et ultrapotassiques et des roches pyroclastiques subordonnées ayant peut-être fait éruption à partir de fissures formées le long de failles en bordure de bassin. Les conglomérats de sédiments alluviaux et les brèches de coulées boueuses intercalés correspondent à un remaniement subaérien de ces dépôts. Un épisode ultérieur de soulèvement et de formation de failles sans volcanisme associé a régi le dépôt de la formation de Kunwak sus-jacente, séquence de conglomérats alluviaux et de sédiments de plaines de chenaux anastomosés associés. Ces roches forment des accumulations exceptionnellement épaisses déposées peut-être par une « zone convoyeuse » empilée près d'escarpements de failles à rejet horizontal (?) d'où proviennent les roches.

[1] Department of Geology, University of Western Ontario, London, Ontario N6A 5B7.

INTRODUCTION

Investigations during the latter part of July and August 1989 included a continuation of 1 : 50 000 scale mapping of the lower Dubawnt Group in the Dubawnt Lake area initiated in 1988 (Peterson et al., 1989). Emphasis was to further delineate the regional distribution and stratigraphic relationships of the rocks of the Kunwak and Christopher Island formations and to characterize their depositional mechanisms. This paper is intended as an accompaniment to Peterson and Rainbird (1990) and will provide additional constraints on the tectonic evolution of early Proterozoic basins in northern Churchill Province.

GENERAL GEOLOGY

The Dubawnt Group (Donaldson, 1965) is a succession of terrestrial clastic and volcanic rocks which were deposited in a series of roughly east-northeast-trending fault-bounded basins. They occur in a 100-150km wide belt extending from Dubawnt Lake in the southwest to Baker Lake, 400km to the northeast (LeCheminant et al., 1979, 1987; Blake, 1980; Peterson et al., 1989; Peterson and Rainbird, 1990; *see* Fig. 1). Tectonic aspects of the region are discussed in more detail by Peterson and Rainbird (1990).

The lower Dubawnt Group includes, in ascending stratigraphic order, the South Channel-Kazan, Christopher Island and Kunwak formations and is unconformably overlain by the middle and upper Dubawnt Group which includes the Pitz and Thelon formations (Fig. 2). In the Dubawnt Lake area, lower Dubawnt Group strata unconformably overlie a complex assortment of Archean and granitic rocks.

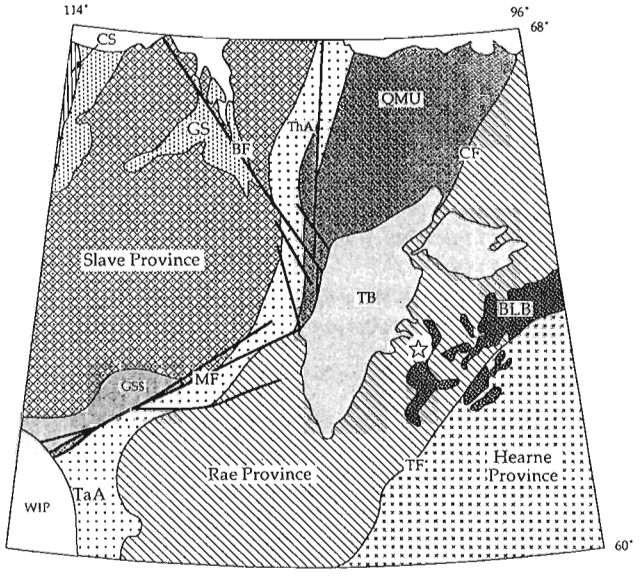

Figure 1. Tectonic elements in the region of the Slave and Churchill provinces. Dubawnt Lake is located by a star. BF = Bathurst Fault; CF = Chantrey Fault zone; MF = McDonald Fault; TF = Tulemalu Fault zone; CS = Coronation Supergroup; GS = Goulbourn Supergroup; GSS = Great Slave Supergroup; QMU = Quenn Maud Uplift; TaA = Taltson Arc; ThA = Thelon Arc; WIP = Western Interior Platform; BLB = Baker Lake Basin; DLB = Dubawnt Lake Basin; TB = Thelon Basin. Adapted from Hoffman (1988).

CHRISTOPHER ISLAND FORMATION

The Christopher Island Formation consists of potassic alkaline lava flows interbedded with subordinate intrabasinal volcaniclastic rocks. These rocks are associated with compositionally similar minette dykes and syenite stocks with a U-Pb zircon age of 1850 +30/−10 Ma (Tella et al., 1985). Maximum cumulative thickness of the Christopher Island Formation is estimated to be more than 2km in the Dubawnt Lake area based on an almost continuous section through the entire formation located at Lost Boat Island (Peterson et al., 1989; Fig. 4). It is estimated to be greater than 2km thick in the Tulemalu Lake area (Blake, 1980) and 10 km thick in the Tebesjuak Lake area (tectonically stacked; LeCheminant et al., 1979). The Christopher Island Formation outcrops within a series of small partially fault-bounded outliers in the northern and eastern part of the study area and forms part of the larger contiguous Dubawnt Lake Basin (Peterson and Rainbird 1990) to the south (Fig. 1 and 3). Strata trend roughly east-west and dip 45-85° north.

Fine grained volcaniclastic rocks

Sequences of fine grainded (max. clast size <2cm) volcaniclastic rocks up to 5m thick occur intercalated with mafic

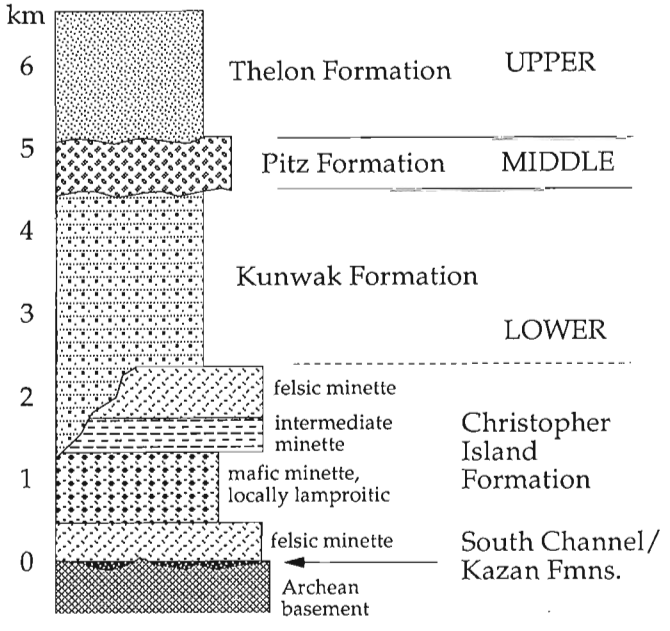

Figure 2. Summary stratigraphic section for the lower Dubawnt Groupe, based on 5 measured sections and additional mapping. Thicknesses of units vary widely and may be uncertain due to fault repetitions; the total thickness of Christopher Island Formation indicated here is a minimum and is based on a nearly complete section at Lost Boat island (Peterson et al., 1989).

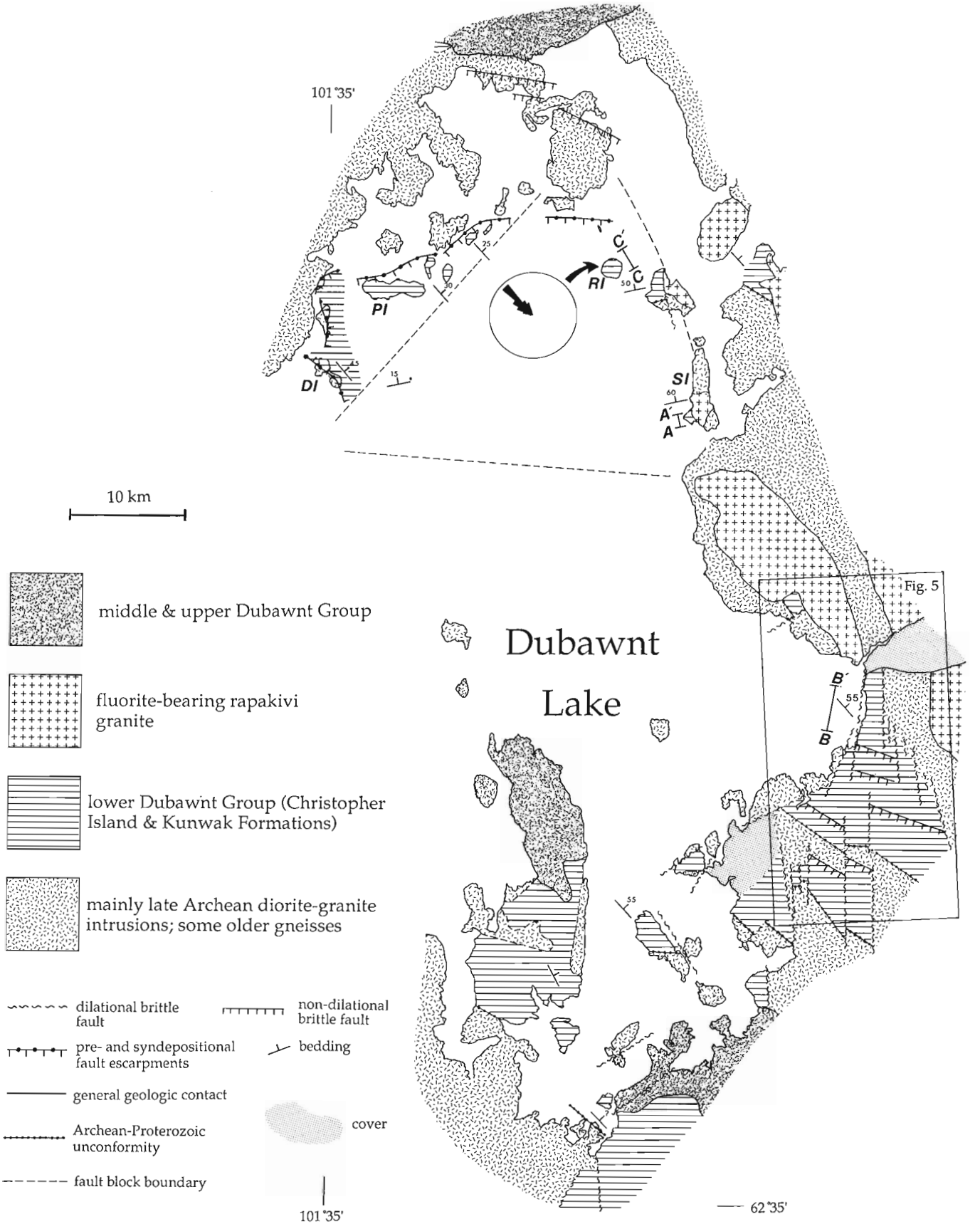

Figure 3. Bedrock geology of the Dubawnt Lake area. DI = Dumbell Island; PI = Peanut Island; RI = Round island; SI = South Long Island. The paleocurrent rose diagram for Round island is based on 37 measurements of planar and trough crossbedding. Mapping by foot and boat traverses during 1988 and 1989, except for the south-central portion which is partly based on mapping by Tella and Eade (1985).

flows and associated flow breccias at South Long Island (Section A-A', Fig. 3 and 4) and in a 100m thick sequence at Slow River (Section B-B', Fig. 3 and 5), where they are associated with coarser grained volcaniclastic rocks (Fig. 6a). A thicker unit of laminated siltites* occurs along strike about 1km to the southeast of the Slow River sequence. It is similar to a sequence on Lost Boat Island both in appearance and stratigraphic position (Fig. 3 and Peterson et al., 1989, Fig. 4). Fine grained volcaniclastic rocks also occur as decimetre-scale lenses and interbeds in breccias and also drapes on the tops of blocky lava flows. Soft-sediment folds are common in the latter suggesting contemporaneous flow movement and sedimentation or perhaps slope-related slumping.

The rocks are poorly- to moderately-well sorted with grain size variation from fine silt to fine pebble size. Parallel stratification is most common with moderate to thick lamination in siltites and thick lamination to thin bedding in arenites. Both normal and reverse grading are common and intergradational (Fig. 6b): sharp-based layers were not observed. Rare 10-20cm thick planar and trough crossbedded arenites interbedded with planar stratified units occur at section "B" (Fig. 5) where they display variable to bipolar sense of transport. Microscopic examination indicates that the detritus is primarily intraformational lithic fragments with a variable but subordinate amount of juvenile ash which is confined to silt rich laminae. Some thin layers within arenites from the middle part of Section "B" (Fig. 5) are composed of more than 40 % phlogopite cystals. The siltite unit southeast of the section "B" is composed of more than 95 % quartz. Outsized lithic blocks up to 20cm occur in several arenite horizons at section "B". Although these may have been emplaced ballistically, pierced laminae below the clasts were not observed.

Several features indicate that these rocks may be of pyroclastic origin. The first is a complete absence of wavy lamination and ripples which are common tractional sedimentary structures in epiclastic sediments under lower flow regime conditions. Crossbedding was noted but could be the product of pyroclastic surge deposition although this is very difficult to prove (*see* Fisher, 1979; Valentine, 1987). Variable paleocurrent trends from limited data likely indicate more than one source for the detritus, perhaps a group of cinder cones.

Generally, the degree of sorting within these deposits is poor which would argue against reworking by water. An exception to this is the quartz-rich siltite unit in which sorting could have been accomplished by elutriation; in which case the rock would be an airfall tuff. A lack of sharply defined stratal boundaries also suggests that deposition was relatively continuous, without any subsequent modification. Fisher and Schminke (1984, p. 166) document studies which indicate that while submarine fallout layers can be sharp-based, primary airfall layers from a single eruptive episode typically display intergradational grain size variation reflecting fluctuations in eruption energy, wind velocity and direction.

* wherever possible non-genetic terminology is employed.

At section "A" (Fig. 4) fine-grained units drape flow-tops supporting an airfall mechanism (Cas and Wright, 1987, p. 94). They also are interbedded with massive minette flows with no features, such as hyaloclastite, which

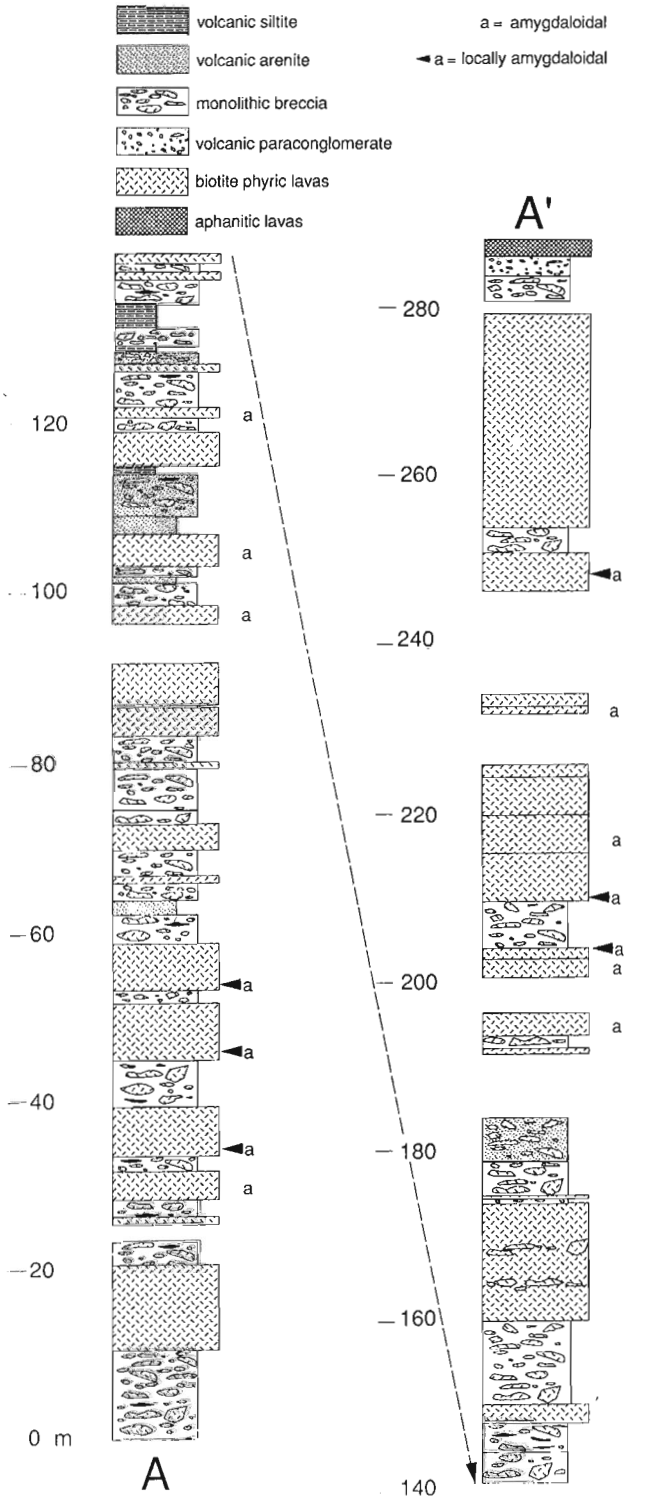

Figure 4. Section "A": stratigraphic section for the Christopher Island Formation on South Long Island (SI, Section A-A' on Fig. 3). Note the predominance of minette flows and associated breccias relative to volcaniclastic rocks.

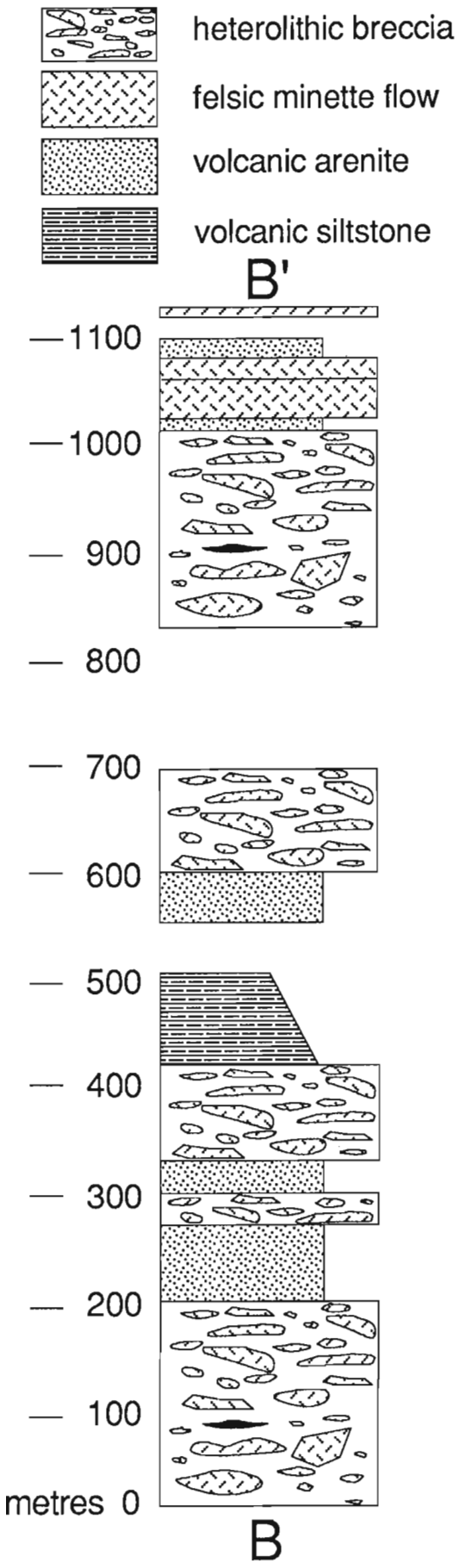

would indicate subaqueous deposition. Finally, Fisher and Schminke (1984, p. 22) pointed out that pyroclastic deposits, especially ash flows and fallout ashes are very common is successions derived from silica undersaturated alkalic magmas.

Arguments against a pyroclastic origin include an absence of welding and a lack of any associated deposits which could be interpreted as ash flow deposits. The relative paucity of pumice, scoria or any glassy juvenile fragments is also peculiar but may indicate that explosive volcanism was dominantly phreatomagmatic (Cas and Wright, 1987, p. 335).

Coarse grained volcaniclastic rocks

Type 1: heterolithic breccia

Texturally immature coarse grained heterolithic breccias represent less than 5 % of section "A" where they occur in association with the finer grained units described above (Fig. 4). In contrast they are extremely abundant at section "B" where they account for more than 70 % of the sedimentary pile (Fig. 5). The framework is generally clast-supported. Clasts are angular to very well rounded and display an almost complete size gradation from fine silt up to boulders exceeding one metre in diameter; modal clast size is about 15cm. Some clasts exhibit extremely irregular outlines with large deep re-entrants and overhangs. Matrix is composed of poorly sorted sand-size lithics with up to 20 % phlogopite crystals which are aligned parallel to bedding. Component clasts at section "B" include about 60 % mafic minette and 30 % felsic minette along with a minor amount of intraformational sedimentary rocks. A few accidental fragments of granitic basement were observed at the base of both sections. It is notable that the basal unit at section "B" also contains about 30-40 % grey aphanitic intermediate minette clasts, similar to flow units mapped stratigraphically below and less than 1km to the southeast. A distinct population of very dark green to black recessive-weathering fragments occurs sporadically throughout the sequence (Fig. 7). They are very angular with high aspect ratios and longest dimension parallel to bedding. Most are 5-15cm long. Their composition appears to be essentially chlorite suggesting that they were originally glassy but were devitrified. On the basis of these observations and by comparison with published photographs (cf. Fisher and Schminke, 1984, p. 187 and Cas and Wright, 1987, p. 252) these fragments resemble fiamme, formed by rapid burial, compaction and welding of glassy juvenile ejecta. Their association with massive, non-welded lithic debris suggests that they were probably resedimented.

Heterolithic breccia units are massive to parallel-bedded. The basal 100m of section "B" is entirely massive and may represent one complete bedding unit. Elsewhere,

Figure 5. Section "B": stratigraphic section for the Christopher Island Formation from an outcrop on the eastern shore of Dubawnt Lake, south of the mouth of the Slow River (Section B-B' on Fig. 3). Note the predominance of volcaniclastic rocks relative to minette flows.

massive and stratified breccia are interbedded in roughly equal proportions with individual units rarely exceeding 20m. Massive breccia is uncommon at section "A" where stratified breccia is interbedded with the fine grained units described previously. Normal, and less commonly reverse, graded bedding is common within the parallel stratified units but crossbedding was not recognized. Contacts between bedding units are generally diffuse although sharp, irregular lower contacts on massive units were observed in several instances at both study sections.

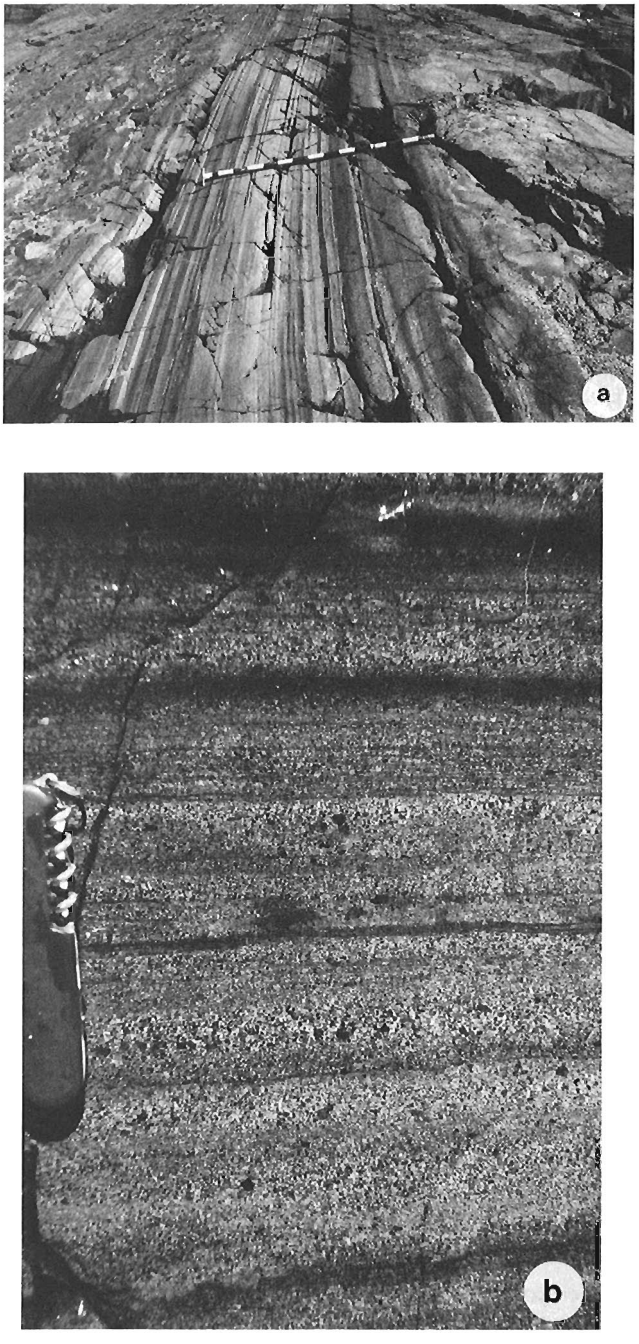

Figure 6. Christopher Island Formation fine grained volcaniclastic rocks from section "A". (a) Two metre thick interlayer of well bedded graded arenites and siltites. The unit occurs at about 130m of section "A" and is bounded by monolithic breccia. (b) Close-up of unit in (a) illustrating well defined normal to reverse and reverse to normal grading in volcanic arenites and siltites. Stratigraphic top is toward the top of the photo. Pocket knife for scale is about 10cm long.

Coarse grained units described above are interpreted as debris flows formed by the deposition of gravitationally unstable sediment, including ejecta, which accumulated on the flanks of a volcanic edifice. The parallel-stratified breccias could be proximal pyroclastic deposits but they lack any of the pumice or scoria fragments which typify these deposits and they also are not depleted in fines (Walker, 1983). Certainly the irregular bases on some of the massive units indicate loading caused by rapid deposition, perhaps by relatively dense sediment gravity flows. Also, the problem of co-existing well-rounded and angular blocks is perplexing if a strictly pyroclastic origin is invoked. Neither the eruption process nor mass-flow transportation would allow enough abrasion to produce the high degree of rounding displayed by some clasts. This relationship could have been accomplished if the debris flows overrode and incorporated unconsolidated epiclastic detritus.

Type 2: volcanic conglomerate

Fifty metres of volcanic conglomerate occurs about 200m stratigraphically above the top of section "A". This sequence overlies about 15m of massive grey aphanitic minettes similar to those at the top of section "A" and to those interbedded with conglomerates on Lost Boat Island (Peterson et al., 1989). The rock is a pebble to cobble orthoconglomerate composed of subangular to rounded clasts set in a matrix of fine sand. Maximum clast size is about 50cm with modal size of about 15cm. Clasts comprise greater than 90% intraformational mafic and felsic minettes with the remainder being a mixture of basement granites and metasedimentary rocks. Textural and compositional maturity increase and average grain size decreases up section. A similar trend was noted in comparable strata from the sec-

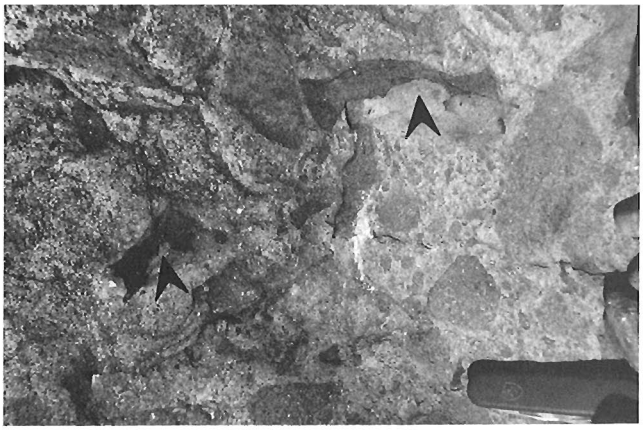

Figure 7. Deformed chloritic fragments (arrowed) in heterolithic breccia from approximately 150m point of section "B". The fragments were likely glassy ejecta which were compacted, devitrified and incorporated into subaerial debris flows. Pocket knife is about 10cm long.

tion on Lost Boat Island (*see* Peterson et al., 1989, Fig. 4). Although low-angle trough crossbeds define some broad shallow channels, planar bedding is the most common stratification style.

Stratification style, coarse grain size and relative textural maturity suggest these conglomerates were deposited by streams on broad alluvial aprons draining volcanic highlands. The fining-upward trend probably reflects channel infill and concommitant waning current deposition.

Lava flows and interflow breccias

Lavas of the Christopher Island Formation are silica undersaturated potassic to ultrapotassic rocks which are interpreted as a lamproite-minette suite (Peterson and Rainbird, 1990). For the purposes of field mapping the rocks were subdivided into mafic and felsic end members with a less common group of grey aphanitic which have an intermediate composition.

Mafic minette flows are typically maroon-brown, dark-brown or dark-green and contain 10-40 % phlogopite phenocrysts ranging in size from a few millimetres up to 15mm in diameter. The phenocrysts are randomly oriented except at flow bases where they are aligned parallel to bedding. Less common are phenocrysts of clinopyroxene which typically comprise less than 10 % of the mafic minettes; a conservative estimate considering that many of the clinopyroxenes are altered or are so small that they are indistinguishable from the groundmass. Previous studies indicate that the groundmass comprises stubby microlites of K-feldspar (>50 %) surrounding microphenocrysts of biotite, clinopyroxene and minor albite (LeCheminant et al., 1979; 1987). Rare feldspar and quartz xenocrysts 2-8mm long were noted in the basal mafic flows at section "A".

Felsic minette flows are distinguished by their distinctive red to reddish-brown colour and cherty habit. Compared to their mafic counterpants they contain fewer phlogopite phenocrysts and clinopyroxene is virtually absent. K-feldspar (sanidine?) phenocrysts form 0-20 % of the rock as stubby euhedra 2-4mm long.

Amygdules, principally calcite, are common in all lavas but are particularly common to the mafic flows at section "A" (Fig. 4) They are typically concentrated at flow margins and especially at flow bases, where they exhibit strong flattening (Fig. 8a). Very small (<5mm) irregular patches resembling amygdules, and containing an as yet unidentified white to light green mineral, possibly a zeolite, make up to 40 % of some mafic flows near the top of section "A" (Fig. 8b). These features were also noted in both mafic and felsic lavas at several localities on the mainland to the southeast.

Individual flow units range in thickness from 1-15m in the mafic minettes at section "A". Two felsic minette flows at the top of section "B" are 20 and 35m thick. Le Cheminant et al. (1979) reported flow thicknesses from the Christopher Island Formation in the Tebesjuak Lake area of 10-250m. It should be emphasized that flow boundaries are difficult to recognize away from water-washed outcrops so that some of the very thick flows could be composite.

Flow contacts are generally planar except in one instance where foundering of a flow into unconsolidated, possibly wet, sediment is indicated by the development of flame structures. Irregular contacts also exist where flows drape blocky auto-brecciated flow-tops. Flow boundaries are most easily recognized between amygdaloidal and massive flows. Lateral continuity and thickness variations could not be determined due to restricted exposure. The flows may occur as a single felsic-mafic-felsic cycle up to 2km thick (Peterson and Rainbird, 1990). LeCheminant et al. (1987) recognized cycles that began with pyroclastic followed by lava eruption, but this relationship was not observed at Dubawnt Lake.

An unusual type of interflow breccia was recognized at section "A" where it represents about 40 % of the section, almost equal to the thickness of minette flows. The rock is not a typical breccia in that the fragments are quite irregular and well rounded with very irregular outlines and diffuse margins suggesting they were plastically deformed while still hot. Their compositions appear to be identical to the

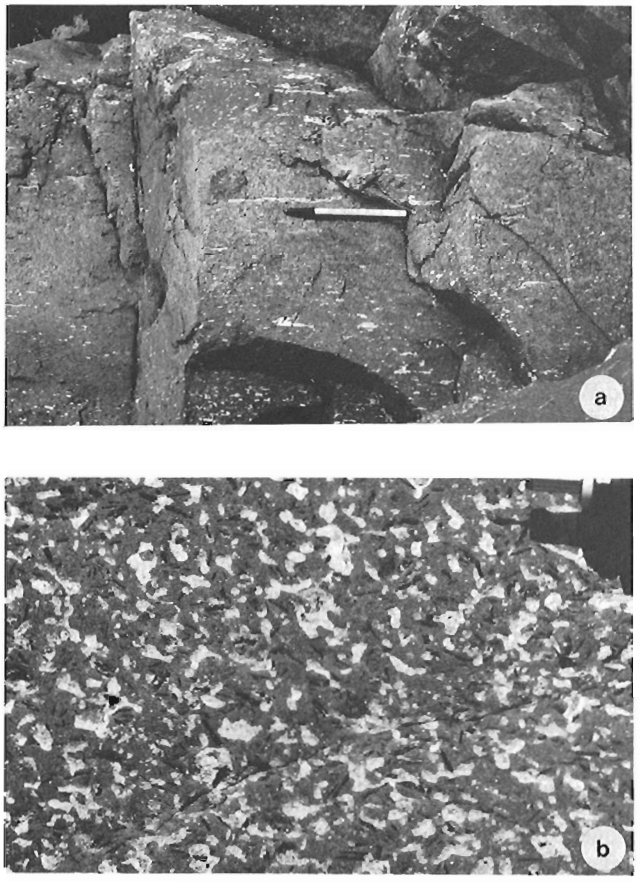

Figure 8. Christopher Island Formation mafic minette flows from section "A". (a) Deformed calcite-filled amygdules formed by shear at the base of a flow. Approximately 210m of section "A". Pen is 15 cm long. (b) Irregular patches (amygdules?) in mafic minette flow from approximately 250 m of section "A". Patches contain a fine granular, as yet unidentified mineral (zeolite?). Black laths are phlogopite phenocyrsts. Drafting pen tip in upper right corner is about 1cm long.

adjacent flows implying local derivation. Rare angular black fragments up to 10cm long occur within a few of the breccia units and are similar to fragments in the heterolithic breccia. The lava fragments compose about 80-90 % of the rock and are set in a typical non-amygdaloidal mafic minette matrix. The matrix also includes rare wisps and layers of deformed fine sediment and in at least one instance this material appears to have infiltrated downwards between the fragments.

Contacts between flows and interflow breccias are diffuse and irregular; in several instances pods of breccia appear to have been dragged down into the underlying flow. Breccia units are 1-10 m thick and generally are thinner than the flows. Apart from lavas these units are less commonly interbedded with the pyroclastic units described previously (eg. at 130m of section "A", Fig. 4).

Most of the described features support the conjecture that these units represent autobreccias formed during movement of the lava flows. A mechanism is invoked in which flows, still hot and therefore plastic, develop joints parallel to flow due to differential rates of internal cooling (Williams and McBirney, 1979, p. 176). Once the joints are developed, continued advance facilitates brecciation. The angular fragments are reincorporated into the flow, deform plastically and are partially reassimilated causing the rounded diffuse outlines. This mechanism does not explain the very high proportion of breccia relative to flows. It also does not account for breccias which occur within fine grained units without any associated flows from which they could have been derived. This suggests the possibility that the breccias may have been transported downslope, beyond the extent of lava flow.

An alternate, and possibly more plausible, theory is that these units might be agglutinates or clastogenic lavas (Cas and Wright, 1987, p. 48). These are vent-proximal deposits created by an accumulation of spatter fragments from lava fountains. This mode of origin might better account for the shape of the fragments in that they would have been hot and plastic at the time of fragmentation. The accumulation would then act like a lava deforming internally and incorporating any airborne ejecta. The fact that clastogenic lavas are regionally restricted might explain why these deposits are unique to section "A". The recognition of these deposits would indicate extreme proximity to a volcanic centre.

Depositional Model for the Christopher Island Formation

The Christopher Island Formation comprises the thickest sequence of subaerial minette lavas anywhere in the world. Lava flows are intercalated with volumetrically lesser, but locally thick, (> 1km) accumulations of volcaniclastic rocks.

Three areas studied in detail offer a varied cross-section through the volcano-sedimentary pile and allow the development of a facies model for deposition of these rocks. The stratigraphic succession at section "A" exhibits features consistent with eruptions close to a volcanic centre, possibly a series of fissure volcanoes. This is indicated by the high proportion and frequency of lava flows relative to sedimentary units and by the recognition of possible clastogenic lavas formed by lava fountaining.

Section "B" differs from section "A" in that it is dominated by coarse sedimentary strata. The remarkable thickness, coarse grain size and compositional immaturity of these deposits suggests proximity to an explosive volcanic centre where material would have accumulated and was periodically redistributed by slope processes.

The succession at Lost Boat Island (Peterson et al., 1989) is interpreted as a valley-fill sequence which explains the co-existence of relatively thick lava flows with an equal abundance of locally-derived alluvial conglomerates and sandstones.

The local environments represented by each of these successions could have formed contemporaneously across a fault-bounded basin such as the Colima-Zacoalco-Chapala graben system in the southwestern Mexican volcanic belt where minettes also occur (cf. Allen, 1986). Volcanic centres such as fissure volcanoes and cinder cones would have developed at the basin margin, close to faults, whereas valley-fill lava flows and alluvium would have been deposited in the axial regions of the basin. This interpretation does not imply that all three sequences represent portions of the same basin fill sequence. Mapping indicates that deposition likely occurred within a series of relatively narrow east-northeast-trending basins (Peterson and Rainbird, 1990).

KUNWAK FORMATION

The Kunwak Formation consists of coarse alluvial redbeds derived from unconformably to conformably underlying Christopher Island Formation strata and older basement rocks. It was deposited in a series of southeast- to northeast-trending fault-bounded troughs such as the Wharton Basin (LeCheminant et al., 1981) which display abrupt local facies and thickness variations. It is estimated to be more than 10km thick adjacent to a basin margin fault situated along the northern shore of Dubawnt Lake, but thins abruptly to the south (Peterson et al., 1989).

Regional mapping in 1989 confirms that the Kunwak Formation is largely restricted to a series of island outcrops which form a 20-30km wide east-northeast-trending zone at the north end of Dubawnt Lake (Fig. 3). Several outcrops of Kunwak conglomerate occur along the shore of a prominant peninsula in southern Dubawnt Lake. The Kunwak Formation was studied in detail on Round Island in the northeast part of Dubawnt Lake where the strata dip 30-40° north (section C-C', Fig. 3 and 9).

Lithofacies

Lithofacies observed in 1989 are similar to those described in 1988 (Peterson et al., 1989). Notable exceptions are the overall finer grain size and more variable clast compositions of the conglomerates.

Two principle coarse grained facies are exposed at section "C": massive to faintly-stratified clast-supported

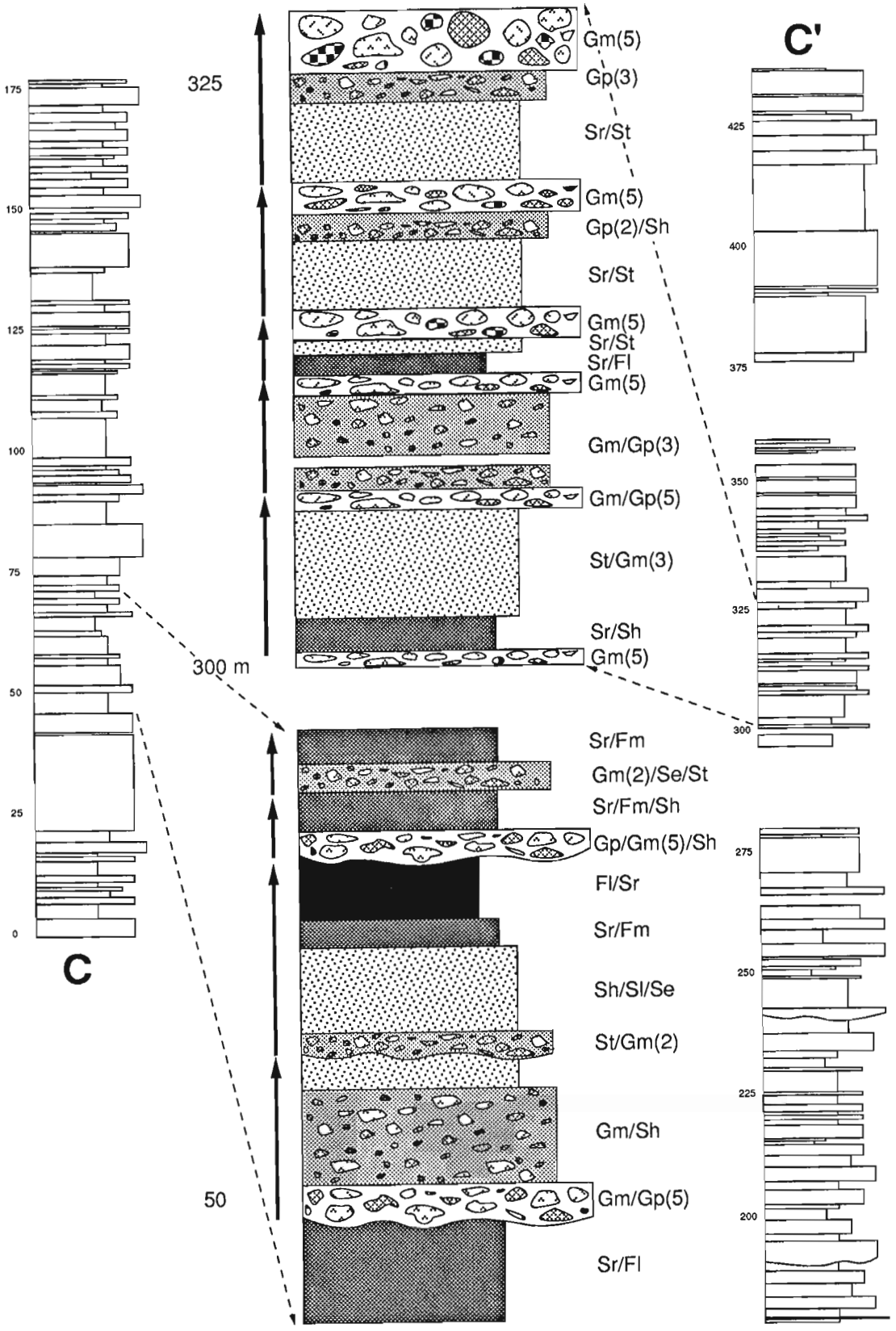

Figure 9. Section "C": stratigraphic section for the Kunwak Formation at Round Island (RI, section C-C' on Fig. 3) showing details of both fining-upward cycles (lower section blow-up) and coarsening-upward cycles (upper section blow-up). FL = parallel laminated silstone, Fm = Fl with desiccation features, Sr = ripple-crosslaminated fine sandstone, St = trough-crossbedded sandstone, Se = sandstone with erosional scours and intraclasts, Sl = low-angle crossbedded sandstone, Sh = horizontally-stratified sandstone, Gm = horizontally-stratified to massive orthoconglomerate, Gp (3) = planar-crossbedded orthoconglomerate with maximum clast size of 3cm. Lithofacies identifiers are from Miall (1978).

conglomerate (Gm); and planar-crossbedded conglomerate (Gp), which is transitional from clast-supported to sandy matrix-supported. Trough-crossbedded conglomerate is rare. Massive to faintly stratified conglomerate is the most abundant coarse grained lithofacies. Maximum clast size at section "C" does not typically exceed 20cm and most units do not have any clasts greater than 5cm. Clast types include roughly equal amounts of volcanic rocks derived from the Christopher Island Formation, pink quartz arenite (Amer Group?) and basement granitic rocks. The clasts of Christopher Island Formation are the largest and are well rounded; the remainder are angular to subrounded. The matrix, which composes from 20-30 % of the rock, is a poorly sorted mixture of sand and hematitic silt which imparts a strong red colour to the rock. Conglomerates exhibit parallel bedding which is most evident in units that contain higher proportions of sand. Conglomeratic lithofacies are gradational with coarse grained sandstone lithofacies but show are scoured basal contacts with silstone units.

Sandstone lithofacies include horizontally-stratified sandstone (Sh), trough- and planar-crossbedded sandstone (St, Sp, Sl, Se) and ripple-crosslaminated, fine grained sandstone (Sr). Crossbedded sandstones are generally coarse grained and poorly sorted, pebbly lithic arenites. Horizontally stratified units are both fine- and coarse-grained. All sandstone facies occur in approximately equal proportions. Other sedimentary structures include primary current lineation (Sh lithofacies), flaser to wavy bedding (Sr lithofacies) and load structures.

Fine grained lithofacies are primarily parallel-laminated red siltstones with minor mudstone interlaminations. Desiccation features such as mud cracks, mud curls (Fm) and associated rip-up breccias are common throughout the section. Typically, parallel-laminated siltstones is interstratified with ripple-crosslaminated, fine grained sandstone (Sr).

In general, it is difficult to recognize a pattern to the vertical arrangement of these lithofacies, although five coarsening-upward cycles were noted between 300-325m of section "C" (Fig. 9). Cycles begin with fine grained, rippled sandstone and pass gradationally upward through parallel-stratified and crossbedded sandstone into parallel-stratified and planar-crossbedded, pebbly sandstone and conglomerate. Also, fining-upward cycles occur between 50-75m of section "C" (Fig. 9). These cycles vary from 3 to 10m thick and commence with an erosive-based conglomerate containing rip-ups. This passes up though horizontally bedded and trough-crossbedded sandstone into rippled fine sandstone and finely laminated siltstone.

Paleocurrent data from crossbedding at section "C" indicate strong unimodal transport to the northwest (Fig. 3); almost opposite to the weaker trend observed at Peanut Island (Peterson et al., 1989; PI on Fig. 3).

Depositional Model for the Kunwak Formation

The well developed coarsening-upward cycles at the Peanut Island section (Peterson et al., 1989; Fig. 7) were interpreted as proximal alluvial fan deposits which formed in response to repeated uplift along a basin-margin fault zone. The fault zone is located on the northern side of a string of island outcrops in the northern part of Dubawnt Lake (Fig. 3; *see* Peterson et al., 1989). The lithofacies described at section "C" are considered to be part of the same depositional system but likely represent a more distal alluvial fan to braidplain setting. Stacked coarsening-upward cycles at section "C" are much less evident than at Peanut Island and there is an overall higher percentage of fine grained lithofacies. Also, at section "C" there is a notable absence of coarse, massive conglomerates interpreted as subaerial debris flows, an essential lithofacies in proximal alluvial fan deposits (Rust and Koster, 1984). Crossbedded and parallel-stratified conglomerates are the most common lithofacies suggesting traction currents were the most important depositional mechanism. The erosive-based fining-upward cycles in the lower part of the section are typical of braidplain as opposed to alluvial fan deposition (cf. Walker and Cant, 1984).

Paleocurrent data (Fig. 3) indicate that the source region, possibly a basin margin fault zone, lay to the southeast and that alluvium deposited along the zone was shed to the northwest. The east-west distribution of the Kunwak Formation combined with thickness estimates and paleocurrent information from 1988 lead us to the tentative hypothesis that the Kunwak Formation was deposited in a narrow fault-bounded trough, possibly an oblique-slip basin, where "conveyor belt"-type sedimentation allowed the accumulation of very thick but regionally restricted coarse alluvial deposits (cf. Crowell, 1974, and Steel and Gloppen, 1980).

SUMMARY

The lower Dubawnt Group comprises a succession of potassic to ultrapotassic volcanic rocks (Christopher Island Formation) and terrestrial sedimentary rocks (Kunwak Formation) deposited between about 1.9-1.8 Ga in a series of narrow, east-northeast-trending fault-bounded basins. Some of these basins are exposed along the northern and southeastern margins of Dubawnt Lake.

The Christopher Island Formation consists of a mafic to felsic suite of minette lavas probably erupted from fissure volcanoes which developed close to faults along the basin margins. Localized accumulations of possible pyroclastic rocks suggest contemporaneous exposive volcanism. Reworking of lava flows and pyroclastic debris is recorded in thick, subaerial debris flows deposited on the flanks of volcanoes. Coarse alluvial conglomerates were likely deposited on alluvial aprons between volcanic centres with finer grained equivalents forming braided stream and ephemeral lake deposits in the axial portions of the basin.

A subsequent episode of uplift and faulting, with no associated volcanism, controlled deposition of the Kunwak Formation, a varied assemblage of terrestrial redbeds. These sediments were cannibalized, mainly from roughly east-west-trending fault scarps and shed inward to form alluvial fans, alluvial braidplains and associated braided river deposits. The presence of exceptional thicknesses of coarse sedimentary rocks at the northern margin of one basin may be a consequence of "conveyor belt"-type stacking which

has been documented within basins developed along strike-slip faults.

ACKNOWLEDGMENTS

The authors thank Bruce Kjarsgaard, Natalie Morisset and Bob Spark for their tireless efforts and enthusiasm in the field. Paul Wallace of the University of California offered many helpful comments regarding physical mechanisms and features of minette volcanism. We also thank Tony LeCheminant for his continued support and advice on various aspects of Dubawnt Group geology. The manuscript was critically reviewed by Rob Hildebrand, with additional comments by Maurice Lambert and Tony LeCheminant.

References

Allan, J.F.
1986: Geology of the northern Colima and Zacoalco grabens, southwest Mexico: late Cenozoic rifting in the Mexican Volcanic Belt; Geological Society of America, Bulletin, v. 97, p. 473-485.

Blake, D.H.
1980: Volcanic rocks of the Paleohelikian Dubawnt Group in the Baker Lake-Angikuni Lake area, District of Keewatin, N.W.T.; Geological Survey of Canada, Bulletin 309, 39 p.

Brantley, S.R. and Waitt, R.B.
1988: Interrelationships among pyroclastic surges, pyroclastic flows and lahars in Smith Creek valley during the first few minutes of the 18 May 1980 eruption of Mount St. Helens, USA; Bulletin of Volcanology, v. 50, p. 304-326.

Cas, R.A.F. and Wright, J.V.
1987: Volcanic Successions, Modern and Ancient; Allen and Unwin, London, 528 p.

Crowell, J.C.
1974: Origin of late Cenozoic basins in southern California; *in* Tectonics and Sedimentation, W.R. Dickenson; ed., Society of Economic Paleontologists and Mineralogists, Special Publication 22, p. 190-204.

Donaldson, J.A.
1965: The Dubawnt Group, District of Keewatin and Mackenzie; Geological Survey of Canada, Paper 64-20, 11 p.

Fisher, R.V.
1979: Models for pyroclastic surges and pyroclastic flows; Journal of Volcanology and Geothermal Research, v. 6, p. 305-318.

Fisher, R.V. and Schminke, H.-U.
1984: Pyroclastic Rocks: Spriger-Verlag, Berlin, 472 p.

Hoffman, P.F.
1988: United plates of America, the birth of a craton: Early Proterozoic assembly and growth of Laurentia; Annual Review of Earth and Planetary Sciences, v. 16, p. 543-603.

LeCheminant, A.N., Lambert, M.B., Miller, A.R., and Booth, G.W.
1979: Geological studies: Tebesjuak Lake map area, District of Keewatin; *in* Current Research, Part A. Geological Survey of Canada Paper 79-1A, p. 179-186.

LeCheminant, A.N., Ianelli, T.R., Zaitlin, B., and Miller, A.R.
1981: Geology of Tebesjuak Lake map area, District of Keewatin: a progress report; *in* Current Research, Part B, Geological Survey of Canada, Paper 81-1B, p. 113-128.

LeCheminant, A.N., Miller, A.R. and LeCheminant G.M.
1987: Early Proterozoic alkaline igneous rocks, District of Keewatin, Canada: petrogenesis and mineralization; *in* Geochemistry and Mineralization of Proterozoic Volcanic Suites, ed. T.C. Pharaoh, R.D. Beckinsale and D. Richard; Geological Society of London, Special Publication 33, p. 219-240.

Miall, A.D.
1978: Fluvial sedimentology: an historical review; *in* Fluvial Sedimentology, ed. A.D. Miall; Canadian Society of Petroleum Geologists, Memoir 5, p. 1-47.

Peterson, T.D., LeCheminant, A.N., and Rainbird, R.H.
1989: Preliminary report on the geology of northwestern Dubawnt Lake area, District of Keewatin, N.W.T.; *in* Current Research, Part C, Geological Survey of Canada, Paper 89-1C, p. 173-183.

Peterson, T.D. and Rainbird, R.H.
1990: Tectonic and petrological significance of regional lamproite-minette volcanism in the Thelon and Trans-Hudson hinterlans: *in* Current Research, Northwest Territories, Part C, Geological Survey of Canada, Paper 90-1C.

Rust, B.R. and Koster, E.H.
1984: Coarse alluvial deposits; *in* Facies Models, ed., R.G. Walker, Geoscience Canada Reprint Series 1; Geological Association of Canada, p. 53-69.

Steel R.J. and Gloppen, T.G.
1980: Late Caledonian (Devonian) basin formation, western Norway: signs of strike-slip tectonics during infilling; *in* Sedimentation in oblique-slip mobile zones, ed. P.F. Balance and H.G. Reading; International Association of Sedimentologists, Special Publication 4, p. 79-103.

Tella, S. and Eade, K.E.
1985: Geology, Kamilukuak Lake, District of Keewatin, Northwest Territories; Geological Survey of Canada, Map1629A, scale 1:250 000.

Tella S., Heywood, W.W., and Loveridge, W.D.
1985: A U-Pb age on zircon from a quartz syenite intrusion, Amer Lake area, District of Keewatin, N.W.T.; *in* Current Research, Part B, Geological Survey of Canada, Paper 85-1B, p. 367-370.

Valentine, G.A.
1987: Stratified flow in pyroclastic surges; Bulletin of Volcanology, v. 49, p. 616-630.

Walker, G.P.L.
1983: Ignimbrite types and ignimbrite problems; Journal of Volcanology and Geothermal Research, v. 17, p. 65-88.

Walker, R.G. and Cant, D.J.
1984: Sandy fluvial systems; *in* Facies Models, ed. R.G. Walker; Geoscience Canada, Reprint Series 1, Geological Association of Canada, p. 71-89.

Williams, H. and McBirney, A.R.
1979: Volcanology; Freeman and Cooper, San Francisco, 397 p.

Stratigraphy, sedimentation, dome and basin basement-cover infolding, and implications for gold in the Hurwitz Group, Hawk Hill-Griffin-Mountain Lakes area, District of Keewatin, N.W.T.[1]

Lawrence B. Aspler[2] and Terry L. Bursey[3]

Aspler, L.B. and Bursey, T.L. Stratigraphy, sedimentation, dome and basin basement-cover infolding, and implications for gold in the Hurwitz Group, Hawk Hill-Griffin-Mountain Lakes area, District of Keewatin, N.W.T.; in Current Research, Part C, Geological Survey of Canada, Paper 90-1C, p. 219-230, 1990.

Abstract

The Hurwitz Group represents aborted rift and cratonic basin sedimentation that was interrupted by flexural bulge emergence and flexural depression drowning (either thrust load or intraplate stress induced). Lateral facies changes in shoaling upward sequences indicate lateral variations in amplitude of multiple bulge/depression pairs. Shortening was by thick-skinned folding, not detachment; NE and E-trending folds cross NW-trending folds generating dome and basin interference. Folding was primarily by flexural slip; minor thrusts, cross faults, disharmonic folds, and fold and cleavage fans are space-accommodating. Changes in basement lithology and structure provided anisotropies that influenced Hurwitz thickness and facies and guided Proterozoic strain. Structural control of pyrite-arsenopyrite-chalcopyrite-Au in fractured Kinga quartz arenite at sheared basement contacts (similar to the past gold producer near Cullaton Lake), and near cross faults (Watterson Formation), suggest a genetic link between folding, cross faulting, jointing and mineralization.

Résumé

Le groupe de Hurwitz est le résultat d'une sédimentation en rift avorté et bassin cratonique interrompue par une émergence de bourrelets par flexion et une submergence par dépression flexurée (soit par chargement de poussée axiale ou contrainte intraplaque induite). Des changements de faciès latéraux dans les séquences à déprofondissement vers le haut indiquent des variations d'amplitude latérale de multiples paires bourrelet-dépression. Le raccourcissement est le résultat d'un plissement de couverture épaisse et non pas d'un détachement; les plis à direction nord-est et est traversent des plis à direction nord-ouest produisant une interférence de dômes et de bassins. Le plissement est principalement dû à un glissement par flexion; les chevauchements secondaires, les failles transversales, les plis disharmoniques et les plis et clivages en éventail se répartissent dans cet espace. Des modifications de la lithologie et de la structure du socle ont produit des anisotropies qui ont influé sur l'épaisseur et le faciès du groupe de Hurwitz et orienté la déformation protérozoïque. Le contrôle structural de l'association pyrite-arsénopyrite-chalcopyrite-or dans l'arénite quartzeuse de Kinga fracturée aux contacts de socle cisaillés (semblable à l'ancienne zone aurifère productrice près du lac Collaton) et près de failles transversales (formation de Watterson) indique un lien génétique entre les plis, les failles transversales, les joints et la minéralisation.

[1] Contribution to the Canada-Northwest Territories Mineral Development Agreement 1987-1991. Project carried jointly by Geological Survey of Canada (Mineral Resources Division), Indian and Northern Affairs Canada (Yellowknife) and Government of the Northwest Territories (Energy Mines and Resources Secretariat)

[2] 215 Fifth Avenue, Ottawa, Ontario, K1S 2N1

[3] Department of Geology, Carleton University, Ottawa, Ontario K1S 5B6

INTRODUCTION

The Hawk Hill-Griffin-Mountain Lakes area constitutes a synclinorium of Hurwitz Group infolded with basement; one of many that extend from Hudson Bay to Ennadai Lake (Fig. 1, Hoffman, 1989). Outstanding problems pertaining to the Hurwitz Group include: more precise determination of stratigraphic and facies relationships to establish basin configuration, subsidence mechanisms and tectonic significance; questions of regional structure (relative importance of thrusting versus basement-cover infolding; significance of inconsistent vergence), evaluation of economic potential, and relationship of regional structure to known deposits. Below we address these problems, based on preliminary analysis of 1:50 000-scale mapping (Fig. 1, Aspler, 1989).

STRATIGRAPHY AND SEDIMENTOLOGY OF THE HURWITZ GROUP

Descriptions and environmental interpretations of units mapped are summarized in Figure 1 and Table 1. The following focusses on stratigraphic and facies relationships. Due to slip during basement-cover infolding, the Hurwitz Group is semi-allochthonous with respect to basement, except southeast of Hawk Hill Lake, where the Padlei and Kinga formations are interpreted to be entirely autochthonous (see Structural Geology). The sub-Hurwitz unconformity is not exposed in the area, but is implied by clast compositions in Padlei conglomerates (Table 1) and the structural discordance between basement (steeply-plunging, downward-facing folds) and cover (shallowly plunging, upward-facing folds).

Notable basement-Padlei-Kinga relations (Fig. 2) are the lens-like character of the Padlei Formation and direct overlap of the Whiterock Member on basement. At the top of the P2 member, Maguse-like quartz (+/− feldspar) granulestone interbeds indicate a conformable contact/lateral facies transition between the P2 and Maguse members. The Padlei Formation appears to be preserved as valley-fills in a rugged basement paleotopography; the Maguse Member is a transgressive marine lag that reworked coeval Padlei alluvium. Maximum thickness of the Maguse Member (100m) is in the autochthon. Elsewhere in the map area the unit forms thin lenses scattered along the Hurwitz-basement contact. To what extent the lenses represent depositional pinchouts between Whiterock Member and basement, versus variation in the level at which the Hurwitz Group slipped over basement, is uncertain.

The name "Hawk Hill Member" is introduced for interbedded hematitic silcrete and fluvial sediments that overlie the Whiterock (Table 1).The type area is southeast of Hawk Hill Lake; upper and lower contacts are exposed at UTM 274658. Transition from the Whiterock Member is over an interval of 0.5 m and is marked by the appearance of clay alteration in fractures and around detrital quartz grains, and of maroon oxidation spots in the quartz arenite. Contact with the Ameto Formation is gradational, with all components of the member (with the exception of slate) disappearing over a thickness of 1m. The member is 18m thick on the eastern limb of a doubly-plunging syncline and 5m thick on the western limb; it is absent elsewhere in the area. Although the member is developed regionally (Bell, 1970b; Eade, 1974; Young, 1988) individual occurrences appear to be of only local extent.

In the southern part of the map, the Ameto Formation shoals upward (Table 1); the transition with the overlying Watterson Formation is conformable, as indicated by appearance of local dm-scale cryptalgal laminate interbeds within slates and arkoses. However, in the Griffin Lake area, the Ameto Formation is missing, and the Watterson Formation was observed in abrupt but conformable contact with the Whiterock Formation (cryptalgal laminates lying concordantly on a pristine quartz arenite bedding surface).

Precise definition of thickness and of vertical and lateral transitions of members within the Watterson Formation is inhibited by poor outcrop in the central part of the map area. At southern Griffin Lake, cryptalgal laminates of the Watterson Formation pass conformably up-section to rocks of the Tavani Formation, with the appearance of quartz arenite and intraformational conglomerate interbeds. At central and western Griffin Lake only, fine grained rocks (Ducker Formation) form a wedge between the Watterson and Tavani formations (Fig. 3).

Figure 1B illustrates a qualitative sea level curve implied by cycles in the Hurwitz Group. Changes north toward Griffin Lake (Fig. 3) imply significant north-south variation in relative emergence including (in terms of paleohighs and paleolows): northward disappearance of Hawk Hill silcretes (north low, south high); northward disappearance of the Ameto Formation and appearance of a conformable Kinga-Watterson contact (north high, south low); northward disappearance of W2 member (north high, south low); and northward appearance of the Ducker Formation (north low, south high). Accompanying these stratigraphic and sedimentological changes are important changes in basement rock type and structural grain, as well as changes in Proterozoic strain, suggesting a feedback mechanism (see below): basement, to sedimentary cover, to basement-cover deformation.

STRUCTURAL GEOLOGY

Folds, faults and fractures

Northwest-trending, upright D1 folds are refolded by east- and northeast-trending, upright (and locally inclined) D2 cross folds, generating dome and basin Ramsay Type I (and locally mushroom-like Type I-II) interference patterns (see Ramsay and Huber, 1987). The east-west structures are considered to be "D2" because they locally refold northwest-trending D1 axial surfaces and D1 limbs, and D2 cleavage is not deflected about D1 trends.

D1 folds are predominant in the area west of Mountain Lake between Hawk Hill and Griffin Lakes. They are open to gentle, symmetric and approximate concentric morphologies, with rounded to flat hinge zones, and rounded limbs (Fig. 5). Meso-scale cleavage related to D1 is only locally developed. Minor disharmonic folds may be space-accommodating structures related to concentric folding.

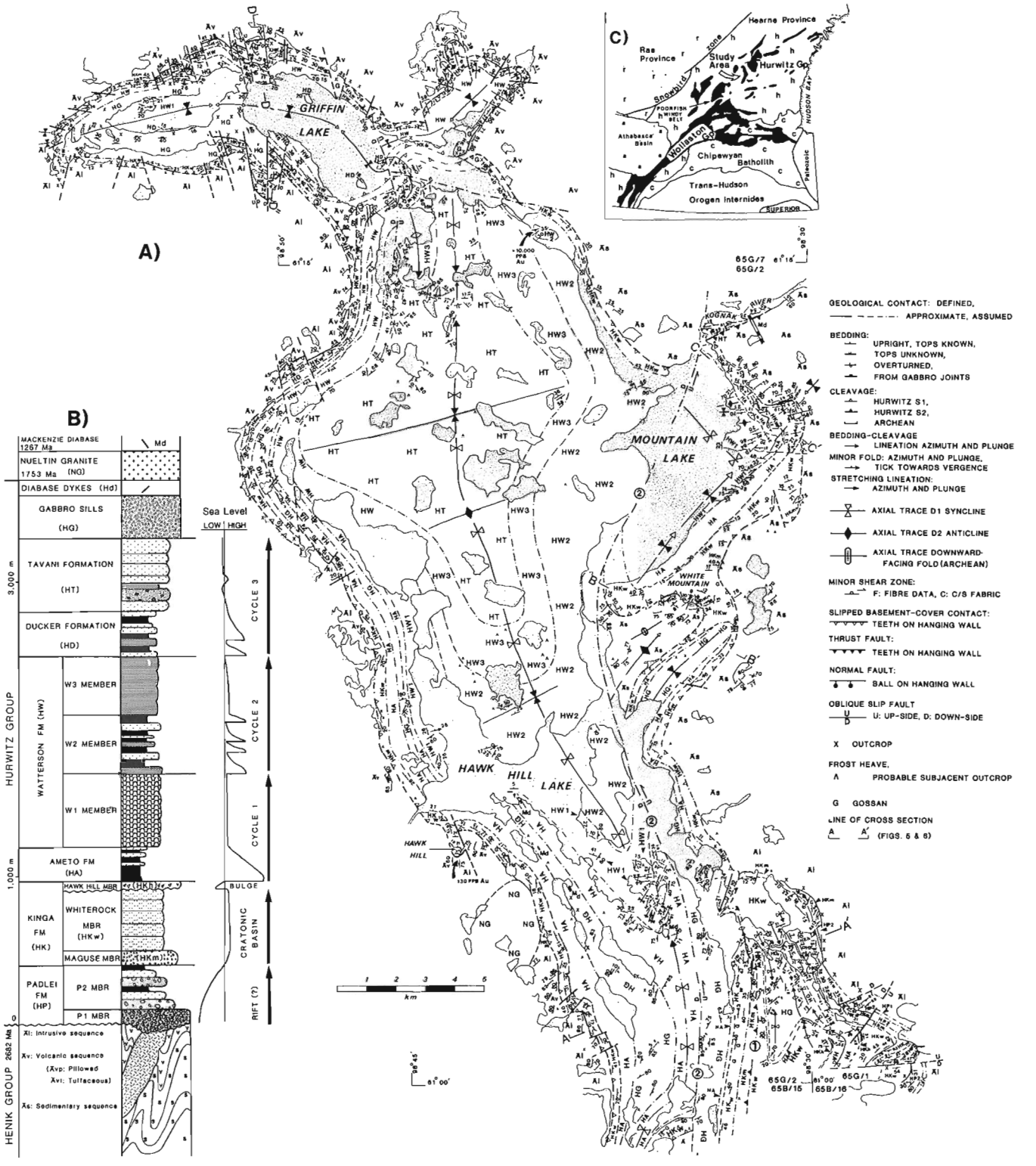

Figure 1. A) Generalized geology Hawk-Hill-Mountain-Griffin lakes. B) Stratigraphic column; thicknesses are estimates based on map data, see Table 1 for sources of geochronological data. C) Location of study area, generalized after Hoffman (1989). Reduced from Aspler (1989).

Table 1. Description and interpretation of map units, Hawk Hill-Mountain-Griffin lakes area.

UNIT			DESCRIPTION	INTERPRETATION	COMMENTS
Mackenzie Diabase			Diabase, coarse-grained, non-foliated, unmetamorphosed, with northwest trend		U-Pb baddeleyite 1267 ± 2 Ma (LeCheminant and Heaman, in press)
Nueltin Granite			Granite, granodiorite, non-foliated		U-Pb zircon 1753 +3/-2 Ma (Loveridge et al., 1988)
Diabase			Rare near-vertical fine-grained diabase dykes cutting tilted Kinga Fm., following joint sets (hence of variable trend). Contain xenoliths with internal joints slightly rotated from host quartz arenites	Post-Hurwitz Group folding, post joint development in Kinga Formation	
HURWITZ GROUP	Gabbro		Gabbro sills, generally green weathering, coarse-grained, commonly with joints parallel to bedding in enclosing Hurwitz strata. Locally well-foliated; chloritic shear zones common	Post-Ducker Formation, pre-Hurwitz Group folding. Relationship to Tavani Fm. is uncertain	Entirely within Ameto Fm. in south, absent in northeast; but within Watterson in northwest (Fig. 3)
	Tavani Fm		Tan and grey weathering quartz arenite and subarkose with rare interbeds of green shale and mudchip breccia. At base, dm-m-scale beds and lenses of orange cryptalgal laminate and intraformational conglomerate bearing clasts of quartz arenite and carbonate floating in a quartz arenite to calcarenite matrix.	Quartz arenites and subarkose as shallow subaqueous to subareal deposits; cryptalgal laminates as isolated intertidal flats and intraformational conglomerates from reworking of early-cemented adjacent sediments	Watterson to Tavani transition is conformable in the map area although to the east is a basin-margin sub-Tavani unconformity that cuts into progressively deeper stratigraphic levels (Bell, 1970a)
	Ducker Fm		Cm to dm-scale fining-upward cycles of grey and tan arkose to blue argillite; discrete beds of arkose with parallel-stratification and ripple cross stratification. Local dm-m-scale interbeds of orange cryptalgal laminate	Below wave base mass flows alternating with shallow water siliciclastic sheetfloods and local algal patches	Only in central and western Griffin Lake area; elsewhere in the map area, the Watterson Formation is conformably overlain by the Tavani Formation
	Watterson Fm.	W_3	Orange-weathering cryptalgal dolostone with rare arkose and shale interbeds.	Shallow subtidal to intertidal carbonate flats with local tidal pools (lagoons?)	
		W_2	Mixed siliciclastic and carbonate in ratios from 2/8 to 8/2. Carbonate massive or cryptalgal, orange dolostone in layers from 10 cm to 2 m. Siliciclastic component; grey arkose and shale as cm-dm-scale discrete beds or in dm-scale arkose to shale fining-upward cycles. Local mm-cm-scale arkose to shale rhythmites; carbonate chip breccias	Below wave base siliciclastic mass flows alternating with shallow subtidal to intertidal carbonate flats. Shoaling-upward aggradational cycles (?)	Three informal members probably equivalent to those described by Eade and Chandler (1975) in the Watterson Lake Area
		W_1	Rose, flesh and cream stromatolitic (Fig. 4F) and cryptalgal dolostone, locally silicified. Stromatolites typically close, laterally linked, bulbous to nodular hemispheroids. Local massive or stratified breccia with angular carbonate and (rarely) well rounded quartz arenite clasts; rare dm-scale ripple-marked red arkose and blue-green siltstone.	Intertidal to supratidal stromatolite patches cut by tidal channels with local channel collapse breccias; rare siliciclastic flooding	
	Ameto Fm.		At base, red, blue, green slate with local mm-cm-scale parallel-stratified arkose. Arkose increases up-section with the development of cm-dm-scale fining-upward cycles (erosional base, parallel stratified or massive medium grained arkose, cross-stratified arkose to blue slate. Fig. 4D) and rare wave (?) ripple cross-stratification (Fig. 4E). Abundant cm-scale massive sulphide concretions and local cryptalgal laminates near top of section	At base, quiet, starved below wave-base sedimentation interrupted by turbidity-like currents; shoaling-upwards such that storm (?) waves rework sandy component and cryptalgal laminates develop	Sudden change from shallow water supermature quartz arenites to deep water slates and non-quartzose arenites is striking.
	Kinga Fm	Hawk Hill Mbr	Interbeds of massive maroon chert; laminar white chert, maroon breccia with quartz arenite and laminar chert clasts in maroon chert cement (with specular hematite void fills) (Fig. 4C), and m-scale fining-upward sequences of framework intact conglomerate (with maroon chert granules and pebbles) to red sandstone to shale. Interbedding is concordant with adjacent units	Hematitic siliceous regolith development alternating with fluvial reworking	New unit (see text)
		Whiterock Mbr	White ridge and cliff-forming fine-medium grained homogeneous quartz arenite. Large areas are devoid of obvious sedimentary structures with the exception of bedding manifested by variation in spacing and continuity of fractures (due to subtle bedding-parallel anisotropy?). Commonly with variably oriented ripple marks (Fig. 4B); local parallel-stratified heavy minerals, dm-scale cross stratification, ripple marks; rare possible adhesion structures and raindrop molds/casts. Notable absence of tidal structures	Wave-dominated platform deposits, at least in part formed under near-emergent depths	" a distinctive and resistant stratigraphic marker of inestimable value" (Eade, 1974, p. 22)
		Maguse Mbr	Grey and white quartz +/- feldspar granulestone and granule-pebble conglomerate, well sorted and rounded, framework intact, with quartz arenite matrix. Sheet interbeds of rose, grey and white quartz arenite	May represent transgressive marine lag from reworking of laterally equivalent Padlei Formation	
	Padlei Fm	P2 Mbr	Maroon, green and grey arkose, with dm-scale trough cross beds (Fig. 4A). Dm-scale grit to arkose to red siltstone to red green and blue slate fining-upward cycles. At base, dm-m-scale, framework intact conglomerate with well-rounded pebbles and cobbles of granitoid rock, jasper and milky quartz in a coarse arkose matrix. Local dm-scale layers with rhythmites of mm-cm-scale arkose and mudstone	Probably fluvial, with rhythmite lenses representing deposition in ponds between fluvial channels	Although diagnostic criteria are lacking, P1 may represent glacigenic mass flows and P2 may represent proglacial sedimentation (see Bell, 1970 a,b; Young, 1988)
		P1 Mbr	Polymictic paraconglomerate with angular to subrounded granitoid, mafic volcanic, milky quartz, jasper, iron formation and quartz arenite clasts floating in a grey-black mud-rich matrix	Mass flow of undeterminate origin	
HENIK GROUP	Intrusive Sequence		Grey, white and pink, generally well-foliated granodiorite; locally with large sedimentary enclaves. Satellite dykes cut volcanic sequence. Local gabbro bodies cut granodiorite		
	Volcanic Sequence		Dark grey, green massive mafic volcanic, locally pillowed (rarely variolitic), local mafic tuff, agglomerate, slatey and calcareous interflow sediments, felsic volcanics. Cut by narrow well-foliated gabbro dykes and sills. Spinifex-textured ultramafic rocks with Cu-Ni sulphides in cumulate layers, overlain by magnetite-gruneritic BIF (with local pyritic alteration) north of map area (A.R. Miller, p. comm. 1989). Type exposures of spinefex are at UTM 046003, Cu-Ni sulphides at 064012; and BIF at 080007		Stratigraphic relationship between sedimentary and volcanic sequence is uncertain (see Eade, 1974, p. 11-12). Assumed to be Archean on the basis of ages on felsic volcanic rocks of the Kaminak Group (2697 ± 1.4 Ma, 2692 ± 1 Ma, Mortensen and Thorpe, 1987) and of similar rocks in northeastern Saskatchewan (2682 ± 5.9 Ma, Chiarenzelli and Macdonald, 1986)
	Sedimentary Sequence		M-scale, massive, grey, coarse-grained arkose with disseminated pyrite; dm-scale arkose (+/- grits) to dark grey, black and green slate fining-upward sequences. Local load casts, flame structures, rare dm-scale carbonate layers. Lower greenschist facies, with pervasive cleavage, near-vertical bedding/cleavage lineations and common downward-facing folds		

Similarly, the east-vergent thrust in southeastern Hawk Hill Lake (fault 1, Fig. 5) is considered an "out of syncline thrust" (see Dahlstrom, 1970).

Folded rocks in the footwall of fault 1 are assumed to be autochthonous because of low apparant strain adjacent to the basement contact. Westward extension of Padlei and Maguse rocks is uncertain; stratigraphic pinchouts are illustrated in Figure 5 (cf Fig. 2). Fault 1 cuts up-section north of the line of Figure 5, but further north, cuts through the south-plunging hinge zone of the footwall syncline to emplace Whiterock quartz arenites directly over basement (break-back thrusting of Butler, 1987). Basement lithology may have exerted a control on development of the autochthonous footwall syncline and positioning of the overlying thrust: the syncline is cut off close to the transition between basement arkoses and slates (north) and massive granitic and gabbroic rocks (south).

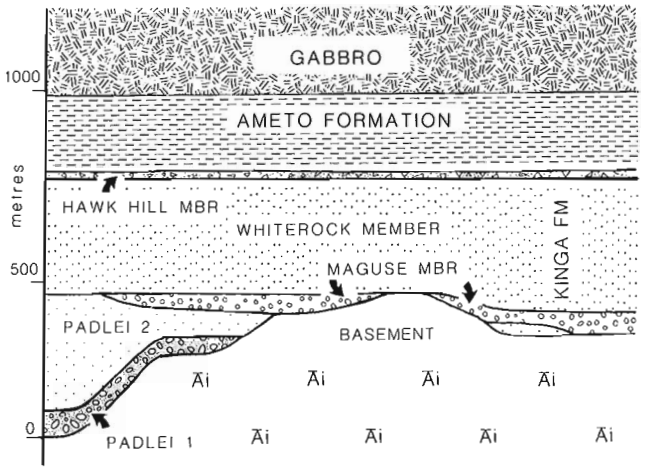

Figure 2. Schematic facies relations, Padlei and Kinga formations, southeast Hawk Hill Lake.

Like D1 folds, D2 folds are open to gentle, concentric and symmetric; minor folds on flat hinge zones of major folds have rounded hinges and limbs (Fig. 6, cf. figs. 4-8 in Bell, 1968). North of Griffin Lake is a D2 box fold around which is a convergent minor fold fan in competent quartz arenites. As with D1, disharmonic D2 folds (eg. Fig. 6) are space accommodating.

There are marked increases in amplitude and decreases in wavelength of D2 folds from south to north such that at Griffin Lake the northwest trend of the D1 synclinorium is replaced by the east and northeast trend of D2. The change in predominant fold set coincides with a change in basement rock type and structural grain. North of Griffin Lake are well foliated mafic volcanic rocks with predominantly east and northeast contacts; south of the lake are less well foliated granitic rocks in which contacts are predominantly northwest-trending. Changes in basement may have influenced Proterozoic deformation both by exerting a control on stratigraphic thickness and facies (see above) and by providing anisotropies that guided deformation (see below and eg. Stewart, 1987).

Southeast of Hawk Hill Lake, D2 axial surfaces are inclined southward and refolding has produced a transitional Type I-II mushroom-like interference pattern. The localization of this pattern south of the transition between the Archean sedimentary and intrusive sequences (Fig. 1) suggests basement control.

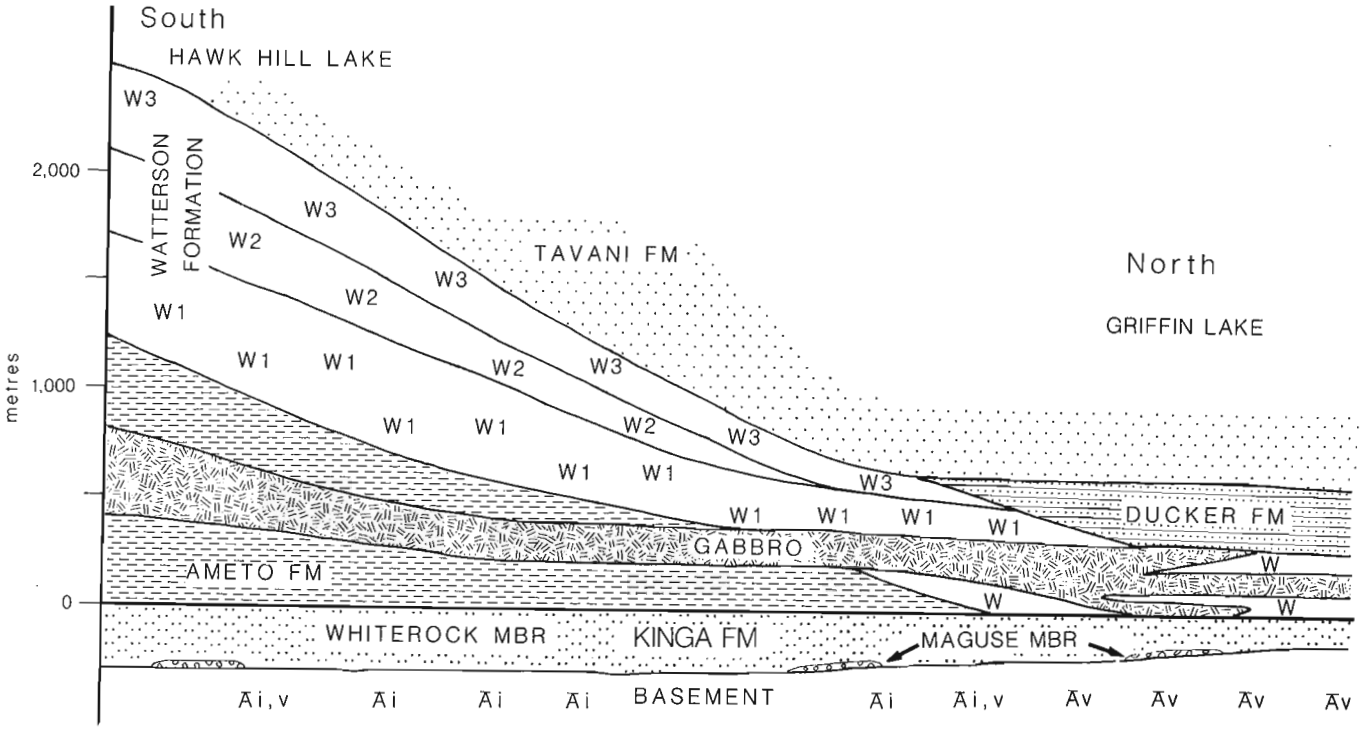

Figure 3. Schematic facies relations, Hurwitz Group, Hawk Hill to Griffin Lake.

In contrast to D1 a regional pressure solution cleavage is related to D2. The cleavage is slaty in mudrocks and appears as insoluble residue stripes in carbonate rocks (Fig. 7). Whiterock quartz arenites are notably cleavage-free; in less competent units the cleavage defines a divergent fan (Fig. 6, C-C').

Active brittle basement involvement during D2 is indicated by concordant faults and cross faults. On the south side of Griffin Lake, a south-vergent low angle (20° at surface) thrust, apparantly rooting in basement, repeats the Whiterock/basement contact (fault 3, Fig. 6, D-D''). This thrust is considered a manifestation of up-dip, out-of-syncline movement. The implied intrabasement detachment

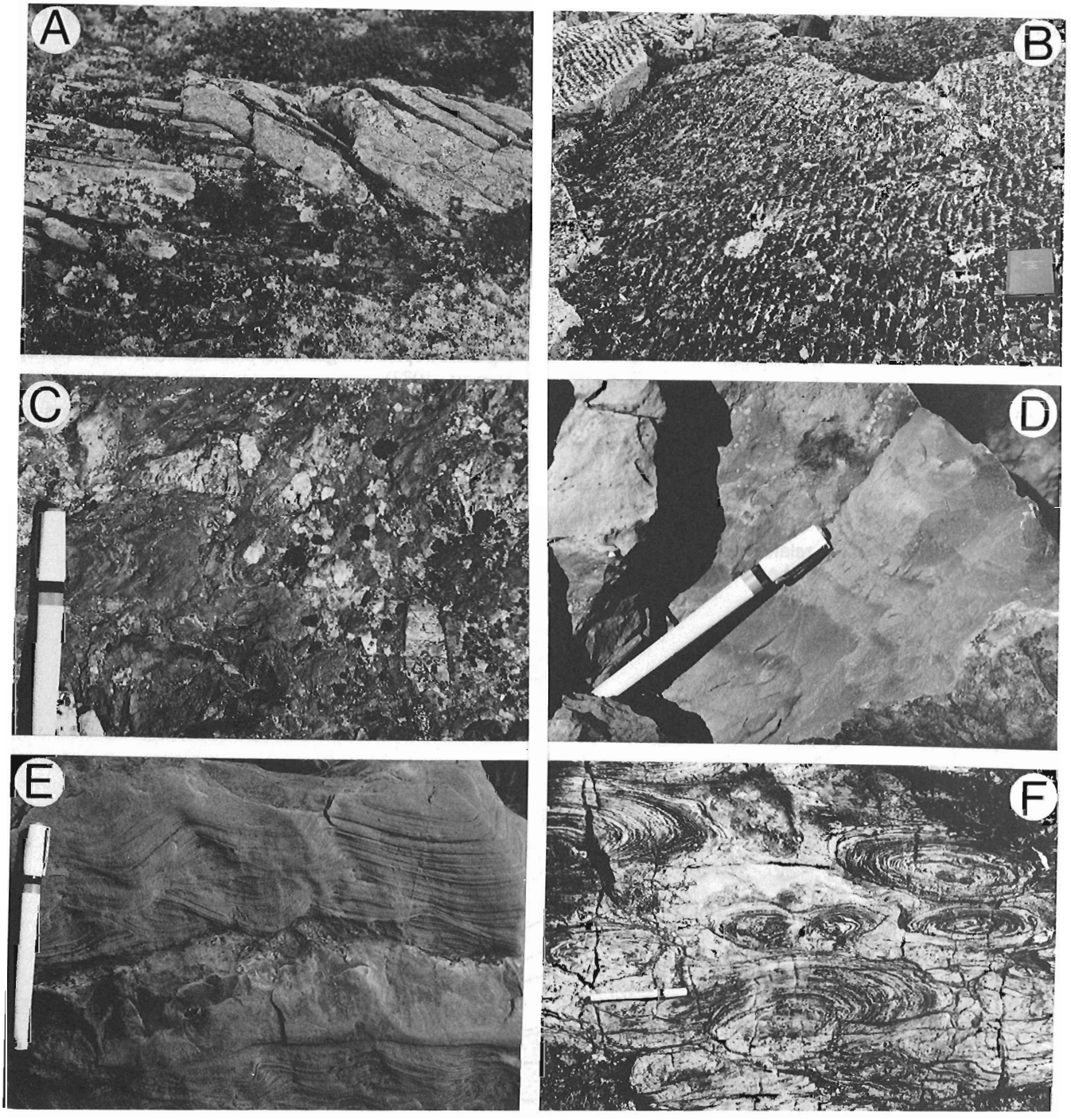

Figure 4. A) Trough crossbeds, P2 arkose; B) different ripple orientations on successive bedding surfaces, Kinga quartz arenite; C) breccia of laminar white chert clasts in maroon chert cement, Hawk Hill member; D) arkose to slate fining-upward sequences, Ameto Formation; E) wave (?) cross-stratification, upper Ameto Formation; F) bulbous stromatolites, Watterson Formation.

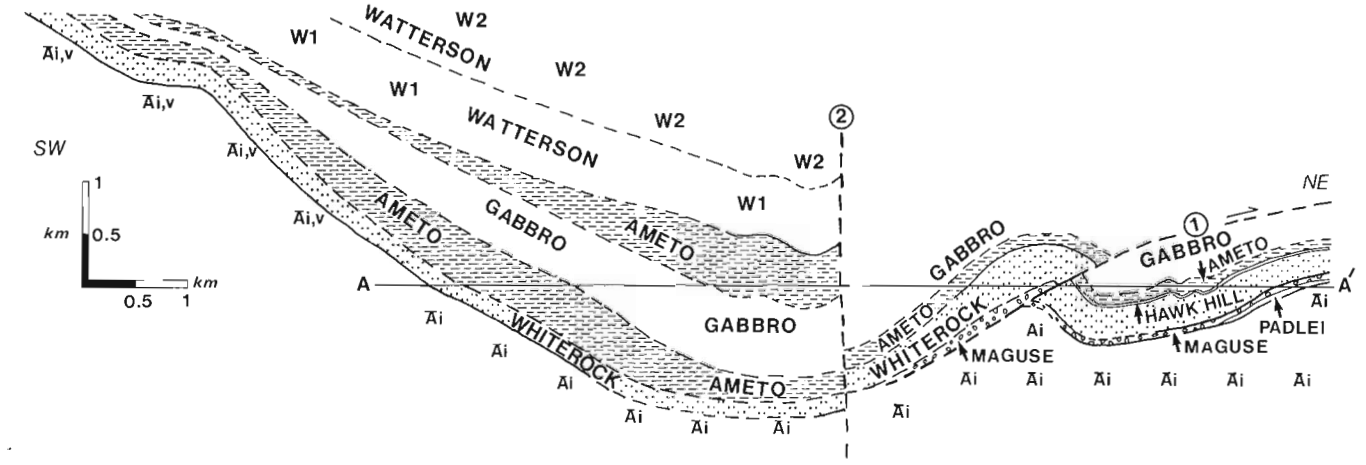

Figure 5. Cross section through D1 fold. East of fault 1, section plunges south; west of fault 2, section plunges north and downplunge data have been added.

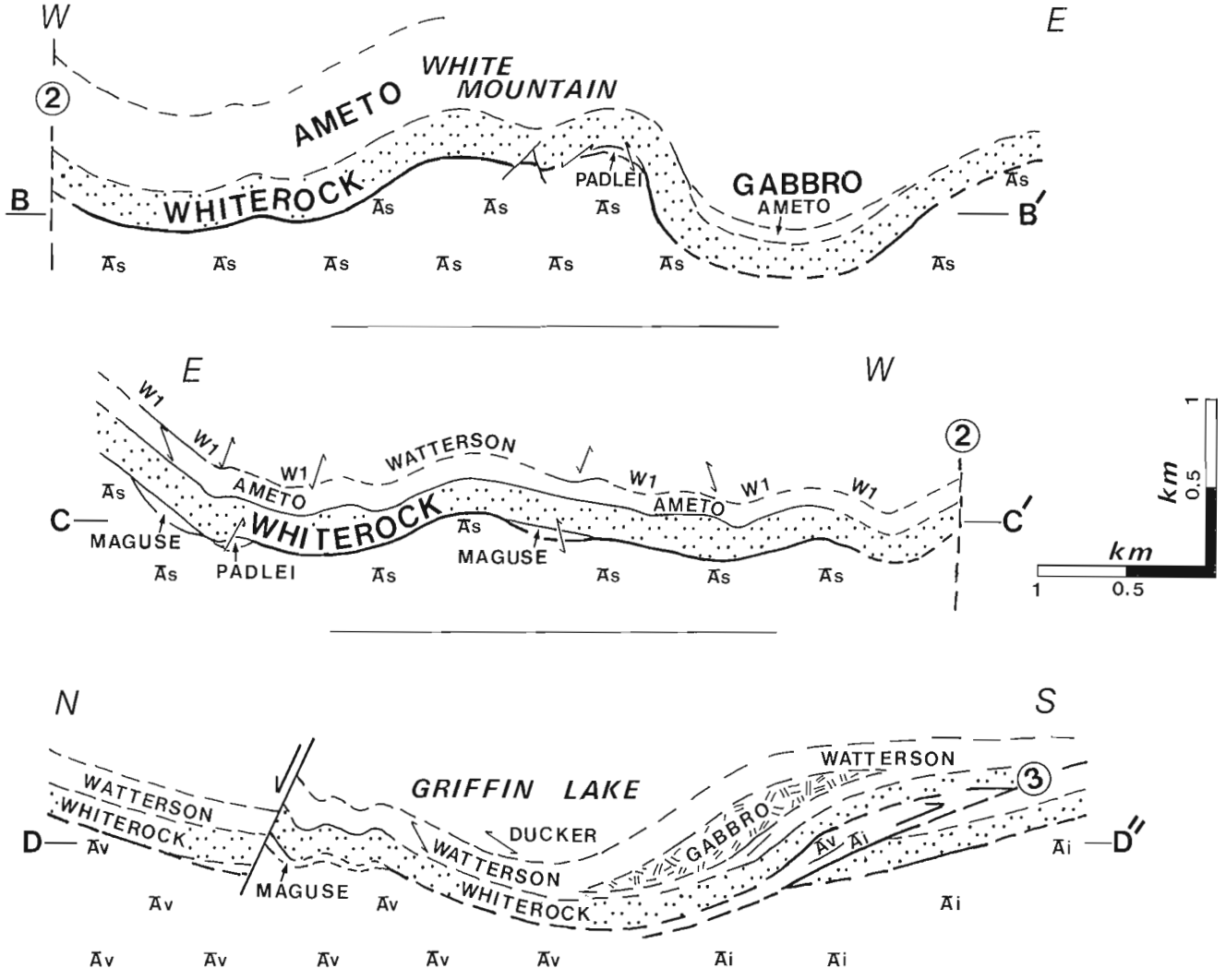

Figure 6. Cross sections through D2 folds: B-B' White Mountain; C-C' northern Mountain Lake (due to plunge reversal inherited from F1, view in B-B' is to north and in C-C' is to south; eastern syncline on C-C' is western syncline on B-B'); D-D'' western Griffin Lake.

may have formed close to, and as a consequence of, the contact between granitic and mafic volcanic rocks (Fig. 6, D-D''). Again, stratigraphic thickness may have exerted an influence on positioning of the detachment within basement and reactivation of an old structure may be indicated. North of Griffin Lake is a concordant, north-dipping high angle (66°) normal fault that cuts through the south-dipping limb of the syncline (Fig. 6 D-D'') and may reflect extension due to northward out of syncline movement.

Oblique-slip cross faults that cut the basement-cover contact are common, particularly in the Griffin Lake area, where such faults fan around the main D2 fold and are consistent with north-south shortening across the limbs of the fold (NNW and NNE) and with outer arc extension in the hinge zone (WNW and ENE; see also horst in hinge zone of D2 syncline at White Mountain, Fig. 6, B-B'). Elsewhere cross faults appear to be primarily minor tears related to D2 warps. Minor near-vertical, NNE-trending sinistral chloritic shear zones in Hurwitz gabbros (Fig. 1), are consistent with north-south shortening due to D2. The arcuate NNW to NNE-trending fault (fault 2) is not exposed, but is demanded by disappearance of Whiterock Member and Archean rocks in the D2 anticline-syncline pair west from White Mountain. The fault appears to have a sinistral-oblique, east-side up sense and is assumed to be genetically related to NNW-SSE shortening during D2.

Hurwitz metamorphism throughout the area is chlorite grade, except at the southeast margin of a wedge of Tavani Formation at Kognak River (Fig. 1), where tremolite-actinolite (?) is developed in carbonate lenses. The southeastern boundary of this wedge is considered a (hot) basement over cover thrust.

Although Kinga quartz arenites at the basement contact do not bear a cleavage related to either D1 or D2, they are intensely fractured. These fractures are sites of pyrite-arsenopyrite-chalcopyrite growth (see Economic Geology below). Fractures were measured continuously as part of mapping (selection method of Goldstein and Marshak, 1988). Preliminary processing of the data suggests that fracture orientations are not consistent regionally, but reflect heterogeneous strain during both D1 and D2 (Fig. 8).

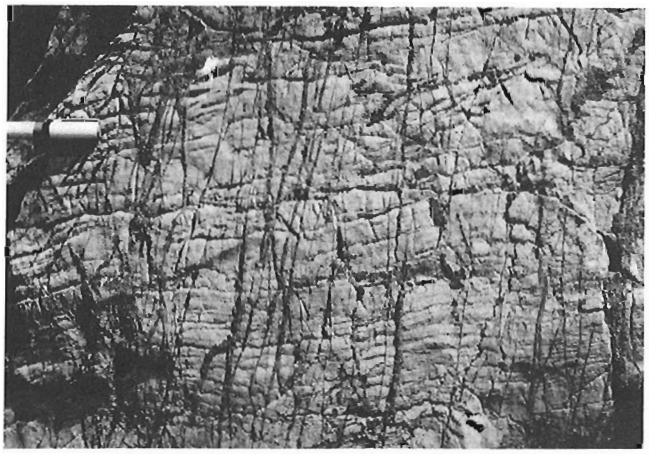

Figure 7. D2 striped pressure-solution cleavage, Watterson cryptalgal laminates.

D1 and D2?

Dome and basin structures have alternatively been interpreted as the result of 2-stage polyphase folding or the product of a single phase, interference being attributed to differential shortening along the length of a fold, diapirism, and high-strain constriction (see Ramsay and Huber, 1987). In the present example a 2-stage model is preferred because: 1) the D2 cross folds and not the D1 folds, have an associated cleavage (changes in plunge are not merely the result of passive deflection about east-west trends, but from active north-south shortening); 2) of the abrupt amplification of D2 folds north toward Griffin Lake, resulting in an abrupt change in predominant fold set, suggesting that the D2 folds are discrete entities with no genetic relationship to the D1 structures; and 3) D2 faults (basement-involved, both concordant and cross) and joints suggest active north-south shortening.

Whether superposed folding was episodic or progressive is unclear. The general similarities of low metamorphic grade, fold style and low apparant strain are consistent with progressive strain. However, cleavage associated with D2 suggests a slight change in physical conditions between D1 and D2, possibly indicating episodic strain. Moreover, the 90° difference between principal strain axes implied by D1 and D2 structures seems extreme for progressive strain.

Basement-cover infolding, cover-over-basement slip and implications

Folding of basement with cover is indicated by the folded basement-cover contact (Fig. 1; eg. White Mountain, Fig. 6, B-B') and by the centripetal pattern that a pre-existing basement fabric makes, (see below). Concentric folding, out of syncline thusting of opposite sense on opposite limbs, fanning of D2 cross faults, minor D2 convergent fold fans and D2 divergent cleavage fans are consistent with a flexural slip (plus tangential longitudinal strain) mechanism.

The basement-cover contact is regarded as having been a site of slip (rather than having been welded) on the basis of: A) the continuation of fault 1 from southern Hawk Hill Lake northward to where it juxtaposes Whiterock directly onto basement; B) local development of a foliation defined by crude alignment of intensely microfractured feldspars in basement granitic rocks adjacent to the contact; C) development in Kinga quartz arenites within 2m of the contact, of thin (0.5-10 cm), bedding-parallel chloritic shear zones with an oblique (locally sigmoidal) internal fabric (Fig. 10) that indicates opposite slip on opposite limbs; up-synclinal dips (eight stations, Fig. 1); D) absence of features typically developed along unslipped Proterozoic-Archean unconformities (despite good exposure close to the contact along a significant strike length); and E) the deflection pattern of basement fabrics at the contact.

The essential elements of the Archean cleavage pattern are: 1) in plan view the cleavage traces are centripetal, following the limbs of both D1 and D2 folds and locally encircling D2 hinge zones (exceptions to the latter are D2 hinges at White Mountain and at northern Mountain Lake, where the cleavage persists at a high angle into the basement-cover contact); 2) close to the contact the cleavage dips at 20-45°

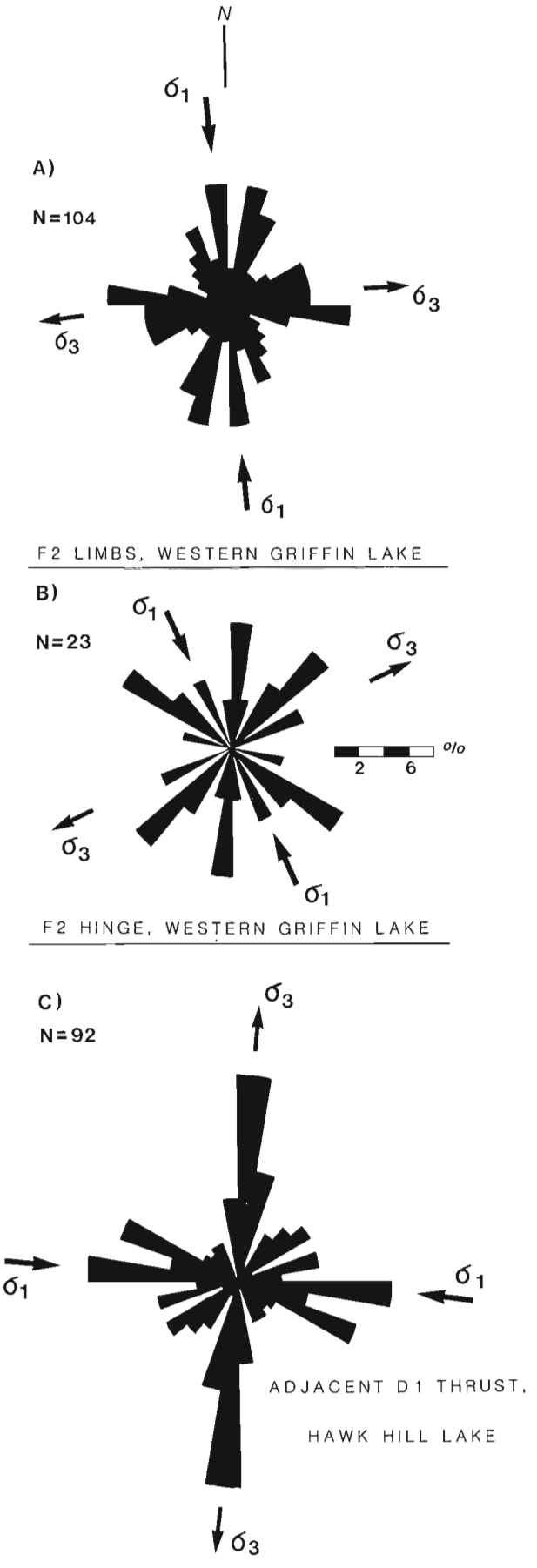

Figure 8. Preliminary interpretation of fracture histograms, Kinga quartz arenites. Principal stress interpretations assume that longitudinal fractures bisect the ca 60° angle between conjugate pairs. The fractures are steep and have not been rotated to account for bedding dip (generally less than 30°)

consistently toward the contact (ie. dipping toward synclinal axes), but steeper than the contact; and 3) locally, dips become progressively flatter as the contact is approached (Fig. 9), suggesting progressive steepening with depth below the contact (a pattern observed in drill core through the Hurwitz-basement contact southwest of Cullaton Lake, A.R. Miller, pers. comm. 1989). In ideal flexural slip, the hinge zone is predicted to be a site of no strain (eg. Ramsay and Huber, 1987), possibly explaining the absence of deflection at White Mountain and northern Mountain Lake. Hinge zones where the centripetal pattern is maintained (eg. box fold, northern Griffin Lake) may reflect tangential longitudinal strain, refolding of an already slipped contact, or hinge line migration.

The open to gentle concentric style of infolding in the present example is in marked contrast to those of cuspate-lobate geometry (megamullions of Tricart and Lemoine, 1986 see also Ramsay, 1982, Harris et al., 1987, Hoffman et al., 1988, Lucas and St-Onge, 1989). The style is more analogous to examples from the Bear Creek Hills (D3 folds of Tirrul, 1985), the Wauchope fold belt, central Australia (Stewart, 1987) and possibly to southern Cape Smith fold belt. Cuspate-lobate forms result from buckling of layers (or interfaces) of low but finite viscosity contrast (low viscosity cusps; high viscosity lobes); the style in the present example resembles buckling with high viscosity contrast (see Ramsay, 1982; Ramsay and Huber, 1987). Ramsay (1982) described changes in rheology, and switches in viscosity, during metamorphism. The high apparent viscosity contrast in the present example may have been maintained because there was no "strong" thermal event during deformation that could have smoothed out rheological differences.

Hoffman et al. (1988) cited several examples of Proterozoic orogens in the Canadian Shield in which thick-skinned folding was preceded by thin-skinned thrusting (see also Harris et al., 1987). We have no evidence from the present map area to demonstrate similar pre-folding nappes,

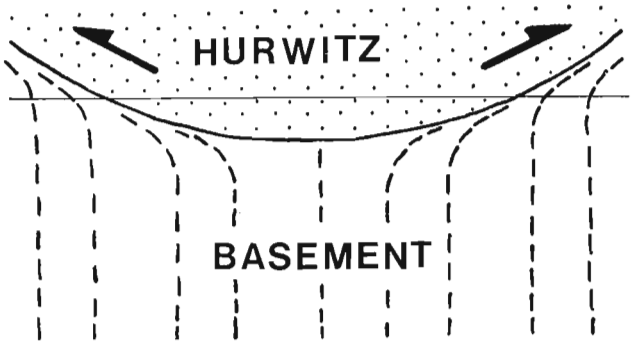

Figure 9. Schematic interpretation of Archean cleavage deflection at contact with Hurwitz Group.

although we cannot rule out the possibility. Crustal shortening by buckling, rather than thrust detachment, may reflect the absence of a sub-Hurwitz weak horizon (eg. evaporites, mudrocks) and the presence of stiff Whiterock quartz arenites that, with anisotropies in basement, guided the folding. Geometric constraints of concentric folding (Dahlstrom, 1970) suggest intrabasement detachment (see Stewart, 1987, Hoffman et al., 1988). The northeast-trending south-dipping (30°) "260" fault discovered at depth during exploration of the Cullaton "B" zone (Raman et al. 1986) may be an example; the southeastern boundary of the Tavani wedge at Kognak River may be where a similar fault breached to surface.

Basement anticlinoria, with a wavelength of about 35 km, separate the present area from synclinoria east at Ducker Lake and west at Watterson Lake. Farther west, low grade Hurwitz rocks in the Poorfish-Windy belt increase in metamorphic grade to the southeast. We speculate that the link between the present area (and the Watterson area) to the Poorfish-Windy belt may be an intrabasement detachment that cut to the surface to emplace hot basement over cold cover immediately east of the Poorfish-Windy belt.

ECONOMIC GEOLOGY

Sites of pyrite, arsenopyrite, chalcopyrite and local gold are (1) at sheared Hurwitz-basement contacts (along the contacts and in fractures that cut Kinga Formation quartz arenites) similar to the past gold producer near Cullaton Lake (Shear Lake deposit, Raman et al., 1986; Miller, 1989) and (2) in the Watterson Formation near cross faults (as fracture-fills and carbonate replacements) (see Fig.1).

Samples from these sites are currently being analyzed. Elevated gold values to date are from two localities shown in Figure 1. Sample 100-11A is from an island in a dried portion of the river between Griffin and Mountain Lakes (UTM 177915): > 10 000 ppb Au (with 1400 ppm Ti, 260 ppm Ni, and 18 ppm As; fire assay DCP by X Ray Assay Laboratories). The sample is quartz-pyrite-veined, sheared calcareous arkose from the Watterson Formation adjacent to a D2 cross fault. Gold fills microfractures in pyrite (up to 20 μm wide and 200 μm long, Fig. 11), forms 0.1-5 μm-sized disseminations in pyrite and 10 μm-sized grains in fractures (with Fe-oxides). The principal exploration targets in the area have been Archean supracrustal sequences (especially BIF) and fractured quartz arenite at the basement-cover contact. The above results indicate that units higher in the Hurwitz Group, adjacent to favourable structures, may be potential hosts for gold (Aspler, 1988; Aspler et al., 1989).

Sample 87-11 is from the southern slope of Hawk Hill (UTM 152703): 130 ppb Au, accompanied by 1300 ppm Cu. The sample is from a quartz vein that cuts Archean granitic rocks close to an intrusive contact with mafic volcanic rocks. Numerous gossans at the top of the Ameto Formation in the Hawk Hill area represent the presence of early diagenetic, (pre-compaction) massive pyrite concretions. Preliminary geochemistry on samples of these rocks did not yield anomalous gold or base metals.

Structural analysis (see above) suggests a regional genetic relationship between folding, fracturing and Shear Lake-type mineralization. There may be a similar genetic link between possible intrabasement detachment ("260 fault"?) and Cullaton "B" zone gold.

DISCUSSION

The discontinuous nature of the Padlei Formation may indicate rift sedimentation. Regional thickening of the Kinga Formation westward from Hudson Bay and eastward from Watterson Lake (ie. toward the centre of the basin, Bell, 1970a) and absence of a typical shelf-slope-rise triad (eg. Ingersoll, 1988) suggests subsequent sedimentation in a cratonic basin (eg. White and McKenzie, 1988) rather than a fully-evolved passive margin.

Previously, Aspler et al. (1989) interpreted the stratigraphy of the Hurwitz and Kiyuk groups in terms of a collision-related foredeep model, with Hurwitz-Kiyuk cycles related to rates of thrust front migration/loading (see also Young, 1988). Below we amplify on this model, but in addition, introduce a non-collision-related intraplate stress model currently being evaluated.

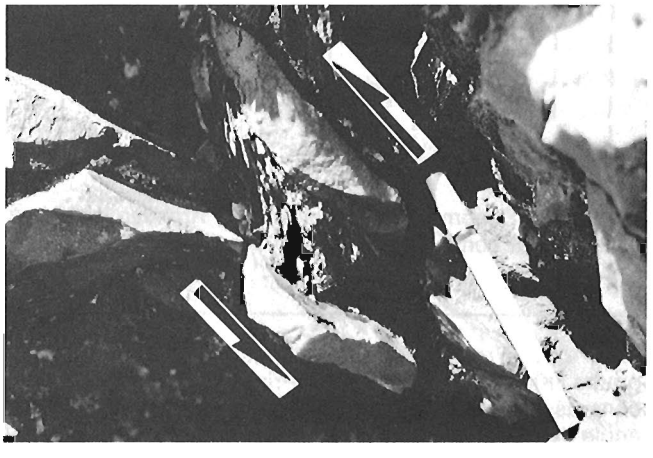

Figure 10. Chloritic shear zone with oblique sigmoidal internal fabric, Kinga quartz arenite.

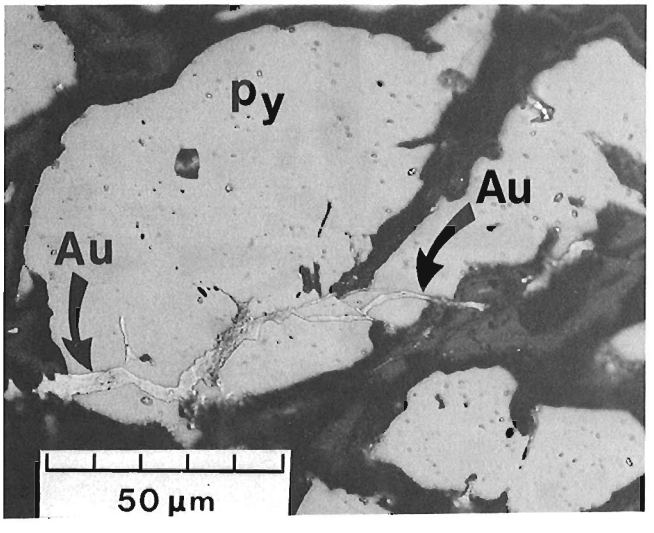

Figure 11. Gold in microfractures and disseminated in pyrite, sheared calcareous arkose (Watterson Formation).

The Foredeep Model

Hematitic silcretes of the Hawk Hill Member coupled with sudden appearance of deep water mudrocks and non-quartzose arenites in the Ameto Formation, suggest interruption of cratonic basin sedimentation, and forebulge emergence coupled with foredeep drowning (see Beaumont et al., 1988). Absence of the silcretes at Griffin Lake is coupled to absence of the Ameto Formation, and a conformable transition from Kinga Formation to Watterson Formation, suggesting that a northward decrease in amplitude of the forebulge/foredeep pair permitted uninterrupted Kinga to Watterson sedimentation. Non-quartzose debris in Ameto Formation arenites may reflect local basement exposure due to bulging; implicit stripping of Kinga may account for local quartz arenite cobbles in Watterson Formation breccias. Shoaling upward of the Ameto Formation to the W1 member may indicate a longer term viscoelastic response to loading, and forebulge retreat (eg. Tankard, 1986) or retreat due to thermal effects of loading (Kominz and Bond, 1986).

The W2 to W3 member stratigraphy suggests a similar second cycle (resumed thrust loading) but of lower forebulge/foredeep amplitude (viscoelastic relaxation from first load impedeing elastic migration due to the second load?). Regional variation of the Watterson Formation (Bell, 1970a) may reflect dynamic interplay between multiple forebulge/foredeep pairs. A third cycle is indicated by fine-grained rocks of the Ducker Formation, shoaling upward to rocks of the Tavani Formation which, east at Pork Peninsula, provide evidence of basin margin sub-Tavani stripping to basement (Bell, 1970a) (due to subareal exposure of the thrust front) and west, in the Poorfish-Windy belt and in the present map area, indicate concurrent uninterrupted sedimentation.

Fine grained rocks of the Hurwitz "H" unit in the Poorfish-Windy belt mark the start of a fourth cycle inferred to represent sudden deepening before arrival of basement-cored thrust sheets, an erosional front and coarse-clastic sedimentation of the Kiyuk Group, which was subsequently thrust-fold deformed (in part cannibalized?) by continued westward migration of the thust complex (Aspler et al., 1989). If the foredeep model is not generally applicable to the Hurwitz Group, the only true foredeep deposits would be those of this fourth cycle.

The question of timing

Previously we assumed that foredeep evolution was genetically linked to 1.91-1.85 Ga collisional events in the Trans-Hudson Orogen (Aspler et al., 1989). A stratigraphic arguement calls this assumption into question. Young (1988) suggested a correlation between the Huronian Supergroup and the Hurwitz Group (glacigenic Gowganda Formation equivalent to the Padlei Formation; Lorrain Formation equivalent to Kinga Formation). The Nippising diabase is younger than the Lorrain Formation and is ca 2.22 Ga (Andrews et al., 1986), suggesting that if Young's correlation is valid, the Kinga is pre-2.22 Ga. Observation at Griffin Lake of a conformable contact between the Watterson and Kinga demands that the two be partly coeval and hence, again if Young's correlation is valid, implies that the Watterson Formation is pre-ca 2.22 Ga. From this it follows that the units attributed above to indicate initial forebulge emergence (Hawk Hill Member) and foredeep drowning (Ameto Formation) are pre-2.22 Ga and cannot be related to known collisional events in Trans Hudson Orogen. This implies that either the foredeep model is not applicable or there is an older, cryptic event to which it is related.

Alternative to the foredeep model: intraplate stresses

Cloetingh (1988) has shown that stresses of sufficient magnitude to cause vertical crustal deflections can be generated in plate interiors, even in non-collisional settings (lacking slab pull forces, but with ridge push). When superposed on an existing subsidence process (eg. thermal subsidence in a cratonic basin) flexural bulges, comparable in amplitude to forebulges, and depressions may develop; bulge/depression migration may simulate forebulge/foredeep interaction (Cloetingh, 1988). Changes in Hurwitz Group stratigraphy might reflect intraplate stress processes (substituting flexural bulge for forebulge and flexural depression for foredeep).

CONCLUDING REMARKS

If geochronology demonstrates that the Hurwitz Group is older than collisional events in Trans Hudson Orogen, and evidence for a cryptic ca 2.22 Ga collision is not found, an intraplate stress model may be more appropriate. Effects of Trans-Hudson Orogen may have been limited to Hurwitz "H"-Kiyuk Group sedimentation and deformation of the entire cover sequence.

In addition to geochronology, a map of silcrete occurrences, and of other sites of a direct Kinga to Watterson transition, on a palinspastic base, (possible only through detailed mapping of the entire Hurwitz belt) may establish bulge wavelengths (and amplitudes?) which may help to differentiate between the foredeep and intraplate stress models as well as shed light on mechanical properties of the Proterozoic crust.

ACKNOWLEDGMENTS

This is a co-operative project supported jointly by: Mineral Resources Division, Geological Survey of Canada; Indian and Northern Affairs Canada (Yellowknife); and Energy Mines and Resources Secretariat, Government of the Northwest Territories, as part of the Canada-Northwest Territories Mineral Development Agreement 1987-1991. C.W. Jefferson and W.A. Padgham were instrumental in securing funding. Discussions with C.W. Jefferson, and J.R. Henderson helped to point out serious flaws in an early interpretation. Richard Lancaster's efficiency permitted preliminary petrography and geochemistry. A.R. Miller generously provided unpublished data on Archean rocks from north of the map area and petrographic help. Expediting and radio contact were by Ingrid Brooks and Gary Gurke of Treeline Lodge, Nueltin Lake. J.R. Chiarenzelli shared geochronological data and H.S. Thompson reprints. We appreciate R.T. Bell's early work in the Hurwitz Group, and his thoughtful critical review of the paper. L. Currie gave deadline assistance.

REFERENCES

Andrews, A.J., Masliwec, A., Morris, W. A., Owsiacki, L. York, D.,
1986: The silver deposites at Cobalt and Gowganda, Ontario. II: An experiment in age determinations employing radiometric and paleomagnetic measurements; Canadian Journal of Earth Sciences, v. 23, p. 1507-1518.

Aspler, L.B.,
1988: Analysis of gossans, exploration guides, and economic evaluation, Poorfish-Windy thrust/fold belt, Ennadai Lake area, District of Keewatin; Indian Affairs and Northern Development Canada Open File, EGS 1988-4, 43 p.
1989: Geology of the Hawk Hill-Griffin-Mountain Lakes Area, District of Keewatin; Indian Affairs and Northern Development Canada Open File, EGS 1989-22, scale, 1:50 000.

Aspler, L.B., Bursey,T.L., and Miller, A.R.,
1989: Sedimentology, structure, and economic geology of the Poorfish-Windy thrust-fold belt, Ennadai Lake area, District of Keewatin, and the shelf to foredeep transition in the foreland of Trans-Hudson Orogen; *in* Current Research, Part C, Geological Survey of Canada, Paper 89-1C, p. 143-155.

Beaumont, C., Quinlan, G., and Hamilton, J.,
1988: Orogeny and stratigraphy: numerical models of the Paleozoic in the eastern interior of North America; Tectonics, v. 7, p. 389-416.

Bell, R.T.,
1968: Preliminary notes on the Proterozoic Hurwitz Group, Tavani (55K) and Kaminak Lake (55L) areas, District of Keewatin; Geological Survey of Canada, Paper 68-36, 17p.
1970a: The Hurwitz Group-a prototype for deposition on metastable cratons; *in* A.J. Baer (ed.) Symposium on basin and geosynclines of the Canadian Shield, Geological Survey of Canada Paper 70-40, p. 159-169.
1970b: Preliminary notes on the Hurwitz Group, Padlei map area, Northwest Territories; Geological Survey of Canada Paper 69-52, 13 p.

Butler, R.W.H.
1987: Thrust sequences; Journal of the Geological Society of London, v. 144, p. 619-634.

Chiarenzelli, J.R., and Macdonald, R.,
1986: A U-Pb zircon date for the Ennadai Group; *in* Summary of Investigations 1986, Saskatchewan Geological Survey, Saskatchewan Energy and Mines Miscellaneous Report 86-4, p. 112-113.

Cloetingh, S.,
1988: Intraplate stress: a new element in basin analysis; *in* K. Kleinspehn and C. Paola (ed.) New Perspectives in Basin Analysis, Springer-Verlag, New York, p. 204-230.

Dahlstrom, C.D.A.,
1970: Structural geology in the Eastern margin of the Canadian Rocky Mountains; Bulletin of Canadian Petroleum Geology, v. 18, p. 332-406.

Eade, K.E.,
1974: Geology of Kognak River area, District of Keewatin, Northwest Territories; Geological Survey of Canada Memoir 377, 66 p.

Eade, K.E., and Chandler, F.,
1975: Geology of Watterson Lake (west half) map area, District of Keewatin; Geological Survey of Canada, Paper 74-64, 10p.

Goldstein, A. and Marshak, S.
1988: Analysis of fracture array geometry; *in* S. Marshak and G. Mitra (ed.) Basic Methods of Structural Geology, Prentice-Hall, p. 249-267.

Harris, C.W., Gibson, R.G., Simpson, C. and Eriksson, K.A.,
1987: Proterozoic cuspate basement-cover structure, Needle Mountains, Colorado; Geology, v. 15, p. 950-953.

Hoffman, P.F.,
1989: Precambrian geology and tectonic history of North America; *in* A.W. Bally and A.R. Palmer, (ed), The Geology of North America- An Overview, Geological Society of America, Boulder, p. 447-512.
in press: Subdivision of the Churchill Province and extent of the Trans-Hudson Orogen; *in* J.F. Lewry and M.R. Stauffer (ed.) The Early Proterozoic Trans-Hudson Orogen of North America, Geological Association of Canada Special Paper.

Hoffman, P.F., Tirrul, R., King, J.E., St-Onge, M.R., and Lucas, S.B.,
1988: Axial projections and modes of crustal thickening, eastern Wopmay orogen, northwest Canadian Sheild; *in* S.P. Clark Jr., B.C. Burchfiel, and J. Suppe (ed.) Processes in Continental Lithospheric Deformation, Geological Society of America Special Paper 218, p. 1-19.

Ingersoll, R.V.,
1988: Tectonics of sedimentary basins; Geological Society of America Bulletin, v. 100, p. 1704-1719.

Kominz, M.A. and Bond, G.C.,
1986: Geophysical modelling of the thermal history of foreland basins; Nature, v. 320, p. 252-256.

LeCheminant, A.N. and Heaman, L.M.
in press: Mackenzie igneous events, Canada: Middle Proterozoic hotspot magmatism associated with ocean opening; Earth and Planetary Science Letters.

Loveridge, W.D., Eade, K.E., and Sullivan, R.W.,
1988: Geochronological studies from Precambrian rocks from the southern District of Keewatin; Geological Survey of Canada Paper 88-18, 36 p.

Lucas, S.B. and St-Onge, M.R.,
1989: Structural evolution of the Cape Smith Belt from initial thrusting to basement-involved folding; Geoscience Canada, v. 16, p. 122-134.

Miller, A.R.,
1989: Highlights of gold studies in the Churchill Structural Province, Kaminak greenstone belt and Hurwitz Group, District of Keewatin, NWT; *in* Current Research, Part C, Geological Survey of Canada, Paper 89-1C, p. 127-134.

Mortensen, J.K., and Thorpe, R.I.,
1987: U-Pb zircon ages of felsic volcanic rocks in the Kaminak Lake area, District of Keewatin; *in* Radiogenic Age and Isotopic Studies: Report 1, Geological Survey of Canada, Paper 87-2, p. 123-128.

Raman, S., Kruse, J., and Tenney, D.,
1986: Geology, geophsics and geochemistry of the Cullaton B-zone gold deposit, N.W.T., Canada; *in* L.A. Clark (ed.) Gold in the Western Shield, Canadian Institute of Mining and Metallurgy Special Volume 38, p. 307-321.

Ramsay, J.G.,
1982: Rock ductility and its influence on the development of tectonic structures in mountain belts; *in* K.J. Hsu (ed.) Mountain Building Processes, Academic Press, London, p. 111-128.

Ramsay, J.G. and Huber, M.I.,
1987: The techniques of modern structural geology, V. 2. Folds and Fractures, Academic Press, London, 462 p.

Stewart, A.J.,
1987: Fault reactivation and superimposed folding in a Proterozoic sandstone-volcanic sequence, Davenport Province, central Australia; Journal of Structural Geology, v. 9, p.441-455.

Tankard, A.J.,
1986: On the depositional response to thrusting and lithospheric flexure: examples from the Appalachian and Rocky Mountain basins; *in* P.A. Allen and P. Homewood (ed.) Foreland Basins, International Association of Sedimentologists Special Publication, 8, Blackwell Scientific, Oxford, p. 369-392.

Tirrul, R.,
1985: Nappes in Kilohigok Basin and their relation to the Thelon Tectonic Zone, District of Mackenzie; *in* Current Research, Part A, Geological Survey of Canada, Paper 85-1A, p. 407-420.

Tricart, P. and Lemoine, M.
1986: From faulted blocks to megamullions and megaboudins: Tethyan heritage in the structure of the western Alps; Tectonics, v. 5, p. 95-118.

White, N., and McKenzie, D.,
1988: Formation of the "Steer's Head" geometry of sedimentary basins by differential stretching of the crust and mantle; Geology, v. 16, p. 250-253.

Young, G.M.,
1988: Proterozoic plate tectonics, glaciation and iron formations; Sedimentary Geology, v. 58, p. 127-144.

Quartzose arenites and possible paleoplacers in Slave Structural Province, N.W.T.[1]

S.M. Roscoe
Mineral Resources Division

Roscoe, S.M. Quartzose arenites and possible paleoplacers in Slave Structural Province, N.W.T.; in Current Research, Part C, Geological Survey of Canada, Paper 90-1C, p. 231-238, 1990.

Abstract

Quartzose arenites and orthoconglomerate, present at bases and upper parts of many Archean supracrustal successions commonly contain concentrations of heavy minerals dominated by pyrite and containing small amounts of uranium and gold. They may be marked by bands of quartz pebbles or rusty-weathering bands and by elevated levels of radioactivity. The most uraniferous and auriferous of those found in 1989 are in the Jackson Lake Formation on the Giant Gold Mine property at Yellowknife (230 ppb Au, 103 ppm U) and in quartz clast conglomerates near the south end of Takijuak Lake (250 ppb Au, 80 ppm U).

Résumé

Les arénites quartzeuses et les orthoconglomérats contenus dans les parties inférieure et supérieure de nombreuses successions supracrustales archéennes contiennent en général des concentrations de minéraux lourds où la pyrite domine et l'uranium et l'or se trouvent en petite quantité. Ils sont marquées par des bandes de cailloux de quartz ou des bandes d'altération rouillée et par une radioactivité élevée. Les roches les plus uranifères et aurifères, parmi celles découvertes en 1989, se situent dans la formation de Jackson Lake à la mine Giant Gold à Yellowknife (230 ppb Au, 103 ppm U) et dans des conglomérats de clastes quartzeux près de l'extrême sud du lac Takijuak (250 ppb Au, 80 ppm U).

[1] Contribution to Canada-Northwest Territories Mineral Development Agreement 1987-1991. Project carried by Geological Survey of Canada.

INTRODUCTION

Fieldwork in 1989 was focused on Archean metaquartzite-bearing formations and possibilities that some of these may contain economically significant paleoplacers. Extensions of the Beniah Formation (Roscoe et al., 1989) found in 1989 in the Beaulieu River supracrustal belt by D. Roach and by M. Stubley and similar rocks found by D. James at Brown Lake in the Cameron River belt were examined. Other hosts and localities of reported or suspected quartzose arenites visited include the Keskarrah Formation at Point Lake, a narrow belt of metasediments extending 100 km south of Point Lake, quartzose clastic metasediments near the south end of Tukiyuak (Tukijuq) Lake reported by Padgham (1985) and the Likely Formation, a local lowermost unit in the Yellowknife supracrustal belt. Slightly elevated levels of radioactivity marking concentrations of heavy detrital minerals associated with pyrite were found in thin lenses at most of these localities. Gold and uranium are slightly concentrated in some of these as reported herein.

At various times, S.M. Roscoe was joined in the field by the following collaborators who contributed special skills in sedimentological and structural studies: D.G.F. Long, Department of Geology, Laurentian University, Sudbury; R.J. Rice, J.A. Donaldson and W.K. Fyson of Carleton-Ottawa Geoscience Center, Ottawa; and E.A. deKemp of Ottawa-Carleton Research Institute. Long and Rice worked almost exclusively on sedimentological studies of three metasedimentary successions reported separately (Rice et al., 1990) in this volume. Rice sampled radioactive heavy mineral-bearing beds discovered by Roscoe at the base of the Jackson Lake Formation on the Giant Gold Mine property at Yellowknife. For comparative purposes, quartz arenite-bearing successions at Wallace Lake in Manitoba and at Eyapamikama Lake in northwestern Ontario, respectively, were examined by Rice and Roscoe and by deKemp and Roscoe enroute between Ottawa and the field area in the Slave Structural Province (Fig. 1).

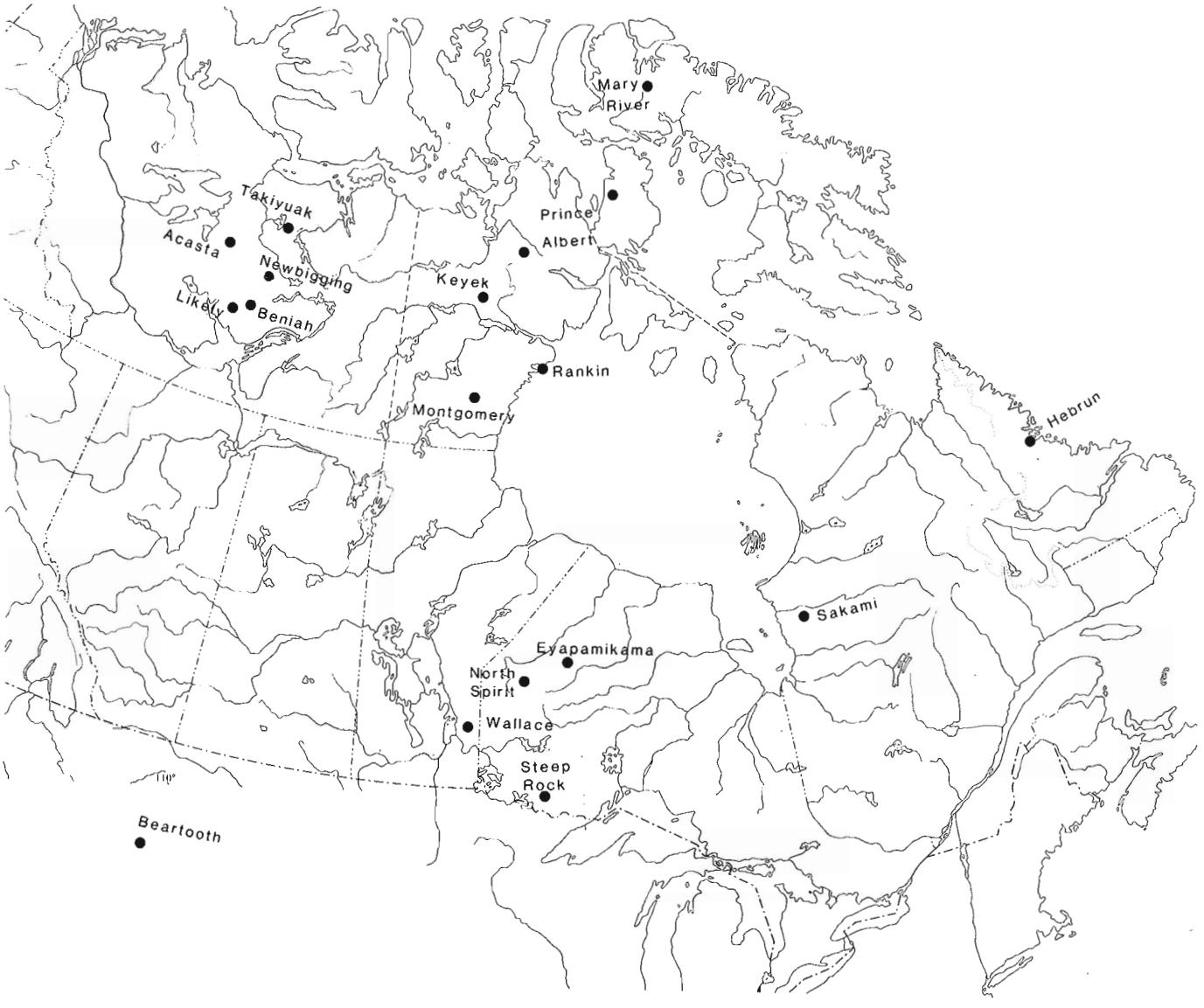

Figure 1. Locations of some Archean successions containing quartz arenites in the Canadian Shield

BENIAH FORMATION

In June 1989, D. Roach (pers. comm.) mapped an east-northeasterly-trending segment of the Beniah Formation centred at 63°17'N, 112°09'W, 4 km southeast of Beniah Lake (Fig. 2; *see* also Fig. 2 in Roscoe et al., 1989). Steeply-dipping metaquartzite beds at the north side of a gneissic terrane are overlain by iron formation and capped by north-facing pillow lava. As in other areas of the Beniah Formation southwest of Beniah Lake, the assemblage includes gabbro and ultramafic rock. Pyrite and slight variations in radioactivity were noted in quartz arenite but no significant heavy mineral bands were observed. Widely scattered exposures of quartzite amid more abundant gabbro outcrops extend through a narrow zone north of Drybones Lake to Clidden Lake near the north end of the Lockhart Lake map sheet (NTS 85P/9) and have been mapped by M. Stubley. The formation is extensively exposed at 63°38.8'N, 112°28.0'W and well-preserved trough crossbeds were noted 1.5 km south of this point. Some ultramafic rock is present near the north end of Drybones Lake in addition to steeply-dipping metasedimentary rocks, including quartzite, siltstone, and polymictic conglomerate, that are flanked to the east by gneissic rocks and overlain to the west by iron formation and pillow lava. Near Clidden Lake, the Beniah Formation is flanked to the east as well as to the west by metavolcanic rocks. No heavy mineral concentrations warranting sampling were found in 85P/9.

SUPRACRUSTAL ROCKS IN RUPP LAKE AREA (85P/16)

The presence of isolated outcrops of quartz arenite in drift covered terrain at 63°56.5'N, 112°17.2'W was reported by Roscoe et al., (1989). Reconnaissance in 1989 was restricted to areas of relatively abundant outcrops near the south border of the Rupp Lake map sheet. No rocks similar to those in the Beniah Formation were observed but some arenaceous metasediments are present at 63°56'N, 112°24'W between outcrop areas of gneissic and granitic rocks to the west and fragmental volcanic rocks that may include ash flow tuffs to the east. Polymictic orthoconglomerate, not unlike conglomerate units in the Beaulieu Rapids formation, is associated with deformed pillow lava at 63°58.6'N, 112°21.8'W.

MCRAE LAKE AREA (85P/10)

Information from M. Stubley (pers. comm., 1989) led to a visit to a locality near the west side of a lake at 63°40'N, 112°40' W. Here, bodies of metagabbro, gossanous sulphide-rich rocks and possibly ultramafic rocks, marked by an aeromagnetic high, occur along a contact between massive granitic rocks to the west and gneisses to the east (see Miller et al. 1951). The gneisses are quartz-rich, contain thin mica and hornblende layers and are intruded by pegmatite. They are apparently paragneisses derived from quartzose sediments. It is possible that they are correlative in part with the Beniah Formation or that they represent basement rocks that predate strata in the Beaulieu River belt including the Beniah Formation.

BROWN LAKE (85P/7)

During 1989, D. James (pers. comm., 1989) mapped a previously unknown lens of quartz rock at the south shore of Brown Lake (63°22.5'N, 113°00'W) along the contact between gneiss and granitic rocks to the northeast and Cameron River metavolcanic rocks to the southwest. It is capped by a thin layer of banded chert-magnetite-amphibole iron formation. Its position in the succession, gneiss-quartzite-iron formation-metavolcanic rock, at the west side of an anticlinorium mirrors that of the Beniah Formation 24 km away at the east side. The quartz rock lacks unequivocal sedimentary structures as do most exposures of the Beniah Formation. Vague banding interpretable as layering is present in places, however, and this together with the presence of green fuchsitic zones, disseminated pyrite, and slight variations in radioactivity likely produced by heavy detrital minerals supports the proposition that the occurrence at Brown Lake can be correlated with the Beniah Formation.

LIKELY FORMATION, YELLOWKNIFE VOLCANIC BELT

Information from Clarke Isachsen and Hendrik Falck led to a tour, guided by Isachsen, of a locality at 62°41.1'N, 114°18.9'W, which is 25 km north of Yellowknife. Here a steeply-dipping lens of quartz arenite and feldspathic quartzite about 70 m thick is flanked by granitic rocks to the west and is overlain stratigraphically by about 20 m of banded chert-magnetite-amphibole iron formation to the east. This lens, which has been termed Likely Formation (see Padgham, 1987, Fig. 10), occurs locally below the Kam Group and is the lowest known stratigraphic unit in the Yellowknife supracrustal belt. Crossbeds, silty beds, coarse grained beds, heavy mineral-bearing pyritic and slightly radioactive layers, and spectacular green fuchsitic zones are present. The succession and associations of lithologic units are remarkably similar to those of the Beniah Formation some 150 km to the northeast.

NEWBIGGING LAKE (86A/8)

Abundant quartz-rich bands were noted in gneiss on islands and shores in the southern part of Newbigging Lake. This is at the east flank of the southern extension of the Point Lake supracrustal belt and about 5 km northeast of an area of clastic metasedimentary rocks mapped by Rice et al. (1990). Fraser (1968) noted mylonitized migmatite south of the lake. This occurrence is at the north end of an extensive area of quartzofeldspathic rocks and gabbro. Some of these apparently quartz-rich felsic rocks may be metarhyolite and/or mylonitized metarhyolite and granite, but some appear to be metaquartzite intruded, like the Beniah Formation, by abundant gabbro dykes.

ACASTA GNEISS (86F/1)

Bowring et al., (1989) have reported extremely ancient Pb-U dates of 3,962 $\pm$ 3 Ma and ca 3.6 Ga obtained for zircons in tonalitic gneiss in the Acasta River area at the extreme westerly edge of the Slave Province about 150 km west of

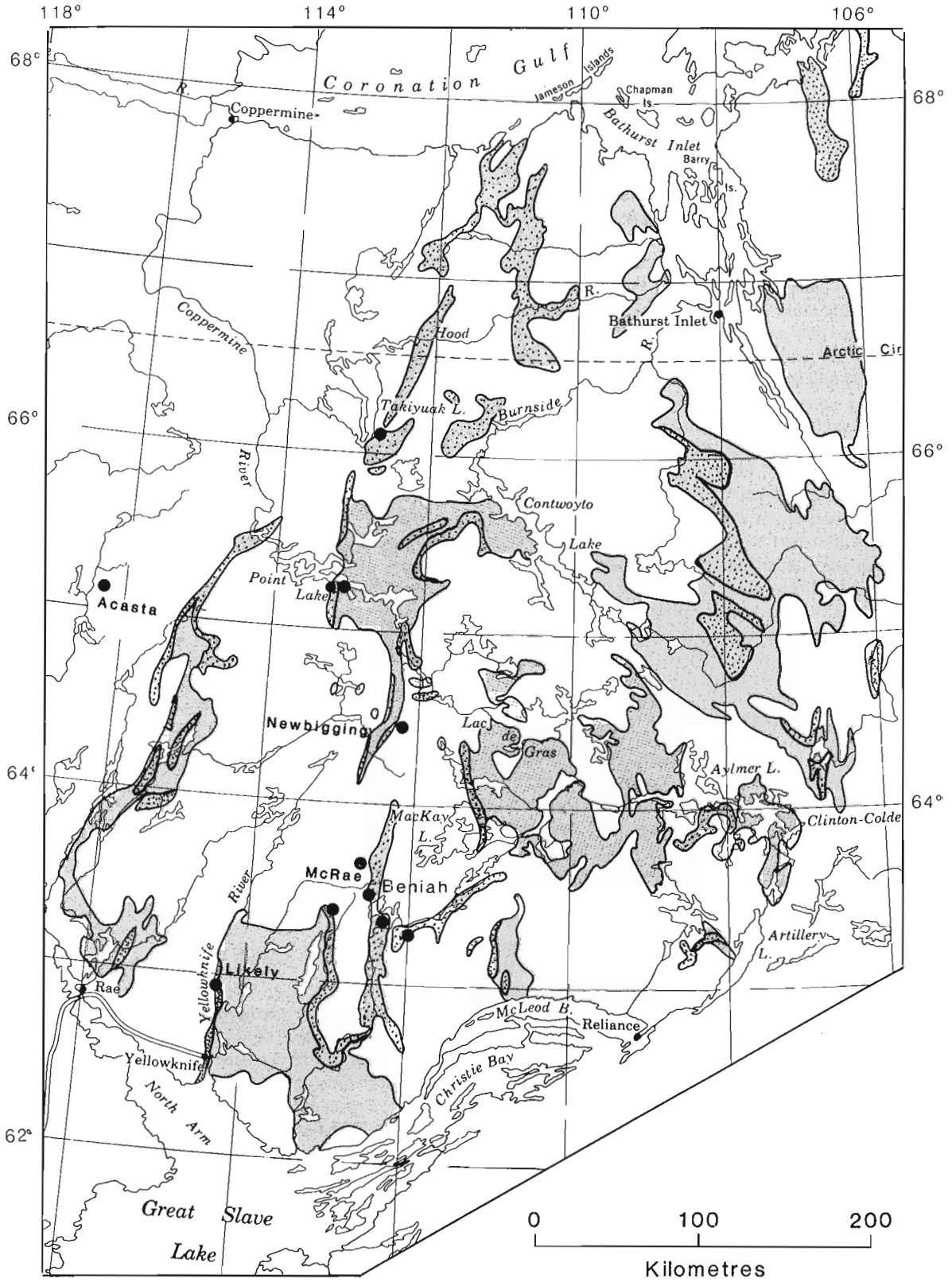

Figure 2. Locations of some quartzose arenites in Archean supracrustal belts in the Slave Structural Province. Finely stippled (grey) areas are underlain mainly by metasedimentary rocks; coarsely stippled areas, by metavolcanic rocks.

the ca 2.7 Ga Point Lake supracrustal belt. Quartzose lenses and ferruginous lenses in the gneiss suggest that it may have been derived in part from an ancient sedimentary terrane that included quartzose arenite (Padgham, pers. comm., 1989).

TAKIYUAK LAKE AREA (86I/2)

Padgham (1985) described quartz-rich clastic rocks near the south end of Takiyuak (Takijuq) Lake. These highly deformed rocks were examined by Donaldson, deKemp and Roscoe in 1989. They include thick arenite and oligomictic orthoconglomerate units. Clasts include rhyolite as well as quartz or metaquartzite. Trough crossbedding is preserved in places. Rusty weathering patches, common on many outcrops, reflect widespread, if not ubiquitous, occurrence of small amounts of fine grained pyrite. Black, highly 'graphitic' and pyritic cherty rock is present along the east side of the metasedimentary belt. The quartzose metasediments are distinctly more radioactive than volcanic and other rocks in the area. Some pyritic pebbly layers in arenites and bands in conglomeratic units are particularly radioactive. Analyses of two samples given in Table 1 provide evidence of concentrations of gold, zircon and uranium, thorium, titanium, rare earth and phosphate minerals.

BASAL POINT LAKE FORMATION AT POINT LAKE

At 65° 15.5'N, 113°16'W, according to Easton et al., (1982), 50 to 100 cm of quartz pebble conglomerate is present between mafic tuff of the Point Lake Formation and "strongly weathered, friable migmatitic gneiss". Unfortunately, it was not possible to visit this locality in 1989. It is 90 km south of, and on strike with, the occurrences of radioactive and auriferous quartz clast conglomerate at Tukiyuak Lake. Ultramafic rocks have been mapped (Bostock, 1980) near the conglomerate locality. This suggests a possible parallel between the initial deposition of supracrustal rocks along the east margin of the Point Lake belt and that of the Beniah Formation in the Beaulieu River belt which hosts most of the ultramafic rocks known in the Slave Province. Iron formation, the most faithful partner of quartz arenite in basal Archean successions, however, has not been reported along the east margin of the belt.

JACKSON LAKE FORMATION, YELLOWKNIFE

The Jackson Lake Formation unconformably overlies the Kam Group in the Giant Mine section at Yellowknife. The formation is fluvial (Padgham, 1985) like the somewhat similar Beaulieu Rapids formation (Rice et al, 1990). A paleoweathered zone can be discerned locally in Kam metavolcanic rocks below the unconformity and chemical variations through it have been studied by Falck (pers. comm.) who provided guidance for our examination of the Jackson Lake Formation. Extensive radioactive layers a few centimetres thick were found at the base and within the lowermost 2 metres of the formation. These are pyritic although they are not conspicuously gossanous.

Analysis of ten samples (Table 1) show that gold, uranium, thorium, titanium, rare earth elements, phosporpus, zirconium and chromium were substantially concentrated in the radioactive layers. Factor analysis shows that abundances of these elements and - in addition - hafnium, sulphur, antimony, boron and cobalt are controlled entirely or largely by Factor I of 5 factors. This factor must represent the process of hydraulic concentration of heavy minerals. Abundances of some elements, such as nickel and vanadium, are partly controlled by Factor I and partly by one or more other factors. Table 2a shows high correlation coefficients for 8 of the elements that are sympathetically concentrated, evidently as a result of hydraulic segregation of heavy minerals. Table 2b shows low correlation coefficients amongst a group of elements that are commonly associated, singly or multiply, with gold in epigenetic concentrations. Of these elements, B alone correlates with Au but it also correlates more closely with REE, Ti, Zr and Cr than with As, Cu, Zn and Pb so it is more likely present in detrital resistate tourmaline than in epigenetic tourmaline. The data do not support any idea that the low concentrations of gold in radioactive clastic sedimentary strata are related to nearby structurally controlled epigenetic gold ores and prospects on the Giant Mine property. They are entirely consistent with a proposition that gold and pyrite, along with zircon, chromite, rare earth-bearing minerals and rutile, are of placer origin.

KESKARRAH FORMATION, POINT LAKE (86H/8)

The Keskarrah Formation, mainly polymictic orthoconglomerate, unconformably overlies the Point Lake Formation and deformed, altered granodiorite at Point Lake. The formation resembles the Jackson Lake and Beaulieu Rapids formations and all three post date the main periods of volcanic eruptions in their respective supracrustal belts. Clastic metasedimentary strata in the southern part of the Point

Table 1. Analyses of selected radioactive specimens from Archean quartzose meta-arenites

Analyses by X-Ray Assay Laboratories Limited, multi-method, multi-element package, S reported as Fe S_2; Fe as FeS_2 and FeO, analyses obtained for numerous elements are omitted.

89RFTJ1 and 3 - quartz pebble conglomerate, Takiyuak Lake

89RFCJL6 and 89RF301-309 - pebbly layers near base of Jackson Lake Formation, Giant Yellowknife Mines.

88RF40, 42, 43 - conglomeratic lenses, Beniah formation (from Roscoe et al, 1989, Table 1)

88RF47-53 - conglomeratic lenses, Beaulieu Rapids formation (from Roscoe et al,1989, Table 1)

89RF200, 201 - grit layer in quartz arenite Eyapamikama Lake.

89RFC1A, 1B - basal 4 cm of quartz arenite formation at Eyapamikama Lake, northwestern Ontario (Figure 1)

89 RF21 - arkose, San Antonio Formation, Manitoba, containing epiogenetic uranium concentration

Table 2. Correlation coefficients, selected elements, Jackson Lake Formation

(a) Heavy detrital mineral association

	Zr	Cr	Ti	La	Th	U	S	Au
Zr	1							
Cr	.977	1						
Ti	.838	.876	1					
La	.911	.867	.852	1				
Th	.985	.975	.779	.831	1			
U	.901	.818	.713	.938	.845	1		
S	.975	.977	.795	.813	.989	.817	1	
Au	.795	.705	.561	.882	.727	.92	.712	1

(b) Common epigenetic gold associates

	As	W	Cu	Zn	Pb	Ni	B	Au
As	1							
W	-.247	1						
Cu	-.231	-.24	1					
Zn	-.484	-.589	.667	1				
Pb	-.864	.201	-.255	.231	1			
Ni	.705	.459	-.235	-.813	-.689	1		
B	.334	.276	-.843	-.723	.067	.421	1	
Au	.631	.332	-.639	-.852	-.354	.749	.881	1

Lake belt also include polymictic orthoconglomerate and they may have been deposited within the same relatively late time interval but are interpreted by Rice et al. (1990) to have been deposited on submarine fans whereas the Beaulieu Rapids formation was deposited on a subaerial fan. Keskarrah arenite at 65°06.5'N, 113°06.3'W (Henderson, 1988) contains trough crossbeds. Disseminations of pyrite and variations in weak radioactivity suggest that some heavy mineral concentrations may be present but none were identified positively.

CONLEY FORMATION, RICE LAKE GROUP, WALLACE LAKE, MANITOBA

W.D. McRitchie and W. Weber provided indispensible guidance for an examination of the quartz arenite-bearing Conley Formation in the Rice Lake Group at Wallace Lake near Bissett. The Rice Lake Group is in the Uchi Subprovince of the Superior Province about 100 km west of Red Lake. According to McRitchie (1971), the Conley Formation disconformably overlies metavolcanic rocks of the Big Island Formation and includes in ascending order, calc-silicate rocks, iron formation, thin pillow basalt flows, ferruginous pelite, trondhjemite clast conglomerate and metaquartzite. It is intruded by ultramafic rocks. The assemblage is like the metaquartzite-bearing successions at Sakami Lake (Roscoe and Donaldson, 1988) and Beniah Lake (Roscoe et al 1989) but the order of succession of units, as interpreted, is the reverse of the order found in other areas where quartz arenite is the basal sedimentary unit and is overlain by iron formation and carbonate or calc-silcate rocks that in turn are overlain by a major volcanic succession. Crossbeds are well preserved in many places in the arenites which contain disseminated pyrite. No heavy mineral concentrations were discovered, but the search for these was not effective as our scintillometer was inoperative.

EYAPAMIKAMA LAKE, NORTHWESTERN ONTARIO

Metavolcanic and metasedimentary rocks at Eyapamikama Lake, 170 km north of Pickle Lake are in the Sachigo Subprovince of the Superior Province. Rocks near the west end of Eyapamikama Lake have been described by deKemp (1987) who guided our field studies in the area in 1989. A thin quartz arenite unit unconformably overlies paleoweathered metavolcanic rocks (Agutua Arm metavolcanics) and is overlain by a thin unit of laminated siltstone that contains

stromatolites. This is capped by a few metres of banded chert-magnetite-siderite-amphibole iron formation. The metasedimentary rocks (Keeyask Lake metasediments) are overlain by komatiite and mafic volcanic rocks that are overlain unconformably by conglomerate and immature arenites (Eyapamikama metasediments). The Keeyask Lake metasedimentary formation, deposited between 2,980 and 2,870 Ma, is the most tightly dated of Archean quartz arenite-bearing units. Trough crossbeds and ripples are well preserved. Radioactive pyrite-bearing pebble layers are present at and near the base of the formation. Pyrite, radioactive minerals, rutile, and zircon are concentrated also within dark layers containing climbing ripples and in stromatolitic layers. Analyses of 4 specimens of radioactive rocks are given in Table 1. Sample 89RF201 is particulary rich in zircon, rutile, thorium-uranium minerals and phosphates.

DISCUSSION

It is becoming increasingly apparent that the history of many, but by no means all, Archean supracrustal belts includes a fragmentary record of an important early period during which mature and supermature clastic sediments derived from deeply weathered cratonic terrains were deposited on stable or metastable supracratonic platforms. This 3.0 - 2.7 Ga period in the Canadian Shield corresponds with the interval in South Africa when thick quartz-rich clastic sedimentary formations containing rich gold paleoplacers were deposited. Minor thin lenses containing detrital heavy minerals, and slight concentrations of gold and uranium, associated with pyrite and quartz pebbles have been found in most of the Archean quartzose arenite formations that have been specifically examined for their presence. These are very low grade analogs of the South African and Huronian gold and uranium paleoplacers. Their gold:uranium ratios, similar to those of sub-ore grade Huronian paleoplacers, are two orders of magnitude lower than those in some South African ores.

Pyritic, uraniferous and auriferous heavy mineral suites are also concentrated in some clastic sedimentary successions deposited late in the depositional history of Archean supracrustal belts. Most favourable are fluvial quartzose formations deposited in proximal parts of alluvial fans.

It is noteworthy that appreciable concentrations of gold (2 orders of magnitude) were formed in clastic metasediments that are older than any known possible lode sources of particulate gold. Gold concentrations in the Jackson Lake Formation at Yellowknife are probably largely, if not entirely, within pyrite that is evidently of detrital origin. A source for detrital auriferous pyrite apparently existed prior to the formation of known epigenetic gold concentrations in rocks of the Yellownife supracrustal belt.

No magnetite has been documented as an allogenic component of heavy mineral suites concentrated in coarse mature Archean clastic metasediments, although it or derived hematite is typically very abundant in younger suites. Magnetic susceptibility measurements on outcrops and hand specimens in this study yielded no evidence that it is present in Slave province arenites

Locations worth exploring for gold paleoplacers in the Slave province would have to contain beds far richer as well as much thicker than any of the radioactive pyritic beds found to date. It should not be concluded, however, that they cannot exist. Only recently has any thought been given to the possibility that even sub-ore grade paleoplacers might exist. This study shows that very low grade concentrations of gold and uranium with pyrite are common, formed as a normal consequence of sedimentation and diagenesis in all situations where heavy minerals were concentrated in Archean strata. The Sakami Lake pyritic uranium paleoplacer prospect (Roscoe and Donaldson, 1988) is sufficently rich and large to serve as an illustration that Archean paleoplacer ores could be present in Canadian Shield localities where no extensive favourable host formations have been mapped and no credible sources are known.

Excepting the conglomerate-bearing section near Takiyuak Lake, the margins of westernmost supracrustal belts in the Slave province have not been evaluated for possible favourable paleoplacer host strata. This should be done.

ACKNOWLEDGMENTS

This project has been furthered by efforts of many individuals. Principal participants in field work, W.K. Fyson, E. deKemp, D.G.F. Long, R.J. Rice, M. Stubley, D. Roach W.D. McRitchie, W. Weber, J.A. Donaldson, H. Falck, and C. Isachsen - and some of their roles, have been cited through the text. The interest of B. Timler, Acting Chief Geologist of Giant Yellowknife Mine and the company's permission to obtain samples of Jackson Lake Formation rocks and to publish analyses of these is appreciated. The staff of LaRonge Aviation and Rod Stone, our expeditor, were most helpful. The manuscript was reviewed by R.T. Bell.

REFERENCES

Bostock, H.H.
1980: Geology of the Itchen Lake area, District of Mackenzie; Geological Survey of Canada, Memoir 391.

Bowring, S.A., Williams, I.S. and Compston, W.
1989: 3.96 Ga gneisses from the Slave province, Northwest Territories, Canada; Geology, v. 17, No. 11, p. 971-975.

deKemp, E.A.
1987: Geochronology, stratigraphy and structural geology of the western Eyapamikama Lake Archean supracrustal sequence; unpblished MSc thesis, Carleton University, 100 p.

Easton, R.M., Boodle, R.L., and Zalusky, L.
1982: Evidence for gneissic basement to the Archean Yellowknife Supergroup in the Point Lake area, Slave Structural Province, District of Mackenzie; *in* Current Research, Part B, Geological Survey of Canada, Paper 82-1B, p.33-41.

Fraser, J.A.
1968: Winter Lake, District of Mackenzie; Geological Survey of Canada, Geological Map 1219 with marginal notes.

Henderson,J.B.
1988: Geology, Keskarrah Bay Area, District of Mackenzie, NWT.; Geological Survey of Canada, Map 1679A scale 1:50,000

McRitchie, W.D.
1971: Geology of the Wallace Lake-Siderock Lake Area: A Reappraisal; Manitoba Mines Branch Publication 71-1, Report 4, p.107-122.

Miller, M.L., Barnes, F.Q., and Moore, J.G.C.
1951: Carp Lakes; Geological Survey of Canada, Paper 51-8, map with marginal notes by J.G.C.Moore.

Padgham, W.A.
1985: Observations and speculations on supracrustal successions in the Slave Structural Province *in* Evolution of Archean supracrustal sequences, Ed. L.D. Ayres, P.C. Thurston, K.D. Card, and W. Weber, Geological Association of Canada, Special Paper 28, p. 133-151.

Padgham, W.A.
1987: The Yellowknife volcanic belt: setting and stratigraphy; *in* Yellowknife Guide Book, Ed. W.A.Padgham, p.11-20.

Rice, R.J., Long, D.G.F., Fyson, W.K., and Roscoe, S.M.
1990: Sedimentological evaluation of three Archean metaquartzite-and conglomerate-bearing sequences in the Slave structural province, NWT.: *in* Current Research, Part!C, Geological Survey of Canada, Paper 90-1C.

Roscoe, S.M. and Donaldson, J.A.
1988: Uraniferous pyritic quartz pebble conglomerate and layered ultramafic intrusions in a sequence of quartzite, carbonate, iron formation and basalt of probable Archean age at Lac Sakami, Quebec; *in* Current Research, Part C, Geological Survey of Canada, Paper 88-1C, p. 117-121.

Roscoe, S.M.,Stubley, M., and Roach, D.
1989: Archean quartz arenites and pyritic paleoplacers in the Beaulieu River supracrustal belt, Slave Structural Province, N.W.T.; *in* Current Research, Part!C, Geological Survey of Canada, Paper 89-1C, p. 199-214.

Bi-Co-Cu-Au-As and U occurrences in metasediments of the Snare Group and felsic volcanics of the southern Great Bear magmatic zone, Lou Lake, Northwest Territories [1]

S.S. Gandhi and D.R. Lentz[2]
Mineral Resources Division

Gandhi, S.S. and Lentz, D.R., Bi-Co-Cu-Au-As and U occurrences in metasediments of the Snare Group and felsic volcanics of the southern Great Bear magmatic zone, Lou Lake , Northwest Territories; in Current Research, Part C, Geological Survey of Canada, Paper 90-1C, p. 239-253, 1990.

Abstract

Arsenopyrite veins and disseminations with associated notable amounts of Bi, Co, Cu and Au, occur near Lou Lake along a 4 km strike zone in sandy and argillaceous metasedimentary rocks of the Aphebian Snare Group and in unconformably overlying felsic volcanic and volcaniclastic units of the southern Great Bear magmatic zone. Magnetite is closely associated with arsenopyrite and also occurs separately as thin layers and lenses in the metasedimentary rocks and as veins commonly containing chlorite and/or quartz. The host rocks are cut by numerous dykes of quartz-feldspar porphyry and quartz monzodiorite. The arsenopyrite mineralization is epigenetic, and is interpreted as related to hydrothermal activity stemming from the felsic volcano-plutonic complex and localized at the unconformity between chemically reactive metasedimentary units and volcaniclastic rocks. Pitchblende veins occur in later fractures subsidiary to a major northeast-trending fault along Lou Lake. These veins and giant quartz veins carrying local concentrations of pyrite, chalcopyrite and sphalerite represent younger metallogenic episodes.

Résumé

Des filons et des dissémination d'arsénopyrite associés à des quantités notables de Bi, Co, Cu et Au, sont présents près du lac Lou, le long d'une zone longitudinale de 4 km dans des roches sédimentaires métamorphisées sableuses et argileuses du groupe de Snare de l'Aphébien et dans des unités discordantes sus-jacentes de roches volcaniques et volcanoclastiques felsiques dans le sud de la zone magmatique de Great Bear. La magnétite est étroitement associée à de l'arsénopyrite et se présente également sous forme de couches minces et de lentilles dans des roches sédimentaires métamorphisées et sous forme de filons contenant généralement de la chlorite et(ou) du quartz. Les roches encaissantes sont recoupées par de nombreux dykes de porphyre quartzo-feldspathique et de monzodiorite quartzifère. La minéralisation en arsénopyrite est épigénétique et serait liée à une activité hydrothermale issue du complexe volcano-plutonique felsique, et située à la discordance entre des unités sédimentaires métamorphisées chimiquement réactives et des roches volcanoclastiques. Des filons de pechblende occupent des fractures formées ultérieurement et subsidaires d'une importante faille à direction nord-est longeant le lac Lou. Ces filons et les immenses filons de quartz contenant des concentrations locales de pyrite, chalcopyrite et sphalérite correspondent à des épisodes métallogéniques plus récents.

[1] Contribution to Canada-Northwest Territories Mineral Development Agreement 1987-1991. Project carried by the Geological Survey of Canada.
[2] Ottawa-Carleton Geoscience Centre, University of Ottawa, Ottawa, Ontario, K1N 6N5

INTRODUCTION

Promising Bi-Co-Cu-Au prospects have been known in the Lou Lake area since 1965. The main prospect has drill-indicated resources of 195 000 tonnes, averaging 0.162 % Bi and lesser values in Co, Cu and Au (Padgham et al., 1978). A 56 kg bulk sample from it contained 0.14 oz/t Au, 2.36 % Co, 0.63 % Bi, 40.8 % As, 22.5 % Fe and 16.0 % S (Mathieu, 1966). Several other occurrences of these metals and uranium were discovered in the area more recently (Thomas and Olson, 1978; Bryan, 1981, 1982). The present study was undertaken as a continuation of the regional metallogenic study of the southern Great Bear magmatic zone started in 1987 under a Canada — Northwest Territories Mineral Development Agreement (Gandhi, 1988, 1989).

PREVIOUS WORK

Regional mapping in the southern part of the Great Bear magmatic zone was conducted by Kidd (1936), Lord (1942), Wilson and Lord (1942), Fraser (1967), and McGlynn (1968, 1977, 1979). It revealed the presence of Aphebian Snare Group strata and of felsic porphyries, believed to be intrusive, in Lou Lake area (Lord, 1942). In uranium exploration work by Thomas and Olson (1978) for Eldorado Nuclear Limited, however, it was recognized that the Snare Group is unconformably overlain by a sequence of felsic volcaniclastic and volcanic rocks at the south end of Lou Lake. This significant observation was confirmed by the present work, and the unconformity is now extended beyond the small area (LOO, BW and C claims) covered by Thomas and Olson. Several uranium occurrences were discovered during this exploration, but they are small and no further exploration was undertaken. Arsenopyrite occurrences in the area have been explored intermittently since their discovery in 1965. One of the two main zones within the original CAB claim area was bulk sampled by Precambrian Mining Services Limited for metallurgical testing by the Mines Branch, Ottawa (Mathieu, 1966). Further exploration by New Athona Mines Limited during 1968-69 included mapping, EM and magnetometer surveys, trenching and drilling of 21 holes totalling 1413 m (Byrne, 1968; Hall, 1969). The drilling intersected rocks that yielded several high Bi, Co and Au values, comparable to those encountered in trenches, and the resources announced were based on these results. During 1978-81 Noranda Exploration Company Limited staked the GAR claims that covered the ground previously held by New Athona Mines Limited and a number of new occurrences in the surrounding region and at Burke Lake 6 km southeast of Lou Lake. An extensive program of detailed geological mapping and sampling was carried out by the company within the claim area (Bryan, 1981, 1982). The GAR claims lapsed in 1989, and were restaked by Brian Weir of Yellowknife.

GEOLOGY OF THE LOU LAKE AREA

Strata of the Snare Group in Lou Lake area form an east-southeast-trending belt, and dip moderately to steeply to the northeast (Fig. 1 and 2). They are overlain unconformably by volcanic strata of the Great Bear magmatic zone that are relatively little deformed, are tilted gently to moderately to the north, and have an aggregate thickness of approximately 1 km. All these rocks are surrounded by granodiorite, quartz monzonite and granite intrusions of the Great Bear magmatic zone (Fig. 1). Basement to the Snare Group is not recognized in the study area, but the group unconformably overlies Archean rocks east of the Wopmay fault (Lord, 1942; Wilson and Lord, 1942; Frith et al., 1977; McGlynn, 1977). The group has been intruded by the Hepburn suite of granitic plutons that are not reported west of the fault, but it is conceivable that they may be present there and are not readily distinguishable from the younger plutons of the Great Bear magmatic zone. A prominent northeast-trending fault along Lou Lake post-dates the intrusive activity. Its northwest side is downfaulted with a small right lateral displacement.

The lithological units distinguished in the present study are mostly those recognized by Thomas and Olson (1978) in the LOO, BW and C claims, with some modifications and additions. Within the GAR claims, mapping done during exploration did not lead to recognition of the unconformity between the Snare Group and the felsic volcanic sequence; instead the latter were regarded as interbedded with the Snare Group (Bryan, 1982). Individual lithological units, however, were clearly distinguished on maps covering arsenopyrite occurrences. These distinctions facilitated application of the legend adopted here to the map areas.

Lithological units

Snare Group (units 1 and 2):

The metasedimentary rocks of this group are broadly divided into a generally uniform, fine grained, thinly bedded siltstone (unit 1), and a lithologically variable quartzite-argillite (unit 2). The siltstone (unit 1) is composed of alternating grey, buff-white and pale pink layers and lenses which are up to 10 mm wide. The layering is essentially primary, but in places is highly attenuated due to tight folding.

The quartzite-argillite (unit 2) comprises three lithological sub-units. The quartzite (sub-unit 2a) is distinctive and massive with variable content of mafic silicates, mainly biotite. It is grey, mature, fine- to medium-grained sandstone. Bedding is well developed in some places. Thin argillaceous layers with variable chlorite contents are common in quartzite, and with an increasing proportion of these it grades into argillites (sub-units 2b and 2c). The argillites are commonly thinly bedded, schistose, and are characterized by the presence of magnetite-rich layers as much as 2 cm thick. The chlorite-rich variety (sub-unit 2c) is distinctively green, and predominates in some areas, but gradations to chlorite-poor argillite are common and the distinction between them in many places is rather arbitrary.

Felsic volcanic and volcaniclastic sequence (units 3 to 12)

At the base of this sequence is an agglomerate-lithic tuff-conglomerate unit of variable lithological character and thickness (unit 3). The unit is referred to as 'polymictic volcanic conglomerate' by Thomas and Olson (1978) and as 'laharic breccia' by Bryan (1982). Angular to subrounded

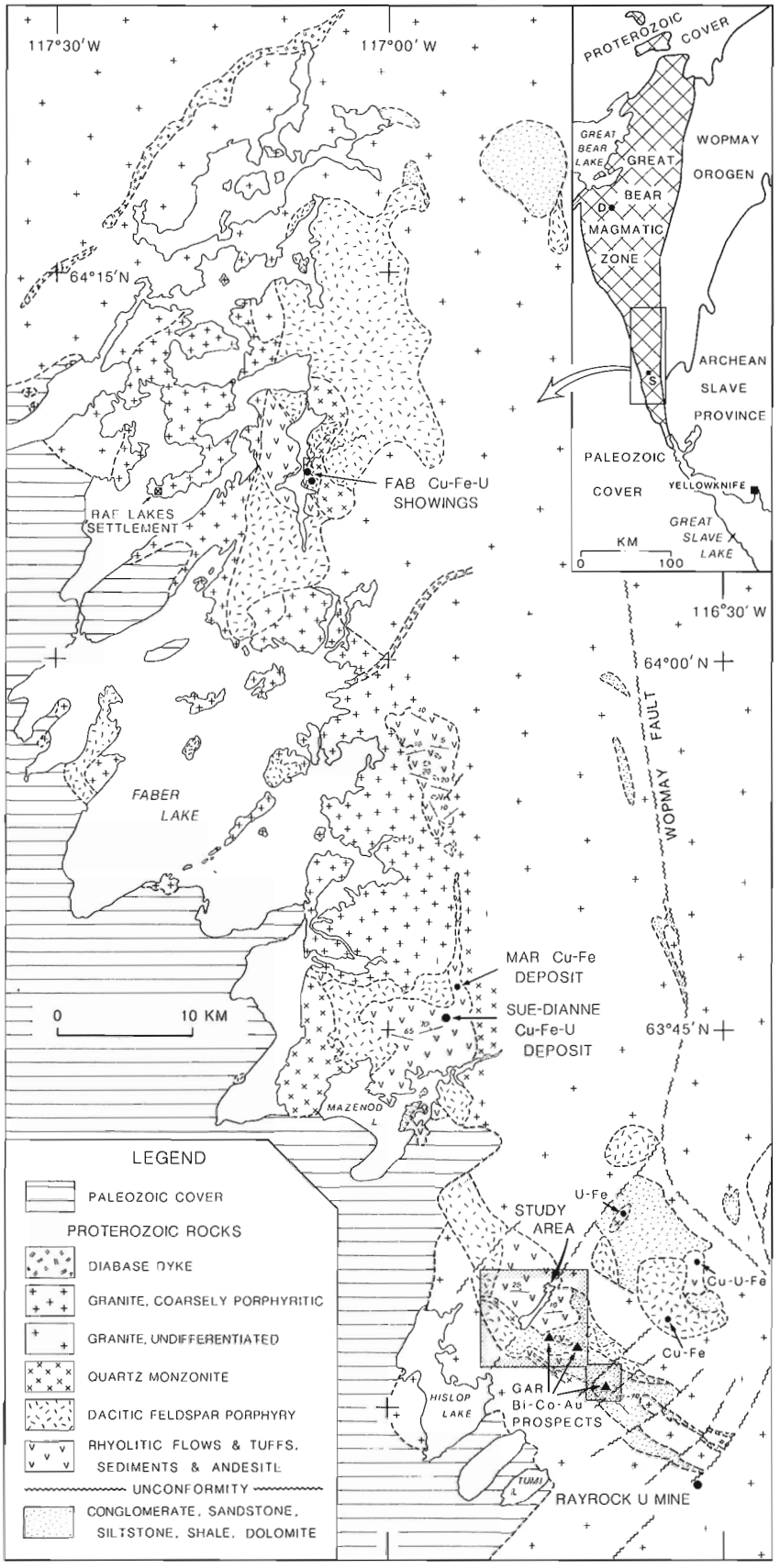

Figure 1. General geology of the southern Great Bear magmatic zone and location of the study area.

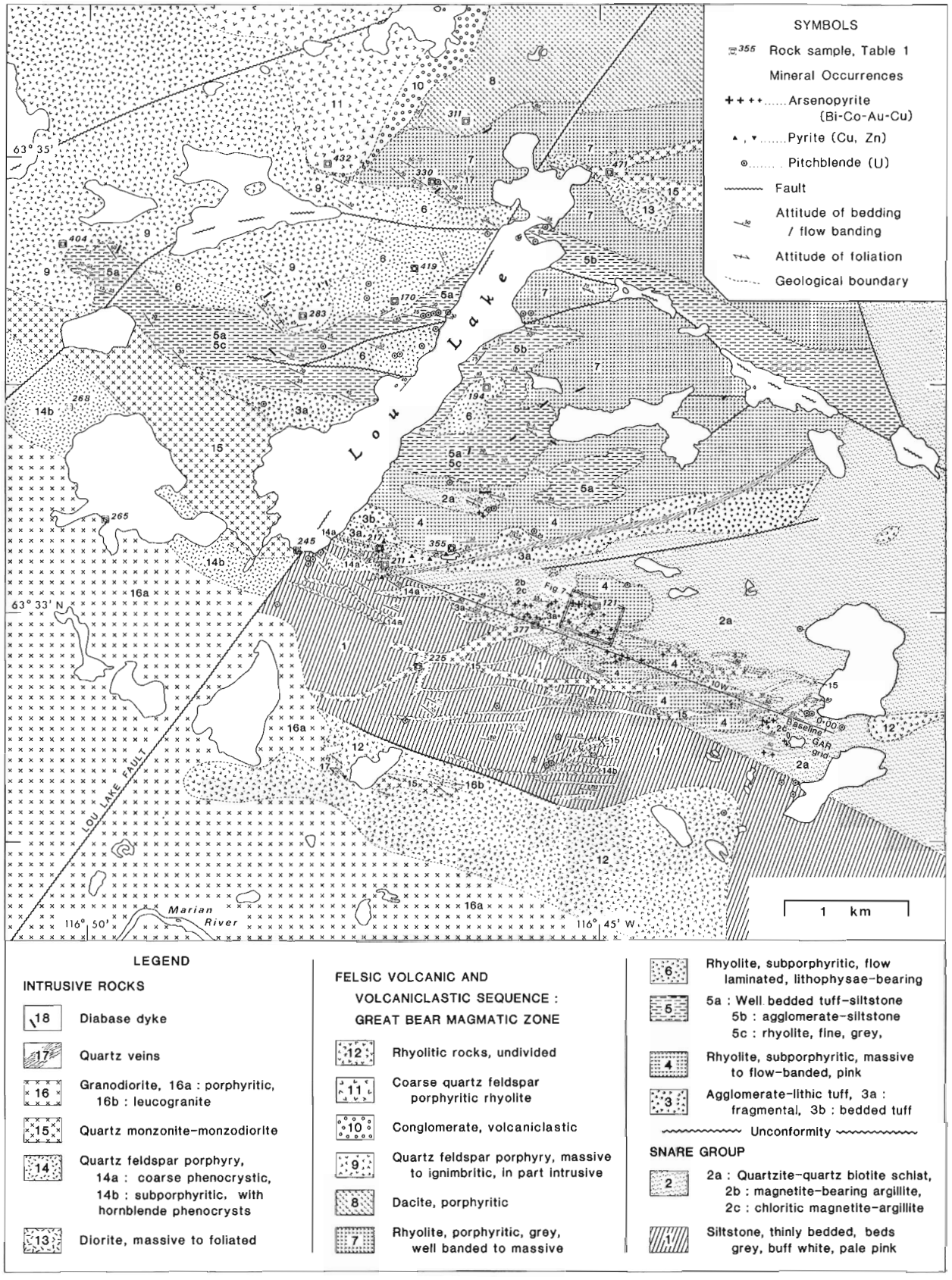

Figure 2. Geology and mineral occurrences of the Lou Lake area, Northwest Territories (after Thomas and Olson, 1978, and Bryan, 1982).

Table 1. Whole-rock chemical analyses of volcanic and plutonic rocks in the Lou Lake area, N.W.T.

Analysis No.		1	2	3	4	5	6	7	8	9	10	11	12	13	14	15	16	17	18	19
Sample No.		121	355	211	170	194	419	330	311	283	404	432	217	268	245	225	377	265	471	261
Map Unit		4	4	5b	6	6	6	7	8	9	9	11	13	13	14	14	14	15	15	15
SiO2	%	72.70	70.30	72.70	74.60	70.00	72.50	75.20	63.10	71.10	70.70	66.00	72.60	70.10	61.10	63.70	70.40	65.90	59.90	70.60
Al2O3	"	13.80	14.30	15.00	14.00	15.50	13.60	13.30	15.20	13.20	14.70	15.10	13.90	15.10	17.50	14.70	13.30	16.20	18.80	14.80
TiO2	"	0.07	0.05	0.14	0.11	0.27	0.11	0.10	0.49	0.10	0.26	0.48	0.12	0.27	0.63	0.54	0.26	0.43	0.61	0.29
FeO	"	0.80	1.20	1.40	0.30	1.20	1.00	0.30	2.10	1.80	1.00	2.80	1.40	1.30	2.90	4.50	2.40	2.40	2.40	1.90
Fe2O3	"	0.30	1.00	1.00	1.10	2.10	2.30	2.00	4.80	4.50	2.00	1.70	1.20	0.70	2.00	1.70	1.00	1.00	2.00	0.90
MnO	"	0.00	0.02	0.04	0.01	0.01	0.01	0.03	0.10	0.00	0.01	0.08	0.03	0.02	0.09	0.03	0.02	0.11	0.04	0.03
MgO	"	0.31	0.40	1.03	0.32	0.44	0.38	0.43	2.42	0.15	0.54	2.37	0.54	0.42	1.95	2.33	0.93	1.56	2.14	0.45
CaO	"	0.03	0.22	0.29	0.06	0.74	0.17	1.06	3.80	0.29	0.50	2.82	0.61	1.04	3.69	0.80	0.43	0.22	3.42	0.55
Na2O	"	0.20	0.30	3.70	0.20	5.00	0.20	2.00	3.50	4.70	2.60	3.00	2.90	3.30	3.30	2.10	1.20	2.10	3.30	4.40
K2O	"	11.57	11.77	3.00	8.31	4.25	8.38	4.65	3.00	3.88	7.02	3.81	5.53	6.76	4.04	7.95	9.00	8.04	5.14	5.62
P2O5	"	0.03	0.03	0.04	0.05	0.10	0.06	0.05	0.12	0.05	0.07	0.11	0.06	0.07	0.15	0.12	0.07	0.10	0.18	0.10
H2O	"	0.60	0.50	1.70	1.40	0.70	1.10	0.60	1.30	0.50	0.80	1.30	1.10	0.90	2.30	1.50	0.90	2.00	1.60	0.80
CO2	"	0.10	0.10	0.00	0.10	0.00	0.10	0.10	0.30	0.00	0.10	0.10	0.10	0.00	0.40	0.20	0.10	0.00	0.30	0.10
S	"	0.00	0.00	0.00	0.00	0.00	0.06	0.00	0.00	0.00	0.00	0.00	0.00	0.00	0.00	0.00	0.02	0.00	0.00	0.02
Total	"	100.5	100.2	100.0	100.6	100.3	99.9	99.8	100.2	100.3	100.3	99.7	100.1	100	100.1	100.2	100	100.1	99.8	100.6
Ba	ppm	1232	1470	239	2107	797	2619	472	453	743	902	498	682	1072	801	1011	910	892	1205	590
Be	"	0.5	2	4.1	4	2.3	2.3	4	2.2	3	2.3	2.7	4.1	2.1	2.5	2.7	2.4	1.7	2.5	1.8
Co	"	6	4	6	2	4	4	4	17	3	5	19	5	5	15	12	8	8	16	8
Cr	"	6	10	10	7	18	13	10	35	13	14	37	10	10	30	40	18	21	34	13
Cu	"	20	8	7	7	8	4	6	4	4	10	8	14	4	28	8	190	6	15	70
La	"	24	7	53	31	42	29	37	37	17	65	37	35	42	45	27	27	44	35	49
Nb	"	20	41	46	34	31	32	39	28	30	41	21	23	62	34	15	33	50	35	57
Ni	"	17	9	8	9	9	12	7	21	6	10	24	8	5	20	25	13	15	19	7
Rb	"	233	261	131	358	152	395	245	124	129	281	194	221	256	157	319	233	220	237	135
Sr	"	0	35	0	0	40	3	74	127	70	75	181	57	86	274	42	23	59	439	8
V	"	1	1	3	4	24	16	5	94	25	16	65	8	4	60	77	30	30	59	16
Y	"	33	59	78	26	62	68	66	74	58	26	61	27	54	64	58	57	34	54	35
Yb	"	1.4	3	2.6	2.3	1.6	2	2.1	2.3	2.1	2.5	2	2.3	1.9	2.1	1.6	2	1.6	1.4	3.2
Zn	"	2	22	29	6	21	11	7	36	26	30	68	28	34	75	26	20	120	36	16
Zr	"	114	119	244	108	172	101	122	170	101	187	175	95	262	284	173	131	351	352	227

Notes : 1) Analyses by the Analytical Chemistry Section, Mineral Resources Division, Geological Survey of Canada, Ottawa.
2) All analyses by x-ray fluorescence method except FeO, H2OT, CO2T and S by rapid chemical methods and Be, Co, Cr, Cu, La, Ni, V, Yb and Zn by ICP-MS method.
3) Fe2O3 is calculated using the formula : Fe2O3 = Fe2O3 (XRF) - 1.11134 X FeO (Volumetric).
4) Sample locations in Figure 2 (analyses 1 to 18), except for sample number 261 (analysis 19) which is from Burke Lake west shore, near tip of peninsula at approximately 63 31' 08" N, 116 42' 49" W (Fig. 8 inset).

fragments of aphanitic, pale pink, feldspathic rock, regarded as felsic volcanic in origin, are most abundant. Clasts of thinly bedded siltstone and quartzite occur in the lower part of the unit. The clasts commonly range in size from 1 to 10 cm, but larger clasts are abundant in places, particularly in the lower part of the unit. The clasts are matrix supported, and the matrix is fine grained, buff-white to light grey and silty. Some thinly bedded siltstone lenses occur locally, and are more common in the upper part. The unconformity is exposed at several localities southeast of Lou Lake, where quartzite forms paleotopographic highs. Large subrounded clasts of quartzite, up to a metre long, occur here in the agglomerate-conglomerate unit. Parts of the unit are rich in magnetite; the magnetite is inherent in some clasts, but in others it was introduced later as veins and irregular patches, commonly with pyrite and chalcopyrite.

A porphyritic, flow-banded rhyolite (unit 4) overlies the agglomerate-lithic tuff and dips gently north (Fig. 3). It is a distinctive pink and is highly potassic (Table 1). In places it looks massive, but in thin section flowage texture is evident.

Well bedded volcaniclastic siltstone-tuff with some interbedded agglomerates and thin, aphyric rhyolites (unit 5), overlie unit 4 east of Lou Lake, and unit 3 west of the lake. The siltstone beds, up to a few centimetres thick, are generally grey to buff-white, but in places are varicoloured. The agglomeratic beds and lenses are as much as a few metres thick, and contain subangular clasts of porphyritic felsic volcanic rocks and some finer grained varieties, in a silty matrix (Fig. 4). The rhyolites are up to a few metres thick, and occur at various intervals. They are grey and flinty, have apparently gradational boundaries with the siltstones, and in a few places show ignimbritic texture.

The overlying rhyolite (unit 6) is buff-white, porphyritic, massive to flow laminated, and in many places contains quartz-rich lithophysae, up to 5 cm in diameter and with magnetite at the core (Fig. 5). Another feldspar-phyric grey rhyolite (unit 7) exposed near the north end of Lou Lake has well developed banding in many places (Fig. 6) and grades into more massive and streaky varieties elsewhere.

Figure 3. Flow banded rhyolite, unit 4, sample 355 (Fig. 2). Looking north. GSC Photo 205021-B.

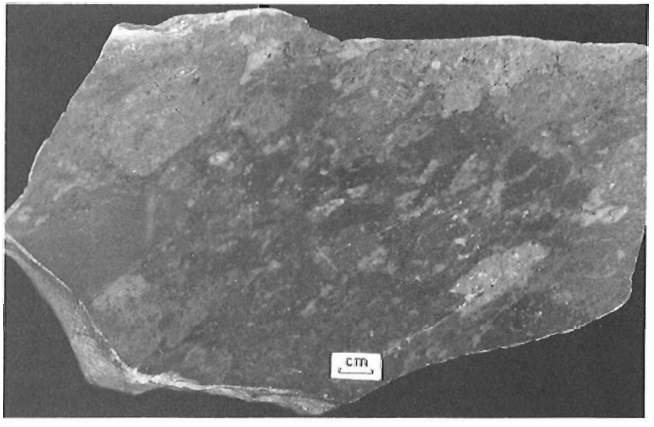

Figure 4. Agglomerate, unit 5b, near shore of Lou Lake approximately 0.5 km N 35° E of sample 194 (Fig. 2).

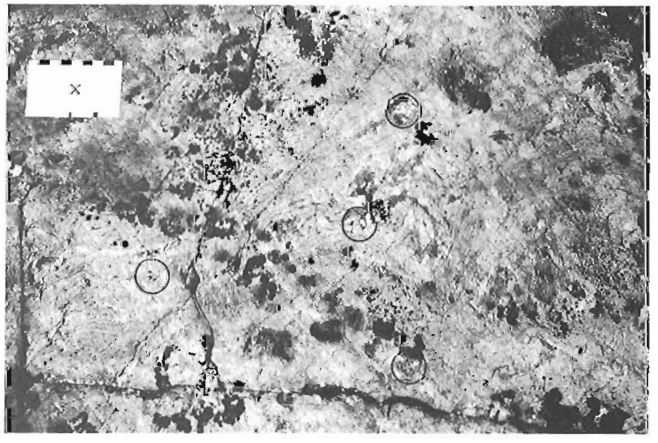

Figure 5. Rhyolite, unit 6, 250 m east of sample 419 (Fig. 2). Note lithophysae in circled areas and folding of flow lamination. GSC Photo 205021-H.

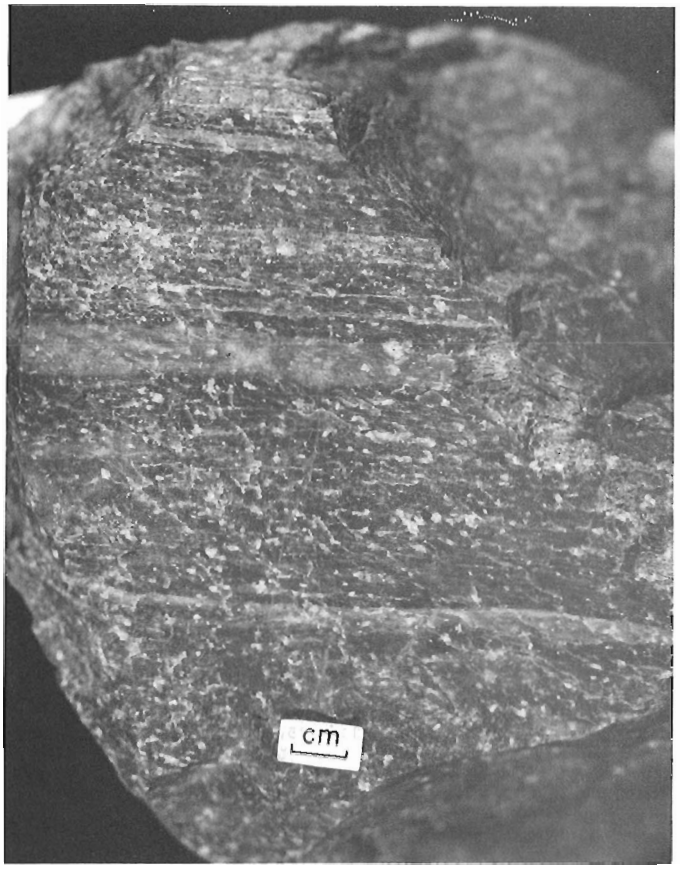

Figure 6. Well banded porphyritic rhyolite, unit 7, sample 330 (Fig. 2).

A dacite to the north (unit 8) is the most mafic volcanic unit encountered in the study area. It was regarded as andesite by Thomas and Olson (1978), but chemical analysis of a representative sample shows that it is dacite. The unit is characterized by abundant plagioclase, some hornblende phenocrysts, a strongly magnetic character and reddish brown weathering. A quartz-feldspar porphyry (unit 9) northwest of Lou Lake is, in part, intrusive but grades into zones that show ignimbritic texture and a lithic fragmental character. The rock has a variable proportion of phenocrysts in a fine grey matrix.

A volcaniclastic conglomerate (unit 10) overlies units 6, 7 and 8, and is characterized by cobbles of porphyritic felsic volcanic rocks. A quartz-feldspar porphyritic rhyolite (unit 11) is the uppermost unit of the volcanic sequence in the area. It is generally massive, grey, and is characterized by coarse phenocrysts, except at the base where it is fine grained. Some of the quartz phenocrysts are embayed and partly resorbed.

Undivided felsic volcanic rocks (unit 12) south of Lou Lake are fine grained to porphyritic rhyolite. Those to the southeast and east of Lou Lake were outlined on a regional sketch map by Bryan (1981, 1982).

Intrusive rocks (units 13 to 18)

The stratified sequences in the Lou Lake area have been intruded by numerous dykes and several plutons, which are broadly grouped into units 13 to 18. Many of the dykes are too small to show on Figure 2.

A small body of coarse diorite (unit 13) occurs at the north end of Lou Lake. It is highly altered adjacent to the Lou Lake fault, and is biotite-rich and foliated along the contact with younger quartz monzonite (unit 15b). A large number of quartz-feldspar porphyritic dykes (unit 14a) occur southeast of Lou Lake. They are as much as 50 m wide, and commonly trend easterly, subparallel to the trend of the Snare Group strata. They are characterized by coarse euhedral phenocrysts of quartz and feldspar. A larger body of porphyry (unit 14b) southwest of Lou Lake, which contains smaller subhedral phenocrysts, also contains hornblende phenocrysts.

Quartz monzonite-monzodiorite (unit 15a) occurs as numerous easterly trending dykes and as a larger body at the south end of Lou Lake. It is characterized by well developed phenocrysts of feldspar. A few small felsitic dykes cut the larger body. A seriate-textured rock (unit 15b) in the northern part of the area, which was considered granite in the field, is a quartz monzonite on the basis of chemistry and petrography (Table 1). A porphyritic granodiorite (unit 16) is intrusive into the porphyry (unit 14b) and other units in the southwestern part of the area. Small bodies of leucogranite occur near its boundary, and these are regarded as related intrusions.

A prominent giant quartz vein and several smaller ones (unit 17) transect various units in the area. Diabase dykes (unit 18), which are are generally less than a metre wide and have various orientations, are sparsely distributed.

Petrochemistry of volcanic and intrusive rocks

Chemical analyses of 11 rocks representing the volcanic sequence (Table 1) show its compositional range from dacite to rhyolite and its calc-alkaline character. The sequence is dominantly rhyolitic. The alkali contents vary considerably, and two rhyolite samples of unit 4 are extremely rich in potash and poor in soda. These rocks have undergone alkali metasomatism. Their proximity to the arsenopyrite occurrences suggests that this phenomenon is related to the hydrothermal activity that formed these occurrences.

Analyses of two intrusive porphyries show rhyolitic composition, with potash dominant over soda (Table 1, analyses 12 and 13). Since they are evidently related to the felsic volcanic rocks, their alkali contents reflect the overall potassic nature of the felsic magmatism. Three samples of quartz monzonite-monzodiorite from the southern part of the area show a variation in silica and alkalis from west to east that may, in part, reflect a differentiation trend from pluton to dykes, and in part potash enrichment closer to the mineralized area (Table 1, analyses 14, 15, and 16). The porphyritic granodiorite (unit 16a) is chemically akin to the quartz monzonite, and is also similar chemically and texturally to the quartz monzonite-granodiorite intrusion reported 20 km to the northwest by Gandhi (1989). They apparently belong to the same suite of intrusions. The sample from Burke Lake (Table 1, analysis 19) is relatively more granitic in chemical and mineralogical composition, but may represent a differentiate of the same granodioritic suite.

MINERAL OCCURRENCES

Several arsenopyrite occurrences containing notable amounts of Bi, Co, Cu and Au, are distributed along a zone 4 km long and 1 km wide in a quartzite-argillite unit of the Snare Group near Lou Lake (Fig. 2 and 7), and similar occurrences are found at Burke Lake approximately 4 km to the southeast along the strike of these strata (Fig. 8). A group of arsenopyrite occurrences, located 1 km northwest of the main showing (Fig. 2), were discovered during the present study. Also present in the Lou Lake area are several fracture-controlled radioactive occurrences, and a few concentrations of pyrite, chalcopyrite and sphalerite in giant quartz veins (Fig. 2).

Bi-Co-Cu-Au occurrences

General features

Arsenopyrite is the predominant mineral in all these occurrences. It is commonly coarse, subhedral to euhedral, and forms disseminated grains, aggregates and veins. The veins range in thickness from 1 to 40 cm, and are most common in competent host rocks, mainly quartzite, and in a few places, rhyolite (Fig. 9). Disseminated arsenopyrite occurs in the vicinity of the veins, and is particularly widely distributed in quartzite. In the argillaceous chlorite- and/or magnetite-rich host rocks, arsenopyrite forms thin layers and lenses subparallel to the bedding or foliation. Pyrite and chalcopyrite occur in some places as coarse aggregates with arsenopyrite. Bismuth minerals are rarely recognized in hand specimen. Scheelite was identified in a few samples during the present study by portable ultraviolet lamp. Weathered surfaces of arsenopyrite are usually dull grey, hence the mineral is obscure in many places, but deeply weathered massive aggregates show the bright green colour of scorodite ($FeAsO_4.2H_2O$). Pink cobalt stain due to erythrite ($Co_3As_2O_8.8H_2O$) although observed, is uncommon.

Magnetite occurs in many of the arsenopyrite veins and aggregates. In some of the magnetite-rich argillaceous host rocks, distinction between magnetite inherent in the host rock and the magnetite which is associated with arsenopyrite aggregates and disseminations, is often difficult. The picture is further complicated by the presence of magnetite veinlets, ranging from thin stringers to veins as thick as 2 cm, whose age relation with the arsenopyrite is not clear. Hematite occurs as an alteration product of magnetite, and also forms thin layers, lenses and vein-like aggregates in biotite-rich and/or chlorite-rich metasedimentary host rocks of arsenopyrite occurrences.

The mineralized zones tend to be parallel to the regional trend of the metasedimentary strata, for lengths of several tens of metres and widths of a few metres. Abundance and distribution of arsenopyrite are, however, highly variable in

all occurrences. At a few places the veins are clearly localized in major fractures or faults; elsewhere their trend and distribution are erratic. Irregular to lensoid aggregates of arsenopyrite are common in argillaceous host rocks. Thin argillaceous sedimentary beds in quartzite tend to be preferentially mineralized in comparison with the surrounding rock. Chloritic and magnetite-rich beds are locally tightly folded on a scale of metres, and arsenopyite in such places occurs mainly as cross-cutting veinlets. The metasedimentary host rocks of the Burke Lake grid include some highly calcareous beds (Fig. 8), and are in general coarser grained than those near Lou Lake. These rocks also contain some vein-like masses of very coarse hornblende, with disseminated coarse arsenopyrite. Most of the occurrences in this grid area appear to be small compared with those in the Lou Lake grid area, but they are not yet tested by drilling or trenching.

Multi-element analyses and mineralogy

Multi-element analyses of 20 arsenopyrite samples, including 6 chip samples from trenches, are presented in Tables 2 and 3. A mineralogical study, including microprobe analyses, of 24 polished sections of arsenopyrite-bearing samples collected by the authors, was carried out by D.C. Harris of the Geological Survey of Canada. The polished sections represent the samples analyzed or similar material in their vicinity. The metallic mineral phases encountered are listed in Table 4.

Analyses of 6 chip samples ranging in widths from 0.3 to 1.5 m show significantly high values in Au, Bi and Co (Table 2). These data confirm the assay results reported by exploration companies. Selected grab samples representing high grade material, also yielded analytical results that are comparable to those given in exploration reports. Contents of copper are generally low, with a few exceptions. Nickel contents are remarkably low considering its geochemical affinity to As and Co. The contents of Ag, Pt, and Pd were below their detection limits. Fe and S contents correspond in part to the As content, reflecting the abundance of arsenopyrite, and in part to the abundance of magnetite, hematite, pyrite and chalcopyrite. Contents of other metals reported in Tables 2 and 3 may represent those inherent in the rock or only slight enrichments, at parts per million levels, due to mineralization. The major oxides of 10 of the samples reported in Table 3 are indicative of altered host rocks. Thus high MgO and CaO contents of a sample from Burke Lake grid indicate a dolomitic character. It is

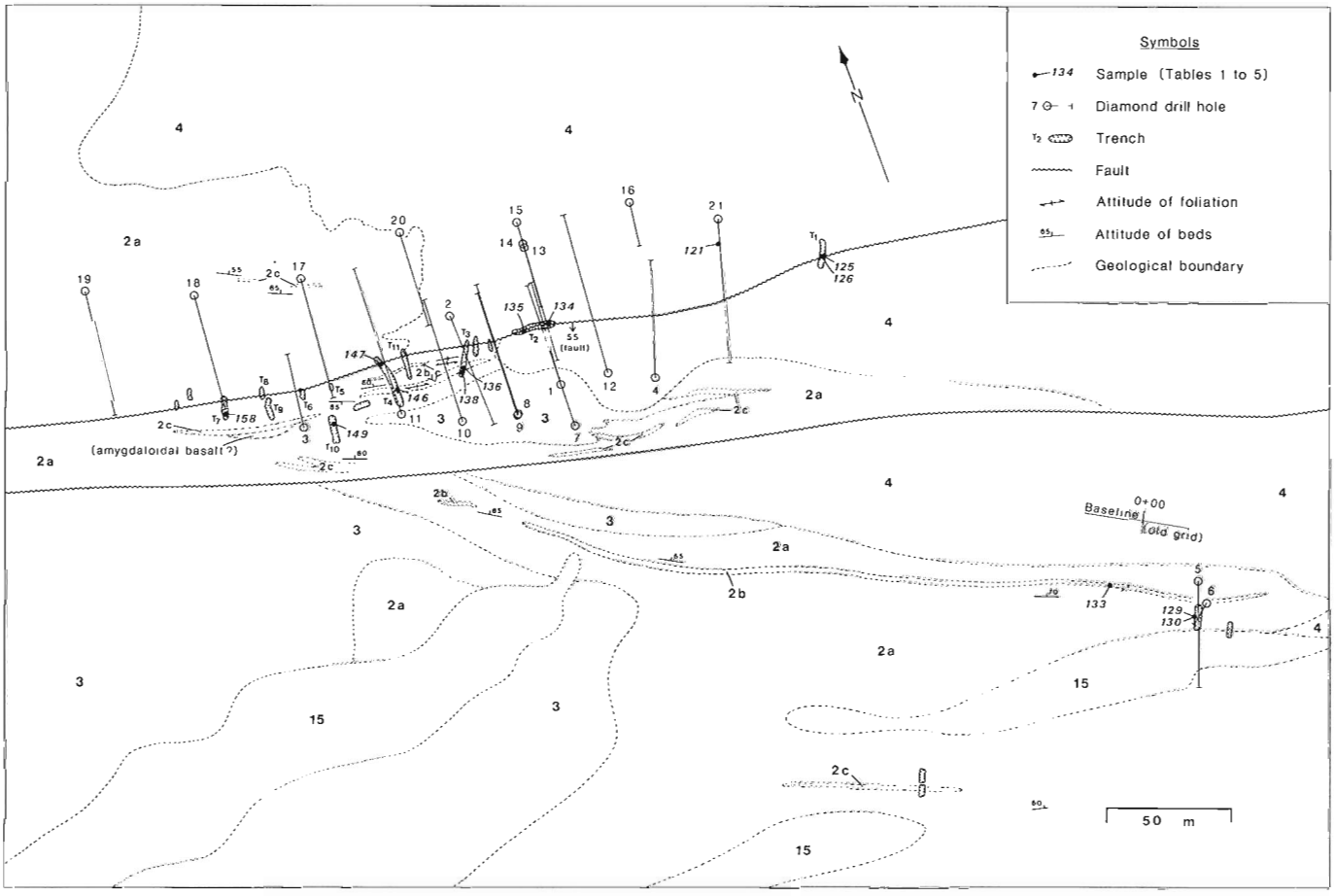

Figure 7. Map of the main Bi-Co-Au prospect showing trenches and drill holes, Lou Lake area, Northwest Territories (after Bryan, 1982). Legend as in Figure 2.

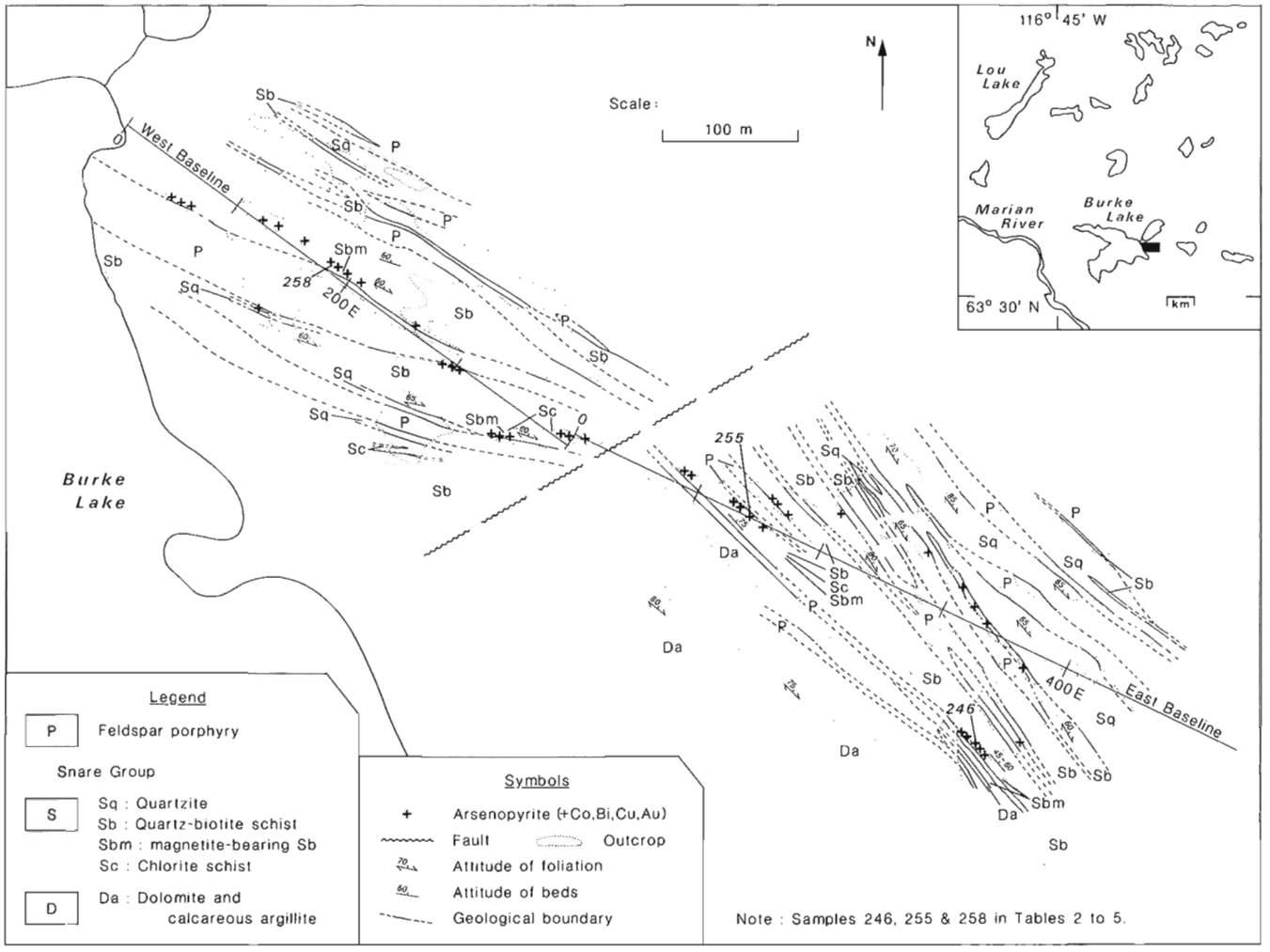

Figure 8. Map of the Burke Lake area showing arsenopyrite occurrences, Northwest Territories (after Bryan, 1982).

Figure 9. Photograph of Trench 2 (Fig. 7), showing massive arsenopyrite vein dipping moderately to south in rhyolite of unit 4. Looking east. GSC Photo 205021-C.

noteworthy that in terms of silicate mineralogy, the rocks contain high potash and low soda relative to their amounts of alumina and silica. This suggests that potash metasomatism accompanied mineralization.

Mineralogical examination of the polished sections revealed that the major phases are arsenopyrite, pyrite and magnetite-hematite, with minor to trace amounts of chalcopyrite, bismuthinite, native bismuth, emplectite, pyrrhotite and rare native gold, which were reported by Mathieu (1966), and in addition cobaltite, loellingite, wittichenite, tennantite, molybdenite, scheelite and wolframite (Table 4). Arsenopyrite, which is very abundant, is cobalt-bearing with as much as 14.7 weight percent Co (Table 5). It is commonly highly fractured and partially replaced by secondary iron arsenate minerals, principally scorodite. Pyrite and magnetite abundances vary considerably. Pyrite has been replaced to varying degrees by magnetite (Fig. 10), with the latter being partially replaced by hematite in places (Fig. 11). Some magnetite aggregates contain numerous minute

Table 2. Multi-element chemical analyses of arsenopyrite-bearing samples from the Lou Lake - Burke Lake area, Northwest Territories.

Sample number	As wt. %	S wt. %	Fe wt. %	Bi wt. %	Co wt. %	Au ppm	Ag ppm	B ppm	Be ppm	Cd ppm	La ppm	Ce ppm	Sm ppm	Nd ppm	Eu ppm	Tb ppm	Yb ppm	Lu ppm	Cu ppm	Mo ppm	Ni ppm	Sb ppm	Sc ppm	Se ppm	U ppm	V ppm	W ppm	Zn ppm
125	9.68	3.55	13.60	1.25	0.59	4.80	<0.5	40	10	21	15.6	29	2	<20	1.2	<2	2.6	<0.5	58	58	39	160	4.2	130	24	<10	<400	6
129	29.50	14.60	20.60	1.00	1.69	5.20	-	-	-	-	-	-	-	-	-	-	-	-	<1	20	260	240	-	-	<2	-	-	240
130	36.40	14.90	26.30	0.99	1.37	14.09	-	-	-	-	-	-	-	-	-	-	-	-	<1	20	190	270	-	-	<2	-	-	230
134	20.30	7.28	14.80	0.63	0.37	0.87	<0.5	20	5	35	42.9	64	2.6	<30	<1	<2	4.6	0.4	54	24	2	230	1.9	<40	37	<10	<400	4
136	11.80	5.88	24.20	0.05	0.29	0.31	<0.5	20	10	13	35.7	57	2.4	<20	<1	<2	4.4	0.6	2200	24	27	240	11.6	<10	<20	50	<400	19
138	18.80	11.80	21.00	0.07	0.33	0.37	-	-	-	-	-	-	-	-	-	-	-	-	9950	30	<2	180	-	-	<2	-	-	220
146	18.20	8.66	17.50	0.50	0.24	0.26	<0.5	40	5	10	14.7	23	1	<20	1.1	<2	2.7	0.4	29	19	9	520	3.6	<40	<20	20	<400	6
147	36.70	16.50	24.60	0.66	0.872	1.10	-	-	-	-	-	-	-	-	-	-	-	-	1490	40	20	300	-	-	<2	-	-	260
158	37.60	16.60	27.47	0.03	1.2	0.08	<0.5	10	10	40	<100	<60	<5	<50	<5	<10	<10	<2.6	120	9	9	630	1.7	130	<60	10	<1000	14
246	0.25	0.10	16.20	<0.01	0.01	<0.01	<0.5	20	5	<1	11.8	23	2.9	11	1	0.7	2.7	0.4	150	<1	8	15	14.2	<3	8	50	<100	58
255	1.10	0.45	17.00	<0.001	0.092	0.22	-	-	-	-	-	-	-	-	-	-	-	-	<1	<2	<2	50	-	-	<2	-	-	290
258	4.20	1.74	19.30	0.46	0.109	0.48	-	-	-	-	-	-	-	-	-	-	-	-	<1	<2	<2	100	-	-	<2	-	-	250
290	21.60	8.33	19.80	0.14	2.3	4.60	<0.5	20	10	40	<100	<60	<5	<50	<5	<10	<10	<2.6	88	1	110	330	7.5	<100	<80	30	<400	10
294	4.16	1.92	16.90	<0.001	0.102	0.75	-	-	-	-	-	-	-	-	-	-	-	-	<1	<2	<2	<3	-	-	<2	-	-	250
300	4.90	0.92	20.80	0.07	0.13	4.00	<0.5	20	10	11	39.2	72	4.9	29	1.4	1.3	6.2	1	80	2	28	110	16.7	<3	19	50	<100	17
351	0.06	3.09	3.74	<0.001	0.008	0.07	-	-	-	-	-	-	-	-	-	-	-	-	1310	<2	<2	<3	-	-	<2	-	-	230
372	10.20	3.52	17.10	2.00	1.4	0.05	<0.5	100	150	12	29	104	40.1	INF	20.1	27.9	104	15.4	16	5	49	340	7.2	<10	50	40	<400	11
373	3.28	1.52	27.00	0.18	0.365	0.00	-	-	-	-	-	-	-	-	-	-	-	-	<1	<2	<2	50	-	-	<2	-	-	240
381	5.12	2.35	24.00	0.03	0.092	3.10	-	-	-	-	-	-	-	-	-	-	-	-	<1	<2	50	30	-	-	<2	-	-	200
384	9.00	4.29	26.90	<0.01	0.11	0.19	<0.5	20	15	7	45.1	64	9.5	35	3.1	3.8	9.3	1.2	28	17	40	85	13.7	<3	12	30	<100	3

Notes: 1) Analyses by X-ray Assay Laboratories Limited, Toronto, except for S analyses by Analytical Chemistry Section, Geological Survey of Canada, Ottawa.

2) Analytical methods : As, Fe & S by x-ray fluorescence; Bi & Pb by induced current plasma; Be, Cd, Co, Mo, Ni, V & Zn by direct current plasma; Au by fire assay- direct current plasma; Ag by atomic absorption; B, Ce, Eu, La, Lu, Nd, Sb, Sc, Se, Tb & Yb by neutron activation; S by combustion-infra red detection.

3) Sample location :

GFA-'89-125 : Chip sample, Trench 1, width o.5 m, across vein, main zone, GAR grid (Fig. 7)
-129 : Grab sample, Trench 200 m southeast of Trench 1, from muck on west side, GAR grid (Fig. 7).
-130 : -- as above -- (stained green, whereas 129 is stained pink), GAR grid (Fig. 7).
-134 : Chip sample, Trench 2, width 0.4 m across vein, main zone, GAR grid (Fig. 7).
-136 : Chip sample, Trench 3, width 1.5 m, 3.0 to 4.5 m from south end, GAR grid (Fig. 7).
-138 : Grab sample, Trench 3, 3 m from south end, Lou Lake main zone, GAR grid (Fig. 7).
-146 : Chip sample, Trench 4, width 0.4 m, 7.0 to 7.4 m from south end, GAR grid (Fig. 7).
-147 : Grab sample, Trench 7, 16.5 m from south end, Lou Lake main zone, GAR grid (Fig. 7).
-158 : Grab sample, Trench 7, south centre, Lou Lake main zone, GAR grid (Fig. 7).
-246 : Grab sample, 3 + 55 E, 0 + 75 S, Burke Lake east grid (Fig. 8).

GFA-'89-255 : Grab sample, on eastern baseline, 1 + 38 E, Burke Lake grid (Fig. 8).
-258 : Grab sample, 1 + 80 E, 0 + 05 N, Burke Lake west grid (Fig. 8).
-290 : Chip sample , Trench at 3 + 00 W, 2 + 00 S, width 0.3 m, Ralph 'A' zone, GAR grid (Fig. 2).
-294 : Grab sample, 3 + 25 W, 3 + 30 S, Ralph 'B' zone , GAR grid (Fig. 2).
-300 : Chip sample, outcrop at 4 + 25 W, 0 + 65 S, Ralph 'C' zone, GAR grid (Fig. 2).
-351 : Grab sample, approximately 35 + 00 W, 2 + 00 N, GAR grid (Fig. 2).
-372 : Grab sample, 24 + 40 W, 2 + 05 N, GAR grid (Fig. 2).
-373 : Grab sample, 24 + 25 W, 2 + 15 N, GAR grid (Fig. 2).
-381 : Grab sample, 25 + 95 W, 0 + 13 N, GAR grid (Fig. 2).
-384 : Grab sample, 27 + 25 W, 1 + 08 N, GAR grid (Fig. 2).

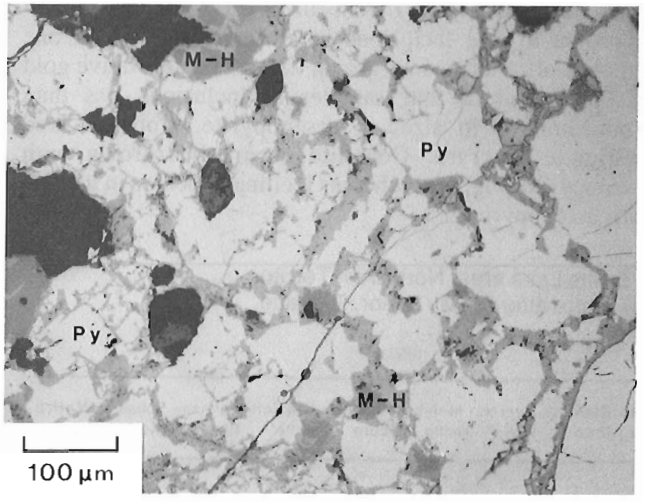

Figure 10. Photomicrograph showing pyrite (Py) partially replaced by magnetite-hematite (M-H); sample GFA-'89-126 (Table 4).

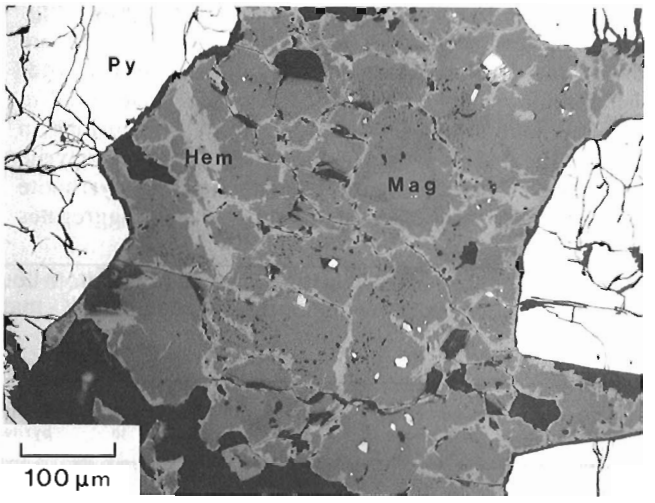

Figure 11. Photomicrograph showing magnetite (Mag) partially replaced by hematite (Hem), and fractured pyrite (Py); Sample GFA-'89-126 (Table 4).

Table 3. Major, minor and selected trace element analyses of arsenopyrite-bearing samples from the Lou Lake - Burke Lake area, Northwest Territories.

Sample No.		125	134	136	146	158	246	290	300	372	384
SiO2	wt.%	46.70	36.60	35.00	45.30	1.73	31.60	29.00	36.00	45.30	39.30
Al2O3	"	6.30	7.05	4.20	2.41	0.34	5.72	2.50	6.58	4.46	3.34
TiO2	"	0.05	0.05	0.17	0.10	<0.01	0.28	0.14	0.36	0.32	0.27
Fe2O3T	"	19.50	21.20	34.60	25.00	39.30	23.10	28.30	29.80	24.50	38.50
MnO	"	0.02	<.01	0.01	0.02	INF	0.36	0.03	0.12	0.03	0.05
MgO	"	1.94	0.30	2.56	1.20	<0.01	5.52	1.94	8.21	2.15	2.49
CaO	"	0.14	<.01	1.19	<0.01	<0.01	20.00	1.31	1.83	0.13	1.73
Na2O	"	0.24	0.23	0.29	0.19	<0.01	0.50	0.26	0.36	0.25	0.32
K2O	"	4.78	6.57	1.90	1.32	0.02	1.34	1.60	3.77	2.86	1.81
P2O5	"	0.03	0.03	0.05	0.04	<0.01	0.06	0.04	0.09	0.07	0.06
LOI	"	16.90	28.50	20.00	24.40	INF	6.08	32.60	6.85	15.80	12.20
Total	"	96.7	100.6	100.1	100	INF	94.6	97.8	94.1	96	100.1
Ba	ppm	480	803	231	197	10	<10	237	184	192	175
Cr	"	85	27	21	21	INF	<10	21	44	92	38
Nb	"	<10	18	18	15	<10	10	<10	17	21	29
Rb	"	<10	<10	49	86	INF	50	77	411	178	100
Y	"	24	<10	<10	14	<10	12	<10	15	572	34
Zr	"	91	82	65	97	<10	57	100	126	140	85

Note: Sample location in footnote of Table 2. Analyses by X-ray Assay Laboratories Limited, Toronto. Analytical method : X-ray fluorescence. INF : Insufficient fusion of sample.

inclusions of pyrite, pyrrhotite and arsenopyrite (Fig. 12). In a few sections minute grains of magnetite are concentrated along streaks and laminae of argillite. Bismuthinite occurs as fine to coarse grains interstitial to arsenopyrite crystals (Fig. 13), as minute inclusions in arsenopyrite and in gangue along fractures in arsenopyrite and pyrite. Native bismuth, bismuthinite and pyrrhotite occur as randomly distributed minute grains and aggregates in arsenopyrite (Fig. 14). Scheelite is erratically distributed as coarse to fine inclusions in arsenopyrite, and in one sample wolframite is intergrown with scheelite. Native gold was identified in four samples as inclusions less than 5 micrometres in size, in arsenopyrite. Cobaltite and loellingite are rare. Cobaltite occurs intergrown with arsenopyrite (Fig. 15), whereas loellingite occurs in gangue with arsenopyrite.

Table 4. Mineralogy of polished sections of samples from Lou Lake - Burke Lake area, Northwest Territories, with abundances of mineral phases indicated as: X - major, X(a) - major altered, M - minor, T - trace, and R - rare.

Sample Number	Gold (native)	Arseno-pyrite	Loelli-ngite	Cobalt-ite	Pyrite	Magnet-ite	Hemati-te	Chalco-pyrite	Bismuth (native)	Bismuth inite	Pyrrho-tite	Molybd-enite	Emple-ctite	Wittich-enite	Tennan-tite	Schee-lite	Wolfra-mite
126	R	X(a)			M	X	X	T	T	T							
129	R	X(a)					M		T	M							
130		X(a)					M		T	M							
133		X(a)				X	M										
135		X(a)					M	T	R								
138		X				M	M	R	R	R	R	T					
147		X(a)						T	T	T							
149		X				T	T		T	M							
158		X(a)			T			T	T					R		M	M
220					M	X	R	T									
246						M	T	T									
255							M										
258		M						R	R	R	R		R				
289C	R	X			X	X		T	R	T	R						
289E	R	X			M	M	T	R	R	R	R						
294		X			M	X	X	T	R	R							
301		T	X				M		R				R				R
351					M	M		M									
372		M			T	T	X	T	T		T						
373		X		M	M	X	M	T	T	M	T						R
381		M			T	M		R		T							
383		X			X	X		T									
384		X			T	X		T		R	R		R				R
467		X(a)						T		T			R				

Note : Location of 14 of the samples in footnote of Table 2 ; the remaining 8 are located as follows : 126 - Trench 1, Lou Lake main zone (Fig. 7); 133 - Approximately 175 m southeast of sample 126 (Fig. 7); 135 - Trench 2, south contact of arsenopyrite vein, Lou Lake main zone (Fig. 7); 149 - Trench 10, 25 cm wide arsenopyrite vein in quartzite, Lou Lake main zone (Fig. 7); 220 - Approximately 50 m northeast of sample 217 (Fig. 2; Table 1), magnetite-rich arsenopyrite-bearing fragmental rock of unit 3; 289C and 289E - Location same as that of chip sample 290 (Table 2); 301 - Character sample of the chip sample 300 (Table 2), approximately 2 m east of it; 383 - Approximately 2 m west of sample 384 (Table 2); 467 - Sample from a group of arsenopyite occurrences discovered during the present study, located approximately 1 km northwest of Lou Lake main zone (Fig. 2). representing arsenopyrite veinlets in quartzite of unit 2.

Table 5. Microprobe analyses of arsenopyrite samples, Lou Lake - Burke Lake area, Northwest Territories.

Sample Number	Co wt.%	Fe wt.%	As wt.%	S wt.%	Total	Co wt.% (range)
126	1.4	33.2	46	20.1	100.7	0.9-2.3
129	3.4	30.7	46.8	19.4	100.3	2.9-4.3
130	3.5	30.4	47.1	19	100	3.1-4.4
135	0.5	33.8	47	19.8	101.1	0.3-0.9
138	1.1	33.4	46.6	20.1	101.2	0.5-1.7
147	1	32.9	45.7	20.1	99.7	0.3-2.2
149	0.2	34.2	46.4	20.3	101.1	0.15-0.21
158	1.5	32.5	45.9	20	99.9	0.8-3.2
258	1.8	32.3	46.8	19.2	100.1	0.5-3.1
294	2	32.1	47.4	19.4	100.9	1.0-2.5
301	0.3	33.3	47.4	18.7	99.7	0.3
372	5.1	28.3	50.5	16.6	100.5	4.5-5.5
373	12.7	21.1	49.1	17.5	100.4	9.5-14.5
381	1.1	33.4	45.4	20.3	100.2	0.4-1.4
383	0.6	33.2	46	20.1	100.3	0.04-1.4
384	0.4	33.9	45.8	20.1	100.2	0.2-0.5
467	0.3	33.3	48.2	18.4	100.2	0.3
289C	2.6	31.5	47.2	19	100.3	2.1-4.0
289E	2.7	31.8	47.3	19.2	101	2.3-3.4

Note : Sample locations in footnotes of Tables 2 and 4.

Metallurgical testing on a bulk sample by flotation, cyanidation and acid leaching, conducted by Mathieu (1966), showed some difficulties in concentration and recovery of Au, Bi and Co. The textural relations noted above explain these difficulties. The bulk sample contained the following mineral phases in addition to the ones mentioned above: native silver, ilmenite, anatase, quartz, mica, scorodite and chlorite (Mathieu, 1966).

Quartz-sulphide veins

Coarse aggregates of pyrite occur in the prominent, east-northeast-trending giant quartz vein near the south end of Lou Lake. They are in patches as much as a few metres long and a metre or so wide. A few of the patches are trenched. Traces of chalcopyrite and malachite stains, and weak radioactivity, up to 5 times background, were noted in the trenches. Siltstone of unit 1 adjacent to them is tightly folded and highly chloritized. Another noteworthy occurrence was discovered during the present study about 2 km south of Lou Lake, and contains some coarse sphalerite, which is unusual in this type of occurrence.

Uranium occurrences

Anomalously high radioactivity is encountered along many fractures in various rock units in the study area (Fig. 2). Hematite is common along the fractures, and the wall rocks are generally red due to hematization. Pitchblende and yellow secondary uranium minerals occur in several places, notably in well bedded siltstone (unit 5) near the west shore of Lou Lake, and also on the shore at the south end of the lake. Massive pitchblende veins and aggregates up to 2 cm wide are found at these two localities. Polished sections of two samples from these localities contain botryoidal aggregates of pitchblende, and minor amounts of chalcopyrite and bornite. Analyses for Au, Pt and Pd (by X-ray Laboratories Limited, Toronto, using a fire assay-direct current plasma method) revealed 2.000 and 0.580 ppm Au, respectively, and <0.010 ppm Pt and <0.003 ppm Pd contents in both.

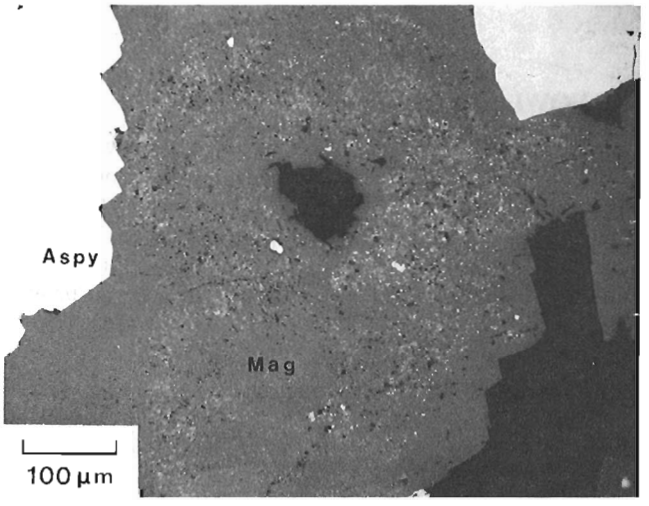

Figure 12. Photomicrograph showing coarse magnetite (Mag) with numerous inclusions, and arsenopyrite (Aspy); sample GFA-'89-289C (Table 4).

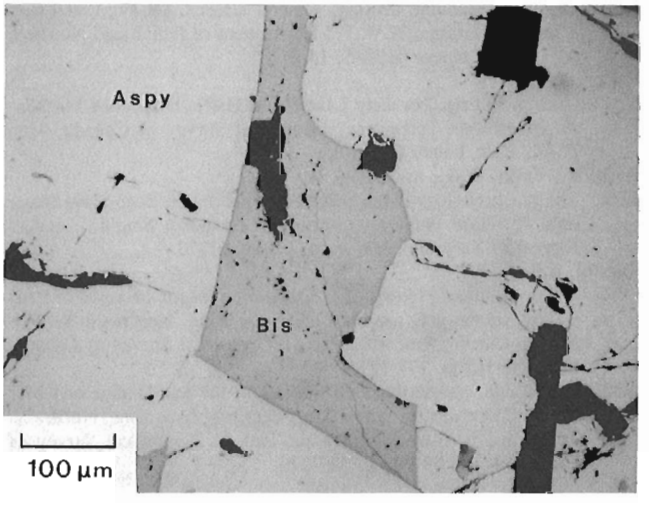

Figure 13. Photomicrograph of coarse bismuthinite grain (Bis) interstitial to arsenopyrite (Aspy); sample GFA-'89-129 (Table 4).

The host fractures commonly trend between east-northeast and southeast, and dip moderately to steeply. They are evidently subsidiary to the major northeast-trending Lou Lake fault. The fractures in the vicinity of the fault at the south end of the lake are parallel to or at low angle to the major fault. Concentration of the occurrences in the vicinity of the fault is noteworthy. A group of radioactive boulders of rhyolite was discovered during the present study on the west side of the fault near a narrow part of the lake. These boulders contain mineralized fractures, and may have come from the fault zone. One occurrence nearby, on the north shore of a small peninsula, is different in that pitchblende here is in a coarse granitic vein that cuts rhyolite.

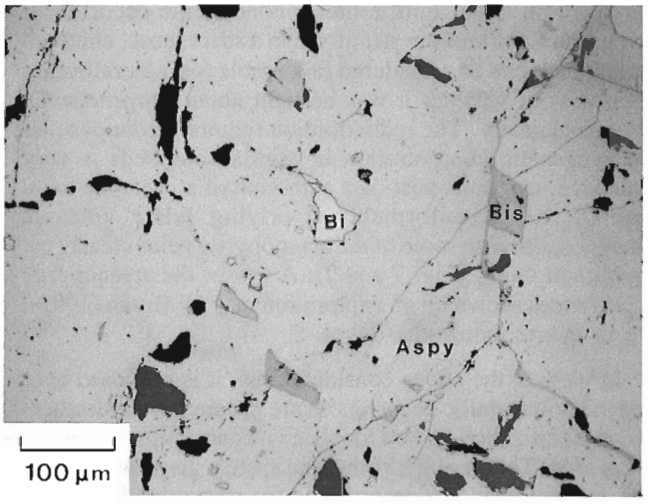

Figure 14. Photomicrograph of bismuthinite (Bis) and native bismuth (Bi) inclusions in arsenopyrite (Aspy); sample GFA-'89-129 (Table 4).

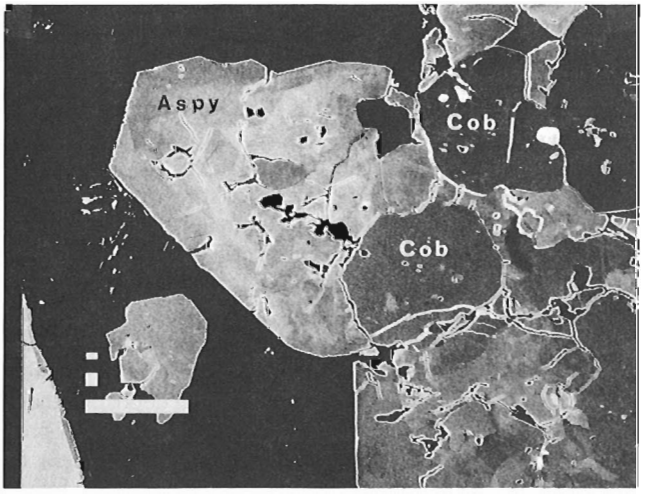

Figure 15. Electron backscattered image of cobaltite (Cob) intergrown with arsenopyrite (Aspy); sample GFA-'89-373 (Table 4). Note various shades of grey in arsenopyrite that are due to variable cobalt contents. The bar scale is 100 micrometres.

METALLOGENY

Polymetallic arsenopyrite veins and disseminations in Lou Lake area are closely associated with magnetite-rich argillaceous beds of the Snare Group. This led to a hypothesis of syngenetic sedimentary concentration of the metals in the beds and their remobilization during deformation and intrusive activity leading to the present distribution (Bryan, 1982). This served as a working hypothesis during the exploration done in 1978-81, and was implied in the guide to exploration suggested earlier by Shegelski and Thorpe (1972). The beds represent environments favourable for concentration of Au and As, akin to some in Archean gold-bearing iron-formations known in many parts of the world. Bi, Co and Cu are, however, not generally characteristic of such accumulations, particularly in the proportions encountered at Lou Lake. Furthermore, none of the occurrences in the Lou Lake area are stratiform in a strict sense, although certain beds can be considered favourable for mineralization regardless of whether it was brought about syngenetically or epigenetically. The redistribution required from postulated syngenetic concentration in argillaceous beds is very extensive, and must post-date extrusion of at least the basal part of the unconformably overlying felsic volcanic sequence, because some of the arsenopyrite veins clearly cut rhyolite of unit 4 (Fig. 7 and 9). A few of the arsenopyrite occurrences shown on an exploration map by Bryan (1982), are in quartz monzonite dykes.

In view of the above considerations, it is proposed here that the polymetallic occurrences are products of hydrothermal mineralization related to felsic volcano-plutonic activity in the area. The large hydrothermal system generated during this activity would be responsible for transportation of the metals and their deposition near the unconformity in response to lithological and structural changes encountered by the mineralizing solution. Intense potash metasomatism of volcanic rocks near the unconformity is attributed to the alteration effect of the hydrothermal solution. This hypothesis is supported by observations on regional metallogeny of the Great Bear magmatic zone, which is characterized by many polymetallic occurrences, including some iron oxide deposits that contain Cu, Au and other metals (Gandhi, 1988, 1989). Magnetite veins in the Lou Lake area, some of which cut the the Snare Group, can thus be readily interpreted as products of the felsic magmatism. Co, Ni and As are associated with some of the magnetite-rich veins and breccia fillings that are widely distributed in the northern Great Bear magmatic zone and in the east arm of Great Slave Lake. It would appear, then, that the Lou Lake arsenopyrite occurrences represent one variant of iron-oxide dominated deposits within the magmatic zone. It is conceivable that the mineralizing solution may have scavenged some of the elements from the metasedimentsary strata and deposited them at favourable sites. This scavenging and redeposition process is comparable in some respects with the process of redistribution of the metals invoked in the syngenetic hypothesis discussed above, but differs from it in terms of timing and the relative importance of the source rocks.

The quartz-sulphide veins and pitchblende veins are clearly epigenetic and post-date the faulting that affected the felsic volcanic sequence and the plutons in the area. Fractures subsidiary to the Lou Lake fault have localized pitchblende deposition. It is probable that copper and gold in the veins have been derived from the arsenopyrite occurrences in the area.

CONCLUSIONS

The felsic volcanic sequence of the Great Bear magmatic zone in the Lou Lake area unconformably overlies the metasedimentary strata of the Snare Group. Hydrothermal solutions generated by subvolcanic magmatic activity formed the Bi-Co-Cu-Au-bearing arsenopyrite veins and disseminations. These are localized near the unconformity, which is thus a favourable target for further exploration. The quartz-sulphide veins and pitchblende veins are controlled by brittle faults which post-date the Great Bear magmatic activity

ACKNOWLEDGMENTS

Mineral identifications and microprobe analyses were carried out by D.C. Harris of the Geological Survey of Canda. The writers thank R.T. Bell and R.I. Thorpe of the Geological Survey of Canada for many helpful discussions and also critical review of the manuscript. Financial support for the study, which included fieldwork for four weeks, was provided by the Canada-Northwest Territories Mineral Development Agreement, under sub-project C.1.2.5 of project 711-7771.

REFERENCES

Bryan, D.
1981: Geological report, GAR 1-3 claims (Jan.-Nov. 1980), Lou lake area, District of Mackenzie (85-N-10); Department of Indian and Northern Affairs, Document 081145, 12 p.
1982: Geological report, GAR 1-5, 7 and 9 claims (Jan.-Dec. 1981), Lou Lake area, District of Mackenzie (85-N-10); Department of Indian and Northern Affairs, Document 081422, 16 p.

Byrne, N. W.
1968: Details of diamond drilling, mineral claim CAB #1, Lou Lake, Marian River area, N.W.T.; Department of Indian and Northern Affairs, Document 018845, 14 p.

Fraser, J.A.
1967: Geological map, Hardisty Lake (West Half); District of Mackenzie, Northwest Territories; Geological Survey of Canada, Map 224A, scale 1 inch to 4 miles.

Frith, R., Frith, R.A., and Doig, R.
1977: The geochronology of the granitic rocks along the Bear-Slave Structural Province boundary, northwest Canadian Shield; Candian Journal of Earth Science, v.14, p.1356- 1373.

Gandhi, S.S.
1988: Volcano-plutonic setting of U-Cu bearing magnetite veins of FAB claims, southern Great Bear magmatic zone, Northwest Territories; in Current Research, Part C, Geological Survey of Canada, Paper 88-1C, p. 177-187.
1989: Rhyodacite ignimbrites and breccias of the Sue-Dianne and Mar Cu-Fe-U deposits, southern Great Bear magmatic zone, Northwest Teritories; in Current Research, Part C, Geological Survey of Canada, Paper 89-1C, p. 263-273.

Hall, B.
1969: Diamond drill hole logs, holes 69-5 to 69-21, CAB claim group, Lou Lake area, N.W.T.; Department of Indian and Northern Affairs, Document 060406.

Kidd, D.F.
1936: Rae to Great Bear Lake, Mackenzie District, N.W.T.; Geological Survey of Canada, Memoir 187, 44 p.

Lord, C.S.
1942: Geological Map, Snare River, District of Mackenzie, Northwest Territories; Geological Survey of Canada, Map 690, scale 1: 253 440.

Mathieu, G.I.
1966: Investigation of a gold-cobalt-bismuth ore from the Marian River area for Precambrian Mining Services Limited, Yellowknife, N.W.T., Canada; Department of Energy, Mines and Resources, Mines Branch Investigation Report TR 66-83, 13 p.

McGlynn, J.C.
1968: Tumi Lake, District of Mackenzie; Geological Survey of Canada, Map 1230A, scale 1: 63 360.
1977: Geology of Bear-Slave Structural Provinces, District of Mackenzie; Geological Survey of Canada, Open File 445, map, scale 1: 1 000 000.
1979: Geology of the Precambrian rocks of the Riviere Grandin and in part of the Marian River map areas, District of Mackenzie; in Current Research, Part A, Geological Survey of Canada, Paper 79-1A, p. 127-131.

Padgham, T., Hughes, D.R., Kennedy, M.W., Caine, T.W., Jefferson, C.W., and Murphy, J.D.
1978: Mineral Industry Report, 1969 and 1970, Volume 3 of 3; Department of Indian and Northern Affairs, Economic Geology Series, Report 1978-6, 168 p.

Shegelski, R.J. and Thorpe, R.I.
1972: Study of selected mineral deposits in the Bear and Slave Provinces; in Report of Activities, Part A , April to October, 1971; Geological Survey of Canada, Paper 72-1, p. 93-96.

Thomas, M. and Olson, R.A.
1978: Exploration — 1977 and 1978; LOO, BW and C mineral claims, Lou Lake, Mackenzie Mining District, N.W.T.; Department of Indian and Northern Affairs Document 080960, 6 p.

Wilson, J.T. and Lord, C.S.
1942: Geological Map, Ingray Lake, District of Mackenzie, N.W.T.; Geological Survey of Canada, Map 697A, scale 1: 253 440.

Preliminary Sm-Nd isotopic analyses of scheelites from Val d'Or gold deposits, Quebec

C.D. Anglin
Mineral Resources Division

Anglin, C.D. Preliminary Sm-Nd isotopic analyses of scheelites from Val d'Or gold deposits, Quebec; in Current Research, Part C, Geological Survey of Canada Paper 90-1C, p. 255-259.

Abstract

Nine scheelite separates from the Sigma, Perron-Pascalis and Siscoe Extension gold deposits in the Val d'Or area have been analyzed for their Sm-Nd isotopic compositions. Coarse-grained scheelite is a common gangue mineral in these deposits and appears to predate gold in vein paragenesis. The data define a good linear array on a Sm-Nd isochron diagram with an MSWD = 2.1. The slope of the array corresponds to an age of 2602±20 Ma which is interpreted to represent the age of the gold mineralization.

Résumé

Neuf groupes de particules de scheelite provenant des gisements aurifères de Sigma, Perron-Pascalis et Siscoe Extension de la région de Val d'Or ont été analysés pour déterminer leur composition isotopique Sm-Nd. Dans ces gisements, la scheelite, à grain grossier, est un minéral commun de la gangue et elle semble être antérieure à l'or dans la paragénèse des filons. Les données produisent une zone linéaire nette sur le diagramme isochrone Sm-Nd avec MSWD de 2,1. La pente de la zone correspond à un âge de 2602 ± 20 Ma qui équivaudrait à l'âge de la minéralisation aurifère.

INTRODUCTION

The Sm-Nd isotopic systematics of scheelite from Archean gold deposits in the Timmins area were examined by Bell et al. (1989) to test the feasibility of using this system for dating auriferous hydrothermal activity. The results of that study were promising in terms of the technique, but yielded a much younger age (2400 Ma) of hydrothermal activity than was anticipated or previously indicated by ^{40}Ar-^{39}Ar analysis of alteration minerals at these deposits (2560 to 2633 Ma; Masliwec et al, 1985). In order to further test the applicability of the method for dating gold deposits, scheelite samples were collected from gold-bearing veins underground in the Val D'Or camp in the fall of 1988 at the Sigma, Perron-Pascalis and Siscoe Extension Mines.

The Val d'Or area is located in northwestern Quebec and forms the southeastern part of the Abitibi Belt (Robert et al., 1983). The Sigma, Perron-Pascalis and Siscoe Extension deposits are hosted by rocks of the Malartic Group consisting of steeply dipping easterly striking ultramafic to felsic volcanic rocks (Fig. 1). Numerous diorite to monzonite (most commonly quartz diorite and granodiorite) intrusions crosscut the volcanics. The large Bourlamaque Batholith, which hosts the Perron-Pascalis deposits, is composed dominantly of diorite and quartz diorite and is subvolcanic (Wong et al., 1989).

At the Sigma Mine, the gold-bearing veins are hosted dominantly by a porphyritic diorite stock which has intruded andesitic volcanic rocks. A younger swarm of feldspar porphyry dykes, postdating the regional folding event, intrudes these rocks and is in turn crosscut by the gold-bearing quartz-tourmaline veins (Robert et al., 1983). The geological relationships at the Siscoe Extension deposit are similar to those at Sigma, with a dioritic body cross-cutting the volcanics, later porphyritic and aplite dykes crosscuting the diorite, and late gold-bearing quartz-tourmaline veins superimposed on all of these earlier lithologies.

The scheelites sampled were largely coarse-grained (> 2 cm diameter) masses (some with euhedral crystal outlines) hosted in quartz, commonly associated with, and intergrown with, fine-grained tourmaline needles, and commonly closely associated with pyrite and/or carbonate. Robert and Brown (1986) have detailed the vein paragenesis at the Sigma Mine and have identified scheelite as a relatively early phase in vein filling. They noted that "Quartz grains, tourmaline needles and pyrite cubes typically surround or are attached to scheelite crystals. Scheelite is commonly fractured and veined by quartz, calcite and more locally by gold... Scheelite cyrstals also show deformation, annealing and various degrees of recrystallization in their internal substructures". (Robert and Brown, 1986; p. 597). The vein paragenesis at the Perron-Pascalis and Siscoe Extension Mines appear to be similar to those described from the Sigma Mine.

ANALYTICAL METHODS

The analytical methods have been described in Bell et al. (1989). Dissolutions were performed in the clearn laboratory at Carleton University and isotopic ratio measurements were made on Carleton's multicollector Finnigan-MAT261 mass spectrometer. The reproducibility of the isotopic ratios

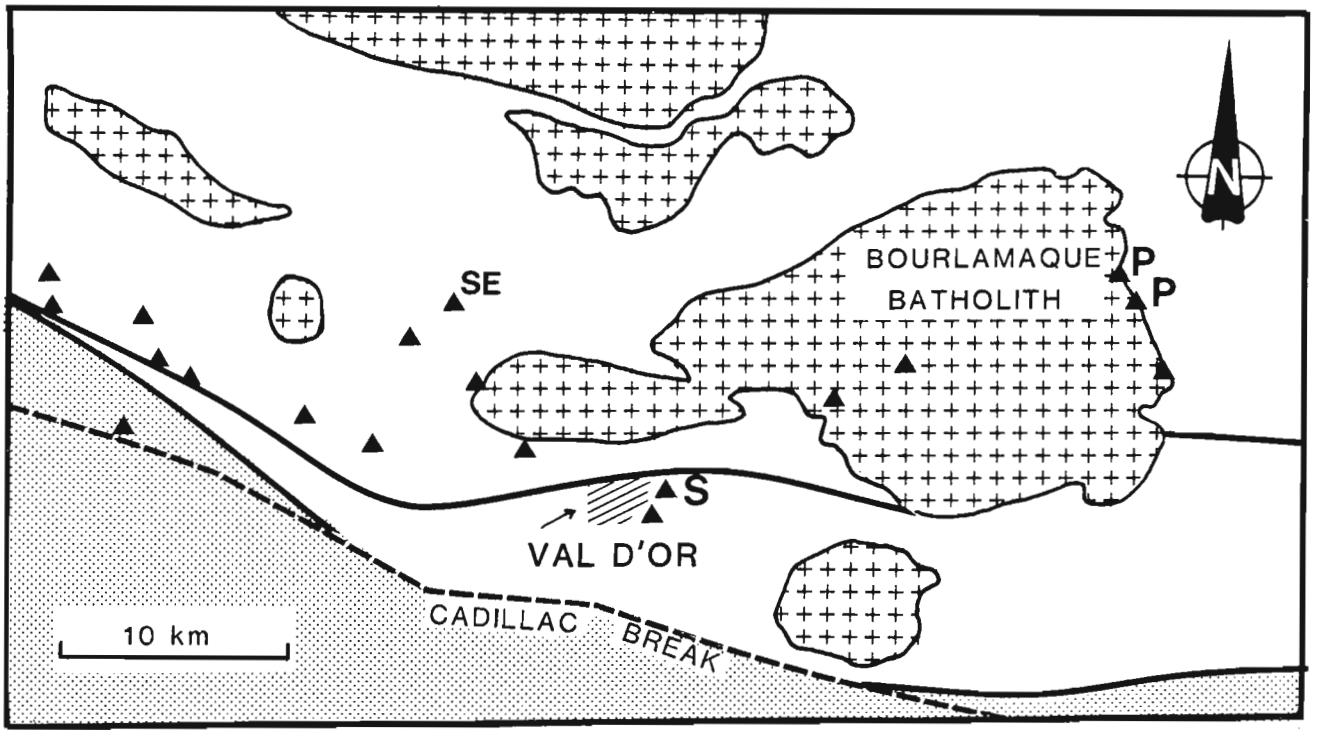

Figure 1. Geology of the Val D'Or area (modified after Robert et al., 1983). Symbols: crosses - felsic intrusions; shaded - sedimentary rocks; white - volcanic rocks; triangles = gold deposits; P = Perron-Pascalis Mine; S = Sigma Mine; SE = Siscoe Extension Mine.

is about 0.003 % at the two-sigma level; the precision for Nd and Sm concentrations at the two-sigma level is about +/- 0.5 % of the quoted values. The La Jolla standard gives a 143Nd/144Nd value of 0.51186 +/- 0.00002. Blanks average 0.02 ng for Nd and Sm. Nd ratios were normalized to a 146Nd/144Nd ratio of 0.7219.

RESULTS

The results of the isotopic ratio and concentration measurements are given in Table 1 and plotted in Figure 2. The decay constant for 147 Sm of 6.54×10^{-12} a^{-1} was used for the age calculation. Linear regression of the data was done using the method of York (1969) and one-sigma uncertainties.

The nine data points define a linear array on a Sm-Nd isochron diagram with a slope of 0.017165 +/- 0.00013, an intercept of 0.50938 +/- 0.00004, and an MSWD of 2.1. A straight line on a Sm-Nd isochron plot may represent an isochron, or may be produced by mixing of two components with different $^{143}Nd/^{144}Nd$ and Sm/Nd ratios. In the case of mixing, the slope of the line has no meaning. Interpreting the linear array as an isochron, the slope corresponds to an age of 2602 +/- 20 Ma. The corresponding $\in$-Nd value is +2.3, calculated using the method of Fletcher and Rosman (1982) and the present-day values of CHUR of Jacobsen and Wasserburg (1980).

DISCUSSION

A geochronological framework for the Sigma deposit has been developed by Wong et al. (1989). U-Pb zircon data indicate volcanism at 2705 +/- 1 Ma, porphyritic diorite intrusion at 2703 +/- 3 Ma and intrusion of the Bourlamaque Batholith at 2699 +/- 1 Ma (consistent with its interpretation as subvolcanic) and 2694 +/- 2 Ma for the feldspar porphyry dykes in the mine. This last age puts a lower limit on the timing of deformation of the volcanics and diorite because the feldspar porphyry dykes are undeformed. In addition, ^{40}Ar-^{39}Ar studies of metamorphic hornblende (Hanes et al., 1988) and U-Pb studies on metamorphic rutile (Wong, et al., 1989) define an age of ca. 2680 Ma for regional metamorphism.

A coarse muscovite from the quartz veins at Sigma yielded an age of 2579 +/- 3 Ma (Ar-Ar plateau date; Hanes et al., 1988) and hydrothermal rutile from a vein alteration halo yielded a U/Pb age of 2592 +/- 2 Ma (Wong et al., 1989). This rutile age is in agreement within analytical error of the Sm-Nd age on scheelites from the veins in the Val D'Or area. A similar age was obtained by Jemielita et al. (1989) on hydrothermal rutile at the Lamaque deposit. It is interesting to note that independent isotopic systems on different hydrothermal mineral phases have indicated the same age for the gold mineralizing event in the Val D'Or area. This supports the validity of the Sm-Nd technique for dating of hydrothermal mineralizing events (ie. the interpretation of the linear array in Fig. 2 as an isochron) as well as having important implications for models of formation of Archean lode gold deposits.

The positive $\in$-Nd value suggests that the source reservoir of the fluids was depleted in Nd relative to CHUR (DePaolo and Wasserburg, 1976). This increased Sm/Nd ratio is a characteristic of depleted mantle and is similar to the $\in$-Nd value observed for the scheelites from the Timmins gold deposits (Bell et al., 1989).

IMPLICATIONS AND CONCLUSIONS

An important constraint on theories of the genesis of gold deposits that has previously been lacking from most proposed models has been that of the age of the deposits themselves. Field relationships and structural mapping have identified the relative timing of events but, without absolute age constraints, determining the importance of spatial relationships of certain rock types or structural features to the mineralization has had to rely on inference and interpretation. Various models of gold genesis have been proposed

Table 1. Sm-Nd isotopic composition of Val D'Or scheelites.

DEPOSIT	SAMPLE	Sm ppm	Nd ppm	143Nd/144Nd	147Sm/144Nd	LABEL	
Sigma	012	92.8	162.1	0.51535	0.346	S	
	S-04	21.5	34.7	0.51584	0.373	S	
	S-11	20.7	31.1	0.51626	0.402	S	
	049	80.9	139.3	0.51544	0.353	S	
	049(II)	80.4	138.7	0.51543	0.352	S	r
	051			0.51547			
	051(II)	120.6	205.2	0.51546	0.355	S	r
P-P	036	76.7	102.0	0.51715	0.453	P	
	P-30	90.0	122.3	0.51702	0.445	P	
	P-37	78.1	97.7	0.51765	0.483	P	
Siscoe	E.SE-1	43.5	130	0.51286	0.203	SE	

S = Sigma Mine
P = Perron-Pascalis Mine
SE = Siscoe Extension Mine
r = repeat sample, including dissolution

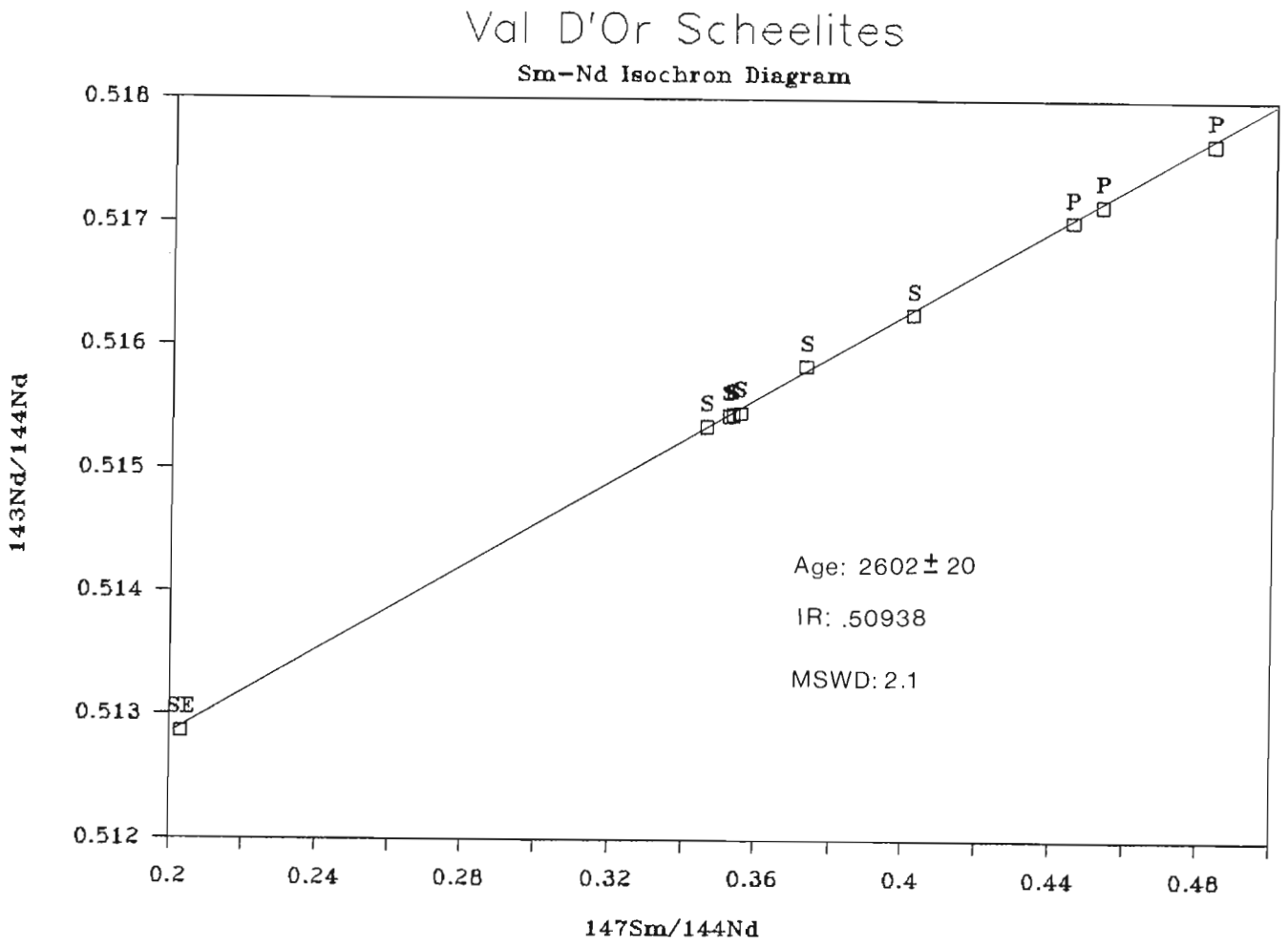

Figure 2. Sm-Nd Isochron Plot of Val D'Or Scheelites. Labels the same as that for deposits marked in Figure 1.

for Archean lode gold deposits including magmatic, metamorphic and syngenetic processes. Recent isotopic work in the Val D'Or area (Hanes et al., 1988; Wong et al., 1989), including the preliminary results presented in this paper, has indicated that gold mineralization may be as much as 90 to 100 Ma younger than porphyry intrusion and regional metamorphism. Therefore, these deposits do not appear to be closely related to spatially associated intrusive rocks or metamorphic events, and are clearly not syngenetic in origin. Much more isotopic data are needed to better constrain the structural, metamorphic and mineralizing events in gold camps to determine the factors of prime importance to the formation of these enigmatic deposits.

REFERENCES

Bell, K. Anglin, C.D. and Franklin, J.M.
1989: Sm-Nd and Rb-Sr isotope systematics of scheelites: possible implications for the age and genesis of vein-hosted gold deposits; Geology, v. 17, p. 500-504.

DePaolo, D.J. and Wasserburg, G.J.
1976: Nd isotopic variations and petrogenetic models; Geophysical Research Letters, v. 3, p. 249-252.

Fletcher, I.R. and Rosman, K.J.R.
1982: Precise determination of initial $\in$-Nd from Sm-Nd isochron data; Geochimica et Cosmochimica Acta, v. 46, p. 1983-1987.

Hanes, J.A. Archibald, D.A. Hodgson, C.J. and Robert, F.
1988: Preliminary $^{40}Ar/^{39}$ Ar Geochronology of the Sigma Mine, Val D'Or Quebec, and its implications for the timing of Archean gold mineralization, Current Research 1988.

Jacobsen, S.B. and Wasserburg, G.J.
1980: Sm-Nd evolution of chondrites. Earth and Planetary Science Letters, v. 50, p. 139-155.

Jemielita, R.A. Davis, D.W. Krogh, T.E. and Spooner, E.T.C.
1989: Chronological constraints on the origin of Archean lode gold deposits in the southern Superior Province from U-Pb isotopic analyses of hydrothermal rutile and titanite; Abstracts with Programs, Geological Society of America Annual Meeting, p. 351.

Latulippe, M.
1980: An overview of the geology of gold occurrence and developments in northwestern Quebec; in R.W. Hodder and W. Petruck, ed., Geology of Canadian gold deposits; Canadian Institute of Mining and Metallurgy special volume 24, p. 9-14.

Masliwec, A. York, D. Kuybida, P. and Hall, C.M.
1985: Grant 233 - The dating of Ontario's gold deposits; in V.G. Milne, ed., Summary of Research 1984-1985, Ontario Geological Survey Miscellaneous Paper 127, p. 223-228.

Robert, F. and Brown, A.C.
1986: Archean gold-bearing quartz veins at the Sigma Mine, Abitibi Greenstone Belt, Quebec: Part II. Vein paragenesis and hydrothermal alteration; Economic Geology, v. 81, p. 593-616.

Robert, F. Brown, A.C. and Audet, A.J.
1983: Structural control of gold mineralization at the Sigma Mine, Val D'Or, Quebec; Canadian Mining and Metallurgical Bulletin, v. 76, p. 72-80.

Wong, L. Davis, D.W. Hanes, J.A. Archibald, D.A. Hodgson, C.J. and Robert, F.
1989: An integrated U-Pb and Ar-Ar geochronological study of the Archean Sigma gold deposit, Val D'Or, Québec; Geological Association of Canada, Program with Abstracts, v. 14, p. A45.

York, D.
1969: Least squares fitting of a straight line with correlated errors; Earth and Planetary Science Letters, v. 5, p. 320-324.

Alkaline magmatism at Kirkland Lake, Ontario: product of strike-slip orogenesis

Eion M. Cameron
Mineral Resources Division

Cameron, E.M. Alkaline magmatism at Kirkland Lake, Ontario: product of strike-slip orogenesis; in Current Research, Part C, Geological Survey of Canada, Paper 90-1C, p. 261-269, 1990.

Abstract

The Kirkland Lake - Larder Lake fault zone (KLLLF) is the western termination of a major, east-west, strike-slip fault, the Larder Lake - Cadillac fault. It is the site of one of the world's major gold camps. The KLLLF is filled with sedimentary and alkaline volcanic rocks of late Archean age, the Temiskaming Group, which resemble, in structure and sedimentology, sequences deposited in modern strike-slip basins. Alkaline intrusions, which are uncommon in Archean terranes, are a major rock type within the fault zone and in the country to the south. It is argued that these features are the product of ''end effect'' on a strike-slip fault with sinistral displacement. A broad zone of lithosphere along and to the south of the KLLLF was stretched. This extension formed strike-slip (pull-apart) basins. In the mantle there was adiabatic upwelling, causing partial melting of carbonated peridotite to yield alkaline magmas and CO_2-rich fluid. CO_2 was the base for the solvent that carried gold.

Résumé

La zone de failles de Kirkland Lake Larder Lake (KLLL) est l'extrémité ouest d'une importante faille de décrochement est-ouest, la faille de Larder Lake-Cadillac. C'est à cet endroit que se trouve l'un des plus importants districts miniers aurifères dans le monde. La KLLL est remplie de roches sédimentaires et volcaniques alcalines de la fin de l'Archéen, soit le groupe de Temiskaming, qui ressemblent, par leur structure et leur sédimentologie, à des séquences déposées dans des bassins de décrochement modernes. Les intrusions alcalines qui sont peu fréquentes dans les terranes archéens constituent un type de roche important contenu dans la zone de failles et au sud de celle-ci. Ces éléments seraient le produit d'un ''effet d'extrémité'' sur une faille de décrochement à déplacement senestre. Une vaste zone de la lithosphère s'étendant le long et au sud de la KLLL a été étirée. Cet étirement a créé des bassins de décrochement (d'extension). Dans le manteau, il s'est produit une remontée adiabatique, causant la fusion partielle de la péridotite carbonatée d'où des magmas alcalins et un fluide à haute teneur en CO_2. Le CO_2 a servi de base au solvant qui a transporté l'or.

INTRODUCTION

Following the widespread acceptance of plate tectonic concepts, emphasis was initially given to subduction and orogenesis involving orthogonal vectors of plate convergence. In reality, plate motions with a significant degree of obliquity is the dominant condition at the present day (Woodcock, 1986). The lateral component of oblique subduction is accommodated by movement on strike-slip faults in the overriding plate (Fitch, 1972). These movements lead to the assembly, transport, and accretion of allochthonous terranes and to the modification of the orogenic belts so formed. In the Cenozoic it has been difficult to unravel the effects of strike-slip movement, notwithstanding the benefit of multidisciplinary approaches that include paleontology and paleomagnetism. Thus it is not surprising that only recently has emphasis been placed on the interpretation of strike-slip processes in Archean terrane.

The southern part of the Superior Province is one of the most intensively studied regions of Archean age. East-trending, elongate belts (subprovinces) of metavolcanic and granitic rocks (greenstone belts) alternate with metasedimentary belts. Major, linear faults or "breaks", which also approximate an easterly trend, occur within subprovinces or form the boundary between subprovinces. Some are now interpreted as strike-slip faults, such as those marking the boundary between the Quetico metasedimentary belt and the flanking Wabigoon and Wawa greenstone belts (e.g., Corfu and Stott, 1986). Percival and Williams (1989) considered that Quetico belt was a sedimentary prism between accreting arcs during oblique subduction. To the east, the Abitibi subprovince is the most important gold- producing greenstone belt in the world. Most of its major deposits occur along the Porcupine-Destor and Larder Lake-Cadillac faults, now interpreted as sinistral strike-slip faults formed during oblique convergence (Hubert et al., 1984).

These observations suggest that major strike-slip faulting played an important part in the construction of the southern Superior Province and in the formation of major quartz-carbonate gold deposits. In places, alkaline volcanic rocks and/or intrusions are present along these faults in association with gold. The most notable such occurrence is at Kirkland Lake. It is widely recognized that understanding the causes for alkaline magmatism may be important to comprehending the origins of Archean mesothermal quartz-carbonate deposits. By definition, these deposits were formed by CO_2-rich fluids; CO_2 is involved in the formation of melts of alkaline composition in the mantle (e.g., Meen, 1987). Further, alkaline magmas have a close spatial and temporal relationship to other types of gold deposit, such as the important epithermal deposits at Cripple Creek, Colorado, and Lihir, Papua New Guinea. This paper describes the tectonic conditions that produced the alkaline magmatism at Kirkland Lake, which lies at the western termination of the Larder Lake - Cadillac fault. The application of these conclusions to the genesis of the Kirkland Lake gold deposits will be treated in a later paper.

A variety of terms are used for strike-slip faults; not always consistently. Sylvester (1988) recommended *transform* be applied to major faults that cut the lithosphere and *transcurrent* to faults that terminate in the crust. But only rarely can penetration be estimated. Because of the weak rheology of the lower crust, most continental strike-slip faults likely terminate there in detachments. In this paper *strike-slip* is used to avoid inference about depth extent.

STRIKE-SLIP OROGENIC BELTS

Strike-slip movements, where the velocity is sufficiently high and long-lived, cause uplift and/or subsidence at some points along the length of the faults. Such effects are minor where the fault is straight and is parallel to the horizontal trace of plate movement. However, faults commonly are curved, which results in subsidence at releasing bends and uplift at restraining bends (Fig. 1). There are a number of other forms which subsidence may take, including basins formed by fault overstep or divergent splays (Fig. 1). There are equivalent convergent features that cause uplift. There may be dynamic change along a fault, with uplift of former basins or vice versa. While most strike-slip faults commonly show both uplift and subsidence at points along their length, faults with a consistent strike across the trace of plate movement will be dominated by either features of convergence (transpression) or of divergence (transtension).

Orogenic belts can form as a result of strike-slip movement (Lowell, 1972; Mitchell and Reading, 1978; Reading, 1980). The initial phase of the cycle is transtension, leading to basin formation and sedimentation, followed by a transpressional phase where the basins and their contained sediments are uplifted and folded. Strike-slip orogenic belts, which have been intensively studied because of their importance as repositories of petroleum, have characteristic features that have been cogently summarized by Reading (1980).

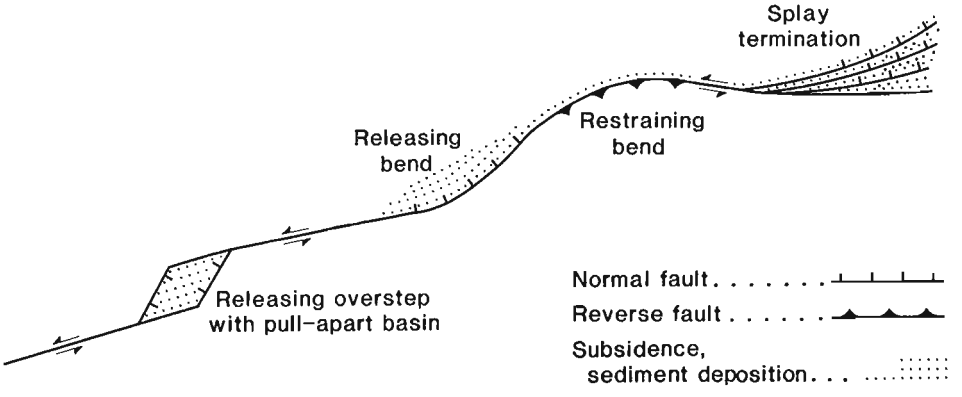

Figure 1. Sinistral strike-slip fault showing features that cause subsidence and/or sedimentation.

Extensional basins (strike-slip or pull-apart basins) along major strike-slip faults are relatively small but deep. Subsidence is rapid; 13 km of sediment were deposited in the Ridge basin, California, in 7 Ma. (Crowell and Link, 1982) and the Ventura basin, California, subsided 4 km during the past 1 Ma. (Yeats, 1978). This high energy environment is reflected in the nature of the sediment fill. Thus basins above sea level may be bordered by alluvial fans that pass rapidly through fluvial deposits into lacustrine sediments. Rapid facies change is a principal characteristic. Marine basins are filled by subaqueous mass-gravity transport of coarse clastics, deposited, in part, on submarine fans. During subsidence, normal faulting dominates, while in the transpressive phase of uplift it is reverse and thrust faults. For strike-slip orogenic belts, Reading (1980) characterized magmatic activity as minor, almost entirely confined to the transtensive phase, and metamorphism as feeble.

VOLCANISM IN STRIKE-SLIP OROGENIC BELTS

Volcanic rocks are found in a minority of strike-slip basins. Where present, they are commonly of alkaline composition. One example is the Erzincan Basin along the active North Anatolian Fault in Turkey (Fig. 2). This basin is filled with fluvial deposits bordered by alluvial fans and aprons (Hempton and Dunne, 1984). There is an evapouritic component in the form of salt playa. Volcanic cones of highly potassic rhyolite flows and volcaniclastic deposits occur along the master faults. Another example is along the Strait of Sicily fault zone, the site of major strike-slip displacement during Early Pliocene to Recent time (Cello, 1987). The submarine Pantelleria Trough (Fig. 3) has a volcanic complex on the island of Pantelleria which comprises a basic to felsic sequence of alkaline rocks, including basalt, hawaiite, benmoreite, mugearite, and peralkaline rhyolite and trachyte, the latter two dominating (Calanchi et al., 1989). The suite formed by fractional crystallization of mantle-derived basalt (Civetta et al., 1984).

The sparing occurrence of volcanic rocks in strike-slip basins, their restriction to the transtensive phase, and their alkaline nature, can all be related to the model of McKenzie and Bickle (1988) for generation of basaltic magma by extension of the lithosphere. Extension causes the adiabatic rise of mantle. In so doing, mantle may cross solidus boundaries causing partial melting. Where there is major extension, such as at continental margins, upwelling of mantle is greatest. Large volumes of basalt of tholeiitic composition are generated at shallow levels, representing a high melt fraction of the rising mantle. Where extension is less, the rise of mantle is not as marked and partial melting, if that occurs, is a small melt fraction, of alkaline composition, at greater depth. The amount of extension needed to generate melt depends on a number of conditions, principally the potential temperature (T_p) of the mantle. For T_p of 1480°C, extensive melting, to produce alkali basalt, occurs only when extension (ß) is 1.5 to 2.0 (Fig 4).

Strike-slip movements do not usually involve the separation of crust, and therefore result in only low levels of extension during transtension. J.A. Andrews and M.S. Steckler (in Pitman and Andrews, 1985) examined extension within basins along the transform boundary between the North America and Pacific plates, where the transform velocity is 4-6 cm/a. They found that maximum ß is about 1.6. This is near the lower bound of extension required for partial melting by the McKenzie and Bickle model. Thus most strike-slip basins will form in crust with extension less than the minimum required for partial melting and will not contain volcanic rocks. Where extension does reach the critical value of ß, the volcanism will be alkaline.

Support for this interpretation of moderate lithospheric extension during strike-slip movement as a cause for alkaline volcanism is found in the above mentioned Strait of Sicily fault zone. This is a region where final closure of an ocean basin is occurring (Ben-Avraham et al., 1987). Some of the motion between the African plate and plates to the north is taking place by dextral strike-slip faulting within the African plate: the eastern Mediterranean fault system (Fig. 3, inset). Extension is occurring near the ends of this system; to the east within the Gulf of Suez, to the west in

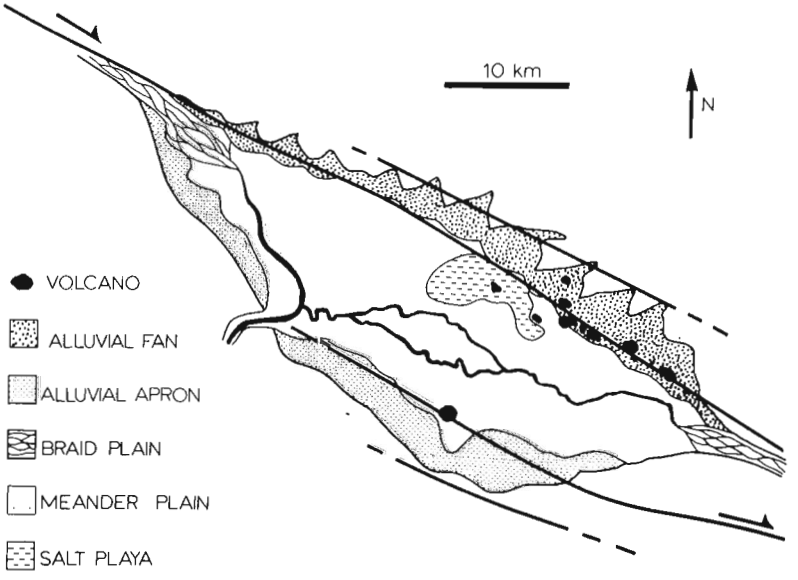

Figure 2. The Erzincan basin, Turkey. An example of a basin along a major strike-slip fault (North Anatolian fault) with alkaline volcanism. From Hempton and Dunne, 1984. By permission, Journal of Geology

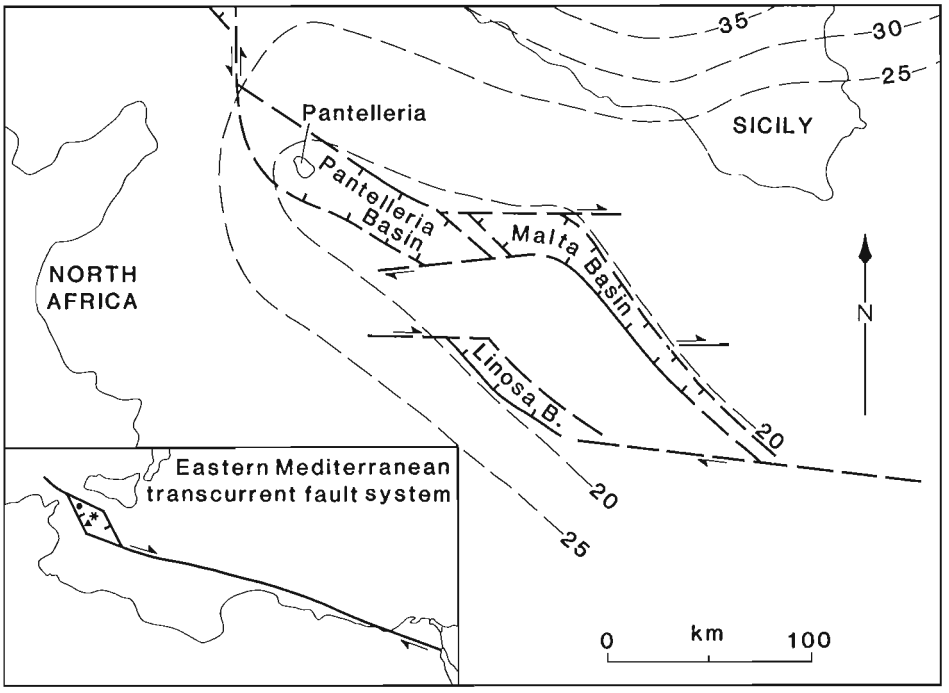

Figure 3. Basins formed in the Strait of Sicily as a result of movement along the eastern Mediterranean transcurrent fault system (from Reuther and Eisbacher, 1985, and Ben-Avraham et al., 1987). Alkaline volcanism on the islands of Pantellaria and Linosa and Bannock seamount, shown on the inset as a dot, triangle and star respectively. Contours are depth (km) to Moho (from Boccaletti et al., 1984).

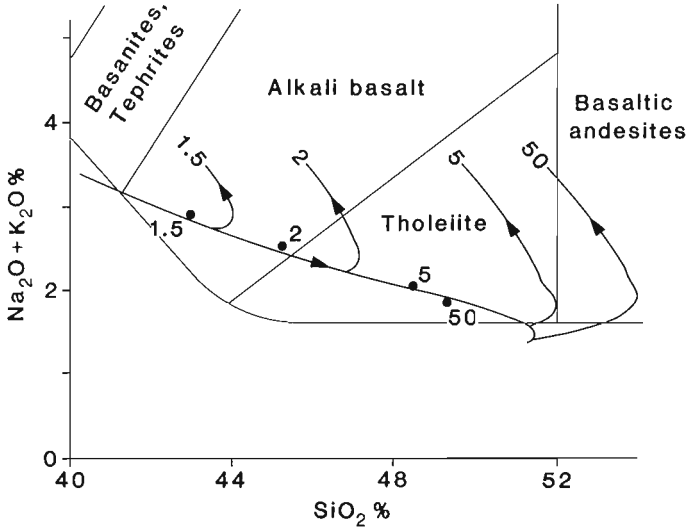

Figure 4. Relationship of basalt type to melting under varying degrees of lithospheric extension. The points and curves are labelled for different values of ß. The curves with arrows show point average compositions of melts as depth of melting decreases. Solid dots are point and depth averages. For T_p of 1480°C; mechanical boundary layer thickness of 100 km; and viscosity of 4 x $10^{15}m^2s^{-1}$. From McKenzie and Bickle (1988).

the Tyrrhenian Sea and the series of strike-slip basins in the Strait of Sicily that include the Pantelleria basin (Ben-Avraham et al., 1987). The crust is 30 to 35 km thick under Sicily, but thins to less than 20 km under the basins in the Strait of Sicily (Fig. 3). This is associated with high heat flow, 100 Mw/m^2 (Boccaletti et al., 1987) and by alkaline volcanism on the island of Linosa and Bannock seamount, in addition to that on Pantelleria.

KIRKLAND LAKE - LARDER LAKE FAULT ZONE

Kirkland Lake is one of the major gold camps of the world. To 1986, ten mines at Kirkland Lake (Teck Township) had produced 723 t of gold (Grabowski et al., 1987). The Kerr Addison mine at Larder Lake (Fig. 5) has produced 318 t. The district has been described in classic reports by J.E. Thomson of the Ontario Department of Mines: Thomson (1950) for Teck Township and Thomson et al. (1950) for the main ore zone. The following geological summary is mainly derived from these sources.

The principal feature of the district is the Kirkland Lake-Larder Lake Fault zone (KLLLF), which is the western termination of the Larder Lake - Cadillac fault. The latter is one of the principal structural features of the Abitibi belt, running east-west for 150 km from Kenogami, near Kirkland Lake, to Cadillac in Quebec. To the north of the KLLLF, there are tholeiitic basalts and sediments of the Kinojevis Group, which are overlain by calc- alkaline basalts and andesites of the Blake River Group. To the south there are komatiitic and tholeiitic basalt of the Larder Lake Group that also contains lesser amounts of conglomerate, greywacke, and iron-formation. The youngest of these groups, the Blake River Group, has been dated at 2703 ±2 Ma by U-Pb zircon methods (Nunes and Jensen, 1980).

The KLLLF is about 50 km long and up to 5 km wide and is largely occupied by the Timiskaming Group: a sequence of interbedded sedimentary and alkalic volcanic rocks, which lies unconformably on the older basaltic rocks. In this report the KLLLF is subdivided into three sectors or "basins" (Fig. 5). In the west, the Kirkland basin trends approximately 067°; in the east, the Larder basin has a variable trend, but in the vicinity of the Kerr Addison mine the strike of the basin is 060° to 070°. The Kirkland and Larder basins are linked by the Dobie basin, which trends

106°. A maximum thickness of 3500 m has been estimated by Hyde (1980) for the Timiskaming Group, which forms a south-dipping homocline. In the mines at Kirkland Lake the Timiskaming rocks have an average dip of 60°, which flattens to 20° in places. The south margin is entirely a fault contact of Timiskaming against the uplifted Larder Lake Group, while the north margin is, in part, an unconformity of Timiskaming on the Kinojevis Group and elsewhere a fault. Formerly, Timiskaming rocks were believed to extend south of the KLLLF. However, sedimentary rocks to the south are now believed to be part of the Larder Lake Group (Jensen and Langford, 1985).

Hyde (1980) subdivided the sedimentary component of the Timiskaming Group into a non-marine series and a resedimented series. The former consists of interbedded conglomerate and sandstone, believed to have formed in a braided river environment; thin to medium- bedded sandstone, siltstone, and argillite, deposited in a floodplain; and thick-bedded sandstone, which may represent eolian dunes. A conglomerate member 1200 m thick was identified by Hewitt (1963) near Kirkland Lake. The resedimented group principally consists of a thick sequence, 1800 m, of proximal turbidites with conglomerate, probably formed within a submarine fan. The non-marine rocks occur mainly in the Kirkland basin to the west and the marine facies in the Larder basin, to the east. Hewitt (1963) found the pebble assemblage in the conglomerates to contain basic to felsic volcanic and plutonic rocks from the underlying greenstone terrane and alkaline flow rocks, tuffs, and sandstones from the Timiskaming Group. Red jasper pebbles form a small but constant proportion of the conglomerates. Pebbles of green carbonate rock occur within a conglomerate within the uppermost part of the Timiskaming in the Kirkland basin.

Alkaline rocks within the Timiskaming Group comprise basic to felsic flows, including pseudoleucite-bearing rocks (Cooke and Moorehouse, 1969) and pyroclastic rocks. Flow rocks include alkali-olivine basalt, trachybasalt, tristianite, hawaiite and mugearite (Basu et al., 1984). The district is also notable in containing major intrusions of alkaline composition, which are scarce in Archean terrane. Outside of the KLLLF these are large rounded plutons, such as the Otto and Lebel stocks (Fig. 5). While these intrusions contain mafic to felsic units, the mafic rocks are present in only small proportion. In the Otto stock, for which there is a zircon U-Pb age determination of 2680 ±1 Myr (Corfu et al., in press), Smith and Sutcliffe (1988) identified syenite as the dominant rock type, with quartz syenite, porphyritic syenite, mafic syenite, and hornblendite. In the Murdock Creek

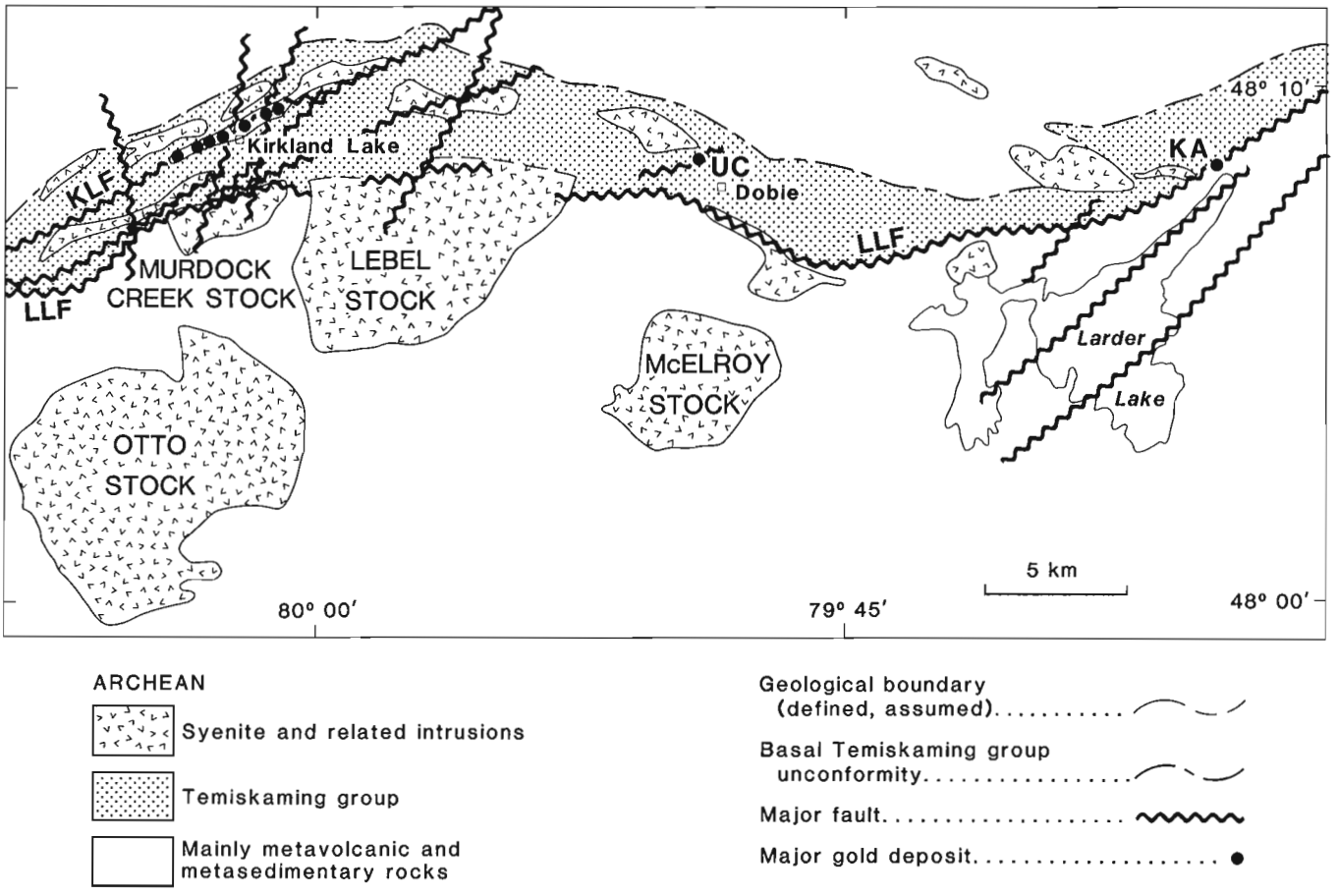

Figure 5. Geology of Kirkland Lake - Larder Lake fault zone (KLLLF). LLF = Larder Lake fault; KLF = Kirkland Lake fault; UC = Upper Canada mine; KA = Kerr Addison mine. Modified from Thomson (1950).

stock, near the KLLLF (Fig. 5), S.M. Rowins, A.E. Lalonde and E.M. Cameron (unpublished data) found alkali-feldspar syenite to be the dominant rock type, with melasyenite, melamonzodiorite, meladiorite, hornblendite, and clinopyroxenite. Within the KLLLF there are similar intrusions of mafic syenite and syenite; also feldspar porphyry. But these differ from intrusions outside the KLLLF in that they are strongly elongate along the strike of the basins. Thin lamprophyre dykes cut the Timiskaming Group and the syenitic intrusions.

Regional metamorphism of rocks underlying the Timiskaming is subgreenschist (e.g., prehnite-pumpellyite) to greenschist grade. Jolly (1978) showed that the Timiskaming is less than sub-greenschist grade, characterized by a diagenetic assemblage, with clay minerals and white mica as the only secondary minerals. Clasts within the Timiskaming contain prehnite- pumpellyite (Jolly, 1978), implying that regional metamorphism of the underlying groups preceded deposition of the Timiskaming.

Faulting in the KLLLF is well defined for the Kirkland basin by Thomson (1950) and Thomson et al. (1950) because of excellent exposure in mines. There are three groups of fault: strike faults, diagonal faults, and cross faults. Strike faults are of most economic importance, since on these lie the major gold veins. Seven major deposits are spaced along a 4 km length of the Kirkland Lake fault. This fault strikes at 067°, parallel to the strike of the Kirkland basin, and dips south at 75° to 80°. It has a reverse component in that the south side has moved upward. At the west end of the camp, where this fault is a single structure, pre-ore displacement is about 460 m; to the east it breaks into a number of faults, each with smaller displacement. The gold deposits are mostly within an elongate, steeply south-dipping, intrusion of mafic to felsic syenite cut by the Kirkland Lake fault. The long axis of the intrusion coincides with the strike of this fault and with the long axis of the Kirkland basin. The strike faults, including the Larder Lake fault, created a series of parallel blocks, each of which rose relative to the block to the north. Diagonal faults have a variable trend, which approximates north-northeasterly. Some experienced both pre-and post-ore movement and, in places, contain gold. Cross faults are post-ore, north-trending normal faults, which offset earlier faults and gold-bearing veins.

Outside of the Kirkland basin the major deposits lie on faults sub-parallel to the Kirkland Lake fault. The Kerr Addison deposit in the Larder basin lies along the Larder Lake fault, which trends 060° - 070° and has a near vertical dip. In the Dobie basin there is only one important deposit, the Upper Canada mine, that has produced 43 t Au. Ore bodies in this mine are associated with steeply-dipping faults that trend 073° to 080°.

A notable feature of the KLLLF is extensive carbonatization, that has altered pre-existing lithologies, particularly basic rocks, into silicious carbonate rock. Carbonate minerals are mainly iron-rich dolomite and calcite. Green mica gives altered zones a characteristic tinge. Carbonatization was structurally controlled along strike and diagonal faults (Thomson, 1950), with particularly strong carbonatization along the Larder Lake fault. Syenitic intrusions are affected by carbonatization, but also, in places, cut carbonatized zones (Thomson, 1950). This, together with Hewitt's (1963) finding of pebbles of carbonatized rock in upper beds of the Timiskaming, suggests a long period of CO_2 fluxing. In ore-bearing sections, carbonatization was followed by pyritization of wall rocks; then precipitation of quartz; and introduction of calcite. Finally, there was deposition of sulphides, tellurides and native gold.

Table 1. Comparison of criteria for strike-slip mobile belts (mainly after Reading, 1980) with characteristics of Timiskaming Group and structures, Kirkland Lake - Larder Lake fault zone.

Criteria, Strike-slip Mobile Belts	Timiskaming Group
Terrestrial Sedimentation Alluvial fans, fluvial sediment, lacustrine deposits. Often thick conglomerates.	Braided river, floodplain and eolian deposits; conglomerate units to 1300 m.
Marine Sedimentation Mass-gravity transport of coarse clastics to submarine fans, basin plains, slope aprons.	Thick proximal turbidites, conglomerates; probably deposited on submarine fan.
Facies Change Extreme lateral facies variation.	Rapid local facies change; alluvial fan/fluvial sediments to turbidites, <25 km.
Stratigraphic Thickness Great stratigraphic thickness in relation to basin size.	3500 m in basin with maximum width of 5 km.
Metamorphism Little or none.	Less than sub-greenschist.
Igneous Activity Generally absent; where present, usually alkaline.	Abundant alkaline rocks as flows, pyroclastic rocks and intrusions.
Faulting during Transtensional Phase Normal faults; extensional fractures.	Normal faults? Alkaline intrusions entered extensional fractures.
Faulting during Transpressional Phase Reverse and thrust faults.	Reverse faults.

INTERPRETATION

The sedimentary rocks, alkaline flows and pyroclastic rocks of the Timiskaming Group are interpreted to have been deposited within narrow, deep basins formed during extension by strike-slip movement. In Table 1 the characteristics of the Timiskaming Group and structures within the KLLLF are compared to that of typical strike-slip mobile belts. There is a close correspondence.

The Kirkland basin, for which there is the most information, could have formed during sinistral transtension along the east-trending Larder Lake -Cadillac fault. At about 067°, the axis of the basin is at an appropriate orientation for extension by normal faulting during east-west sinistral transtension (Sanderson and Marchini, 1984). The axes of elongate syenite intrusions, such as that hosting the ore at Kirkland Lake (Fig. 6a) have a similar orientation. These are interpreted to have been passively intruded into extensional fractures (Fig. 6b) at a late stage of sinistral transtension, after the Timiskaming had been tilted to the south. Strike faults, as defined by Thomson (1950), are reverse faults. Since their orientation is the same as the basin axis and the long axis of the syenite intrusions, they are tentatively interpreted to have formed by reactivation of earlier normal faults during a compressional phase that followed the earlier sinistral transtensional fracturing. Gold was introduced along the reverse faults during this compressional phase.

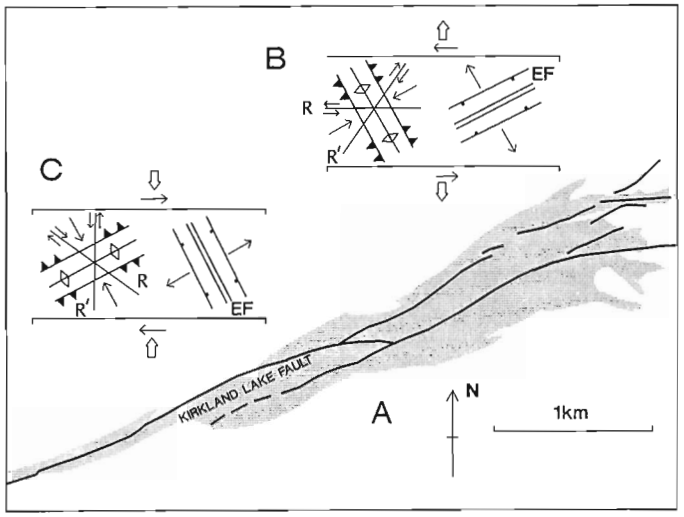

Figure 6. (A) Surface plan of composite syenitic intrusion that hosts most of the gold ore at Kirkland Lake. The Kirkland Lake fault is also shown. (B) Orientation of structures formed by sinistral transtension; EF = extensional fracture. (C) Orientation of structures formed by dextral transpression. (A) is from Thomson et al. (1950); (B) and (C) are from Sanderson and Marchini (1984).

The Larder basin has a similar orientation and structural features as the Kirkland basin and is interpreted to have formed during the same sinistral transtensional event. The 106° orientation of the Dobie basin is not consistent with its formation during east- west sinistral transtension.

The important structural study of Hubert et al. (1984) was carried out in the Rouyn-Noranda area directly east of Kirkland Lake. They identified two important periods of deformation in the region between the Porcupine-Destor and Larder Lake -Cadillac faults. The first is represented by west-northwest folds that they relate to sinistral movement along these major strike-slip faults. This was followed by folding along east-west axes caused by compression normal to these faults.

The Shebandowan belt in western Ontario lies along the boundary between the Quetico and Wawa subprovinces. The belt contains Timiskaming- type sedimentary rocks and alkaline pyroclastic rocks. Corfu and Stott (1986) described a D1 deformation of the underlying rocks, which has not affected the Timiskaming. Both the Timiskaming and the underlying rocks were affected by a D2 deformation that involved shortening and shearing caused by major, oblique, subhorizontal compression along a northwest-southeast axis. This D2 deformation is associated with carbonatization and gold mineralization.

The model given here is not the first for basin formation along the KLLLF. Hopkins (1949) suggested that the Timiskaming at Kirkland Lake, after folding, was dropped into a deep graben. Toogood and Hodgson (1985) carried out a comprehensive structural study of the region. They suggested that the Dobie basin was formed as a pull-apart during dextral transpression; sedimentation and volcanism within the other parts of the deformation zone took place during this dextral event. Their scenario of: 1. dextral transpression accompanied by sedimentation and volcanism; 2. a compressive phase, with beds becoming vertical before intrusion of syenite, differs from that given above. However, dextral transpression is one possibility for the formation of the 067°-trending reverse faults (Fi. 6c). In the Larder Lake Group, south of the KLLLF, Toogood and Hodgson identified D_1 and D_2 folds; the first with north-northwest-trending axial folds, the second trending northeast. Intrusion of syenite dykes occurred between D_1 and D_2 and some lamprophyre dikes appeared to have been intruded comtemporaneously with D2. Earlier, Hodgson (1982) recognized the possibility of extension during sinistral displacement along the Larder Lake-Cadillac and the Porcupine-Destor faults. Colvine et al. (1988) noted that the Timiskaming Group near Timmins may have been deposited in a strike-slip basin.

The Larder Lake-Cadillac fault terminates near Kirkland Lake, with a subsidiary fault, possibly a splay, continuing at 240° towards Matachewan. Large-scale extension and compression can be associated with the terminations of major strike-slip faults. These "end effects" were modelled by Chinnery (1961). In Figure 7 his results, giving the elevation or depression of the ground surface, have been modified to show the left half of a sinistral fault. North of the fault termination there is compression and thickening of the lithosphere, causing the ground to rise. To the south of the fault there is extension. It is to the south of the termination of the Larder Lake - Cadillac fault, near Kirkland Lake, that the alkaline intrusions occur. These are interpreted to be the product of a moderate degree of lithosphere thinning during extension that caused upwelling of the mantle and low degrees of partial melting. Chinnery's model is based on an elastic medium. In part, the upper crust will respond to

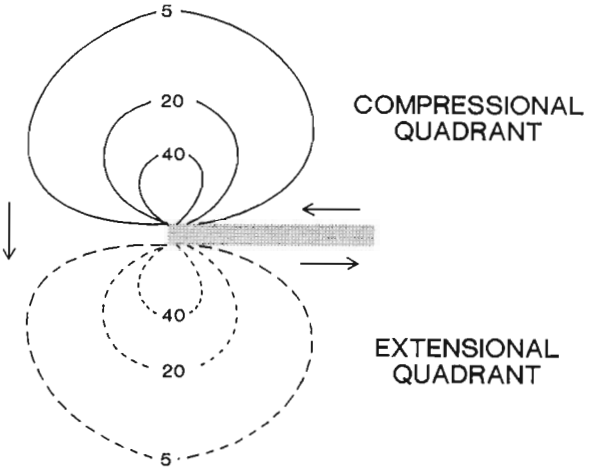

Figure 7. Plan view of vertical displacements (υ] around the termination of a strike-slip fault. Drawn to scale with half of the total length of the fault shown. Depth of the fault is equal to the total length. Contours for υ are expressed in units of 10^{-3}U, where U is the total relative displacement of the two sides of the fault. Solid contours indicate elevation; interrupted contours, depression. Modified from Chinnery (1961).

extension by brittle failure. The principal expression of brittle failure is interpreted to be the basins that comprise the KLLLF. The subsidiary fault or splay to Matachewan may be another expression of extension.

The alkaline magmas generated during extension were forcefully emplaced as diapirs in the country south of the KLLLF and also rose within the shear zone to be passively emplaced in the KLLLF. This accounts for the circular shape of the plutons south of the KLLLF, compared to the elongate nature of intrusions within the KLLLF. An analogous situation has been described by Davies (1982) for alkaline and calc-alkaline granites associated with the Ajjaj shear zone in northern Saudia Arabia.

It is now widely believed that alkaline magmas are generated during or following metasomatism of the upper mantle. One scenario, described by Meen (1987), usefully illustrates the co-generation of alkaline magma and CO_2. For volatile-bearing (CO_2 and H_2O) peridotite, carbonate is stable on the solidus only at pressures >17 kbar. A partial melt formed along the solidus at 30 to 40 kbar can be carbonated and will rise to intersect an inflection on the solidus above the 17 kbar level (see Meen, 1987, Fig. 1). There the melt will react to produce a carbonate-free peridotite or pyroxenite and a CO_2-rich fluid. This CO_2-rich fluid may rise and cannot be fixed in the solid assemblages until it reaches the crust. It will tend to dehydrate the rocks through which it passes, becoming a CO_2- H_2O fluid. Repeated impingement of carbonated melts on the <17 kbar solidus will lead to enrichment of the peridotite in alkali and other elements and, eventually, may cause partial melting to form alkali basalt that is enriched in these elements. This basalt may rise and differentiate into more felsic alkaline rocks.

The evidence summarized above indicates a long period of CO_2-fluxing up the KLLLF that both preceded and continued after intrusion of the alkaline rocks. It was in the latter stages of fluxing, when the CO_2-H_2O fluid carried a sulphide ligand (indicated by deposition of sulphide minerals), that gold was introduced. This was during the second stage of strike-slip orogenesis, when basin extension changed to compression. Fluids were injected up reverse-slip faults, which are speculatively suggested to be reactivated normal-slip (extensional) faults that parallel the long axis of the basin. This structural setting is in accord with the elegant mechanism for the formation of mesothermal gold-quartz veins by Sibson et al. (1988). They showed that veins are associated with reverse faults that dip too steeply to be accounted for by the expected stress fields. Two of the solutions that they proposed for this enigma are: 1. reactivation of normal faults when an originally extended area is shortened; 2. transpression across a vertical strike-slip fault.

CONCLUSIONS

Major strike-slip movement along the Larder Lake -Cadillac fault occurred at a late stage in the history of the Abitibi greenstone belt, subsequent to regional metamorphism. The fault terminated near Kirkland Lake. Given the initial sinistral displacement along the fault, this termination caused lithospheric extension ("end effect") within a broad zone that encompassed the KLLLF and the country to the south. This caused the formation of strike-slip (pull-apart) basins along the fault zone within which the Timiskaming Group was deposited. Lithospheric extension also led to partial melting in the mantle with the generation of magmas of alkaline composition. The magmas, after differentiation, were extruded as flows and pyroclastic deposits to form part of the Timiskaming Group, and were intruded: passively into the shear zone and forcefully outside the shear zone. With the alkaline magmas there was co- generation of a CO_2-H_2O fluid which rose through the ductile shear zone. In the later stages of devolatalization this fluid contained a sulphide ligand, which could dissolve and transport gold. This was during a second, compressional, phase of strike-slip orogenesis, with the fluids directed up reverse faults.

The modelling of Chinnery (1961) shows the possibility for a broad area of extension at the termination of a major strike-slip fault. This is consonant with the large volume of alkaline magma introduced into the crust near Kirkland Lake (Fig. 5), relative to other occurrences in the Superior Province. Extension along the length of strike-slip faults, such as at releasing bends and fault oversteps, can reach sufficiently high levels of ß for alkaline magmas to form, but probably not in as large volumes as at Kirkland Lake. Even where extension is less than that required for magma to appear in the crust, upwelling may be sufficient for decarbonation reactions to take place in the mantle releasing CO_2.

ACKNOWLEDGMENTS

The stimulus to consider these topics came from joint studies with colleagues at the University of Ottawa, Bill Carrigan, André Lalonde, Guy Levesque, and Steve Rowins, on the relationship of the alkaline intrusions at Kirkland Lake to the gold. I am most grateful to Jack Henderson, André Lalonde, John Percival and Steve Rowins who provided constructive comment on the manuscript.

REFERENCES

Basu, A.R., Goodwin, A.M. and Tatsumoto, M.
1984: Sm-Nd study of Archean alkalic rocks from the Superior Province of the Canadian Shield; Earth and Planetary Science Letters, v. 70, p. 40-46.

Ben-Avraham, Z., Nur, A. and Cello, G.
1987: Active transcurrent fault system along the north African passive margin; Tectonophysics, v. 141, p. 249-260.

Boccaletti, M., Nicolich, R. and Tortocici, L.
1984: The Calabrian Arc and the Ionian Sea in the dynamic evolution of the Central Mediterranean; Marine Geology, v. 55, p. 219-245.

Calanchi, N., Colantoni, P., Rossi, P.L., Saitta, M. and Serri, G.
1989: The Strait of Sicily continental rift systems: Physiography and petrochemistry of the submarine volcanic centres; Marine Geology, v. 87, p. 55- 83.

Cello, G.
1987: Structure and deformation processes in the Strait of Sicily "rift zone"; Tectonophysics, v. 141, p. 237-247.

Chinnery, M.A.
1961: The deformation of the ground around surface faults; Seismological Society America Bulletin, v. 51, p. 355-372.

Civetta, L., Cornette, Y., Crisci, G., Gillot, P.Y., Orsi, G. and Requiejo, C.S.
1984: Geology, geochronology and chemical evolution of the island of Pantelleria; Geological Magazine, v. 6, p. 541-562.

Colvine, A.C., Fyon, J.A., Heather, K.B., Marmont, S., Smith, P.M. and Troop, D.G.
1988: Archean lode gold deposits in Ontario; Ontario Geological Survey, Miscellaneous Paper 139, 136p.

Cooke, D.L. and Moorehouse, W.W.
1969: Timiskaming volcanism in the Kirkland Lake area, Ontario, Canada; Canadian Journal of Earth Sciences, v. 6, p. 117-132.
Corfu, F. and Stott, G.M.
1986: U-Pb ages for late magmatism and regional deformation in the Shebandowan belt, Superior Province: a U-Pb zircon and titanite study; Journal of Geology, v. 95, p. 87-105.
Corfu, F., Krogh, T.E., Kwok, Y.Y., Marmont, S. and Jensen, L.S.
(in press): U-Pb geochronology in the southwestern Abitibi greenstone belt, Superior Province; Canadian Journal of Earth Sciences.
Crowell, J.C. and Link, M.H. (editors)
1982: Geologic history of the Ridge basin, southern California; Society of Economic Paleontologists and Mineralogist, Pacific Section, Guidebook, 309p.
Davies, F.B.
1982: Pan-African granite intrusion in response to tectonic volume changes in a ductile shear zone from northern Saudia Arabia; Journal of Geology, v. 90, p. 467-483.
Fitch, T.J.
1972: Plate convergence, transcurrent faults and internal deformation adjacent to southeast Asia and the western Pacific; Journal of Geophysical Research, v. 77, p. 4432-4460.
Grabowski, G., Lovell, H.L., Guindon, D. and Bath, A.
1987: Kirkland Lake Resident Geologist's area; Ontario Geological Survey, Miscellaneous Paper 138, p. 251-284.
Hempton, M.R. and Dunne, L.A.
1984: Sedimentation of pull-apart basins: Active examples in eastern Turkey; Journal of Geology, v. 92, p. 513-530.
Hewitt, D.F.
1963: The Timiskaming Series of the Kirkland Lake area; Canadian Mineralogist, v. 7, p. 497-523.
Hodgson, C.J.
1982: Gold deposits in the Abitibi belt, Ontario; Ontario Geological Survey, Miscellaneous Paper 106, p. 192-197.
Hopkins, H.
1949: Structure at Kirkland Lake, Ontario, Canada; Geological Society of America Bulletin, v. 60, p. 909-922.
Hubert, C., Trudel, P. and Gelinas, L.
1984: Archean wrench fault tectonics and structural evolution of the Blake River Group, Abitibi belt, Quebec; Canadian Journal of Earth Sciences, v. 21, p. 1024-1032.
Hyde, R.S.
1980: Sedimentary facies in the Archean Timiskaming Group, Abitibi greenstone belt, northeastern Ontario, Canada; Precambrian Research, v. 12, p. 161-195.
Jensen, L.S. and Langford, F.F.
1985: Geology and petrogenesis of the Archean Abitibi belt in the Kirkland Lake area, Ontario; Ontario Geological Survey, Miscellaneous Paper 123, 130p.
Jolly, W.T.
1978: Metamorphic history of the Archean Abitibi belt; *in* Fraser, J.A. and Heywood, W.W., eds., Metamorphism in the Canadian Shield, Geological Survey of Canada, Paper 78-10, p. 63-78.
Lowell, J.D.
1972: Spitsbergen Tertiary orogenic belt and the Spitsbergen fracture zone; Geological Society of America Bulletin, v. 83, p. 3091-3102.
McKenzie, D. and Bickle, M.J.
1988: The volume and composition of melt generated by extension of the lithosphere; Journal of Petrology, v. 29, p. 625-679.
Meen, J.K.
1987: Mantle metasomatism and carbonatites; an experimental study of a complex relationship; Geological Society America Special Paper 215, p. 91-100.
Mitchell, A.H.G. and Reading, H.G.
1978: Sedimentation and tectonics; *in* H.G. Reading, ed., Sedimentary Environments and Facies, Blackwell, Oxford, England, p. 439-476.
Nunes, P.D. and Jensen, L.S.
1980: Geochronology of the Abitibi metavolcanic belt, Kirkland Lake area - progress report; Ontario Geological Survey, Miscellaneous Paper 92, p. 40-45.
Percival, J.A. and Williams, H.R.
1989: The late Archean Quetico accretionary complex, Superior Province, Canada; Geology, v. 17, p. 23-25.
Pitman, W.C. and Andrews, J.A.
1985: Subsidence and thermal history of small pull-apart basins; *in* K.T. Biddle and N. Christie-Blick, ed., Strike-slip Deformation, Basin Formation, and Sedimentation, Society of Economic Geologists and Paleontologists and Mineralogists, Special Publication 37, p. 45-49.
Reading, H.G.
1980: Characteristics and recognition of strike-slip fault systems; *in* P.F. Ballance and H.G. Reading, ed., Sedimentation in oblique-slip mobile zones, International Association of Sedimentologists, Special Publication 4, p. 7-26
Reuther, C.D. and Eisbacher, G.H.
1985: Pantelleria Rift - crustal extension in a convergent intraplate setting; Geologische Rundschau, v. 74, p. 585-597.
Sanderson, D.J. and Marchini, W.R.D.
1984: Transpression; Journal of Structural Geology, v. 6, p. 449-458.
Smith, A.R. and Sutcliffe, R.H.
1988: Project number 88-08. Plutonic rocks of the Abitibi subprovince; Ontario Geological Survey, Miscellaneous Paper 141, p. 188-196.
Sibson, R.H., Robert, F. and Poulsen, K.H.
1988: High-angle reverse faults, fluid pressure cycling, and mesothermal gold-quartz deposits; Geology, v. 16, p. 551-555.
Sylvester, A.G.
1988: Strike-slip faults; Geological Society of America Bulletin, v. 100, p. 1666-1703.
Thomson, J.E.
1950: Geology of Teck Township and the Kenogami Lake area, Kirkland Lake gold belt; Ontario Department of Mines, Annual Report, v. 57, p. 1- 53.
Thomson, J.E., Charlewood, G.H., Griffin, K., Hawley, J.E., Hopkins, H., MacIntosh, C.G., Ogrizlo, S.P., Perry, O.S. and Ward, W.
1950: Geology of the main ore zone at Kirkland Lake; Ontario Department of Mines, Annual Report, v. 57, p. 54-188.
Toogood, D.J. and Hodgson, C.J.
1985: Grant 227. A structural investigation between the Kirkland Lake and Larder Lake gold camps; Ontario Geological Survey, Miscellaneous Paper 127, p. 200-205.
Woodcock, N.H.
1986: The role of strike-slip fault systems at plate boundaries; Royal Society of London, Philosophical Transactions, series A, v. 317, p. 13- 29.
Yeats, R.S.
1978: Neogene acceleration and subsidence rates in southern California; Geology, v. 6, p. 456-460.

The sub-Thelon Formation paleosol, Northwest Territories[1]

Q. Gall[2] and J.A. Donaldson[2]
Mineral Resources Division

Gall, Q. and Donaldson, J.A., The sub-Thelon Formation paleosol, Northwest Territories; in Current Research, Part C, Geological Survey of Canada, Paper 90-1C, p. 271-277, 1990.

Abstract

The sub-Thelon Formation paleosol developed on a variety of protoliths following extrusion of the 1.76 Ga Pitz Formation rhyolite, and prior to 1.72 Ga diagenetic apatite formation in the Thelon Formation. The saprolitic paleosol ranges in thickness from 1 to 100 m. The paleosol characteristically displays a colour zonation from a green-grey base to a red top, and an upward increase in disruption of original protolith textures. Lithochemical trends in paleoweathered gneiss and granite show a consistent upward increase in SiO_2, Fe_2O_3/FeO, and CIA values, and upward decrease in MnO, MgO, CaO, Na_2O, K_2O, V, Rb and Ba.

Résumé

Le paléosol au-dessous de la formation de Thelon s'est formé sur diverses roches originelles après l'extrusion de la rhyolite de la formation de Pitz daté à 1,76 Ga et avant la formation à 1,72 Ga de l'apatite diagénétique de la formation de Thelon. L'épaisseur du paléosol saprolitique varie de 1 à 100 m. Le paléosol présente un horizon coloré caractéristique passant de vert-gris à la base à rouge au sommet, et une modification vers le haut des textures originelles. Les tendances lithochimiques dans le gneiss et le granite paléo-érodés indiquent une augmentation continue vers le haut des teneurs en SiO_2, Fe_2O_3/FeO et CIA et une diminution vers le haut de MnO, MgO, CaO, Na_2O, K_2O, V, Rb et Ba.

[1] Contribution to Canada — Northwest Territories Mineral Development Agreement 1987-1991. Project carried by the Geological Survey of Canada.

[2] Ottawa-Carleton Geoscience Centre, Department of Earth Sciences, Carleton University, Ottawa, Ontario K1S 5B6

SUB-THELON FORMATION PALEOSOL

The Thelon Basin comprises quartz arenite and conglomerate of the Thelon Formation, the uppermost siliciclastic unit of the Dubawnt Group (Wright, 1955; Donaldson, 1965). In most places the Thelon Formation overlies either paleoweathered sedimentary and volcanic rocks of the Pitz Formation, or paleoweathered Archean and Early Proterozoic basement rocks. Basal sedimentary rocks of the Thelon Formation contain lithic grains of pedogenic origin, indicating that weathering occurred before deposition of the Thelon Formation.

A maximum age for the sub-Thelon Formation paleoweathering is given by a 1.76 Ga U-Pb zircon age (LeCheminant et al., 1987) from weathered volcanic rocks of the Pitz Formation. A minimum age of 1720 ± 6 Ma comes from U-Pb analysis of diagenetic apatite cement from the base of the Thelon Formation (Miller et al., 1989).

The sub-Thelon Formation paleosol appears to be laterally extensive under much of the Thelon Basin as it has been observed in outcrop along the eastern margin of the basin, and has been intersected by drilling in both the western and eastern parts of the basin. Profile thicknesses range from less than 1 m of hematitic alteration in quartzite to 100 m in schistose rocks. The paleoweathering profiles are actually erosional remnants of thicker profiles, as indicated by lithic grains of paleosol in the basal Thelon Formation; only lowermost C (saprolite) and R (consolidated bedrock) weathering horizons have been identified.

To date, nine profiles (Fig. 1) have been sampled, providing examples of paleosols developed on: granitoid augen gneiss (profiles 1 and 2), megacrystic granite (profile 3), felsic volcanic rock (profiles 4 and 5), garnet-bearing gneiss (profile 6), peridotite (profile 7) and semipelitic metasedimentary rock (profiles 8 and 9). Profile 6 from the Boomerang Lake uranium prospect, plus core from altered metasedimentary rocks from the Kiggavik uranium deposit and adjacent properties, were collected for subsequent study to seek criteria for distinguishing between the alteration produced by unconformity/paleosol-related uranium and precious metal mineralization, and protolith alteration due to paleoweathering.

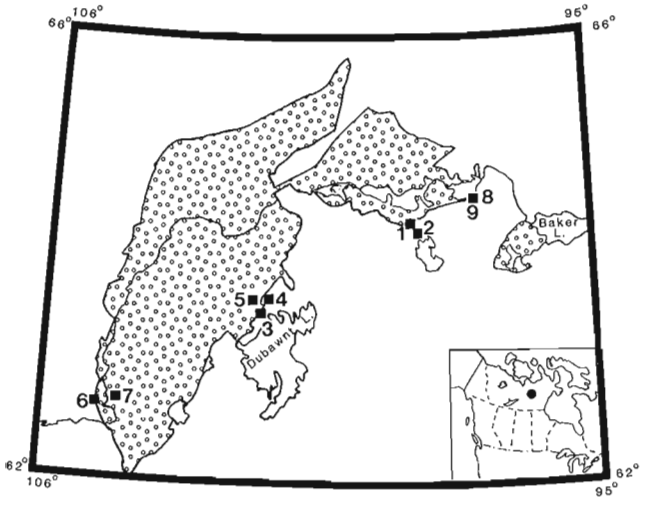

Figure 1. Sampling localities of 9 paleoweathering profiles of sub-Thelon Formation paleosol.

Detailed petrographic studies have been completed on the paleosol where it is developed on granitoid augen gneiss (profiles 1 and 2) and megacrystic granite (profile 3). The mineral assemblage of the augen gneiss is plagioclase and potassic feldspar, quartz, hornblende, biotite, zircon and apatite. As the augen gneiss becomes progressively weathered towards the contact with the overlying Thelon Formation, the feldspars lose their augen shape and twinning, and become illitized. Microcrystalline quartz cement is more abundant towards the top of the paleosol. The quartz cement occurs both in the corroded feldspar augen and interstitially. Hematite is present in all the paleosol samples, and typically is concentrated along the gneissosity, where the fabric persists, and overprints the other minerals. Veins, filled by kaolinite and quartz, post-date the hematite cement. From X-ray diffractograms, the clay-fraction assemblage of the paleosol is illite, quartz, hematite and kaolinite, and minor chlorite. The gneissic fabric of the protolith is progressively destroyed with increased weathering. The paleosol becomes unstructured and starts to develop angular, feldspar-rich peds in a quartz-clay-hematite matrix. The Thelon Formation sandstones in profiles 1 and 2 contain monocrystalline and polycrystalline quartz grains, feldspar grains, and a variety of lithic grains including silicified paleosol. Interstitial material, in order of development, is quartz cement, kaolinite, minor illite and hematite cement.

The granite protolith in profile 3 consists of perthitic microcline megacrysts in a fine- to medium-grained matrix of quartz, plagioclase, biotite, zircon, apatite and magnetite. At the base of the paleosol the feldspar becomes increasingly illitized and biotite becomes hematized, especially along cleavage planes. At the top of the paleosol quartz and feldspar becomes corroded, fractured and disrupted by quartz cement. Fibrous illite occurs on feldspar grains, and to a lesser extent on kaolinite and quartz cement. Hematite cement overprints all the remnant protolith mineralogy, quartz cement, kaolinite and illite. X-ray diffractograms indicate that the clay-size fraction mineral assemblage of the paleosol is quartz, kaolinite, illite and hematite. The Thelon Formation pebble conglomerate and sandstone in profile 3 contains polycrystalline quartz grains, feldspar grains, and metamorphic and igneous lithic grains. Interstitial minerals, in order of development, are chert, kaolinite and hematite.

One of the most striking features of the paleosol in profiles 1, 2, 3, 8 and 9, is the vertical colour transitions with increasing depth from red paleosol (5R 5/4, Munsell colour system), to red-grey-green (5YR 6/1), to green-grey (10GY 5/2), to fresh protolith. As substantiated by thin section petrography, the upper red zone reflects extensive hematite cement, which overprints all other minerals; the lower green-grey zone reflects a relative abundance of chlorite and illite and a paucity of late-stage hematite cement. These colour zones are inferred to have resulted from downward-percolating weathering fluids, including late oxidizing fluids which have hematized earlier-formed chlorite. Discrete silicified and hematized pedogenic lithic grains in the basal Thelon Formation surrounded by diagenetic cements,

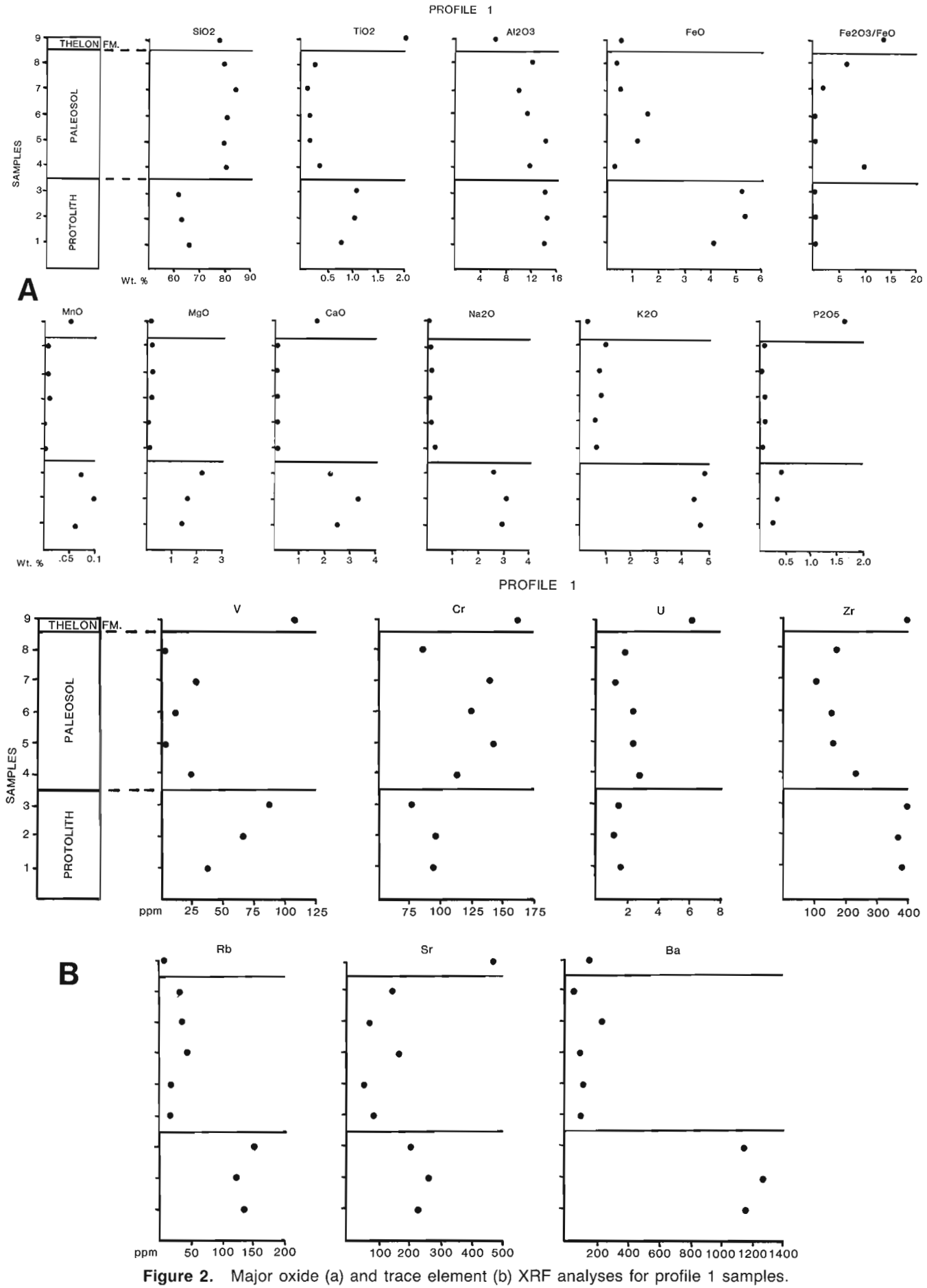

Figure 2. Major oxide (a) and trace element (b) XRF analyses for profile 1 samples.

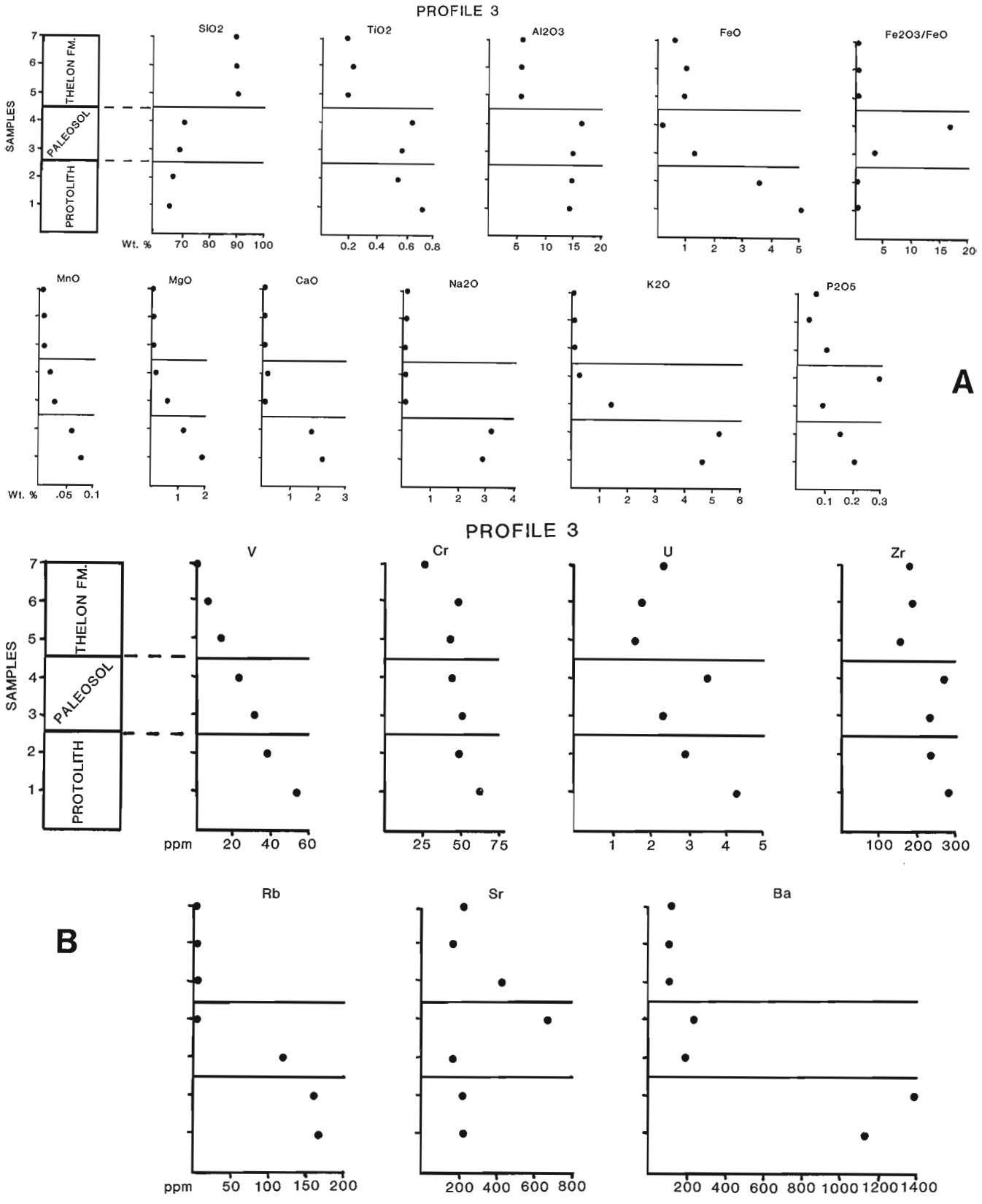

Figure 3. Major oxide (a) and trace element (b) XRF analyses for profile 3 samples.

plus chemical profile trends (Table 1, Fig. 2 and 3), suggest that the vertical colour transitions are a true paleoweathering feature and not a product of diagenetic overprinting during cementation of the Thelon Formation. This is a critical feature in the identification of paleosols (Retallack et al., 1984). Similar vertical colour transitions have been described from paleosols beneath the Athabasca Basin (MacDonald, 1980) and Kombolgie Formation in the Northern Territories, Australia (Miller et al., in press). However, in distinctly coloured lithologies, such as the red Pitz Formation rhyolite, the colour transition is not developed. In this case the red groundmass and white phenocrysts grade from fresh, dark red (10 R 3/4), to grey-red (10 R 4/2), to pale red (10 R 6/2) with increased weathering.

Major oxide and trace element analyses have been completed on profile 1 and profile 3 (Table 1 and Fig. 2 and 3). Both profiles were sampled from outcrop, with approximately 10m between each profile 1 sample locality, and approximately 1m between each profile 3 sample locality. In both profiles SiO_2 and Fe_2O_3/FeO increase upward within the paleosol, reflecting increasing quartz and hematite cementation with increased weathering. Uranium tends to remain unchanged in both profiles despite the presence of hematite cement. The slight increase in Cr in profile 1 may be due to the destruction of ferromagnesian minerals, and subsequent adsorption of Cr onto clay minerals (cf. Aubert and Pinta, 1977). MnO, MgO, CaO, Na_2O, K_2O, V, and Ba consistently decrease upward in the profiles, commonly in an abrupt fashion, reflecting the increase in element leaching with increased weathering. The other major oxides and trace elements either remain unchanged or decrease with increased weathering. The chemical index of alteration (Nesbitt and Young, 1982) for the two profiles

Table 1. Major oxide and trace element chemistry and CIA for paleoweathering profiles developed in augen gneiss (profile 1) and megacrystic granite (profile 3).

PROFILE 1		Major Elements (wt. %)										
Sample #		SiO2	TiO2	Al203	Fe203/FeO	FeO	MnO	MgO	CaO	Na20	K20	P205
Thelon Fm.	9	77.91	2.08	6.08	14.14	0.51	0.05	0.13	1.60	0.00	0.29	1.63
Paleosol	8	79.84	0.23	12.00	6.94	0.32	0.01	0.13	0.05	0.05	0.93	0.09
"	7	83.79	0.13	9.87	2.33	0.51	0.01	0.16	0.06	0.17	0.72	0.02
"	6	80.89	0.18	11.49	0.03	1.57	0.01	0.14	0.06	0.09	0.79	0.07
"	5	79.90	0.19	13.18	0.29	1.12	0.00	0.00	0.05	0.13	0.60	0.09
	4	80.22	0.36	11.94	10.20	0.25	0.00	0.02	0.05	0.25	0.63	0.05
Gneiss	3	61.89	1.18	14.23	0.36	5.24	0.07	2.16	2.16	2.55	4.84	0.42
"	2	62.62	1.08	14.50	0.35	5.38	0.10	1.56	3.28	3.05	4.42	0.32
"	1	65.85	0.80	14.19	0.29	4.14	0.06	1.34	2.46	2.87	4.62	0.22

	Trace Elements (ppm)								
Sample #	V	Cr	U	Zr	Rb	Sr	Ba	LOI(wt%)	CIA
9	107	161	6.2	396	5	473	156	3.89	65.36
8	3	85	1.9	169	30	146	57	3.70	91.05
7	26	138	1.3	100	34	71	121	3.16	89.42
6	5	123	2.4	152	43	163	91	3.74	91.17
5	3	141	2.4	158	17	52	117	4.35	93.25
4	23	112	2.8	231	16	88	97	3.93	90.98
3	85	75	1.6	392	151	203	1154	1.41	51.58
2	66	95	1.2	368	124	260	1267	0.89	47.91
1	37	94	1.5	375	135	229	1158	0.80	49.99

PROFILE 3		Major Elements (wt. %)										
Sample #		SiO2	TiO2	Al203	Fe203/FeO	FeO	MnO	MgO	CaO	Na20	K20	P205
Thelon Fm.	7	89.67	0.18	5.33	0.29	0.56	0.01	0.06	0.06	0.03	0.04	0.06
"	6	90.05	0.21	5.20	0.28	0.97	0 01	0.07	0.06	0.05	0.05	0.04
"	5	90.10	0.18	5.27	0.42	0.89	0.01	0.06	0.06	0.02	0.04	0.10
Paleosol	4	70.87	0.64	16.29	16.86	0.15	0.02	0.12	0.12	0.03	0.25	0.29
"	3	69.48	0.57	14.96	3.57	1.26	0.03	0.60	0.07	0.03	1.35	0.09
Granite	2	67.50	0.54	14.83	0.28	3.54	0.06	1.18	1.75	3.16	5.27	0.15
"	1	65.65	0.72	14.34	0.19	5.02	0.08	1.91	2.16	2.87	4.66	0.20

Sample #	V	Cr	U	Zr	Rb	Sr	Ba	LOI(wt%)	CIA
7	0	25	2.3	175	0	220	115	2.03	96.35
6	6	48	1.8	185	0	161	105	1.90	95.49
5	12	43	1.6	159	0	413	116	1.93	96.60
4	22	45	3.4	273	0	662	227	5.78	96.80
3	31	50	2.3	238	118	179	189	5.05	90.13
2	37	48	2.9	237	156	219	1386	0.64	51.29
1	53	62	4.2	282	163	220	1131	0.95	51.16

was also calculated (CIA, Table 1 and Fig. 4). This index measures the degree of Na_2O, K_2O and CaO leaching during weathering relative to Al_2O_3 using molecular proportions. Alumina is considered to be stable in the weathering environment compared to most other elements (Birkeland, 1974), and indeed does not appear to have been leached as much as the sodium, potassium and calcium in both profiles. An increase in the CIA value reflects increased Na_2O, K_2O and CaO leaching, and consequently increased weathering. Profiles 1 and 3 display sharp increases in CIA values upwards within the paleosol. This provides additional evidence that the sub-Thelon Formation paleosol is a true paleoweathering horizon.

Many of the other paleosol profiles also show an upward increase in disruption of pre-existing metamorphic and igneous fabrics. A feature, particularly well developed in paleoweathered outcrops of Pitz Formation rhyolite, is a hackly, polyhedral structure (Fig. 5) considered to be the result of extensive mineral dissolution and/or shrinkage. A crude horizontal parting, observed in paleoweathered Pitz Formation (Fig. 6), subtle mineral flattening, and stylocumulates in paleoweathered megacrystic granite (Fig. 7), are considered to be compaction features related to loading caused by accumulation of the Thelon Formation on structurally weakened paleosol.

Silcretes have been documented in Thelon Formation and underlying paleosol by Chiarenzelli (1983) and Ross and Chiarenzelli (1985). Although the existence of these silcretes is not contested, caution must be exercised in their field identification. This is because of the widespread occurrence of fault-associated quartz veins in both basement rocks and Thelon Formation that show features similar to silcretized outcrop, and the possibility of mistaking one for the other. These features include several generations of fracturing and silica deposition, zonation of megaquartz and chalcedony, and brecciated host rock, where the fragments have not moved more than a few centimetres from their place of origin. On exposed horizontal surfaces of paleosol adjacent to faults, the vein distribution is similar to the subparallel "quartz stringers" described by Ross and Chiarenzelli (1985). Northwest of Dubawnt Lake, the widest quartz veins are generally subvertical and are parallel to the subvertical northeast-trending (040-055°) faults. This trend approximates the orientation of a regional set of faults that cut the Thelon Formation throughout the Thelon Basin.

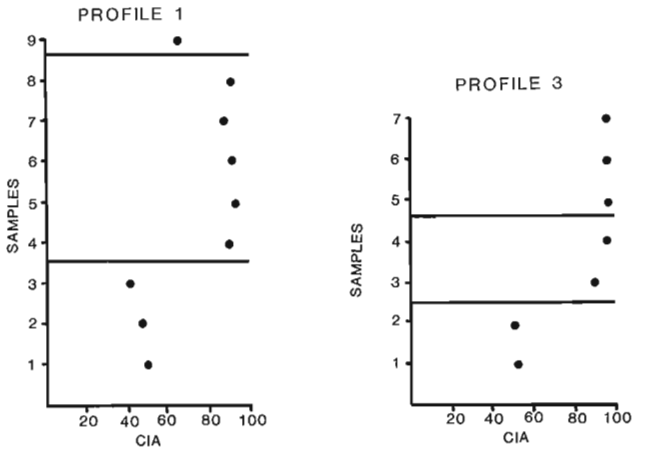

Figure 4. CIA trends for profile 1 (a) and profile 3 (b) samples. (CIA = $[Al_2O_3/(Al_2O_3 + CaO^* + Na_2O + K_2O)]$ 100, CaO* is amount of CaO in the silicate fraction of the rock).

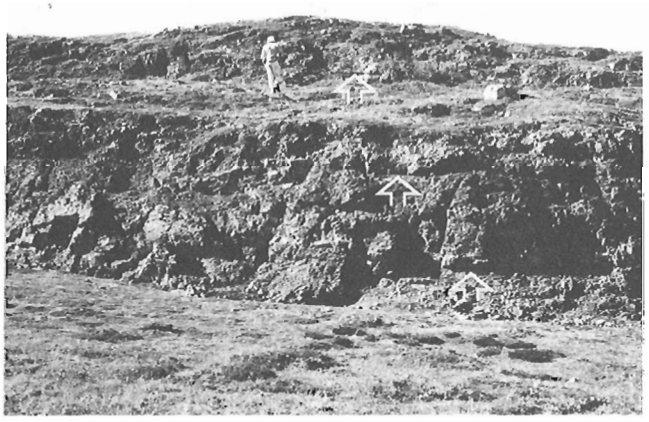

Figure 6. Crude horizontal parting (arrows) developed in paleoweathered Pitz Formation feldspar- quartz phyric rhyolite.

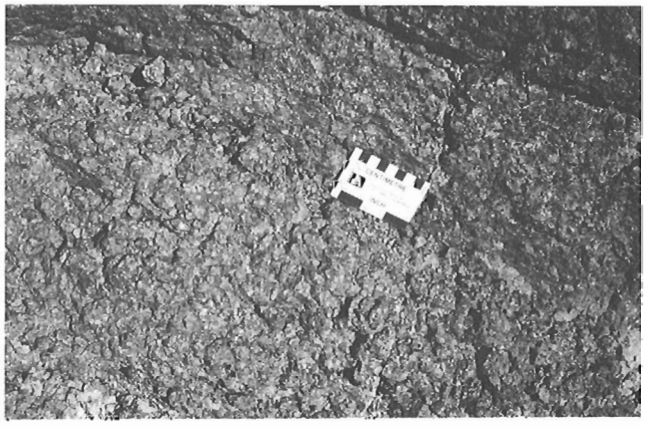

Figure 5. Polyhedral structure in paleoweathering rhyolite. Vertical section.

Figure 7. Compaction-induced stylocumulates (arrows) in megacrystic granite. Field of view is 3 mm wide.

Identifying fault associations and trends, or features such as silcrete caps and lenses as described by Ross and Chiarenzelli (1985), may be important guides for distinguishing fault-related quartz veins in paleosol from silicified paleosol in the field.

CONCLUSIONS

The foregoing preliminary description of the sub-Thelon Formation paleosol leads to the following conclusions:

(1) The paleosol profiles developed on a variety of protoliths display saprolite (C horizon) weathering, but are missing A, B and K soil horizons; which, if they formed, were likely eroded.

(2) Physicochemical manifestations of protolith paleoweathering are a descending colour change from red (extensive paleosol hematization), to red-grey-green, to green-grey, to fresh protolith, especially in metasedimentary protoliths; and development of a hackly, disrupted texture with increased weathering of the Pitz Formation.

(3) Petrographic features in the protoliths, paleosol and Thelon Formation, including grains of paleosol in the Thelon Formation and chemical trends in the profiles, suggest that phyllosilicate mineral growth, silicification and hematization within the protoliths all occurred during paleoweathering, and pre-date diagenetic silicification, phyllosilicate growth and hematization within the overlying Thelon Formation.

(4) Paleosol profile geochemical trends from gneiss and granite protoliths show a consistent depletion in many of the major oxides and trace elements towards the unconformity; except for silica and ferric iron which show an increase with increased paleoweathering and reflect pedogenic silicification and hematization. CIA values and profiles similarly reflect paleoweathering of these two protoliths beneath the Thelon Formation.

ACKNOWLEDGMENTS

We thank T.D. Peterson (GSC/LCSD) and members of his mapping team for supplying a friendly field base for our work. We also gratefully acknowledge Power Reactor and Nuclear Fuel Development Corporation (PNC) for giving us the opportunity to sample the paleosol in drill core. R.T. Bell, P.F. Hoffman, A.N. LeCheminant, A.R. Miller and S.M. Roscoe are thanked for their constructive comments on an earlier version of this paper.

REFERENCES

Aubert, H. and Pinta, M.
1977: Trace Elements in Soils; Elsevier, 395 p.

Birkeland, P.W.
1974: Pedology, Weathering, and Geomorphological Research; Oxford University Press, 285 p.

Chiarenzelli, J.R.
1983: Mid-Proterozoic chemical weathering, regolith and silcrete in the Thelon Basin, Northwest Territories; unpublished M. Sc. thesis, Carleton University, Ottawa, 197 p.

Donaldson, J.A.
1965: The Dubawnt Group, Districts of Keewatin and Mackenzie; Geological Survey of Canada, Paper 64-20.

LeCheminant, A.N., Miller, A.R. and LeCheminant, G.M.
1987: Early Proterozoic alkaline igneous rocks, District of Keewatin, Canada: petrogenesis and mineralization *in* Geochemistry and Mineralization of Proterozoic Volcanic Suites, ed. T.C. Pharaoh, R.D. Beckinsale and D. Rickard; Geological Society, Special Publication No 33, p. 219-240.

MacDonald, C.
1980: Mineralogy and geochemistry of a Precambrian regolith in the Athabasca Basin; unpublished M. Sc. thesis, University of Saskatchewan, Saskatoon, 151 p.

Miller, A.R., Needham, R.S. and Stuart-Smith, P.G.
In Press: Pre-Kombolgie (~ 1.69-1.65 Ga) saprolitic weathering in the Pine Creek Geosyncline, Northern Territory, Australia; *in* Early Organic Evolution and Mineral and Energy Resources, ed. M.M. Kimberley; Springer-Verlag.

Miller, A.R., Cumming, G.L. and Krstic, D.
1989: U-Pb, Pb-Pb and K-Ar isotopic study of uraniferous phosphate-bearing rocks in the Thelon Formation, Dubawnt Group, Northwest Territories, Canada; Canadian Journal of Earth Sciences, v. 26, p. 867-880.

Nesbitt, H.W. and Young, G.M.
1982: Early Proterozoic climates and plate motions inferred from major element chemistry of lutites; Nature, v. 299, p. 715-717.

Retallack, G., Grandstaff, D. and Kimberley, M.
1984: The promise and problems of Precambrian paleosols; Episodes, v. 7, p. 8-12.

Ross, G.M. and Chiarenzelli, J.R.
1985: Paleoclimatic significance of widespread Proterozoic silcrete in the Bear and Churchill provinces of the northwestern Canadian Shield; Journal of Sedimentary Petrology, v. 55, p. 196-204.

Wright, G.M.
1955: Geological notes on central District of Keewatin, Northwest Territories; Geological Survey of Canada, Paper 55-17.

A new source for carvingstone (soapstone) near Baker Lake, N.W.T.

R.T. Bell
Mineral Resources Division

Bell, R.T. A new source for carvingstone (soapstone) near Baker Lake, N.W.T.; in Current Research, Part C, Geological Survey of Canada, Paper 90-1C, p. 279-280, 1990.

Abstract

Massive, clay-alteration zone material outside of unconformity uranium deposits may provide useful white carvingstone (soapstone). Southwest Grid deposit in Baker Lake area of District of Keewatin provides an example.

Résumé

Un matériau massif, de zone d'altération argileuse, à l'extérieur de gisements d'uranium discordants, pourrait être utilisé comme pierre à savon (''stéatite''). Le gisement Southwest Grid dans la région du lac Baker (district de Keewatin) est présenté à titre d'exemple.

A possible source of "soapstone" or more properly carvingstone was encountered this summer while conducting routine resource evaluation studies on Kiggavik, nearby uranium deposits and occurrences in Central Keewatin District.

Reports of carvingstone are few. The most comprehensive and widely accessible is by Gibbins (1988), in which he outlined the characteristics, rough composition and aesthetic attributes. More importantly he discussed the economic aspects. In this regard, a typical Inuit community which ranges from roughly 300 to 800 permanent residents typically gains a net income from carving in the order of $100 000. In some cases it exceeds $ 1 000 000 per settlement. Consequently soapstone carvings provide an important source of income in northern communities.

In the early days of soapstone carving much of the raw material was shipped in from southern Quebec. Now most settlements have very distinct local materials, e.g. "Black soapstone" at Baker Lake or laminated to layered soapstone (argillite, hornfels) at Sanikiluaq.

Typically "carvingstone" ranges from black and dark gray through to medium greenish grey (most common) to pale yellow-green, pale grey and pale green. A very few carvings are very pale grey to buff and are restricted to massive aphanitic limestone, dolomite or marble. Other than these and ivory carvings, white carvings by Inuits artists are either extremely rare or else non-existent.

The Southwest Grid drilling project (Urangesellschaft Canada, Ltd, operator) intersected significant white clay-alteration zones, parts of which extent outside of the uranium mineralized zones. Here as well as elsewhere clay alteration zones are a distinctive feature (*see* Fuchs and Hilger, 1989) of virtually all unconformity type uranium deposits, but commonly (almost always?) the originally layered or foliate nature of the protolith as well as later shear-deformation results in a strongly foliated material, quite unsuitable for carving.

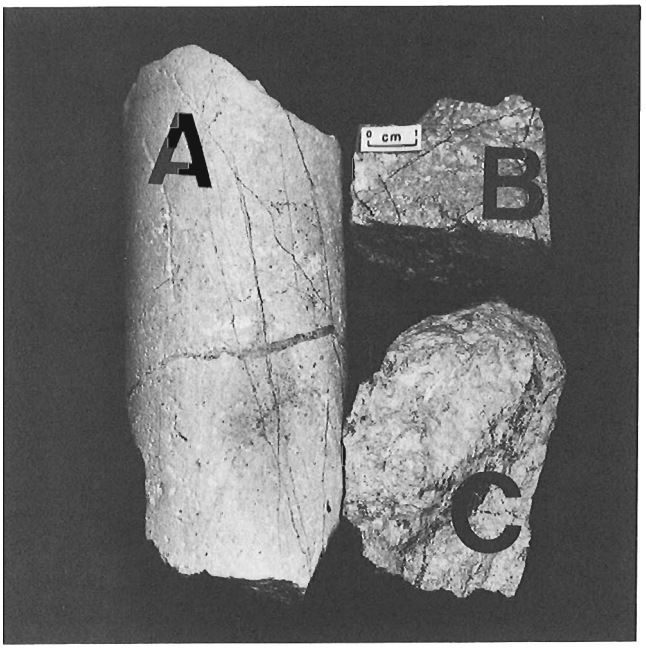

Figure 1. Specimens from Southwest Grid drill site, 15 km southwest of Kiggavik, all several hundred feet below surface, letters on specimens are keyed to Table 1. (GSC 204995)

Table 1. Samples from drillholes from Southwest Grid and other areas.

SPECIMEN	MINERALOGY	LOCATION	ASPECT
A*	illite, kaolinite	DH 11, 595ft	white, soft massive
B*	quartz, illite, kaolinite	DH 04, 517ft	very pale grey, medium soft, massive
C*	quartz, illite	DH 11, 722ft	very pale grey medium soft, massive
Argillite**	talc, chlorite minor calcite	Sanikiluaq Tukarak Isl.	green, hard layered
"Soapstone"**	chlorite, talc	Sanikiluaq Co-op (imported?)	grey medium soft, typical soapstone
"Soapstone"**	talc, chlorite	Sanikiluaq Co-op (imported?)	grey, soft, typical soapstone

* See Figure 1
** Samples from Carvings

In the case at Southwest Grid (about 15 km southwest of Kiggavik) some of the original protolith was thick, structurally massive syenite to granite dykes which have not undergone shearing deformation. Accordingly as these retain a massive and non-foliate characteristic, those portions of this lying at depths of several hundreds of feet and outside the uranium deposit proper, may provide an economic by-product in the form of white artistic carvingstone.

Figure 1 illustrates three samples. Table 1 summarizes the composition of these samples from drillholes in the Southwest Grid and for comparison three other carvingstones.

The only detriments to the feasibility of using these materials is that hardness may vary due to late (post-mineralization) quartz veinlets and some may have relict pale brown redox fronts, as well that the material for carving must be carefully segregated from the ore zone completely.

G. LeCheminant, A. Roberts and R. Delabio made mineralogical determinations. A.R. Miller (GSC) and M. Stuart (Urangesellschaft) made comments that improved this note. Urangesellschaft Canada, Limited has permitted the publication of this short note.

REFERENCES

Fuchs, H.D. and Hilger, W.
1989: Kiggavik (Lone Gull): an unconformity related uranium deposit in the Thelon Basin, Northwest Territories, Canada; *in* Uranium Resources and Geology of North America, International Atomic Energy Agency, Vienna, IAEA — TECDOC-500 p. 429-454.

Gibbins, W.A.
1988: Carvingstone, the foundation of a northern economy; Inuit Art Quarterly, Fall 1988, p. 4-8 (also circulated in EGS 1987-7, Department of Indian and Northern Affairs, 22 p).

Vapour-induced partial melting in the gabbroic part of the Lac des Iles Complex, Ontario and the genesis of platinum group element mineralization[1]

G.E. Brügmann[2] and A.J. Naldrett[2]

Brügmann, G.E. and Naldrett A.J. Vapour-induced partial melting in the gabbroic part of the Lac des Iles Complex, Ontario and the genesis of platinum group element mineralization; in Current Research, Part C, Geological Survey of Canada, Paper 90-1C, p. 281-291, 1990.

Abstract

The gabbroic part of the Lac des Iles Complex consists mainly of gabbroic and gabbro-noritic cumulates. Gradational chemical variations indicate a continuously fractionating magma chamber rather than the two phases of intrusion proposed by previous studies. The high grade PGE mineralization in the texturally complex Roby Zone is associated with pegmatitic and mafic-ultramafic dykes, and is strongly enriched in Au, Pd and Pt relative to Ir and Os. Pd/Ir ratios exceed 10 000 and high Pd/Pt ratios indicate fractionation of Pt from Pd. Constitutional zone refining, whereby the high volatile content of residual magma induced partial melting of gabbroic cumulates, accounts for textural and compositional variations.

Résumé

La partie gabbroïque du complexe du lac des Îles est principalement constituée de cumulats gabbroïques et gabbro-noritiques. Des variations chimiques progressives indiquent la présence d'une chambre magmatique à fractionnement continu plutôt que des deux phases d'intrusion proposées dans des études antérieures. La forte minéralisation en éléments du groupe du platine ÉGP qu'on trouve dans la zone de Roby à texture complexe, est associée à des dykes pegmatitiques et mafiques et ultramafiques; elle est en outre fortement enrichie en Au, Pd et Pt par rapport à Ir et Os. Les rapports Pd/Ir dépassent 10 000 et des rapports Pd/Pt indiquent un fractionnement Pt à partir de Pd. Le raffinement de la zone constitutionnelle, au moyen duquel la forte teneur en matières volatiles du magma résiduel a provoqué la fonte partielle des cumulats gabbroïques, explique les variations de texture et de composition.

[1] Contribution to the Canada Ontario Mineral Development Agreement 1985-1990. Project carried by the Geological Survey of Canada.

[2] Department of Geology, University of Toronto, Toronto, Ontario M5S 3B1

INTRODUCTION

The Lac des Iles (LDI) complex lies within an Archean granite/granite gneiss terrane which belongs to the Wabigoon Subprovince. Several mafic intrusions within the area appear to define the perimeter of a circle about 20 km in diameter, the centre of which is occupied by hornblende and biotite tonalite rocks (Sutcliffe, 1986). The LDI complex which is the largest of the mafic bodies has been mapped by Pye (1968), and Sutcliffe and Sweeney (1985, 1986) and consists of an ultramafic part (UMP) around Lac des Iles and a gabbroic part (GP) to the south (Fig. 1).

The gabbroic part is well known because of its Cu-Ni mineralization which has been explored by several mining companies since its discovery in 1963. Gunnex Ltd. investigated 8 mineralized zones (A to H zones). The Roby Zone comprising the E, C, and part of the F-zone contains estimated reserves of 20 400 000 tonnes of ore with an average grade of 6.17 ppm total PGE (Northern Miner, Nov. 10, 1986).

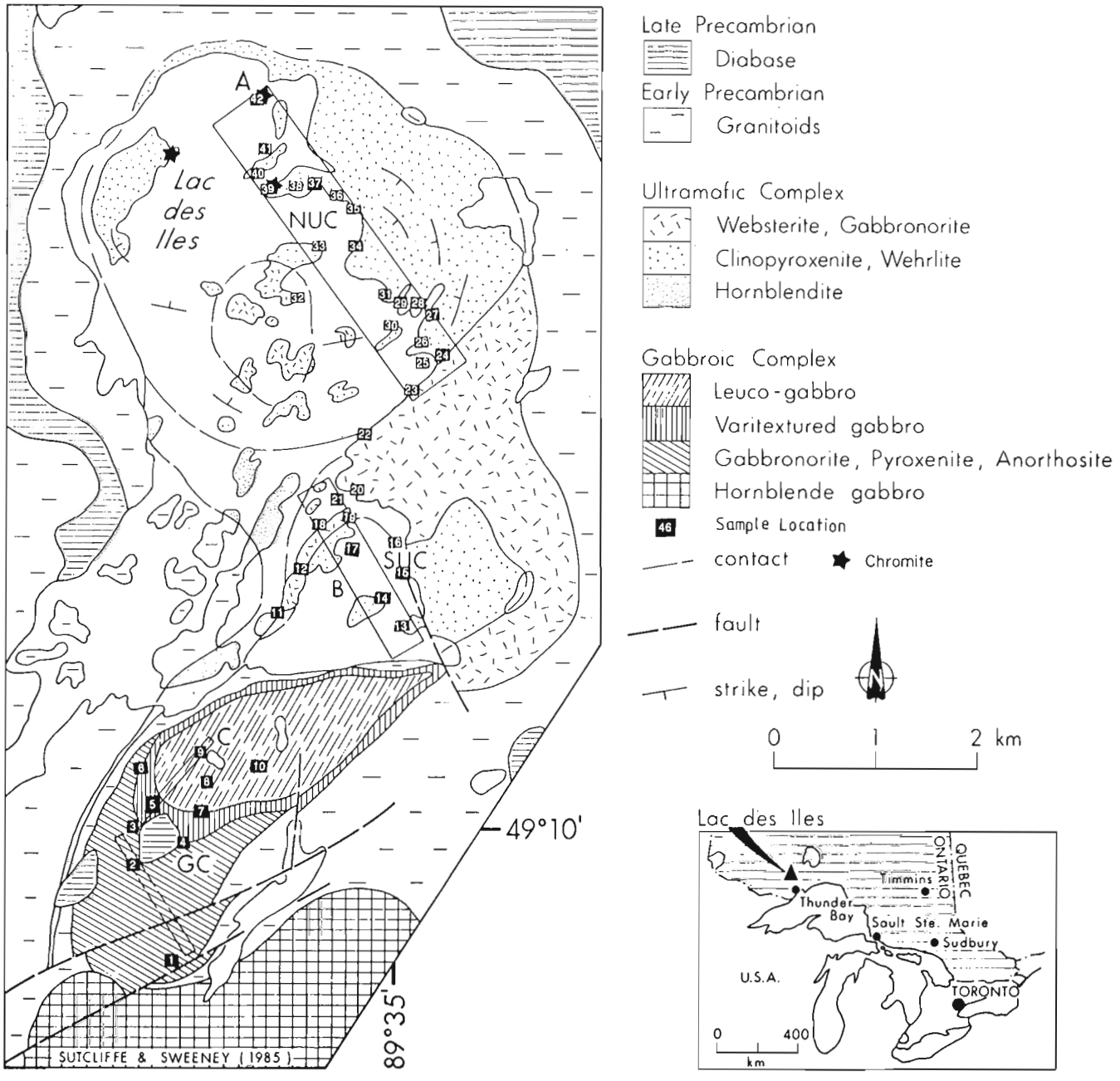

Figure 1. Location and geology of the Lac des Iles Complex, and sample locations (modified from Sutcliffe and Sweeney, 1985). GC: gabbro complex; SUC: southern ultramafic complex; NUC: northern ultramafic complex; The Roby zone is at location 5 in the GC.

GEOLOGY AND PETROGRAPHY OF THE GABBROIC PART OF THE LAC DES ILES COMPLEX

Previous studies of the gabbroic part of the LDI complex concentrated on occurrences of PGE-bearing sulphide mineralization especially the Roby Zone (Location 5, Fig. 1; Dunning, 1979; Watkinson and Dunning, 1979; Talkington and Watkinson, 1984; Macdonald, 1985, 1987; Sweeney and Sutcliffe, 1986; Sweeney and Edgar, 1987). Based on mineralogical and chemical differences, Dunning (1979) distinguished two intrusive phases: an oxide-rich and sulphide-poor eastern gabbro and a sulphide-rich and oxide-poor, norite- and gabbronorite-bearing western gabbro. However, the primary mineralogy of the gabbroic part is rarely preserved, as plagioclase is altered to albite, sericite, epidote and chlorite, and pyroxenes are replaced by fibres of actinolite or blades of hornblende. Hornblende pseudomorphs are often rimmed by actinolite or chlorite. The alteration appears to be most intense in the centre of the mineralized Roby Zone and less intense in the unmineralized portions of the gabbro to the east. Rocks to west and southwest (including the mineralized C-zone) are only moderately altered or, in some cases, even fresh.

No unequivocal intrusive contacts between the eastern and western gabbroic phases defined by Dunning (1979) have been observed. Furthermore, recent field studies of Macdonald and Lawson (1987) have revealed that the eastern phase contains orthopyroxene-bearing cumulates, and that the western phase contains magnetite-rich gabbro. Macdonald et al. (1989) observed similar major element trends in both gabbroic phases and suggested that variations are caused by fractional crystallization of a common parental magma. Sm-Nd isotope studies support this idea because samples from the eastern and western part have similar ε_{Nd} values of about 1.7, suggesting a comagmatic origin (Brügmann et al., unpublished data). Thus it appears to be less certain than previously thought that the eastern and western gabbro represent different intrusive phases.

Based on detailed mapping of the Roby Zone, Macdonald (1985, 1987), Sweeney and Sutcliffe (1986) and Sweeney and Edgar (1987) have shown that the assumed interface between eastern and western gabbro (where the Roby Zone is located) is lithologically and texturally very complex and heterogeneous on a centimetre and metre scale. It consists of melanocratic to leucocratic, medium-grained to coarse-grained gabbro and is intruded by fine to medium grained pyroxene-rich dykes, pegmatitic gabbro and tonalite dykes. This zone has been mapped as one unit called varitextured gabbro (Macdonald, 1985, 1987). The economically most important ore metals are Pd, Pt and Au and based on their abundances and the lithological association of the mineralization, Macdonald et al. (1989) distinguished three categories:

1) low grade mineralization (less than 1000 ppb PGE+Au) occurring in pegmatoidal gabbro, and leucocratic gabbro;
2) mineralization with up to 15 ppm PGE+Au associated with a pyroxenitic dyke;
3) high grade mineralization (up to 35 ppm PGE+Au) in gabbro pegmatite dykes.

Sweeney and Sutcliffe (1986) interpreted the Roby Zone as a zone of mixing between a volatile-rich eastern gabbro and a sulphide-rich western gabbro magma. As an alternative to the two gabbro hypothesis, Macdonald et al. (1989) suggested that mineralization was formed by mixing of a gabbroic, ultramafic and tonalite magma, which caused sulphide liquation. The degree of the noble metal enrichment in gabbro to pegmatite rocks reflects increasing fractionation of the contaminated gabbro melt. Watkinson and Dunning (1979) and Talkington and Watkinson (1984) also suggested a primary magmatic origin of the sulphides. However, they believed the PGM and the intense alteration indicate that late deuteric and hydrothermal fluids have mobilized and further concentrated the PGE.

SAMPLES AND ANALYTICAL TECHNIQUES

The locations of the rock samples analyzed in this study are shown in Figure 1. Sampling concentrated on the Roby Zone but also included nonmineralized portions of the intrusion, to allow the investigation of the background PGE distribution and the formation of sulphide mineralization.

Major elements, S, and Cu have been determined by X-Ray Assay Ltd. by conventional X-ray fluorescence analysis (XRF). The trace element concentrations of Cr, Ni, V, Rb, Sr, Zr and Y have been determined by XRF at the Department of Geology, University of Toronto. For these elements a 10 % error is expected for concentrations of 100, 30, 100, 15, 15, 20 and 15 ppm, respectively. REE, Co and Sc determinations have been performed by instrumental neutron activation analysis (INAA) at the Slowpoke Reactor, University of Toronto. The 2s standard deviation for the REE data is better than 30 %, for Co and Sc it is better than 5 %. The accuracy of the data has been controlled by routinely analyzing an in-house standard (UTB-1).

Concentrations of the noble metals Au, Pd, Pt, Ir, Os and Ru, as well as the chalcophile elements As and Se have been determined by radiochemical neutron activation analysis (RNAA) as described by Brügmann et al. (1987, 1989). Samples have been irradiated at the Slowpoke Reactor for 16 hours in a thermal neutron flux of $2\times10^{11}ns^{-1}cm^{-2}$, or at the Nuclear Reactor, McMaster University, for 52 hours in a thermal flux of $3\times10^{13}ns^{-1}cm^{-2}$. Under the best of conditions detection limits for Au are 0.004 ppb, for Ir 0.03 ppb, for Pt 1.5 ppb, for Pd 2 ppb, for Os 0.4 ppb, for Ru 2 ppb, As 0.2 ppb and Se 5 ppb. Precision (defined as the 2s error of the peak area) is best for Au (< 1-10 %), followed by Ir, As, Pt,and Se (5-20 %) and Pd, Os and Ru (10-50 %). As cited by Brügmann et al. (1987, 1989) the accuracy of the data as determined on rock and meteorite standards is better than 10 %.

RESULTS

The results of major and trace element analyses are summarized in Table. 1. This table reports only data for samples which have been analyzed for PGE. The results of the remaining major and lithophile trace element analyses are available upon request from the senior author. Although Ru concentrations are reported, it is emphasized that these data

Table 1. Major and trace element contents of samples from the gabbroic part of the Lac des Iles Complex.

		LDI-03	LDI-06	LDI-08	LDI-55	LDI-57	LDI-63	87-02	87-03	87-04	87-06	87-08	87-09	87-10	87-14	87-15	85-31	85-52a	86-118	86-125	86-203	86-211	86-224
Rock-Type		Ga-No	Ga-No	Ga	Ma-Dy	Ga	Ga	Ga-No	Ga-No	Peg-Dy	Ga-No	Ga-Dy	Ma-Dy	Ma-Dy	Peg-Dy	Ga	Peg-Ga	Peg-Dy	Peg-Ga	Ga-No	Ma-Dy	Ga	Peg-Dy
Loc.		3	8	9	5	10	2	5	5	5	5	7	8	8	5	5	5	5	5	5	5	5	5
SiO2	wt.%	51.06	51.02	50.52	51.27	51.58	53.66	51.73	51.68	50.71	52.12	51.54	50.07	49.97	51.41	50.30	52.32	50.33	52.34	52.50	49.19	50.05	51.15
TiO2		0.09	0.27	0.19	0.29	0.16	0.15	0.12	0.23	0.20	0.13	0.09	0.42	0.16	0.09	0.07	0.10	0.44	0.07	0.10	0.04	0.13	0.16
Al2O3		18.62	14.46	25.07	8.38	17.13	17.31	13.92	7.71	9.47	14.01	27.09	10.51	15.04	12.17	15.97	11.65	16.12	12.21	15.86	23.00	19.37	18.54
FeO		6.73	9.17	4.94	16.14	9.35	7.30	9.23	14.20	16.03	8.86	2.51	10.11	9.54	9.85	7.58	9.55	10.23	11.46	8.45	6.06	6.93	7.77
MnO		0.12	0.16	0.07	0.29	0.14	0.15	0.17	0.25	0.26	0.16	0.05	0.20	0.18	0.18	0.13	0.14	0.19	0.19	0.21	0.12	0.09	0.13
MgO		10.82	9.37	4.37	15.93	11.42	8.39	14.43	17.53	15.93	14.73	2.15	16.55	11.33	17.85	15.56	12.90	8.11	15.71	11.69	8.35	7.84	9.77
CaO		10.50	13.65	11.56	6.57	8.57	10.38	8.65	6.83	5.45	8.39	12.22	10.62	11.75	6.60	7.99	11.96	10.54	7.24	7.61	8.08	12.04	9.88
Na2O		1.63	1.76	2.93	0.51	1.47	2.45	1.31	1.00	1.28	1.34	3.66	1.17	1.66	1.16	1.09	0.68	2.13	0.00	2.35	1.52	2.15	1.72
K2O		0.41	0.11	0.32	0.17	0.16	0.19	0.12	0.09	0.08	0.22	0.67	0.27	0.34	0.17	0.49	0.34	0.36	0.25	0.94	2.62	0.58	0.69
P2O5		0.01	0.02	0.03	0.02	0.02	0.02	0.02	0.02	0.02	0.02	0.02	0.09	0.02	0.02	0.02	0.00	0.05	0.01	0.00	0.01	0.04	0.02
S		0.02	0.01	0.00	0.44	0.00	0.00	0.29	0.45	0.56	0.02	0.00	0.00	0.00	0.51	0.81	0.35	1.50	0.51	0.28	1.01	0.77	0.18
LOI		2.4	0.5	1.8	3.1	0.8	1.0	0.7	0.7	0.5	1.5	1.3	2.3	1.4	1.2	1.9	2.3	3.1	4.6	3.2	0.4	2.4	2.8
Mg#		0.74	0.65	0.61	0.64	0.69	0.67	0.74	0.69	0.64	0.75	0.60	0.74	0.68	0.76	0.79	0.71	0.59	0.71	0.71	0.71	0.67	0.69
Cr	ppm	205	38	121	292			398	398	336	421	63	2530	477	429	550		148	350	229	247		200
Ni		499	81	131	2082			2800	980	900	525	94	473	202	1700	3100	1602	2459	842	540	3070	1462	416
Cu								1450	1000	1250	237	69	87	178	1990	3330	1484	3635	2216	516	3939	1933	431
Co		46	67	33	112			86					59		109		72	140	67	65	74	50	50
V		89	305	106													167	212	100	103	48	89	122
Rb		13	0	8	4	4	3								18								0
Sr		192	170	357	42	207	294										172	217	69	182	177	200	198
Zr		5	9	14	14	6	11																0
Y		2	4	2	5	3	4										5	6	4	4	0	5	4
Sc		24	74	16	48			33					37		36		53	27	30	28	9	24	30
La		0.7	0.81	2.1	1.32			1					3.7		0.8		2.1	4.4	0.89	1.1	1.4		1.6
Ce		1.4	1.9	4	2.8			2					8.1		0		4.4	8.7	1.9	2	2.3		3.4
Sm		0.14	0.47	0.31	0.54			0.2					1.7		0.2		0.97	0.91	0.21	0.27	0.2		0.43
Eu		0.21	0.24	0.24	0.24			0.2					0		0		0.29	0.32	0.15	0.19	0.14		0.22
Yb		0.22	0.58	0.19	0.68			0.3					0.9		0		0.44	0.55	0.34	0.3	0.18		0.32
Lu		0.05	0.08	0.03	0.13			0.05					0.1		0		0.07	0.09	0.05	0.05	0.04		0.06
Ir	ppb	0.11	0.04	0.08	0.41	0.43	0.33	0.71	0.78	0.48	0.34	0.19	0.34	1.06	0.6	1.79	1.82	0.93	0.27	0.15	0.62	0.67	0.1
Os		1.1	0	0.4	0	1.6	1.5	0.9	0.5	1.2	2.1	0.7	1.1	1.8	2	3.4	1.3	0	0	0	0	1.1	0
Ru		3	7	12	16	15	9	23	8	80	5	12	15	29	102	0	13	39	9	7	6	11	9
Pt		109	29	35	372	38	42	510	316	263	105	14	21	64	413	903	272	574	23	37	902	1110	45
Pd		1010	0	20	7200	0	85	6200	0	1800	0	0	55	170	5800	9600	1130	8500	26	21	12000	2400	360
Au		21	1.98	1.56	613	6.96	0.98	724	454	297	75.3	4.93	8.45	10.6	479	852	168	266	47	16.3	973	415	27.3
As		75	49	189	0	108	110	17499	1278	1339	3059	0.1	1411	182	2663	70	258	0	1042	338	0	1273	
Se	ppm	1.35	0.49	0.12	5.97	0.25	0.35	9.8	5.28	6.5	1.55	0.36	0.35	0.49	13.2	27.9	4.9	13.3	3.9	1.4	13.2	6.48	0.87

major element data are normalized to 100% anhydreous; 0 values: below detection limit; blank values: not determined; loc: refers to sample locations in Fig. 1

Ga: Gabbro; Ga-No: Gabbronorite; Peg-Ga: Pegmatoidal Gabbro; Ma-Dy: Mafic Dyke; Peg-Dy: Pegmatite Dyke; Ga-Dy: Gabbro-Dyke.

are of poor quality. This is because Ru concentrations have not been corrected for ^{103}Ru, which has been produced by fission of U during irradiation. U concentrations in the samples are very low (< 100 ppb) and not detectable with INAA. Nevertheless, 100 ppb U may produce about 14 ppb Ru. Therefore, the reported Ru concentrations are expected to be too high (Table.2, 3).

In contrast to the ultramafic part to the north the gabbroic part is significantly altered and the primary mineralogy is rarely preserved: however thin section examination suggests that the GP consists mainly of gabbroic and gabbronoritic cumulates. Many of the gabbronorites represent intrusive phases, which cut gabbroic cumulates. The normative mineralogy (Fig. 2) implies that the rocks consist of clinopyroxene, plagioclase *and* orthopyroxene. This probably indicates the presence of interstitial orthopyroxene and magmatic hornblende, which are not observable in thin section due to the alteration. The distribution of elements such as Al_2O_3 and Sc (Fig. 3), which are commonly regarded as immobile during alteration, supports this conclusion, assuming that the cumulates consist of plagioclase , clinopyroxene and relatively large amounts of interstitial liquid containing approximately 10 wt.% Al_2O_3 and 30 ppm Sc. However, the low abundances of incompatible elements, such as the REE or Zr (Table 1) imply that the cumulates contained less than 10% pore liquid. Therefore, the most likely explanation of the Sc-Al_2O_3 distribution is that the gabbroic cumulates contained significant amounts of orthopyroxene and possibly hornblende.

There is no obvious difference in the normative mineralogy between samples from the eastern or the western parts of the intrusion. Comparison of major and trace elements (e.g. Mg#, REE) do not reveal evidence for two chemically different gabbroic intrusions (Macdonald et al., 1989)
Noble metal contents in samples from the gabbroic complex are highly variable, ranging from 50 ppb total PGE in non-mineralized rocks to 15 ppm in mineralized samples from the Roby Zone (Table 1, Fig. 4). Pyroxenitic dykes and pegmatitic dykes tend to have higher PGE concentrations than gabbro (Fig. 4). Analysis of variation coefficients indicate that the concentration range of Pd and Au is significantly greater than that of Ir and Os. For example, whereas Pd concentrations vary by about 3 orders of magnitude, Ir concentrations vary by just 1 (Fig. 4). Nevertheless, there is reasonably good correlation between PGE and S or Se contents (Fig. 4a, Table 2), which suggests that sulphide phases are controlling the distribution of the PGE. Correlation between Ni, Cu, Pd, Au and Pt are good (Table 2), however, correlation between Ir and these three PGE is less significant (Fig. 4d, Table 2).

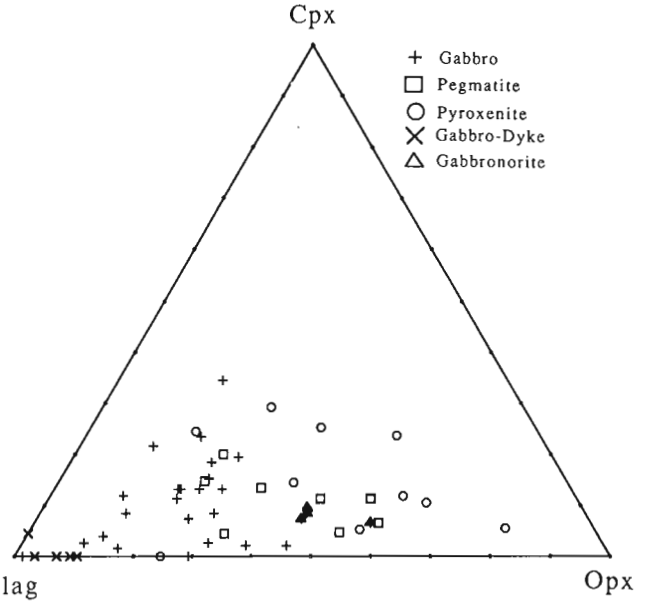

Figure 2. Variations in the normative mineralogy of samples from the gabbroic part of the Lac des Iles Complex.

Table 2. Correlation coefficients for Cr, PGE and chalcophile elements in the gabbroic part of the Lac des Iles Complex.

	Cr	Ni	Cu	Co	Ir	Os	Ru	Pt	Pd	Au	As	Se	S
Cr	1.000	-.051	-.266	-.115	.096	.057	.015	-.097	-.203	-.072	.024	-.054	.058
Ni		1.000	**.868**	**.663**	**.593**	.503	.205	**.816**	**.931**	**.908**	*.531*	**.864**	**.687**
Cu			1.000	.582	.432	.548	.173	**.761**	**.865**	**.731**	.058	**.814**	**.884**
Co				1.000	.399	*.791*	*.584*	.303	**.686**	.455	.434	**.740**	*.608*
Ir					1.000	*.535*	.194	*.530*	.399	*.478*	.048	**.653**	.444
Os						1.000	.352	.344	*.683*	.375	-.143	**.669**	.297
Ru							1.000	.156	.209	.230	.118	*.522*	.270
Pt								1.000	**.760**	**.835**	.244	**.780**	**.690**
Pd									1.000	**.910**	.419	**.833**	*.661*
Au										1.000	*.516*	**.820**	*.507*
As											1.000	.207	-.101
Se												1.000	**.653**
S													1.000

Numbers in bold and italics refer to correlations which are significant at the 99% and 95% level, respectivily

DISCUSSION

As indicated above, PGE concentrations in the grabboic part vary by up to 3 orders of magnitude. Background samples from outside the Roby Zone have PGE abundances and mantle-normalized chalcophile element patterns similar to unmineralized samples from the ultramafic part of the Lac des Iles complex (Brügmann and Naldrett, 1990). The patterns of gabbroic cumulates (ldi-08, ldi-63, 86-125) overlap with those of unmineralized mafic dykes (samples 87-09, 87-10, Fig. 5). Sample 87-09 may represent a liquid composition and could provide some constraints for the PGE abundances of the parental liquids forming the ultramafic and gabbroic parts, as Pt/Ir, Pd/Ir, or Pd/Pt ratios (62, 160, 2.6, respectively) are not uncommon for sulphur undersaturated mafic magmas.

The differences between the geological setting and distribution of PGE in the gabbroic and the ultramafic parts of the LDI complex and other important PGE-rich maficultramafic complexes (e.g. Bushveld and Stillwater) suggest that the genesis of the sulphide mineralization and the concentration of PGE was different in each case, although there is always a close connection between sulphides and PGE. This is supported by the identical Pd/Se, Au/Se and Pd/Au variations for both ultramafic and mafic intrusive phases of the LDI complex (Fig. 4a, b). However, at comparable Au and Pd abundances, Ir and Pt contents of the GP are lower than those of the UMP (Fig. 4c, d). This suggests that besides their concentration in the sulphide liquid there is an additional process which controls the abundances of Ir and Pt. A comparison with Stillwater and Bushveld sulphide liquid compositions also demonstrates a relative depletion in Ir and Pt in the sulphides from the Roby Zone. This can also be seen if the data are normalized to a primitive mantle composition: mineralized samples from the Roby Zone are highly enriched in Pd, Pt and Au relative to Ir, Os and Ni (Fig. 5). In fact their Ir and Os abundances are overlapping with those of the unmineralized samples and display a significantly smaller variation than elements like Au and Pd. This causes extremely variable and high Pd/Ir ratios in the order of 10 000 (Fig. 6). Pd/Pt ratios are also unusually high (10. Fig. 4c). Diagrams where Pt- or Pd- or Au/Ir ratios are plotted against Pt or Pd or Au (Fig. 6) show a positive correlation. Given that the PGE have similar silicate/sulphide partition coefficients we would expect a slope of 0. The positive slope in these diagrams implies that besides the concentration of PGE in a sulphide liquid there is another process controlling the PGE abundances which cause an enrichment of Pd, Pt and Au relative to Ir, as overall enrichment of PGE proceeds.

Macdonald et al. (1989) suggested that intensive fractional crystallization, which depleted Ir and Os, but enriched Pd, Pt and Au in the residual liquid led to the high Pd/Ir ratios. Concentration of the PGE by a supercritical fluid offers another possible explanation. It has been suggested on thermodynamic grounds that Pt and Au can be mobilized hydrothermally (Lydon, 1987). Furthermore, the discordant PGE-rich pipes in the Bushveld Complex are evidence that Pt can be transported hydrothermally, and Stumpfl and Ballhaus (1986) and Boudreau et al. (1986) have proposed that hydrothermal fluids have played a major role in concentrating PGE in the sulphides of the Merensky and J-M Reefs. The presence of pegmatitic textures and the extensive deuteric alteration is evidence of a volatile-rich environment in the Roby Zone, which led, as previously outlined, to the suggestion that PGE were remobilized and concentrated by fluids (Watkinson and Dunning, 1979; Talkington and Watkinson, 1984; Sweeney and Edgar, 1987). However, in the southern part of the Roby Zone (C-zone), the primary mineralogy is well preserved and this zone exhibits all the characteristic features of the mineralization, including pegmatites with high grade mineralization. This would argue against a direct genetic relationship between PGE concentration and alteration processes. Although the activity of the volatiles certainly has redistributed the PGE in the central part of the Roby Zone, the strong association of PGE with sulphides in gabbro, the association of sulphides with pegmatite dykes and the identical variations of Au and Pd in the gabbroic and ultramafic parts suggests that the PGE concentration is not purely

Table 3. Ni-Cu and platinum-group element composition of sulfide liquids from mafic-ultramafic complexes. Data for Bushveld Stillwater, and Noril'sk intrusions are from Naldrett (1981).

	Lac des Iles	Merenskey-Reef	Stillwater	Noril'sk
Ni wt. %	4-10	10.9	13.2	7.6
Cu wt. %	6-14	4.6	6.5	10.9
Au ppm	20-60	21	75	2
Pd ppm	100-300	102	4876	42
Pt ppm	10-30	258	939	15
Ir ppm	0.01-0.03	4.3	3.5	?

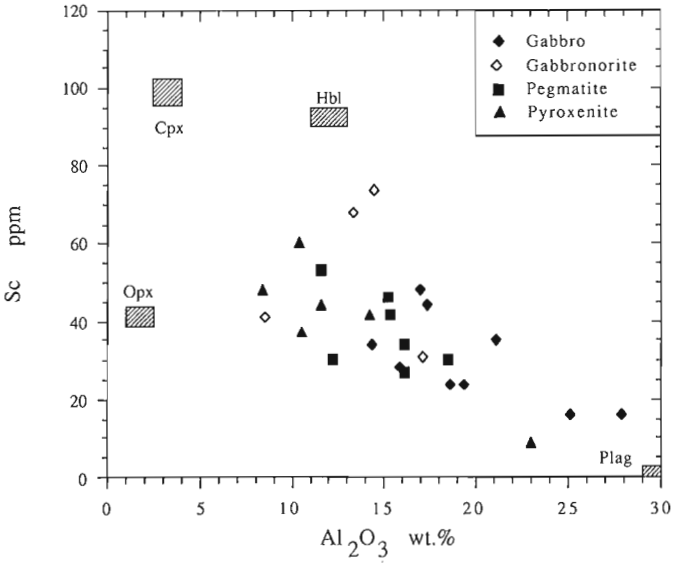

Figure 3. Sc-Al_2O_3 variation in the gabbroic complex, Lac des Iles. Note that Sc-Al_2O_3 contents of the cumulates can be explained if significant amounts of orthopyroxene (interstitial), together with plagioclase and clinopyroxene, are present. Sc data for orthopyroxene clinopyroxene and plagioclase are from this study; Sc and Al_2O_3 data for magmatic hornblende are from Luhr and Carmicheal (1980)

hydrothermal, but is bound up in the magmatic history of the gabbro complex.

FORMATION OF PGE-RICH SULPHIDES BY CONSTITUTIONAL ZONE REFINING (CZR)

Many aspects of the ore zone in the Roby Zone suggest localized remelting of the original complex. These include

i) the ubiquitous presence of breccia zones, in which melagabbro, gabbro, anorthositic gabbro and anorthositic segregations occur in a matrix which varies from mela to anorthositic gabbro.
ii) pyroxenitic dykes which, outside the ore zone and in cooler areas within it are cross cutting, but in other areas are cut by late stage pegmatites, and, on the scale of an outcrop, can be seen ranging from discrete dykes to irregular blob-like masses to fragments in a gabbroic matrix. Our interpretation of these observations is that in places the gabbro could fracture when the pyroxenite intruded, in places the gabbro was fluid so that one had one liquid intruding the other, and in places remelting of gabbro cut by pyroxenite occurred to give rise to the fragments in the gabbro matrix.
iii) a large number of pegmatites cut other rock types. Locally pegmatoids can be traced along strike undergoing a transition to pegmatites.
iv) cuspate contacts and interfingering phases of leucocratic to melanocratic gabbro, which suggest the presence of coeval liquid phases.

McBirney (1987) suggested that if water comes into contact with overlying hot cumulates, the cumulates will partially melt. This zone of volatile-induced melting can progress upwards through the cumulate leaving behind a

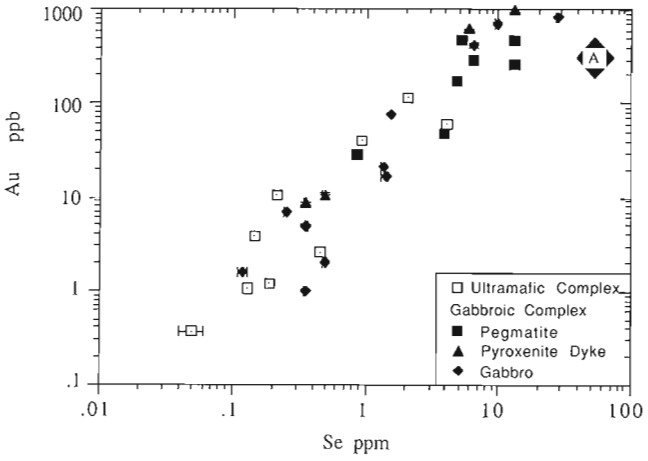

a. Au-Se; the reasonable good correlation with Se suggests that sulfides are controlling the distribution of the PGE

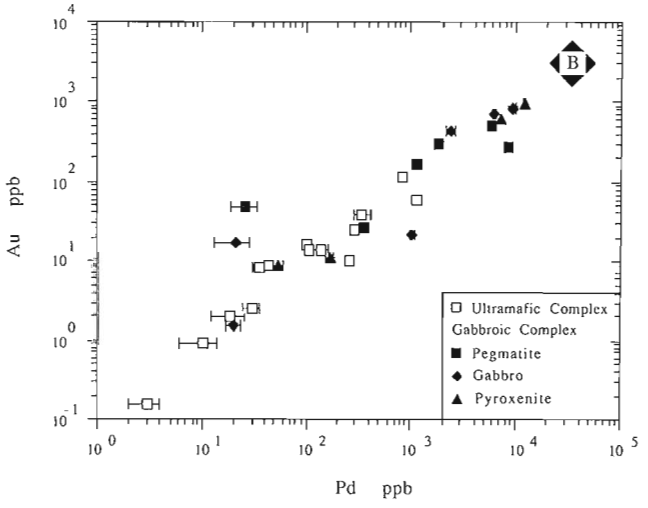

b. Au-Pd; note the identical variation for gabbro and ultramafic samples

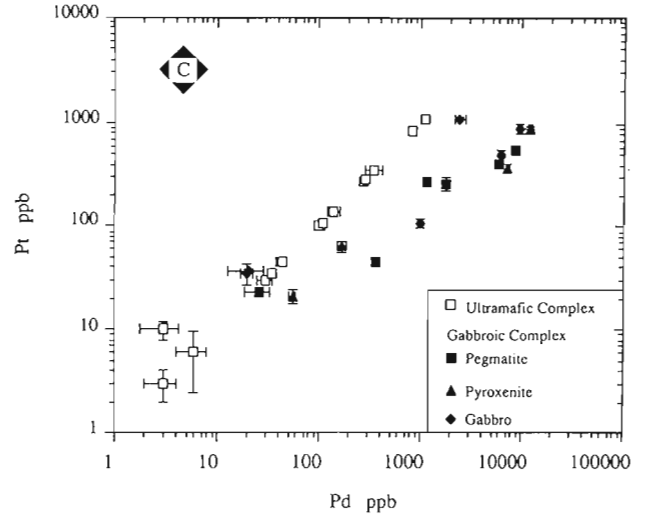

c. Pd-Pt; note that samples from the gabbroic part form a trend suggesting lower Pt concentrations compared to the trend for ultramafic samples

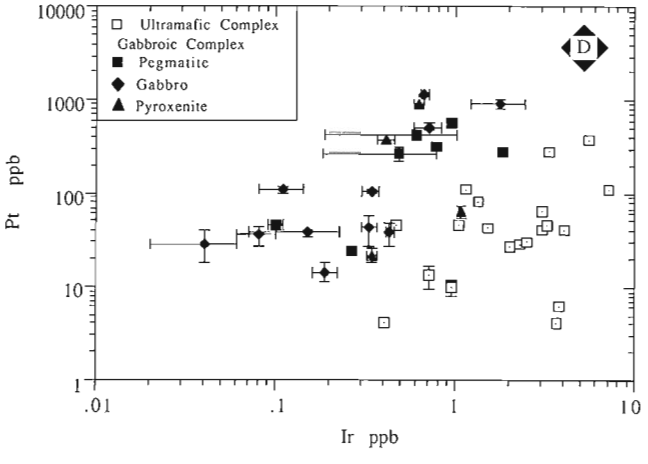

d. Pt-Ir; note that for gabbro plot on trend suggesting lower Ir concentrations compared to the trend for ultramafic samples

Figure 4. Variation diagrams of PGE and Se concentrations in the gabbroic part of the Lac des Iles Complex and comparison with PGE abundances in the ultramafic part. Error bars represent 2 σ standard deviation.

residue of more refractory unmelted material, plus material crystallizing from the secondary melt, as the more volatile-rich phase proceeds upward. As McBirney pointed out, this process is analogous to industrial zone refining. The effect will be the same: the cumulates are purged of incompatible elements which become highly concentrated in the advancing partial melt. So long as the partial melt is undersaturated in sulphur, sulphides in the cumulates will be dissolved in the melt, as will Au, Pd and Pt. Iridium, Os and Ru are thought to behave compatibly and thus their concentrations will not build up nearly so rapidly, if at all, in the melt. Thus in addition to concentrating Pt, Pd and Au in the melt phase, zone refining will also fractionate them from Ir, Os and Ru. Platinum is also thought to be somewhat less incompatible than Pd, so that one would expect that Pd became more concentrated than Pt in the partial melt, causing high Pd/Pt ratios. Once the partial melt becomes saturated with respect to sulphur, sulphides will be left behind in the residue. These sulphides will retain most of the PGE and thereby becoming PGE-rich. We suggest that the Roby Zone at LDI, with evidence of high volatile contents and subsequent remelting, represents the dumping ground of PGE scavenged from the gabbro cumulates by zone refining.

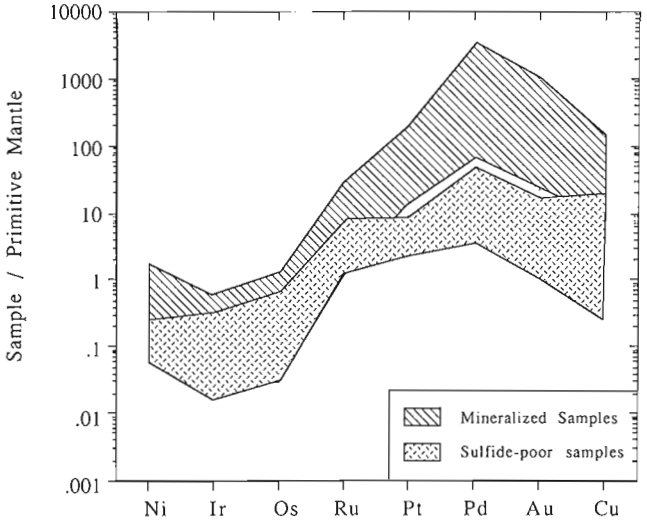

Figure 5. Mantle normalized Ni, Cu, and PGE patterns of mineralized and sulfide-poor samples from the gabbroic complex, Lac des Iles. Primitive mantle (PM) values from Brügmann et al. (1987)

Zone refining in nature is unlikely to be the uniform, controlled process that it is in industry. On a local scale different areas are likely to be remelted to different degrees and the extraction of the partial melt is not likely to be uniform. We suggest that the varitextured gabbro, which forms the matrix of the ore zone, represents the residue of variable melting due to the zone refining process. Pegmatoids, pegmatites, plagioclase-rich gabbro segregations and dykes represent the product of zone refining. Zone refining may pass through an area and cause a diminution in PGE. It is only where sulphides remain behind that the PGE will be concentrated. It should be pointed out that any rocks within the zone of melting, which contain pre-existing sulphide, such as for example the pyroxenitic dykes, will not lose their sulphides once the zone refining melt has become sulphide saturated; these sulphides may, however, act as a sink for Pt, Pd, and Au and thus become very enriched themselves.

It is also important to stress that Pt, Pd, and Au will only behave incompatibly while sulphides are dissolving and do not remain behind in the residue. Once sulphides remain behind all of the PGE become highly compatible. Thus one should not necessarily expect a correlation between PGE and other incompatible elements in the gabbro body that has been subjected to zone refining.

CONCLUSIONS

The gabbroic part of the Lac des Iles Complex consists mainly of cumulates of gabbroic and gabbronoritic composition. The primary mineralogy has been replaced by secondary minerals due to an intensive deuteric alteration. Major

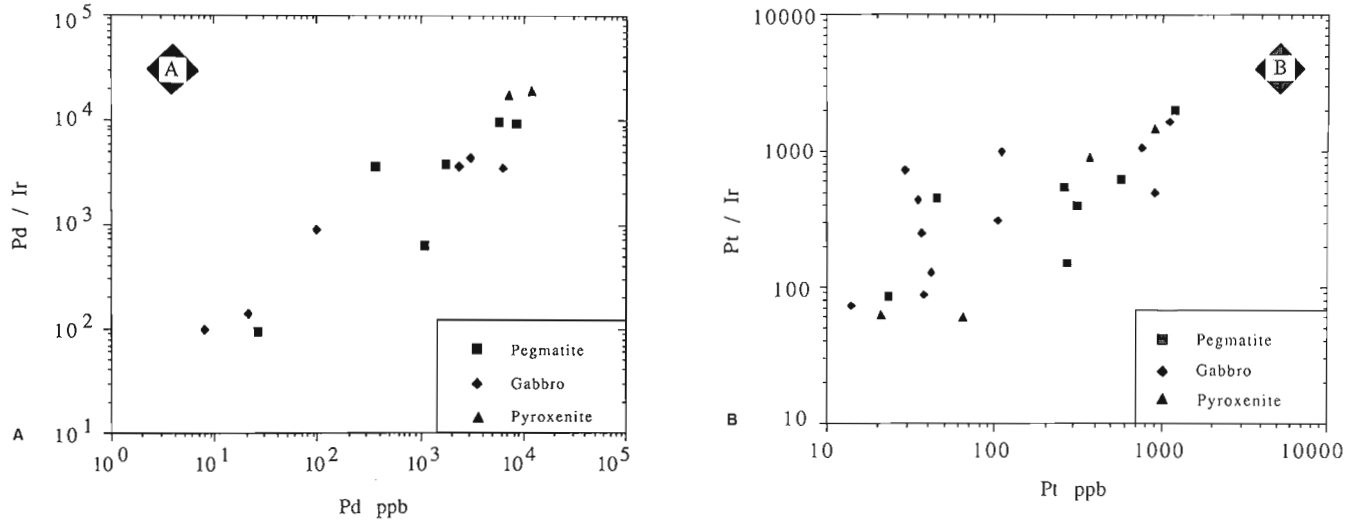

Figure 6. Diagrams of (a) Pd/Ir versus Pd and (b) Pt/Ir versus Pt. The distinct positive slope in these diagrams suggests that Pt, and Pd behave incompatibly relative to Ir.

and trace elements variations can be explained by continuous fractional crystallization of one batch of magma and do not support the existence of two separate gabbro phases (Macdonald et al., 1989).

The PGE mineralization in the Roby Zone occurs in the centre of the gabbric pluton and is associated with varitextured gabbro. Distinctive features of the Roby zone are the occurrence of pegmatitic rocks and textures suggesting partial melting of the original gabbro cumulates. The occurrence of pegmatites and the intensive deuteric alteration of the primary mineralogy suggest the existence of an aqueous fluid phase, probably exsolved from the volatile saturated residual liquid in the magma chamber.

The high grade PGE mineralization is associated with pegmatitic phases as well as with irregularly shaped bolder and dyke-like pyroxenite bodies. Mineralized samples have a very distinct mantle normalized PGE pattern characterized by a strong enrichment in Pt, Pd and Au relative to Ir, Os and Ru, giving rise to very high Pd/Ir ratios in the order of 10 000. PGE variations such as the Pd/Ir versus Pd, or Pt/Ir versus Pt suggest that PGE abundances in the Roby zone are controlled by their concentration in a sulphide liquid and by a second process which buffered the concentrations of the less incompatible PGE (Ir, Os, Ru) and/or enriched the more incompatible PGE (Pd, Pt). Zone refining as defined by McBirney (1987) might explain these PGE characteristics. It assumes that a volatile-rich mafic liquid is able to remelt surrounding gabbro cumulates. Sources for the PGE are either intercumulus liquid or more likely finely dispersed sulfide minerals in the gabbroic cumulates. Where there was sufficient partial melt to dissolve all of the sulfides, Au, Pd, and Pt behaved incompatibly and dissolved in the melt phase, whereas Ir, Os and Ru were retained in residual minerals. The melt proceeded through the gabbro cumulates dissolving sulphides and leaving a residue enriched in Ir, Os and Ru, but concentrating Au, Pd and Pt, until it became saturated in sulphide. At this point sulphides were retained in the residue and concentrated the PGE out of the silicate liquid, giving rise to the deposit with its very high Pd/Ir ratio. Ratios such as Pd/Ir and Pd/Pt would strongly depend on the degree of partial remelting and fractional crystallization until the time of sulphide liquation.

We interpret the matrix of the varitextured gabbro as residuum of the partial melt formed by zone refining. Pegmatoids, pegmatites, segregations of leucocratic gabbro and incompatible element-rich plagioclase and quartz -bearing gabbro dykes may represent crystallization products of the partial melt.

Acknowledgments

We are grateful to P. Sheridan of Madelaine Mines Ltd. for access to the property and permission to collect samples, and to R. Sutcliffe and A.J. Macdonald for introducing us to the Lac des Iles Complex. We greatly appreciate the assistance of the staff of the reactors at the SLOWPOKE, University of Toronto, and the McMaster University, Hamilton, during neutron activation analysis. This research has been supported by the GSC through DSS contract No. 34SZ.23233-7-1083 with to A.J. Naldrett. Additional support came from OGRF grant 276 (1986/87) and NSERC operating grant A4244 also to A.J. Naldrett.

REFERENCES

Boudreau, A.E., Mathez, E.A., and McCallum, I.S.
1986: Halogen geochemistry of the Stillwater and Bushveld complexes: Evidence for transport of the platinum group elements by Cl-rich fluids; Journal of Petrology, v. 27, p. 967-986.

Brügmann, G.E. and Naldrett, A.J.
1990: Origin of Cu-Ni-PGE mineralization in the ultramafic part of the Lac des Iles Complex, Ontario; *in* Current Research, Part C, Geological Survey of Canada, Paper 90-1C.

Brügmann, G.E., Arndt, N.T., Hofmann, A.W., and Tobschall, H.J.
1987: Noble metal abundances in komatiite suites from Alexo, Ontario, and Gorgona Island, Colombia; Geochimica et Cosmochimica Acta, v. 51, p. 2159-2169.

Brügmann, G.E., Gorton, M.P., and Hancock, R.G.V.
1989: Simultaneous determination of noble metals, Re, Se, As and Sb by radiochemical neutron activation analysis; Journal of Geochemical Exploration., in press.

Dunning, G.R.
1979: The geology and platinum group element mineralization of the Roby Zone, Lac des Iles complex, northwestern Ontario: M.Sc. Thesis, University of Ottawa, Ontario, 129 p.

Luhr, J.F., and Carmichael, I.S.E.
1980: The Colina volcanic complex, Mexico. I. Post-caldera andesites from volcan Colima; Contributions to Mineralogy, Petrology, v. 71, p. 343-372.

Lydon, J.W.
1987: Potential for hydrothermal platinum deposits; Canadian Mining Journal, March, p. 24-25.

Macdonald, A.J.
1985: The Lac des Iles platinum-group element deposit, Thunder Bay District, Ontario; *in* J.Wood et al. (ed.), Summary of Field Work and Other Activities 1985, Ontario Geological Survey, Misc. Paper, 126, p. 80-81.
1987: The Lac des Iles platinum group metal deposit, Thunder Bay District; *in* O.L. White, R.B. Barlow, and A.C. Colvine (ed.) Summary of Field Work and Other Activities 1985, Ontario Geological Survey, Misc. Paper 126, p. 235-241.

Macdonald, A.J. and Lawson, G.E.
1987: Lac des Iles (Pt-Pd-Au) deposit: Geology of the mineralized zone, contact phenomena and mafic/ultramafic dikes within the gabbroic complex; *in* R.B. Barlow, et al. (ed.) Summary of field work and other activities 1987, Ontario Geological Survey, Misc. Paper 37, p. 281-285.

Macdonald, A.J., Brügmann, G.E., and Naldrett, A.J.
1989: Coeval felsic, mafic and ultramafic magmas: Magma mixing during formation of PGE-rich Ni-Cu sulfides at Lac des Iles, Ontario, Canada; *in* M.D. Prendergast and M.J. Jones (ed) Magmatic sulfides - the Zimbabwe volume, Institute of Mining and Metalurgy, London, p. 139-150.

McBirney
1987: Constitutional zone refining of layered intrusions; *in* I.Parsons (ed.), Origin of Igneous Layering, Nato ASI Series C, v. 196, p. 437-452.

Pye, E.G.
1968: Geology of the Lac des Iles area, District of Thunder Bay; Ontario Department of Mines, Geological Report 64, 47 p.

Stumpfl, E.F. and Ballhaus, C.G.
1986: Stratiform platinum deposits: New data and concepts: Fortschritte des Mineralogie, v. 64, p. 205-214.

Sutcliffe, R.H.
1986: Regional geology of the Lac des Iles area, District of Thunder Bay; *in* P.C. Thurston, et al. (ed.) Summary of Field Work and Other Activities 1986; Ontario Geological Survey, Miscellaneous Paper, 132, p. 70-75.

Sutcliffe, R.H. and Sweeney, J.M.

1985: Geology of the Lac des Iles Complex, District of Thunder Bay; *in* J.Wood et al. (ed.) Summary of Field Work and Other Activities 1985, Ontario Geological Survey, Miscellaneous. Paper, 126, p. 47-53.

1986: Geology of the Lac des Iles Complex, District of Thunder Bay; Ontario Geological Survey Map P.3047.

Sweeney, J.M. and Edgar, A.D.

1987: The geochemistry, origin and economic potential of platinum group element bearing rocks of the Lac des Iles complex, northwestern Ontario; *in* V.G. Milne (ed.) Geoscience Research Grant Program, Summary of Research 1986 1987, Ontario Geological Survey, Miscellaneous Paper, 136, p. 140-152.

Sweeney, J.M. and Sutcliffe, R.H.

1986: Geology and platinum-group element mineralization of the Roby Zone, Lac des Iles; *in* P.C. Thurston et al. (ed.) Summary of Field Work and Other Activities 1986, Ontario Geological Survey, Miscellaneous Paper, 132, p. 82-84.

Talkington, R.W. and Watkinson, D.H.

1984: Trends in the distribution of the precious metals in the Lac des Iles Complex, northwestern Ontario; Canadian Mineralogist, v. 22, p. 125-136.

Watkinson, D.H. and Dunning, G.

1979: Geology and the platinum group mineralization, Lac des Iles complex, northwestern Ontario; Canadian Mineralogist, v. 17, p. 453-462.

Origin of copper-nickel-platinum group element mineralization in the ultramafic part of the Lac des Iles Complex, Ontario[1].

G.E. Brügmann[2] and A.J. Naldrett[2]
Mineral Resources Division

Brügmann, G.E. and Naldrett, A.J., Origin of copper-nickel-platinum group element mineralization in the ultramafic part of the Lac des Iles Complex, Ontario; in Current Research, Part C, Geological Survey of Canada, Paper 90-1C, p. 293-303, 1990.

Abstract

The northern intrusive phase of the ultramafic part of the Lac des Iles Complex consists of at least 8 cyclic units which, where complete, comprise the sequence dunite, wehrlite to olivine clinopyroxenite, clinopyroxenite, websterite and, locally, gabbro-norite. PGE-bearing sulphide mineralization occurs at the top of cyclic units in websterite and orthopyroxenite cumulates and is enriched in Au, Pd, Pt and Cu relative to Ni, Ir, Os and Ru with Pd/Ir ratios in the order of 250. Sulphide saturation was caused by mixing of fractionated residual melt with more primitive liquid which entered the magma chamber. Sulphur-poor pyroxenites at the centre of cyclic units can contain elevated PGE concentrations with low Pd/Ir ratios (9 to 40). This enrichment resulted from segregation of very small amounts of sulphide liquid from a silicate magma that became saturated during continuous crystallization.

Résumé

La phase intrusive nord de la partie ultramafique du complexe du lac des Îles est constituée d'au moins huit unités cycliques qui, lorsqu'elle sont complètes, comprennent la séquence dunite, wehrlite à clinopyroxénite à olivine, clinopyroxénite, webstérite et, par endroits, gabbronorite. La minéralisation sulfurée riche en ÉGP se trouve au sommet des unités cycliques dans des cumulats de webstérite et d'orthopyroxénite et est enrichie en Au, Pd, Pt et Cu par rapport au Ni, Ir, Os et Ru, avec des rapports de Pd/Ir de l'ordre de 250. La saturation en sulfures a été causée par le mélange du magma fondu résiduel, fractionné, et d'un liquide plus primitif qui a pénétré dans la chambre magmatique. Des pyroxénites pauvres en soufre, se trouvant dans la partie centrale des unités cycliques, peuvent présenter de fortes concentrations d'ÉGP avec des faibles rapports de Pd/Ir (de 9 à 40). Cet enrichissement est le résultat d'une séparation de très petites quantités d'un liquide sulfuré provenant d'un magma silicaté qui a été saturé au cours d'une cristallisation continue.

[1] Contribution to the Canada-Ontario Mineral Development Agreement 1985-1990. Project carried by the Geological Survey of Canada.

[2] Department of Geology, University of Toronto, Toronto, Ontario M5S 3B1

INTRODUCTION

The Lac des Iles Complex (LDIC) is located about 80 km NNW of Thunder Bay in northwestern Ontario (Fig. 1). It lies within an Archean granite/granite gneiss terrane of the Wabigoon Subprovince. The LDIC is the largest of several mafic intrusions in the area which lie subparallel to the Wabigoon-Quetico subprovince boundary (Sutcliffe, 1986). It has been mapped by Pye (1968), and Sutcliffe and Sweeney (1985, 1986) who distinguished an ultramafic part (UMP) around Lac des Iles and a gabbroic part (GP) to the south of it (Fig. 1). The ultramafic part has been further subdivided into southern (SUP) and northern (NUP) intrusive phases (Sutcliffe and Sweeney, 1985). The NUP has been mapped in detail by Linhard and Bues (1987). The SUP has been dated by Brügmann and Naldrett (1987) using the Sm-Nd isotope dating technique. A combined mineral and whole-rock isochron gives an age of 2738 ± 27 Ma. Although age relationships are not well constrained by field evidence, it is believed that the gabbroic and ultramafic intrusive phases are coeval.

Geology and Petrography of the Ultramafic part of the Lac des Iles Complex

The intense deformation seen in the Quetico Subprovince to the east has not been observed in rocks of the LDIC and the primary mineralogy - with the exception of olivine-bearing cumulates- is generally well preserved. The SUP consists of a wehrlite to clinopyroxenite core, surrounded by websterite to gabbro-norite cumulates (Fig. 1; Sutcliffe and Sweeney, 1985). The NUP is built up of several cycles of peridotite (olivine, clinopyroxene, ± orthopyroxene cumulates), clinopyroxenite, websterite and minor amounts of orthopyroxenite and gabbronorite cumulates (Fig. 1; Sutcliffe, 1986; Linhard and Bues, 1987; Brügmann and Naldrett, 1987). Due to the poor outcrop in some areas it is, however, possible that the NUP is composed of more than 8 cyclic units as suggested in Figure 2. The cyclic units are defined by the re-appearance of high-temperature minerals, such as olivine or clinopyroxene, and by chemical variations (Fig. 2). Several thin (< 1 cm) chromite seams have been found at the base of cyclic units (Fig. 1, 2).

Peridotites occur as 0.5 to 5 m thick layers, lenses and dyke-like bodies. Peridotite layers commonly form the base of cyclic units. They are strongly altered to serpentine, tremolite, hornblende and minor talc and calcite. Primary textures are rarely preserved. Original olivine formed 0.2-2 mm large euhedral to subhedral grains. They are often enclosed in massive serpentine or patches of tremolite-actinolite or hornblende. Although these amphiboles probably replaced pyroxenes, it is not known whether orthopyroxene or clinopyroxene were the primary phases. The peridotitic cumulates also contain up to 1% idiomorphic chromite crystals 0.05 to 0.3 mm in size, which sometimes have a thin margin of magnetite.

Olivine-clinopyroxenite and clinopyroxenite are the most prominent rock types and form up to 80 m thick horizons which are either in gradational contact with basal peridotitic cumulates or occur at the base of the cyclic units. Olivine is generally replaced by serpentine. In serpentine-rich zones, clinopyroxene is strongly altered to tremolite-actinolite-calcite assemblages, whereas in serpentine-free cumulates, pyroxene grains are fresh to moderately altered. The mineral grains are 0.2 -2 mm in size, are subhedral, and indicate an adcumulate texture. Clinopyroxene cumulates at the interface of cyclic units often indicate a mesocumulate texture as they contain interstitial orthopyroxene (hypersthene). They may also contain a few large subhedral grains of bronzite (≤3 mm), which have small subhedral inclusions of clinopyroxene, and sometimes olivine. Clinopyroxene crystals occasionally have olivine or orthopyroxene cores. In all cases clinopyroxene contains abundant exsolution lamellae of orthopyroxene.

Websterite cumulates commonly form the top of a cyclic unit and their primary mineralogy is well preserved. Orthopyroxene grains are idiomorphic, subhedral to euhedral and are 0.2 to 1.5 mm in size. They show a strong neutral to reddish pleochroism, and hence are of hypersthene composition. Clinopyroxene grains are subhedral to euhedral and usually are larger (0.5 to 3 mm) than orthopyroxene. Whereas hypersthene is clear and free of inclusions, clinopyroxene has exsolution lamellae of orthopyroxene. Near the top of these cumulates plagioclase occurs as interstitial, 0.2-1 mm large crystals or as oikocrysts up to 5 mm in diameter enclosing pyroxene grains. At the interface of cyclic unit 7/8 and at the northern margin of the SUP (LDI-19, 21) websterite cumulates contain inclusions of olivine, sometimes forming aggregates of 1 cm size. These olivine grains are strongly fractured, partly altered to serpentine and are replaced around their margins by hypersthene. Here clinopyroxene and orthopyroxene grains contain large numbers of subhedral to euhedral inclusions of clinopyroxene, orthopyroxene and plagioclase.

The top of cycles 2 and 7 consists of orthopyroxene cumulates (Fig. 2). They show meso- to adcumulate textures with subhedral to euhedral hypersthene grains and variable amounts of interstitial clinopyroxene. Samples LDI-43 and 46 from cycle 8 also contain strongly fractured, anhedral olivine grains, partly altered to serpentine together with thin seams of chromite (≤ 1 cm). The appearance of orthopyroxene cumulates at the top of cyclic units 2 and 7 poses a problem because here they overlie websterite cumulates, and the implied crystallization sequence of clinopyroxene+orthopyroxene, followed by orthopyroxene has not been observed in experimental studies of the system olivine-clinopyroxene-quartz-plagioclase (Irvine, 1970). Our interpretation of this observation will be discussed in a later section.

The ultramafic centres also contain PGE-bearing sulphide mineralization, but so far this is of minor economic interest. Sulphide minerals occur throughout the ultramafic complex (see geological map of Linhard and Bues, 1987), but most of them represent isolated occurrences which can only be followed for a few metres. Exceptions are sulphide mineralization at locations 26 and 38 (Fig. 1, 2), which are the focus of current exploration activities in the UMP. At location 26, sulphide mineralization occurs in a reef, which can be followed for more than a kilometer, and, to date, this

constitutes the most important PGE mineralization (up to 3 ppm total PGE; Linhard and Sutcliffe, 1986). Along the profile A sulphide minerals have also been found at locations 30, 29, and 41 (Fig, 1, 2). The PGE-bearing sulphide mineralization usually occurs at the interface of two cyclic units, in websterite and orthopyroxenite cumulates, which are overlain by peridotite or bronzite and olivine-bearing clinopyroxenite cumulates (Fig. 2). The main sulphide minerals are pyrrhotite, chalcopyrite and pentlandite. PGM have not been observed so far.

SAMPLING AND ANALYTICAL METHODS

The locations of the rock samples are shown in Figure 1 and 2. Sampling depended on outcrop conditions, which gave rise to an uneven sample distribution with distances between samples ranging from several to hundreds of metres. Sampling included mineralized and nonmineralized portions of the intrusions and represents the lithological sequence of the different intrusive phases.

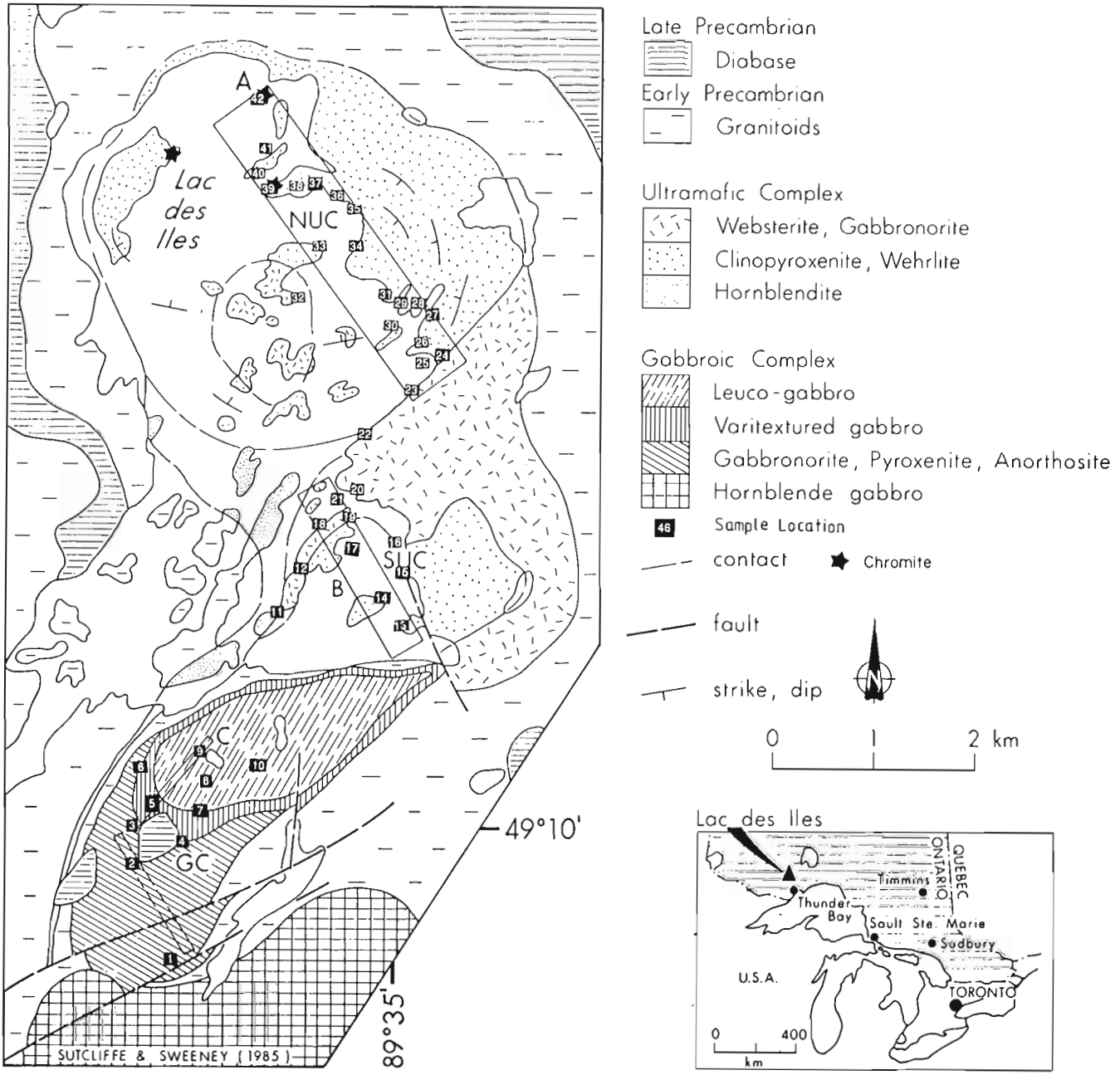

Figure 1. Location and Geology of the Lac des Iles Complex, and sample locations (modified from Sutcliffe and Sweeney (1985). GC: gabbro complex; SUC: southern ultramafic complex; NUC: northern ultramafic complex; A, B, C: outline of sections through the different intrusive parts.

Major elements, S, and Cu have been determined by X-Ray Assay Ltd. by conventional X-ray fluorescence analysis (XRF). Trace element concentrations of Cr, Ni, V, Rb, Sr, Zr and Y have been determined by XRF at the Department of Geology, University of Toronto. For the trace elements a 10 % error is expected for concentrations of 100, 30, 100, 15, 15, 20 and 15 ppm, respectively. REE, Co and Sc determinations have been made by instrumental neutron activation analysis (INAA) at the Slowpoke Reactor, University of Toronto. The precision of the REE is generally poor due to the very low concentration found in the rock samples, but the 2s standard deviation is better than 30 %. The precision of the Co and Sc data is always better than 5 %. The accuracy of the data has been controlled by routinely analyzing an in-house standard (UTB-1).

Concentrations of Au, Pd, Pt, Ir, Os, Ru, As and Se have been determined by radiochemical neutron activation analysis (RNAA) as described by Brügmann et al. (1987, 1989). Samples have been irradiated at the Slowpoke Reactor for 16 hours in a thermal neutron flux of $2*10^{11}ns^{-1}cm^{-2}$, or at the Nuclear Reactor, McMaster University, for 52 hours in a thermal flux of $3*10^{13}ns^{-1}cm^{-2}$. Under the best of conditions, the detection limits are 0.004 ppb for Au, 0.03 ppb for Ir, 1.5 ppb for Pt, 2 ppb for Pd, 0.4 ppb for Os, 2 ppb for Ru, 0.2 ppb for As and 5 ppb for Se. Precision (defined as the 2s error of the peak area) is best for Au (< 1-10 %), followed by Ir, As, Pt,and Se (5-20 %) and Pd, Os and Ru (10-50 %). As cited by Brügmann et al. (1987, 1989) the accuracy of the data as determined on rock and meteorite standards is better than 10 %.

RESULTS

The results of major and trace element analysis on samples from the ultramafic parts are summarized in Table 1 and Figures 2, 3 and 4. Although Ru concentrations are reported, it is emphasized that these data are of poor quality. This is because Ru concentrations have not been corrected for ^{103}Ru, which has been produced by fission of U during

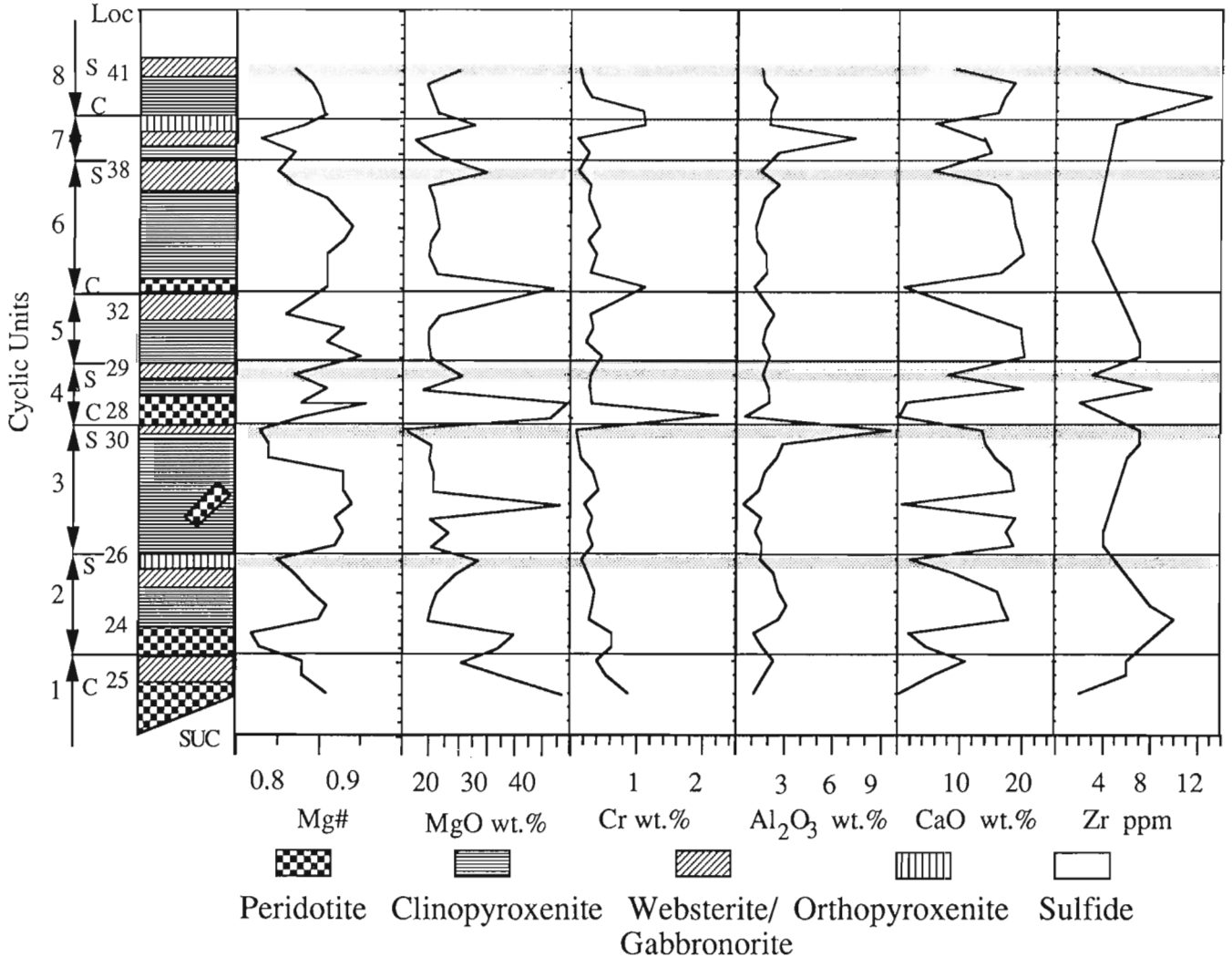

Figure 2. Major and trace element variations along a section A of Figure 1 through the northern ultramafic complex, Lac des Iles. Note that vertical axes is not to scale. Mg# has been calculated by using the total FeO content; S: sulphide occurrences; C: chromite; loc: refers to sample locations in Figure 1.

Table 1. Major and trace element contents of samples from the ultramafic part of the Lac des Iles Complex.

	LDI-19	LDI-21	LDI-22	87-27	LDI-27	LDI-26	87-28	87-29	87-30	LDI-30	87-32	LDI-32	LDI-34	LDI-36	LDI-35	LDI-37	LDI-38	LDI-39	LDI-41	87-46	87-45	87-44	LDI-45
Loc*	18	19	25	24	24	24	24	24	26	26	26	30	28	28	28	28	29	29	32	38	38	38	41
SiO2 wt.%	50.82	49.37	42.73	44.65	52.74	53.08	52.10	53.63	54.00	51.85	53.58	52.03	51.43	40.61	45.86	52.80	53.91	52.78	52.64	52.93	48.88	52.61	53.75
TiO2	0.22	0.21	0.08	0.15	0.27	0.27	0.26	0.21	0.12	0.10	0.10	0.23	0.19	0.15	0.07	0.16	0.15	0.19	0.22	0.21	0.13	0.20	0.13
Al2O3	15.60	8.66	1.09	1.65	2.63	3.17	2.66	2.35	1.52	1.20	1.40	2.53	9.50	2.06	0.53	2.00	1.64	2.05	2.35	2.65	1.50	2.58	1.54
FeO total	6.74	9.11	12.29	16.06	6.38	5.95	7.13	9.62	12.62	5.68	5.03	9.27	8.07	14.51	7.95	5.63	10.05	4.15	9.20	7.93	13.16	8.23	9.67
MnO	0.15	0.19	0.19	0.24	0.16	0.16	0.18	0.24	0.31	0.17	0.17	0.21	0.19	0.27	0.19	0.15	0.27	0.13	0.23	0.19	0.21	0.20	0.26
MgO	10.36	18.54	43.32	32.10	19.75	20.30	21.27	24.53	28.63	23.36	20.64	19.99	16.06	40.86	45.15	18.83	25.73	20.17	21.76	19.68	29.91	20.80	25.01
CaO	13.66	12.66	0.20	4.72	17.68	16.76	15.93	9.05	2.07	17.39	18.66	15.50	13.43	1.35	0.11	19.96	8.04	20.17	13.34	15.91	5.64	14.89	9.18
Na2O	1.61	0.65	0.06	0.38	0.35	0.28	0.43	0.33	0.33	0.23	0.40	0.22	0.72	0.11	0.09	0.39	0.19	0.34	0.24	0.44	0.41	0.44	0.18
K2O	0.57	0.24	0.01	0.02	0.03	0.02	0.02	0.02	0.01	0.01	0.02	0.01	0.20	0.01	0.02	0.06	0.01	0.01	0.01	0.03	0.04	0.01	0.01
P2O5	0.02	0.02	0.02	0.02	0.01	0.01	0.01	0.01	0.01	0.01	0.01	0.01	0.01	0.02	0.02	0.01	0.01	0.01	0.01	0.02	0.02	0.01	0.01
S	0.25	0.36	0.02	0.00	0.00	0.00	0.00	0.00	0.38	0.00	0.00	0.00	0.19	0.04	0.00	0.01	0.00	0.00	0.00	0.00	0.11	0.03	0.26
LOI	1.2	2.7	12.2	8.5	1.8	2.5	1.8	1.5	0.1	4.0	2.5	0.8	0.5	13.2	14.8	1.5	0.1	1.2	0.4	0.6	6.6	0.8	0.0
Mg#	0.73	0.78	0.86	0.78	0.85	0.86	0.84	0.82	0.80	0.88	0.88	0.79	0.78	0.83	0.91	0.86	0.82	0.90	0.81	0.82	0.80	0.82	0.82
Cr ppm	987	1562	8662	6290	2820	3285	3620	2580	1680	2608	4190	1631	909	22834	3540	2854	3124	4680	3010	2970	1110	2740	1350
Ni	314	801	1403	1460	394	445	354	454	2060	302	282	259	461	2004	1803	323	418	391	415	430	1100	399	592
Cu				26			2	161	2270		38									55	611	207	
Co	51		109		50			84	117			58	68					84			67	55	90
V	170	158	76		214	221				113		239	190	106	43	122	131	130	201				144
Rb	8	3	0		0	0				0		0	2	0	0	0	0	0	0				0
Sr	319	172	2		28	24				25		16	227	4	3	39	13	36	19				12
Zr	10	10	2		10	8				4		6	7	2	0	8	3	7	6				3
Y	5	6	0		9	9				4		7	6	0	2	6	3	7	6				3
Sc	45		11		80			64	40			81	60					53			71	76	58
La	0.7		0.63		0.57				0			0.42	0.51				0.2					0.3	0.2
Ce	2		1.1		2.9				0			1.5	1.8				0					0	1.3
Sm	0.66		0.24		4.15				0.1			1.07	0.71				0.4					1.1	0.5
Eu	0.31		0.09		0.42				0			0.23	0.29				0					0.3	0.2
Yb	0.57		0.26		0.82				0			0.59	0.44				0.3					0.6	0.56
Lu	0.09		0.05		0.12				0			0.1	0.08				0					0.1	0.1
Ir ppb	1.9	3	4.5	*2.25*	4	1	*0.47*	*1.04*	5.46	0.8	*0.94*	3.2	7	3.7	3.8	2.5	1.5	0.4	2	1.33	3.28	1.15	3
Os	0	0	5	0	0	0	0	0	2.8	0	0	4	8	3.2	4.1	2.3	0.9	0.7	2.5	2.8	12.4	2.1	2
Ru	0	0	0	*19*	0	0	*9*	*8*	8	0	*22*	0	0	0	0	0	0	0	0	11	16	11	
Pt	0	40	0	*29*	40	0	*44*	*44*	365	0	*10*	45	109	4	6	30	42	4	26	80	284	110	64
Pd	44	102	0	*20*	35	10	*12*	*102*	1120	18	*10*	110	290	0	3	0	0	0	30	270	830	350	140
Au	8.7	16.2	0.1	*1.2*	8	2	*0.36*	*2.5*	58.8	2	*1.04*	13.7	24	0.1	0.2	5.4	6.9	0.8	2.6	10.5	112	39.1	13.9
Se ppm				*0.19*			*0.05*	*0.46*	4.12		*0.13*	0.46	1.1	0.06		0.29	0.48	0.15	0.21	0.22	2.09	0.93	0.66

samples are ordered with stratigraphic height; major element data are normalized to 100% anhydreous; 0 values: below detection limit; blank values: not determined; loc: refers to sample locations in Fig. 1

the irradiation of the samples. U concentrations in the samples are, however, low (< 100 ppb) and not detectable with INAA. Nevertheless, 100 ppb U may produce about 14 ppb Ru, therefore, the Ru concentrations reported in Table 1 are expected to be too high.

Geochemistry of the northern ultramafic part

CIPW normative and observed mineralogy in websteritic and clinopyroxene cumulates are in very good agreement and indicate that secondary alteration processes did not significantly change the chemical composition of these rock samples. This is, however, not well established for peridotitic cumulates for their poor preservation state does not allow a reasonable comparison of calculated and observed data.

Figures 2 and 3 show the variation of selected major and trace element concentrations along a section of the NUP (Fig. 1). The cyclic character of the intrusion is displayed by jumps in the Mg-number (Mg#), MgO, Ni and Cr contents. High MgO, Cr and Ni contents at the bottom of cyclic units indicate the crystallization of olivine and minor amounts of chromite, whereas an increase in CaO indicates the beginning of clinopyroxene crystallization. An increase in MgO associated with a further decrease in Mg# and CaO indicates the crystallization of orthopyroxene and the formation of websteritic cumulates. Finally high Al_2O_3 contents indicate the appearance of plagioclase at the top of a cyclic unit. Some interfaces of cyclic units display a gradational increase in Mg#, Ni and Cr (e.g. cycle 3/4, 5/6, 7/8; Fig. 2).

The cumulates have very low abundances of incompatible elements such as Zr (Fig. 2) or REE (Table 1). When normalized to a primitive mantle composition REE contents of these rocks show low enrichment factors between 0.3 and 3.

Sulphide mineralization is delineated by S, Se, Ni, Cu and PGE anomalies (Fig. 3). Due to the high Ni background (olivine and pyroxene contain high concentrations of Ni), Ni is less reliable as a pathfinder for the sulphide-bearing horizons. This is also reflected by the rather low correlation coefficient between Ni and PGE, Se and S (Table 2). Selenium displays a strong correlation with PGE and the PGE are strongly correlated with each other (Fig.4, Table

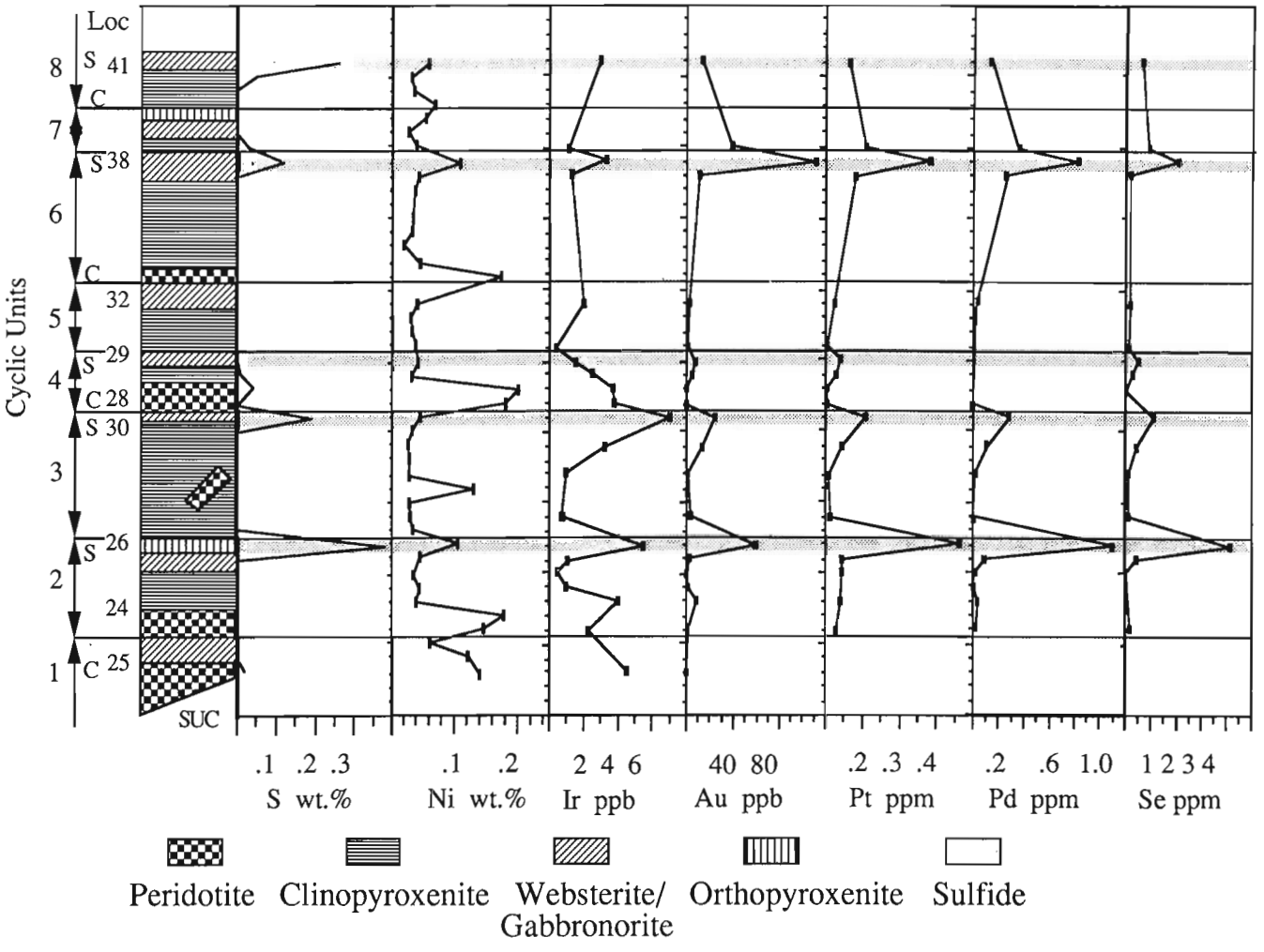

Figure 3. Variation of S, Se, Ni, and PGE along section A of Figure 1 through the northern ultramafic complex, Lac des Iles. (Abbreviations as for Figure 2)

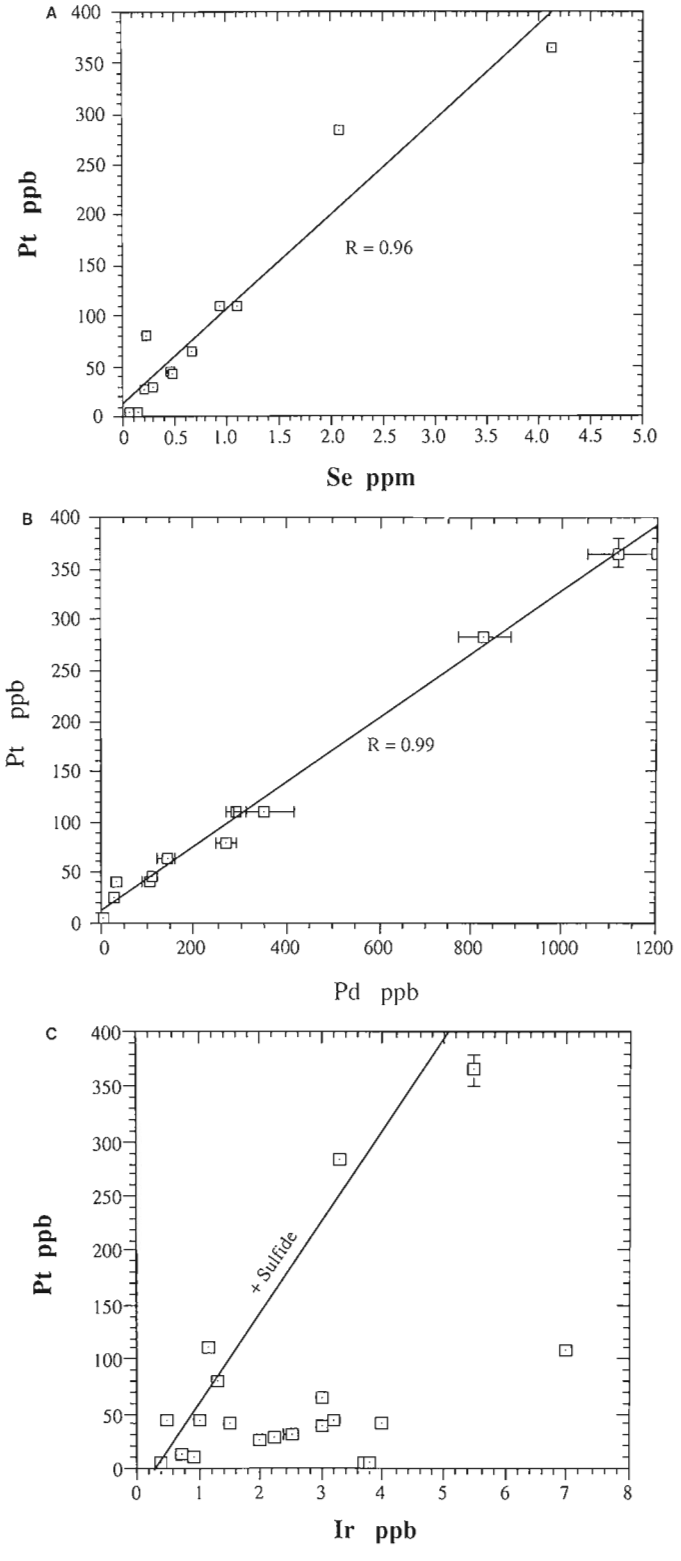

Figure 4. Variation diagrams of PGE , S, Ni, Cu and Se concentrations in the gabbroic and ultramafic parts of the Lac des Iles Complex. Error bars represent 2 σ standard deviation

a. Pt-Se correlation; b. Pd-Pt; c. Pt-Ir; regression line indicates the trend of PGE enrichment caused by sulphides; note that sulphur-poor samples plot along trends suggesting lower Pt/Ir ratios than sulfide-bearing samples

2)). Correlation between S and Se is only significant at the 95 % probability level. The maximum sulphide content found in this study is about 1 wt. % , but none of the analyzed mineralized rocks contain economic grades of PGE. The highest contents were found at location 26 (sample 87-30), with up to 1120 ppb Pd, 365 ppb Pt, 58.8 ppb Au, 5.5 ppb Ir, 3 ppb Os, 2060 ppm Ni, and 2270 ppm Cu. Elevated chalcophile element abundances are also found at the top of cyclic units 3, 4, 6 and 8.

DISCUSSION

Based on their profiles in mantle normalized diagrams, sulphur-poor (< 100 ppm S) samples from the UMP can be divided into two groups (Fig. 5):

a. Peridotitic cumulates enriched in Ir, Os, and Ni compared to Pt, Pd Au, Cu (samples ldi-35, ldi-36)
b. Pyroxenitic and gabbronoritic cumulates enriched in Pd, Pt, Au and Cu relative to Ni, Ir, and Os (e.g. samples ldi-27, ldi-41).

These different patterns can be interpreted in terms of the known behaviour of PGE and Au during fractional crystallization of a mantle derived magma. Iridium, Os and Ru behave like compatible elements and although the cause of this behaviour is currently debated (for a detailed discussion of the existence of PGE-bearing alloys and their influence on the fractionation behaviour of these elements refer to Keays and Campbell (1981), Barnes et al. (1985), Brügmann et al. (1987)). Agiorgitis and Wolf (1978), Naldrett and Barnes (1986) and Brügmann et al. (1987) have suggested that Ir and probably also Os and Ru, resemble Ni in being compatible in mafic silicates and oxides such as olivine and chromite, so that the Ir concentration in a magma decreases as it crystallizes. The type (a) pattern is therefore to be expected of sulphide-free olivine + chromite cumulates in which only a small fraction of interstitial liquid is retained. High concentrations of Ir and Os in S-poor pyroxenites (e.g. samples LDI-32, LDI-41) could imply that these elements are compatible in pyroxene as well, although to a much lesser degree than in olivine. The even higher concentrations of Pt, Pd, and Au in these rocks are explicable in terms of their levels being controlled by either the amount of trapped intercumulus liquid or the presence of small amounts of sulphides. The low abundances of incompatible trace elements (REE, Zr, Rb) indicate that these rocks only contain a small amount of intercumulus liquid. Therefore, small amounts of sulphides control their PGE pattern. This is also indicated in Figure 4c, where these samples define a Pt-Ir trend with a lower Pt-Ir ratio than those of the higher grade mineralization. This trend implies either a preferred Ir enrichment or a Pt (and also Au and Pd) depletion in the parental silicate magma in which these sulphides formed. As Se, Pd and Pt concentrations of all samples plot along identical trends (Fig.4a, b), which suggest a sulphide control, Pt depletion in the parental liquid cannot explain the low Pt/Ir ratio in the sulphur-poor samples. This is more likely due to additional Ir in silicate phases such as clinopyroxene and orthopyroxene or in metal alloys.

Mantle normalized PGE patterns of the sulphide-bearing samples are typical of magmatic Ni-Cu sulphide deposits

Table 2. Correlation coefficients for Cr, PGE and chalcophile elements in the ultramafic part of the Lac des Iles Complex.

	Cr	Ni	Ir	Os	Pt	Pd	Au	Se	S
Cr	1.000	*.532*	-.103	-.134	-.306	-.385	-.285	-.310	-.464
Ni		1.000	*.524*	.190	.386	*.611*	.231	*.597*	.087
Ir			1.000	-.084	**.747**	**.756**	.370	**.876**	.530
Os				1.000	.491	.362	**.701**	.345	-.038
Pt					1.000	**.996**	**.869**	**.962**	.385
Pd						1.000	**.853**	**.952**	.056
Au							1.000	**.728**	.138
Se								1.000	*.745*
S									1.000

Numbers in bold and italics refer to correlations which are significant at the 99% and 95% level, respectivily

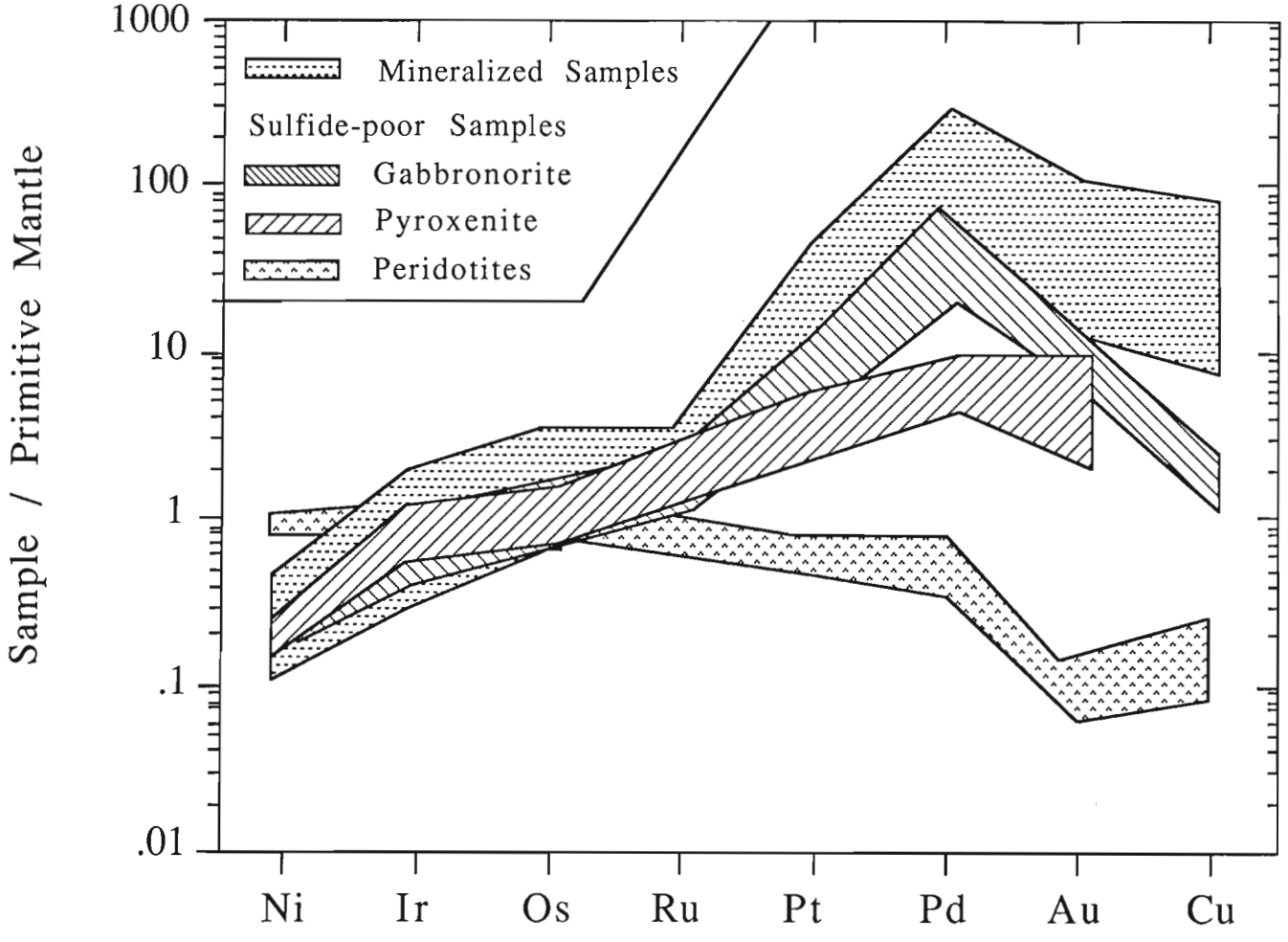

Figure 5. Mantle normalized Ni, Cu, and PGE patterns of unmineralized and sulphide-bearing samples from the ultramafic complex, Lac des Iles; primitive mantle (PM) values from Brügmann et al. (1987)

(Naldrett and Duke, 1980), which are depleted in Ni, Ir, Os, and Ru relative to Pt, Pd, Au and Cu (Fig. 5). Higher grade mineralization (total PGE + Au ≥ 500 ppb) has higher Pd/Ir ratios (205 - 304) than sulphide-free and sulphide-poor samples (0.8 to 41).

The cause of sulphide immiscibility in the parental magma of the UMP.

PGE-rich sulphides have been found at 5 horizons within the NUP (Fig. 3). In each case the mineralization occurs at the interface of cyclic units in orthopyroxenite or websterite cumulates and is associated with a decrease in Mg# of the bulk-rock. Four possible factors could contribute to such a decrease:

- — the presence of a Fe-rich oxide such as magnetite or chromite
- — the presence of sulphides,
- — the original trapping of large amounts of pore fluid, which caused the formation of Fe-rich margins at the silicate grains,
- — fractional crystallization.

Primary magnetite and chromite are not observed in these rocks, indeed these horizons are Cr-"lows", which also argues against the presence of chromite. In the case of the sulphide zone at the top of cycle 2, the amount of sulphide present would mean that the Mg# calculated for the silicates including the Fe in the sulphide would be by 0.02 lower than if this Fe is excluded. In all the other cases, where the sulphide-bearing zones have lower S contents, the difference would be even less significant. The principal explanation for the low Mg# must therefore lie in the fractional crystallization towards the top of the cycles plus the increased trapping of intercumulus liquid. The progressive change in Mg#, shown in cycles 2, 4, 6 and 8 below the mineralized horizons for instance, could be due to fractionation, particularly because Al_2O_3 and Zr concentrations show little change or even decrease suggesting a minor influence of the pore liquid. The abrupt decrease of the Mg# in cycle 3 (loc 30) is more readily explained as being partly due to high proportions of intercumulus liquid because of the high concentration of Al_2O_3 and incompatible elements, such as Zr (Fig. 2).

The occurrence of the sulphide horizons at the top of cyclic units, just below where new magma became involved in the crystallization of the succeeding cycle, suggests that it is the introduction of this new magma that triggered the formation of an immiscible sulphide liquid.

Naldrett and Von Grünewaldt (1989) have discussed the mixing of primitive and fractionated magma with reference to a postulated sulphide solubility curve (Fig. 6). Mixing of primitive magma of composition A with well fractionated magma such as that lying on the sulphide saturation curve at D, can result in a mixture being saturated with sulphide as at AD. Such a model would explain the formation of PGE-rich mineralization like these of the Bushveld and Stillwater complexes (Naldrett and Von Grünewaldt, 1989). The case of the LDIC is probably more like mixing of A with a less fractionated magma such as C which does not yet crystallize plagioclase. The mixture then lies at AC, and will segregate a small amount of sulphide. Continuous input of A will mean that the mixture will move from AC towards A and thus become undersaturated with sulphide. This would explain the lack of sulphides at the base of the overlying cycle. Ultimately, with further fractionation, this cycle will become enriched in S again and may eventually segregate small amounts of sulphides. This would explain the elevated PGE contents in S-poor clinopyroxenites in the centre of cyclic units 2 and 4. Since both magma compositions D and C lie on the solubility curve, segregation of sulphides will occur before mixing causes an increase in the sulphur content again. This will mean that the magmas will be poor in PGE, since these metals partition so readily into sulphide phases. PGE will therefore have to be scavenged from the new input, which is presumed to be unsaturated in sulphide.

Mineralization at the top of cycle 2 is unique in that it occurs in an orthopyroxenite cumulate which overlies websterite and is overlain by clinopyroxenite. This relationship suggests a crystallization sequence of clinopyroxene + orthopyroxenite, orthopyroxene and clinopyroxene. In Figure 7 the normative mineralogy of the UMP samples is shown in the plagioclase-projection of the system olivine-clinopyroxene-plagioclase-quartz, together with its phase relationships (after Irvine, 1970). A hypothetical liquid such as A, lying within the triangle olivine-clinopyroxene-C crystallizes olivine until it reaches at B the olivine-clinopyroxene cotectic line. Further cooling causes the liquid to reach C where crystallization of clinopyroxene and orthopyroxene produces websteritic cumulates. Eventually plagioclase might join the liquidus to give rise to gabbronorite cumulates. This is the crystallization sequence commonly observed in the UMP. In order to form

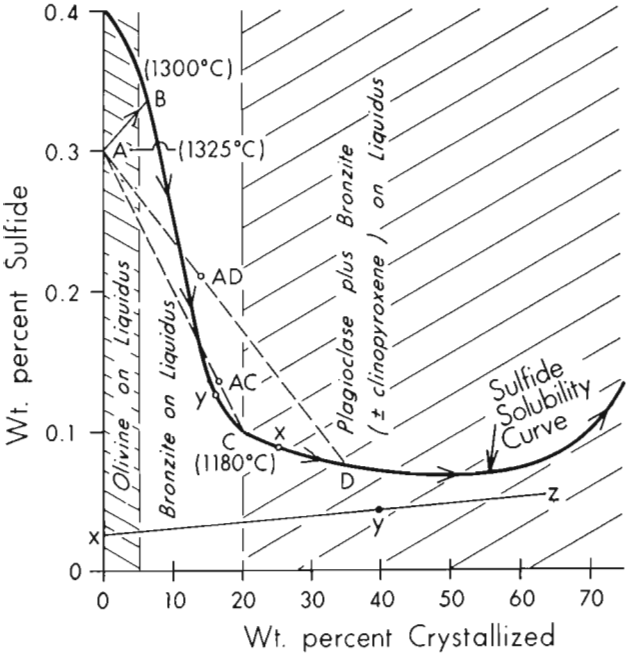

Figure 6. Schematic diagram illustrating the variation in the sulphide solubility of a fractionating mantle magma (after Naldrett and Von Grünewaldt, 1989)

commonly observed in the UMP. In order to form orthopyroxenite cumulates a different parental magma composition, lying within triangle olivine-orthopyroxene-C, has to be inferred. This would yield the cumulate sequence dunite, orthopyroxenite, websterite, gabbro-norite. Although neither a basal dunite nor an overlying websterite cumulate is found in our special case, it is still possible that a new magma with a composition close to the reaction line olivine-orthopyroxene intruded the magma chamber, giving rise to orthopyroxenites, but further evolution was prevented due to the input of a new batch of magma. However, there is an alternative explanation, which relates the formation of sulphide mineralization to that of orthopyroxene crystallization. Suppose a magma chamber with a resident magma D (Fig. 7) was replenished with a magma such as A which mixed with D. This mixing could produce a hybrid magma such as E, which would be able to form orthopyroxene cumulates. This hybrid liquid would also be sulphide saturated as outlined previously and thus has given rise to the formation of sulphide mineralization. Unfortunately, the parental magma compositions forming the UMP cumulates are not well constrained, because chilled margins have not been observed, and mass balance calculations are impossible because the stratigraphic profile through the magma chamber is incomplete. Interestingly, however, the composition of some mafic dykes (Fig. 7), which intruded the GP and the UMP and could represent feeder dykes for individual cyclic units, lie very close to the line olivine-C. These liquids would be the ideal candidates to form orthopyroxene cumulates, since even a small amount of contamination with a magma such as D could produce a hybrid magma which crystallizes orthopyroxene.

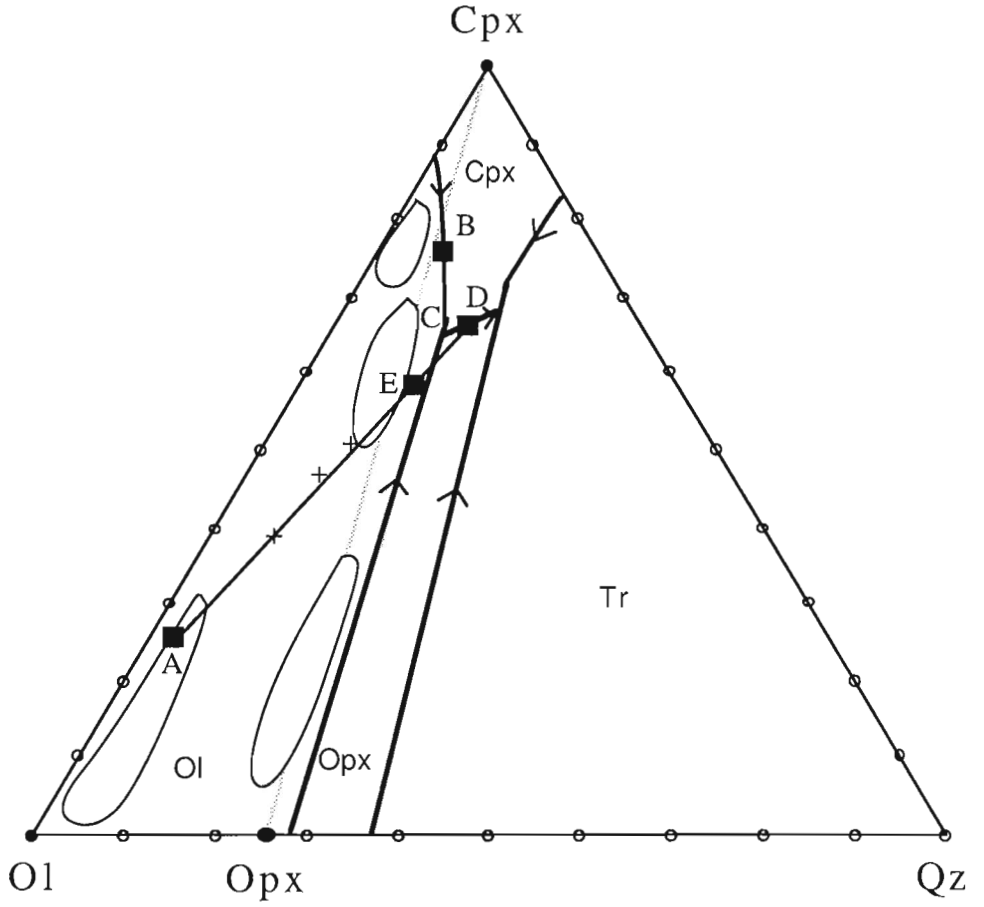

Figure 7. Phase relationships in the plagioclase projection of the system olivine-clinopyroxene, plagioclase-quartz (after Irvine, 1970). Heavy lines represent phase boundaries for quartz (Tr), orthopyroxene (Opx), clinopyroxene (Cpx) and olivine (Ol); outlined areas represent cumulate compositions; line A-B represents a mixing line between magma compositions such as A and D to produce hybrid magmas such as E, which would crystallize Opx; + represent compositions of mafic dykes.

SUMMARY

The Lac des Iles Complex in northwestern Ontario consists of several mafic and ultramafic intrusive phases, which contain economically interesting PGE-bearing Cu-Ni sulphide mineralization.

The ultramafic part mainly consists of peridotites, pyroxenites, and minor gabbro-norites. The lithological sequence suggests a crystallization sequence of olivine + clinopyroxene, clinopyroxene, clinopyroxene + orthopyroxene and clinopyroxene + orthopyroxene + plagioclase. The different ultramafic intrusive phases probably represent magma chambers which were periodically refilled with fresh, more primitive magma. Gradational chemical variation trends across a contact between two cyclic units, and the incorporation of olivine crystals and aggregate into gabbronorite at the top of such an unit suggest that the fresh input of magma mixed with residual evolved liquid.

Sulphide mineralization occurs in websterite, gabbronorite and orthopyroxenite cumulates at the top of cyclic units. Maximum ore grades are about 3 ppm total PGE+Au. Their mantle normalized PGE pattern is typical for magmatic sulphide ores, in that it is enriched in Au, Pd and Pt relative to Ir, Os and Ru with Pd/Ir ratios in the order of 250. It is proposed that sulphide saturation was achieved during replenishment of the magma chamber by mixing of fractionated with primitive liquid.

ACKNOWLEDGMENTS

We are grateful to R. Sutcliffe and A.J. Macdonald for introducing us to the Lac des Iles Complex. We appreciate the assistance of the staff of the reactors at the SLOWPOKE, University of Toronto,and the McMaster University, Hamilton, during neutron activation analysis. This research has been supported the GSC through by DSS contract No. 34SZ.23233-7-1083 to A. J. Naldrett. Additional support came from OGRF grant 276 (1986/87) and NSERC operating grant A4244 also to A.J. Naldrett.

REFERENCES

Agiorgitis, G., and Wolf, R.
1978: Aspects of osmium, ruthenium and iridium contents in some greek chromitites: Chemical Geology, v. 23, p. 267-272.

Barnes, S.-J, Naldrett, A.J., and Gorton, M.P.
1985: The origin of the fractionation of platinum-group elements in terrestrial magmas; Chemical Geology, v. 53, p. 303-325.

Brügmann, G.E. and Naldrett, A.J.N.
1987: Platinum-group element abundances in mafic and ultramafic rocks: preliminary geochemical studies at the Lac des Iles complex, District of Thunder Bay: *in*: (ed.) Geoscience Research Grant Program, Summary of Research 1986-1987, ed. V.G. Milne, Ontario, Geological Survey Miscellaneous, Paper, v. 136, p. 99-114.

Brügmann, G.E., Gorton, M.P., and Hancock, R.G.V.
1989: Simultaneous determination of noble metals, Re, Se, As and Sb by radiochemical neutron activation analysis: Journal Geochemical Exploration.

Brügmann, G.E., Arndt, N.T., Hofmann, A.W., and Tobschall, H.J.
1987: Noble metal abundances in komatiite suites from Alexo, Ontario, and Gorgona Island, Colombia; Geochimica et Cosmochimica Acta, v. 51, p. 2159-2169.

Campbell, I.H., Naldrett, A.J., and Barnes, S.J.
1983: A model for the origin of the platinum-rich sulfide horizons in the Bushveld and Stillwater complexes; Journal of Petrology, v. 24, p. 133-165.

Dunning, G.R.
1979: The geology and platinum-group element mineralization of the Roby Zone, Lac des Iles complex, northwestern Ontario; M, Sc, unpublished thesis, Carleton University, Ottawa, Ontario, 129 p.

Irvine, T.N.
1970: Crystallization sequences in the Muskox intrusion and other layered intrusions: *in* Symposium on the Bushveld Igneous Complex and Other Layered Intrusions, ed. D.J.L. Visser and G. Von Grünewaldt; Geological Society South Africa, Special Publication, v. 1, p. 441-476.

Keays, R.R. and Campbell , I.H.
1981: Precious metals in the Jimberlana intrusion, western Australia: Implications for genesis of platiniferous ores in layered intrusions: Economic Geology, v. 76, p. 1118-1141.

Linhard, E. and Bues, C.C.
1987: Geology of the northern Lac des Iles complex, District of Thunder Bay; *In* Summary of Field Work and Other Activities 1987, ed. R.B. Barlow, M.E. Cherry, A.C. Colvine, B.O. Dressler, and O.L. White; Ontario, Geological Survey, Miscellaneous. Paper, v. 137, p. 281-285.

Naldrett, A.J. and Barnes, S-J.
1986: The behavior of platinum group elements during fractional crystallization and partial melting with special reference to the composition of magmatic sulfide ores: Fortschritle due Mineralogic, v. 64, p. 113-133.

Naldrett, A.J. and Campbell. I.H.
1979: The influence of the silicate: sulfide ratios on the geochemistry of magmatic sulfides; Economic Geology, v. 74, p. 1503-1506.

Naldrett, A.J. and Duke, J.M.
1980: Platinum metals in magmatic sulfide ores; Science, v. 208, p. 1417-1424.

Naldrett, A.J. and Von Grünewaldt G.
1989: The association of PGE with chromitite in layered intrusions and ophiolite complexes; Economic Geology.

Naldrett, A.J., Gasparrini, E.C., Barnes, S.J., Von Grünewaldt, G., and Sharpe, M.R.,
1986: The upper critical zone of the Bushveld Complex and the origin of Merensky-type ores; Economic Geology, v. 81, p. 1105-1117.

Pye, E.G.
1968: Geology of the Lac des Iles area, District of Thunder Bay; Ontario, Department Mines, Geological Report., v. 64, 47 p.

Sutcliffe, R.H.
1986: Regional geology of the Lac des Iles area, District of Thunder Bay; *in* Summary of Field Work and Other Activities 1986, ed. P.C. Thurston, R.B. Barlow, O.L. White and A.C. Colvine; Ontario, Geological Survey, Miscellaneous, Paper, v. 132, p. 70-75.

Sutcliffe, R.H. and Sweeney, J.M.
1985: Geology of the Lac des Iles Complex, District of Thunder Bay; *in* Summary of Field Work and Other Activities 1985, J.Wood, R.B. Barlow, O.L. White and A.C. Colvine; Ont. Geol. Surv., Misc. Paper, v. 126, p. 47-53.
1986: Geology of the Lac des Iles Complex, District of Thunder Bay; Ontario, Geological Survey, Map P.3047.

Sedimentological evaluation of three Archean metaquartzite- and conglomerate-bearing sequences in the Slave Province, N.W.T.[1]

R.J. Rice[2], D.G.F. Long[3], W.K. Fyson[2], and S.M. Roscoe
Mineral Resources Division

Rice, R.J., Long, D.G.F., Fyson, W.K., and Roscoe, S.M., Sedimentological evaluation of three Archean metaquartzite- and conglomerate-bearing sequences in the Slave Province, N.W.T.; in Current Research, Part C, Geological Survey of Canada, Paper 90-1C, p. 305-322, 1990.

Abstract

Phyllite, sub-mature metaquartzite and polymictic orthoconglomerate with granitic and volcanic clasts occur in an areally restricted submarine fan system near Newbigging Lake in the southern part of the Point Lake supracrustal belt.

The Beniah Formation, examined near the southwest part of Beniah Lake in the Beaulieu River supracrustal belt 120 km south of Newbigging Lake, contains phyllite, minor beds of oligomictic quartz-pebble orthoconglomerate and dominantly mature metaquartzite deposited on a shallow siliciclastic shelf.

The Beaulieu Rapids Formation in the Beaulieu River supracrustal belt 30 km south of Beniah Lake includes phyllite, metaquartzite and polymictic with minor oligomictic quartz-pebble orthoconglomerate deposited on a subaerial alluvial fan followed by deposits of a deeper sandy fluvial system.

The subaerial alluvial fan environment attributed to most of the Beaulieu Rapids Formations is one that is particularly favourable for pyritic paleoplacer concentrations of gold and uranium. The self environment of the Beniah Formation is less favourable and the submarine fan deposits near Newbigging Lake are unfavourable.

Résumé

Un cône sous-marin spatialement restreint, près du lac Newbigging dans le sud de la zone supracrustale du lac Point, contient de la phyllite, du quartzite métamorphisé sous-mature et de l'orthoconglomérat polygénique à clastes granitiques et volcaniques.

La formation de Beniah, a été analysée près de la partie sud-ouest du lac Beniah, dans la zone supracrustale de la rivière Beaulieu, à 120 km au sud du lac Newbigging. Elle contient de la phyllite, des couches secondaires d'orthoconglomérat à cailloux de quartz oligogéniques et du quartzite métamorphisé en grande partie mature déposé sur une plate-forme silicoclastique peu profonde.

La formation de Beaulieu Rapids dans la zone supracrustale de la rivière Beaulieu, à 30 km au sud du lac Beniah, contient de la phyllite, du quartzite métamorphisé et un peu d'orthoconglomérat polygénique à cailloux de quartz oligogéniques déposés d'abord sur un cône alluvial subaérien et ensuite, dans un système fluvial sableux plus profond.

Le milieu de sédimentation de la grande partie de la formation de Beaulieu Rapids est celui d'un cône alluvial subaérien, milieu particulièrement favorable à la formation d'or et d'uranium en gisements alluvionnaires pyritiques. Le milieu de sédimentation de la formation de Beniah, soit sur une plate-forme continentale, est un milieu moins favorable et les sédiments déposés dans un cône sous-marin près du lac Newbigging ne constituent pas un milieu favorable.

[1] Contribution to Canada-Northwest Territories Mineral Development Agreement 1987-1991. Project carried by the Geological Survey of Canada.
[2] Ottawa-Carleton Geoscience Centre, Ottawa, Ontario, K1S 5B6
[3] Department of Geology, Laurentian University, Sudbury, Ontario, P3E 2C6

INTRODUCTION

The report of quartz arenite in the Beaulieu River supracrustal belt by Covello et al. (1988) was the first to note such compositionally mature clastic metasediments in the Slave Province. Roscoe et al. (1989) briefly discussed additional examples of similar rocks in the Beaulieu River belt and stressed the significance of the mature clastic rocks for providing clues to the early tectonic history of the Slave Province as well as for possible paleoplacer gold exploration targets.

This paper outlines the results of more detailed work on three clastic metasedimentary sequences in two supracrustal belts of the Slave Province. Two of the sequences, the Beniah and Beaulieu Rapids formations, are in the Beaulieu River supracrustal belt; they were named and discussed in Roscoe et al. (1989). An additional clastic metasedimentary sequence was examined near Newbigging Lake in the southern extension of the Point Lake supracrustal belt. The objective of the more thorough examination is a sedimentological evaluation of depositional environment(s) and consequently the tenability of the rocks as exploration targets for paleoplacer gold mineralization.

Pyritic oligomictic conglomeratic beds in the Witwatersrand succession in South Africa have been by far the most important source of the world's gold and, together with similar conglomerates in earliest Aphebian Huronian strata in Canada, they are also major sources of uranium. The origin of gold, uranium and pyrite concentrations within and associated with oligomictic orthoconglomerates has long been a subject of debate but it is accepted that they are associated with undoubted heavy detrital minerals concentrated in high energy depositional environments and that a paleoplacer model provides an essential guide for exploration.

Paleoplacer ores must be very much richer and larger than most exploitable placers in unconsolidated sediments, so many depositional environments favourable for recent placer deposits are unlikely to have produced economically interesting heavy mineral concentrations in Archean strata. The Newbigging, Beniah and Beaulieu Rapids successions are examined herein on the basis of the possibility that they, or unexamined extensions, may include sediments deposited in environments similar to those favourable for pyritic paleoplacers in South Africa and in Huronian rocks in Canada. These are mainly, if not entirely, proximal fluvial environments found particularly in the upper and middle reaches of subaerial fans, or fan-deltas, that fed repositories filled largely by coarse quartz-rich sands (Minter, 1981; Roscoe, 1981). Other factors, such as the existence of sources of particulate gold, may be important or critical but they are more speculative and are beyond the scope of this paper.

SOUTHERN EXTENSION OF THE POINT LAKE SUPRACRUSTAL BELT

A narrow tract of supracrustal rocks extends 100 km south from latitude 65 N in the Point Lake area (Fig. 1). The only description of this portion of the Point Lake supracrustal belt is given by Fraser (1968) although Stockwell (1933) described the geology of the Winter-Little Marten-Starvation-Point lakes region lying immediately to the west. Fine-grained clastic metasediments are widespread whereas metavolcanics, metaquartzites and conglomerates outcrop more locally. The metasediments were examined at three localities (1, 2 and 3, Fig. 1). Poor exposures resulted in only brief visits to locations 1 and 2.

Lithological description

Location 1 (64° 49′, 112° 25′, NTS 86A)

Pale brown weathering, medium- to coarse-grained, highly sheared metaquartzite is poorly exposed around a small lake 8 km west of Lake Providence. Greyish weathering conglomerates at this locality are highly deformed (4:1 axial ratios in horizontal sections) clast supported and polymict. Clast percentage is estimated as 20-25 % with an arenaceous matrix. Clasts are well-rounded and vary from granule to boulder grade. Granitoid (dominant), tonalite and mafic to intermediate volcanic lithologies are represented. Phyllite does not outcrop and is presumed to underlie low-lying tundra covered areas.

Location 2 (64° 36′, 112° 20′, NTS 86A)

Traverse were run from the southwest and southeast corners of a lake immediately west of Beauparlant Lake. Metavolcanics and high grade metasediments were encountered to the southwest. The metavolcanics are mafic to intermediate, locally pillowed with tops to the southeast and locally highly deformed. Metasediments (hornblende-muscovite schists) are interstratified with the metavolcanics on a scale of metres. Hornblende gneiss replaces the schists as granitic rock bordering the supracrustal rocks is approached. Southeast of the lake, mafic metavolcanics are locally pillowed and intruded by a small granitoid body; deformation is too high to determine reliable tops. Schists along the contact of volcanics with the granitoid body are possibly of sedimentary origin. Locally exposed highly sheared conglomerates are cobble grade, polymict (granitic and mafic volcanic) and clast supported (20-30 % clasts).

Location 3 (64° 23′, 112° 28′, NTS 86A)

Metasediments and metavolcanics immediately east of an irregular shaped lake, 10 km southwest of Newbigging Lake, were sufficiently exposed to permit detailed mapping of a small area (40 km^2, Fig. 2). The sequence from bottom to top consists of phyllite, metaquartzite, conglomerate and mafic metavolcanics, which are associated with small gabbroic intrusions. A prominent schistosity strikes northeasterly through the area parallel or at a low angle to the bedding. Both bedding and schistosity are near vertical. Conglomerate clasts are flattened within the plane of schistosity; horizontal axes are commonly 3:1. Cordierite and garnet in the finer grained metasediments indicate amphibolite grade metamorphism. Small folds are present in fine-grained rocks in the southern portion of the area.

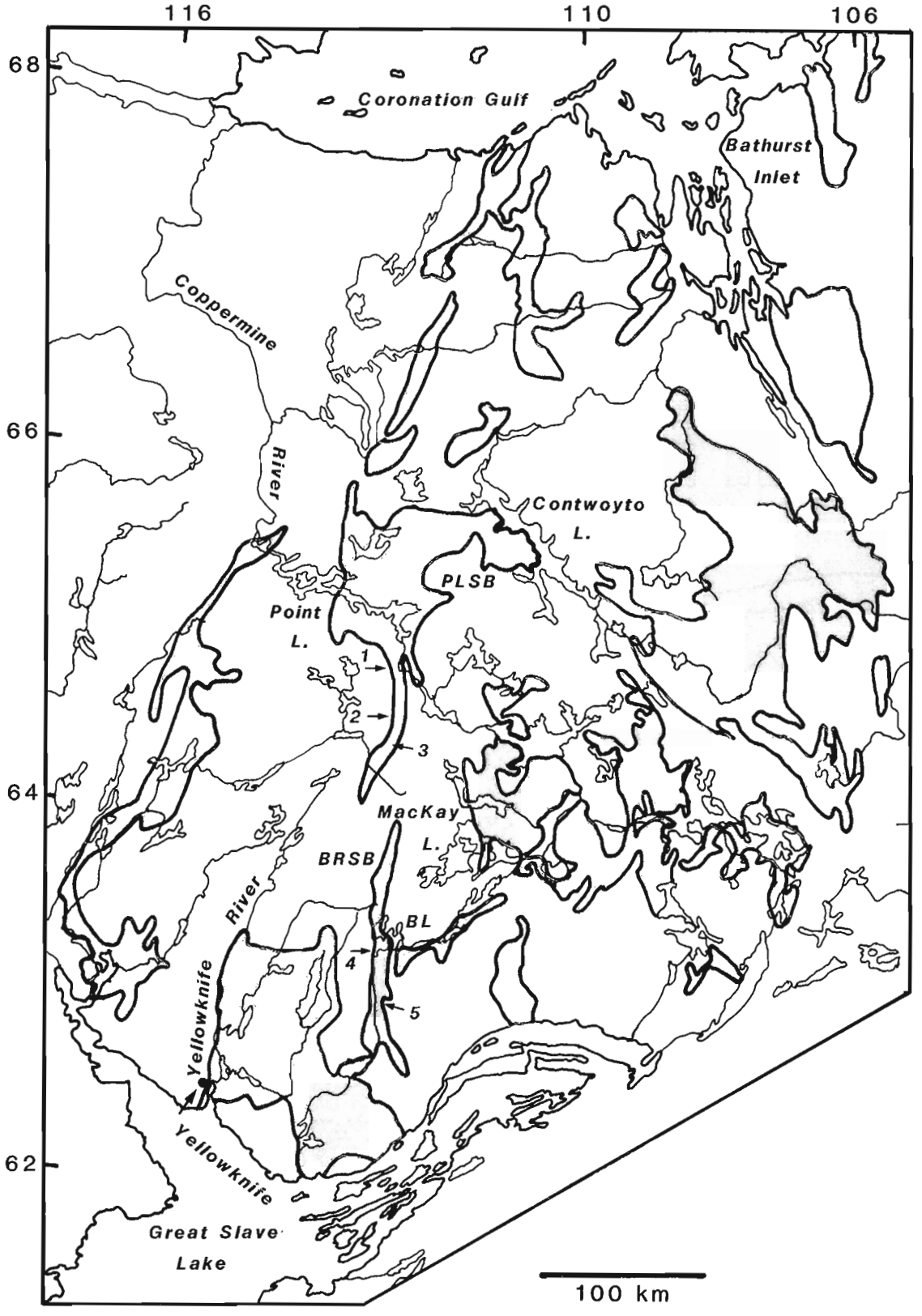

Figure 1. Archean supracrustal belts in the Slave Structural Province, Northwest Territories. Locations 1-5 in the Point Lake (PLSB) and Beaulieu River (BRSB) supracrustal belts are discussed in the text (BL — Beniah Lake). Modified after Figure 1 of Roscoe et al. 1989.

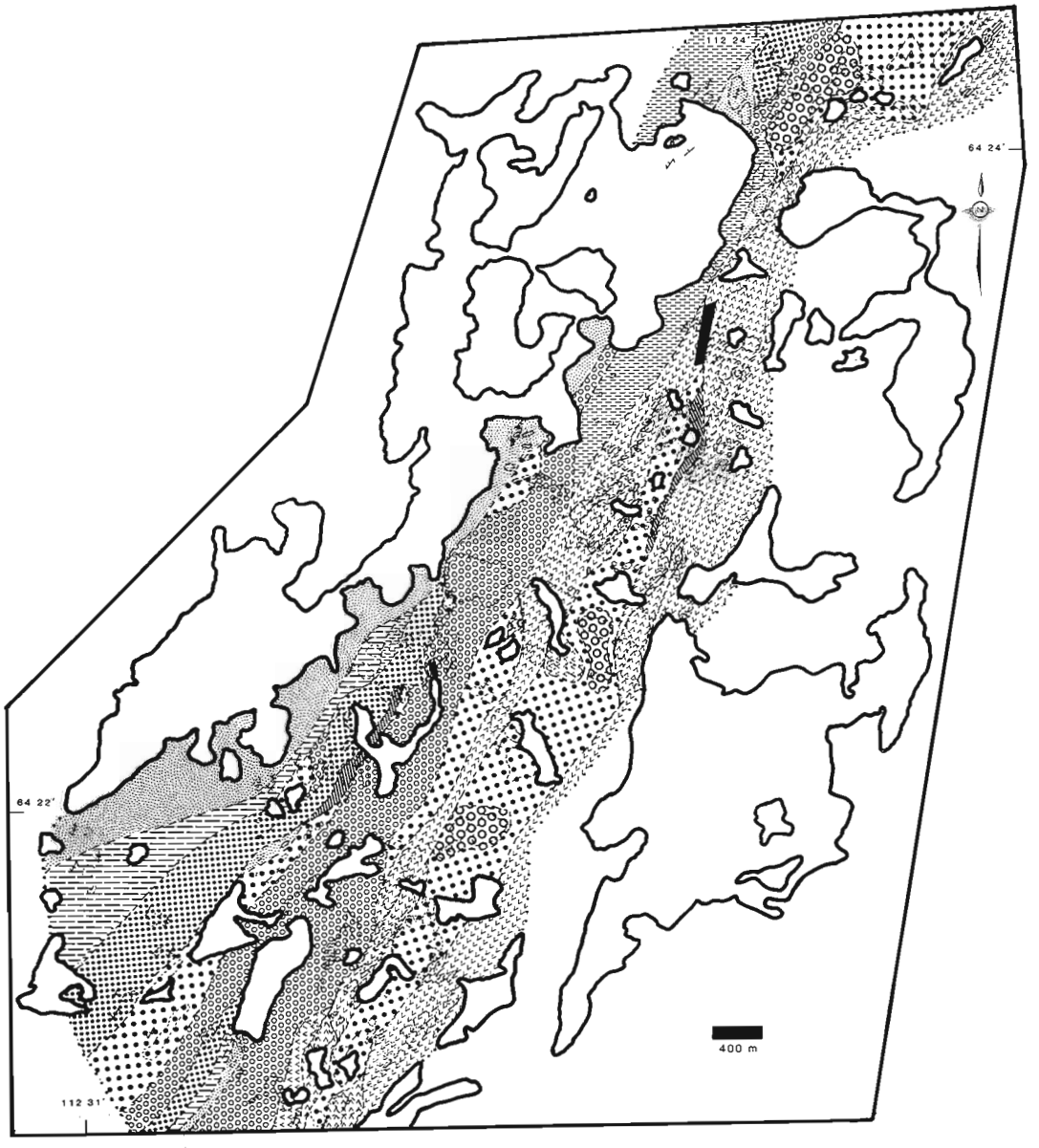

LEGEND

Metasedimentary & Metavolcanic Rocks

- phyllite
- phyllite interstratified with metaquartzite
- metaquartzite
- metaquartzite interstratified with granule to pebble grade polymictic orthoconglomerate
- granule grade polymictic orthoconglomerate
- pebble to cobble grade polymictic orthoconglomerate
- cobble to boulder grade polymictic orthoconglomerate
- interstratified metabasalt and pebble to boulder grade polymictic orthoconglomerate
- pillowed metabasalt
- massive metabasalt
- agglomerate

Intrusive Rocks

- gabbro
- hornblende-plagioclase dyke

Symbols

- outcrop: small, area
- lithological contact: defined, assumed
- bedding (tops known): inclined, vertical, pillows
- bedding (tops unknown): inclined, vertical
- foliation: inclined, vertical
- limit of detailed mapping

Note: 1. all dip angles are near vertical
2. metasediments are at greenschist grade

Figure 2. Detailed geological map of the metasedimentary and metavolcanic sequence at location 3, 10 km southwes of Newbigging Lake in the southern extension of the Point Lake supracrustal belt.

Geopetals in the finer grained metasediments and metavolcanics indicate that depositional tops are to the southeast over most of the area, except at the northern extremity where juxtaposed northwesterly and southeasterly tops suggest an anticlinal structure.

Metasediments and metavolcanics are interstratified, locally down to a scale of several metres, in the eastern, upper part of the stratigraphic section. Pillows are common in the metavolcanics, but deformation prohibits top determinations. Agglomerates at two localities (Fig. 2) include scattered granitoid clasts. Fine stratification in the mafic metavolcanic rock suggests pyroclastic deposition (Fig. 3c). Polymictic orthoconglomerate (Fig. 3a) ranging from granule- to boulder-grade is widely distributed throughout the map area, locally interstratified with the volcanics. Clasts are rounded or, less commonly, angular and are dominantly granitic and mafic volcanic in composition. The largest clasts are 1-2 m granitic boulders.

Metaquartzite (Fig. 4a-c) is widely distributed, either in isolation, or interstratified with phyllite or conglomerate. Relative to that in the Beniah and Beaulieu Rapids formations (locations 4 and 5, respectively, Fig. 1) it is less compositionally mature. Primary sedimentary structures are rare, with only a few small-scale sets of trough cross-lamination or normal grading suggesting depositional tops. Possible rippled contourites occur only where the metaquartzite is interstratified with phyllite (Fig. 3b), which is restricted to the western margin of the map area (Fig. 2). Farther westward, beyond the map area, phyllite predominates, indicating an overall westward fining trend to the metasedimentary sequence.

Interpretation

Locations 1 and 2

Poor exposure of the metasediments combined with high metamorphic grade prohibited any speculation concerning the depositional setting.

Location 3

The phyllite-metaquartzite-conglomerate sequence is best interpreted as indicating deposition of an areally restricted submarine fan system. The intimate association of metasediments with pillowed mafic metavolcanics indicates that sedimentation and subaqueous volcanism were contemporaneous lending support to this interpretation. Furthermore, the east-west (down section) progression from boulder-grade conglomerates to phyllite readily fits the proximal-distal lithological variation expected in a prograding fan setting. Additional interpretive detail is speculative:

1. The presence, at one locality, of 1-2 m boulders in the conglomerate suggests that a fan may have been headed in a canyon, presumably marine.

2. Three areas of boulder-grade conglomerate occur along strike with each other (Fig. 2) suggesting the possibility of several fan-head regions and a system of small coalescing fans.

3. The down section transition from boulder-grade conglomerate to phyllite occurs over a distance of only 2 km. Using this stratigraphic thickness as a scale for the lateral extent of the fan system, a rapid reduction in transport energy is indicated, not unlike that anticipated for a small fan emanating from a canyon eroded into a submarine escarpment.

BENIAH FORMATION

Lithological description

The structurally complex geological setting of the Beniah Formation (Roscoe et al., 1989) in the Beniah Lake area has been described by Covello et al. (1988) and Roscoe et al. (1989). Roscoe et al. (1989) described two areas (north and south) of the formation, both of which are extensively intruded by gabbro making stratigraphic reconstruction speculative. The southern area, 3 km west of the south end of Beniah Lake, was revisited in 1989 for more detailed sedimentological study (location 4, Fig. 1). The Beniah Formation at this location consists of at least 230 m of metaquartzite, phyllite and conglomerate (Fig. 5a, b).

The lower 137 m (cumulative) of the sequence (Fig. 5a) consists of isolated blocks of metasediment separated by gabbro. Block size varies from a few square metres to several tens of square metres. Relative stratigraphic position is determined from geopetals in the metasediments aided by the locally consistent strike. Preliminary petrographic examination indicates that metaquartzite in the lower portion is compositionally mature (Fig. 4g-i) relative to that in the upper portion which is slightly feldspathic. The lithofacies are dominated by nonstratified metaquartzite and fining-upward couplets of metaquartzite and phyllite varying from 2 – 25 cm in thickness. Metaquartzite and phyllite weather white and pale green, respectively. The upper phyllitic part of a couplet usually is only a few centimetres thick. Commonly this part is absent and an amalgamation (erosional) surface takes its place representing erosion accompanying emplacement of the basal portion of the succeeding couplet. Isolated phyllite units are featureless and relatively rare varying from 2 – 17 m thickness. Conglomerate is absent from this portion of the sequence. Primary sedimentary structures are only rarely preserved in the couplets of metaquartzite and phyllite, where both ripples and cross-stratification occur in the metaquartzite. The ripples are preserved as micro trough cross-lamination and are slightly asymmetrical in sets several centimetres thick forming cosets several centimetres to 20 cm (rarely) thick. Sporadic cross-stratification forms trough cross-laminated sets up to 20 cm thick. A few isolated layers of distinctly coarser-grained metaquartzite (coarse to very coarse) several centimetres in thickness are present within couplet intervals.

The upper 94 m of the sequence (Fig. 5b) is dominated by a series of phyllites (up to 11 m thick) interbedded with units of quartz pebble conglomerate, pebbly metaquartzite and submature metaquartzite. A 7.5 – 11 m thick unit of grey-green weathering, parallel laminated phyllite, which overlies the metaquartzite sequence (Fig. 5a) is conformably overlain by 7 – 10 m of thinly bedded, massive to plane

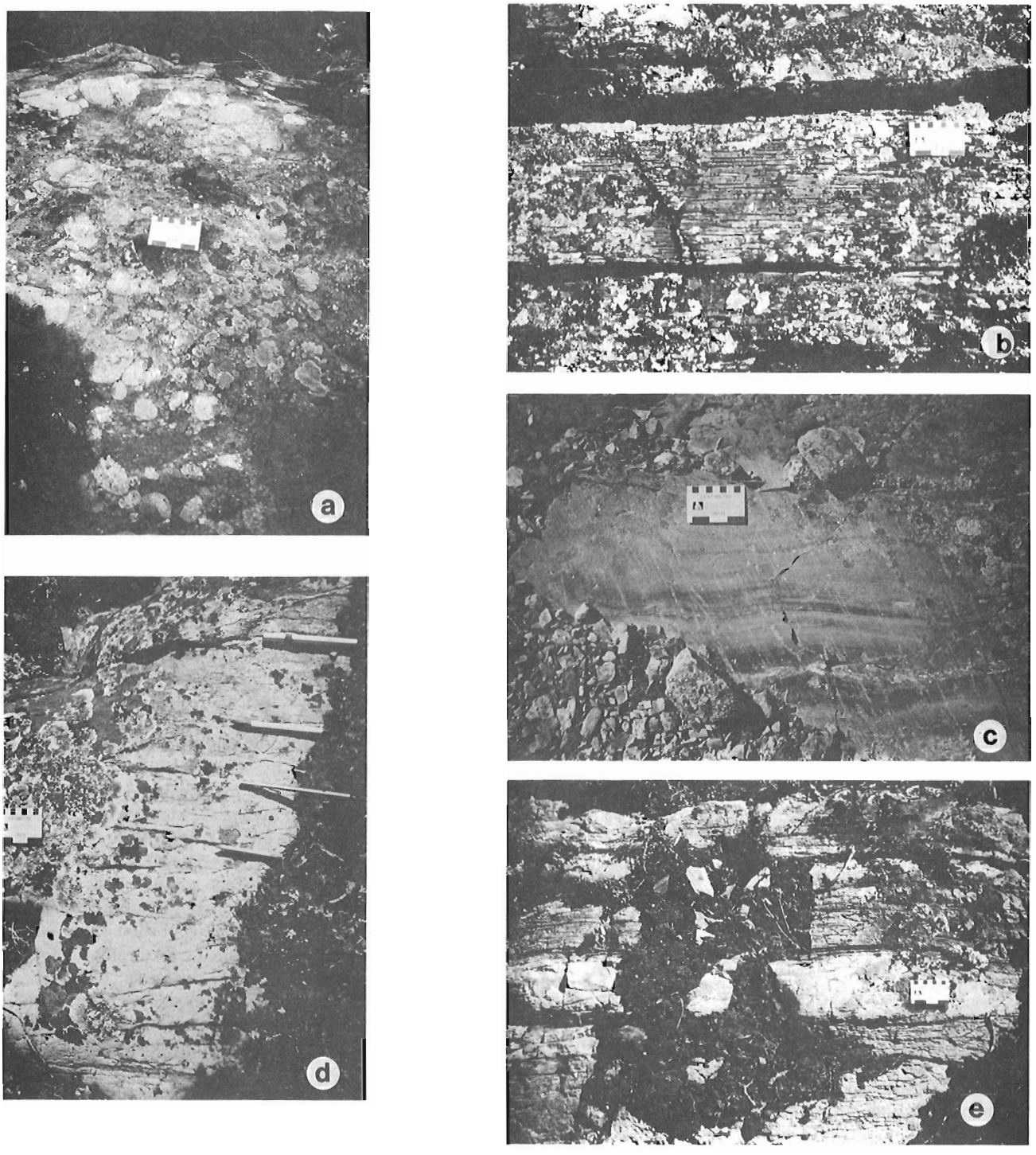

Figure 3. a-c-. Metasediments and metavolcanics in the Point Lake supracrustal belt at location 3 (8 cm scale): a) Pebble to cobble grade polymictic orthoconglomerate b) Interstratified arenite (metaquartzite) and mudstone/siltstone (phyllite) possibly representing contourites 0.5 – 2 cm thick. c) Possible pyroclastic stratification in metabasalt

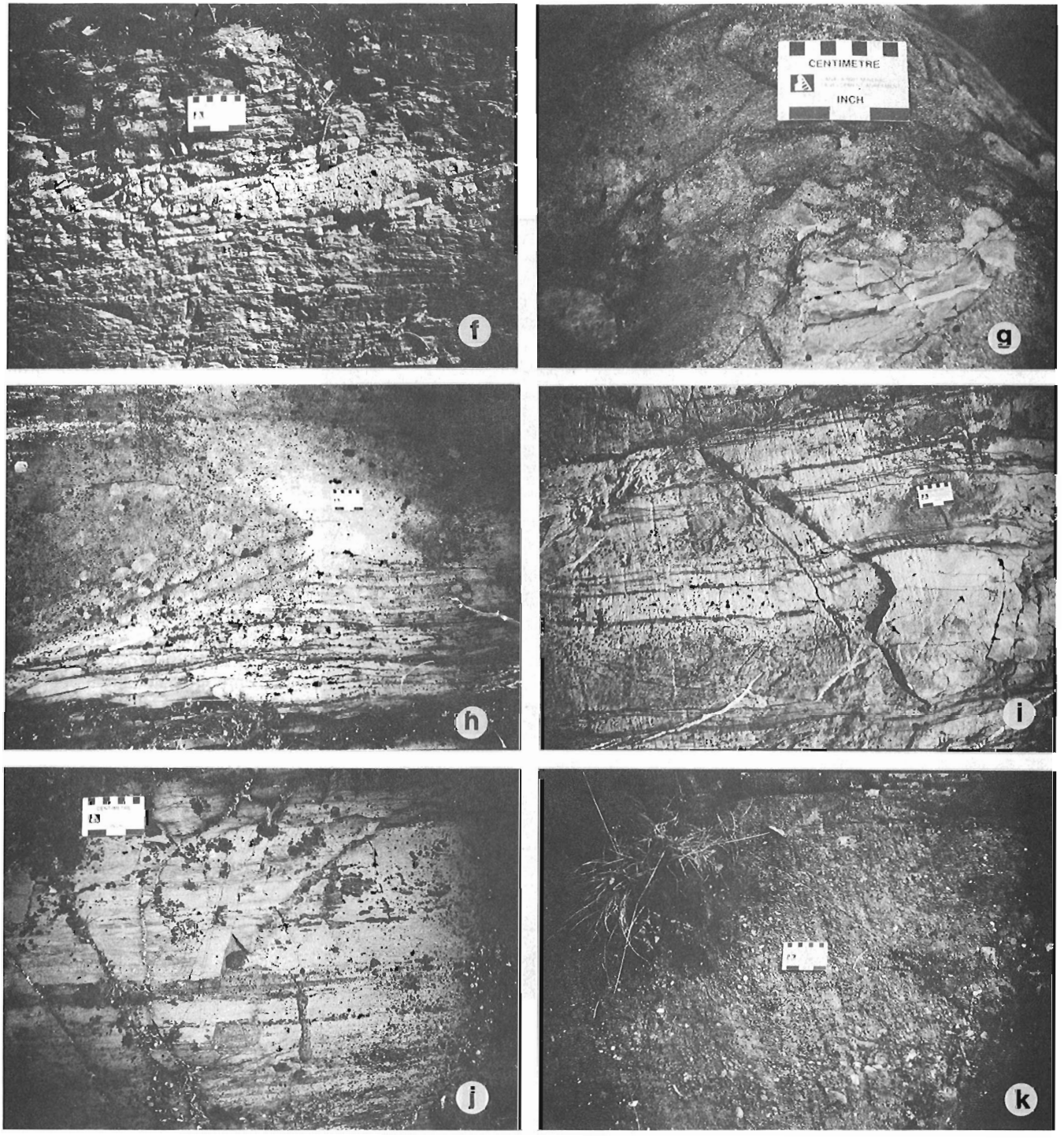

d – f. Features of the basal 137 m of the Beniah Formation near the south end of Beniah Lake in the Beaulieu River supracrustal belt (8 cm scale): d) A sequence of thin fining-upward couplets of metaquartzite and phyllite with pencils marking couplet boundaries e) A coarse- to very coarse-grained metaquartzite possibly representing a storm unit (scale is on the unit) f) A rare occurrence of large scale trough cross-stratification

g – k. Features of the basal 314 m of the northern exposure of the Beaulieu Rapids Formation along the Beaulieu River 30 km south of Beniah Lake in the Beaulieu River supracrustal belt (8 cm scale): g) A large angular clast of silicified siltstone forming part of a lag horizon in metaquartzite h) One-half of a broad channel scour in very thin to thinly bedded metaquartzite i) Metaquartzite with dark phyllite laminae j) Thin (1-3 cm) fining-upward couplets of metaquartzite and rippled phyllite possibly representing distal ephemeral stream deposition k) Granule- to pebble-grade conglomerate with angular to rounded, intermediate to felsic volcanic lithics, rounded quartz grains and rare glass suggesting a combined pyroclastic/epiclastic origin.

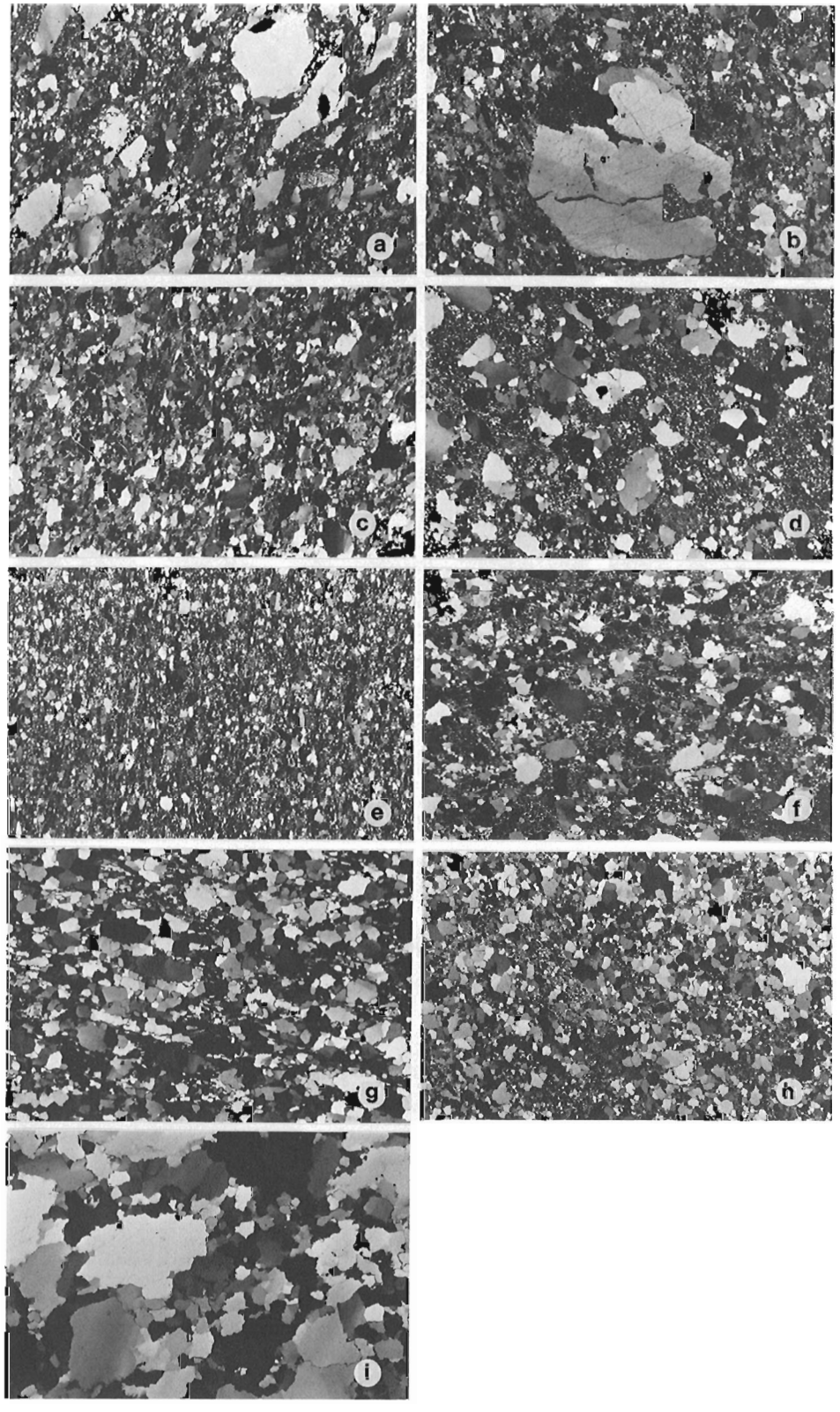

Figure 4. a – c. Compositionally submature metaquartzite from location 3 in the Point Lake supracrustal belt. Photomicrograph 4b shows a large strained quartz grain that has retained some crystal faces and is embayed, possibly indicating a volcanic provenance. Height of field of view is 3.6 mm. d – f. Metaquartzite from the lower, intermediate and upper portion of the basal 314 m of the Beaulieu Rapids Formation in the northern region of its outcrop belt (location 5, Fig. 1). Height of field of view is 3.6 mm. g – i. Compositionally mature metaquartzite from the basal, intermediate and upper portion of the lower 137 m of the Beniah Formation (location 4). Height of field of view is 3.6 mm.

bedded quartz pebble conglomerate with minor beds of pebbly very coarse metaquartzite and rare mudstone (phyllite) drapes. The sharp basal contact of these clast supported conglomerates with the phyllites, combined with the presence of mudstone intraclasts indicates an erosional contact between these units. Clasts within the conglomerate are typically medium to small pebble grade, consisting mainly of subrounded to well-rounded pebbles of quartz, with minor siltstone (phyllitic) intraclasts and rare volcanic pebbles (Fig. 7a).

Pebbly, medium- to very coarse-grained metaquartzites interbedded with the quartz pebble conglomerates are typically massive. Like the orthoconglomerates, they contain minor mudstone intraclasts, and are locally draped by discontinuous mudstone layers up to 1 cm thick. In thin section the metaquartzites appear to have been both quartz arenites and subarkoses. In the latter feldspar grains have been replaced by a mixture of microcrystalline white mica and hornblende.

The conglomerate sequence appears to be overlain by 2 – 5 m of light grey-green weathering, laminated phyllite. This is similar in composition to the unit below the conglomerate and similarly lacks metaquartzite interbeds.

The phyllite sequence is conformably overlain by approximately 10 m of massive, slightly pebbly to pebbly metaquartzite, in planar sets 5 – 60 cm thick, separated by minor units of metaquartzite and phyllite. Local rusty weathering units near the base of the section may include concentrations of up to 8 ppm uranium and 30 ppb gold (Covello et al., 1988). The small to medium pebbles which form 1 – 20 % of the gravelly units are similar to those in the orthoconglomerate. Subrounded polycrystalline quartz clasts predominate with only minor volcanic and granitic clasts. Patches of quartz, mica and hornblende in the matrix of these metaquartzites may represent degraded feldspar and/or volcanic rock fragments. Massive and ripple cross-laminated, very fine- to medium-grained metaquartzites interbedded with the pebble-bearing units appear to be subarkosic.

The pebbly metaquartzite sequence is overlain by, and may grade into, a further 4 – 10 m of variably feldspathic, poorly sorted, medium- to very coarse-grained metaquartzite, characterized by local planar and trough cross-stratification in sets 5 – 50 cm thick (Fig. 7b). This is apparently overlain by at least 3 m of dark grey weathering laminated phyllite with minor linsen of very finegrained metaquartzite (Fig. 7c) which increase in abundance towards the top of the unit.

Conformably overlying the phyllite unit are 6 – 13 m of interbedded feldspathic fine- to very coarse-grained metaquartzite and phyllite. The metaquartzites include massive, plane-laminated and ripple-laminated varieties, most of which occur in graded sets 5 – 30 cm thick (Fig. 7d, e).

The upper 7.5 m of the sequence is dominated by laminated strata of phyllite to very fine grained metaquartzite. Interbedded with these are a few thin beds of ripple laminated very fine grained metaquartzite with local bimodal opposed cross-laminae.

Interpretation

The lithofacies sequence in the basal 137 m of the Beniah Formation (Fig. 5a) is best interpreted as an accumulation of detritus in a middle to outer shelf environment. The absence of conglomerate reflects the lower energy associated with a more distal shelf setting relative to the upper 94 m of the formation (see below). Four genetic units constitute this portion of the formation:

1. Fining-upward couplets of arenite (metaquartzite) and mudstone (phyllite) (Fig. 3d)

The process represented by this genetic association is repetitive waning flows. The presence of these couplets could represent either 1) fortuitous preservation above fair weather wave base in an area of the shelf characterized by reduced ambient energy permitting fines deposition or 2) deposition by return flows, associated with coastal set-down following a storm in a sub-storm wave base position promoting preservation of the fines. The latter interpretation is favoured in this report.

2. Isolated, thin (5-15 cm) horizons of normally graded coarse- to very coarse-grained arenite (Fig. 3e)

The normal grading and coarser grain size associated with these occasional units is interpreted to represent deposition from a waning flow associated with a particularly strong flow event on the shelf, possibly a storm. Preservation of such units suggests deposition below storm wave base.

3. Isolated thick mudstone units

Isolated mudstone units could represent either a lateral facies shift to a region of a shelf characterized by lowered ambient energy or a seaward facies shift to a more distal shelf position significantly below storm wave base. The thickness (2 and 17 m) of the mudstone units favours a distal shelf interpretation.

4. Nonstratified arenite

The absence of primary sedimentary structures in these units is problematical. It could be associated with the transformation of arenite into metaquartzite (but why only these units), or might only be apparent, caused by the absence of fines delineating stratification surfaces. Favouring the latter, these units are considered to represent periods of deposition by weak traction currents in a below fair weather wave base — above storm wave base position on a shelf. The more shoreward, slightly higher energy position (relative to a sub-storm wave-base position suggested for the couplets of arenite and mudstone) would account for the absence of fines as would the occasional reworking of the sediment surface due to storm activity.

With the above interpretations the lithofacies sequence displayed in Figure 5a can be attributed to fluctuations in relative sea level as given below:

Transition	Response
couplets to nonstratified	slight shoaling
couplets to mudstone	slight deepening
nonstratified to mudstone	marked deepening
nonstratified to couplets	slight deepening
mudstone to nonstratified	marked shoaling
mudstone to couplets	slight shoaling

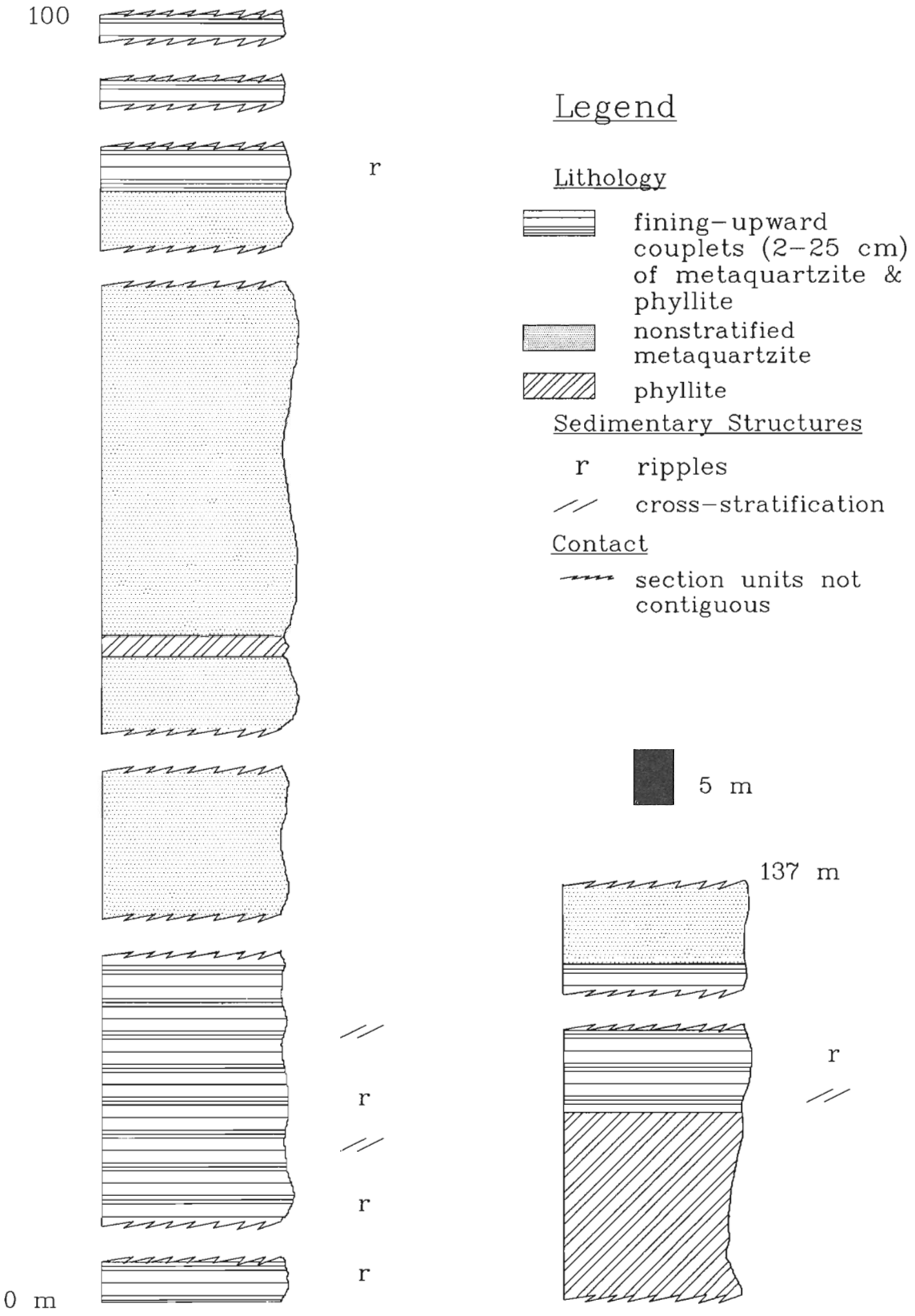

Figure 5. a) Basal 137 m of the Beniah Formation near the southern end of Beniah Lake in the Beaulieu River supracrustal belt (location 4). b) Upper 94 m of the Beniah Foramtion near the southern end of Beniah Lake (location 4).

Strata in the upper 94 m of the sequence are best interpreted as products of deposition on an inner to mid-shelf setting. Laminated mudrocks (phyllites) at the base of the upper sequence reflect deposition on a muddy shelf, below storm wave-base. The absence of flasers in the arenite (metaquartzite) or linsen in the upper part of the mudstone sequence, combined with the evidence for erosion at the base of the overlying quartz pebble conglomerates suggests a period of tectonic uplift or depression of sea level on the shelf. The presence of discontinuous mud drapes within the conglomerate unit suggests deposition in a nearshore, subtidal or intertidal setting.

The high lateral continuity of laminae in the overlying mudstone sequence indicates a return to sub-wave base conditions. A second regressive phase led to deposition of the overlying pebbly arenite sequence in a nearshore shallow marine environment. Deposition of cross-stratified arenites in the upper part of this sequence indicates deposition above storm wave base. A further transgressive phase is indicated by the presence of laminated mudrocks above this sequence. The presence of isolated ripples and discontinuous laminae (linsen) of sand-grade material in the upper part of the sequence suggests the action of storm-induced currents, below normal wave base. Shoaling to within maximum storm wave base is indicated by the presence of graded, laminated to ripple-laminated arenites in the overlying sequence. While no hummocky cross-stratification was observed, the structure sequence is consistent with deposition under waning flow conditions. The presence of abundant laterally continuous mud drapes indicates deposition below normal wave-base, as these would be lost in depths where persistent longshore currents were generated.

The upper 10 m of the sequence appears to reflect a further phase of deepening on the shelf. The few ripple cross-laminated units present indicate minor tidal influence in the form of bimodal opposed cross-lamination.

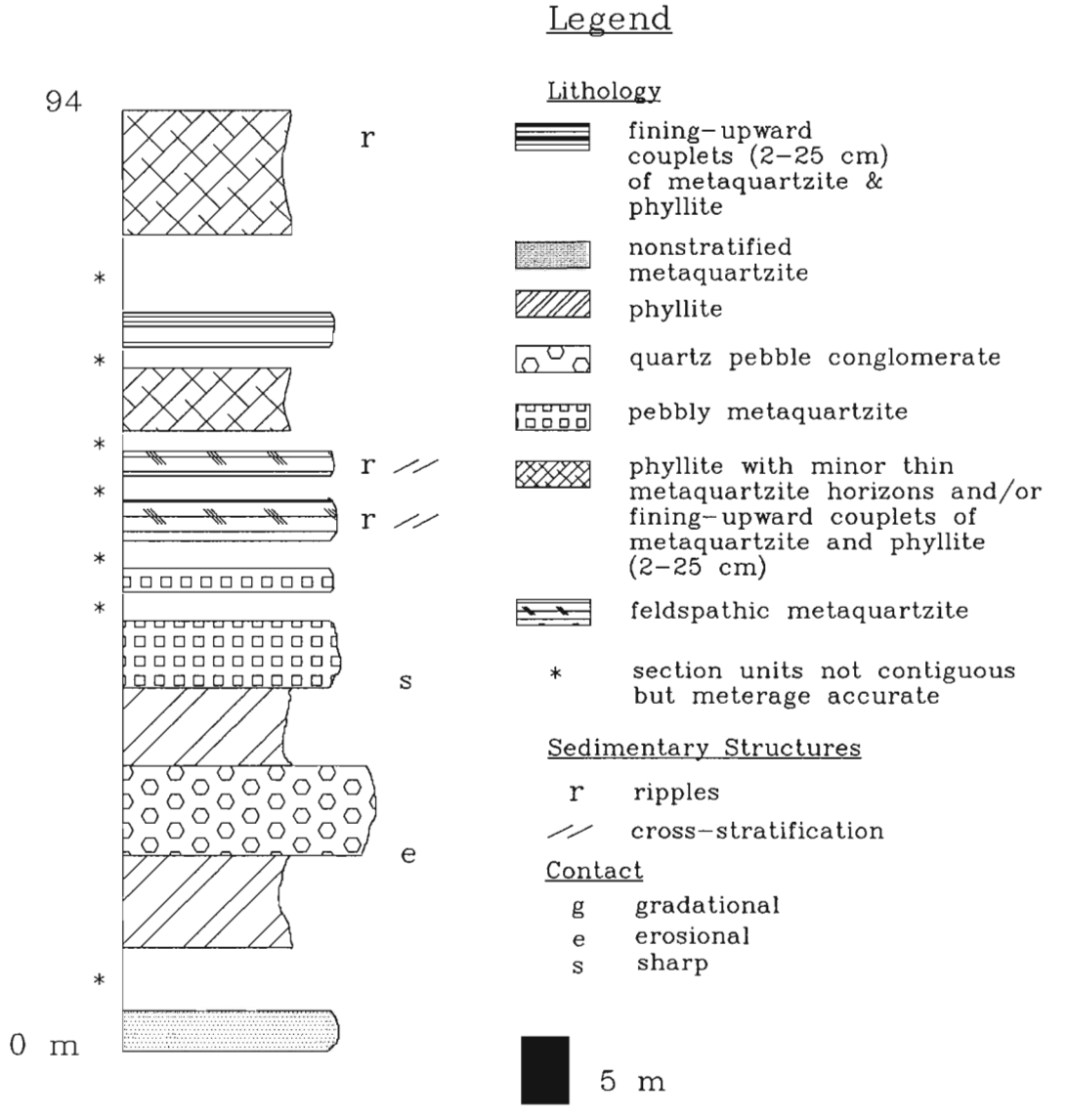

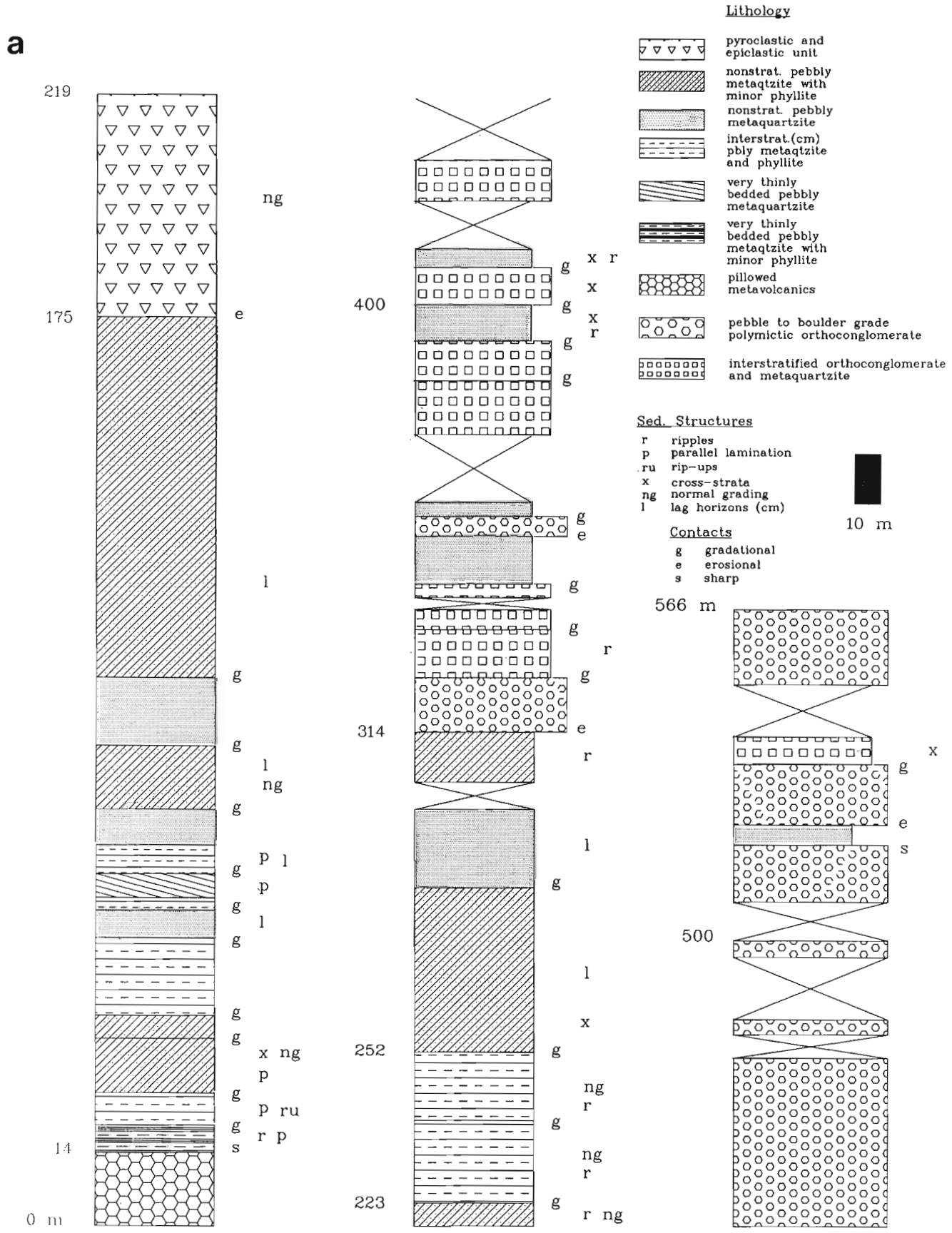

Figure 6. a) The Beaulieu Rapids Formation on the Beaulieu River 30 km south of Beniah Lake in the Beaulieu River supracrustal belt (location 5). b) The Beaulieu Rapids Formation on the Beaulieu River 4 km south of exposures examined for Figure 6a (location 5).

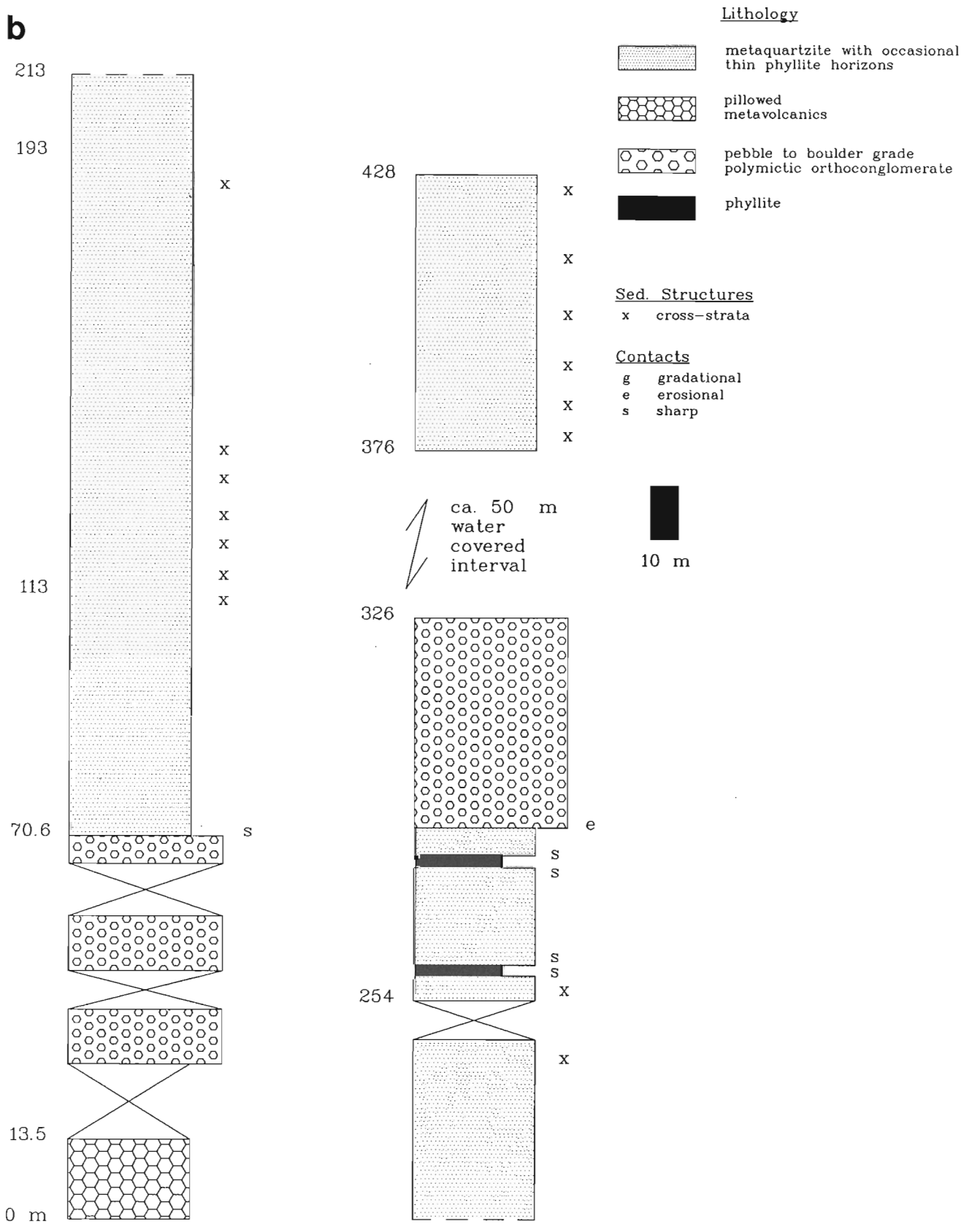
b
213
193
113
70.6
13.5
0 m
428
376
326
254
ca. 50 m water covered interval
10 m
Lithology
metaquartzite with occasional thin phyllite horizons
pillowed metavolcanics
pebble to boulder grade polymictic orthoconglomerate
phyllite
Sed. Structures
x cross-strata
Contacts
g gradational
e erosional
s sharp

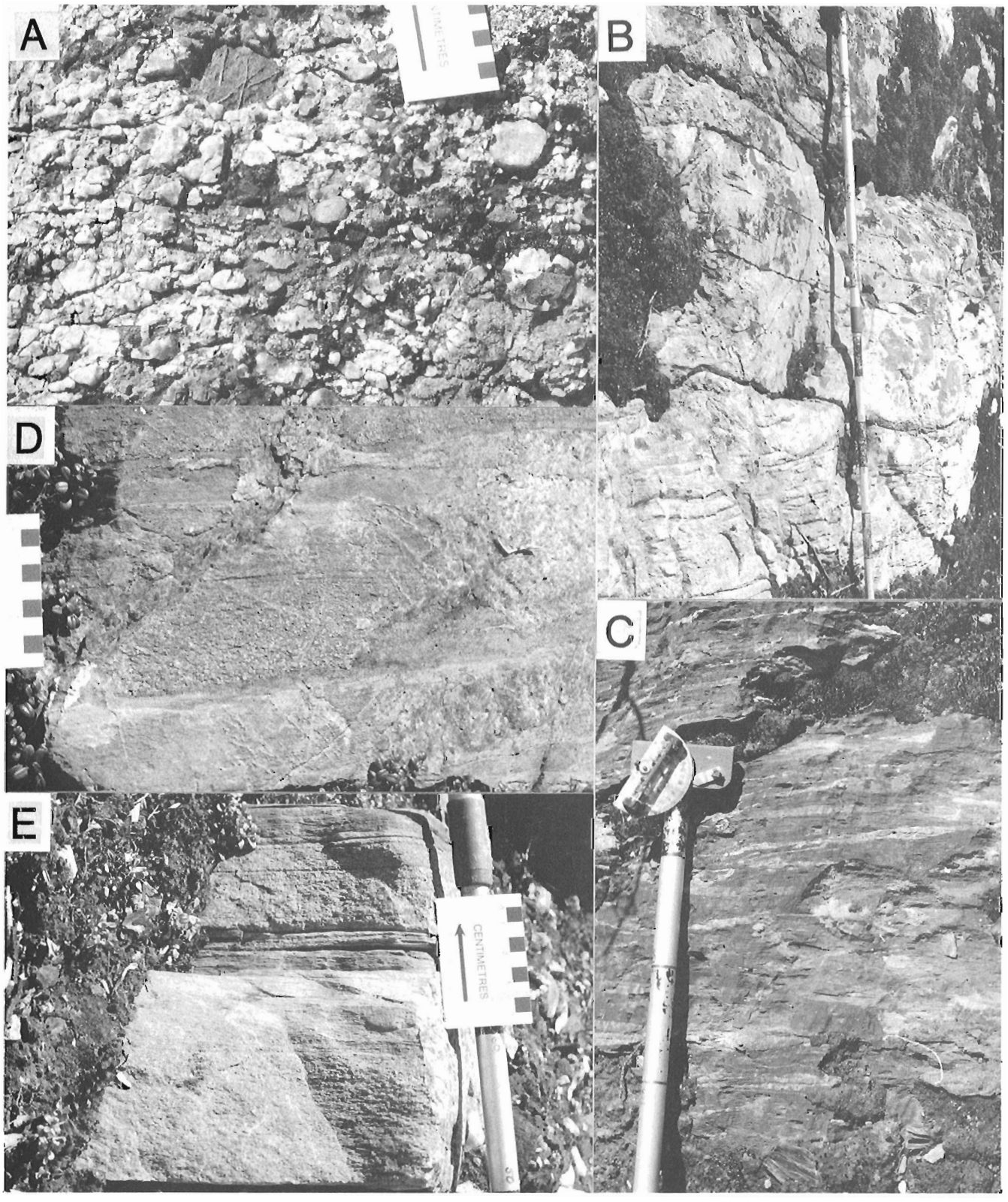

Figure 7. Features from the upper 94 m of the Beniah Formation near the southern end of Beniah Lake in the Beaulieu River supracrustal belt (location 4): a) Medium to large pebble-grade conglomerate unit. Note rounded clasts of quartz (white) and metavolcanic rocks (dark) b) Plane bedded (top) and planar cross-stratified medium-grained sandstone c) Thick-laminated phyllite with arenite linsen d, e) Graded stratified sets of very coarse to fine arenite of probable storm origin.

BEAULIEU RAPIDS FORMATION

Lithological Description

The geological setting of the Beaulieu Rapids Formation, determined from mapping by M. Stubley along an 8 km stretch of the Beaulieu River 30 km south of Beniah Lake, was described in Roscoe et al. (1989). A composite stratigraphic section (Fig. 6) in the latter paper depicts the formation as consisting of ca. 1.3 km of metaquartzite and conglomerate lying unconformably on pillowed metavolcanics (Roscoe et al., 1989, Fig. 6). This location (location 5, Fig. 1) was revisited in 1989 for a more detailed sedimentological evaluation utilizing the structural interpretation of Stubley in Roscoe et al. (1989, Fig. 5). Re-measurement of a northern (Fig. 6a) and southern exposure of the formation (4 km farther south, Fig. 6b) showed it to consist cumulatively of 994 m of metaquartzite, conglomerate and minor phyllite (the uppermost 100 m of Fig. 6 in Roscoe et al. (1989) was not examined).

In the northern part of the outcrop belt 314 m of arenite (metaquartzite) with minor siltstone (phyllite) and volcaniclastics lies between underlying pillowed mafic metavolcanics (unconformable contact) and overlying interstratified arenites and conglomerates (Fig. 6a). This arenite-dominated interval is absent in the southern part of the outcrop belt (Fig. 6b) suggesting significant relief along the unconformity surface. Arenite in this interval is compositionally more mature than that encountered at location 3 in the Point Lake supracrustal belt and slightly less mature than that in the Beniah Formation (Fig. 4d-f). Volcanic lithics are readily identified in hand specimen. The arenites are dominantly medium- to coarse-grained and invariably white weathering whereas weathers pale green to brown. Five lithofacies were identified: 1, 2) nonstratified pebbly arenite with/without minor siltstone laminae 3, 4) very thinly to thinly bedded arenite with (Fig. 3i)/without minor siltstone laminae and 5) centimetre-scale fining-upward couplets of pebbly arenite and rippled siltstone (Fig. 3j). Contacts between the lithofacies are largely gradational. Primary sedimentary structures are uncommon, their identification being difficult due to the presence of three schistosities mapped by Stubley in Roscoe et al. (1989, Fig. 5). Large-scale cross-stratification is absent, only occasional micro-trough cross-lamination attributable to ripple migration is observed. Other less common sedimentary structures include parallel lamination, several centimetres thick normally graded units and lag horizons (Fig. 3g). Clasts in the lag horizons include rounded granule-to pebble-grade quartz and angular (stretched ?) siltstone and mafic, intermediate and felsic volcanic lithics to several centimetres. A dark green weathering, 44 m thick unit of largely volcanogenic origin occurs in the arenite sequence in the northern portion of the outcrop belt (175-219 m, Fig. 6a) and was referred to as a "sharpstone conglomerate" by Roscoe et al. (1989, Fig. 6). Preliminary examination suggests that this unit contains mafic flow(s), epiclastic units dominated by intermediate to felsic volcanic lithics in an apparently non-volcanic matrix and units of combined epiclastic and pyroclastic origin (devitrified glass, rounded quartz clasts and angular volcanic lithics; Fig. 3k).

The erosionally overlying sequence of interbedded polymict, clast-supported, pebble- to boulder-grade conglomerates and pebbly arenites (metaquartzites) thins from 252 m in the north (314-566 m, Fig. 6a), to less than 60 m in the south (13.5-70.6 m, Fig. 6b), where it rests directly on intermediate to mafic metavolcanic rocks without an intervening arenite interval. Most of the conglomerates are sheared and have green-grey weathering colours. In places rusty weathering occurs, perhaps related to the presence of minor sulphides. Prominent rusty weathering is typically associated with shear zones. Conglomeratic units occur in sets from 40 cm to 15 m thick. Most have a contact framework, with subrounded clasts of pebble- to boulder-grade set in a matrix of granular, coarse or very coarse sand grade (Fig. 8a). Matrix-supported varieties are rare. Most beds are massive, although imbrication of mudstone intraclasts was observed in one unit (Fig. 8b). Clasts within the conglomerates include mafic to intermediate volcanic rocks (similar to the local basement), variable amounts of quartz diorite, granodiorite and gneiss and occasional green fuchsitic pebbles. Minor components include quartz and chert. Whereas volcanic clasts predominate (especially in the lower 15 m of the member in the northern part of the outcrop belt), most units are polymict with 20-70 % granitoid clasts and 2-9 % quartz.

Arenite units occur throughout the conglomeratic sequence, being most abundant in the lower half of the member in the northern part of the outcrop belt (Fig. 6a). They are dominated by coarse to very coarse, pebbly and non-pebbly volcanic lithic arenite. These occur as lenticular sets, which can be massive, planar or trough cross-stratified, ripple cross-laminated or plane-bedded (Fig. 8c, d). Minor units of sheared siltstone (phyllite) are present between arenite and conglomerate units in the northern area (400 m level of Fig. 6a). Most are less than 30 cm thick and are highly lenticular (Fig. 8e).

The conglomeratic sequence in the southern part of the outcrop belt is conformably overlain by a 216 m thick sequence of volcanic lithic arenite and feldspathic volcanic lithic arenite, with minor interbeds of siltstone and intraformational conglomerate (Fig. 6b). Arenites near the base of the sequence are typically of medium and fine sand grade. Most beds appear massive, or lack identifiable primary structures due to pervasive shearing but planar and trough cross-stratification in sets 5-80 cm thick are locally conspicuous. Four kilometres farther south (Fig. 6b) a 40 m thick sequence of cobble and boulder conglomerates overlies the arenites with an erosional contact. Clasts in the conglomerate are similar to those in the lower conglomeratic unit, except that no fuchsitic pebbles were noted. The member is dominated by pebbly to cobbly intact framework conglomerates with a matrix of coarse to very coarse volcanic lithic arenite. Interbeds of massive and trough cross-stratified medium and coarse arenite are highly lenticular.

The upper conglomerate member is overlain by at least 100 m of pebbly very coarse-grained arenite and coarse- to very coarse-grained volcanic lithic-rich arkose and feldspathic volcanic lithic arenite. These are characterized by large scale planar and trough cross-stratification up to 1.3 m thick.

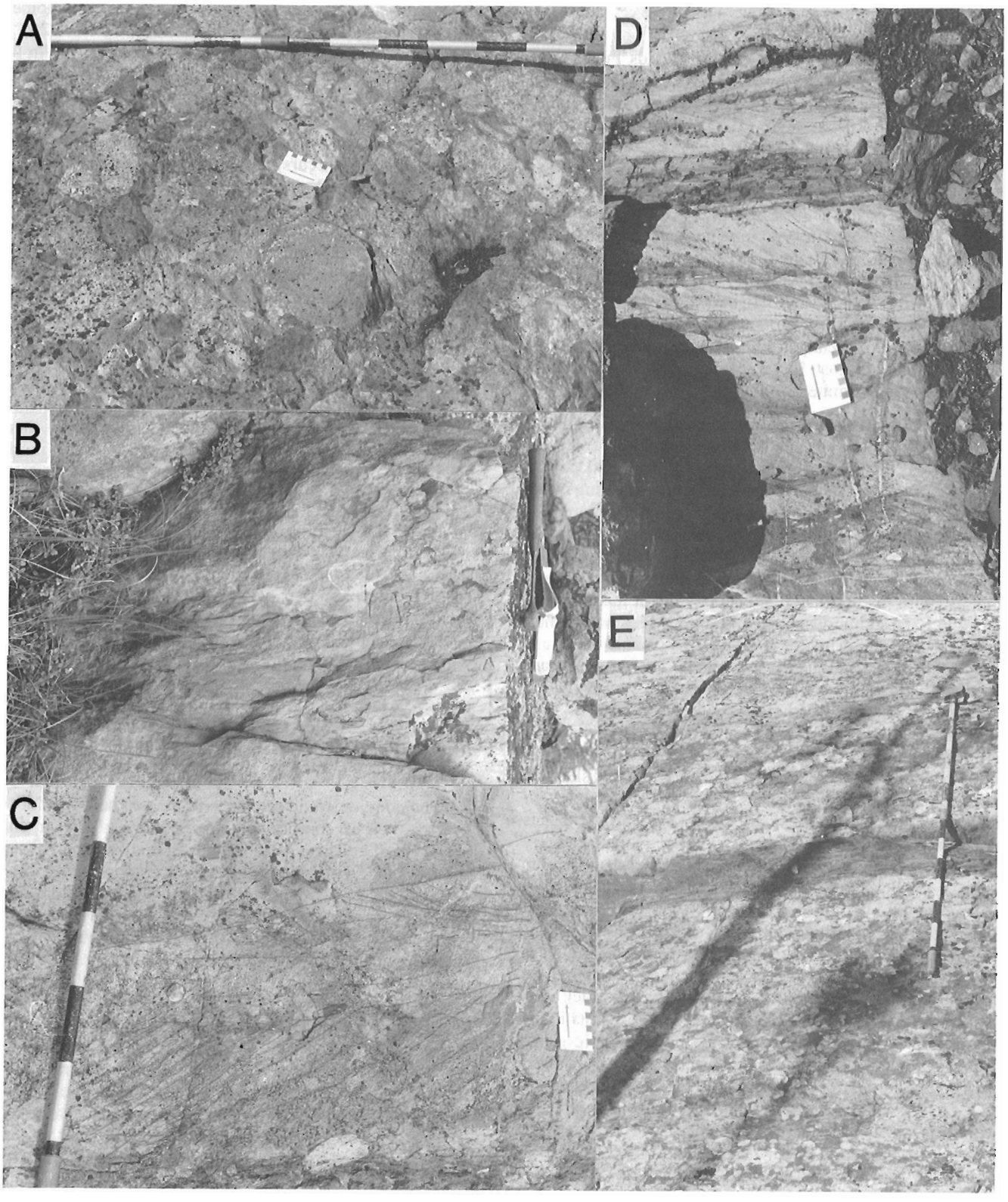

Figure 8. Features of the Beaulieu Rapids Formation from the upper portion (above 314 m) of the northern exposure and from the southern exposure, both located along the Beaulieu River 30 km south of Beniah Lake, in the Beaulieu River supracrustal belt (location 5): a) Clast-supported bouldery cobble conglomerate of alluvial fan origin; lighter clasts — granitoid, darker clasts — volcanic b) Imbricated mudstone cobble conglomerate with granular very coarse sand matrix; apparent flow is eastward c) Planar (base) and trough cross-stratified granular very coarse arenite d) Trough cross-stratified medium- to coarse-grained arenite e) Plane-laminated mudstone interbed between amalgamated sets of bouldery cobble conglomerate.

Gradationally overlying this arenite is a further ca. 100 m of arenite which Roscoe et al. (1989) described as fine grained, massive and thick-bedded with minor quartz clasts.

Interpretation

Arenites and conglomerates in the Beaulieu Rapids Formation appear to have been deposited as part of a subaerial alluvial fan system. Systematic mapping by Stubley (Roscoe et al., 1989, Fig. 5) appears to indicate significant topographic relief at the base of the sequence. This was blanketed by a thick sequence of arenites and conglomerates which was in part derived from a conglomeratic fan system in the northern part of the outcrop belt.

The pebbly arenite sequence at the base of the northern outcrop belt is best interpreted as shallow sheet flood deposits of an ephemeral stream system in the intermediate to distal regions of an alluvial fan, partially analogous to the "Bijou Creek" braided stream profile proposed by Miall (1978).

The sporadic presence of several centimetre-thick fining-upward couplets of pebbly arenite and rippled siltstone (Fig. 3j) suggests periodic deposition in a very distal position on an alluvial fan system.

Evidence that volcanism and tectonic instability were associated with alluvial fan deposition lies in the volcanogenic unit found in this portion of the formation. Such instability would readily account for the transition to conglomerate deposition higher up in the formation.

Conglomeratic strata in the middle and upper parts of the formation are best interpreted as channel fill deposits in the proximal to intermediate region of a wet alluvial fan system, in part analogous to the "Scott Type" of Miall (1978). Lack of abundant matrix-supported conglomerates indicates that debris flows were not important in shaping facies architecture.

The abundance of cross-stratification in arenite interbeds within the conglomerate sequences, and in the overlying arenite-dominated sequences indicates the importance of traction currents. The progressive up-section decrease in grain size of arenites in the sequence overlying the lower conglomerate member suggests deposition in more distal fan or braided stream settings analogous to the "Platt type" of Miall (1978). Minor mudstone (phyllite) interbeds in these sequences could have accumulated in broad shallow channels or local floodponds on the fluvial plain.

Reactivation of the fan system is indicated by the presence of the upper conglomerate unit. Arenites in the unit above this were deposited in braided rivers dominated by straight- to sinuous-crested bars. It is not certain if these indicate distal fan deposits, or the deposits of a trunk stream system.

PALEOPLACERS (CONCENTRATIONS OF GOLD WITH HEAVY MINERALS)

Clearly the Beaulieu Rapids Formation, interpreted to have been deposited mainly on a subaerial alluvial fan, would be considered favourable for paleoplacer exploration even if it were not known to host the small, slightly auriferous, slightly uraniferous, pyritic heavy mineral concentrations reported by Roscoe et al. (1989). Arenites in the formation are much less mature, however, than those in major paleoplacer hosts and unfavourable limited source weathering is also reflected in an abundance of polymictic conglomerates and scarcity of oligomictic (quartz pebble) beds.

Quartz arenite and occurrences of significant beds of quartz pebble conglomerates in the Beniah Formation reflect mineralogical maturities and provenance weathering akin to those of Witwatersrand paleoplacer hosts. The shelf depositional environment attributed to the studied section, however, is less favourable for the development of economically significant paleoplacers. Elsewhere, however, it is possible that the formation may contain units deposited in more favourable proximal environments. This may be the case in the sections 3 km northwest and along the west shore of Beniah Lake that contain thin lenses of radioactive pyritic oligomict conglomerate (Roscoe et al., 1989). On the other hand, scattered outcrops of the formation 3 km south of Beniah Lake (D. Roach, personal communication, 1989) and 9 to 30 km north of Beniah Lake provide no hints of the possible presence of favourable environments for paleoplacers.

The metasedimentary rocks studied near Newbigging Lake were evidently deposited in a submarine fan system and do not warrant prospecting for paleoplacers. They are the least mature clastic metasediments found in any of the three successions. No concentrations of detrital heavy minerals were identified in them.

ACKNOWLEDGMENTS

This study benefited from discussions in the field with Mike Stubley and Dan Roach. Financial support for R. Rice was provided through Natural Sciences and Engineering Research Council of Canada grant A5536 to J.A. Donaldson, Department of Geology, Carleton University and also contract YK-89-90-013 between J.A. Donaldson and Indian and Northern Affairs Canada. Funding for W.K. Fyson was provided by contract YK-89-90-008 with Indian and Northern Affairs Canada. Financial support for D. Long was provided by Natural Sciences and Engineering Research Council of Canada grant A8456. Expediting services were provided by Rod Stone, out of Yellowknife, under contract with the Geological Survey of Canada.

REFERENCES

Covello, L., Roscoe, S.M., Donaldson, J.A., Roach, D., and Fyson, W.K.
1988: Archean quartz arenite and ultramafic rocks at Beniah Lake, Slave Structural Province, N.W.T.; *in* Current Research, Part C, Geological Survey of Canada, Paper 88-1C, p. 223-232.

Fraser, J.A.
1968: Geology of Winter Lake, District of Mackenzie; Geological Survey of Canada, Map 1219A with marginal notes.

Mial, A.D.
1978: Lithofacies types and vertical profile models in braided river deposits: a summary; *in* Fluvial Sedimentology, ed. A.D. Miall; Canadian Society of Petroleum Geologists, Memoir 5, p. 597-604.

Minter, W.E.L.
1981: Examples that illustrate sedimentological aspects of the Proterozoic placer model on the Kaap-Vaal Craton, Witwatersrand, South Africa; *in* Genesis of Uranium-and Gold-bearing Precambrian Quartz-pebble Conglomerates, ed. by F.C. Armstrong; United States Geological Survey, Professional Paper 1161-A-BB.

Roscoe, S.M.
1981: Temporal and other factors affecting deposition of uraniferous conglomerates; *in* Genesis of Uranium- and Gold-bearing Precambrian Quartz-pebble Conglomerates, ed. F.C. Armstrong; United States Geological Survey, Professional Paper 1161-A-BB, p. W1-W17.

Roscoe, S.M., Stubley, M., and Roach, D.
1989: Archean quartz arenites and pyritic paleoplacers in the Beaulieu River supracrustal belt, Slave Structural Province, N.W.T.; *in* Current Research, Part C, Geological Survey of Canada, Paper 89-1C, p. 199-214.

Stockwell, C.H.
1933: Great Slave Lake-Coppermine River area, Northwest Territories; Geological Survey of Canada, Summary Report 1932, Part C, p. 37-63.

Classification and interpretation of the shapes and surface textures of gold grains from till on the Canadian Shield

R.N.W. DiLabio
Terrain Sciences Division

DiLabio, R.N.W., Classification and interpretation of the shapes and surface textures of gold grains from till on the Canadian Shield; in Current Research, Part C, Geological Survey of Canada, Paper 90-1C, p. 323-329, 1990.

Abstract

Scanning electron microscopy has been used to examine gold grains from till from eight localities in order to design a classification scheme for the shapes and surface textures of gold grains. The classification is meant to be simple and graphic - to aid in describing grains. Three main classes of shapes are recognized: pristine, modified, and reshaped. They from a progression from undamaged grains to ones that retain none of their original features. This progression probably represents increasing distance from the bedrock source of the gold, which should assist drift prospecting.

Résumé

La microscopie électronique par balayage a été utilisée pour analyser des grains d'or provenant de till de huit localités, afin d'établir une méthode de classification des formes et des textures superficielles des grains d'or. Cette classification se veut simple et graphique, afin de faciliter la description des grains. Trois classes principales de formes ont été déterminées: pristine, modifiée et refaçonnée. Elles représentent une progression allant de grains non endommagés à des grains ne conservant aucune de leurs caractéristiques originelles. Cette progression correspond probablement à une augmentation de la distance du socle d'origine de l'or et pourra, de ce fait, faciliter la prospection des gisements alluvionnaires.

INTRODUCTION

Since the widespread adoption of drift prospecting in the search for gold deposits, several tens of thousands of till samples have been processed to recover heavy minerals by shaking table, heavy liquid separation, and panning technology (Averill, 1988). In addition to preparing the samples for geochemical analysis, this method permits direct inspection of ore minerals in the heavy concentrates. Inspection of gold grains, in particular, is done to estimate the distance that the grains have been transported from their bedrock source, by observing the degree of rounding, polishing, and bending of the grains. Virtually all these observations have been made using a binocular microscope, which has limited the size of grain and surface feature that could be resolved.

The dominance of silt- and clay-sized gold in Canadian gold deposits and the tills derived from them (DiLabio, 1985, 1988; Shelp and Nichol, 1987; Averill, 1988; Brereton et al., 1988) has prompted laboratories to improve recovery rates for fine gold, mainly by modifying the procedures used with the shaking table and by making slight changes to the design of the table itself. Gold grains that are too small to see on the surface of the table are isolated by panning the heavy mineral concentrate. When examined with a binocular microscope, however, fine gold grains are not seen clearly. In the present study, scanning electron microscopy (SEM) has also been employed, taking advantage of the higher depth-of-field even at high magnification of the SEM (compared to light microscopy) to view the shapes and surface textures of gold grains in greater detail. A scanning electron mircroscope equipped for backscattered electron imaging (BEI) and energy-dispersive spectrometry has the added advantage of discriminating among the ore, gangue, and secondary minerals that may be present; it can also analyze their compositions. In BEI, a phase with a high average atomic number (e.g., gold) appears bright white, and most other phases appear in shades of dull grey. This high contrast allows one to see the true shape and texture of the gold, even where coatings and other minerals partly obscure the gold in normal secondary electron imaging. These SEM observations allow the analyst to interpret the mineralogy and texture of the source mineralization and to infer the transport and weathering history of the gold grains.

Existing classification schemes for the morphology of detrital gold were developed mainly for gold from unglaciated terrain (Hérail, 1984; Freyssinet et al., 1989). The only scheme that is specific to glaciated terrain was devised by S.A. Averill, and is based on many years of binocular microscope examination of grains from till (Averill and Zimmerman, 1986; Sopuck et al., 1986; Averill, 1988; Grant et al., 1989). The new scheme presented here is based on Averill's, but is not intended to replace it. The cost of scanning electron microscopy will restrict the commercial use of this scheme to exceptional cases; however, it may be possible to substitute a powerful optical microscope for the SEM.

In order to make the study representative of different styles of mineralization and different areas of Canada, archived and donated till samples from eight localities were examined. The localities are: Waverley, Nova Scotia; Eastmain River, Quebec; Matachewan, Ontario; Onaman River, Ontario; Beardmore-Geraldton, Ontario; Manigotagan, Manitoba; Wheatcroft Lake, Manitoba; and Yathkyed Lake, District of Keewatin. The suite includes samples from gold-rich dispersal trains and trains containing only rare gold grains. Most of the samples are from shallow test pits and are the oxidized C horizon of soil developed on till. Samples were prepared by shaking table and panning methods; the resulting heavy mineral concentrates were scanned under a binocular microscope and any gold grains were picked out and mounted on adhesive-coated SEM stubs, then carbon-coated, and examined and photographed with an SEM. Electron microprobe analyses of most of the grains have also been completed and will be reported in a future paper.

CLASSIFICATION SCHEME

The scheme (Table 1) is designed to be nongenetic and graphically descriptive, so that someone reading grain descriptions would be able to visualize the variety of shapes and surface textures present in a sample. The vast number of morphological terms that have been applied to detrital gold grains (Boyle, 1979; Hérail, 1984; Freyssinet et al., 1989) has made it difficult to choose terms that are the most useful. The most commonly used were chosen first and a few particularly vivid ones were added. Terms should be used in combination to describe grains as clearly as possible. This is not meant to imply that the classification is complete; users are encouraged to add terms that are suitable. The main shape types and surface textures are described below.

Table 1. Classification of shapes and surface textures of gold grains in till.

Class	Shape	Surface Texture
Pristine	- block - rod - wire - leaf - crystal - star - globule	- smooth surfaces - angular edges - grain moulds clearly visible - thin edges not curled - some striae
Modified	- all shapes, damaged	- pristine shapes visible - leaf edges and wires bent - blunted and thickened edges - grain moulds preserved where protected - moderately striated - felty texture where damaged
Reshaped	- folded rod, wire, flake - rounded block - typical discoid placer flake - nugget	- pristine shapes destroyed - well rounded grain outline - moderately striated - porous, scaly, felty, or spongy

Terms that would describe secondary or supergene gold have been omitted because of the rarity of such grains in till (Warren, 1982; MacEachern and Stea, 1985), although the classification could be expanded in the future to accommodate new terms to describe secondary gold.

Pristine

The pristine class of grains is analogous to the "delicate" class of Averill (1988), but the new name has been used because many pristine grains are not delicate in appearance at all, being robust blocky shapes. The term "fresh" could be substituted for pristine in most cases, but the term "primary" is avoided because of the possibility that some gold crystals are secondary authigenic precipitates in weathered till (Warren, 1982). Euhedral dodecahedral gold crystals (Fig. 1A) were found in one sample, and at first they were believed to be authigenic. Later, similar crystals were observed in fluid inclusions in vein quartz at the Tangier mine in Nova Scotia (Smith and Kontak, 1988) and the Sigma mine in Quebec (Robert and Kelly, 1987), so crystals in till cannot be assumed to be authigenic.

Grains in this class appear not to have been damaged in glacial transport. The most impressive shapes in the group are the angular wires or rods and the delicate leaves that obviously were fracture fillings or grain boundary films in the mineralized rock (Fig. 1B-H). Equant grains such as blocks, blebs, and globules are common, and they do not appear to be pristine until they are viewed at high magnification. All grains in this class retain primary surface textures such as crystal faces or grain molds, which probably held sulphide or gangue minerals that have been broken out or weathered out of the gold. They have smooth surfaces that are bright in reflected light and have surface roughness of the order of 0.1 μ m or less.

The surprising feature of the pristine grains is their abundance. Most samples contained a few pristine grains, and samples collected close to mineralized bedrock are flooded by this type of grain. It is possible, of course, for pristine grains to have weathered out of a carbonate- or pyrite-rich host clast that was glacially transported a great distance, giving a false impression of the nearness of a sample site to mineralized bedrock. This type of problem can be evaluated by comparison of the suspect data to those from nearby sites, and by resampling the original site.

Modified

In the modified class of grains, the original grain shapes are still visible, but all edges and protrusions have been damaged and appear curled, crumpled, blunted, clubbed, and bent, presumably through grain-to-grain impact and abrasion during transport (Fig. 2A-D). Damaged surfaces have a felty texture, having lost their original smoothness. Grain moulds and other primary surface features are preserved only where they were protected in concavities in the grains (Fig. 2E-F).

Although present on some pristine grains, striae (Fig. 2g,h) are much more common on modified ones (Fig. 2G, H). The striae are inferred to be glacial in origin; only in a few cases could the striae have been formed during sample collection (e.g., drill-induced abrasion) or processing. Most artificial striae were formed during mounting of the grains, when excessive pressure with a probe scratched the topmost part of the grains. Tectonic striae have also been ruled out because the striae are found in isolated patches on grain protrusions and not on whole sides of grains, and because they form randomly oriented overlapping sets, not consistently oriented sets. The striae are 1.0 to 0.1 μm across and appear in sets that give the surfaces the appearance of spread butter or wax. The striae probably were not cut by individual grains in the 1.0 to 0.1 μm size range, but were cut by the surface roughness of larger grains, which would account for the extremely small size of the striae.

Striated gold grains are strong evidence of glacial transport, but inferring an absolute distance of transport from them is difficult. It is safe to say that where such grains are abundant (well above local background abundance), the bedrock source should be up-ice and "nearby", probably within a few hundred metres to a few kilometres. Of course, where striated pristine grains are abundant, the source should be closer. Based on data from three localities, samples containing >90 % pristine grains were collected within 200 m of their sources.

Reshaped

Reshaped grains retain none of their pristine shapes or textures. Most have a rounded outline. The term rounded is used here solely to denote the silhouette of the grains and it does not necessarily imply abrasion rounding in the sedimentological sense. Many are simple rounded blocks and others can be seen to be repeatedly folded leaves, wires, and rods. The end-product shape of reshaped grains seems to be the classic placer flake, a flat or toroidal disc (Fig. 3A-D). Classic "nuggets" are placed in this group, although some retain enough primary surface textures in recesses to warrant their inclusion in the modified group.

The surface of these grains is characteristically scaly or felty, presumably from abrasion. Some of them are riddled with fine pores about 0.1 μm in diameter. The most porous have a spongy appearance. Electron microprobe analysis of polished sections of the porous grains show that a porous rim of high fineness gold, usually 1 to 5 μm thick, surrounds a massive core of primary gold that contains significant silver. The leaching of silver from the rim, not the secondary precipitation of gold, is indicated by the presence of pores through glacially striated surfaces, because the striae would have been obscured by secondary gold. The silver-depleted rim on placer gold grains is well known (Desborough, 1970; Giusti, 1986; Knight and McTaggart, 1986); these results indicate that silver removal has been going on rapidly during the 10 000 years or so that the tills have been weathering, if one assumes that the striae are late glacial and the pores are Holocene in age. The destruction of primary surface textures by silver leaching might make it difficult to recognize pristine or modified grains, but the survival of striated surfaces indicates that most original surface textures will be visible on grains that have been weathered.

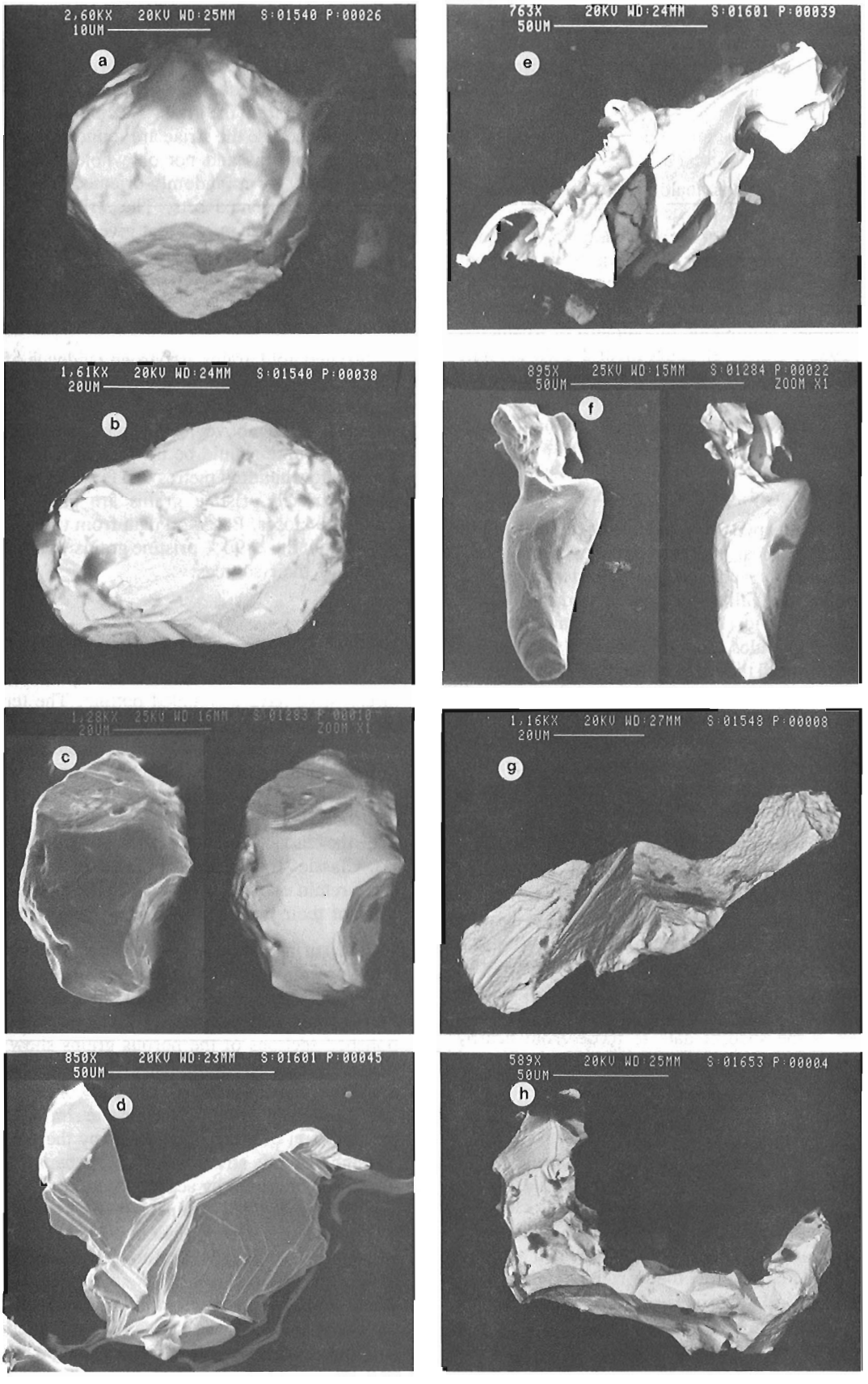

Figure 1. Pristine gold grains. Scale bar in μm at top of each photo.

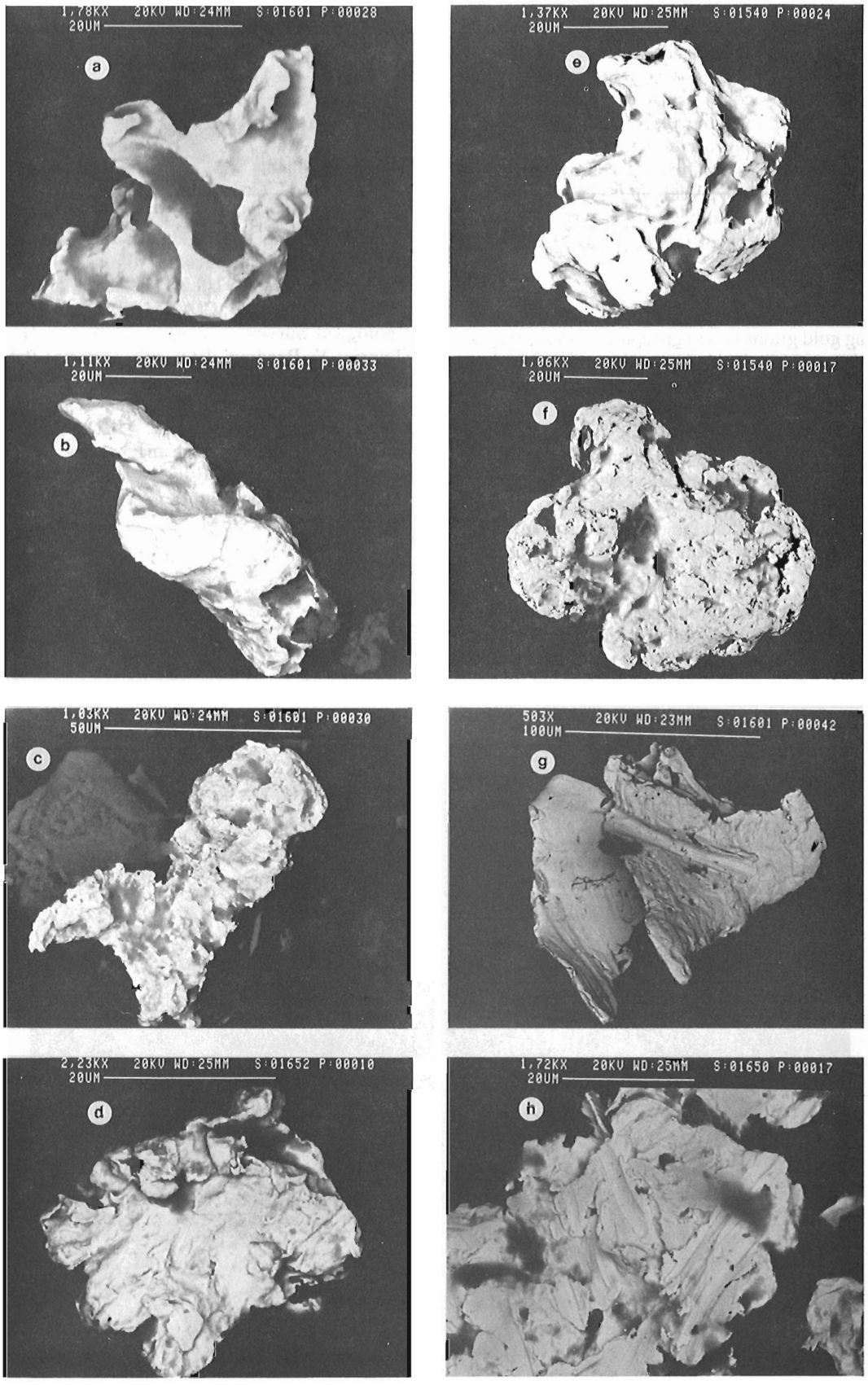

Figure 2. Modified gold grains. Scale bar in μm at top of each photo.

Reshaped grains are present in small numbers in many of the samples processed for this study. According to Averill (1988), they are the "background" detrital gold that is essentially ubiquitous in surficial sediments. The history of these grains and their ultimate source are usually difficult to estimate, because they could have been recycled many times over a long period, even the entire Quaternary. They can be problematic where they are found in large numbers, as happened in the Munro esker, Ontario, where gold grains were concentrated by glaciofluvial and glaciolacustrine action into small placers that have no discrete, known sources (Ferguson and Freeman, 1978, p.167, 171).

Discussion

The classification scheme given in Table 1 is intended as an aid in describing gold grains and in grouping them into types that represent the stages in the history of the grains. Moving from pristine to reshaped should represent increased distance of transport, so the relative proportions of the types should indicate nearness to the bedrock source, at least qualitatively (Averill, 1988). When the number of grains in each sample is large, say about 100 at a typical frequency of > 10/kg, then the counting statistics should be representative enough to be reliable, and the mapped distribution of gold abundances can be used directly as a guide to mineralized bedrock.

This classification does not prejudge the issue of the possible supergene origin of large, globular or smooth, ovoid nuggets that have been found in Canada's glaciated terrain. It is aimed more at assisting communication and at interpreting distances of glacial transport.

A French version of this classification is being prepared by the staff of Consorminex, Inc., Gatineau, Quebec.

ACKNOWLEDGMENTS

The author thanks S.A. Averill (Overburden Drilling Management, Ltd., Ottawa) for suggesting the study of gold grain shapes and for commenting on the manuscript. Overburden Drilling Management and Consorminex, Inc., Gatineau, Quebec, processed the samples. Samples were donated for this study by: E. Nielsen, Manitoba Department of Energy and Mines; C.A. Kaszycki and L.H. Thorleifson, Geological Survey of Canada; E.H. van Hees, Timmins, Ontario; K. Reading, Thornhill, Ontario; R.H. McMillan, Westmin Resources, Toronto; and E. Dillman, Mississauga, Ontario. L.H. Thorleifson made several valuable comments on the manuscript. M.E. Villeneuve and D.A. Walker commented on the manuscript and performed the scanning electron microscopy at the Geological Survey of Canada; this project would not have been possible without their work on the SEM.

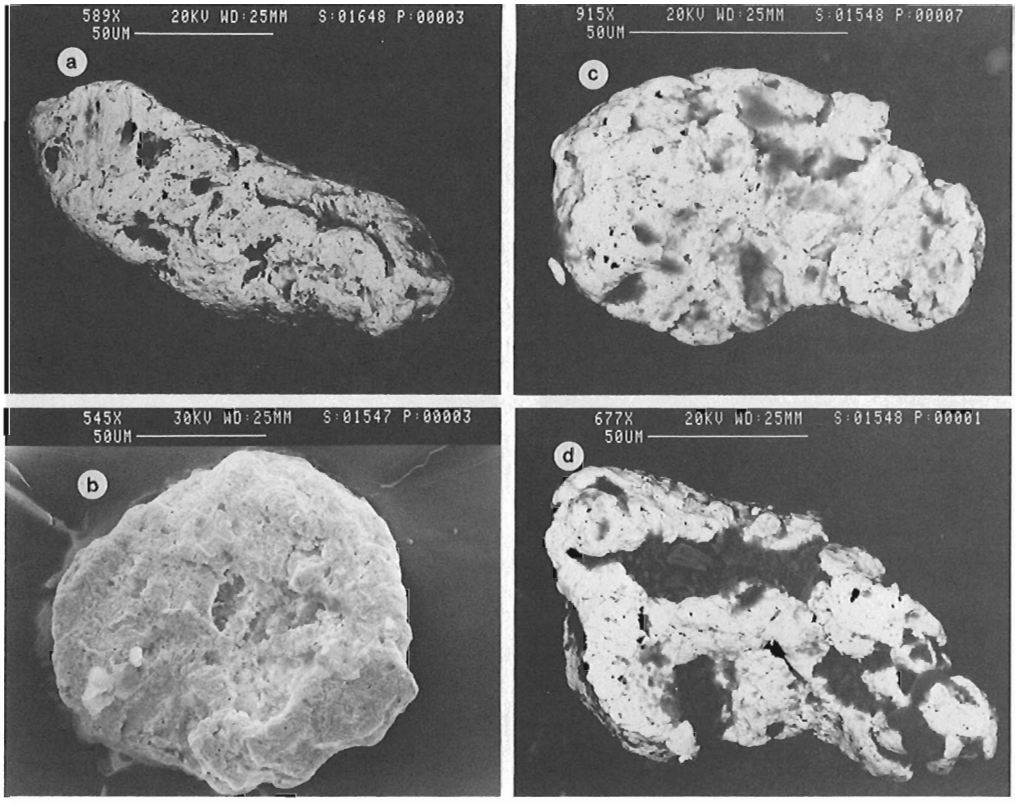

Figure 3. Reshaped gold grains. Scale bar in μm at top of each photo.

REFERENCES

Averill, S.A.
1988: Regional variations in the gold content of till in Canada; *in* Prospecting in Areas of Glaciated Terrain — 1988; D.R. MacDonald and K.A. Mills (ed.); Canadian Institute of Mining and Metallurgy, p. 271-284.

Averill, S.A. and Zimmerman, J.R.
1986: The Riddle resolved: the discovery of the Partridge gold zone using sonic drilling in glacial overburden at Waddy Lake, Saskatchewan; Canadian Geology Journal of the Canadian Institute of Mining and Metallurgy, v. 1, p. 14-20.

Boyle, R.W.
1979: The geochemistry of gold and its deposits; Geological Survey of Canada, Bulletin 280, 584 p.

Brereton, W.E., Briggs, D.N., and Rollinson, J.P.
1988: Till prospecting in the area of the Farley Lake gold deposits, northwestern Manitoba, Canada; *in* Prospecting in Areas of Glaciated Terrain - 1988; D.R. MacDonald and K.A. Mills (ed.); Canadian Institute of Mining and Metallurgy, p. 225-239.

Desborough, G.A.
1970: Silver depletion indicated by microanalysis of gold from placer occurrences, western United States; Economic Geology, v. 65, p. 304-311.

DiLabio, R.N.W.
1985: Gold abundances vs. grain size in weathered and unweathered till; *in* Current Research, Part A; Geological Survey of Canada, Paper 85-1A, p. 117-122.
1988: Residence sites of gold, PGE, and rare lithophile elements in till; *in* Prospecting in Areas of Glaciated Terrain — 1988; D.R. MacDonald and K.A. Mills (ed.); Canadian Institute of Mining and Metallurgy, p. 121-140.

Ferguson, S.A. and Freeman, E.B.
1978: Ontario occurrences of float, placer gold, and other heavy minerals; Ontario Geological Survey, Mineral Deposits Circular 17, 214 p.

Freyssinet, Ph., Zeegers, H. and Tardy, Y.
1989: Morphology and geochemistry of gold grains in lateritic profiles of southern Mali; Journal of Geochemical Exploration, v. 32, p. 17-31.

Giusti, L.
1986: The morphology, mineralogy, and behaviour of "fine-grained" gold from placer deposits of Alberta: sampling and indications for mineral exploration; Canadian Journal of Earth Sciences, v. 23, p. 1662-1672.

Grant, A.H., Lavin, O.P., and Nichol, I.
1989: The morphology and chemistry of transported gold grains as an exploration tool (abstract); Abstracts, XIII International Geochmeical Exploration Symposium, p. 158-159.

Hérail, G.
1984: Géomorphologie et gîtologie de l'or détritique, piémonts et bassins intramontagneux du nord-ouest de l'Espagne; Centre National de la Recherche Scientifique, Paris, 456 p.

Knight, J. and McTaggart, K.C.
1986: The composition of placer and lode gold from the Fraser River drainage area, southwestern British Columbia; Canadian Geology Journal of the Canadian Institute of Mining and Metallurgy, v. 1, no.1, p. 21-30.

MacEachern, I.J. and Stea, R.R.
1985: The dispersal of gold and related elements in tills and soils at the Forest Hill gold district, Guysborough County, Nova Scotia; Geological Survey of Canada, Paper 85-18, 31 p.

Robert, F. and Kelly, W.C.
1987: Ore-forming fluids in Archean gold-bearing quartz veins at the Sigma mine, Abitibi greenstone belt, Quebec, Canada; Economic Geology, v. 82, p. 1464-1482.

Shelp, G.S. and Nichol, I
1987: Distribution and dispersion of gold in glacial till associated with gold mineralization in the Canadian Shield; Journal of Geochemical Exploration, v. 28, p. 315-336.

Smith, P.K and Kontak, D.J.
1988: Meguma gold studies II: vein morphology, classification, and information, a new interpretation of "crack-seal" quartz veins; *in* Mines and Minerals Branch, Report of Activities, 1987, Part B; Nova Scotia Department of Mines and Energy, Report 88-1, p. 61-76.

Sopuck, V.J., Schreiner, B.T., and Averill, S.A.
1986: Drift prospecting for gold in the southwestern Shield of Saskatchewan, Canada; *in* Prospecting in Areas of Glaciated Terrain — 1986; Institution of Mining and Metallurgy, London, p. 217-240.

Warren, H.V.
1982: The significance of a discovery of gold crystals in overburden; *in* Precious Metals in the Northern Cordillera; Association of Exploration Geochemists, Special Publication No. 10, p. 45-51.

Évidences d'un écoulement glaciaire sud, antérieur à l'écoulement sud-ouest du Wisconsinien supérieur, région de Chapais, Québec

G. Prichonnet[1] et L. M. Beaudry[1]
Division de la science des terrains

Prichonnet, G., et Beaudry, L.M., Évidences d'un écoulement glaciaire sud, antérieur à l'écoulement sud-ouest du Wisconsinien supérieur, région de Chapais, Québec; dans Recherches en cours, Partie C, Commission géologique du Canada, Étude 90-1C, p. 331-338, 1990.

Résumé

Un nouvel écoulement glaciaire du nord vers le sud a été identifié dans la région de Chapais, au sud-est de la baie James. Cet écoulement est clairement situé entre les écoulements vers le sud-est (ESE puis SE et enfin SSE) et vers le sud-ouest. Il faut en déduire que les centres de dispersion ou les lignes de partage des glaces se sont déplacées, dans le sens horaire, depuis un secteur situé au sud de la baie James vers le Nouveau Québec. Ces mouvements glaciaires peuvent être rattachés à l'évolution du dernier inlandsis du Wisconsinien. Les nouvelles données de terrain recueillies semblent montrer que la région est un secteur-clé pour la compréhension des événements reliés à l'englaciation et à la déglaciation du Wisconsinien supérieur, et en particulier pour mieux situer les lignes de partage des glaces ou leurs dômes.

Abstract

A new ice flow direction from the north to the south has been identified in the Chapais region, southeast of James Bay. This flow direction is clearly situated between the ice movements toward the southeast (ESE, then SE and finally SSE) and those toward the southwest. We must conclude from this that the dispersal centres or ice divides shifted in a clockwise direction from a sector south of James Bay toward New Quebec. These ice movements may be linked to the evolution of the last Wisconsinan ice sheet. The new field data seem to suggest that this region is a key sector in understanding the events related to glaciation and deglaciation during the Late Wisconsinan, particularly in locating the ice divides and domes.

[1] Département des sciences de la Terre, Université du Québec à Montréal, Montréal (Québec)

INTRODUCTION

La région de Chibougamau-Chapais a connu un développement économique intensif depuis les années 50, grâce à l'exploration minérale et à l'exploitation forestière. Un meilleur accès au territoire a favorisé, entre autres, une meilleure connaissance des phénomènes géologiques du Quaternaire: en particulier, l'un des faits majeurs de mieux en mieux établis est le mouvement glaciaire NE-SO, responsable de l'érosion et du fuselage général des terrains dans la même direction (Mawdsley, 1936; Norman, 1938; Ermengen, 1957; Ignatius, 1958; Prest et coll., 1968; Martineau, 1984; Prichonnet et coll., 1984, fig. 3; Bouchard et Martineau, 1985, fig. 2).

Un travail de cartographie régionale a été réalisé par le ministère de l'Énergie et des Ressources du Québec entre 1982 et 1985. Il a permis de mettre en évidence de nombreuses preuves d'un écoulement NO-SE, antérieur au mouvement SO (Martineau et coll., 1984; Bouchard et Martineau, 1984, 1985; Prichonnet et coll., 1984 ; de Corta,1988). Près de la ligne de partage des eaux, au sud-est et au sud de Chibougameau, on a pu relever également de nombreuses preuves d'un écoulement "tardiglaciaire" vers le sud (de Corta et Prichonnet, 1986; de Corta, 1988). Cet écoulement semble lié à l'influence du relief; en effet, ses traces sont identifiées essentiellement dans le secteur de la ligne de partage des eaux et à l'est de celle-ci, aux endroits où la topographie s'incline vers le sud-est. De plus ce mouvement est bien le dernier à avoir eu lieu.

La présente note a pour objectif de signaler, pour la première fois semble-t-il, l'existence d'un écoulement glaciaire N-S, intermédiaire aux mouvements NO-SE et NE-SO, et d'en discuter la signification; ce mouvement est bien représenté dans la région de Chapais, à l'ouest du secteur de Chibougamau (fig. 1).

Du point de vue méthodologique, on a insisté sur l'identification des troncatures et sur l'étude des stries laissées à proximité des troncatures ou sur les surfaces protégées. Les localités les plus significatives sont reportées au tableau 1.

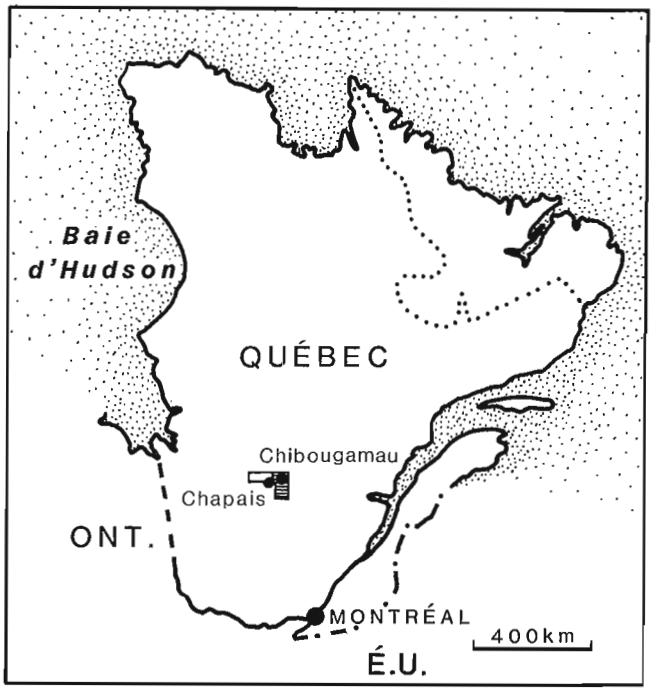

Figure 1. Carte de localisation du secteur à l'étude (en blanc). Le secteur au sud de la ville de Chibougamau représente les zones cartographiées par le ministère de l'Énergie et des Ressources du Québec (1982-1985).

LES CONTEXTES TOPOGRAPHIQUE ET STRATIGRAPHIQUE DE LA RÉGION À L'ÉTUDE

La région offre peu de reliefs majeurs, à l'exception de trois monts bien connus (fig. 2): les monts Opemisca (538m), Springer (540 m) et Michwacho (560 m). On note aussi un secteur caractérisé par la présence de grandes formes fuselées affectant le substratum rocheux au sud-ouest du lac Opemisca, secteur où la différence d'altitude entre les crêtes et les dépressions est de l'ordre de 15 à 50 m. Généralement, la région est relativement plane: la très grande majorité des localités de stries observées sont situées dans des zones très peu accidentées. Le grand nombre de lacs et le réseau de chemins forestiers déjà anciens ont limité l'accès à certains secteurs des cartes étudiées.

Le contrôle des unités stratigraphiques en surface a confirmé la séquence établie dans le secteur sud de Chibougamau (Prichonnet et coll, 1984; Bisson, 1987). Et, à ce jour, on n'a toujours identifié qu'une nappe de till, ce qui impose une limite aux interprétations des mouvements glaciaires discutés ici. On peut retenir aussi que les moraines mineures (ou de De Geer) forment de larges essaims, particulièrement dans plusieurs secteurs du territoire de la carte du lac Lamarck (cartes en préparation).

L'ÉCOULEMENT GLACIAIRE N-S

Plus de 90 localités de surface glaciaire ont été observées sur le territoire couvert par les feuilles topographiques à 1 / 50 000 de Chapais (G.15), du lac Lamarck (G.14) et du lac Dickson (G.11). La majorité est reportée sur la figure 2. Parmi les plus importantes de ces localités, 20 % ont révélé la présence de stries et de sillons franchement N-S ($\pm 5°$), tandis que 10 % montrent des traces d'écoulement glaciaire probablement associées au mouvement N-S ($\pm 10°$) (fig. 3). La figure 3 met aussi en évidence le fait que la "famille" de stries N-S se distingue nettement des autres.

Un certain nombre de cas plus favorables ont permis d'établir, sans aucun doute, que le mouvement N-S, d'une part recoupait l'écoulement NO-SE (tabl. 1: localités 1, 60 et 62; fig. 4) et d'autre part était recoupé par l'écoulement NNE-SSO ou NE-SO (tabl.1: localités 3 et 9; fig. 4 et 5), ou encore était conservé sur des surfaces non touchées par l'écoulement omniprésent de direction NE-SO. Dans quelques cas, il s'agit de traces recoupant le mouvement NO-SE sur des faces orientées vers le sud-ouest, celles-là mêmes qui ont permis de bien établir l'antériorité de l'écoulement SE (stries ascendantes vers le sud-est; queues de rat et têtes de clou; Prichonnet et coll., 1984; Bouchard et Martineau, 1984, 1985).

Tableau 1 Localités de stries: les localités marquées d'un astérisque ont été étudiées en plus grand détail.

No	Troncature* ou face protégée	Polarité spécifique (1) RM = Roche moutonnée	Recoupement indiqué par X	Familles retenues (1) (2)... ordre chronologique
1*	*292-112	RM (SO) Stries ascendantes (SE)	ESE X par SSE et S	(1) SE + SSE (2) S (3) SO
2		Queue de rat (218)		SO
3	*NO-SE Face protégée SO		N-S X par SO	(1) S (2) SO
4	*NO-SE Face protégée SO			(1) SE (2) SO
8	Face protégée SO			SE
9*	*010-190 Face protégée « ouest »	RM (SO) Queue de rat (209) et (213); et (258) têtes de clou (265) et (258)	NS X par NNE SSO NNE-SSO X par ENE-OSO ENE-OSO par E-O	(1) SE (2) S (3) SSO à SO (4) OSO à O
10	*323-143	RM (SO)		SSE/S/SSO/SO
13	*irrégulière NO-SE Face protégée SO			SE/SSE/SO
17			NE-SO X par ESE-OSO	(1) SE (2) SSO à SO (3) OSO
19	Face protégée			(1) SE (2) SO
22*	*310-130 Face protégée SO		NE-SO X par ENE-SSO	(1) SE (2) SO à SSO ?S entre (1) et (2)
30	Face protégée SO			(1) SE (2) SO
31	Face protégée SO			(1) SE (2) SO
32	Face protégée SO			(1) SE (2) SSO à SO
55*	*295-115 *025-205 2 faces protégées SO et O	RM (SO)	NNE-SSO X par ENE-OSO NNO-SSE X par NNE-SSO	(1) SSE (2) SSO (3) SO
56	*NO-SE Face protégée SO			SSO/SO
60*	2 faces protégées étagées (SO)	RM (SO) RM (S)	NNO-SSE X par N-S	(1) SSE (2) S (3) SSO à SO
62*	292-112	Stries ascendantes SE RM (SO)	NO-SE X par N-S	(1) SE (2) S (3) SO
65	Face protégée SO	Queue de rat (215)		(1) SE (2) S (3) SO
68*	*NO-SE Face protégée SO	RM (SO)		(1) SE (2) SO
74	Face protégée SO			(1) SE (2) SO
78*		Marques en croissant (230) RM (SO) Queue de rat (212)		SO
79*	*288-108	Queues de rat (100) et (104) RM (SO)		(1) SE (2) SO ?S entre (1) et (2)

(1) Le moutonnement des affleurements rocheux indiquant un écoulement du nord-est vers le sud-ouest est omniprésent dans la région. Seuls quelques cas plus spécifiques sont signalés ici.

Deux localités sont particulièrement intéressantes (tabl. 1: localités 9 et 55). Elles permettent d'observer soit une troncature N-S (nº 9), soit un large sillon ascendant vers le SSO (nº 55), qui témoignent d'une érosion significative et d'un écoulement vers le secteur sud, puis SSO. Il est à noter que l'écoulement N-S a été relevé à la localité 79, située à plus de 30 km au sud du territoire représenté sur la figure 2. On peut donc affirmer que le secteur dans lequel ces stries se manifestent est assez étendu (sur trois cartes à 1 / 50 000), et considérer que l'évènement est significatif, à l'échelle de la région étudiée.

Enfin, les surfaces glaciaires ne montrent aucun signe d'altération ancienne. Dans quelques cas, les surfaces sont légèrement dégradées par l'altération récente (desquamation, attaque de lichens, micro-soulèvements dans les roches fortement diaclasées), mais le phénomène affecte indifféremment toutes les surfaces striées, jusqu'aux plus récentes. On remarque aussi un aspect de moins en moins net des stries des familles les plus anciennes, sauf sur les surfaces bien protégées.

DISCUSSION SUR LA RELATION DU MOUVEMENT N-S AVEC LES MOUVEMENTS NO-SE ET NE-SO.

Si l'on considère le nombre de troncatures relevées, on note que la direction NO-SE est très bien représentée avec 11 localités identifiées, tandis que deux troncatures seulement résultent de l'intersection entre une érosion N-S et une érosion NE-SO (fig. 6). On peut probablement en déduire que le mouvement NO-SE a marqué plus profondément le substratum rocheux, que ne l'a fait l'écoulement N-S. Et, effectivement, une seule localité montre une érosion très prononcée du nord vers le sud, grâce à la présence de plusieurs sillons (localité 9). On a aussi observé à plusieurs reprises que les stries NNO-SSE ou N-S ne font que recouper les stries NO-SE, sur les faces protégées inclinées vers le sud-ouest (fig.4).

Mais par ailleurs, il faut souligner que le dernier mouvement NE-SO montre un étalement de 30 à 35°, commençant vers 020°; cet écoulement, qui traverse en oblique les marques N-S, et qui a profondément affecté le socle (fig. 7) a probablement eu tendance à en effacer les preuves.

En conclusion, les observations de terrain démontrent que les recoupements se font progressivement de la façon suivante (tabl. 1):

- l'écoulement ESE est recoupé par l'écoulement SSE (et sud);
- l'écoulement SSE est recoupé par l'écoulement sud;
- l'écoulement sud est recoupé par l'écoulement SSO (et SO); et,
- l'écoulement SO est recoupé par l'écoulement OSO (voir aussi Prichonnet et coll., 1984).

On peut en déduire que le déplacement de l'écoulement s'est réalisé dans le sens horaire. Par contre l'importance relative de l'écoulement N-S demeure incertaine malgré le nombre de localités identifiées; la rareté des larges sillons porte à croire intuitivement que l'érosion par l'écoulement vers le sud a été moins prononcée que lors des autres phases d'écoulement glaciaire.

SIGNIFICATION DU MOUVEMENT N-S

L'âge relatif des mouvements glaciaires identifiés, l'ordre de leurs recoupements et leurs sens d'écoulement

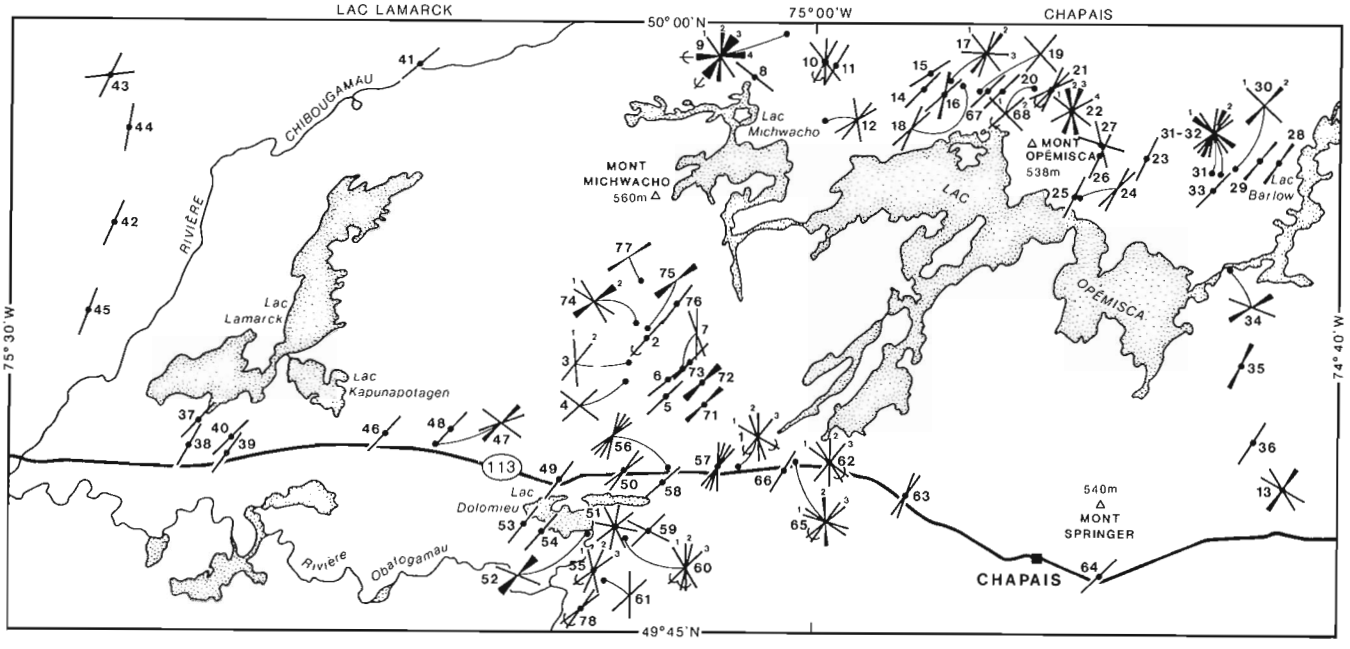

Figure 2. Carte de localisation de l'emplacement des surfaces glaciaires observées: chaque ligne azimutale représente une strie ou un sillon; lorsque plusieurs stries ou sillons sont très rapprochés, le secteur angulaire est représenté en noir.

conduisent à une interprétation paléogéographique plus complexe que celle qu'on avait établie jusqu'à présent. Martineau et coll. (1984) et Bouchard et Martineau (1985) ont proposé l'hypothèse d'un centre local de dispersion qui aurait existé du côté est de la baie James (voir aussi Boulton et coll., 1985). L'un des critères retenus pour une telle localisation est l'absence de roches paléozoïques, ou protéozoïques, affleurant à la baie James et à la baie d'Hudson, dans le till de la région de Chibougamau. Bien que l'argument soit important, il faut remarquer que la distance entre la région de Chapais-Chibougamau et les affleurements des roches sources mentionnées est considérable: plus de 400 km pour les roches carbonatées paléozoïques, et plus de 600 km pour les roches protérozoïques; dans le cas de ces dernières, d'ailleurs, il serait impossible de distinguer les grès et les roches carbonatées de ceux qui proviennent du bassin protérozoïque de Mistassini, du même âge et beaucoup plus rapproché. Dans le cas des roches paléozoïques, on pourrait admettre aussi un écoulement de trop courte durée pour avoir apporté des débris jusqu'à la zone à l'étude; mais les indices d'un tel transport n'ont pas été signalés à ce jour (Hardy, 1976 et 1982; voir aussi la limite d'extension des roches paléozoïques au Témiscamingue et dans l'ouest de l'Abitibi de Veillette, 1986, fig. 12).

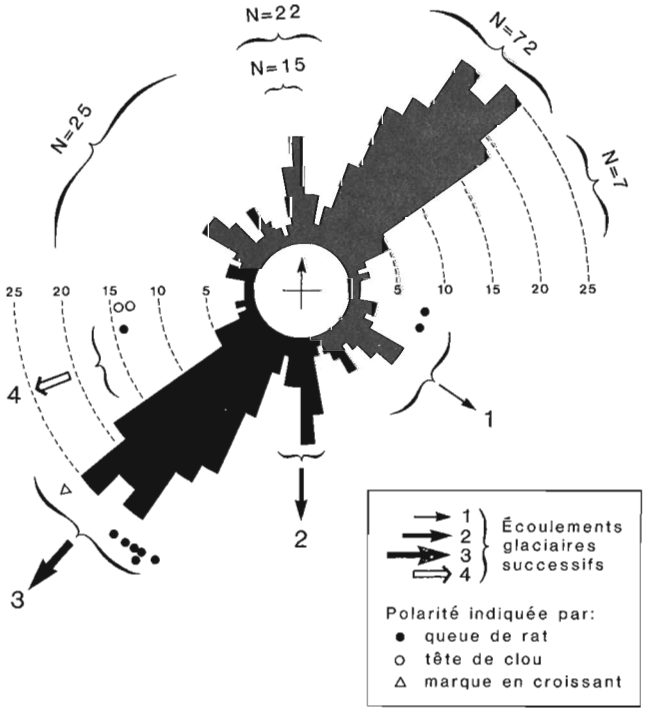

Figure 3. Diagramme rose des vents de fréquence des stries et sillons relevés à 77 localités: au total 271 mesures ont été réalisées, incluant 12 mesures de polarité; les 259 mesures de stries et sillons sont regroupées en 230 valeurs, par classes de 5°. Les flèches 1, 2 et 3 désignent les grands écoulements glaciaires retenus pour fin de reconstitution de la paléogéographie: on notera que l'écoulement dit SE semble bien comporter, en réalité, trois sous-familles (à 105°, 125° et 145°). La flèche 4 désigne l'écoulement tardif de la marge glaciaire, tel que défini par Prichonnet et coll. (1984).

Il faut aussi rappeler la présence de petits affleurements de roches paléozoïques sur le Bouclier, dont ceux de la région de Desmaraisville. Le sens de transport de ces roches pourrait éventuellement servir à préciser les étapes de la dispersion glaciaire. Toutefois l'exiguïté des affleurements restreint les chances d'identifier les traînées distales.

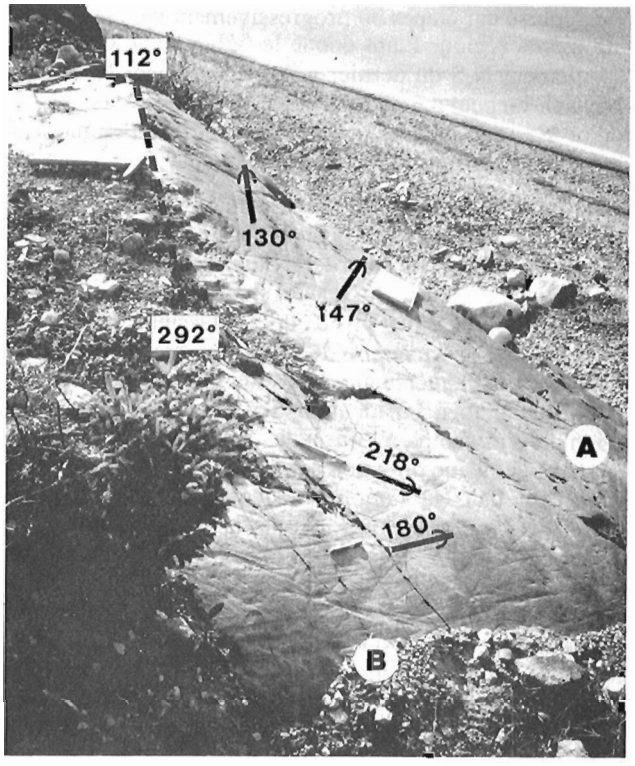

Figure 4. Photo prise au site 62. La troncature est orientée 292°-112°. La face inclinée vers le SO (A) porte de nombreuses stries orientées 130° et 147°. Près de la troncature (B) les stries sont orientées 180° à 184°. La surface supérieure (marteau) est ascendante vers le SO et elle est abondamment striée (038°-218°); ces stries se prolongent parfois au-delà de la troncature (C).

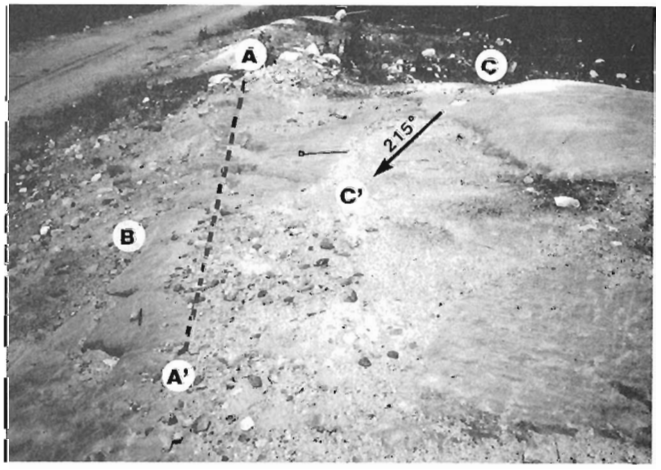

Figure 5. Photo prise à la localité 9. On observe une troncature (AA') et des stries N-S (près de B), un sillon 035°-215° (CC'), et des stries fines vers l'OSO, parallèles au marteau.

Mais, quelle que soit la position de ce centre de dispersion, ou de la ligne de partage des glaces à l'origine d'un écoulement vers le sud-est, il est intéressant d'insister sur son déplacement progressif, dans le sens horaire (fig. 5, A, B, C). En effet, tous les indices de recoupement, comme l'âge relatif des troncatures, indiquent que ce centre, d'abord situé à l'ouest-nord-ouest de la région à l'étude, s'est déplacé par étapes ou progressivement vers le nord de cette même région. Étant donné le faible angle qui sépare l'écoulement N-S du dernier grand écoulement NNE-SSO à NE-SO. on peut même se demander si le centre de dispersion ne s'est pas déplacé continuellement jusqu'au moment où il a été localisé sur le Nouveau Québec.

La position des centres de dispersion ou des lignes de partage des glaces mérite quelques remarques. Boulton et coll. (1985) situent un centre d'épaississement des glaces à l'est de la baie James. Et Dyke et Prest (1987) ont proposé la ligne de partage des glaces de Mistassini (fig. 8). Ces deux modèles permettent d'expliquer, partiellement du moins, les écoulements glaciaires identifiés dans la zone à l'étude. Toutefois, on identifie des stries NO-SE dans la région de Waswanipi, à l'ouest de Chapais (fig.5). De plus, des stries de même direction existent encore plus à l'ouest, notamment dans la région de Desmaraisville (Veillette, comm. pers.) Il apparaît donc que la ligne de partage de Mistassini devrait être localisée plus à l'ouest que ne l'ont proposé Dyke et Prest. Il est possible que cette ligne corresponde à un vrai centre de dispersion, ce qui expliquerait la présence des stries NO-SE sur le vaste territoire où elles ont été signalées (Prichonnet et coll.,1984; Bouchard et Martineau, 1985; la présente étude). Quant à la ligne de partage Hudson et au centre de dispersion D_1 (fig. 8) de Dyke et Prest (1987, carte 1703A), ils permettent d'expliquer les écoulements en provenance du NNO, du N et du NNE.

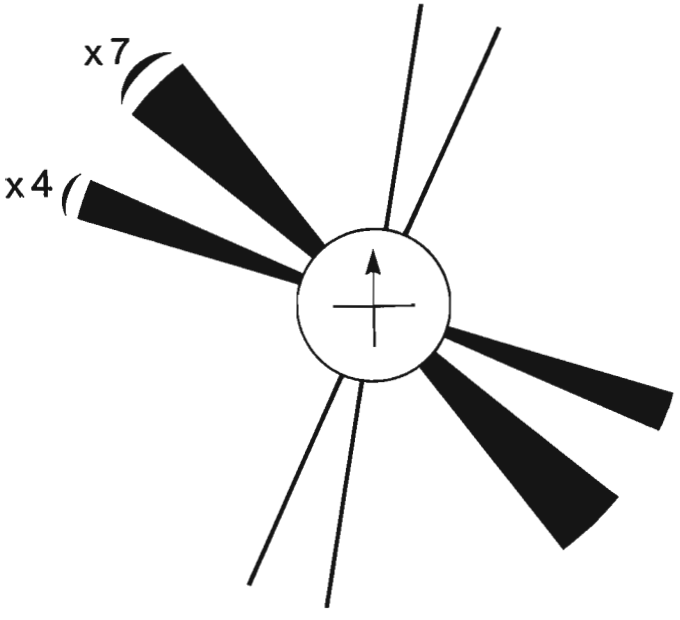

Figure 6. Diagramme des 13 troncatures observées: on notera les deux modes à 110° et 135° (environ), qui peuvent être mis en relation avec deux sous-familles de l'écoulement SE (fig. 2).

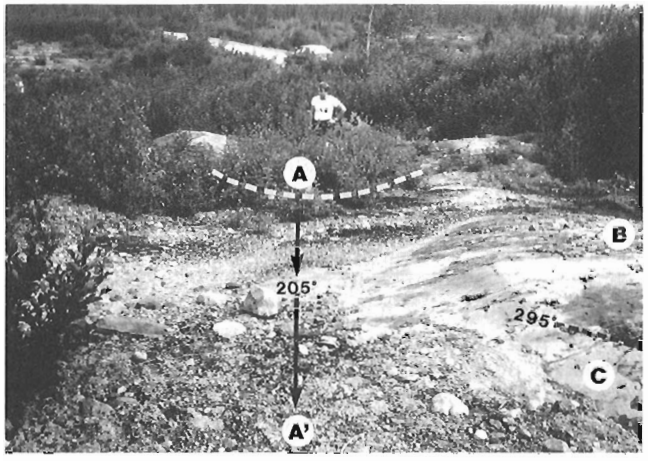

Figure 7. Photo prise au site 55. Le grand sillon (AA') en direction du personnage est ascendant vers le 205°. Côté NE (B) il est recoupé par de très nombreuses stries 054°-234°. Au premier plan à droite (C), on note une surface inclinée vers le SO, limitée par une troncature de direction 295°-115°: cette surface est affectée de stries mal préservées 333°-153° et de petites stries fines 025°-205°.

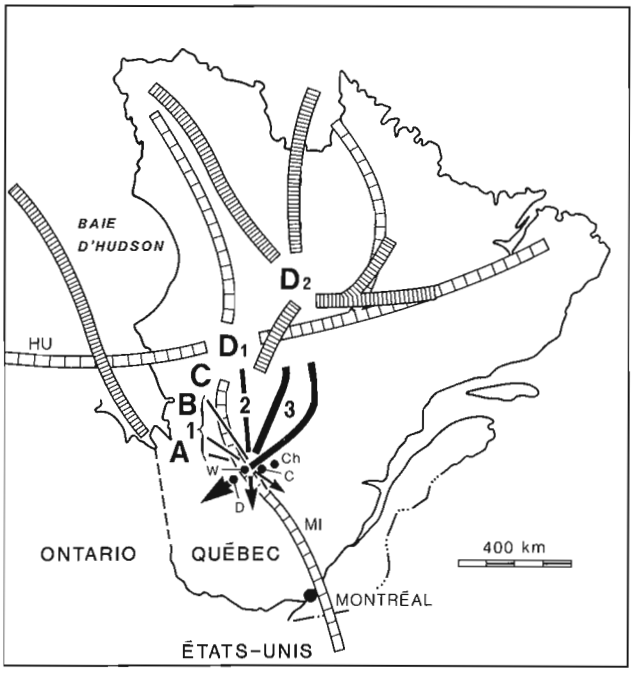

Figure 8. Reconstitution des zones de dispersion glaciaire ayant favorisé les écoulements des glaces sur la région de Chapais-Chibougamau. A, B, C: positions successives pour les écoulements vers l'ESE, le SE et le SSE. Voir figure 3 pour les écoulements correspondants. D_1et D_2 représentent les dômes du Nouveau Québec respectivement vers 18 000 et 8 400 ans, selon Dyke et Prest (1987). Les lignes de partage des glaces des mêmes auteurs sont représentées par des hachures espacées pour 18 000 ans, et par des hachures rapprochées pour 8 400 ans. MI, HU: lignes de partage des glaces de Mistassini et d'Hudson.

Puis le déplacement du dôme du Nouveau-Québec, de D_1 à D_2, pourrait rendre compte du changement progressif des écoulements qui ont touché la région à l'étude, soit un déplacement de l'écoulement NNE-SSO vers le NE-SO. Enfin, le dernier écoulement vers l'OSO, et même localement vers l'ouest, semble être de plus en plus marqué dans le secteur nord de la zone à l'étude par rapport à la région de Chibougamau (Prichonnet et coll.,1984); il se trouve que ce secteur correspond aussi à celui où l'on constate un épaississement des rythmites (varves ?) attribuées au lac Ojibway (carte en préparation). Ainsi se trouverait confirmé le rôle de ce lac, qui aurait attiré la marge glaciaire lors de la déglaciation.

Il est à noter qu'un tel déplacement du sens des écoulements glaciaires n'est pas un phénomène rare puisque des phénomènes analogues sont bien établis dans d'autres régions de l'Est canadien (p. ex., Klassen, 1984; Klassen et Bolduc, 1984, 1986; Prichonnet, 1977 et 1984; Veillette, 1986; Foisy et Prichonnet, 1988).

CONCLUSION

Une étude attentive des recoupements des marques d'érosion glaciaire dans le secteur minier de Chapais-Chibougamau démontre que les écoulements de la glace sont plus complexes qu'on ne l'avait pensé jusqu'à ce jour. D'une part, le mouvement NO-SE pourrait bien correspondre à une suite de mouvements, d'abord de l'ONO vers l'ESE, puis du NO vers le SE et enfin, du NNO vers le SSE. D'autre part, l'écoulement N-S "bien daté", relativement, succède aux écoulements précédents, et précède les écoulements en provenance du NNE et du NE. Un centre de dispersion (ou une ligne de partage des glaces) se déplaçant dans le sens horaire, situé entre la zone à l'étude et la baie James, et se déplaçant en direction du Nouveau Québec, permet d'expliquer les faits observés sur le terrain. Si tous ces évènements ont eu lieu au Wisconsinien supérieur, en un laps de temps relativement court et donc sans retrait des glaces de la zone considérée, il n'est pas surprenant que l'ensemble des surfaces glaciaires observées soient si bien préservées.

Une étude plus approfondie à l'ouest et au nord de la région à l'étude serait utile pour compléter les données présentées ici. Mais ces données nouvelles semblent contribuer de façon significative à la détermination précise des positions successives des centres de dispersion du Wisconsinien (supérieur ?).

REMERCIEMENTS

Cette étude a été rendue possible grâce au soutien financier de trois organisations auxquelles les auteurs désirent exprimer leur reconnaissance: la Division de la science des terrains de la Commission géologique du Canada, l'Université du Québec à Montréal (FIR-PAFAC) et le ministère de l'Enseignement supérieur du Québec (FCAR-équipe). Les auteurs tiennent à souligner les contributions de Mme Michelle Laithier, géocartographe; de M. Jean La Haye, adjoint de recherche; de M. Denis Levasseur, assistant; et, de Mme Andrée Gendron, secrétaire du GEOTERAP. Les auteurs adressent leurs remerciements à M. Jean Veillette qui a revu le texte; ses commentaires, critiques et suggestions leur ont été très utiles. Les idées et les opinions exprimées ici sont la responsabilité des auteurs.

RÉFÉRENCES

Bisson, L.,
1987: Géologie des dépôts quaternaires du Canton de Scott, Chibougamau - Québec. Avec applications à la prospection minérale; Mémoire de maîtrise (inédit), Université du Québec à Montréal, 182 p.

Bouchard, M.A., et Martineau, G.,
1984: Les aspects régionaux de la dispersion glaciaire, Chibougamau, Québec; dans Chibougamau-Stratigraphy and Mineralization, Canadian Institute of Mining and Metallurgy, Spécial volume 34, pp. 431-440.

Bouchard, M.A. et Martineau, G.
1985; Southeastward ice flow in central Quebec and its paleogeographic significance; Canadian Journal of Earth Sciences, v. 22, no 10, pp. 1536-1541.

Boulton, G.S., Smith, G.D., Jones, A.S., et Newsome, J.,
1985: Glacial geology and glaciology of the last mid-latitude ice sheets; Journal of the Geological Society, London, 142, pp. 447-474.

De Corta, H.,
1988: Les dépôts quaternaires de la région Lac Rohault - Lac Boisvert (sud de Chibougamau): aspect de la dispersion glaciaire clastique; Mémoire de maîtrise, Université du Québec à Montréal, 112 p.

De Corta, H., et Prichonnet, G.,
1986: La dispersion clastique dans la fraction grossière des dépôts glaciaires wisconsiniens au sud de Chibougamau, Québec: Association canadienne-française pour l'avancement des sciences, Résumés des communications, v. 56, p. 216.

Dyke, A.S., et Prest, V.K.,
1987: Late Wisconsinan and Holocene history of the Laurentide ice sheet; Géographie physique et Quaternaire, vol. XLI, no 2, pp. 237-263.

Ermengen, S.V.,
1957: Report on glacial geology and geochemical dispersion in the Chibougamau area, Québec, Ministère des l'Énergie et de Ressources, Direction de l'exploration géologique et minérale, DP-26, GM—23803, pp. 1-159.

Foisy, M., et Prichonnet, G.,
1988: Glaciation and deglaciation in the northeastern part of the Caledonian Highlands, New-Brunswick: Glacial dispersal and mineral geochemistry of tills, 13th Annual Review of Activities, Project résumés, S.A. Abbot ed., Division, New-Brunswick Department of Natural Ressources and Energy, Information circular 88-2, pp. 90-92.

Hardy, L.
1976: Contribution à l'étude morphologique de la portion québécoise des basses terres de la Baie de James, Thèse de Ph.D., Université McGill, Montréal, 264 p.

Hardy, L.
1982: Le Wisconsinien supérieur à l'est de la Baie James (Québec); Naturaliste canadien, 109, pp. 333-351.

Ignatius, H.C.,
1958: On the Late-Wisconsin deglaciation in Eastern Canada, Part 1; Acta geographica, v. 16, no 3, pp. 2-34.

Klassen, R.A.,
1984: A preliminary report on drift prospecting studies in Labrador: part II; Current Research, Part A, Geological Survey of Canada, Paper 84-1A, pp. 247-254.

Klassen, R.A., and Bolduc, A.,
1984: Ice flow directions and drift composition, Churchill Falls, Labrador; Current Research, Part A, Geological Survey of Canada, Paper 84-1A, pp. 255-258.

Klassen, R.A., and Bolduc, A.M.,
1986: Ice flow trends and drift composition, Flowers River area, Labrador; Geological Survey of Canada, Paper 86-1A, pp. 697-702.

Martineau, G.,
1984: Géologie du Quaternaire, région de Chibougameau: Ministère de l'Énergie et des Ressources, du Québec, Étude 83-20,15 p.
Martineau, G., Bouchard, M., et Prichonnet, G.,
1984: Southeastward ice flow in Central Quebec and its implication for the location of the Laurentide ice sheet dispersal centers; Geological Association of Canada - Mineralogical Association of Canada, Meetings Abstracts, v. 9, p. 87.
Mawdsley, J.B.,
1936: The washboard moraines of the Opemisca-Chibougamau area, Quebec; Royal Society of Canada, Transactions, v. 30, sect. IV, pp. 9-12.
Norman, G.W.H.,
1938: The last Pleistocene ice-front in Chibougamau district, Quebec; Royal Society of Canada, Transactions, v. 32, sect. IV, pp.69-86.
Prest, V.K., Grant, D.R., and Rampton, V.N.,
1968: Glacial map of Canada; Geological Survey of Canada, Map 1253-A.
Prichonnet, G.,
1977: La déglaciation de la vallée du Saint-Laurent et l'invasion marine contemporaine; Géographie physique et Quaternaire, vol. XXXI, n^{os} 3 et 4, pp. 323-345.
Prichonnet, G.,
1984: Dépôts quaternaires de la région de Granby, Québec: Commission géologique du Canada, Étude 83-30, 8 p., carte annexée à 1 / 50 000.
Prichonnet, G., Martineau, G., et Bisson, L.,
1984: Les dépôts quaternaires de la région de Chibougamau, Québec; Géographie physique et Quaternaire, vol. XXXVIII, no 3, pp. 287-304.
Veillette, J.J.,
1986: Former southwesterly ice flows in the Abitibi-Timiskaming region: implications for the configuration of the late Wisconsinian ice sheet; Canadian Journal of Earth Sciences, v. 23, no 11, pp. 1724-1741.

Precambrian structure and stratigraphy based on seismic interpretation, Colville Hills region, Northwest Territories

D.G.Cook and I.R.Mayers[1]
Institute of Sedimentary and Petroleum Geology, Calgary

Cook, D.G. and Mayers, I.R., Precambrian structure and stratigraphy based on seismic interpretation, Colville Hills region, Northwest Territories; in Current Research, Part C, Geological Survey of Canada, Paper 90-1C, p. 339-348, 1990.

Abstract

Proterozoic strata imaged on publicly available seismic data in the Colville Hills region can be subdivided into two major sequences separated by a regional unconformity. A large tilted fault block, offsetting the deeper sequence I units, is truncated at the unconformity. It is interpreted as being underlain by a steeply dipping, curved, westward-directed, reverse fault. Other, smaller thrust faults also offset sequence I strata; others offset both sequences I and II. Some of the latter appear to have developed through reactivation of the former. Sequence I, below the unconformity, is divided into three sub-units which are tentatively correlated with units mapped on Coppermine Homocline to the east: Ia) Dismal Lakes Group and older; Ib) Copper Creek Formation; and Ic) Husky Creek Formation. Sequence II, above the unconformity, is correlated with the Mackenzie Mountains supergroup, to the west, and the Rae and Shaler groups, to the east. Some sub-horizontal discordant reflections are considered to be intrusive sheets of the same general age as Late Proterozoic diabase dilkes and sills reported on Brock Inlier.

Résumé

Des couches protérozoïques de la région des collines Colville, figurées par des données sismiques accessibles au public, peuvent être subdivisées en deux séquences principales séparées par une discordance régionale. Un gros bloc faillé incliné, décalant les unités de la séquence I plus profonde, est tronqué au niveau de la discordance. Selon l'interprétation donnée, il serait sus-jacent à une faille inverse à fort pendage, courbée et dirigée vers l'ouest. D'autres chevauchements moins importants décalent également les couches de la séquence I tandis que d'autres décalent les séquences I et II. Certains parmi ces derniers semblent avoir été formés par la réactivation des premiers. La séquence I, au-dessous de la discordance, est divisée en trois sous-unités qui ont été provisoirement corrélées à des unités cartographiées sur la structure monoclinale de Coppermine à l'est: Ia) le groupe de Dismal Lakes et des roches plus anciennes; Ib) la formation de Copper Creek; et Ic) la formation de Husky Creek. La séquence II, au-dessus de la discordance, est corrélée au supergroupe de Mackenzie Mountains, à l'ouest, et aux groupes de Rae et de Shaler, à l'est. Certaines réflexions discordantes sub-horizontales devraient correspondre à des nappes intrusives du même âge en général que les dykes et les filons-couches de diabase du Protérozoïque supérieur relevés sur l'enclave de Brock.

[1] Geophysical Consultant, 2216 Longridge Drive S.W., Calgary, Alberta, T3E 5N6

INTRODUCTION

Multifold reflection seismic data released by the Canada Oil and Gas Lands Administration (COGLA) provide an important database for interpreting subsurface Precambrian stratigraphy and tectonics in the Northwest Territories. This report presents very preliminary results of a study in progress, in the region of the Colville Hills (Fig. 1).

Subsurface studies in this region, to date, with a few notable exceptions, have concentrated on Phanerozoic strata. Although many important problems related to the Phanerozoic remain to be solved, the focus of the present study is on the subsurface Precambrian, about which relatively little is known. Two east-west, regional, composite seismic cross-sections, B-B′ (about 220 km long) and C-C′ (about 300 km), and connecting north-south cross-sections, Y-Y′ (about 60 km), Z-Z′ (about 100 km), and line 77A (about 40 km) are key (Fig. 2) among the data being interpreted, and some preliminary conclusions are presented here. Parts of two interpreted seismic lines, Forward Resources Line FR-14 (from C-C′), and Petro-Canada Inc. Line 114X (from B-B′) are reproduced herein (Figures 3 and 4, respectively) to illustrate examples of our current understanding of the area's geology.

More than 800 line kilometres are represented by these five, spliced cross-sections. The data were recorded and processed during the 1970s and early 1980s, using a variety of hardware and software combinations. The most commonly available, and best quality sections are 12-fold, dynamite lines, recorded in the early 1980s, processed to a datum plane of 305 m above sea level (using a datum velocity of 5500 m/sec.) and displayed in structural stack format only.

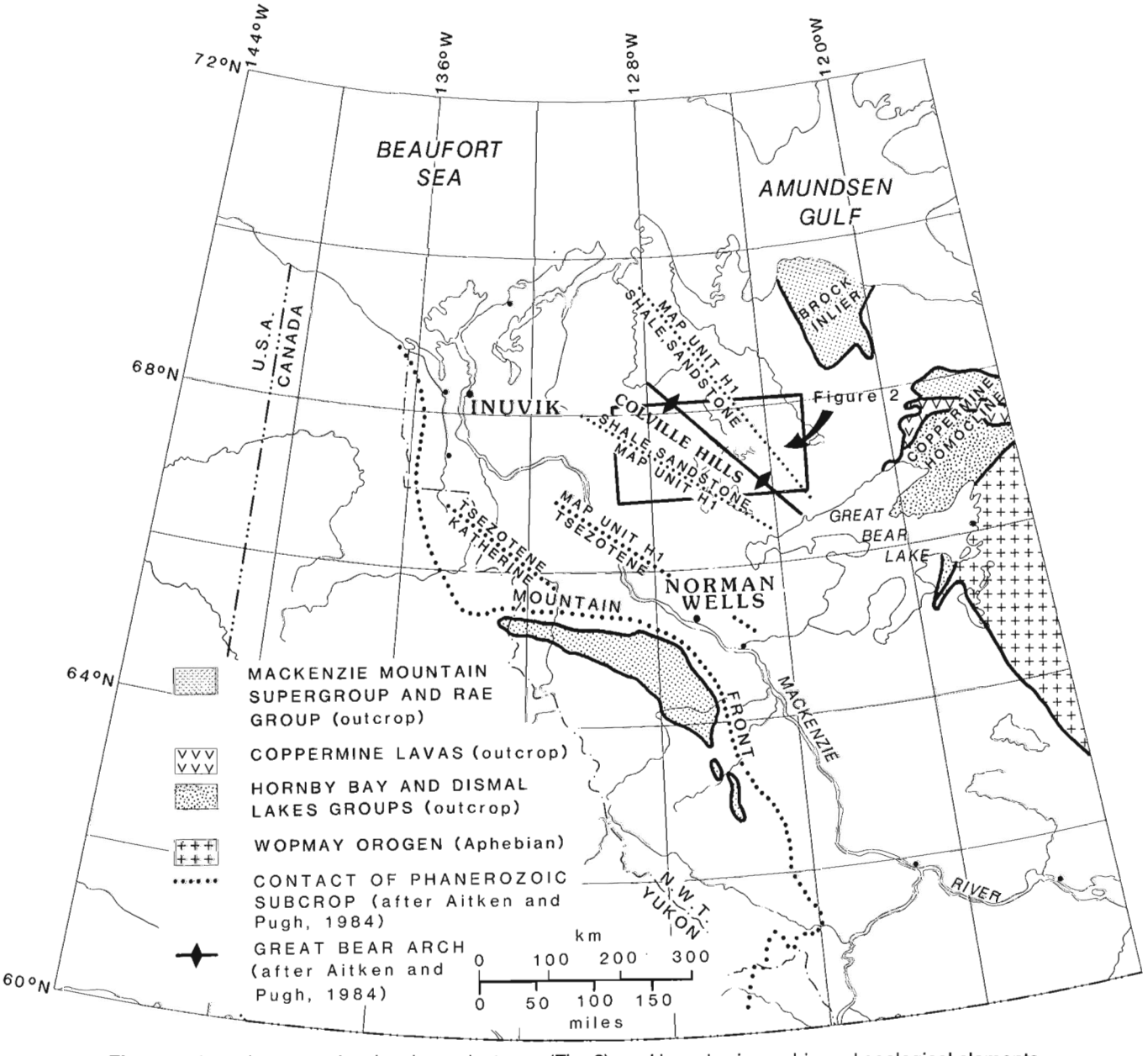

Figure 1. Location map, showing the project area (Fig. 2), and key physiographic and geological elements.

Both of the lines illustrated in Figures 3 and 4 are taken from this 1200 per cent data set. We have not as yet attempted to obtain copies of the original magnetic tapes in order to digitally reprocess and redisplay the lines in a migrated format.

Interval seismic velocities for stratigraphic units are taken from either the released acoustic logs or check shot surveys of the local wells (Vp) or, in the case of the deeper, undrilled zones, estimated (where data quality is adequate) by the Dix Equation (Dix, 1955) from the seismic processing RMS velocities (Vd). These have been used to estimate thicknesses of the subsurface units. Those thicknesses and the interval velocities themselves are used to support tentative correlations with exposed sequences to the west and east. In the area crossed by the two regional lines a coherent stratigraphic and structural rationale is possible particularly in the eastern part. However, cursory inspection of other seismic lines indicates that significantly greater structural complexity occurs to the south and southwest.

Precambrian strata imaged on the two seismic lines, FR-14 and 114X, lie below the regional sub-Cambrian unconformity (marker "F", Figs. 3, 4). On most of the available seismic sections, this unconformity is easily identified as the lowermost reflection of a distinctive set of parallel seismic reflections, that truncates reflections representing the underlying Precambrian strata throughout the area. The Precambrian has been subdivided into two seismic sequences separated by a major unconformity (marker "C", Figs. 3, 4). Sequence I, lying below the unconformity, is locally faulted and folded and has been affected by at least three phases of deformation. Some structures in that sequence are truncated by, and therefore predate, the unconformity; others were initiated prior to the unconformity, but were reactivated later to affect sequence II. Sequence II, above unconformity "C", is mildly deformed by at least two phases of deformation. Phanerozoic rocks, mainly Cambrian to Devonian, unconformably overlie Precambrian strata, and have been affected by at least one phase of deformation, that which generated the isolated ridges of the Colville Hills (see Cook and Aitken, 1971; Davis and Willott, 1978).

F.A.Cook (1988a, b) analysed a number of seismic lines from east of Colville Hills and interpreted Precambrian flat thrust faults on the basis of reflection discontinuities and apparent structural repetition of layered strata. Cook considered these thrusts to represent an east verging, Proterozoic, thin-skinned thrust and fold belt, which he linked, via a regional, sub-horizontal detachment, to Proterozoic thrusting documented in the Inuvik area to the northwest (F.A. Cook et al., 1987). In the present study, we recognize the need for some measure of horizontal shortening, but we do not recognize his specific thrust faults.

Other studies of the Proterozoic in the region deal mainly with surface exposures in Mackenzie Mountains to the west and Brock Inlier and Coppermine Homocline to the east (Fig. 1). Our tentative correlations of seismic sequences with exposed sequences in the region (Fig. 5) are in general agreement with those of F.A. Cook (1988a) with important differences regarding the placement of the sub-Rae Group unconformity, and the identification of major thrust fault repeats. Williams (1986) provided an outline of the general lithostratigraphy in the subsurface of Mackenzie River

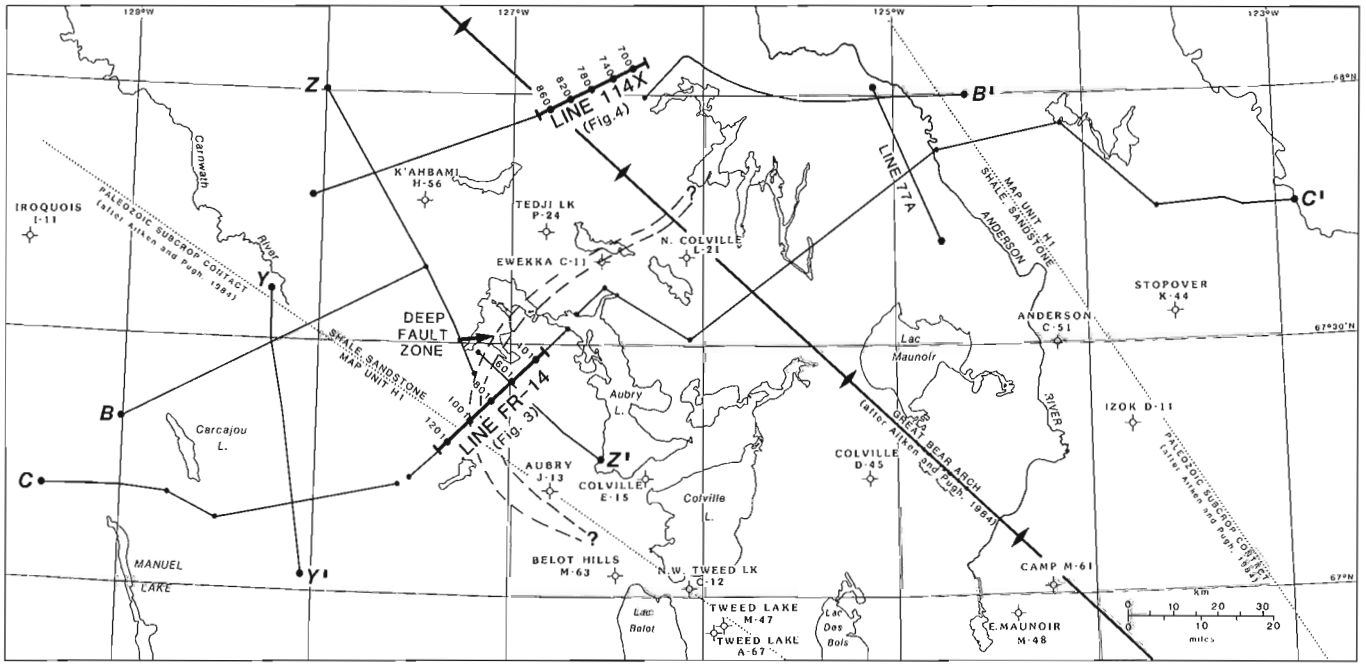

Figure 2. Project area, showing: wells penetrating the sub-Cambrian; seismic transects B-B', C-C', Y-Y', Z-Z', and line 77A; the displayed seismic sections FR-14 (Fig. 3), and 114X (Fig. 4); and a deep fault zone.

corridor and discussed possible links to outcrops to the west, and to the east. Aitken and Pugh (1984) correlated subsurface Proterozoic strata of the Colville Hills region with the informal Mackenzie Mountains supergroup, which has been extensively studied by Aitken (e.g., 1982; Aitken et al., 1978a, b). Aitken (1982) has also tentatively correlated the Mackenzie Mountains supergroup with strata of the Shaler Group exposed in Brock Inlier to the east (Fig. 1). Similarily, Young et al. (1979) correlated the lower part of the Mackenzie Mountains supergroup with the Rae Group in Coppermine Homocline, northeast and east of Great Bear Lake. There, Precambrian rocks mapped by Baragar and Donaldson (1973a, b), and Ross and Kerans (in press), occur in four gross packages. The oldest is composed of the highly deformed sedimentary, volcanic and intrusive rocks of the Lower Proterozoic Wopmay Orogen. These are unconformably overlain by sandstones, conglomerates, shales and dolomites of the Hornby Bay Group. These strata are unconformably overlain in turn by a third package comprising the Dismal Lakes Group, (mainly dolomite in the upper part and mainly siliciclastic rocks in the lower part) and the Coppermine River Group (mainly basalt). The youngest sequence, the Rae Group, comprising various clastic, carbonate, and minor gypsum beds, unconformably overlies all of the other packages.

The regional subsurface unconformity interpreted and illustrated herein (marker "C", Figs. 3, 4) presumably is equivalent to one or more of the unconformities noted above, and is considered most likely to be equivalent to that underlying the Rae Group. Seismic sequence II, accordingly, is correlated with some or all of the Mackenzie Mountains supergroup, the Rae Group, and the Shaler Group. Two of three seismic units below the subsurface unconformity are correlated, in downward succession, with the Husky Creek Formation and the Copper Creek Formation. A third basal unit is believed to represent the Dismal Lakes Group and/or the Hornby Bay Group, but may include strata equivalent to formations in the highly deformed Wopmay Orogen.

SEISMIC STRATIGRAPHY AND STRUCTURAL ANALYSIS

Proterozoic sequence 1

The lower seismic sequence is divided into three sub-units (Figs. 3, 4).

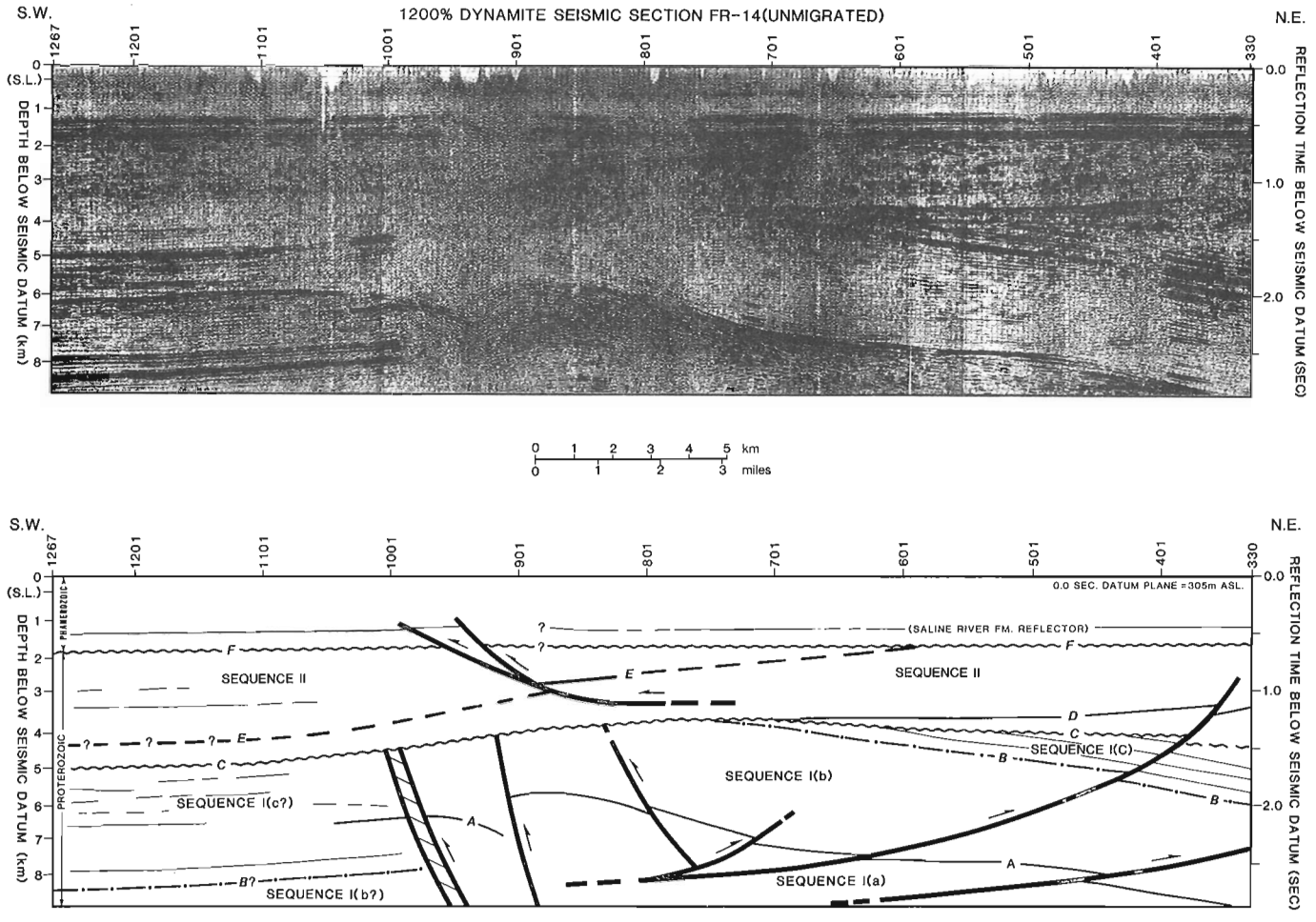

Figure 3. Upper part: Uninterpreted Forward Resources Seismic Section FR-14 (partial). Lower part: Line-drawing interpretation of line FR-14, showing key structural and stratigraphic elements.

Unit Ia

Unit Ia typically is characterized by indistinct, hummocky, wispy seismic patterns as in Figures 3 and 4, although elsewhere it is locally differentiated into parallel and subparallel seismic markers. The top of unit Ia is a very strong reflection (marker "A", Figs. 3, 4) that can be carried over the eastern portion of the study area, and is the most consistent seismic marker in the Proterozoic sequences studied. Few distinct, continuous reflections are identifiable in unit Ia, on sections examined to date, with the exception of two prominent parallel reflections (S1 and S2, Fig. 4), which are identifiable on both lines B-B' and C-C' east of 126° W. These discordant reflections are discussed below as possible intrusive sheets. Dix Interval Velocities calculated for unit Ia vary between 6500 and 7500 m/sec., but at these depths (greater than 2.5 sec., or 8 km) the seismic processing velocities from which these were calculated are often unreliable.

West of the large, deep fault zone (Figs. 2, 3), unit Ia is believed to be deeper than the bottom of the display on most of the available seismic sections. This huge fault appears to have an uplifted and rotated hanging wall on its east side and will be discussed more fully below.

Potential correlation with rocks of the Wopmay Orogen and Coppermine Homocline will also be discussed below.

Unit Ib

Unit Ib is an interval of fairly constant thickness (1.0 - 1.2 sec.) characterized by a weak or semi-transparent pattern of parallel reflections. Based on its relatively uniform Dix seismic velocity of 6 to 6.5 km/sec. this unit is calculated to be 3 to 3.5 km thick over most of the study area. However, near the east side of the area, on lines not illustrated here, the unit thickens abruptly from 3 to 4 km over a distance of about 27 km. This sudden thickening may be depositional

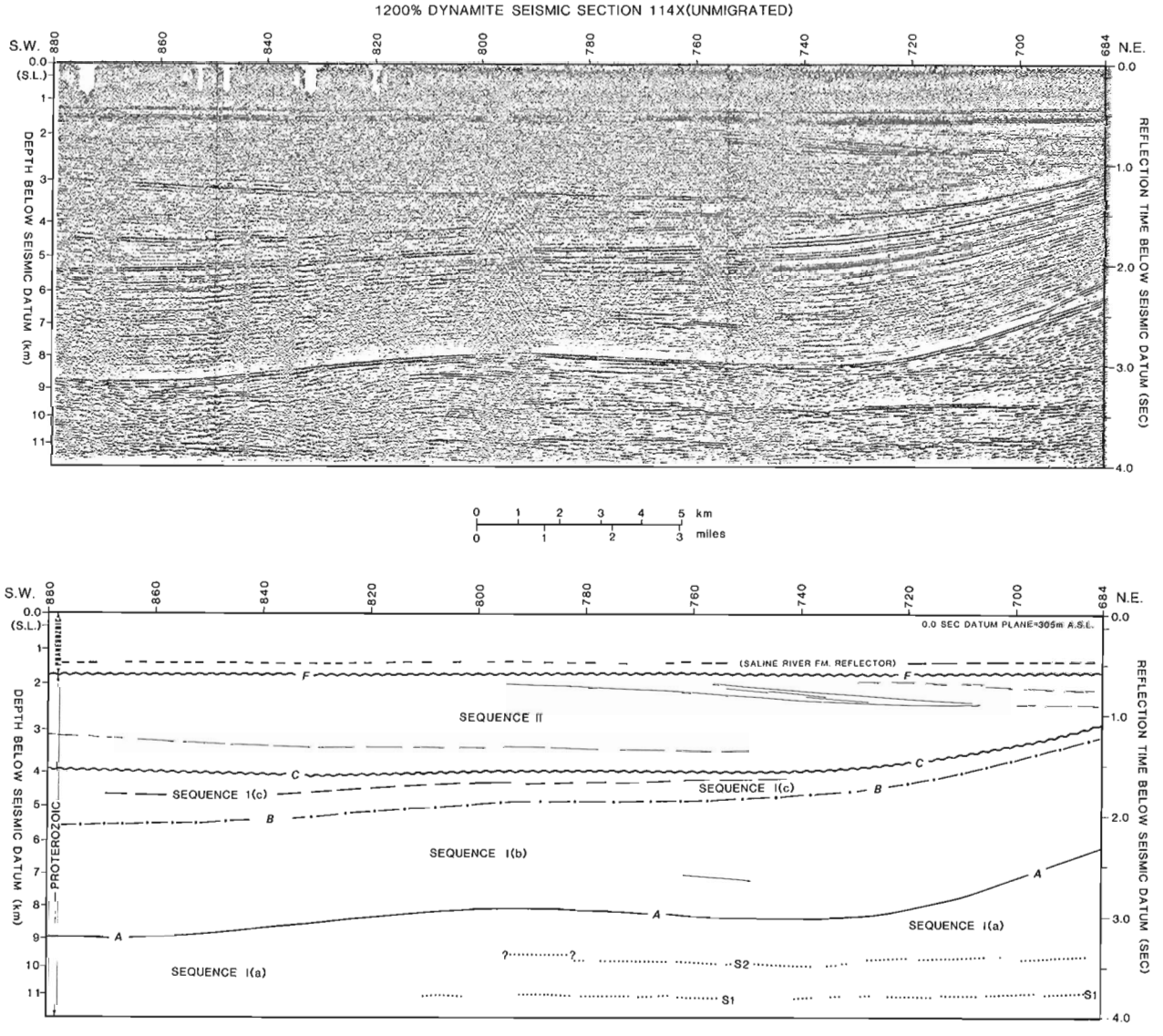

Figure 4. Upper part: Uninterpreted Petro-Canada Inc. Seismic Section 114X (partial). Lower part: Line-drawing interpretation of line 114X, showing key structural and stratigraphic elements.

TENTATIVE CORRELATION CHART

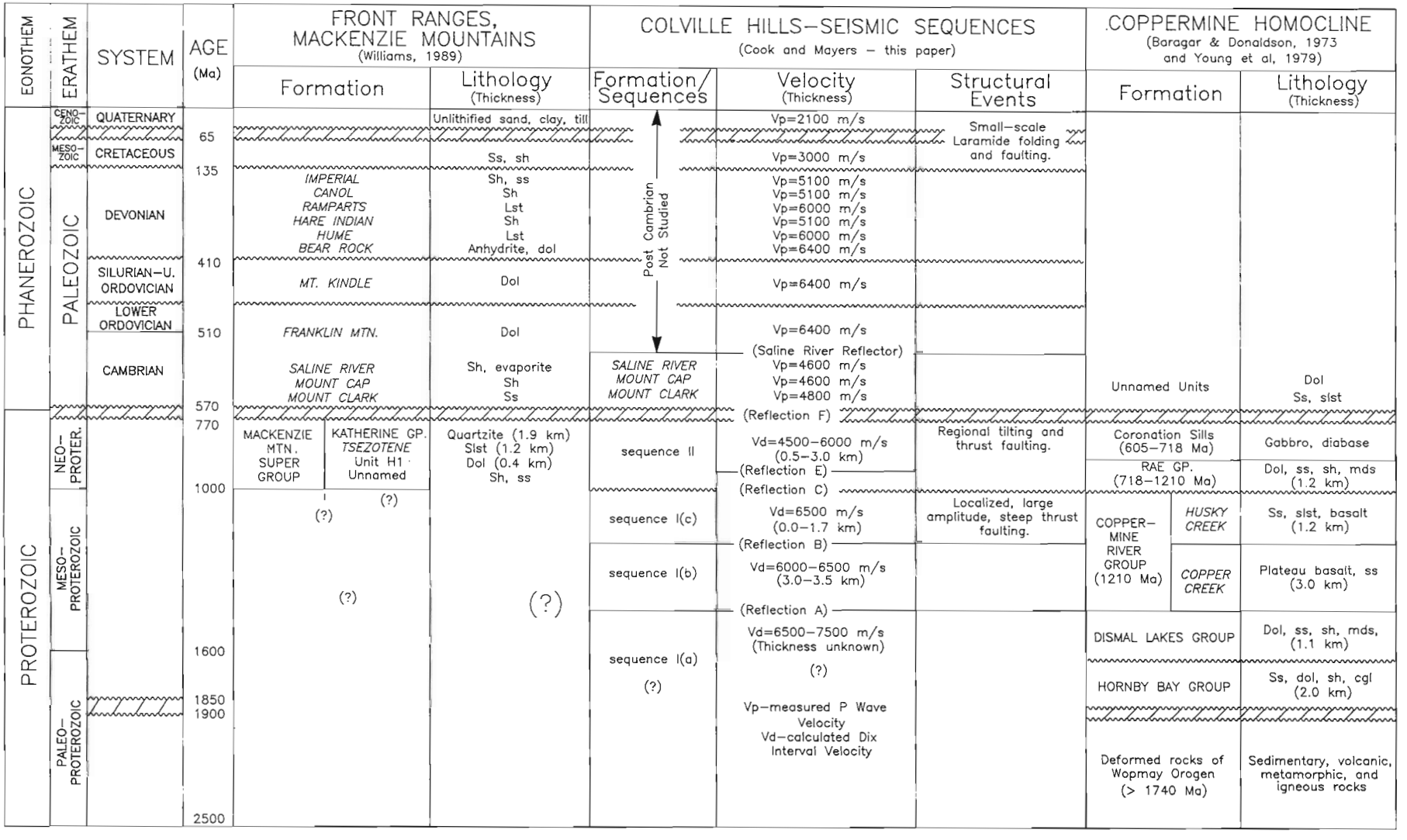

Figure 5. Provisional correlation chart showing the interpreted relationships between the seismic sequences and sequence boundaries in the report area and exposed rocks in the Mackenzie Mountains (west) and the Coppermine Homocline (east).

or may be due to structural causes. The upper contact with unit Ic is transitional into a zone of strong parallel seismic markers, and the boundary is selected as the lowest, consistently strong reflection (marker "B", Figs. 3, 4). This reflection is subparallel to marker "A" over the eastern part of the study area. It is tentatively correlated westward, across the large fault shown in Figure 3, to the lowermost strong marker.

Potential correlation of unit Ib with the Copper Creek Formation in Coppermine Homocline will be discussed below.

Unit Ic

Seismic unit Ic is a zone of strong parallel reflections, which varies in thickness from zero to 1.2 seconds (zero to 3.5 km) because of truncation by an overlying regional unconformity (marker "C", Figs. 3, 4). The truncation is best seen in the hanging wall of a large tilted fault block shown in Figure 3. The unit is tentatively identified west of the fault, as indicated. In this interpretation the unit thickens dramatically across the fault because of greater preservation in the footwall block and erosional truncation in the hanging wall block.

Potential correlation of unit Ic with the Husky Creek Formation in Coppermine Homocline will be discussed below.

Major fault

A large fault, expressed as a broad zone of disruption of seismic markers, has been identified. It is well displayed on Forward Resources Line FR-14 (Fig. 3), but through cursory examination of a number of adjacent lines it has been traced as a curvilinear zone at least 100 km long (Fig. 2). No seismic markers can be traced with confidence across the fault and, unfortunately, the fault zone largely coincides, on this line, with a zone of very poor energy returns. This zone of poor record affects all levels in the section, including the Phanerozoic, and probably is not due primarily to structural complexities at depth. Whatever the cause, discrete reflections are absent in the critical zone of interpretation. Nonetheless, from general considerations of the overall structure, a number of conclusions can be drawn. Firstly, the upthrown eastern block is a large tilted or rotated mass with a minimum structural relief of 3 km, as measured on the "A" and "B" markers. Rotation of the hanging wall block implies that it is underlain by a curved, eastward dipping thrust fault as interpreted in Figure 3. Secondly, the strata imaged in the western, footwall block, terminate abruptly at the fault zone and do not project beneath the hanging wall block. The fault appears, therefore, to be a deeply rooted, curved reverse fault. It may be analogous to the intra-cratonic, crustal-scale, Laramide uplifts of the Rocky Mountain foreland of mid-western U.S.A. (e.g., Matthews 1978). Considering its geometry and its northwestward sense of transport, the fault appears to be incompatible with a regional, "thin-skinned", eastward directed thrust belt interpreted by F.A. Cook (1988a, b) in the eastern part of our study area.

Lesser thrusts

Sequence I is also cut by smaller-scale thrust faults. Considered over the entire study area they are mostly eastward verging, and therefore may not be related to the phase of deformation that produced the westward verging, large rotated block of Figure 3. Others are younger, because they offset the unconformity (marker "C", Figs. 3, 4) separating sequences I and II. One such fault is interpreted and is shown on the east side of Figure 3. Some of these faults, on lines not reproduced here, show greater offset of markers below the unconformity than of those above, indicating reactivation of earlier-formed structures.

REGIONAL UNCONFORMITY

Sequence I is separated from sequence II by a regional unconformity (marker "C", Figs. 3, 4). Locally, the unconformity is angular and truncates large structures affecting sequence I (e.g., Fig. 3). It is nonetheless difficult to trace with precision across the entire region because locally it is paraconformable, and does not everywhere correspond to an observable velocity contrast. However, in most sections, some discontinuity and truncation of the underlying strata can be detected (e.g., Fig. 4).

PROTEROZOIC SEQUENCE II

Sequence II has an indistinct seismic character, but clearly represents a stratified sequence. A few strong, internal, discontinuous reflections occur across the region. Examples are an unnamed, gently east-dipping reflection on the left side of Figure 4 (at 1.0 to 1.5 sec.) and a reflection labelled "D" on Figure 3.

Marker "E" on Figure 3 is problematical in that it cuts upsection eastward across sequence II. This is a prominent reflection, identifiable on a number of adjacent lines to the south of FR-l4, but we have been unable to trace it regionally. Dix velocities decrease eastward across it. East of the intersection, between reflections E and F (-shotpoint 601, Fig. 3), the sequence II strata below "F" have lower velocities (4500-5000 m/sec.), whereas immediately to the west they are slightly higher (5000-5500 m/sec.). Reflection "E" may represent an eastward directed thrust fault. If so, it must be listric into an unseen detachment surface above reflection "C", because underlying reflections are not displaced. Alternatively, "E" might represent an unconformity dividing sequence II into two entirely different stratigraphic packages of different lithologies. A third possibility is that it is related to a contact between map-unit H1 dolomites (on the west) and unnamed shale and sandstone (on the east), interpreted by Aitken and Pugh (1984), from sparse well control. Their contact crosses line FR-14 (see Fig. 2) at about shotpoint 1101. This possibility seems unlikely because reflection "E" cuts diagonally across, more or less, the entire sequence II package.

As will be discussed below, sequence II probably correlates with the Mackenzie Mountains supergroup to the west, and with the Shaler and Rae groups to the east.

INTRUSIVE SHEETS

Two reflections (S1 and S2, Fig. 4) at depths of 3.4 to 3.8 seconds, or 9.5 to 11.0 km, are sub-horizontal and parallel to each other. They occur in sequence Ia and cut discordantly across a westward dipping panel. Similar sub-horizontal parallel reflections on lines in the eastern part of the area were interpreted by F.A. Cook (1988a, b) as representing stratigraphic layering in the footwall of a flat, large-displacement thrust fault. An alternative interpretation, offered here, is that these sub-horizontal reflections represent intrusive sheets. If so, the need for the lower of Cook's flat thrust faults is obviated. Diabase sills intrude the Mackenzie Mountains supergroup to the west, and the Shaler, Rae, Coppermine, Dismal Lakes and Hornby Bay groups to the east. Consequently, they are to be expected in the Precambrian rocks imaged on these sections. If reflections S1 and S2 (Fig. 4) do represent intrusive sheets, the intrusions cross-cut, and therefore postdate, the tilted panel of sequences I and II. They would, therefore, be younger than sequence II, and may have been emplaced in the same general period as diabase dikes and sills mapped by Cook and Aitken (1969), intruding strata equivalent to the Shaler Group on Brock Inlier.

PHANEROZOIC STRATA

Phanerozoic strata in the study area include those of Cambrian, Ordovician, Silurian, Devonian, and Cretaceous ages. The Phanerozoic is easily identified on most sections because the lower part of the section, comprising sandstones, shales, and evaporites of the Mount Clark, Mount Cap, and Saline River formations, is expressed as a distinct band of parallel reflections. That band, moreover, is commonly discordant to, and truncates reflections in the underlying Proterozoic section. Phanerozoic strata are locally offset by faults, as for example between shotpoints 901 and 1001 on Figure 3. In that case, the structure is local and must be listric, becoming bedding-parallel at a very shallow depth. Other faults cutting the Phanerozoic affect much larger blocks and must root deeper in the section than the one illustrated in Figure 3. Faults that disrupt the Phanerozoic commonly occur above a zone of disruption in the Precambrian, and have probably been localized by the presence of older structures. The details of any such relationship have not as yet been established.

STRUCTURAL CONSIDERATIONS

At least three phases of compressive deformation are displayed in the seismic records of this area. First, sequence I is disrupted by the large northwestward directed fault illustrated in Figure 3, and that deformation predates deposition of sequence II. Second, sequences I and II are cut by eastward directed thrust faults with relatively minor displacements, such as that illustrated on the east side of Figure 3. The relationship between these thrusts and the large northwestward directed fault of Figure 3 is unknown. Regional tilting of both major sequences occurred, as shown, for example, at the right or east side of Figure 3. Truncation eastward of unit Ic by the major unconformity (marker "C") indicates that tilting was initiated prior to deposition of sequence II, and was reactivated following deposition of sequence II. Minor thrusts and large-scale tilting postdate deposition of sequence II, and predate Phanerozoic deposition. Third, Phanerozoic strata are affected by folds and faults that may have been localized by earlier structures. Structures forming the Colville Hills (Cook and Aitken, 1971) were generated during this last phase of deformation.

In the eastern part of the study area, F.A. Cook (1988a, b) has interpreted two sub-horizontal detachments in an east-verging Proterozoic thin-skinned thrust and fold belt, with at least 50 to 90 km of horizontal shortening. We agree that the Proterozoic strata have experienced more-or-less east-west horizontal shortening, and the large reverse fault interpreted in Figure 3 could, no doubt, be accommodated in a primarily eastward-directed kinematic system. However, at this point in our preliminary investigations we do not recognize his stratigraphic repetitions (particularly for the upper thrust fault), and, accordingly, we do not recognize his bedding-parallel thrusts. The lower of his two thrusts is required if a set of sub-horizontal reflections, here considered to represent intrusive sheets, in fact represent stratigraphic layering as he interpreted.

REGIONAL CORRELATIONS

The uppermost Proterozoic rocks (sequence II) are considered to correlate, on the west, with the Mackenzie Mountains supergroup. Strata immediately underlying the sub-Cambrian unconformity are penetrated by a number of wells in the region. Wissner (1986) identified the Tsezotene Formation of the Mackenzie Mountains supergroup in the PCI Sammons H-55 well, which is situated on Imperial Anticline west of the Mackenzie River. Aitken and Pugh (1984) correlated Precambrian rocks encountered in fifteen wells with formations comprising the Mackenzie Mountains supergroup. They interpreted the regional subCambrian structure as a broad, westward dipping homocline, truncated by erosion at the sub-Cambrian unconformity. They suggested that the homoclinal dip reversed across a broad anticlinal axis (Great Bear Arch) in the Colville Hills area (see Figs. 1, 2). None of their correlations can be specifically confirmed by the present study, with the possible exception of one of their stratigraphic contacts, which crosses line FR-14 (Fig. 3) at about shot-point 1100, and which, as discussed but discounted above, may correspond to marker "E". Our two regional cross-sections do, however, confirm Aitken and Pugh's (1984) suggestion that uppermost Proterozoic strata (sequence II) occur in a westward dipping homocline, although their broad anticlinal Great Bear Arch, which should be recognizable at the left side of Figure 4, has not been identified. Because sequence II thins eastward to zero thickness within the study area, such an arch, or alternatively a large fault, seems to be required somewhere between the study area and Brock Inlier where interpreted correlatives of sequence II are exposed.

The thickness of sequence II varies from a maximum of 4 km in the west to zero in the east (where it is truncated by the sub-Cambrian unconformity). Because the lowermost unnamed shale and sandstone of Aitken and Pugh (1984) in the subsurface is virtually unseen in the Mackenzie

Mountains, no direct thickness comparisons can be made with measured thicknesses in the Mackenzies. Katherine Group and older units of the Mackenzie Mountains supergroup vary from 1.6 to 3.5 km in thickness (Aitken, et al., 1973). This supergroup has been correlated in a general way (Young et al., 1979) with the Rae Group exposed in Coppermine Homocline and the Shaler Group on Victoria Island. Similarily Aitken (1982) correlated the supergroup with unnamed units on Brock Inlier and to the Shaler Group on Victoria Island. Accordingly, sequence II also presumably correlates on the east, at least in part,with the Rae and Shaler groups. The existence of a major unconformity at the base of the Rae Group (Baragar and Donaldson, 1973a, b), which would correlate with our unconformity "C", supports that conclusion. It is noteworthy that the sub-Rae Group unconformity, as mapped by Baragar and Donaldson, is paraconformable over part of its surface trace, but elsewhere cuts rapidly downsection. The unconformity, identified here, appears to be significantly lower than the sub-Rae Group unconformity indicated by F.A. Cook (1988a), and probably occurs near the base of his reflection sequence V (see his Figure 3).

If strata of the Coppermine Homocline extend westward beneath Anderson Plains and Colville Hills, then sequence I probably represents some part or all of the Coppermine River, Dismal Lakes, and Hornby Bay groups. Tentative correlations (Fig. 5) of sequence I correspond more or less directly with F.A.Cook's (1988a) seismic sequences as applied in his central region. Because we do not recognize his thrust repeats in his eastern region, one-to-one correspondence between our units and his cannot be made there. Unit Ib corresponds generally with F.A. Cook's seismic sequence III, and correlates with the Copper Creek Formation volcanic rocks, which are largely plateau basalts. Its relatively uniform thickness of about 3 km, Dix seismic velocity of 6.0 to 6.5 km/sec., and uniform reflection character, compare favourably with a measured thickness (Baragar and Donaldson, 1971) of 3 km for the Copper Creek Formation and expected velocities of 4 to 6 km/sec. for volcanic rocks. This correlation implies that the Coppermine basalts extend westward into the subsurface for at least 300 km, and would more than double their known lateral extent. This correlation supports Davis and Willot (1978) who attributed magnetic anomalies, coincident with Colville Hills structures, to the folded or faulted involvement of Coppermine basalts in the structures.

If unit Ib correlates with the Copper Creek Formation, it follows that the overlying, multilayered unit Ic correlates with the interbedded clastic and volcanic rocks of the Husky Creek Formation in Coppermine Homocline. Unit Ic corresponds with F.A. Cook's (1988a) seismic reflection sequence IV (see his Fig. 3).

Unit Ib is underlain by high velocity unit Ia, which could represent high velocity dolomites of the Dismal Lakes Group. Unit Ia, however, is much thicker than known thicknesses of the Dismal Lakes Group. The group may thicken dramatically westward, as the Hornby Bay Group is known to do southwestward [one of the Hornby Bay units has a tenfold thickness increase across 400 km from Coppermine Homocline to Cap Mountain to the southwest (G.M.Ross, pers. comm., 1989)]. Conversely, unit Ia could include rocks equivalent to one or both of the Hornby Bay Group and complexly deformed rocks of the Wopmay Orogen. Because we cannot identify a reflection that might represent crystalline basement, our unit Ia is undivided and corresponds to F.A. Cook's (1988a) sequences I and II combined.

CONCLUSIONS

Initial seismic interpretation across a 30 000 km^2 region of the Colville Hills indicates that:

1. From reflection seismic records, the Proterozoic rocks in the northern part of the Colville Hills can be subdivided into two major sequences (I and II) separated by a locally angular, locally paraconformable unconformity (marker "C") that appears to correlate with that mapped at the Coppermine River Group - Rae Group boundary in the Coppermine Homocline to the east. Unit Ia of sequence I is correlated with the Dismal Lakes Group, but may include rocks equivalent to the Hornby Bay Group and/or highly deformed rock units of the Wopmay Orogen. Sequence Ib is correlated with the plateau basalts of the Copper Creek Formation, and unit Ic is correlated with the Husky Creek Formation. Sequence II unconformably overlies sequence I and is correlated with the Mackenzie Mountains supergroup, to the west, and with the Rae and Shaler groups, to the east.

2. The seismic data examined to date confirm that in the Colville Hills area younger Proterozoic strata occur in a westward dipping homocline, as interpreted by Aitken and Pugh (1984). However, we do not recognize the broad anticlinal reversal (Great Bear Arch) that they interpreted along the eastern side of the study area.

3. The shallower, sub-Cambrian unconformity that has been mapped in outcrop and penetrated by exploration wells is readily detected on the seismic profiles (reflection "F").

4. Proterozoic rocks have been deformed by three periods of compression directed roughly east-west. The earliest of these postdates strata that may correlate with the Husky Creek Formation, and affected only sequence I strata. The most significant early structure is a large rotated or tilted fault block interpreted as being underlain by a steeply dipping, curved reverse fault. Gross geometry of the structure seems to be analogous to, although at a smaller-scale than, that of intracratonic, crustal scale uplifts typical of Wyoming. A second compressional deformation was less intense, and postdates strata correlated with the Mackenzie Mountains supergroup and the Rae Group. It affected both sequences I and II. The third, and last, compressional deformation was post Early Cretaceous, and is probably related to the Tertiary Laramide orogenic development of the Mackenzie and Franklin Mountains to the southwest. Displacements during this phase of deformation were relatively small and were probably localized by underlying earlier structures.

5. We agree with F.A.Cook that Proterozoic strata have been subjected to east-west horizontal shortening, but we do not recognize two large displacement sub-horizontal detachments interpreted by him (1988a, b). Resolution of the lower of his faults is dependant on the identification of a number of strong, sub-horizontal reflections that are considered here to be post-orogenic igneous intrusions, but which were considered by F.A. Cook to be pre-orogenic footwall strata.

6. If the above-noted reflections represent intrusive sheets, they are younger than sequence II strata.

REFERENCES

Aitken, J.D.
1982: Precambrian of the Mackenzie fold belt - A stratigraphic and tectonic overview. Geological Association of Canada, Special Paper 25, p. 1439-1461.

Aitken, J.D., Long, D.G.F., and Semikhatov, M.A.
1978a: Progress in Helikian stratigraphy, Mackenzie Mountains; *in* Current Research, Part A, Geological Survey of Canada, Paper 78-1A, p. 481-484.
1978b: Correlation of Helikian strata, Mackenzie Mountains - Brock Inlier - Victoria Island. *in* Current Research, Part A, Geological Survey of Canada, Paper 78-1A, p. 485-486.

Aitken, J.D., Macqueen, R.W., and Usher, J.L.
1973: Reconnaissance studies of Proterozoic and Cambrian stratigraphy, lower Mackenzie River area (Operation Norman), District of Mackenzie. Geological Survey of Canada, Paper 73-9, 178 p.

Aitken, J.D. and Pugh, D.C.
1984: The Fort Norman and Leith Ridge structures: major, buried, Precambrian features underlying Franklin Mountains and Great Bear and Mackenzie Plains. Bulletin of Canadian Petroleum Geology, v. 32, p. 139-146.

Baragar, W.R.A. and Donaldson, J.A.
1971: Coppermine and Dismal Lakes map-areas. Geological Survey of Canada, Paper 71-39, 20 p.
1973a: Geology, Coppermine, District of Mackenzie. Geological Survey of Canada, Map 1337A, scale 1:250 000.
1973b: Geology, Dismal Lakes, District of Mackenzie. Geological Survey of Canada, Map 1338A, scale 1:250 000.

Cook, D.G. and Aitken, J.D.
1969: Geology, Early Lake, District of Mackenzie. Geological Survey of Canada, Map 5-1969, scale 1:250 000.
1971: Geology, Colville Lake map-area and part of Coppermine map-area Northwest Territories. Geological Survey of Canada, Paper 70-12, 42 p.

Cook, F.A.
1988a: Middle Proterozoic compressional orogen in northwestern Canada. Journal of Geophysical Research, v. 93, p. 8985-9005.
1988b: Proterozoic thin-skinned thrust and fold belt beneath the interior platform in northwestern Canada. Geological Society of America, Bulletin, v.100, p. 877-890.

Cook, F.A., Coflin, K., Lane, L., Dietrich, J., and Dixon, J.
1987: Structure of the southeast margin of the Beaufort-Mackenzie Basin, Arctic Canada, from crustal seismic data. Geology, v. 15, p. 931-935.

Davis, J.W. and Willott, R.
1978: Structural geology of the Colville Hills. Bulletin of Canadian Petroleum Geology, v. 26, p.105-122.

Dix, C.H.
1955: Seismic velocities from surface measurements. Geophysics, v. 20, p. 68-86.

Matthews, Vincent, III, (editor)
1978: Laramide folding associated with basement block faulting in the western United States. Geological Society of America, Memoir 151, p. 313-336.

Ross, G.M. and Kerans, C.
in press: Geology, Hornby Bay and Dismal Lakes groups, Coppermine Homocline, District of Mackenzie, Northwest Territories. Geological Survey of Canada, Map 1663A, scale 1:250 000.

Williams, G.K.
1986: Proterozoic, Mackenzie corridor. Geological Survey of Canada, Open File 1273.
1989: Tectonic Evolution of the Fort Norman area, Mackenzie corridor, N.W.T. Geological Survey of Canada, Open File 2045.

Wissner, U.
1986: A new look at the Imperial Anticlinorium, Mackenzie Plain, Northwest Territories. (abstract). Canadian Society of Petroleum Geologists 1986 Convention, Calgary, Alberta. Program and Abstracts, p. 97.

Young, G.M., Jefferson, C.W., Delaney, G.D., and Yeo, G.M.
1979: Middle and Late Proterozoic evolution of the northern Canadian Cordillera and Shield. Geology v. 7, p. 125-128.

Geological setting of stratabound gold occurrences in the Archean Fish-hook — Turner lakes belt, Bathurst Inlet area, District of Mackenzie, N.W.T.[1]

C.W. Jefferson, M.N. Henderson, J.R. Henderson[2], and S. Schaan[3]
Mineral Resources Division

Jefferson, C.W., Henderson, M.N., Henderson, J.R. and Schaan, S., Geological setting of stratabound gold occurrences in the Archean Fish-hook — Turner lakes belt, Bathurst Inlet area, District of Mackenzie, N.W.T.; in Current Research, Part C, Geological Survey of Canada, Paper 90-1C, p. 349-361, 1990.

Abstract

Three deformation phases are documented in the belt. Where distinguishable, S_1 is parallel to S_0 and is crenulated by S_2. The latter is marked by alignment of metamorphic minerals (cordierite and andalusite) which include S_1, indicating that the peak of metamorphism occurred during D_2. An upright, southwest-plunging D_3 antiform preserves reclined F_2 and F_1 on its hinge, implying horizontal transport during D_1 and D_2. Tonalites were intruded during late stages of D_3. The stratigraphy of the supracrustal sequence, from the base, is: (1) greywacke, (2) iron-formation, (3) angular unconformity, (4) polymictic conglomerate (James Falls Conglomerate), (5) complex sequence of arenite, conglomerate, volcanic, hypabyssal and volcaniclastic rocks, (6) greywacke. High strain zones border a central belt dominated by sequence (5). Stratabound gold prospects spatially coincide with macroscale F_3 hinges in sulphidic iron-formation (Fish-hook Lake) and sulphidic arenite (Turner Lake).

Résumé

Trois phases de déformation affectent cette zone. Lorsqu'elle est visible, S_1 est parallèle à S_0 et crénulée par S_2. Cette dernière se distingue par l'alignement des minéraux métamorphiques (cordiérite et andalousite) qui renferment des inclusions de S_1, indiquant un maximum métamorphique pendant D_2. Un antiforme droit D_3, plongeant vers le sud-ouest, préserve des plis inclinés F_2 et F_1 dans sa charnière, témoignant d'un transport horizontal pendant D_1 et D_2. Des tonalites sont intrusives vers la fin de D_3. La stratigraphie de la succession supracrustale comprend de bas en haut: 1) grauwacke, 2) formation ferrifère, 3) discordance, 4) conglomérat polymicte (conglomérat de James Falls), 5) série complexe d'arénite, de conglomérat, de roches volcaniques, hypabyssales et volcanoclastiques et 6) grauwacke. Des zones fortement déformées limitent une zone centrale dominée par la série 5). Les indices d'or connus coïncident avec les charnières de plis macroscopiques F_3 et sont situés dans des formations ferrifères à sulfures (lac Fish-hook) et arénites à sulfures (lac Turner).

[1] Contribution to Canada-Northwest Territories Mineral Development Agreement 1987-1991. Project carried by the Geological Survey of Canada.
[2] Continental Geoscience Division
[3] Ottawa-Carleton Geoscience Centre, Ottawa, Ontario K1N 6N5

INTRODUCTION

The Fish-hook — Turner lakes supracrustal belt is overlain to the east and south by the Early Proterozoic Goulburn Group, bordered on the west by Late Archean tonalite and truncated with sinistral deflection on the north by the Bathurst Fault (Fig. 1). The purpose of this study is to map the belt, and provide constraints on the origin of various known gold occurrences. Detailed studies of the Turner Lake (S. Schaan, M.Sc at University of Ottawa; S. Fumerton, internal research for Chevron Minerals Ltd.) and Pistol Lake (R. Wyllie, M.Sc. at University of New Brunswick) prospects are underway. Ford (1988) has compared the Pistol Lake prospect to the Lupin Mine and other prospects in the Slave Province. Documentation of the structure and stratigraphy of the Fish-hook — Turner lakes supracrustal belt will provide a context for these local studies.

This progress report is based on six traverse days in 1988, about five man-months of traversing in 1989, and some compilation as indicated in Figure 1. A stratigraphic summary is based on mapping of the Fish-hook Lake (JRH, MNH and CWJ) and Turner Lake (SS and CWJ) areas. This mapping also provided information on some high strain zones transecting the belt (CWJ).

ACKNOWLEDGMENTS

S.M. Roscoe introduced CWJ to the area and forwarded unpublished material. We greatly appreciated logistical help and geological discussions from Chevron Minerals Ltd. (G.Walton, S. Fumerton and R.Wyllie). Indian and Northern Affairs Canada (W. Padgham) supported the concept of the project, and employed S. Schaan and assistant S. Penny. R. Johnstone (Government of the N.W.T.), mapping in the Torp Lake belt about 50 km to the north of our camps (Johnstone 1989), exchanged geological information most enthusiastically. T.O. Wright (NSF, Washington D.C.) collaborated in the mapping, and shares credit for many of the observations and interpretations related to the Fish-hook Lake area. W.K. Fyson is supervising S. Schaan's M.Sc in the Turner Lake area. Polar Continental Shelf provided 20 hours of helicopter time. Canada Centre for Remote Sensing (A. Fabbri and C. Kushigbor) provided undistorted 1:10 000 and 1:20 000 scale SPOT and SAR images for base maps, as part of a research project on the use of remote-sensed data in this area (Fabbri et al., 1989). Rod Stone and Lynn Parney provided perfect expediting. A visit by Otto van Breemen (GSC) to collect rocks for geochronology was much enjoyed professionally and socially. J.A. Kerswill critically read the manuscript and made many constructive suggestions.

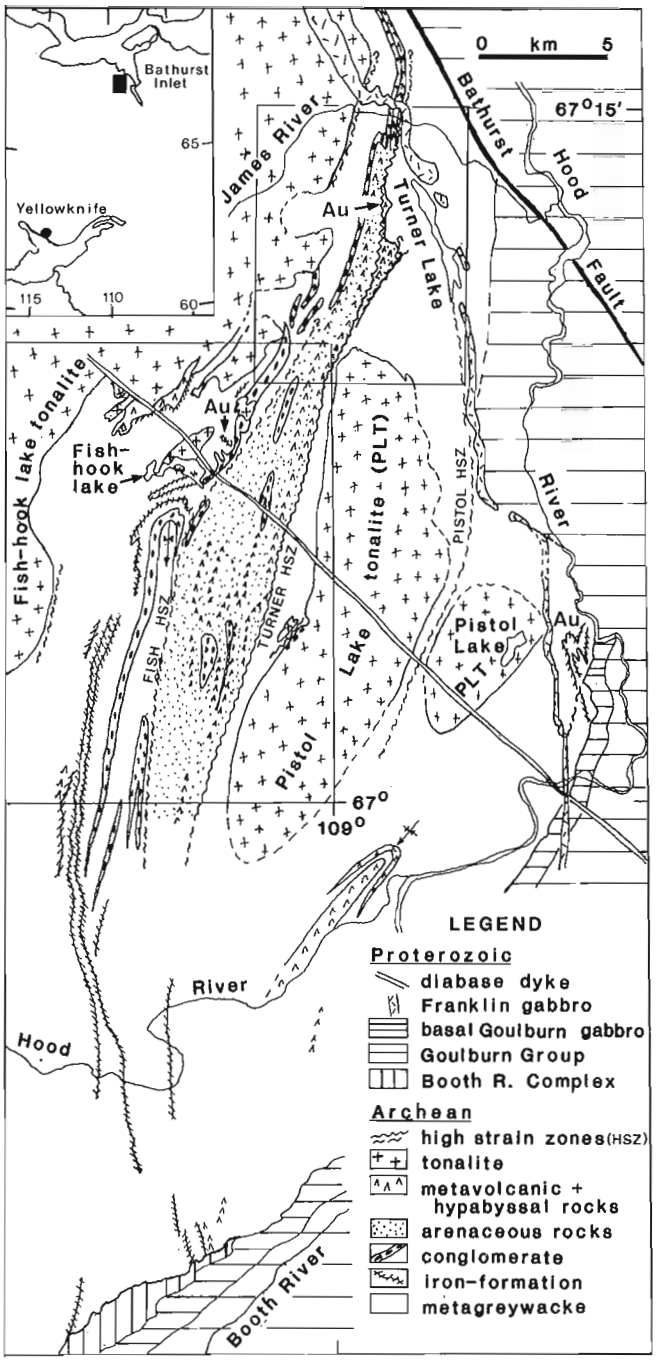

Figure 1. Location (inset, black box) and geological sketch map of the region of the Turner Lake belt. Modified from Geological Survey of Canada Map 45-1963, Figure 1 of Roscoe et al. (1989), and unpublished maps of Silver Hart Mines Ltd. properties by E.A. Hardy, C. Clode and S. Bishop. The Fish-hook Lake (Fig. 2) and Turner Lake (Fig. 7) map-areas are outlined, as are high strain zones (HSZ) and auriferous zones (Au).

ROCK UNITS

All rocks in the belt are metamorphosed, from lower greenschist to cordierite + andalusite grade. The stratigraphy is generalized as follows, in roughly ascending order based on numerous younging indicators.

1. *Argillaceous greywackes* predominate in the western, southern and eastern parts of the supracrustal belt (Fig. 1, 2, 7). These typically comprise two facies: (a) massive, poorly graded beds of argillaceous wacke, 10-300 cm thick, separated by minor pelites, and (b) alternating graded arenites and laminated pelites each 2-10 cm thick. Turbidites are interbedded with relatively continuous magnetic iron-formation and in some areas have thin silicate iron-formation (variously amphibolitic, garnetiferous) interbeds. Much of the greywacke sequence is poorly graded, so that younging directions are difficult to obtain. Bedding is commonly obscured by the fairly strong S_2 fabric and the planar orientation of cordierite and andalusite which are generally 2-3 cm long and locally up to 10 cm.

2. *Banded iron-formations* are located near the top of the lower greywacke sequence. At Pistol Lake, Silver Hart Mines Ltd. (1985), Ford (1988) and G. Walton (pers. comm., 1989) have reported a lower, continuous, silicate-sulphide-dominated auriferous iron-formation separated by approximately 100 m of greywacke (in two drillholes) from an upper, continuous, silicate-magnetite iron-formation which has auriferous sulphidic alteration zones. The magnetite-silicate zone outcrops on Hood River, but the silicate-sulphide zone has not been recognized on Hood River. In the Fish-hook Lake map area (Fig. 2) only the very continuous magnetite-silicate iron-formations have been mapped for this study. Other thin, sulphidic and magnetic, less continuous iron-formations are contained in the upper greywacke interval. Local thin felsic and mafic tuffs are within 10s of metres of iron-formation on the west side of the belt at 67° N and near Booth River. Iron-formation is also adjacent to volcanic rocks northwest of Fish-hook Lake. Tuffs have also been recognized in greywackes near the iron-formations in the Pistol Lake area (G. Walton, pers. comm., 1989). Gold and arsenopyrite have been found in the sulphidic parts of the iron-formations (Roscoe et al., 1988).

3. *Polymict orthoconglomerate* was earlier described by Roscoe (1983), C. Clode (1987) and Roscoe et al. (1988, the James Falls Conglomerate). They recognized the flattening of clasts, the possibility of structural and stratigraphic repetition and a variety of clast compositions. We have confirmed this flattening, the stratigraphic as well as structural repetitions, and have observed clast sizes from granule to boulders larger than 1 m. Clasts include variably abundant felsic-volcanic, hypabyssal and sedimentary rocks indistinguishable from units in the same belt (described below). No basalt clasts have been recognized. Despite much searching, no clasts with pre-F1 fabrics were noted, therefore it is unlikely that any of the clasts represent a much older basement.

The James Falls Conglomerate (Fig. 9) is exposed with some discontinuities for about 36 km south of Bathurst Fault (Fig. 1) along the western margin of the central arenite-volcanic sequence. Separate lenses of very similar polymict conglomerate are dispersed within the central arenite belt, on the margin of the volcanic belt NW of Fish-hook Lake, and on the west margin of the Pistol Lake tonalite. In the vicinity of Fish-hook Lake (Fig. 2), the conglomerate unconformably overlies the lower greywacke and iron-formation. At the Outlet Stream the unit is a breccia composed entirely of greywacke and iron-formation fragments that seemingly passes conformably upward into polymict orthoconglomerate.

4. *Rusty weathering, sulphidic quartz-rich arenites* are located stratigraphically below, above and intercalated with volcanic, volcaniclastic, hypabyssal and conglomeratic rocks. Cross beds and fine planar laminations are the most common sedimentary structures. Graded beds with flame structures are subordinate in this non-pelitic facies; ripple-drift cross-laminae and wavy crested ripples are rare. A shallow water depositional environment is inferred.

5. *Volcanic and volcaniclastic rocks* range in composition from magnesium-rich basalt (S. Fumerton, pers. comm., 1989) to rhyolite and are located, together with arenites and conglomerates, mainly in a central north-south zone. Mafic compositions are most common, although felsic crystal tuffs attain thicknessess of more than 100 m. Volcanic textures include pillows, tabular flows and monomict breccias. Volcaniclastic rocks characteristically have monomict, coarse-to-fine, sub-angular clasts, laminations and planar to trough-cross beds.

6. *Hypabyssal gabbro, medium- to fine-grained diorite and tonalite* in tabular to anastamosing peneconcordant sheets and lenses are also present mainly in the central arenite belt. The diorite and tonalite have very finely crystalline chill margins where well exposed (at James Falls and west of Turner Lake). Thick diorites in the same areas contain central zones with coarse feathery amphiboles. Some gabbros are typically pitted on weathered surfaces. A series of thin-to-thick, white-weathering, rhyolite sills outline a prominent southwest-plunging isoclinal syncline north of Hood River (Fig. 1). Most of these rocks contain the same fabrics as the supracrustal units, hence are interpreted as syn-volcanic hypabyssal intrusions.

7. *Argillaceous greywackes* overlying the conglomerate at James River Falls (Fig. 9) and in the "hook fold complex" southwest of Turner Lake (Fig. 8) are lithologically indistinguishable from those that underlie the same strata. Greywackes between the hook fold complex and Turner Lake contain thin, poorly exposed silicate-sulphide iron-formation whose stratigraphic position is yet undetermined.

8. *The Pistol Lake tonalite* (Fig. 1, 2, 7) is interpreted (CWJ) to be one of the oldest large plutons in the study area, pre-dating F1 because its margins and associated sills are transected by both S1 and S2. Although this tonalite is segmented by high strain zones (described below), the central parts of the segments are only weakly foliated.

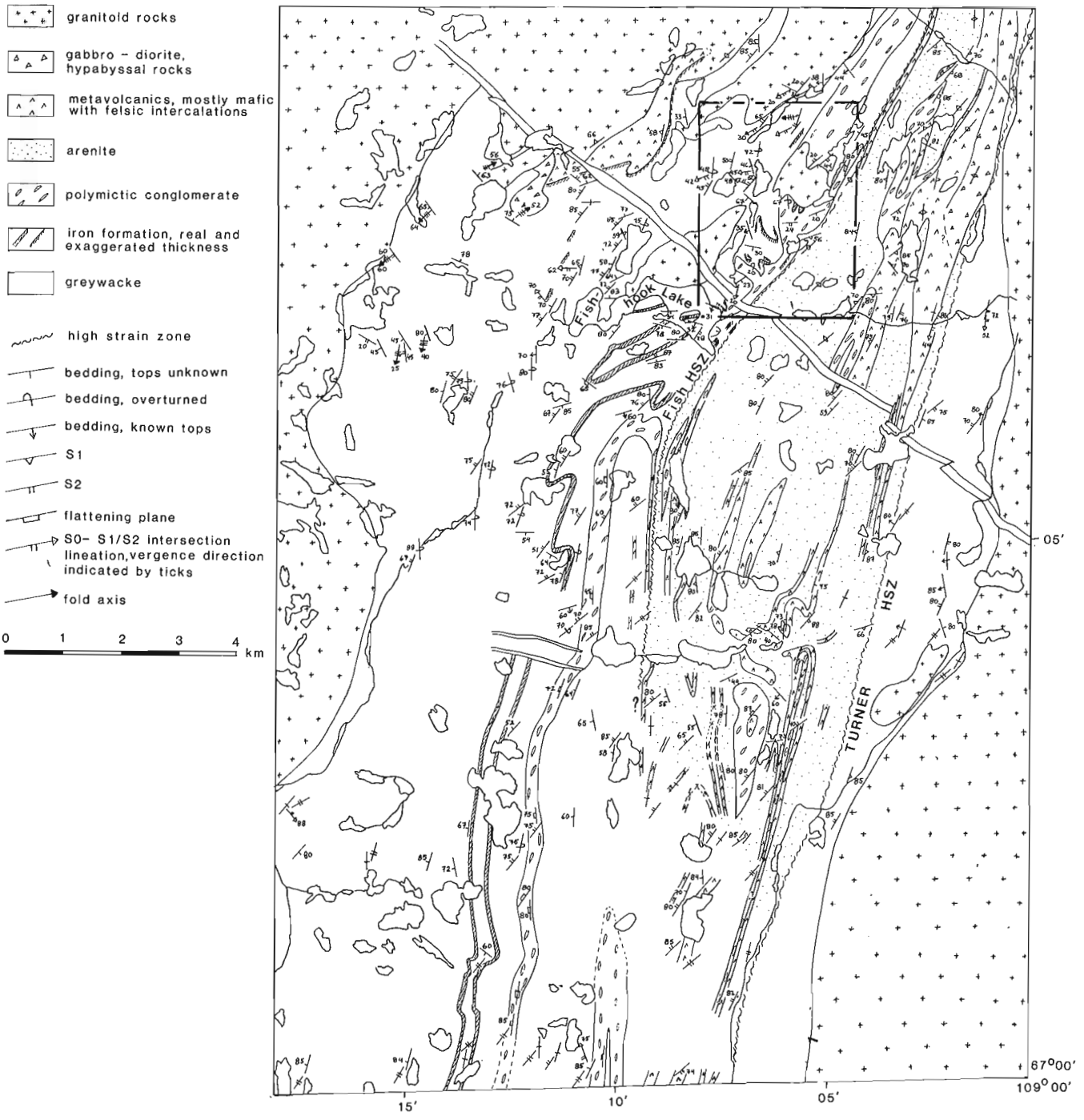

Figure 2. Geological map of the Fish-hook Lake area (Fig. 1). The abundant pegmatite bodies and narrow diabase dykes are omitted for clarity. The largest Mackenzie dyke in the area is shown (it intersects the east border of the map at 67° 05′N). The Outlet Stream area (Fig. 3) is indicated by the rectangle.

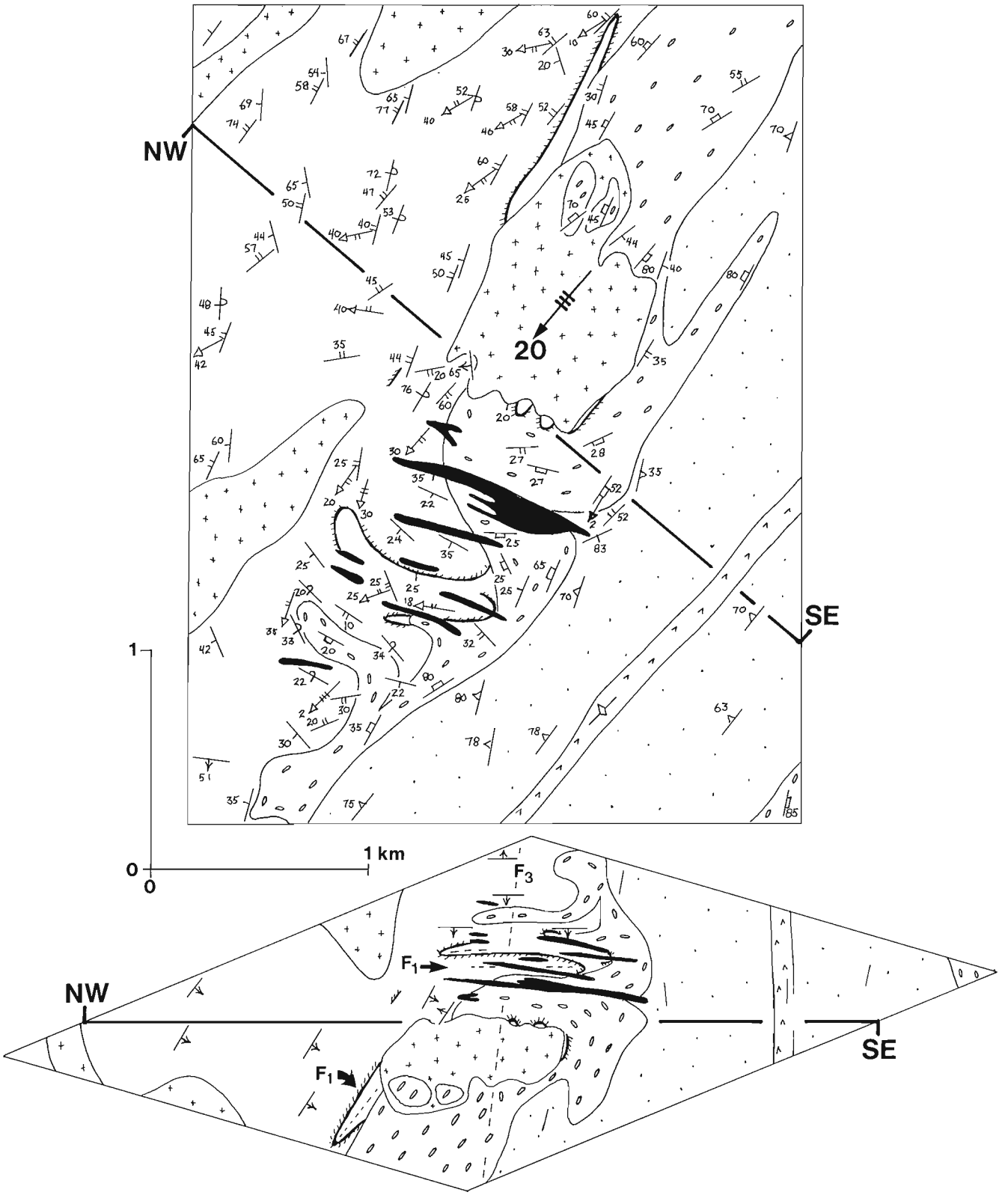

Figure 3. Detailed structural map of the Fish-hook Lake Outlet Stream area (Fig. 2) and tectonic profile of the map projected onto the plane labelled NW-SE. Symbols and patterns correspond to Figure 2, except that pegmatitic tonalite sheets are black and iron-formation is hachured for emphasis. The Mackenzie dyke is omitted. See text for discussion.

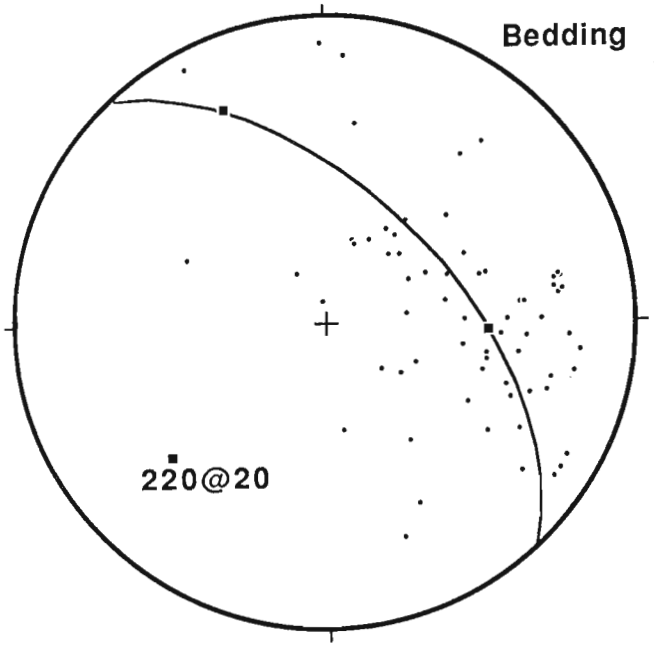

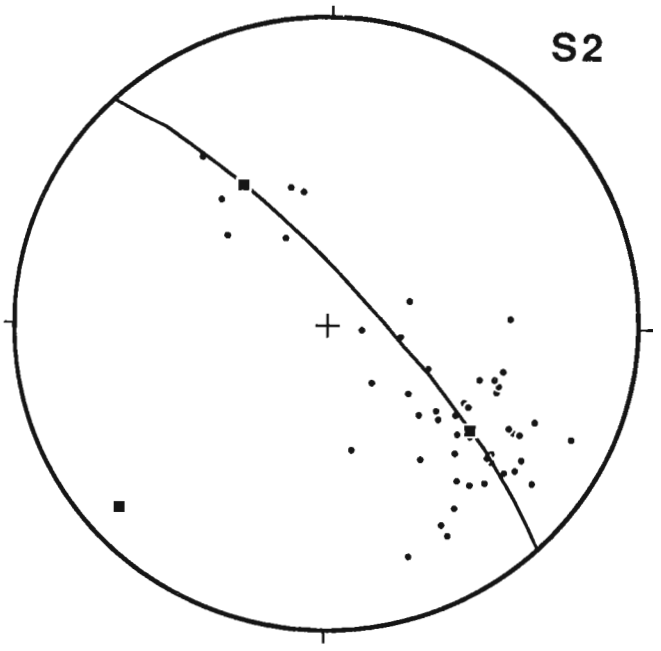

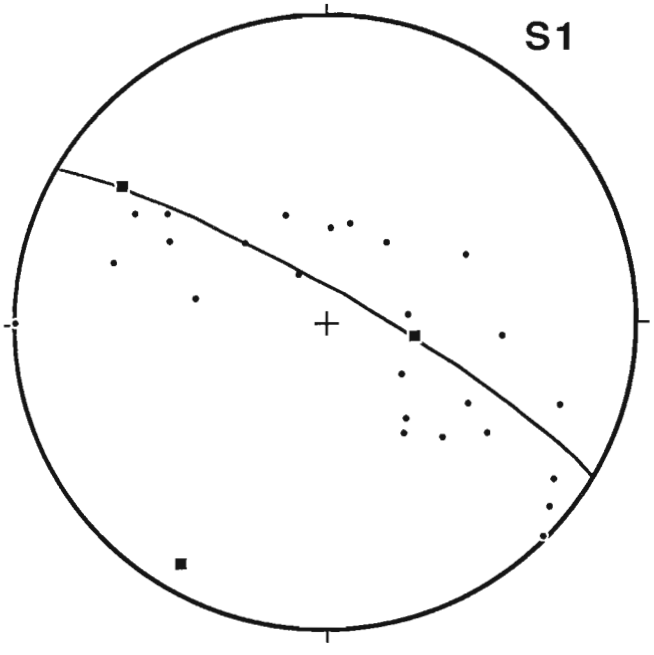

Figure 4. Equal area plots of data collected from the Fish-hook Lake Outlet Stream area (Fig. 3). Plots of poles to S_0, S_1, and S_2 with the best-fit great circles and fold axes are shown. The bedding axis (220°/20°) was used to construct the tectonic profile of the map (Fig. 3). See text for discussion.

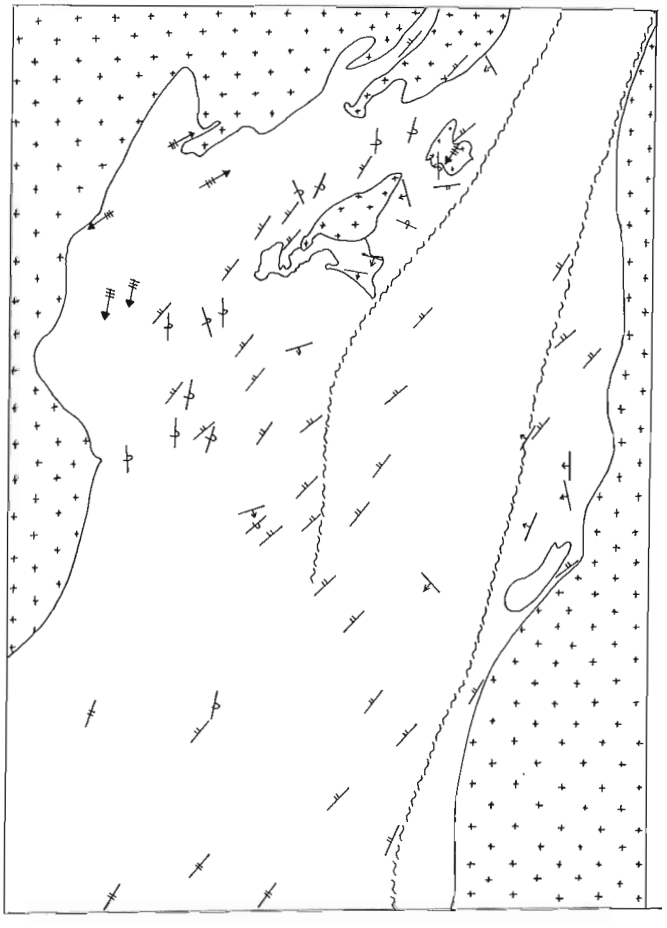

Figure 5. Map of the Fish-hook Lake area showing S_0 facing directions, S_2 cleavage orientations and F_3 axes. The wavy lines enclose the bulk of the volcanic, hypabyssal, and associated arenites and coarse clastic rocks (Fig. 2). See text for discussion.

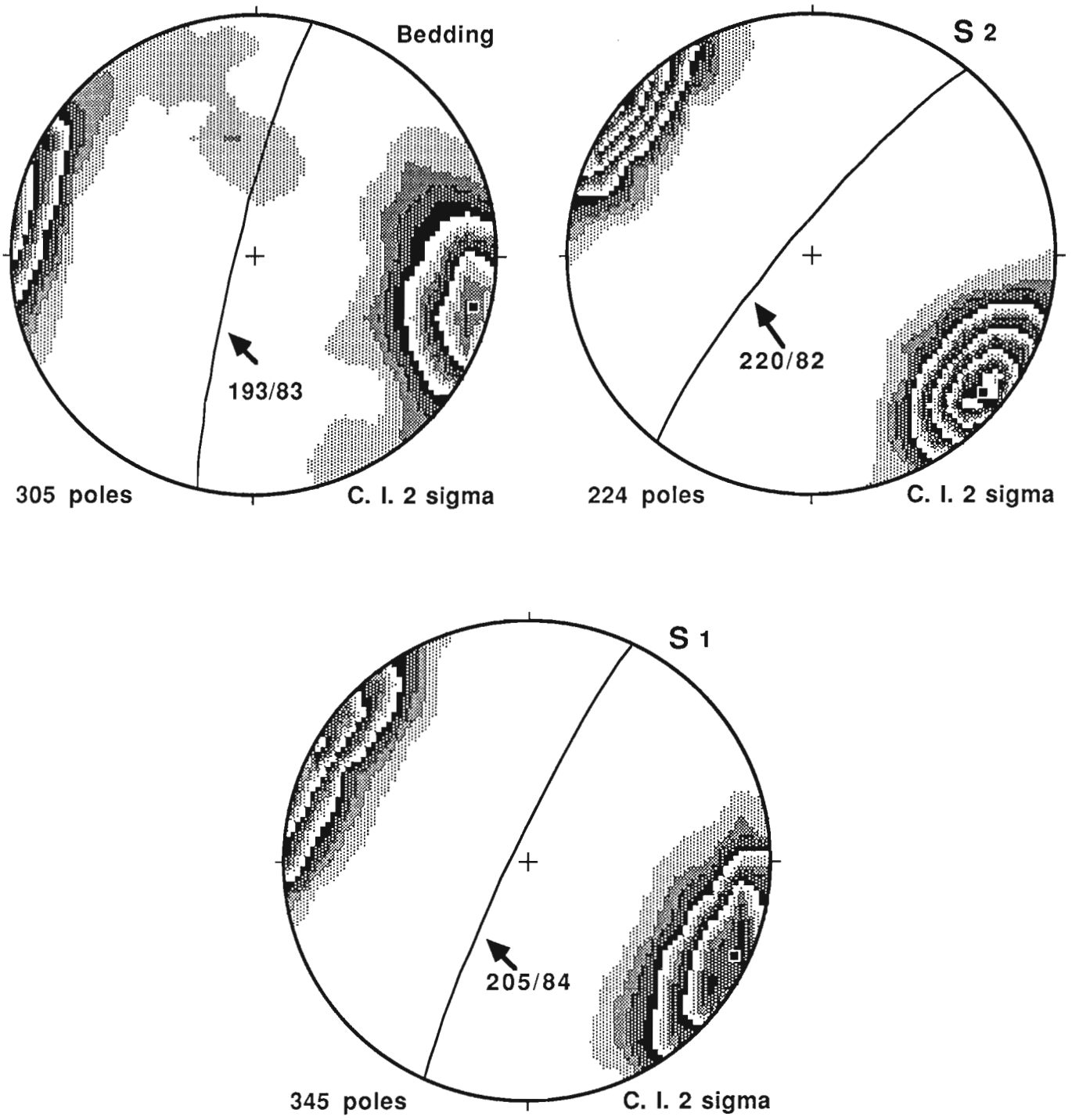

Figure 6. Equal area plots of S_0, S_1, and S_2 with great circles showing the dominant trend of each fabric plane in the Fish-hook Lake area (data from F3 hinge regions are omitted). Note that S_2 strikes clockwise of S_0 and S_1 (this can also be seen by inspection of Fig. 2.). See text for discussion.

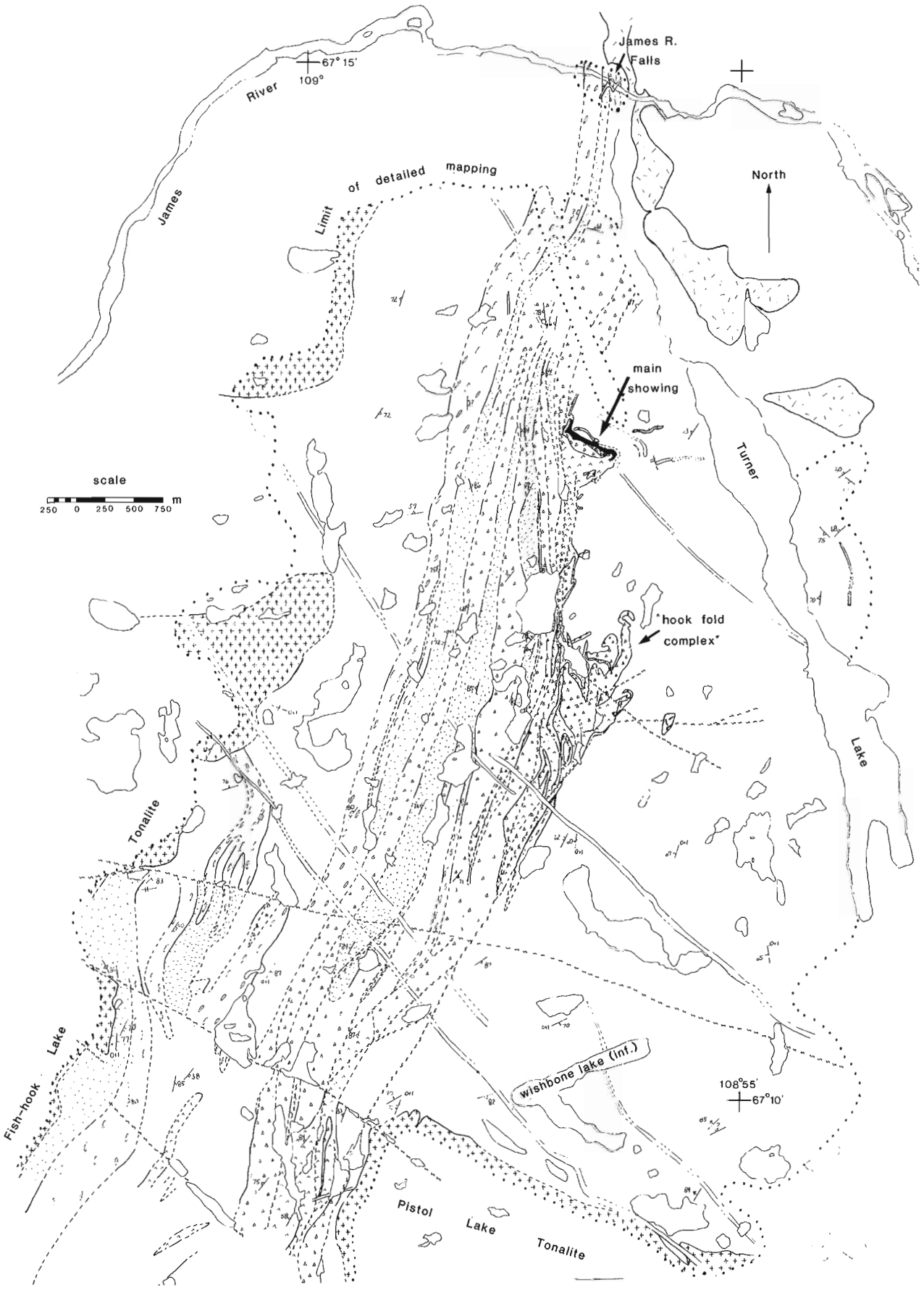

Figure 7. Geology of Turner Lake area, incorporating data from unpublished map by C. Clode and S. Bishop. Legend as in Figures 1 and 2. Figures 8 and 9 provide more detail of the hook fold complex and James River Falls section.

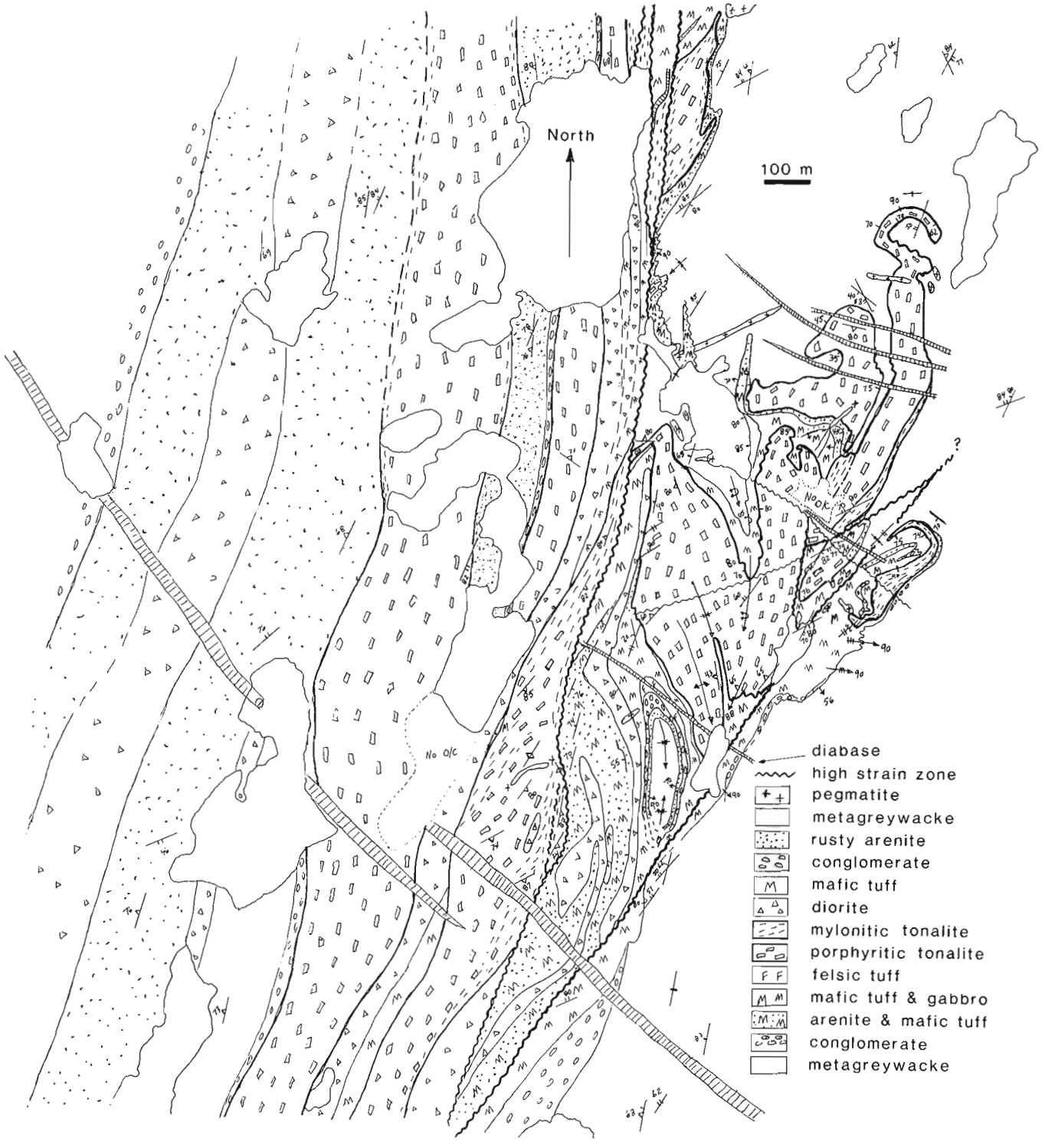

Figure 8. Detailed geology of the "hook fold complex", central Turner Lake area (Fig. 7), illustrating change in structural style and truncation of lithological units across the Turner high-strain zone and its splays. Legend shows mapped lithological sequence in this locality.

9. *Pegmatite sheets* in the Turner Lake area are irregular, gently to steeply dipping, deformed (F_1?) bodies as exposed at James River falls (Fig. 9) and around the main showing west of Turner Lake (Fig. 7). These bodies comprise at least two pegmatite phases. The older phase, northerly trending and tonalitic, is characterized by Z-folded, rhythmically graded layering with distinct cusp-and-lobe structures. Tourmaline is consistently enriched toward the east sides of layers (hachured lines in Fig. 9) which are subparallel to the walls of the dyke.

10. *The Fish-hook Lake tonalite* is only weakly foliated (S_3?) and cuts angularly across mapped F_1 and F_2 folds and fabrics (*see* Fig. 3 and discussion below). The main body marks the western margin of the supracrustal belt. Several satellite bodies, as well as related east-west pegmatitic dykes, occur in the Fish-hook Lake area (Fig. 2, 3). The dykes increase markedly in abundance toward the west, are very abundant close to and within the tonalite, and similarly transect S_1 and S_2.

FISH-HOOK LAKE AREA

Figure 2 summarizes the geology of this part of the belt. The structure is complex; three periods of folding are recognized which have associated fabric elements. A bedding-parallel foliation is the earliest tectonic fabric. In several places mesoscale isoclinal folds were seen that appear to have an axial-planar S_1 foliation. The most convincing evidence to date of the reality and significance of F_1, however, is shown in Figure 3, discussed as follows.

In the area of Figure 3, bedding (S_0), S_1, and crenulation cleavage (S_2) are all nearly coaxially folded parallel to an F_3 antiform axis plunging toward 220° at 20° (Fig. 4). The three fold sets are not perfectly coaxial, and the tectonic profile should be taken qualitatively, although it was constructed using quantitative techniques pioneered by Stockwell (1950). The same perspective can be obtained by viewing the map from NE to SW at an angle of 20° (cf. Mackin, 1950).

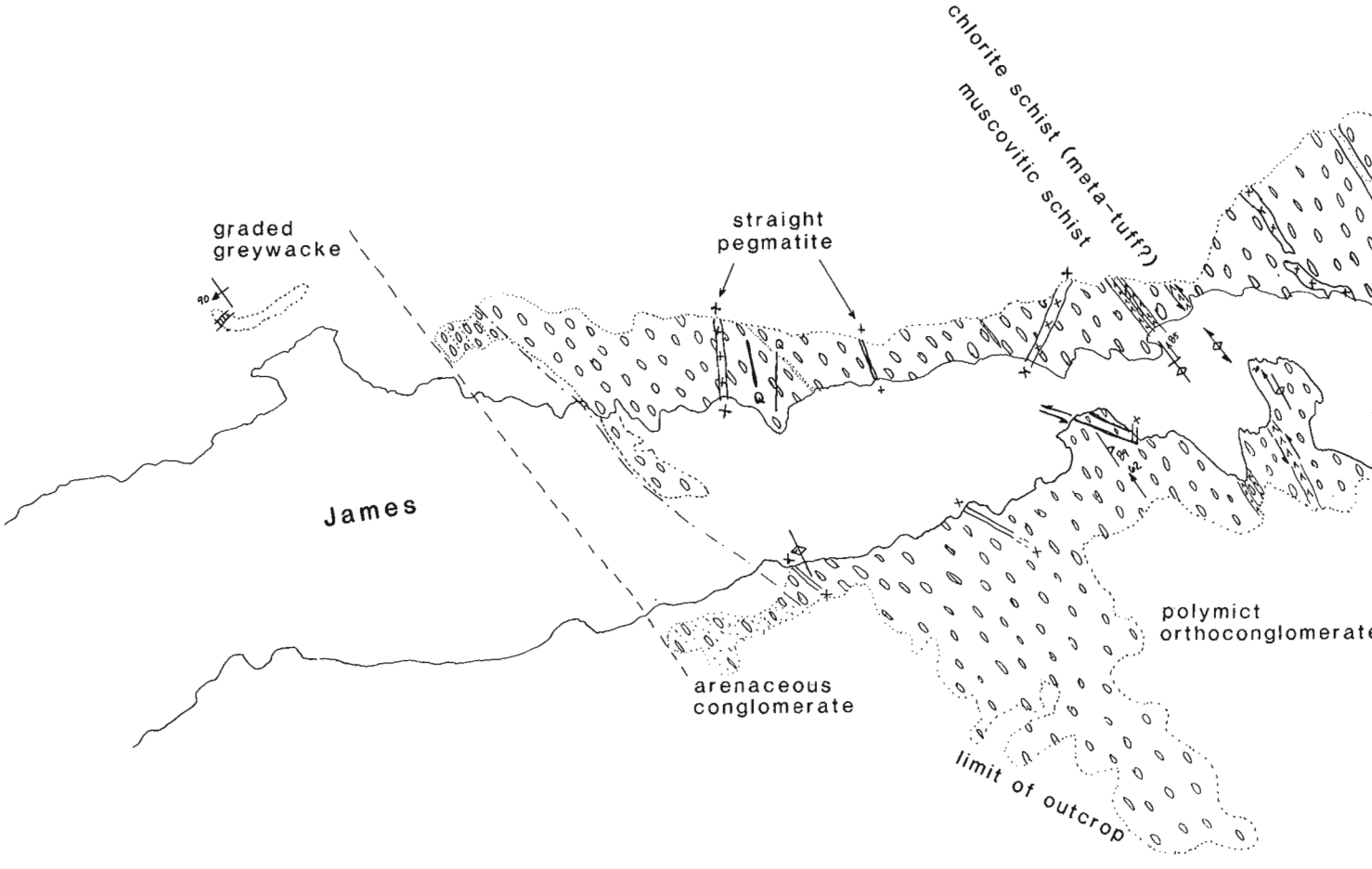

Figure 9. Detailed geology of the James River Falls section (symbols as in Fig. 2, location in Fig. 7).

The metagreywacke succession in the NW (Fig. 3) is overturned and faces SE toward the iron-formation and conglomerate (*see* Fig. 5). The iron-formation displays an isoclinal F_1 syncline on the NW limb of the F_3 antiform (labelled on the profile, Fig. 3), and it is overlain unconformably by the conglomerate. Note that the succession is generally downward-facing on the F_3 antiform. On the crest of the F_3 antiform is a reclined F_1 anticline with its lower limb truncated by the unconformity at the base of the conglomerate.

Numerous inclined-plunging F_2 folds occur within the greywacke sequence on the NW limb of the F_3 antiform (Fig. 3), and they are revealed by the changing vergence of SW-plunging crenulations of S1 cleavages (S1/S2 intersection lineations). Given sufficient time, these macroscale F_2 folds could be mapped by tracing individual metagreywacke beds on the aerial photographs. In contrast to the greywacke-dominated NW limb of the F_3 antiform, the quartz-arenite- and volcanic-rock-dominated SE limb has no mapped F_2 folds or cleavages in the area of Figure 3. In this domain, a single tectonic fabric plane, for simplicity labelled S_1, is very well developed. It is believed that this domain is a zone of high strain resulting in F_3 transposition of S_0 and S_2. This high-strain zone is shown by the wavy line in Figures 1, 2 and 5. Steeply-dipping limbs of F_3 characterize the structural pattern of most of the Fish-hook Lake area.

The macroscopic geometry of S_2 in the Fish-hook Lake area is shown in Figures 5 and 6. The stereonets (Fig. 6) indicate a strong tendency, except in F_3 fold hinges, for S_2 planes to dip steeply toward the NW, and to strike clockwise of more northerly-striking S_0 and S_1. It should be noted that F_2 structures, like F_1, are reclined on the crest of the F_3 antiform. If this hinge region retains the orientation of F_1 and F_2 prior to F_3, then thrust and nappe tectonics had a role in the early development of the deformed belt. Inspection of Figure 5 (and Fig. 2) reveals a stratigraphic-facing reversal in the centre of the Fish-hook Lake belt indicating that the supracrustal belt forms a major syncline bordered by tonalite. This feature is transected by the regional fabric labelled S_2 (Fig. 5).

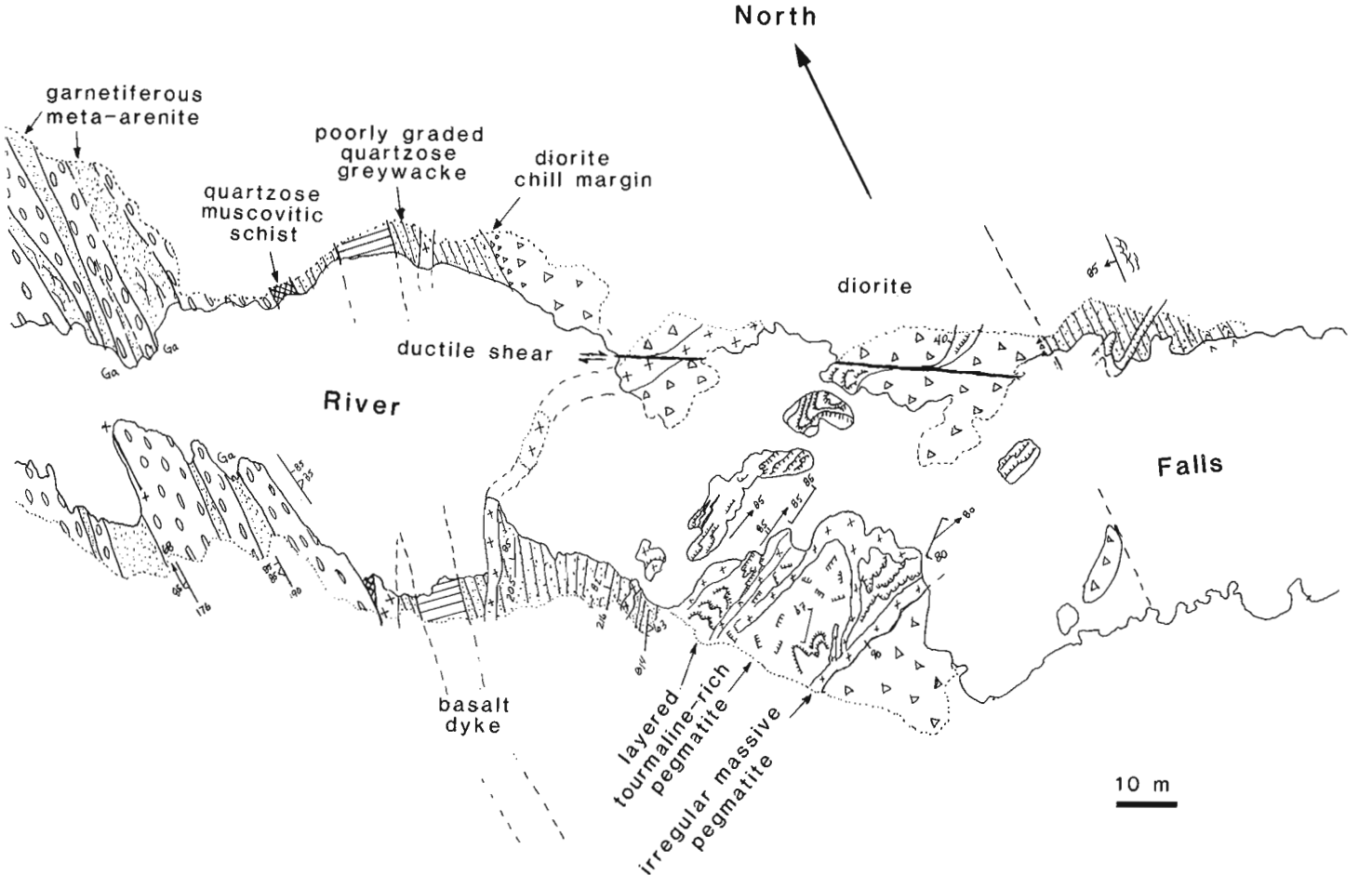

Localization of numerous semi-concordant tonalite sheets on the crest of the F_3 antiform (Fig. 3) indicates that this was a region of vertical extension during formation of the fold, permitting synkinematic intrusion of the sheets. U-Pb zircon dating of this tonalite, if successful, will date the important F_3 event here.

Evidence of prospecting in the Fish-hook Lake area is widespread. Nearly all rusty-weathering outcrops show evidence of surface sampling and have recently been flagged. However, the only area of diamond drilling observed is on the crest of the F_3 antiform in the Outlet Stream area (Fig. 3) where the holes were collared in conglomerate containing rusty-weathering, sulphidic iron-formation boulders.

TURNER LAKE AREA

Figure 7 summarizes the geology of this part of the belt. The main structural elements here (S_0, S_1, S_2) and rock types are identical to those present in the Fish-hook Lake area. S_2 transects doubly plunging F_1 isoclines as well the high strain zones and most other structures in the area of Figure 8, with overall steep NW dips and strikes clockwise of the more northerly striking S_0 and S_1.

This area differs from the Fish-hook Lake area in (i) the complexity of F_1 folds visible east of the Turner high strain zone (Fig. 8), (ii) the absence of southwesterly plunging F_3 folds, and (iii) the presence of very steep to vertical E-W (F_3) folds in the area from the "hook fold complex" (Fig. 8) to the main showing (Fig. 7). These are domainal structures that fold S_2, tighten F_1 isoclines, and contain local axial-planar crenulation cleavage (100°/90°). This cleavage is, in turn, weakly deformed by steeply dipping, north-trending crenulations. The E-W folds are unique to this area and are relatively tight close to the Turner high strain zone, but become more open and die out toward the east. These folds are not present west of the high strain zone and appear to be rooted in it. Their timing with respect to the Fish-hook Lake F_3 folds is not known.

The Turner Lake main gold showing (Silver Hart Mines Limited, 1985) is located on the south-facing (younging inward) north limb of the largest E-W fold. S. Fumerton of Chevron Minerals Ltd. (pers. comm. 1989) has mapped the prospect as a series of arenite lenses within epiclastic and high-magnesium volcanic rocks. The arenites are transected by various quartz veins with adjacent garnet+hornblende alteration. Gold is visible in the quartz veins and is located on the boundaries of microscopic pyrrhotite disseminated in the arenite.

HIGH STRAIN ZONES (*HSZ*)

A number of northerly trending valleys have linear to lenticular surface fabrics visible on 1:20 000 colour air photographs. Three of these linear zones (HSZ on Fig. 1) have been partially investigated in the course of mapping for this project. The central, Turner HSZ was previously interpreted (e.g. Clode, 1987) as a shear zone. It, and the Fish HSZs are approximately coincident with: 1) facies changes from the central arenite-volcanic sequence to the eastern and western greywacke-iron-formation sequences, 2) changes in structural style from northerly trending in the centre to variable (locally east-west) on the margins of the arenite-volcanic facies belt, and 3) the angular unconformity between conglomerate and iron-formation in the Fish-hook Lake area. The Pistol HSZ is a zone of highly foliated wackes that separates the eastern and western lobes of the Pistol Lake tonalite. Other zones are shown only as lineaments and lack field observations. Epidote and chlorite alteration and local intense quartz veining with associated disseminations of pyrrhotite and arsenopyrite are exposed in a number of places along the shear zones.

The Turner HSZ is marked by broad to narrow linear valleys which are characterized by intense development of regional fabrics (flattening of cobbles, steep S_1 and S_2 foliations in all rock types transected by them), local mylonite, and abundant quartz veins in supracrustal rocks. The east-west structural change across the Turner HSZ is illustrated in Figure 8. Complex isoclinal F_1 folds are transected by S_2 cleavage, on both sides of this HSZ but are refolded by mesoscopic to macroscopic, vertical, F_3 (?) folds only on the east side of the HSZ.

Numerous minor "S" and "Z" folds and "pull-aparts" are developed in the quartz veinlets that pervade the Turner HSZ. Intersecting fabrics that superficially resemble C/S are best developed near and in the high strain zones, in homogeneous competent rocks such as felsic crystal tuffs and arenites. No stretching lineations, only the ubiquitous, near-vertical intersection lineations of S_1/S_2, have been observed. The net amount and direction of movement across the Turner HSZ cannot be ascertained without more diagnostic criteria.

The Fish HSZ (Fig. 1, 2) is a less distinct zone of relatively strong foliation across which lithological units and fold structures cannot be traced (see discussion of D_3 in the Fish-hook Lake Outlet Stream area).

The Pistol HSZ, a screen of intensely foliated greywacke containing large lenticles of tonalite, partitions the Pistol Lake tonalite into two large lobes but has not been defined to the north or south. Cusp-and-lobe structures mapped at the northwest end of the Pistol Lake tonalite (Fig. 7) contain similar fabrics to those of the Turner HSZ. Vertically plunging lobes of tonalite project into greywacke, and cusps of highly foliated greywacke project a few to tens of metres into the tonalite. One or both margins of the cusps include thin mylonite and abundant quartz veins. The plunges of the lobes vary from near-vertical to overturned. Steeply dipping S_2 transects the cusps with a strike clockwise to that of both limbs. The natures of the foliations, quartz veins and thin mylonites are very similar to those noted at the northeast corner and western margin of the tonalite where it is transected by the continuous Turner HSZ. The cusp-and lobe structures are roughly symmetrical and there is no horizontal offset of the enveloping east-west tonalite-wacke contact.

RELEVANCE TO MINERAL EXPLORATION

Much mineral exploration, including drilling, has been concentrated on the Fish-hook Lake F_3 hinge. We have observed that drill targets have included not only iron-formation, but also sulphidic parts of the James Falls conglomerate that have incorporated clasts of iron-formation above an unconformity. Similarly, the Turner Lake main gold showing is located in a late macroscale fold which deforms S_0, S_1 and S_2. The Turner Lake showing differs by being hosted in sulphidic arenites and the structure is the steep north limb of the vertically plunging, east-closing fold. Both exploration areas are bounded on one side by high strain zones that trend approximately 020° and contain intense foliation, abundant quartz veins, local mylonite and local arsenopyrite. The Fish and Turner high strain zones approximately outline a central sequence, dominated by conglomerate, arenite and volcanic rocks, which is bounded to the east and west by greywacke with iron-formation.

The auriferous iron-formations at Pistol Lake are also complexly folded, hosted by greywacke and apparently transected by high strain zones. The writers and R. Wyllie intend to further investigate the variety of structural-stratigraphic associations that appear to be favourable for gold in this belt.

REFERENCES

Clode, C.
1987: The geology of the Turner Lake gold prospect, Bathurst Inlet, Northwest territories; unpublished M.Sc. thesis, Queen's University, 50 p.

Fabbri, A.G., Kushigbor, C.A., Wang. L., Baker, A.B., and Roscoe, S.M.
1989: Integration of remotely sensed and ancillary geological data for assessing mineral resources in the Bathurst Inlet area, N.W.T., Canada; *in* Proceedings of the 21st Application of Computers and Operations Research in the Mineral Industry (APCOM). Las Vegas, Nevada, Feb. 27 — Mar 2, 1989, Society of Mining Engineers Inc., p. 1109-1120.

Ford, R.C.
1988: Comparative geology of gold-bearing Archean iron-formation, Slave Structural Province, Northwest territories; unpublished M. Sc. thesis, The University of Western Ontario, London, Ontario, 233 p.

Fraser, J.A.,
1964: Geological notes on northeastern District of Mackenzie, Northwest Territories Geological Survey of Canada, Paper 63-40, 16 p. (report and Map 45-1963).

Johnstone, R. M.
1989: Preliminary geology of the Torp Lake area NTS 76 N/5, 6 Torp Lake metasedimentary belt, NWT (EGS 1989-7); NWT Geology Division, Indian and Northern Affairs Canada.

Mackin, J. H.
1950: The down-structure method of viewing geological maps; Journal of Geology, v. 58, p. 55-72.

Roscoe, S.M.,
1983: Assessment of mineral resource potential in the Bathurst Inlet Area, NTS 76J,K,N,O, including the proposed Bathurst Inlet National Park; Geological Survey of Canada, Open File 788.

Roscoe, S.M., Staargaard, C.F. and Fraser S.
1988: Stratigraphic setting of gold concentrations in Archean supracrustal rocks near the west side of Bathurst Inlet, N.W.T.; *in* Current Research, Part C, Geological Survey of Canada, Paper 88-1C, p. 367-372.

Silver Hart Mines Limited
1985: 1985 Annual Report, Silver Hart Mines Ltd., Sherwood Park, Alberta, 21 p.

Stockwell, C. H.
1950: The use of plunge in the construction of cross-sections of folds; Geological Association of Canada, Proceedings, v. 3, p. 97-121.

AUTHOR INDEX

Geological Survey of Canada, Paper 90-1, Current Research is published as six parts, listed below, that can be purchased separately.

Recherches en cours, une publication de la Commission géologique du Canada, Étude 90-1, est publiée en huit parties, énumérées ci-dessous ; chaque partie est vendue séparément.

Part A, National and general programs
Partie A, Programmes nationaux et généraux

Part B, Eastern and Atlantic Canada
Partie B, Est et région atlantique du Canada

Part C, Canadian Shield
Partie C, Bouclier canadien

Part D, Interior Plaines and Arctic Canada
Partie D, Plaines intérieures et région arctique du Canada

Part E, Cordillera and Pacific Margin
Partie E, Cordillère et marge du Pacifique

Part F, Frontier Geoscience Program, Cordilleran and offshore basins, British Columbia
Partie F, Programme géoscientifique des régions pionnières, bassins de la Cordillère et extracôtiers, Colombie-Britannique